Pediatr Radiol (2018) 48 (Suppl 1):S1–S298
https://doi.org/10.1007/s00247-018-4130-z

The Society for Pediatric Radiology introduced its new logo August 15, 2013. The logo communicates both the warmth of the Society community and the strength of the members' commitment to excellent and thoughtful care of the pediatric patient.

The first official logo for the SPR was designed by Tamar Kahane Oestreich of Cincinnati, Ohio in 1985. Thank you, Mrs. Oestreich.

Founded in 1959
The Society for Pediatric Radiology

61st Annual Meeting & Postgraduate Course
May 15-19, 2018

The Omni Nashville Hotel
Nashville, Tennessee, United States

Pediatric Imaging Technologist Program
May 17-19, 2018

Jointly provided by the American College of Radiology

This supplement was not sponsored by outside commercial interests; it was funded entirely by the Society's own resources.

TABLE OF CONTENTS

(T) Indicates an Imaging Technologist Program Submission.

WELCOME MESSAGE

I am extremely pleased to welcome you to the 61st meeting of The Society for Pediatric Radiology in the beautiful, vibrant city of Nashville, Tennessee.

We live in exciting, dynamic and challenging times. The world of medicine continues to evolve and advance at a remarkable and hectic pace. Radiology is at the center of this turmoil and affected in myriad ways. Imaging technology advances at a pace that is difficult to manage. New machines obtain more numerous and better images. New techniques allow for imaging of structures and diseases previously thought impossible. Imaging increasingly guides intervention and therapy. Imaging and imaged-guided interventional procedures are truly integral to modern pediatric healthcare delivery.

Many challenges persist. We constantly strive to achieve better images more efficiently (time and money), safely and with compassion. We challenge ourselves to maximize patient throughput, decrease reporting turn-around time, manage and limit radiation exposure, use contrast judiciously and safely, and address increasing concern with the use of sedation and anesthesia in children. Our clinical colleagues ask tough questions and want answers. Our researchers continually push the envelope of discovery.

Many important themes run through this meeting. Everything, however, comes back to the overriding theme of "Value-added Pediatric Radiology." Everything that we do in our daily work is aimed at improving the healthcare of the children that we serve. Everything that you will see and experience at this meeting will aid you to become a better pediatric radiologist or pediatric imaging technologist and take better care of your patients.

This meeting occurs at a time when our nation, inexplicably, is taking a deep look into issues of race, gender, diversity and inclusion. The SPR has always prided itself on being a welcoming, diverse, inclusive society. Ill-conceived laws in the states of Tennessee and California have forced the SPR to directly deal with this issue. As a professional society, we welcome this as a positive opportunity. We have created an SPR Diversity and Inclusion Committee, co-chaired by Ashok Panigrahy and Stephanie Spottswood. This important committee will help the SPR to evaluate itself. How are we doing as a society with diversity and inclusion? What can we do better? How can we help members to promote diversity and inclusion in their home institutions and in the care of our patients and their families? Dr. Spottswood, Associate Vice Chair for Diversity in the Department of Radiology at Vanderbilt University and Chair of the Office of Inclusion and Health Equity Advisory Board at Vanderbilt Children's Hospital, will deliver a keynote address "The Power of Diversity: Meeting Today's (and Tomorrow's) Greatest Healthcare Challenges" to the whole society on Wednesday, immediately prior to the Neuhauser lecture. There will be a workshop on diversity on Friday. I think that you will find these presentations thought-provoking and enlightening.

In current times, the health and well-being of children is under substantial threat by a small, but growing swell of child abuse denialism. For those of us that work in children's healthcare, this challenge is difficult to understand and rationalize. We work very hard to diagnose, to treat and to protect children and their families. We are extraordinarily careful to get the diagnosis right, be it child abuse or something else. However, there is much to be learned. We need to be careful, deliberate, regimented, collaborative and compassionate. I am delighted to have Paul Kleinman deliver this year's Neuhauser lecture. The lecture will be a capstone of a remarkable and impactful career. Paul's lecture, "Curious Bones: Sustaining Discovery in the Face of Doubt", will be an erudite look at where we have been, where we are and where we will go in child abuse imaging. A sequence of workshops will also address the important topic of child abuse.

I am indebted to Janet Reid and Jonathan Dillman for organizing and directing a spectacular Postgraduate Course. There will be two concurrent tracks, one on body imaging and the other on general pediatric radiology. Each topic will be a presented by paired speakers as a brief didactic followed by a response with cases. The paired speakers have diligently coordinated their presentations. I think that you will find this novel presentation mode exciting and educational. We are excited to include an updated version of RSNA Diagnosis Live™. We have dedicated a half day of one track to an update on Image Gently, organized by Don Frush and Keith Strauss, Chair and Vice Chair of the Image Gently Alliance, respectively.

You will also be excited to find more educational content in the form of workshops – more time slots and more choices. In addition to traditional sunrise workshops, we have added two "mid-day" (actually late morning) workshops. Ethan Smith and Mahesh Thapa have constructed a wonderfully diverse array of choices that should please everyone. I am very excited about a non-imaging, leadership development/practice of radiology series that runs throughout the workshops.

Please plan your stay until Saturday noon!! On Saturday morning, there are five spectacular sessions of focused learning planned – Education ("The Teaching Portfolio: A Hands-on Workshop on How to Get Promoted as an Educator"), Interventional Radiology ("Young Practitioners: The Future of Pediatric Interventional Radiology"), Oncology, Hands-on Ultrasound and Neuroradiology. These sessions are an integral component of the meeting and allow for greater depth of development of the program in each of these topics than can be achieved elsewhere in the meeting. If you leave early, you will miss out!

George Bisset has carefully recruited two highly qualified, highly competitive teams (again Team E and Team T) to battle it out in a much-anticipated reprisal of Jeopardy. Thanks to George for making this both fun and highly educational (great cases & pearls).

No professional meeting is successful without great science (papers) and education (posters). A heartfelt thanks goes to all of you who have invested hard work into your projects, papers and presentations. All papers will be presented in tri-current sessions this year in order to maximize the schedule and other activities. This reflects the continual growth of our society and our meeting, as well as the need to create more presentation and participation opportunities. Most of the paper sessions will be preceded by a 20-minute keynote address.

Melissa Hilmes (with her local connections to Vanderbilt) and Rich Heller (with his enthusiasm for the practice of radiology) have been charged to invite and coach speakers to address the fundamental theme of our meeting – "Value-added Pediatric Radiology." These talks will focus on how we add value in each realm of our work.

Imaging technologists are integral to our work. I am very pleased that, for the third year, there will be a Pediatric Imaging Technologists' Course, renamed from "Radiographers' Course to reflect its broader content. The course is again organized and directed by Laura Gruber and Christine Harris with guidance from Steve Simoneaux. The Imaging Technologists' Course is a great opportunity to learn and network. Please consider how your radiology department or group can facilitate the attendance of a deserving technologist (or more) who will surely benefit from this great program!

Nashville is an extraordinary city. It is vibrant and full of life. I urge you to take time to explore what Nashville has to offer. The Omni Nashville Hotel is conveniently located close to the rich nightlife of downtown Nashville and close to many great restaurants. Be sure to try the barbecue, Prince's hot chicken and, if to your liking, local libations. Take time to listen to the music! Many choices abound and not just limited to country music. Nashville is a very progressive, diverse, inclusive, welcoming and fun city. It is a perfect environment of our meeting. We thank the people of the city of Nashville and the staff at the truly marvelous Omni Hotel Nashville for their hospitality.

This meeting would not be possible if not for the extraordinary support and work of Angela Davis and Kasey O'Dea. They have been two or three steps ahead of me throughout the process. Angela and Kasey – thank you so much!!!

Lastly, the SPR meeting is about people. Reacquaint yourself with old friends and make some new friends. Please take time to introduce yourself to and get to know new people. Share your experiences and your enthusiasm for the work that we do in Pediatric Radiology. We can all be immensely proud of the work that we do, both individually and collectively as a professional society. Let us take this time to celebrate those successes, but also to learn and to do even better! I wish you a truly productive and fun week in Nashville!

Peter J. Strouse, MD, FACR
President and Program Director
The Society for Pediatric Radiology

DEDICATION

Walter E. Berdon, MD, 1930-2017

Thomas L. Slovis, MD, 1941-2018

The 2018 Society for Pediatric Radiology Meeting is dedicated to the memory of Walter E. Berdon, MD and Thomas L. Slovis, MD.

Walter E. Berdon ("Walter") was a forward-thinking leader for the Society for Pediatric Radiology. Walter served as president of the Society in 1979-1980 (presiding over the Society's meeting in Salt Lake City, Utah in 1980). In 1994, Walter was honored with the Gold Medal of the Society for Pediatric Radiology.

Of his many great accomplishments, one of his most significant was his role as a founding editor of the official journal of the Society, *Pediatric Radiology*, where he served as the sole Editor for the Americas for two decades. Through his role as journal editor, Walter guided our profession from its infancy into the modern era. He worked tirelessly to make the journal an informative and trustworthy source of information on pediatric radiology and to help each and every author make their paper better. He had remarkable insight for new technologies and great wisdom for controversies, new and old. As an editor, he served as an excellent role model, mentor and advisor for his successors.

Walter is best remembered for his boundless enthusiasm, his innate interest in life-long learning and his impact on his colleagues in pediatric radiology. He had a profound intellectual mind, a keen interest in well-performed science, and was an accomplished clinical researcher. He mentored innumerable students, trainees and junior colleagues, creating lifelong friendships and leaving a lasting impact on many careers.

Walter was a "people person." He took an interest in everyone – not just professionally but personally, as well. He wanted to know how you were doing and what you were doing professionally (how could he help?). He loved to talk; he connected with people and he connected people.

Walter was a constant presence at the annual Society for Pediatric Radiology meetings until recently when his health precluded his attendance. Even into his 80's, Walter attended the meeting to learn about new advances in pediatric radiology, to see old friends and to meet and mentor the younger members of our society.

Thomas L. Slovis ("Tom") was an energetic leader for the Society for Pediatric Radiology. Tom served as president of the Society in 1999-2000 (presiding over the Society's meeting in Naples, Florida in 2000). In 2005, Tom was honored with the Gold Medal of the Society for Pediatric Radiology.

Tom served as an assistant editor for *Pediatric Radiology* under Walter Berdon and assumed the role of Editor for the Americas in 2003. Tom served in this role for a decade. With the journal, Tom carried the great work of his predecessor forward. Tom expanded the scope of the journal with greater emphasis on review articles and topic oriented mini-symposia. He maintained high standards for scientific inquiry. He placed great emphasis on images ("they need to jump out at you"). Most importantly, he brought many contributors into the fold as authors, reviewers, editorial board members and assistant editors.

As with his mentor, Tom was blessed with boundless enthusiasm. He was also blessed with energy and determination. Tom got things done. If you were working on a paper or project with Tom, he drove you to get it done and you tried not to disappoint him. Tom was a terrific mentor to his colleagues at Children's Hospital of Michigan and to innumerable members of the Society for Pediatric Radiology.

A pediatrician at the start, Tom was truly driven in the quest to improve the healthcare and well-being of children. His dedication to this goal is an exemplar for all of us. Although there are countless examples, two areas of accomplishment stand out. First, Tom was instrumental in focusing our attention on management of radiation dose in children. He was the principal organizer of the first and subsequent ALARA meetings and saw that the material from these meetings was published in *Pediatric Radiology* for all to benefit from.

Second, throughout his career, and especially recently, Tom always sought to do what is right and to properly diagnose and protect the abused child, the most vulnerable of our patients.

Tom was also an instrumental leader of the Society for Pediatric Radiology. Under Tom's leadership, foundations for the current administrative structure of the Society were laid. He served on the Society for Pediatric Radiology Board of Directors longer than anyone else, wearing the hats of member-at-large and secretary before ramping up to president, chairman of the board of directors and past-president, then adding a few more years as journal editor. Like Walter, Tom was a constant presence at SPR meetings until last year when his health limited his ability to travel.

As you take in this meeting, please remember Walter and Tom and their many contributions to our society, to the healthcare of children and to each of us as individuals. The Society for Pediatric Radiology would not be what it is today without Walter and Tom. It is with immense gratitude that we remember these two great individuals.

Peter J. Strouse, MD, FACR

(Please also refer to: Walter E. Berdon (1930-2017) by Tom Slovis, Terry Levin and Aparna Joshi in the November 2017 issue of *Pediatric Radiology*. An obituary for Dr. Slovis will appear in the May 2018 issue of *Pediatric Radiology.)*

SPR 2018 ORGANIZATION

2018 MEETING CURRICULUM COMMITTEE

Peter J. Strouse, MD, FACR (Program Director and Paper Committee Chair)
Adina L. Alazraki, MD, FAAP (Oncology Session)
George S. Bisset, III, MD, FACR (Jeopardy Session)
Leah E. Braswell, MD (Interventional Radiology Session)
Sarah D. Bixby, MD (Poster Committee Vice Chair)
Taylor Chung, MD (Poster Committee Vice Chair)
Kassa Darge, MD, PhD (Hands-On Ultrasound Session)
Jonathan R. Dillman, MD, MSc (Postgraduate Course Director)
Monica Epelman, MD (Hands-On Ultrasound Session)
Donald P. Frush, MD, FACR (Postgraduate Course – Image Gently Organizer)
Michael S. Gee, MD, PhD (Oncology Session)
Laura A. Gruber, MBA, RT(R), RDMS, RVT (Technologist Program Director)
Roger Harned, MD, FACR (Interventional Radiology Session)
Christine Harris, RT (R) (MR) (Technologist Program Director)
Richard E. Heller, III, MD, MBA (Scientific Session Organizer)
Marta Hernanz-Schulman, MD, FACR (Hands-On Ultrasound Session)
Melissa A. Hilmes, MD (Scientific Session Organizer)
Thierry A. G. M. Huisman, MD (Neuroradiology Session)
Sarah S. Milla, MD, FAAP (Poster Committee Chair)
Helen R. Nadel, MD, FRCPC (Oncology Session)
Susan Palasis, MD (Neuroradiology Session)
Manish N. Patel, MD (Interventional Radiology Session)
Janet R. Reid, MD, FRCPC (Postgraduate Course Director and Education Session)
Dennis W. W. Shaw, MD (Neuroradiology Session)
Ethan A. Smith, MD (Workshop Director)
Keith J. Strauss, MSc, FACR (Postgraduate Course – Image Gently Organizer)
Mahesh M. Thapa, MD (Workshop Director and Education Session)
Stephan D. Voss, MD, PhD (Oncology Session)

ABSTRACT REVIEW COMMITTEE – PAPERS

Peter J. Strouse, MD, FACR, Chair
Taylor Chung, MD, Vice Chair
Sarah D. Bixby, MD
David A. Bloom, MD
Lorna P. Browne, MD
Dorothy I. Bulas, MD, FACR, FAAP
Michael J. Callahan, MD
Christopher I. Cassady, MD, FAAP
Teresa Chapman, MD, MA
Nancy A. Chauvin, MD
Brian D. Coley, MD, FACR, FAIUM
Hisham M. Dahmoush, MBBCh, FRCR
Kassa Darge, MD, PhD
Jonathan R. Dillman, MD, MSc
James S. Donaldson, MD, FACR
Josée Dubois, MD
Monica Epelman, MD
Mark R. Ferguson, MD
Donald P. Frush, MD, FACR
Michael S. Gee, MD, PhD
J. Damien Grattan-Smith, MBBS
Roger Harned, MD, FACR
Mark J. Hogan, MD
Nadja Kadom, MD
S. Pinar Karakas, MD
Beth M. Kline-Fath, MD
Bernadette L. Koch, MD
Neha S. Kwatra, MD
John D. MacKenzie, MD
M. Beth McCarville, MD
Arthur B. Meyers, MD
Robert C. Orth, MD, PhD
John M. Racadio, MD
Janet R. Reid, MD, FRCPC
Cynthia K. Rigsby, MD, FACR
Maura E. Ryan, MD
Jonathan Samet, MD
Sabah Servaes, MD
Ethan A. Smith, MD
Keith J. Strauss, MSc, FACR
Alexander J. Towbin, MD
Andrew T. Trout, MD
Jason P. Weinman, MD
Matthew T. Whitehead, MD
Stephan D. Voss, MD, PhD

ABSTRACT REVIEW COMMITTEE – POSTERS

Sarah S. Milla, MD, FAAP, Chair
Sarah D. Bixby, MD, Vice Chair
Anjum N. Bandarkar, MD
Thangamadhan Bosemani, MD
Kiery A. Braithwaite, MD
Maria A. Calvo-Garcia, MD
Gulraiz A. Chaudry, MBChB, MRCP, FRCR
Kassa Darge, MD, PhD
Nilesh Desai, MD
Paula N. Dickson, MD
Steven Don, MD
Eric Eutsler, MD
Anne Gill, MD

ABSTRACT REVIEW COMMITTEE – POSTERS
(continued)

Leslie E. Hirsig, MD
Thierry A. G. M. Huisman, MD
Nadja Kadom, MD
J. Herman Kan, MD
Rajesh Krishnamurthy, MD
Neha S. Kwatra, MD
Maria F. Ladino-Torres, MD
Shailee V. Lala, MD
Jonathan M. Loewen, MD
Adeka D. McIntosh, MD
Craig S. Mitchell, DO, MA
Helen R. Nadel, MD, FRCPC
Srikala Narayanan, MD
Hansel J. Otero, MD
Daniel J. Podberesky, MD
Janet R. Reid, MD, FRCPC
Susan E. Sharp, MD
Manrita K. Sidhu, MD
Bruno P. Soares, MD
Aylin Tekes-Brady, MD
Stephanie B. Theut, DO
Alexander J. Towbin, MD
Jason Tsai, MD
Jennifer Vaughn, MD
Nghia (Jack) Vo, MD
Ewa M. Wasilewska, MD
Arash R. Zandieh, MD

IMAGING TECHNOLOGIST PROGRAM & ABSTRACT COMMITTEE

Christine Harris, RT (R) (MR) (Technologist Program Director)
Laura A. Gruber, MBA, RT(R), RDMS, RVT (Technologist Program Director)
Stuart Brice
Brian Fox, MBA
Charles R. Fritz, RT, MBA
Lynne Hamer, MEd., RT
Todd Lehkamp
M. Craig Morriss, MD
Stephen F. Simoneaux, MD, Advisor
R. Daniel Smock, BHS RT(R)(MR)(CT), MRSO (MRSC)

CASES OF THE DAY ORGANIZERS

Neil D. Johnson, MBBS
Christopher Sternal- Johnson

MEETING INFORMATION TECHNOLOGY

Safwan S. Halabi, MD, Meeting IT Co-Director
Alexander J. Towbin, MD, Meeting IT Co-Director

MEETING PHOTOGRAPHERS

Alan E. Schlesinger, MD
Mahesh M. Thapa, MD

CONTINUING MEDICAL EDUCATION

ACCREDITATION STATEMENT:

This activity has been planned and implemented in accordance with the accreditation requirements and policies of the Accreditation Council for Continuing Medical Education through the joint providership of the American College of Radiology and Society of Pediatric Radiology. The American College of Radiology is accredited by the ACCME to provide continuing medical education for physicians.

CREDIT DESIGNATION STATEMENT:

The American College of Radiology designates this activity for a maximum of 39.25 *AMA PRA Category 1 Credit(s)* ™ Physicians should claim only the credit commensurate with the extent of their participation in the activity.

TECHNOLOGISTS:

The American College of Radiology is approved by the American Registry of Radiologic Technologists (ARRT) as a Recognized Continuing Education Evaluation Mechanism (RCEEM) to sponsor and/or review Continuing Medical Educational programs for Radiologic Technologists and Radiation Therapists. The American College of Radiology designates this educational activity as meeting the criteria for up to 42.75 Category A credit hours of the ARRT.

MAINTENANCE OF CERTIFICATION

Qualified on January 29, 2018, select sessions from this activity meet the American Board of Radiology criteria for a self-assessment (SAM) activity and is designated for up to 14.50 SAM credits toward the ABR Maintenance of Certification Program.

OBJECTIVES

The 2018 61st Annual Meeting & Postgraduate Course will provide pediatric and general radiologists with an opportunity to do the following:

1. Summarize the most current information on state-of-the-art pediatric imaging and the practice of pediatric radiology.
2. Describe and apply new technologies and imaging findings for pediatric imaging.
3. Discuss trends in research and education concerning the care and imaging of pediatric patients.
4. Identify common challenges facing pediatric radiologists, and possible solutions.
5. Describe and apply basic principles for implementing quality and safety programs in pediatric radiology
6. Evaluate and apply means of managing radiation exposure and the need for sedation/anesthesia during diagnostic imaging and image guided therapy.

At the conclusion of the experience, participants should have an improved understanding of the technologies discussed, increased awareness of the benefits and costs of diagnostic imaging in children and of ways to minimize risks, and an improved general knowledge of pediatric radiology.

DISCLOSURES

In compliance with ACCME requirements and guidelines, the ACR has developed a policy for review and disclosure of potential conflicts of interest, and a method of resolution if a conflict does exist. The ACR maintains a tradition of scientific integrity and objectivity in its educational activities. In order to preserve this integrity and objectivity, all individuals participating as planners, presenters, moderators and evaluators in an ACR educational activity or an activity jointly sponsored by the ACR must appropriately disclose any financial relationship with a commercial organization that may have an interest in the content of the educational activity.

The following planners, presenters, staff and evaluators have disclosed that neither they nor their spouse/partner have any financial interests, arrangements or affiliation in the context of this activity:

PRESENTERS

Patricia T. Acharya, MD
Michael R. Acord, MD
Sudha A. Anupindi, MD
Edward Arroyo, RDMS
Lauren W. Averill, MD
Rama S. Ayyala, MD
D. Gregory Bates, MD
David M. Biko, MD
David A. Bloom, MD, FACR
Tim N. Booth, MD
Scott Borinstein, MD
Samuel L. Brady, MS, PhD
Dana Brinson, BHA RT(R)
Brandon P. Brown, MD
Lorna P. Browne, MBBS
Dorothy I. Bulas, MD, FACR, FAAP
Nikki D. Butler, BMSc, RT(R)(QM)
Michael J. Callahan, MD
Christopher I. Cassady, MD, FAAP
Sherwin S. Chan, MD
Nancy A. Chauvin, MD
Govind B. Chavhan, MD, DNB
Lorraine Chisari, RDMS, RVT
Arabinda K. Choudhary, MD, FACHE, MBA
Asim F. Choudhri, MD
Jeanne Chow, MD
Jason Christensen, MD
Matthew Cooper, MD
Jesse Courtier, MD
Eric J. Crotty, MD
Hisham M. Dahmoush, MD
Jonathan Dallas, BS
Matthew Davenport, MD
John W. Dell, BSRT (R) (MR)
Jie Deng, PhD
Sarah Desoky, MD
Paula N. Dickson, MD
Cristina Dodge, MS
Steven Don, MD
James S. Donaldson, MD, FACR
Lane F. Donnelly, MD
Kevin C. Doyle,
Josee Dubois, MD
Jerry R. Dwek, MD
Brandon Edwards, CEO
Jesse M. Ehrenfeld, MD, MPH
Laura Z. Fenton, MD
Mark R. Ferguson, MD
Robert J. Fleck, MD
Judith Gadde, DO
Lacy Gandor, RDMS
Kimberly A. Garver, MD
Michelle Garza, (RTR)
Maryam Ghadimi Mahani, MD
Anne Gill, MD
Ciji N. Gilley, R.T.(R)
Melissa Goehner, BA RT(R)(CT)
Sarah Beth Gray, CCLS
Jared R. Green, MD
Jesse Green, RT(R)
S. Bruce Greenberg, MD
Mary-Louise Greer, MBBS
Richard B. Gunderman, MD, PhD
Matthew R. Hammer, MD
Nicole Hardin, MD
C. Matthew Hawkins, MD
Laura L. Hayes, MD
Gary L. Hedlund, DO
Lamont Hill, RDMS
Mai-Lan Ho, MD
Victor M. Ho-Fung, MD
Jason Hooper, BS, RDMS, RVT
Brian Hopely, MD
Ramesh S. Iyer, MD
Siddarth P. Jadhav, MD
Camilo Jaimes, MD
Diego Jaramillo, MD, MPH
Delma Y. Jarrett, MD
Craig M. Johnson, DO
Marty Jones, MHA, RT (R)(MR)
Aparna Joshi, MD
Bamidele F. Kammen, MD
Summer L. Kaplan, MD, MS
S. Pinar Karakas, MD
Merima Karastanovic, MS, RT(R)(MR)
Boaz Karmazyn, MD
Sue C. Kaste, DO
Geetika Khanna, MD, MS
Jill Kilkelly, MD
Paul K. Kleinman, MD
Beth M. Kline-Fath, MD
Brandi Kozak, RDMS
Rajesh Krishnamurthy, MD
Peter G. Kruk, MD
Jeannie K. Kwon, MD
Maria F. Ladino-Torres, MD
Tal Laor, MD
David B. Larson, MD, MBA
Bernard F. Laya, DO
Edward Y. Lee, MD, MPH
Gabe Linke, BSRT (R)(MR)
Deborah Lowen, MD
Karen Lyons, MB, BCh, BAO
Robert MacDougall, MS

Joseph MacLean, CNMT
Alexis B. R. Maddocks, MD
Ladonna J. Malone, MD
Peter A. Marcovici, MD
Megan B. Marine, MD
Kelley W. Marshall, MD
Jeffrey E. Martus, MD, MS
Lea Matsuoka, MD, FACS
M. Beth McCarville, MD
Sarah McKenney, PhD
Mariana Meyers, MD
Cindy R. Miller, MD
Leslie Mintz, BSN
David M. Mirsky, MD
David A. Mong, MD
Joëlle A. Moreno, JD
Trudy Morgan, RDMS
Dedrick Moulton, MD
Martha M. Munden, MD
Oscar M. Navarro, MD
Elad Nevo, MS, RT(MR)(N)(CT), CNMT
Beverley Newman, MD, FACR
Anh-Vu H. Ngo, MD
Jennifer L. Nicholas, MD
Joshua Nickerson, MD
Anh-Vu M. O'Hara, MD
James A. O'Neill, MD
Seng H. Ong, MBBS
Robert C. Orth, MD, MPH, PhD
Hansel J. Otero, MD
Jeffrey P. Otjen, MD
Randolph K. Otto, MD
Harriet J. Paltiel, MD
Ashok Panigrahy, MD
Marguerite T. Parisi, MD, MS
Zoltan Patay, MD, PhD
Michael D. Payne, RT
Jeannette M. Perez-Rossello, MD
John Pietch, MD
Kara-Lee Pool, MD
Andrada R. Popescu, MD
Laura Poznick, AAS, RDMS
Georgiena E. Prevett, MS, RT(R)(N) (CT)(MR), CNMT (CT)
Sumit Pruthi, MD
John Racadio, MD
Ray Ramoso, ARRT (r) (vi)
Trista Raymer, RT, (R)(CT)(MR)
Cynthia K. Rigsby, MD, FACR
Kimberly Ritze, BS, RT(R), CT, MR
Gina Roberts, ARRT (R)(CT)(MRI)
Nancy K. Rollins, MD
Veronica J. Rooks, MD
Monica A. Rossleigh, MD
Erika Rubesova, MD
Maura E. Ryan, MD
Pallavi Sagar, MD
David Saul, MD
Dawn E. Saunders, MD
Andrew Schapiro, MD
Gary R. Schooler, MD
Daniel M. Schwartz, MD
Erin S. Schwartz, MD
Ramdas Senasi, MD
Suraj D. Serai, PhD
Susan E. Sharp, MD
Karuna V. Shekdar, MD
Sphoorti Shellikeri, MS
Nicholas Shkumat, MSc
Manohar Shroff, MD
Cicero T. Silva, MD
Stephen F. Simoneaux, MD
Maria Smith, BS, RDMS, RVT
Stephanie E. Spottswood, MD, MSPH
Judy H. Squires, MD
Abhay Srinivasan, MD
Lisa J. States, MD
Stacy T. Tanaka, MD, MS
Richard B. Towbin, MD, FACR
Sheryl A. Tulin-Silver, MD
Unmi K. Udayasankar, MD
Seth E. Vatsky, DO
Teresa Victoria, MD, PhD
Nghia "Jack" Vo, MD
Arastoo Vossough, MD, PhD
Jason P. Weinman, MD
Amy S. Whigham, MD
Jason N. Wright, MD
Deborah Zarnow, MD
Andrew M. Zbojniewicz, MD

PLANNING COMMITTEE & PRESENTER

Adina L. Alazraki, MD, FAAP
George S. Bissett, MD, FACR
Sarah D. Bixby, MD
Leah E. Braswell, MD
Kassa Darge, MD, PhD
Ellen M. Chung, MD
Monica Epelman, MD
Donald. P. Frush, MD, FACR
Michael S. Gee, MD, PhD
Laura Gruber, MBA, RT(R), RDMS, RVT
Christine Harris, RT (R) (MR)
Richard E. Heller III, MD, MBA
Marta Hernanz-Schulman, MD, FACR
Melissa A. Hilmes, MD
Thierry A. G. M. Huisman, MD
Sarah S. Milla, MD, FAAP
Helen R. Nadel, MD, FRCPC
Susan Palasis, MD
Manish N. Patel, DO
Janet R. Reid, MD, FRCPC
Dennis W. W. Shaw, MD
Ethan A. Smith, MD
Keith J. Strauss, MSc, FACR
Peter J. Strouse, MD, FACR
Mahesh M. Thapa, MD
Stephan D. Voss, MD, PhD

STAFF & CME REVIEWER(S)

Angela R. Davis, CAE
Kasey O'Dea
Category 1 - Steven Chmielewski, MD
Category A - Brian Monzon, RT

The planners and presenters listed below have disclosed the following relevant financial relationships. Potential conflicts have been resolved.

PRESENTERS WITH DISCLOSURES

Michael Aquino, MD	Elsevier - Royalties
Susan J. Back, MD	Bracco – Research Grant(s)
Brian D. Coley, MD, FACR	Elsevier – Royalties, NewView – Board Member Philips/Toshiba – Travel Support
R. Paul Guillerman, MD	Guerbet LLC – Consultant, Honoraria
Eric Hoggard, MD	Gore – Consultant, Honoraria
Jill V. Hunter, MBBS	Medico – Consultant, Honoraria; UpToDate - Royalties
Steven J. Kraus, MD, MS, FAAP	Elsevier - Royalties
Ruth Lim, MD	New England PET Imaging System - Officer
Prakash M. Masand, MD	Daiichi Sankyo Inc., Vital Images, Philips MRI – Consultant Honoraria; Toshiba Medical Systems – Speakers Bureau; Amirsys - Royalties
Arnold Carl Merrow, MD	Elsevier – Royalties, Consultant, Honoraria
Arthur B. Meyers, MD	Amirsys – Royalties, Elsevier - Royalties
Eric J. Monroe, MD	Biogen – Advisory Board
Daniel J. Podberesky, MD	Guerbet/GE/Philips/Siemens – Consultant, Honoraria; Toshiba of Americas Medical Systems – Speakers Bureau; Amirsys – Royalties
Caroline D. Robson, MBChB	Elsevier – Royalties
Ehsan Samei, PhD	GE/Siemens – Research Grant(s); MedInt Holdings – Advisory Board
Scott E. Snyder, PhD	Ground Fluor Pharmaceuticals/ United Therapeutics, EMD Sorono (Merck, KGaA) – Research Grant(s)
Alexander J. Towbin, MD	Siemens/Guerbet/Cystic Fibrosis Foundation – Research Grant(s), Applied Radiology, IBM Watson Health - Consultant/Honoraria
Andrew T. Trout, MD	Geurbet - Consultant, Honoraria; Elsevier - Royalites; Siemens/ Toshiba - Research Grant(s); Perpectum Diagnostics – Medical Advisory Board
Shreyas S. Vasanawala, MD, PhD	Arterys - Stock Options, GE Healthcare – Research Grant(s), Stanford - Intellectual Property Rights
Lisa R. Young, MD	Boehringer Ingeleheim - Advisory Board, UpToDate – Royalties

PLANNING COMMITTEE & PRESENTER WITH DISCLOSURES

Jonathan R. Dillman, MD, MSc	Bracoo Diagnostics/Guerbet/Toshiba US/Siemens Medical Solutions USA – Research Grant(s)
Keith J. Strauss, MSc, FACR	Philips Medical Systems – Consultant/Honoraria

ACKNOWLEDGEMENTS

The Society for Pediatric Radiology gratefully acknowledges the support of the of the following companies in presenting the 61st Annual Meeting & Postgraduate Course.

EDUCATIONAL GRANTS
Bayer
Guerbet LLC

EXHIBITORS – *as of April 6th*
AGFA HealthCare
Alexion
Aris Radiology
Bayer
Bracco Diagnostics Inc.
Canon Medical Systems USA
ChiRhoClin,Inc.
Dream Think Imagine
Elsevier, Inc.
Fujifilm Medical Systems USA, Inc.
GE Healthcare
Guerbet, LLC
Imorgan
LMT Medical Systems GmbH
Mindray
Philips Healthcare
Planmed, Inc.
Samsung Neurologica
SealCath
Siemens
Softek Illuminate
SREE Medical Systems
Stratasys
Wolters Kluwer
St. Jude Children's Research Hospital Department Diagnostic Imaging

MEETING SPACE

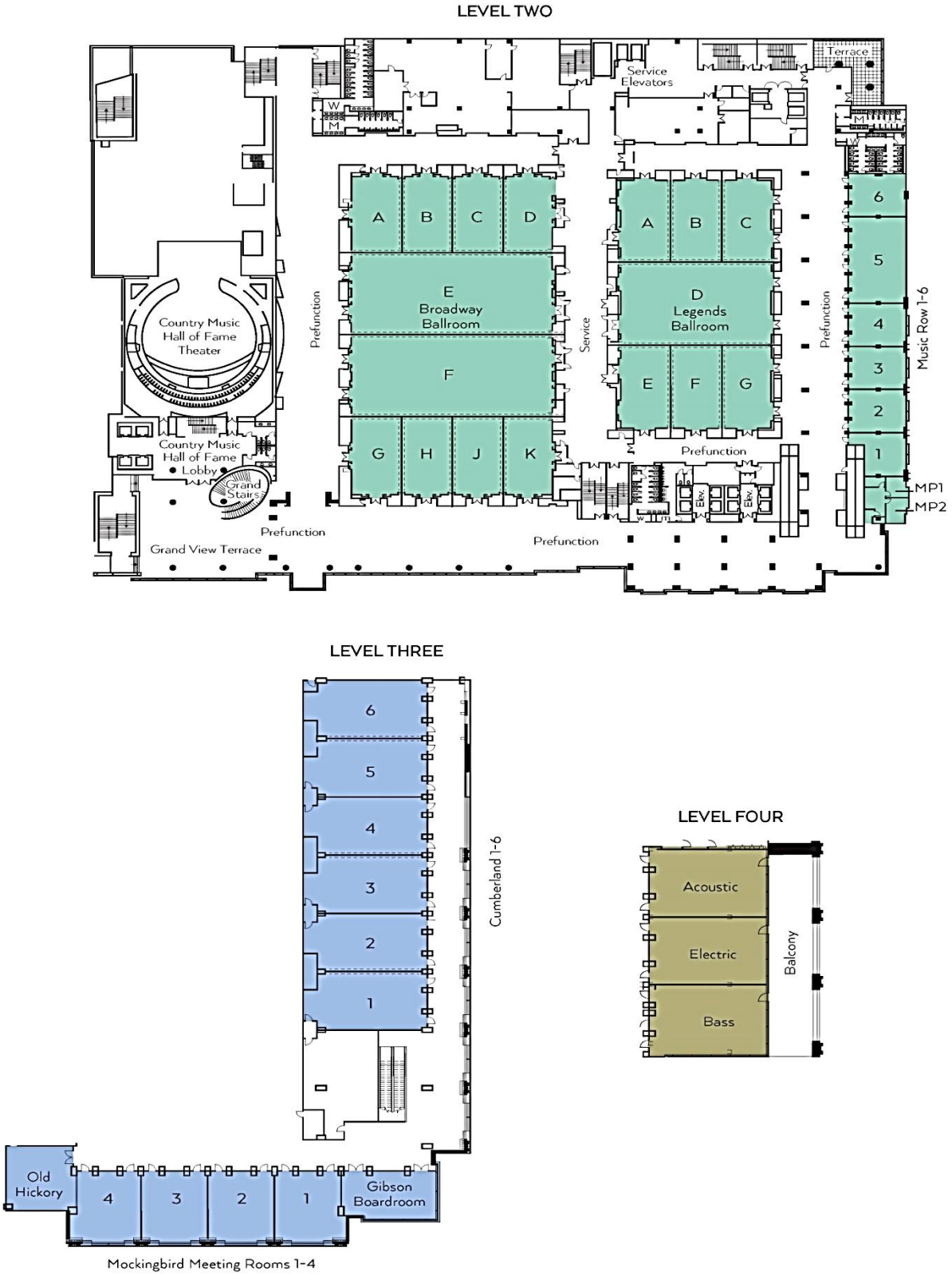

SPR GENERAL INFORMATION

MISSION STATEMENT
The Society for Pediatric Radiology is dedicated to fostering excellence in pediatric health care through imaging and image-guided care.

DIVERSITY & INCLUSION STATEMENT
The Society for Pediatric Radiology actively promotes diversity and inclusion at all levels of training, practice and leadership for the benefit of our patients, our profession and for the Society as a whole.

SPR OFFICERS, DIRECTORS AND COMMITTEES 2017–2018

BOARD OF DIRECTORS

Diego Jaramillo, MD, MPH, Chair
Peter J. Strouse, MD, FACR, President and Editor
Taylor Chung, MD, President-Elect
Christopher I. Cassady, MD, FAAP, 1st Vice-President
J. Damien Grattan-Smith, MBBS, 2nd Vice-President, SPR Research and Education Foundation President
Michael J. Callahan, MD, Secretary
Stephen F. Simoneaux, MD, Treasurer and '15-'17 SCORCH President
Kassa Darge, MD, PhD
Molly E. Dempsey, MD, '17-'19 SCORCH President
Josée Dubois, MD
Laura Z. Fenton, MD
Beth M. Kline-Fath, MD
Susan Palasis, MD
Mary R. Wyers, MD
Richard A. Barth, MD, FACR, FAAP, Past President
Brian D. Coley, MD, FACR, FAIUM, Past President
James S. Donaldson, MD, FACR, Past President
Donald P. Frush, MD, FACR, Image Gently Liaison
Marta Hernanz-Schulman, MD, FACR, ACR Commission Liaison
Benjamin H. Taragin, MD, Web Editor
Maria Gisela Mercado-Dean, MD, '15-'17 AAP Liaison
Sarah S. Milla, MD, FAAP, '17-'19 AAP Liaison
M. Ines Boechat, MD, FACR, WFPI Liaison

ABDOMINAL IMAGING COMMITTEE

Jonathan R. Dillman, MD, MSc, Chair
Sudha A. Anupindi, MD
Lauren W. Averill, MD
Govind B. Chavhan, MD, DNB
Ellen M. Chung, MD
Meryle Eklund, MD
Hansel J. Otero, MD
Daniel J. Podberesky, MD
Anil G. Rao, DMRD, DNB
Gary R. Schooler, MD
Ethan A. Smith, MD
Andrew T. Trout, MD

BYLAWS COMMITTEE

Diego Jaramillo, MD, MPH, Chair
Richard A. Barth, MD, FACR, FAAP
Kassa Darge, MD, PhD
Mary R. Wyers, MD

CARDIAC IMAGING COMMITTEE

Lorna P. Browne, MD, Chair
Mark R. Ferguson, MD
Maryam Ghadimi Mahani, MD
Eric Hoggard, MD
Ramkumar Krishnamurthy, PhD
Karen Lyons, MB, BCh, BAO
Ladonna J. Malone, MD
Prakash M. Masand, MD
Mike Seed, MBBS
Ting Y. Tao, MD, PhD
Gauri S. Tilak, MD, PhD, MPH
Smyrna P. Tuburan, MD
Cynthia K. Rigsby MD, FACR
Laureen M. Sena, MD

CHILD ABUSE COMMITTEE

Sabah Servaes, MD, Chair
Arabinda K. Choudhary, MBBS, MRCP, FRCR Vice Chair
David A. Bloom, MD
Karen Blumberg, MD, FACR
Jonathan Chen, MD
Tejaswini K. Deshmukh, MD
Michael F. Fadell, II, MD
Laura L. Hayes, MD
Gary L. Hedlund, DO
Muhammad N. Khan, MBBS, FCPS
Jeannie K. Kwon, MD
Megan B. Marine, MD
Bradley A. Maxfield, MD
Kenneth L. Mendelson, MD
David M. Mirsky, MD
Joëlle A. Moreno, JD
Sandeep Narang, MD
Susan Palasis, MD
Ashishkumar K. Parikh, MD
Jeannette M. Perez-Rossello, MD
Cory M. Pfeifer, MD, FAAP

CHILD ABUSE COMMITTEE
(continued)

Veronica J. Rooks, MD
Michael D. Rubin, MD
Dana S. Schwartz, MD
Daniel M. Schwartz, MD
Victoria M. Silvera, MD
Heba S. Takrouri, MBBS
Chido Vera, MD
Gregory A. Vorona, MD
Matthew A. Zapala, MD, PhD
Stephen D. Brown, MD, Advisory
Richard I. Markowitz, MD, FACR, Advisory
Thomas L. Slovis, MD, Advisory
Peter J. Strouse, MD, FACR, Advisory

CONTRAST-ENHANCED ULTRASOUND COMMITTEE

M. Beth McCarville, MD, Chair
Susan J. Back, MD, Vice Chair
Patricia T. Acharya, MD
Carol E. Barnewolt, MD
Jamie L. Coleman, MD
Kassa Darge MD, PhD
Jonathan R. Dillman, MD, MSc
Lynn A. Fordham, MD, FACR
Misun Hwang, MD
Annie Lim, DO
Martha M. Munden, MD
Harriet J. Paltiel, MD

CT COMMITTEE

John D. MacKenzie, MD, Chair
Tushar Chandra, MBBS, MD
Kara G. Gill, MD
Prakash M. Masand, MD
Grace S. Phillips, MD
Karuna V. Shekdar, MD
Richard Southard, MD
Jacqueline A. Urbine, MD
Jason P. Weinman, MD
Sjirk J. Westra, MD
Sheila C. Berlin, MD, Advisory

DIVERSITY AND INCLUSION COMMITTEE

Ashok Panigrahy, MD, Co-Chair
Stephanie E. Spottswood, MD, MSPH, Co-Chair
Aparna Annam, DO
Taylor Chung, MD
Gregory L. Compton, MBBS
Sarah Desoky, MD
Melanie B. Levin, MD
Maria-Gisela Mercado-Deane, MD
Cindy R. Miller, MD
Kristi B. Oatis, MD
Tina Young Poussaint, MD, FACR
Peter J. Strouse, MD, FACR
Amit S. Sura, MD
Philip Teitelbaum, MD
Adrienne F. Thompson, MD
Chido Vera, MD

EDUCATION-CURRICULUM COMMITTEE

Christopher I. Cassady, MD, FAAP, Chair
Sarah S. Milla, MD, FAAP, Vice Chair
Michael J. Callahan, MD
Taylor Chung, MD
Peter J. Strouse, MD, FACR, Editor
Monica Epelman, MD
Laura Z. Fenton, MD
Liliane H. Gibbs, MD
Safwan S. Halabi, MD
Angelisa M. Paladin, MD
Daniel J. Podberesky, MD
Sanjay P. Prabhu, MBBS, FRCR
Janet R. Reid, MD, FRCPC
Cynthia K. Rigsby, MD, FACR
Manrita K. Sidhu, MD
Stephen F. Simoneaux, MD
Benjamin H. Taragin, MD
Mahesh M. Thapa, MD
Kevin Wong, DO

EMERGENCY RADIOLOGY & TRAUMA COMMITTEE

Susan D. John MD, FACR, Chair
Michael R Aquino, MD
Tejaswini K Deshmukh, MD
David Dinan, MD
Michael P. George, MD
Ashwin Hegde, MD, FRCPC
Jeanne G. Hill, MD
Victor M. Ho-Fung, MD
Tara L. Holm, MD
Paul J. Iskander, MD
Jennifer H. Johnston, MD
George C. Koberlein, MD
Jonathan M. Loewen, MD
Indu R. Meesa, MD
Michael A. Murati, MD
Michael P. Nasser, MD

FELLOWSHIP PROGRAM DIRECTOR COMMITTEE

Paula N. Dickson, MD, Co-Chair
Sabah Servaes, MD, Co-Chair

FETAL IMAGING COMMITTEE

Teresa Victoria, MD, PhD, Chair
Mariana L. Meyers, MD, Vice Chair
Rama S. Ayyala, MD
Richard A. Barth, MD, FACR, FAAP
Michael A. Breen, MBBCh
Brandon P. Brown, MD
Lucia Carpineta, MD, CM
John A. Cassese, MD
Dorothy I. Bulas, MD, FACR, FAAP
Christopher I. Cassady, MD, FAAP
Patricia Cornejo, MD
Kimberly A. Dannull, MD
Nilesh Desai, MD
Michael S. Gee, MD, PhD
Luis Goncalves, MD
Carolina V. Guimaraes, MD
Camilo J. Cobos, MD
Pamela M. Ketwaroo, MD
Paggie Kim, MD
Beth M. Kline-Fath, MD
Amy B. Kolbe, MD

FETAL IMAGING COMMITTEE
(continued)

Leann E. Linam, MD
David M. Mirsky, MD
Edward R. Oliver, MD
Erika Rubesova, MD
Chetan C. Shah, MD
Gayathri Sreedher, MD

FINANCE COMMITTEE

Avrum N. Pollock, MD, FRCPC, Chair
Richard A. Barth, MD, FACR, FAAP
Christopher I. Cassady, MD, FAAP
Taylor Chung, MD
Randheer Shailam, MD
Stephen F. Simoneaux, MD
Peter J. Strouse, MD, FACR
Dayna M. Weinert, MD

HISTORY COMMITTEE

Alan E. Schlesinger, MD, Historian
N.Thorne Griscom, MD, Consultant

HONORS COMMITTEE

Richard A. Barth, MD, FACR, FAAP, Chair
Brian D. Coley, MD, FACR, FAIUM
James S. Donaldson, MD, FACR

INFORMATICS COMMITTEE

Safwan S. Halabi, MD, Chair
Steven L. Blumer, MD
Michael L. Francavilla, MD
C. Matthew Hawkins, MD
Nadja Kadom, MD
Summer L. Kaplan, MD
Jeannie K. Kwon, MD
Neil U. Lall, MD
Morgan McBee, MD
Saad A. Ranginwala, MD
Takashi Sato, MD, PhD
Evan J. Zucker, MD
Alexander J. Towbin, MD

INTERVENTIONAL COMMITTEE

Manish N. Patel, DO, Chair
Leah E. Braswell, MD
Jared R. Green, MD
Craig M. Johnson, DO
Matthew P. Lungren, MD, MPH
Janice D. McDaniel, MD
Radu Nicolaescu, MD
Jeremiah J. Sabado, MD
Timothy R. Singewald, MD
Ranjith Vellody, MD
Fabiola C. Weber, MD

JUDICIARY COMMITTEE

Thomas L. Slovis, MD, Chair
Richard A. Barth, MD, FACR, FAAP
Dorothy I. Bulas, MD, FACR, FAAP
Neil D. Johnson, MBBS
Richard B. Gunderman, MD, PhD, FACR

MR COMMITTEE

Michael S. Gee, MD, PhD, Chair
Sudha A. Anupindi, MD
Sherwin S. Chan, MD
Tushar Chandra, MBBS, MD
Govind B. Chavhan, MD, DNB
Jesse Courtier, MD
Jorge H. Davila-Acosta, MD
Robert J. Fleck, Jr, MD
Shahnaz G. Koureh, MD
Mai-Lan Ho, MD
Geetika Khanna, MD, MS
Hee-Kyung Kim, MD
Amy B. Kolbe, MD
Archana Malik, MD
Michael M. Moore, MD
Thang Ngo, MD
Hansel J. Otero, MD
Anil G. Rao, DMRD, DNB
Gary R. Schooler, MD
Mitchell L. Simon, MD
Gayathri Sreedher, MD
Unni K. Udayasankar, MD
Matthew J. Winfeld, MD
Taylor Chung, MD, Advisory
Shreyas S. Vasanawala, MD, PhD, Advisory

MUSCULOSKELETAL IMAGING COMMITTEE

Jerry R. Dwek, MD, Chair
Arthur B. Meyers, MD, Vice Chair
Lauren W. Averill, MD
Sebastien Benali, MD
Sarah D. Bixby MD
Tushar Chandra, MBBS, MD
Nancy A. Chauvin, MD
Jonathan Chen, MD
Kirsten Ecklund, MD
R. Paul Guillerman, MD
Siddharth P. Jadhav, MD
Shawn E. Kamps, MD
Hee-Kyung Kim, MD
Archana Malik, MD
Tracey R. Mehlman, MD
Arnold Carl Merrow, Jr, MD
Jie C. Nguyen, MD, MS
Allison K. Person, MD
Jonathan Samet, MD
Amisha J. Shah, MD
Mahesh M. Thapa, MD
Sai G. Yarram, MD

NEONATAL IMAGING COMMITTEE

Rama S. Ayyala, MD, Chair
Emily M. Janitz, DO, Vice Chair
Karen Blumberg, MD, FACR
Judy A. Estroff, MD
Tara L. Holm, MD
Shailee V. Lala, MD
Brooke S. Lampl, DO
David W. McDonald, MD
Richard Parad, MD
Pallavi Sagar, MD
Cassandra M. Sams, MD
Mitchell L. Simon, MD
Jennifer L. Williams, MD

NEURORADIOLOGY COMMITTEE

Dennis W. W. Shaw, MD, Chair
Thierry A. G. M. Huisman, MD, Vice Chair
Mariaem M. Andres, MD
Ravi Bhargava, MD
Timothy N. Booth, MD
Thangamadhan Bosemani, MD
S. Srinivas Ganapathy, MD
Carolina V. Guimaraes, MD
Arzu Kovanlikaya, MD
Susan Palasis, MD
Sumit Pruthi, MD
Rupa Radhakrishnan, MBBS
Raghu H. Ramakrishnaiah, MD
Caroline D. Robson, MBChB
Nancy K. Rollins, MD
Gaurav Saigal, MD
Matthew T. Whitehead, MD
Jason N. Wright, MD
Charles R. Fitz, MD, Advisory

NOMINATING COMMITTEE

Diego Jaramillo, MD, MPH, Chair
Monica Epelman, MD
Judy A. Estroff, MD
Tara L. Holm, MD
Alan E. Schlesinger, MD
Sabah Servaes, MD
Stephan D. Voss, MD, PhD

NUCLEAR MEDICINE COMMITTEE

Helen R. Nadel, MD, FRCPC, Chair
Adina L. Alazraki, MD, FAAP
Deepa R. Biyyam, MBBS
Neha S. Kwatra, MD
Maria R. Ponisio, MD
Victor J. Seghers, MD, PhD
Sabah Servaes, MD
Lisa J. States, MD
S. Ted Treves, MD
Stephan D. Voss, MD, PhD
Jennifer L. Williams, MD

ONCOLOGY COMMITTEE

Adina L. Alazraki, MD, FAAP, Chair
Govind B. Chavhan, MD, DNB
Kelly R. Dietz, MD
Meryle Eklund, MD
Sue C. Kaste, DO
Muhammad N. Khan, MBBS, FCPS
Arzu Kovanlikaya, MD
Irit R. Maianski, MD
M. Beth McCarville, MD
Ajaykumar C. Morani, MD
Erika Pace, MD
Marguerite T. Parisi, MD, MS
Edward J. Richer, MD
Susan E. Sharp, MD
Stephan D. Voss, MD, PhD
Sireesha Yedururi, MD
Geetika Khanna, MD, MS, Advisory

PHYSICIAN RESOURCES COMMITTEE

Rebecca L. Hulett-Bowling, MD, Chair
Kristen B. Thomas, MD, Vice Chair
Ellen M. Chung, MD
Meryle Eklund, MD
Shannon G. Farmakis, MD
Summer L. Kaplan, MD
Brooke S. Lampl, DO
Janice D. McDaniel, MD
Maria-Gisela Mercado-Deane, MD
Debbie J. Merinbaum, MD

POST-MORTEM IMAGING COMMITTEE

Mary P. Harty MD, Chair
Pierre J. Schmit, MD
Micheal A. Breen MBBCh
Sharon W. Gould, MD
Jeanne G. Hill, MD
Tatum S. Johnson, MD
Muhammad N. Khan, MBBS, FCPS
Amy R. Mehollin-Ray, MD
Mark E. Sharafinski, Jr, MD

PROFESSIONALISM COMMITTEE

Brandon P. Brown, Chair
Michael A. Breen, MBBCh
Dorothy I. Bulas, MD, FACR, FAAP
Teresa Chapman, MD, MA
Jeanne G. Hill, MD
Anastasia L. Hryhorczuk, MD
Susan D. John, MD, FACR
Craig M. Johnson, DO
Pamela M. Ketwaroo, MD
Sarah S. Milla, MD, FAAP
Tina Y. Poussaint, MD, FACR
Sabah Servaes, MD
Stephen D. Brown, MD, Advisory

PUBLICATIONS COMMITTEE

Ethan A. Smith, MD, Chair
Andrew T. Trout, MD, Vice Chair
Michael J. Callahan, MD
Srikala Narayanan, MD
Ashok Panigrahy, MD
Sumit Pruthi, MD
Pooja D. Thakrar, MD
Teresa Victoria, MD, PhD
Diego Jaramillo, MD, MPH – *Ex officio*
Peter J. Strouse, MD, FACR, Editor
Brian D. Coley, MD, FACR, FAIUM, Assistant Editor
Geetika Khanna, MD, MS, Assistant Editor
Cynthia K. Rigsby, MD, FACR, Assistant Editor

PUBLIC POLICY COMMITTEE

David W. Swenson, MD, Chair
Neil Anand, MD
Aparna Annam, DO
Richard A. Barth, MD, FACR, FAAP
Kate A. Feinstein, MD, FACR
Michael L. Francavilla, MD
Susan D. John, MD, FACR
Michael E. Katz, MD, FACR
Annie Lim, DO
Anil G. Rao, DMRD, DNB
Summit H. Shah, MD
Jonathan Swanson, MD
Richard M. Benator, MD, FACR, Advisory
Marta Hernanz-Schulman, MD, Advisory

QUALITY AND SAFETY COMMITTEE

Ramesh S. Iyer, MD, Chair
Neil Anand, MD
Einat Blumfield, MD
Tushar Chandra, MBBS, MD
Govind B. Chavhan, MD, DNB
Thomas R. Goodman, MBBCh
Muhammad N. Khan, MBBS, FCPS
Michael M. Moore, MD
Thang Ngo, MD
Christina L. Sammet, PhD
Arta-Luana Stanescu, MD
David W. Swenson, MD
Raymond W. Sze, MD
Chido Vera, MD
Thomas L. Slovis, MD, Advisory

SPR REPRESENTATIVES

Richard A. Barth, MD, FACR, FAAP (ARR)
Donald P. Frush, MD, FACR (ABR)
Richard B. Gunderman, MD, PhD, FACR (ACR)
Sarah S. Milla, MD, FAAP (AAP)
Susan D. John, MD, FACR (RRC)

SPR RESEARCH AND EDUCATION FOUNDATION

J. Damien Grattan-Smith, MBBS, President
Peter J. Strouse, MD, FACR, Vice President
Michael J. Callahan, MD, Secretary
Stephen F. Simoneaux, MD, Treasurer
Sudha A. Anupindi, MD
R. Paul Guillerman, MD
Joseph J. Junewick, MD, FACR
William H. McAlister, MD, FACR
John D. Mackenzie, MD
Janet R. Reid, MD, FRCPC
Stuart A. Royal, MS, MD, FACR

THORACIC IMAGING COMMITTEE

Paul G. Thacker, Jr, MD, Chair
David M. Biko, MD
Matthew Cooper, MD
Sarah Desoky, MD
Meryle Eklund, MD
Monica Epelman, MD
Maryam Ghadimi Mahani, MD
Paul J. Iskander, MD
Manisha Jana, MBBS, MD, FRCR
Arzu Kovanlikaya, MD
Gauri S. Tilak, MD, PhD, MPH
Jason P. Weinman, MD
Evan J. Zucker, MD
Alan S. Brody, MD
Beverley Newman MD, FACR, Advisory

ULTRASOUND COMMITTEE

Monica Epelman, MD, Chair
Andrew S. Phelps, MD, Vice Chair
Christian L. Carlson, MD
Tushar Chandra, MBBS, MD
Harris L. Cohen, MD, FACR
Ricardo Faingold, MD
Rachelle Goldfisher, MD
Kerri Highmore, MD
Melanie B. Levin, MD
Harriet J. Paltiel, MD
Michele Retrouvey, MD
Erica L. Riedesel, MD
Henrietta K. Rosenberg, MD, FACR, FAAP
Cicero T. Silva, MD
Judy H. Squires, MD
Neil Vachhani, MD
Dayna M. Weinert, MD
Jonathan R. Wood, MD
Richard D. Bellah, MD, Advisory

WEBSITE EDITORIAL COMMITTEE

Benjamin H. Taragin, MD, Chair and Web Editor
Peter A. Marcovici, MD, Assistant Web Editor - Unknown Cases
Amy R. Mehollin-Ray, MD, Assistant Web Editor
Anh-Vu H. Ngo, MD, Assistant Web Editor
Mahesh M. Thapa, MD, Assistant Web Editor

SPR PAST PRESIDENTS, PREVIOUS & FUTURE MEETING SITES, AWARDEES & EDWARD B. D. NEUHAUSER LECTURERS

PAST PRESIDENTS & PREVIOUS MEETING SITES

1958-59	Edward B. Neuhauser, MD	Cincinnati, Ohio
1959-60	Frederic N. Silverman, MD	Atlantic City, New Jersey
1960-61	John F. Holt, MD	Miami Beach, Florida
1961-62	Arthur S. Tucker, MD	Washington, D.C.
1962-63	John W. Hope, MD	Montreal, Quebec, Canada
1963-64	R. Parker Allen, MD	Minneapolis, Minneapolis
1964-65	Edward B. Singleton, MD	Washington, D.C.
1965-66	J. Scott Dunbar, MD	San Francisco, California
1966-67	Harvey White, MD	Washington, D.C.
1967-68	M.H. Wittenborg, MD	New Orleans, Louisiana
1968-69	David H. Baker, MD	Washington, D.C.
1969-70	John A. Kirkpatrick, Jr., MD	Miami Beach, Florida
1970-71	Norman M. Glazer, MD	Boston, Massachusetts
1971-72	Bertram R. Girdany, MD	Washington, D.C.
1972-73	Donald H. Altman, MD	Montreal, Quebec, Canada
1973-74	Hooshang Taybi, MD	San Francisco, California
1974-75	John L. Gwinn, MD	Atlanta, Georgia
1975-76	Lawrence A. Davis, MD	Washington, D.C.
1976-77	Marie A. Capitanio, MD	Boston, Massachusetts
1977-78	John P. Dorst, MD	Denver, Colorado
1978-79	Bernard J. Reilly, MB, FRCP (C)	Toronto, Ontario, Canada
1979-80	Walter E. Berdon, MD	Salt Lake City, Utah
1980-81	Andrew K. Poznanski, MD	San Francisco, California
1981-82	N. Thorne Griscom, MD	New Orleans, Louisiana
1982-83	Virgil R. Condon, MD	Atlanta, Georgia
1983-84	Jerald P. Kuhn, MD	Las Vegas, Nevada
1984-85	Lionel W. Young, MD	Boston, Massachusetts
1985-86	John C. Leonidas, MD	Washington, D.C.
1986-87	Derek C. Harwood Nash, MD, DSc & Denis Lallemand, MD (ESPR, IPR'87)	Toronto, Ontario, Canada
1987-88	Beverly P. Wood, MD	San Diego, California
1988-89	John F. O'Connor, MD	San Antonio, Texas
1989-90	E.A. Franken, Jr., MD	Cincinnati, Ohio
1990-91	Donald R. Kirks, MD & Hans G. Ringertz, MD, PhD (ESPR, IPR '91)	Stockholm, Sweden
1991-92	William H. McAlister, MD	Orlando, Florida
1992-93	M. B. Ozonoff, MD	Seattle, Washington
1993-94	Joanna J. Seibert, MD	Colorado Springs, Colorado
1994-95	Eric L. Effmann, MD	Washington, D.C.
1995-96	Kenneth E. Fellows, MD & Paul S. Thomas, MD (ESPR, IPR '96)	Boston, Massachusetts
1996-97	Diane S. Babcock, MD	St. Louis, Missouri
1997-98	Charles A. Gooding, MD	Tucson, Arizona
1998-99	Robert L. Lebowitz, MD	Vancouver, British Columbia, Canada
1999-00	Thomas L. Slovis, MD	Naples, Florida
2000-01	Janet L. Strife, MD & Francis Brunelle, MD (ESPR, IPR'01)	Paris, France
2001-02	Bruce R. Parker, MD	Philadelphia, Pennsylvania
2002-03	Richard B. Towbin, MD	San Francisco, California
2003-04	David C. Kushner, MD	Savannah, Georgia
2004-05	Stuart A. Royal, MS, MD	New Orleans, Louisiana
2005-06	George A. Taylor, MD & Richard Fotter, MD (ESPR, IPR'06)	Montreal, Quebec, Canada
2006-07	Marilyn J. Goske, MD	Miami, Florida
2007-08	Marta Hernanz-Schulman, MD	Scottsdale, Arizona
2008-09	M. Ines Boechat, MD	Carlsbad, California
2009-10	Neil D. Johnson, MBBS	Boston, Massachusetts
2010-11	Dorothy I. Bulas, MD & Catherine M. Owens, MD (ESPR, IPR'11)	London, England
2011-12	Donald P. Frush, MD	San Francisco, California
2012-13	Sue C. Kaste, DO	San Antonio, Texas
2013-14	Richard A. Barth, MD	Washington, D.C.

2014-15	Brian D. Coley, MD	Bellevue, Washington
2015-16	James S. Donaldson, MD, & Karen Rosendahl, MD, PhD (ESPR, IPR' 16)	Chicago, Illinois
2016-17	Diego Jaramillo, MD, MPH	Vancouver, British Columbia, Canada

FUTURE MEETINGS

2019	April 30 – May 4, 2019	San Francisco, California
2020	May 12 – May 16, 2020	Fajardo, Puerto Rico
2021	June 15 – June 19, 2021 (IPR)	Rome, Italy

GOLD MEDALISTS

1988	Frederic N. Silverman, MD
1989	John L. Gwinn, MD
1990	John F. Holt, MD
1991	John A. Kirkpatrick, Jr., MD
1991	Bernard J. Reilly, MB, FRCP
1992	Edward B. Singleton, MD
1993	Hooshang Taybi, MD
1994	Walter E. Berdon, MD
1994	J. Scott Dunbar, MD
1995	Guido Currarino, MD
1995	Derek C. Harwood Nash, MD, DSc
1996	Andrew K. Poznanski, MD
1996	Beverly P. Wood, MD
1997	N. Thorne Griscom, MD
1997	John F. O'Connor, MD
1998	William H. McAlister, MD
1999	E. A. Franken, MD
2000	Eric L. Effmann, MD
2001	Giulio J. D'Angio, MD
2002	David H. Baker, MD
2003	Brinton B. Gay, Jr., MD
2003	William H. Northway, Jr., MD
2004	Diane S. Babcock, MD
2004	Virgil R. Condon, MD
2005	Jerald P. Kuhn, MD
2005	Thomas L. Slovis, MD
2006	Robert L. Lebowitz, MD
2006	John C. Leonidas, MD
2007	Leonard E. Swischuk, MD
2008	Barry D. Fletcher, MD
2009	Charles A. Gooding, MD
2010	Janet L. Strife, MD
2011	Carol M. Rumack, MD
2012	Marilyn J. Goske, MD
2013	Stuart A. Royal, MS, MD
2014	David C. Kushner, MD
2015	George A. Taylor, MD
2016	Jennifer K. Boylan, MA
2017	M. Ines Boechat, MD
2017	Paul K. Kleinman, MD
2018	Dorothy I. Bulas, MD, FACR, FAAP
2018	Neil D. Johnson, MBBS

PIONEER HONOREES

1990	John P. Caffey, MD
1991	M. H. Wittenborg, MD
1992	Edward B. Singleton, MD
1993	Frederic N. Silverman, MD
1994	John P. Dorst, MD
1995	E.B.D. Neuhauser, MD
1996	E. A. Franken, MD
1996	Kazimierz Kozlowski, MD
1996	M. Arnold Lassrich, MD
1997	Arnold Shkolnik, MD
1998	Heidi B. Patriquin, MD
1998	William H. Northway, Jr., MD

2000	Jerald P. Kuhn, MD
2001	Diane S. Babcock, MD
2001	Fred E. Avni, MD, PhD
2003	Walter E. Berdon, MD
2004	G. B. Clifton Harris, MD
2005	Rita L. Teele, MD
2006	Robert L. Lebowitz, MD
2007	Carol M. Rumack, MD
2008	Paul S. Babyn, MD
2009	Kenneth E. Fellows, MD
2010	David K. Yousefzadeh, MD
2011	Massoud Majd, MD
2012	George S. Bisset, III, MD
2013	Barry D. Fletcher, MD
2014	Diego Jaramillo, MD, MPH
2015	William E. Shiels, DO
2016	Mary R. Wyers, MD
2017	H. Theodore Harcke, Jr., MD
2018	Richard B. Towbin, MD, FACR

PRESIDENTIAL RECOGNITION AWARDS

1999	David C. Kushner, MD
2000	Paul K. Kleinman, MD
2001	Neil D. Johnson, MBBS
2001	Christopher Johnson
2002	Jennifer K. Boylan, MA
2002	Thomas L. Slovis, MD
2003	Danielle K.B. Boal, MD
2003	Marta Hernanz-Schulman, MD
2004	Kenneth L. Mendelson, MD
2005	Taylor Chung, MD
2005	J. A. Gordon Culham, MD
2005	Shi-Joon Yoo, MD
2006	L. Christopher Foley, MD
2007	Donald P. Frush, MD
2008	Mary K. Martel, PhD
2008	Connie L. Mitchell, MA, RT(R)(CT)
2008	Harvey L. Neiman, MD
2009	Karen S. Schmitt
2010	Richard A. Barth, MD
2011	Kimberly E. Applegate, MD, MS
2011	Keith Strauss, MS, FACR
2012	David C. Kushner, MD, FACR
2012	Stuart A. Royal, MS, MD
2013	Alan E. Schlesinger, MD
2014	Richard M. Benator, MD
2015	Cynthia K. Rigsby, MD
2016	Vicente Gilsanz, MD, PhD
2017	Tal Laor, MD
2018	Joëlle A. Moreno, JD
2018	Patricia Vario

HONORARY MEMBERS

1985	Jacques Sauvegrain, MD
1987	Bryan J. Cremin, MD
1987	Ole A. Eklof, MD
1987	Clement C. Faure, MD
1987	Andres Giedion, MD
1987	Denis Lallemand, MD
1987	Arnold Lassrich, MD
1987	Ulf G. Rudhe, MD
1998	Frederic N. Silverman, MD
1989	John L. Gwinn, MD
1990	John F. Holt, MD
1990	Richard G. Lester, MD
1991	Gabriel L. Kalifa, MD
1991	Javier Lucaya, MD
1991	John P. Masel, MD

1991	Noemi Perlmutter Cremer, MD
1991	Hans G. Ringertz, MD
1991	John A. Kirkpatrick, Jr., MD
1991	Bernard J. Reilly, MB, FRCP(C)
1992	Edward B. Singleton, MD
1992	Donald R. Kirks, MD
1992	Beverly P. Wood, MD
1992	Walter E. Berdon, MD
1993	Hooshang Taybi, MD
1994	Marie A. Capitanio, MD
1994	E. A. Franken, Jr., MD
1994	John C. Leonidas, MD
1994	William H. McAlister, MD
1994	Andrew K. Poznanski, MD
1994	J. Scott Dunbar, MD
1995	David H. Baker, MD
1992	Derek C. Harwood Nash, MD, DSc
1995	N. Thorne Griscom, MD
1995	Guido Currarino, MD
1996	Francis O. Brunelle, MD
1996	Lloyd L. Morris, MD
1996	Heidi B. Patriquin, MD
1997	John F. O'Connor, MD
1997	Theodore E. Keats, MD
1998	Rita L. Teele, MD
1998	H. Ted Harcke, MD
1999	J. Bruce Beckwith, MD
2000	Joseph Volpe, MD
2001	Ulrich V. Willi, MD
2001	Henrique M. Lederman, MD
2001	Mutsuhisa Fujioka, MD
2002	Eric J. Hall, DSc, FACR, FRCR
2002	Walter Huda, PhD
2003	Michael R. Harrison, MD
2004	Lee F. Rogers, MD
2005	Carden Johnston, MD
2006	Alan B. Retik, MD
2007	Robert R. Hattery, MD
2008	Professor Hassen A. Gharbi
2009	Dolores Bustelo, MD
2009	Pedro A. Daltro, MD, PhD
2009	Cristian Garcia, MD
2009	Antônio Soares de Souza, MD
2010	Stephen Chapman, MD
2011	Catherine M. Owens, MBBS
2011	Madan M. Rehani, PhD
2012	Harvey L. Neiman, MD, FACR
2013	Savvas Andronikou, MBBCh, FCRad, FRCR, PhD
2014	Timothy M. Cain, MBBS
2015	In-One Kim, MD
2015	Professor Guy Sebag (posthumously)
2016	Bernard F. Laya, DO
2017	Gloria Soto Giordani, MD
2018	Fred E. Avni, Jr., MD, PhD
2018	Karen Rosendahl, MD, PhD

EDWARD B. SINGLETON-HOOSHANG TAYBI AWARD

2006	Corning Benton, Jr., MD
2007	Michael P. D'Alessandro, MD
2007	Janet R. Reid, MD
2008	Dorothy I. Bulas, MD
2009	Lane F. Donnelly, MD
2010	Wilbur L. Smith, Jr., MD
2011	Ralph S. Lachman, MD, FACR
2012	Alan Daneman, MD
2013	Lisa H. Lowe, MD
2014	Robert H. Cleveland, MD

2015	Stephen F. Simoneaux, MD
2016	Michael A. DiPietro, MD
2017	Shi-Joon Yoo, MD
2018	John D. Strain, MD, FACR

JOHN A. KIRKPATRICK YOUNG INVESTIGATOR AWARD

This award is given to the author of the best paper presented by a resident or fellow at the SPR meeting. Beginning in 1995, the award became known as the John A. Kirkpatrick Young Investigator Award.

1993	Philipp K. Lang, MD
1993	Stephanie P. Ryan, MD
1994	Sara O'Hara, MD
1995	Philipp K. Lang, MD
1996	Fergus V. Coakley, MB, FRCR
1997	Ronald A. Alberico, MD
1998	Laura J. Varich, MD
1999	A. E. Ensley, BS
1999	R.W. Sze, MD
2000	S. H. Schneider, MD
2001	Valerie L. Ward, MD
2002	Ricardo Faingold, MD
2003	Andrea Doria, MD
2004	Nina M. Menezes, PhD
2005	Lena Naffaa, MD
2006	Courtney A. Coursey, MD
2007	Ashley J. Robinson, MBChB
2008	Hee Kyung Kim, MD
2009	Conor Bogue, MD
2010	Albert Hsiao, MD, PhD
2011	Ethan A. Smith, MD
2012	Saivivek Bogale, MD
2013	Emma Raver, BA
2014	Aarti Luhar, MD
2015	Ashish Parikh, MD
2016	Sila Kurugol, PhD
2017	Ezekiel Maloney, MD

WALTER E. BERDON AND THOMAS L. SLOVIS AWARDS - 2017

The Walter E. Berdon Award recognizes the best clinical research paper submitted to the journal of ***Pediatric Radiology*** in the year preceding the meeting. This award was established to honor Walter E. Berdon who served as the North American Editor of Pediatric Radiology for 30 years and who stepped down as editor on June 30, 2003.

The Thomas L. Slovis Award recognizes the best basic scientific paper submitted to the journal of ***Pediatric Radiology*** in the year preceding the meeting. This award was established to honor Thomas L. Slovis who served as the North American Editor of Pediatric Radiology following Dr. Berdon and who stepped down as editor on December 31, 2012.

Prior to 2012, Walter E. Berdon Awards recognized both the best clinical research paper and the best basic scientific paper.

2017 recipients will be announced at the meeting.

2016

Best Clinical Paper (Walter E. Berdon Award):
Rothman S, Gonen A, Vodonos A, Novack V, Shelef I (2016) Does preparation of children before MRI reduce the need for anesthesia? Prospective randomized control trial. Pediatr Radiol 46:1599-1605

Best Basic Science Paper (Thomas L. Slovis Award):
Jarvis K, Schnell S, Barker AJ, Garcia J, Lorenz R, Rose M, Chowdhary V, Carr J, Robinson JD, Rigsby CK, Markl M (2016) Evaluation of blood flow distribution asymmetry and vascular geometry in patients with Fontan circulation using 4-D flow MRI. Pediatr Radiol 46:1507-1519

2015

Best Clinical Paper (Walter E. Berdon Award):
Choudhary AK, Bradford R, Dias MS, Thamburaj K, Boal DK (2015) Venous injury in abusive head trauma. Pediatr Radiol 45:1803-1813

Best Basic Science Paper (Thomas L. Slovis Award):
Back SJ, Edgar JC, Canning DA, Darge K (2015) Contrast-enhanced voiding urosonography: In vitro evaluation of a second generation ultrasound contrast agent for in vivo optimization. Pediatr Radiol 45:1496-1505

2014

Best Clinical Paper (Walter E. Berdon Award):
Tyson ME, Bohl DD, Blickman JG. (2014) A randomized controlled trial: child life services in pediatric imaging. Pediatr Radiol 44:1426-1432

Best Basic Science Paper (Thomas L. Slovis Award):
Tsai A, McDonald AG, Rosenberg AE, Gupta R, Kleinman PK (2014) High-resolution CT with histopathological correlates of the classic metaphyseal lesion of infant abuse. Pediatr Radiol 44:124-140

2013

Best Clinical Paper (Walter E. Berdon Award):
Punwani S, Cheung KK, Skipper N, Bell N, Bainbridge A, Taylor SA, Groves AM, Hain SF, Ben-Haim S, Shankar A, Daw S, Halligan S, Humphries PD (2013) Dynamic contrast enhanced MRI improves accuracy for detecting focal splenic involvement in children and adolescents with Hodgkin disease. Pediatr Radiol 43:941-949

Best Basic Science Paper (Thomas L. Slovis Award):
Hanquinet S, Rougemont AL, Courvoisier D, Rubbia-Brandt L, McLin V, Tempia M, Anooshiravani M (2013) Acoustic radiation force impulse (ARFI) elastography for the non-invasive diagnosis of liver fibrosis in children. Pediatr Radiol 43:545-551

2012

Best Clinical Paper (Walter E. Berdon Award):
Swanson JO1, Vavilala MS, Wang J, Pruthi S, Fink J, Jaffe KM, Durbin D, Koepsell T, Temkin N, Rivara FP (2012) Association of initial CT findings with quality-of-life outcomes for traumatic brain injury in children. Pediatr Radiol 42:974-981

Best Basic Science Paper (Thomas L. Slovis Award):
Tkach JA, Hillman NH, Jobe AH, Loew W, Pratt RG, Daniels BR, Kallapur SG, Kline-Fath BM, Merhar SL, Giaquinto RO, Winter PM, Li Y, Ikegami M, Whitsett JA, Dumoulin CL (2012) An MRI system for imaging neonates in the NICU: initial feasibility study. Pediatr Radiol 412:1347-1356

2011

Best Basic Science Paper:
Castaneda RT1, Boddington S, Henning TD, Wendland M, Mandrussow L, Liu S, Daldrup-Link H (2011) Labeling human embryonic stem-cell-derived cardiomyocytes for tracking with MR imaging. Pediatr Radiol 41:1384-1392

Best Clinical Research Paper:
Schachar JL, Zampolin RL, Miller TS, Farinhas JM, Freeman K, Taragin BH (2011) External validation of the New Orleans Criteria (NOC), the Canadian CT Head Rule (CCHR) and the National Emergency X-Radiography Utilization Study II (NEXUS II) for CT scanning in pediatric patients with minor head injury in a non-trauma center. Pediatr Radiol 41:971-979

2010

Best Basic Science Paper:
Goo HW (2010) Initial experience of dual energy lung perfusion CT using a dual source CT system in children. Pediatr Radiol 40:1536-1544

Best Clinical Research Paper:
Raissaki M, Perisinakis K, Damilakis J, Gourtsoyiannis N (2010) Eye-lens bismuth shielding in paediatric head CT: artefact evaluation and reduction. Pediatr Radiol 40:1748-1754

2009

Best Basic Science Paper:
Helm EJ, Silva CT, Roberts HC, Manson D, Seed MT, Amaral JG, Babyn PS (2009) Computer-aided detection for the identification of pulmonary nodules in pediatric oncology patients: initial experience. Pediatr Radiol 39:685-693

Best Clinical Research Paper:
Ben Saad M, Rohnean A, Sigal-Cinqualbre A, Adler G, Paul JF (2009) Evaluation of image quality and radiation dose of thoracic and coronary dual-source CT in 110 infant with congenital heart disease. Pediatr Radiol 39:668-676

2008

Best Basic Science Paper:
Wang ZJ, Boddington S, Wendland M, Meier R, Corot C, Daldrup-Link H (2008) MR imaging of ovarian tumors using folate-receptor-targeted contrast agents. Pediatr Radiol 38:529-537

Best Clinical Research Paper:
Hallowell LM, Stewart SE, de Amorim E Silva CT, Ditchfield MR (2008) Reviewing the process of preparing children for MRI. Pediatr Radiol 38:271-279

2007

Best Basic Science Paper:
Maree GJ, Irving BJ, Hering ER (2007) Paediatric dose measurement in a full-body digital radiography unit. Pediatr Radiol 37:990-997

Best Clinical Research Paper:
Silva CT, Daneman A, Navarro OM, Moore AM, Moineddin R, Gerstle JT, Mittal A, Brindle M, Epelman M (2007) Correlation of sonographic findings and outcome in necrotizing enterocolitis. Pediatr Radiol 37:274-282

2006

Best Basic Science Paper:
Goo HW, Suh DS (2006) The influences of tube voltage and scan direction on combined tube current modulation: a phantom study. Pediatr Radiol 36:833-840

Best Clinical Research Paper:
Lee T, Tsai IC, Fu YC, Jan SL, Wang CC, Chang Y, Chen MC (2006) Using multidetector-row CT in neonates with complex congenital heart disease to replace diagnostic cardiac catheterization for anatomical investigation: initial experiences in technical and clinical feasibility. Pediatr Radiol 36:1273-1282

2005

Best Basic Science Paper:
Nield LE, Qi XL, Valsangiacomo ER, Macgowan CK, Wright GA, Hornberger LK, Yoo SJ (2005) In vivo MRI measurement of blood oxygen saturation in children with congenital heart disease. Pediatr Radiol 35:179-185

Best Clinical Paper:
Jones A, Granger S, Brambilla D, Gallagher D, Vichinsky E, Woods G, Berman B, Roach S, Nichols F, Adams RJ (2005) Can peak systolic velocities be used for prediction of stroke in sickle cell anemia? Pediatr Radiol 35:66-72

2004

Best Basic Science Paper:
Peng SS, Lee WT, Wang YH, Huang KM (2004) Cerebral diffusion tensor images in children with tuberous sclerosis: a preliminary report. Pediatr Radiol 34:387-392

Best Clinical Paper:
Babyn PS, Chu WC, Tsou IY, Wansaicheong GK, Allen U, Bitnun A, Chee TS, Cheng FW, Chiu MC, Fok TF, Hon EK, Gahunia HK, Kaw GJ, Khong PL, Leung CW, Li AM, Manson D, Metreweli C, Ng PC, Read S, Stringer DA (2004) Severe acute respiratory syndrome (SARS): chest radiographic features in children. Pediatr Radiol 34:47-58

2003

Best Basic Science Paper:
Xiang J, Holowka S, Sharma R, Hunjan A, Otsubo H, Chuang S (2003) Volumetric localization of somatosensory cortex in children using synthetic aperture magnetometry. Pediatr Radiol 33:321-327

Best Clinical Paper:
Grattan-Smith JD, Perez-Bayfield MR, Jones RA, Little S, Broecker B, Smith EA, Scherz HC, Kirsch AJ (2003) MR imaging of kidneys: functional evaluation using F-15 perfusion imaging. Pediatr Radiol 33:293-304

2002

Best Basic Science Paper:
Nield LE, Qi X, Yoo SJ, Valsangiacomo ER, Hornberger LK, Wright GA (2002) MRI-based blood oxygen saturation measurements in infants and children with congenital heart disease. Pediatr Radiol 32:518-522

Best Clinical Paper:
Lamer S, Dorgeret S, Khairouni A, Mazda K, Brillet PY, Bacheville E, Bloch J, Penneçot GF, Hassan M, Sebag GH (2002) Femoral head vascularisation in Legg-Calvé-Perthes disease: comparison of dynamic gadolinium-enhanced subtraction MRI with bone scintigraphy. Pediatr Radiol 32:580-585

SPR RESEARCH AND EDUCATION FOUNDATION AWARDS

The SPR Research and Education Foundation is dedicated to promoting research and scholarship in pediatric radiology. The SPR Board of Directors has supported research through grants since 1990. The Foundation was established in 1994 with an initial donation from the Society's reserves.

THE JACK O. HALLER AWARD FOR EXCELLENCE IN TEACHING

2005	Alan Daneman, MD
2006	William R. Cranley, MD
2006	John F. O'Connor, MD
2007	Cindy R. Miller, MD
2008	Sara J. Abramson-Squire, MD
2009	Michael A. DiPietro, MD
2010	George A. Taylor, MD
2011	Paul K. Kleinman, MD
2012	Richard I. Markowitz, MD
2013	Gary L. Hedlund, DO
2014	Tal Laor, MD
2014	Carrie B. Ruzal-Shapiro, MD
2015	Laura Z. Fenton, MD
2016	Melvin Senac, MD
2017	Janet R. Reid, MD, FRCPC
2018	Veronica J. Rooks, MD
2018	Yukata Sato, MD, PhD

THE HEIDI PATRIQUIN INTERNATIONAL FELLOWSHIP

2005	Luy Lyda, MD, Angkor Hospital for Children, Siem Reap, Cambodia
2006	Hakima Al-Hashimi, MD Salmaniya Medical Complex, Manama, Bahrain
2006	Pannee Visrutaratna, MD, Chiang Mai University, Chiang Mai, Thailand
2006	Juana Maria Vallejo, MD, Clinica del Country, Bogota, Colombia
2007	Nathan David P. Concepcion, MD, St. Luke's Medical Center, Quezon City, Philippines
2008	Rolando Reyna Lopez, MD, Hospital Santo Tomas, Panama City, Panama
2009	Ahmed Mussa Jusabani, MD, Kilimanjaro Christian Medical Centre, Moshi Town, Tanzania
2010	Omolola Mojisola Atalabi, MD, College of Medicine, University of Ibadan, Nigeria
2011	Kushaljit Singh Sodhi, MD, Postgraduate Institute of Medical Education and Research (PGIMER), Chandigarh, India)
2012	Wambani Sidika Jeska, MBchB, Kenyatta National Hospital, Nairobi, Kenya
2012	Yocabel Gorfu, MD, Addis Ababa University, Addis Ababa, Ethiopia
2013	Regina Nava, MD, St. Luke's Medical Center, Quezon City, Philippines
2013	Olubukola Abeni Omidiji, MBBS, University of Lagos, Lagos, Nigeria
2014	Nneka I. Iloanusi, MBBS, University of Nigeria Teaching Hospital, Enugu, Nigeria
2014	Beatrice Mulama, MBChB, M. Med, Kenyatta National Hospital, Nairobi, Kenya
2015	Nasreen Mahomed, MBBCh, University of the Wiwatersand, Johannesburg, Gauteng
2015	Waseem Akhtar Mirza, MBBS, The Aga Khan University, Karachi, Pakistan
2016	Daniel Zewdneh Solomon, MD, Addis Ababa University, Addis Ababa, Ethiopia
2016	Vikas Yadav, MD, Christian Medical College, Vellore, Tamilnadu, India
2017	Hatíce Ariöz Habíbí, MD, Cerrahpasa Medical, Istanbul University, Turkey
2017	Faizah Mohd Zaki, MD, Universiti Kebangsaan Malaysia Medical Centre, Kuala Lumpur, Malaysia
2018	Bernadette Wambui Muthee, MD, Aga Khan University Hospital, Nairobi, Kenya

SPR RESEARCH AND EDUCATION FOUNDATION GRANTS

The 2017 grant recipients are listed. 2018 grant recipients will be announced at the meeting. For grants from prior years, please see the SPR website.

EDUCATION PROJECT AWARD
Grant: $10,000

"Facilitating a Pediatric Radiology Curriculum in the Global Health Setting Using Tablet Computers" Jennifer Nicholas, MD, Mallinckrodt Institute of Radiology

"Pediatric Cardiovascular CT: A Faculty Development Initiative" Lorna Browne, MBBCH, Children's Hospital of Colorado

MULTI-INSTITUTIONAL PILOT AWARD
Grant: $100,000

"Determination of Normal Liver Stiffness by MR Elastography in Children" Andrew Trout, MD, Cincinnati Children's Medical Center; Kassa Darge, MD, PhD, Children's Hospital of Philadelphia; Michael S. Gee, MD, Phd and Manish Dhyani, MD, Massachusetts General Hospital; Geetika Khanna, MD, MS, Washington University School of Medicine.

SEED GRANT
Grant: $10,000

"*Feasibility of contrast-enhanced transfontanelle ultrasound: comparison with magnetic resonance imaging in the neonate*"- Judy H. Squires, MD, Children's Hospital of Pittsburgh. Co-investigators: Ashok Panigrahy, MD, Toby Yanowitz, MD and Monica Naik, MD

YOUNG INVESTIGATOR
Grant: $30,000

"*In vivo Tau Imaging using 18F-AV-1451 PET Radioligand in a Swine Model of Closed Head Injury*" - Neha S. Kwatra, MD, Children's Hospital, Boston. Mentor: Stephan D. Voss, MD, PhD. Co-investigators: Frederick Fahey DSc and Rebekah Manix, MD, MPH.

PREVIOUS EDWARD B. D. NEUHAUSER LECTURES

1971- John Caffey, MD, Pittsburgh, Pennsylvania: "The Radiologist and Unexplained Injury to Infants: Early History and Current Status"
1972- M. Judah Folkman, MD, Boston, Massachusetts: "Patterns of Discovery Fundamental to Radiology and Biology"
1973- Josef Warkany, MD, Cincinnati, Ohio: "Pediatric Radiology and Syndromology"
1974- Benjamin H. Landing, MD, Los Angeles, California: "Syndromes of Congenital Heart Disease with Tracheobronchial Anomalies"
1975- Frederic N. Silverman, MD, Cincinnati, Ohio: "Viral Diseases of Bone Do They Exist?"
1976- Lynne M. Reid, MD, Boston, Massachusetts: "The Lung Its Growth and Remodeling in Health and Disease"
1977- John F. Holt, MD, Ann Arbor, Michigan: "Neurofibromatosis in Children"
1978- Helen B. Taussig, MD, Baltimore, Maryland: "The Tetralogy of Fallot"
1979- Robert B. Salter, MD, Toronto, Ontario, Canada: "Legg Perthes Disease: The Scientific Basis for the Various Methods of Treatment and Their Indications"
1980- C. John Hodson, MD, New Haven, Connecticut: "Reflux Nephropathy and the Pediatric Radiologist"
1981- Stanley M. Garn, Ph.D., Ann Arbor, Michigan: "Contributions of the Radiographic Image to the Understanding of Human Growth"
1982- Duncan V. B. Neuhauser, Ph.D., Cleveland, Ohio: "Careful Thinking"
1983- J. Bruce Beckwith, MD, Seattle, Washington: "Renal Tumors of Children Pathologic Considerations Relevant to Diagnostic Imaging"
1984- J. Scott Dunbar, MD, Cincinnati, Ohio: "The Accessory Nasal Sinuses"
1985- John A. Kirkpatrick, Jr., MD, Boston, Massachusetts: "The Neuhauser Legacy"
1986- Kurt Hirschhorn, MD, New York, New York: "Recent Advances in Prenatal Diagnosis of Genetic and Congenital Disease"
1987- Andres Giedion, MD, Zurich, Switzerland: "Radiological Syntax of Genetic Bone Disease"
1988- Joseph J. Volpe, MD, St. Louis, Missouri: "Brain Injury in the Premature Infant"
1989- David H. Baker, MD, New York, New York: "Personal Reflections on Men and Machines from Red Goggles to Spin Wobbles"
1990- William H. Northway, Jr., MD, Stanford, California: "Bronchopulmonary Dysplasia and Research in Diagnostic Radiology"
1991- Derek C. Harwood Nash, MD, DSc, Toronto, Canada: "Pediatric Neuroimaging: The Evolution and Revolution of a Sub Specialty"
1992- Walter E. Berdon, MD, New York, New York: "Diseases of the Bone Marrow: MRI Observations"
1993- Morrie E. Kricun, MD, Philadelphia, Pennsylvania: "Paleoradiology: A Look into the Past"
1994- Beverly Wood, MD, Los Angeles, California: "Acute Pulmonary Disease in the Compromised Child"
1995- Frances S. Collins, MD, PhD, Washington, DC: "The Human Genome Project and the Future of Medicine"
1996- M. Judah Folkman, MD, Boston, Massachusetts: "Clinical Applications of Angiogenesis Research"
1997- S. Steven Potter, PhD, Cincinnati, Ohio: "Homeobox Genes and Pattern Formation (Master Genes)"
1998- Roy A. Filly, MD, San Francisco, California: "Fetal Thoracic Surgery"
1999- Harold A Richman, PhD, Chicago, Illinois: "Child Abuse: From a Radiologist's Discovery to a Major Issue of Public Policy. What Have We Wrought?"
2000-William D. Lyman, PhD, Detroit, Michigan: "Prenatal Molecular Diagnosis and Fetal Therapy"
2001- Jerry R. Dwek, MD, Columbus, Ohio: "Médecins Sans Frontiéres/The Doctors Without Borders Experience – Afghanistan"
2002- Eric J. Hall, DSc, FACR, FRCR, New York, New York: "Lessons We Have Learned From Our Children: Cancer Risks From Diagnostic Radiology"
2003- Jeffrey A. Towbin, MD, Houston, Texas: "Molecular Cardiology: Laboratory to Bedside"
2004- Bruce R. Rosen, MD, PhD, Boston, Massachusetts: "New Advances in MRI: A Guide for the Practicing Pediatric Radiologist"
2005- Bruce R. Korf, MD, PhD, Birmingham, Alabama: "Pathobiology and Management of NF1 in the 'Genomic Era'"
2006- Richard M.J. Bohmer, MD, MPH, Boston, Massachusetts: "Evolution, Innovation and the Changing Nature of Healthcare Delivery"
2007- Nogah Haramati, MD, Bronx, New York: "21st Century Radiology: Growth and Development of Our Workflows and Processes"
2008- Emanuel Kanal, MD, FACR, FISMRM, AANG, Pittsburg, Pennsylvania: "MR Technology: Where Are We, Where Are We Going?
2009- Roberta G. Williams, MD, Los Angeles, California: "Cardiology and Radiology: Partners in Producing Healthy Adults with Congenital Heart Disease"

2010- Regina E. Herzlinger, PhD, Boston, Massachusetts: “The Economic Basis of Change in Healthcare”
2011- Sanjiv Gambhir, MD, PhD, Stanford, California: “Molecular Imaging”
2012- William R. Hendee, PhD, Milwaukee, Wisconsin: “Past and Future Patient Benefits of Radiologist/Physicist Collaboration”
2013- James R. Downing, MD, Memphis, Tennessee: “The Pediatric Cancer Genome Project – Implications for Clinical Medicine
2014- Robert Pearl, MD, Oakland, California: “The Future of American Medicine – The Impact of Health Care Reform”
2015- Robert J. Gillies, PhD, Tampa, Florida: “Radiomics and Radiogenomics”
2016- Scott E. Fraser, PhD, Los Angeles, California: "Multimodal Imaging of the Molecular, Cellular and Tissue Events Underlying Embryonic Development”
2017- James H. Thrall, MD, FACR, Boston, Massachusetts: “Roles for Imaging in the Age of Precision Medicine”

SPR 2018 HONOREES

SPR 2018 GOLD MEDALIST

The Gold Medal of The Society for Pediatric Radiology is our most distinguished honor. The SPR Gold Medal is awarded to pediatric radiologists who have contributed greatly to the SPR and our subspecialty of pediatric radiology as a scientist, teacher, personal mentor and leader.

Dorothy I. Bulas, MD, FACR, FAAP, FAIUM

"From the first day I met Dorothy as an incoming fellow, I knew she would be a star!" - *George Taylor, MD*

"Dorothy should be everyone's pediatric radiology hero. She has limitless energy, inspirational passion, unquestioned ethics, a warm inclusiveness. She has a gift for education and a commitment to advocacy." - *Christopher Cassady, MD*

Writing a professional biography about Dorothy I. Bulas MD, FACR, FAAP, FAIUM, Professor of Radiology and Pediatrics and newly appointed Division Chief of Diagnostic Imaging and Radiology at Children's National Health Systems in Washington, DC is like trying to describe a hurricane in a 10 minute weather forecast. As David Kushner MD, who hired her for her first pediatric radiology faculty position said, "She is a force of nature". It is a totally inadequate exercise to describe this extraordinary woman and physician who has dedicated her life to improving the care of children since she completed her pediatric residency in 1983. The breadth of what she has accomplished in fetal and pediatric radiology, education and international outreach is mind boggling. Expertise in any one of these three areas would be noteworthy, but, to innovate and contribute meaningfully in these three areas is truly remarkable.

Dorothy was born in New York City, the middle child of Polish immigrants. Her mother's life story is one of sheer willpower and strength. During World War II, Dorothy's grandparents were deported to Siberia from Lithuania, and their family estates overtaken, first by Russian troops and later by the Nazis. Dorothy's mother survived the war and as a displaced refugee was accepted into the University of Heidelberg's medical school. Her father, who was active in the Polish underground, was also a displaced refugee studying chemistry in Heidelberg. It was there that Dorothy's parents met. Through the kindness of strangers, they found sponsors who helped them come to the United States. While penniless and without family, they both had educations that allowed them to quickly find work. The generosity of these sponsors impacted Dorothy's worldview and continues to inspire her international outreach efforts. Her parents' survival based on a strong education taught her the importance of knowledge and independence.

Growing up, Dorothy fell in love with ballet and until high school, was set on this professional path. A severe case of mononucleosis plus a growth spurt put this dream out of reach. She always enjoyed science and math so her high school guidance counselor encouraged her to apply to a combined college and medical program at the Medical College of Pennsylvania. Leave it to Dorothy to get her BA/MD degree in six years…

During those years she was awarded Phi Beta Kappa and Alpha Omega Alpha Honorary Society, already excelling among her peers.

During medical school, dance would again figure prominently in her life. While performing in a medical school skit, "Chorus Line", she met her future husband, Neal Kurzrok also a medical student at her school.

Dorothy initially completed a residency in pediatrics. During a pediatric radiology rotation with John Dorst at John Hopkins University, she realized how much she loved problem solving and using emerging imaging modalities. Dr. Dorst encouraged her to visit Children's National Medical Center where she met Bill McSweeney, then Chair of Radiology. Dr. McSweeney, after her visit, wrote her a letter that said "…you've been accepted in our pediatric radiology fellowship program. Oh, and by the way, you also need to complete a residency in diagnostic radiology!" Her path was set. She completed her radiology residency at Albert Einstein Hospital in NYC and then moved to Washington DC with her neurologist husband Neal, to complete a pediatric radiology fellowship at her beloved professional home, Children's National.

David Kushner, the new Chair at Children's National described those early years. "I first met Dorothy when I reported for work on my first day as Chief of the Radiology Department. Dorothy was just completing her fellowship in pediatric radiology and, being a "northern type" person, was "in my face" and in my office from the first moment. She had "plans" and it was obvious that there was nothing that would stand in her way. What an excellent attitude for a future faculty member! I offered her a job on the spot."

Her early research was mentored by George Taylor, and included work with Carlos Sivit on trauma related to motor vehicle accidents and cranial ultrasound findings on ECMO. Since her first publications in 1984, she has published 131 papers, one of her most recent as a co-author on "Neuroimaging findings in normocephalic infants with Zika virus" in *Pediatric Neurology*. This paper is an example of her intellectual curiosity on a cutting-edge topic combined with an international collaboration with physicians in Barranquilla, Colombia.

Dorothy views her role in the advancement of fetal imaging as her most significant professional contribution. She sees the progress in fetal medicine as a collaborative effort, and her involvement in this field as "one of the most exciting times". Her enthusiasm to share this knowledge resulted in the Society for Pediatric Radiology supporting a three-day fetal/neonatology meeting during her year as President of the Society for Pediatric Radiology in 2011. These meetings have now become highly successful biannual events. At Children's' she has been director of fetal imaging since she completed her fellowship, helping grow the program from its infancy. Besides numerous papers on fetal imaging, Dorothy is co-author with Beth Kline Fath on the textbook entitled Fundamental and Advanced Fetal Imaging. She has authored 35 book chapters and was prenatal/neonatal section editor with Tom Slovis for the 11th edition of Caffey's Pediatric Imaging. Tom Slovis said of Dorothy, "Dorothy has been an outstanding partner throughout her career in pediatric radiology. She is fun to work with and a superb team member. She represents the best of pediatric radiology."

Dorothy's passion for education is renown. She has been described as an "extraordinary teacher". In 2002, she a received a certificate as a Master Teacher through a George Washington University leadership development program. She has served as Program Director of the Fellowship Program at Children's National (2005- present) where she has impacted medical students, residents and fellows from the United States and abroad. She has served as education track chair for the RSNA and co-chaired the first and subsequent Education Summits of the SPR. She was a committee member of the ACGME radiology residency milestone committee and chaired the pediatric radiology milestone committee. She currently co-chairs the ACR pediatric radiology education committee. She was a founding member of the Image Gently Alliance, chairing the outreach campaign to parents, writing brochures, web material and articles to reach this most importance of audiences. She has been honored as an outstanding teacher with the Singleton-Taybi award from the SPR and this past fall, was awarded the Outstanding Educator from the RSNA.

Dorothy's role in international outreach in pediatric radiology is significant and impactful. In the words of Maria Ines Boechat MD, Founding President of the World Federation of Pediatric Imaging (WFPI), "From the time the concept of the WFPI was raised, Dorothy was a supporter and collaborator, playing an important role in convincing different societies' leadership that the WFPI was a feasible undertaking. As co-President of the London IPR in 2011, Dorothy and Cathy Owens officially launched the organization. She presided over the Education Committee for 4 years." Dorothy is now Chair of the ACR International Outreach Committee. She has given over 200 abstracts and scientific presentations nationally and 42 international invited lectures and 19 visiting professorships. Some of the countries she has taught in include Haiti, Ghana, Eritrea, South Africa, Poland, Russia, Brazil, Colombia, Thailand, Japan, and China. It is notable that for many of the international lectures she has given up to 20 lectures in a single week.

In her words, her involvement with the Society for Pediatric Radiology was a "gamechanger" in developing her career as a researcher, educator and advocate. Dorothy says, "Wonderful mentors such as Joanna Seibert, Janet Strife and Carol Rumack encouraged me to get involved. Working with mentors George Taylor, Tom Slovis and Marilyn Goske has been inspiring and made the work fun. The support SPR members have for new ideas, the flexible infrastructure SPR has for innovation plus the amazing execution by those involved particularly Jennifer Boylan, Karen Schmitt and Angela Davis have been amazing motivators. The SPR has been another family to me through the years."

And what about her real family? Neal, her husband of 35 years is so proud of her as a wife, mother and physician. He has been the stalwart "partner in crime" as they raised their two sons as "thoughtful citizens of the world". Mark, the oldest, has been passionate about outreach in South America. With degrees from Duke, Johns Hopkins and Mt. Sinai, he is currently a psychiatry resident in NYC and engaged to be married to Robyn Fialkow. Adam, a Duke graduate in engineering, did outreach in Tanzania, and currently works at Google on futuristic projects beyond the understanding of his mother. Clearly, the apples do not fall far from the family tree!

When Dorothy walks into a room the energy shifts. It is not just her quick wit, poise and warm physical presence that positively impacts those around her, but her ability to engage with each person as a valued individual, no matter their role in the medical profession or as a parent or patient. As Chris Cassady said, "Dorothy sees the good in people, and their best potential and she encourages both. Above all, you know that in her heart, the first and most important question to answer in any decision is, 'What is best for children?' Who would not want to be that kind of role model?"

For her intelligence and scientific curiosity, mentorship, passion and boundless energy in the care of children at home and around the world, the Society for Pediatric Radiology is proud to award the Gold Medal, the society's highest honor to Dorothy I. Bulas, MD.

Marilyn J. Goske, MD

SPR 2018 GOLD MEDALIST

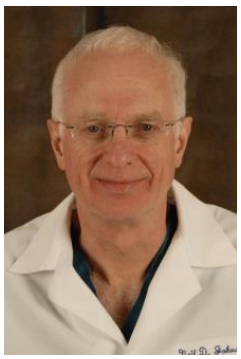

Neil D. Johnson, MBBS

Neil Johnson was born in Ballarat, Australia in 1952, the second of three children to parents who were not materially wealthy but highly valued education, achievement and hard work. Neil won scholarships to a local private school where students with a focus in science and related subjects were strongly supported. He and his older brother taught themselves basic mechanics, electronics, and backyard science. The occasional explosion, model aircraft crash or electrical short circuits were a feature of life in the Johnson household. Their younger sister, on the other hand, was a balancing model of common sense, tolerance and reason.

He attended medical school at the University of Melbourne where he graduated in 1976. During a neurology clerkship, he admitted one of the first patients to be scanned on the first CT scanner in Australia – the original "EMI Scanner". While that revolutionary but primitive machine clunked and rotated around the patient's head, images of a brain tumor with associated hydrocephalus magically appeared on the monitor and his future medical specialty became clear.

Neil moved to Hobart, Tasmania for his intern year where he developed a special interest in orthopedics, approaching it as a human version of motorcycle maintenance, a longtime passion that helped hone his mechanical skills. Neil also developed a passion for a nurse named Lorraine, who would become his lifelong partner and loyal mother of their three children. She may have made a different decision had she known that she and the children would be dragged backwards and forwards across the Pacific and end up in Cincinnati, Ohio!

Moving back to Melbourne in 1977, Neil was a pediatric intern at the Royal Children's Hospital, but decided to switch his career focus from pediatrics back to radiology. He took a year off clinical service and worked as an instructor in anatomy where he helped to develop the teaching materials for a new undergraduate course in radiological anatomy. Moving on to the Royal Melbourne Hospital, Neil completed his radiology training and was lucky enough to do his final year as a trainee of Dr. Ken Thomson, an Australian pioneer of what would become interventional radiology.

Dr. Thomson arranged a fellowship for Neil at the University of Rochester, NY, Strong Memorial Hospital intending that he would return to Melbourne as an adult interventional radiologist. But Neil met and was inspired by Dr. Beverly Wood at Rochester and combined interventional and pediatric radiology training. A month after Neil arrived in Rochester in 1985, an MRI clinical and research magnet was commissioned and for the next two years, some of the earliest work on pediatric MRI was done at Rochester. Neil's 1988 SPR presentation on MRI anatomy of the infant hip was recognized with a Caffey award.

Neil and Lorraine arrived in Rochester in the middle of a blizzard with their first child, Christopher. They departed Rochester to return to Melbourne in 1988 with the addition of Luana and David. Returning to the Royal Children's Hospital in Melbourne, Neil was influenced by Dr. John DeCampo who developed an early radiology information system and who taught and practiced a common sense business approach to the organization of radiology services.

Neil was recruited back to the US in 1988 by Donald Kirks, who patiently waited nearly three years for the family to get green cards. When Don made the first offer while visiting Melbourne, Neil and Lorraine had to rush home and look up an atlas to find out just where Cincinnati was! So the family packed up and crossed the Pacific again in 1991, settling in Cincinnati and planning to look for a "real" pediatric radiology job on one of the coasts. Twenty-seven years later he is still at Cincinnati Children's Hospital, having worn many different hats in addition to that of an outstanding pediatric radiologist.

Neil was appointed Associate Director under Janet Strife and changed the entire workflow, installing the first radiology information system, holding radiologists accountable for timely radiology reports to referring clinicians. Neil proposed the installation of PACS in 1998, which led to filmless operations in 2002, followed by integrated electronic radiology orders and soon after, voice recognition.

In 1993, Neil and his brother's IT company in Australia developed a radiology report rapid word search system named "Radsearch," which enabled fast retrieval of the basic data behind many of the clinical research projects at Cincinnati. Later, with University of Cincinnati business school partners, a system called "Radstream" was developed and patented that prioritized the reading list so that the most urgent radiology studies were read first and also provided effective and rapid communication of radiology repots to referring physicians. Neil was asked to become the first medical director of hospital information systems in 2000 and proceeded to lead the planning and implementation of the hospital's first electronic medical information system, winning the prestigious HIMSS Davies Award in 2003.

He returned to radiology full time in 2007 and then became the first medical director of vascular access, contributing to the organization and implementation of an integrated nursing, interventional radiology and surgical vascular access service, which remains a national model. He also created and led the implementation of a system for prevention of peripheral IV injuries, which has now become widely adopted nationally and internationally.

All the time, Neil was becoming more involved with service to the SPR. He was the first chair of the SPR Informatics Committee. Neil and his son Christopher supported by family and especially by Jennifer Boylan, developed and maintained the SPR web site for many years. Neil and Christopher were awarded the SPR President's award in 2001 for that work.

Neil was President of the SPR in 2010 during the recession, yet was able to raise commercial support to help put on an excellent scientific, educational, and social annual meeting in Boston. Later, as Chair of the SPR Board, Neil convened the first face to face meeting and helped establish what would become Image Gently, as well as supporting the formation of the World Federation, co-chairing the foundation meeting of WFPI at the London IPR.

Despite all his success in systems organization, hospital and SPR leadership, Neil's first professional priority is individual patient care in interventional radiology. He has always been driven by the idea that "we should always do for patients what we would do for our own families and children." He has used his early experiences in orthopedics, medical imaging and motorcycle maintenance to develop a unique system of tools and methods for image-guided orthopedic procedures. He moved the IR service to the operating room in 2000 and helped create and execute the vision to integrate IR fully into the operating room.

Although work, individual patient care and career are important to Neil, mentoring junior colleagues, people and family are more important. Most important is his wife Lorraine, family and friends. The success of his children in their new country has been a great pleasure and comfort. When Neil sees junior colleagues spending a bit too much time and effort at work, one of his favorite sayings is "remember - your family will be at your funeral, but the hospital will not." Lorraine and Neil have been through occasional tough times as first generation immigrants with the nearest grandparents and family nearly 9000 miles away, but the toughest time was when 26 week premie grand-twins were born in Rochester, NY. Lorraine selflessly spent months living in Rochester, supporting the twins and the family. Although they struggled through many obstacles, the twins, who are now almost 9 years old, are excelling physically and academically.

Despite all his many talents, achievements, passion for patient care, and devotion to family and friends, Neil Johnson is really just an odd ball Australian from Ballarat with an attitude for challenging the status quo and questioning everything from an upside down southern hemisphere perspective. And that's why we love him! A heart of gold and a medal to match. Congratulations, Neil! Good on ya mate!

John M. Racadio, MD

SPR 2018 PIONEER AWARD

Pioneer Honorees were first acknowledged in 1990 as a means to honor certain physicians who made special contributions to the early development of our specialty. The Pioneer Award now honors individuals who have advanced pediatric radiology through innovation, forethought and leadership.

Richard B. Towbin, MD, FACR

"I must not fear. Fear is the mind-killer. Fear is the little-death that brings total obliteration. I will face my fear. I will permit it to pass over me and through me. And when it has gone past I will turn the inner eye to see its path. Where the fear has gone there will be nothing. Only I will remain." - *Frank Herbert, Dune*

Richard Towbin, M.D. is being awarded the 2018 Society for Pediatric Radiology Pioneer Award for his significant role in the development and promotion of Pediatric Interventional Radiology. His contributions and commitment to this area of Pediatric Radiology have been influential in changing the way pediatric patients are treated and have benefited thousands of children.

Rich was born and raised in Brooklyn, New York. After high school, he moved to Cincinnati where he pursued his undergraduate studies, and he received a Bachelor of Science degree in Microbiology from the University of Cincinnati. He continued on there for medical school receiving his medical degree in 1974. Like many pediatric radiologists of his generation, Rich first completed a residency in pediatrics at Los Angeles Children's Hospital. However, while there he saw the light, and he returned to the University of Cincinnati to do a second residency in radiology, followed by a fellowship in pediatric radiology. During his radiology residency Rich was introduced to Interventional Radiology. Under the tutelage and mentorship of Dr. Corning Benton, at Cincinnati Children's Hospital, Rich performed his first interventional cases on pediatric patients, and he was hooked. He entered the world of Interventional Radiology in the late 1970's and early 1980's, just as the specialty was coming into its own, as a result of significant advancements in imaging and catheter and device technology. It was not lost on him that most, if not all, of the techniques and procedures being used to treat adult patients could be used to treat pediatric patients as well.

The above quote from Frank Herbert's Dune, one of Rich's favorite books, became a guiding principle for him during his career, and indeed, in his life. Fear of the unknown, fear of failure, fear of complications, fear of ridicule — none of these were seen by him as reasons to accept the status quo. During the early part of his career, spent at Cincinnati Children's Hospital and Children's Hospital of Michigan, he was among the first to introduce GI, biliary, and GU interventions in pediatric patients. He, along with a few others, developed the technique for percutaneous antegrade gastrostomy tube placement. He worked with many of the companies that manufacture the catheters and devices used in IR to modify them for use in pediatric patients. He invented several devices, including a neonatal pigtail catheter, a magnetic catheter, an over-the-wire magnetic catheter, and a button J tube.

During his career Rich has served as the Radiologist-in-Chief at Phoenix Children's Hospital, Children's Hospital of Philadelphia, and Children's Hospital of Pittsburgh, where under his leadership, each of these radiology departments, and in particular the IR sections, flourished and grew. He has published over 225 peer-reviewed articles, over 37 chapters or reviews, and one of the most comprehensive books on pediatric interventional radiology published to date. Recognized as a leader in pediatric interventional radiology, he has given over 250 invited lectures. He is a Fellow of the American College of Radiology, the Society of Interventional Radiology, the American Academy of Pediatrics, and the Society for Gastrointestinal Radiology. He has worked with the ACR and the SIR spearheading the development of standards for the practice of pediatric IR. He has served as the President of the Society for Pediatric Radiology and on the Society's Board of Directors. He has also served as the Treasurer of the Society of Interventional Radiology.

On a personal note Rich is the person who introduced me to the world of Pediatric Interventional Radiology. He has been a mentor, role model, colleague and friend for over 25 years. For me, what stands out about Rich is his boundless energy, his enthusiasm, and his passion for taking care of patients. He is an imaginative and creative individual, both professionally and personally, and he has a wild sense of humor. He has always enthusiastically promoted his trainees and has never been afraid of their successes, but rather, obviously feels a sense of pride in their accomplishments.

Rich has been a tireless advocate for pediatric IR and its continued growth, and he continues to push the boundaries of what can be done for pediatric patients in the IR suite. He has been an outstanding teacher and mentor not only for me, but for dozens of residents, fellows, and colleagues throughout his career. Many people who today practice Pediatric Interventional Radiology have been directly or indirectly influenced by him. It is without a doubt that the field of Pediatric Interventional Radiology would not be what it is today without the contributions of Richard Towbin, MD, FACR.

- *Robin Kaye, MD*

SPR 2018 PRESIDENTIAL RECOGNITION AWARD

The Society bestows Presidential Recognition Awards on members or other individuals whose energy and creativity have made a significant impact on the work of the Society and its service to its members.

Joëlle A. Moreno, JD

The 2018 SPR Presidential Recognition Award is bestowed upon Professor Joëlle Anne Moreno for her ongoing contributions to the protection of abused children and service to the Society.

Joëlle is a native of New York City. She was able to rise above her early education at Stuyvesant High School, a nondescript, provincial institution of little note, to study at Swarthmore College and to receive her J.D. from the University of Pennsylvania Law School. Before beginning her academic career, she served as a federal prosecutor in the Antitrust Division of the United States Department of Justice, where she prosecuted DeBeers and General Electric for price-fixing in the industrial diamonds industry. She is currently the Associate Dean for Faculty and a Professor of Law at Florida International University.

Joëlle has been an invaluable asset to the SPR and a member of its Child Abuse Imaging Committee since the committee was formed almost 20 years ago. From early papers addressing so-called Temporary Brittle Bone Disease to ongoing commentary on the recent flawed AHT report out of Sweden, she has had a hand in almost every project the committee has undertaken. Joëlle has presented her work at numerous medical and legal conferences, including the annual meetings of the SPR, ESPR, AAP, Helfer, ASNR, the National Center on Shaken Baby Syndrome, InterCAP, the Florida Bar, and the Queens DA's Office, and has acted as an unofficial liaison for the SPR on multiple occasions. She received the 2017 Helfer award for best long-form presentation (along with Dr. Gabriel Otterman).

She began her law-teaching career at the New England School of Law in Boston where she first started working with the SPR and the Child Abuse Committee. Among other activities, she ran expert witness training sessions for radiology and pediatric fellows at Hasbro and Boston Children's Hospitals and conducted a symposium on scientific evidence, which included panels on child abuse. She moved to Miami in 2007 and has continued her child abuse work at FIU.

Joëlle's excellence in teaching and dedication to helping others understand issues of the court specific to issues of child abuse are demonstrated by her outstanding presentations at numerous SPR meetings. She honored her commitment to speak at an abusive head trauma meeting in New York City despite the devastation hurricane Irma caused in areas around her home in Miami. She has also volunteered to assist physicians preparing for court in child abuse cases.

Her professional goal is to work together with physician experts to correct the fake news of a "controversy" surrounding the diagnosis of abusive head trauma, which has been promulgated in the courts and the popular media. Her academic writings include a general critique of the Supreme Court's misuse of science, a review of the vaccine linked autism pseudo-controversy, and two articles on the science and law of infant abusive head trauma (co-authored with Brian Holmgren). A selection of her books and articles can be found at https://law.fiu.edu/wp-content/uploads/sites/21/2015/07/Joelle-Moreno.pdf.

In her day job as a law professor, Joëlle teaches Evidence, Criminal Procedure, Scientific & Forensic Evidence, and Alternate Dispute Resolution. She is a longstanding member of the National Committee of Bar Examiners, which means that she writes or edits every essay question on every bar exam administered in 35 states – if the question involves evidence, criminal procedure, or criminal law. She is active on the Membership Committee of the American Association of Law Schools and is a past chair of its Evidence Section. She has also worked as a consultant, testifying as an expert witness in the international litigation involving manipulation of LIBOR benchmark rates.

Last month, Joëlle and Ken Mendelson celebrated their 24th wedding anniversary. Next month their older son Adam will graduate from Carleton College. Their younger son Nathan, who followed in his mother's footsteps to Swarthmore, will graduate in the spring of 2020. Joëlle is not sure of her plans for the future, but is certain that red wine will be playing a role.

Sabah Servaes, MD

SPR 2018 PRESIDENTIAL RECOGNITION AWARD

Patricia Vario

Since 2004, Pat Vario has served as Editorial Assistant for the journal *Pediatric Radiology*. Pat's work has been integral to the sustained success of the journal. Every Society for Pediatric Radiology member who has submitted a paper to Pediatric Radiology since 2004 has knowingly or unknowingly benefitted from Pat's dedication, consistency, professionalism and passion for her work.

Pat is *Pediatric Radiology's* superstar. Every single paper and communication of the American Editorial Office goes through Pat. She has been the "go-to" person for authors, potential authors, reviewers, the assistant editors, the editor and our publisher. Pat knows how things work. She is the repository of the inner workings of the journal, the nuances of maintaining a collegial and fruitful relationship with an overseas partner and the secrets of working cohesively with the publisher. Pat understands the relationship of the journal within the universe of the SPR and ESPR. Pat was the fiber holding the journal together through a seamless editorial transition from Dr. Slovis to Dr. Strouse in 2013. Pat's excellent rapport with all contributors helps to build teamwork so that the journal can continuously advance its mission to improve our understanding of pediatric imaging and its impact on the healthcare of children.

Pat is on the frontline, serving as the chief conduit for communications between authors, reviews, editors and the publishers. She truly realizes the importance to authors of each and every submission to the journal. Her treatment of authors is on the highest plane – fair, helpful, friendly, respectful, professional. Pat seeks to help all authors achieve what they wish to achieve. Some communications are difficult – rejected papers, requests for revisions, edits needed during copy editing or proof correction – in all of these communications and interactions with authors, Pat remains helpful, respectful and empathetic.

Pat has a keen insight into the goodness of people she encounters without being taken in by their agenda. She plays no favorites and even tells the editors like it is. Pat mediates disagreements between both sides of the Atlantic better than many countries' foreign policy. Throughout the challenges of the journalistic process – controversial topics, operational surprises, disgruntled authors and readers, no matter what - Pat has always been focused on the journal and its mission.

Pat keeps us on course without harsh words but instead with gentle firm and consistent guidance. She has been the backbone of our editorial office, maintaining and managing the never-ending, relentless flow of manuscripts, balancing the workflow of the editorial team members and keeping the editors on task. Pat is highly efficient, never overwhelmed and often thinking two or three steps ahead.

Pat is truly gifted in her skills as an editorial assistant – many, many manuscripts have been improved and many errors avoided due to Pat's consistency, thoroughness and keen eye. Pat is intellectually curious and often anticipates changes from the publisher, researching material from/for articles and keeps it all together when the editorial staff is sure that "we are going down the tubes." Pat is an incredibly hard worker willing to devote extra time necessary off hours and on weekends to maintain the flow and timeliness of the editorial office.

Before becoming the journal's Editorial Assistant, Pat was devoted to pediatric healthcare in her work. Pat is passionate for causes which help children and the underdog. Pat worked as an administrative assistant in the Immunology, Rheumatology and Allergy Division of the Department of Pediatrics at the Children's Hospital of Michigan in Detroit from 1980 until 2004. Pat was not a typical administrative assistant though. Beginning in 1983, she also worked with pediatric HIV patients in the immunology clinic. There was no nurse or social worker. Pat held babies for blood draws, went to funerals and comforted the grieving. She worked with the Department of Social Services to facilitate care for families and went to schools to help HIV children get into the classroom. Her efforts were instrumental at a time when resources and support were scarce.

Pat has attended numerous Society for Pediatric Radiology meetings, mainly to support journal Editorial Board and Managing Editors' Meetings, but also to meet many of the people behind the names on title pages of papers and on manuscript reviews. At these SPR meetings, Pat filled her time by volunteering at the registration desk. Pat has also assisted previous editors Dr. Berdon and Dr. Slovis with numerous tasks related to the SPR. Dr. Berdon quickly learned that Pat could be counted on to find and obtain an important, obscure literature reference.

Pat's whole career has been about learning, problem solving and improving the work those she serves. However, it is her example and treatment of others has made each of us better and enriched our lives. Those who have worked with her directly in the editorial process are keenly aware of how much we owe her. We are happy for this opportunity to share this with members of the Society for Pediatric Radiology. Thank you Pat!

Thomas L. Slovis, MD, FACR - Emeritus Editor, Pediatric Radiology *Peter J. Strouse, MD, FACR - Editor, Pediatric Radiology*

SPR 2018 HONORARY MEMBER

The Society extends Honorary Membership to individuals outside of the SPR who have made outstanding contributions to the care of children.

Fred E. Avni, Jr., MD, PhD

La flamme (Fr): enthusiasm, ardor, empathy, sympathy, cordiality, warmth, energy, animation, passion, honor, eclat, verve, zeal, hope

PROFESSOR EPHRAIM (FREDDY) AVNI

I am greatly honored to offer this tribute to Dr. Fred Avni, a leading pediatric radiologist from Belgium and a dear friend to many SPR members.

We know Freddy as a respected imager, teacher, researcher, and writer whose particular interest in fetal and neonatal imaging, ultrasound, and congenital uro-nephropathies has led to remarkable changes within our field and to the training of a new generation of pediatric radiologists. We also know him as a devoted husband of the brilliant and beautiful Jacqueline (Lussan) Avni, and as the proud father of his three accomplished children: Sarah, 28, an architect; Fanny, 27, an accountant; and Nathan, 25, a physiotherapist.

Fred Avni was born in 1951 in Kfar-Saba, Israel. His family moved to Brussels, Belgium in 1959 where he received his formal education through college and then earned his medical degree from the Université Libre de Bruxelles (ULB) in 1976.

ESPR 2010, Cathy Owens, Veronica Donoghue, and Mrs. Francois Diard

Fred's training in Radiology (1976-1980) began in Brussels. After his mentors encouraged him to take the then unusual step of extended study abroad, he continued his training in Paris and Boston. He spent six months working with Professor Jacques Sauvegrain at the Hôpital des Enfants-Malades, the world's first hospital especially established for the treatment of sick children, founded in 1802. Dr. Avni then spent six months at Boston Children's Hospital (BCH) under the charismatic leadership of Dr. John A. Kirkpatrick whose passion for the field is legendary. During both periods of study, Fred formed close and lasting friendships with his French and American counterparts in radiology.

In the early stages of Dr. Avni's career in medicine, radiography was of paramount importance and ultrasound was an emerging, experimental technology. As an "early user" and pioneer in exploring the diagnostic capabilities of ultraound-- especially abdominal, obstetrical, and pediatric ultrasound—Fred pushed the field forward with determination and a level of enthusiasm that was contagious. In fact, he was so gripped by the potential of ultrasound to enable the safe, rapid, accurate diagnosis of so many illnesses affecting women and children, that he returned to the Université Libre de Bruxelles (ULB), and in 1992, completed his PhD, magna cum laude, with the publication of his doctoral thesis on the "Contribution of obstetrical ultrasound to our knowledge of the natural course of some congenital diseases" – a work that simultaneously advanced our understanding of the capacity of obstetric ultrasound to evaluate fetal anomalies, and cemented the role of the pediatric radiologist as a natural fetal imager.

With the mentorship of John Kirkpatrick, Jacques Sauvegrain, and other luminaries in pediatric radiology, Fred developed an ever growing passion for the field during these early years of training—a passion which has not abated with time and is evident in every setting where Dr. Avni has worked.

As Chief of the Department of Pediatric Imaging at Queen Fabiola Children's University Hospital Brussels, from 1997-2002, and then as Chairman of the Medical Imaging Department at Erase Hospital (ULB), Brussels from 2002-2012), Fred has focused on developing Pediatric Radiology as a specialty—one that fosters close collaboration with other medical and surgical disciplines aimed at achieving the best possible outcomes for their young patients. Of Dr. Avni's many accomplishments, perhaps the greatest is his rare ability to cultivate and share his passion for the field, or, as he would say in his native French, "allumer la flamme chez les autres " (ignite the flame in others), especially the next generation of pediatric radiologists.

Photo with John Kirkpatrick: ESPR, Florence, 1984

Dr. Avni is an avid contributor to, and supporter of technological innovation in Radiology. He regularly reviews papers for the most prestigious peer-reviewed journals; he has authored over 170 peer-reviewed articles and over 55 book chapters; and he has edited five books, including his latest textbook, Imaging the Acute Abdomen in Children (2018).

Fred's record of service to radiology societies includes serving as:

- President, European Society of Paediatric Radiology (ESPR) – 1993-1994
- President, 1994 ESPR Annual Meeting and Postgraduate Course (Brussels)
- General Secretary, ESPR (1999-2008)
- Member, Trustees of the Board, ESPR
- Member, Executive Committee, European Society of Radiology, (ESR)
- Chairman, European Society of Radiology Subspecialties Committee
- Course organizer: European Society for Magnetic Resonance in Medicine and Biology (ESMRMB) Annual Pediatric MRI Course (2008-2016)

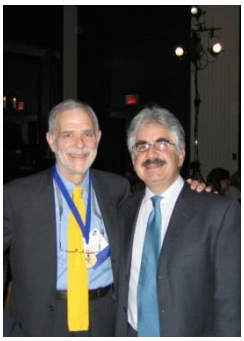

Photo with Bob Lebowitz: IPR 2006

In gratitude, his peers have recognized him with well-earned awards and honorary memberships:

- Jacques Lefebvre Award, ESPR (1985)
- Pioneer Award, SPR (2001)
- Honorary Member , French Society of Radiology (SFR) (2009)
- Honorary Member (2010) and Gold Medal (2013), ESPR

His academic appointments include:

- Chief of the Department of Pediatric Imaging – Queen Fabiola Children's University Hospital– Brussels (1997-2002)
- Chairman of the Medical Imaging Department - Erase Hospital (ULB) – Brussels (2002-2012)
- Chairman of the Radiological Specialty Training Committee (ULB) (2005-2012)

Dr. Avni currently serves as Professor Emeritus in Medical Imaging (ULB-Brussels), and as Senior Consultant and Director of the Ultrasound Division at the Pediatric Radiology Department of the Jeanne de Flanders (Mother and Child) University Hospital in Lille, France. In addition to spending time with his family and close friends, Fred enjoys genealogy, gardening and photography; traveling around the world (most recently practicing his Spanish in Mexico and planning a trip to South America); reading books (especially crime and historical novels); visiting modern art museums and exhibits; and going to the theatre and movies in Brussels and Paris.

When his closest radiologist friends were asked to say a few words about him, they offered these comments:

- Clever free spirit, curious, dynamic and fast, always in action, but unable to stay more than 5 minutes sitting during a congress.
- Passionate, generous with his ideas, having contributed to the formation and education of numerous residents, medical doctors and radiologists, and responsible for numerous careers in pediatric radiology and prenatal imaging.
- Excellent teacher and mentor, constantly participating in scientific societies, appreciated speaker in international meetings, and remaining involved in the day to day clinical work, helping pregnant women, neonates, infants and children.
- Insisting on quality in his work and teaching and able to obtain the best from his colleagues.
- Favoring team work, a constant and efficient leader, able to federate individuals, and always ready to help the youngest and most timid.
- The wisest, most perspicacious, courageous and honorable man.
- Fervent partisan of conciliation and discussion, in opposition to confrontation, and always present for friends and family.
- A friend, who has favorably influenced a generation of radiologists from all over the world.

And finally, in his own words, Fred Avni reminds us:

- Never forget to look back
- Be generous and respectful
- Never let people down
- Admit mistakes
- Remain faithful
- One cannot succeed alone
- Listen to the old and to the young
- Transmit "la flamme"

Dr. Fred Avni, we thank you: Merci mille fois!

Judy A. Estroff, MD

SPR 2018 HONORARY MEMBER

Karen Rosendahl, MD, PhD

Each year the SPR confers honorary membership on "individuals who have made an outstanding contribution to the care of children through scientific innovations which impact pediatric radiology". Karen Rosendahl epitomizes this definition and is one of our honorees this year.

Karen is true native of Bergen, Norway. She was born there, she attended medical school, trained in radiology and defended her PhD thesis locally at the University of Bergen. After moving away for a few short years to explore the world – she returned home and again lives in Bergen, Norway.

Karen is an associate professor at the Institute of Surgical Sciences, Section for Radiology and is a consultant paediatric Radiologist at Haukeland University Hospital in Bergen. She worked as consultant at Great Ormond Street Hospital for Children in London for several years returning to Norway in 2010 to take up her current post.

Early in her career Karen gained an interest in paediatric musculoskeletal radiology. Her PhD thesis entitled "Ultrasound in the developmental dysplasia of the hip in newborns" intensified her focus on the hip joint. As Karen says: 'The hip is our most important organ'. In 1988, she initiated a prospective longitudinal population-based study of more than 12,000 children to understand the pathogenesis of developmental dysplasia of the hips and assess the impact and costs of US screening. Karen is head of the paediatric arm of European Institute of Biomedical Imaging Research (EIBIR) and leads several research groups on juvenile idiopathic arthritis (JIA). Her research initiatives have validated imaging techniques in JIA. Her work has helped established age-based normal MRI standards in children.

Karen works thoroughly and systematically to reach her goals. Her arguments are scientifically based and if she runs out of arguments she simply conducts the studies required to find the answers. Karen's relentless work to search for the truth, particularly for hip dysplasia and juvenile idiopathic arthritis, has resulted in more than 100 papers in peer reviewed journals. Karen has received numerous awards for her scientific work and is honorary member of the Nordic Society of Radiology and the Norwegian Society of Radiology. Karen has mentored ten PhD candidates who have all successfully defended their theses. She was editor for the paediatric section of Acta Radiologica Journal for 10 years and is currently member of the Editorial Board for Pediatric Radiology.

Karen has been a leader and advocate for paediatric radiology both nationally and internationally. She hosted the ESPR in Bergen in 2002 and last year was elected president of the ESPR. Karen showed her true leadership and diplomatic skills as Co-President of IPR in Chicago in 2016. The SPR thanks Karen for her selfless hard work and contributions toward this successful collaboration between our two societies.

Despite her continuous clinical and scientific work for paediatric radiology she finds time to spend with her family and friends. Karen and her partner Alvhild have the most beautiful white wooden house by the fjord in Western Norway and their hospitality is heart-warming. Karen likes to work in her garden. Her passion for garden equipment, particularly motorized, is almost as strong as for hips, and she is very fond of her tractor and her hedge-cutter with a harness.

Karen has raised two fantastic sons who often visit Karen and Alvhild in their childhood home. Karen frequently travels to Oslo to spend as much time as possible with her two beloved grand-daughters Anna and Elise.

The SPR thanks Karen Rosendahl and proudly recognizes her with Honorary Membership.

Lil-Sofie Ording Müller, MD, PhD
James S. Donaldson, MD, FACR

SPR 2018 EDWARD B. SINGLETON-HOOSHANG TAYBI AWARD

The Edward B. Singleton-Hooshang Taybi Award is given in honor of Edward B. Singleton and Hooshang Taybi, in recognition of their personal commitment to the educational goals of the SPR. Initiated in 2006, the Award is presented annually to a senior member of the SPR whose professional lifetime dedication to the education of medical students, residents, fellows, and colleagues has brought honor to him/her and to the discipline of pediatric radiology.

John D. Strain, MD, FACR

Dr. John D. Strain is a Denver native who grew up in a close family with three siblings, a physician father and a great stay at home mom. John's father, Dr. Jim Strain, is an acclaimed pediatrician and former president of the American Academy of Pediatrics.

Growing up, John was a tremendous athlete. He began swimming at age 4, competed in his first out of state swim meet at age 8 and held every state record in freestyle throughout high school. He was a three-sport athlete, also playing football (all state quarterback) and baseball (all state pitcher). He even led the nation (NAIA) in strikeouts and ERA on a talented all-star baseball team. The Minnesota twins were even planning to draft him out of high school, but when his mom received the call, she simply told them not to bother as "Johnny was going to college!"

Instead of joining the major leagues, John attended the University of Northern Colorado on a full ride baseball scholarship, earning a B.S. in Chemistry. Upon graduation, he was unsure about medical school but decided to apply to one. He was accepted at the University of Colorado (CU) School of Medicine and John's first love was surgery. After completing a surgical internship, he knew this would not be a good fit and instead, did ED locums for a year. During that time, he honed his golf game, and even competed in the PGA qualifying tournament in Chicago!

John's final elective in medical school was radiology and he credits Dr. Paul Siebert, Chair of Radiology at the Denver VA, as the spark to his career. John discovered he had a keen eye, could identify abnormalities quickly, and remembered patients through their imaging. After a month rotation during residency at Denver Children's Hospital (now Children's Hospital Colorado, CHCO) under Dr. Jack Campbell, his career path was clear. Upon completion of pediatric radiology fellowship training at CHCO, his goal was to be chairman. Through the SPR, he was mentored by the best pediatric radiologists including Drs. John Kirkpatrick, Ed Singleton, Dave Baker and Walter Berdon. John initially with Drs. Jack Campbell, Chris Foley and Lee Harvey until political challenges at the University led the entire faculty to leave the practice—except him. A model of resilience, John worked as the sole pediatric radiologist at CHCO for eleven months! Following the strong recommendation by Dr. Scott Dunbar, former chairman at Cincinnati Children's Hospital, John was promoted to chairman of pediatric radiology at CHCO and has excelled in this position for 28 years! He spearheaded growth of the faculty from 1 (himself) to the current 23, all with sub-specialty expertise. John is a dedicated visionary and tireless advocate for the faculty, the hospital and the community.

Throughout his career, John has shown exceptional leadership at the local, state and national levels. At CHCO, after serving on numerous committees, he quickly chaired them, including the medical board, board of directors, medical staff nominating committee and numerous task forces. He has been instrumental in organizing, planning and development of hospital informatics. At the state level, he has served as treasurer, president elect and president of the Colorado Radiological Society. At the national level, John has been active in the children's cancer group, the ACR (chairing the imaging appropriateness criteria committee) and especially SCORCH (Society of Chiefs of Radiology in Children's Hospitals), serving as president in 2002-2003.

John is truly one of the giants in pediatric radiology. He is an outstanding "generalist" in an era of sub-specialization. Many of his accomplishments are now utilized in daily practice, notably the utility of oblique chest radiographs to improve detection of rib fractures and the development of indication driven decision support for order entry. John's tireless work ethic and passion for optimizing pediatric imaging are summed up by his colleague of 27 years, Dr. Tom Hay: "I learned how to be a good clinical radiologist from John's guidance and great example. There is no one better".

John is a passionate, gifted and dynamic speaker, who has been invited to give more than 100 lectures over his 30+ year career. He connects with every level of learner from the child to the professional. Our faculty's children even remember John's thoughtful practical teaching while hosting departmental picnics at his home! He sees the big picture, thinks outside the box and offers insight that had often not been considered previously.

As the director of the pediatric radiology fellowship for nearly 20 years, he was a tremendous role model, mentoring over 25 pediatric radiology fellows and countless residents. John has been my strongest mentor and entrusted me to direct the fellowship since 2010. He also holds a CAQ in neuroradiology and helped establish our pediatric neuroradiology fellowship program. John supports education through technology and implemented our Integrated Radiology Imaging System (IRIS) digital teaching file in 2008. The teaching file now has greater than 23,000 cases and will continue to benefit residents and fellows for generations to come. He listens, supports, guides and inspires others to create meaningful solutions to our everyday challenges.

John has been awarded many honors for his commitment and leadership, including the medical board award for outstanding service to CHCO and numerous faculty teaching awards, For 23 consecutive years, John has received Denver's 5280 "Top Doc" award, emphasizing his tremendous standing amongst his peers.

Julie and John have been married for 25 years. Julie is the light of John's life, and the rock of their family. She would often remind him how lucky he was to be able to help children, even when he had to go in at 3am to reduce an intussusception! They are the proud parents of three boys: JJ (currently a freshman at Villanova and on the swim team!) and twins James (swimming and playing basketball) and Jonas (playing basketball and baseball) at Cherry Creek high school.

Dr. John Strain's lifetime of service and dedication to children, education, leadership, and the SPR make him an obvious choice for the 2018 SPR Edward B. Singleton-Hooshang Taybi Award. Dr. Strain encompasses all the ideals this award embraces. We are fortunate to know and work with such a brilliant and compassionate pediatric radiologist! Congratulations John!

Laura Z. Fenton, MD

SPR 2018 JACK O. HALLER AWARD

This award is given in memory of Jack O. Haller who excelled as an educator, mentor and author. His ability and enthusiasm stimulated many young medical students and residents to pursue pediatric radiology. This award is given to an individual who has demonstrated evidence of outstanding ability to educate trainees (medical student, resident and fellow) who has shown sustained substantial excellence in mentorship skills.

Veronica J. Rooks, MD

"If your actions inspire others to dream more, learn more, do more, and become more, you are a leader." - *John Quincy Adams*

The quotation above describes the life and work of the venerated and beloved Jack O. Haller and also the career of Veronica "Roni" Rooks, one of the two recipients of the 2018 Jack O. Haller Award. Throughout a long and varied career as a pediatric radiologist and medical leader in the US Army, Roni has always focused on teaching, mentoring, and inspiring students, resident physicians, and junior faculty members while serving her country.

Born in New Jersey, Roni graduated from Gettysburg College and then went on to earn a master's degree in chemical engineering. She heard the call to the medical profession and, following medical training at the University of Vermont, completed radiology residency at Tripler Army Medical Center (TAMC) and then pediatric radiology fellowship at the Children's Hospital Boston. There she met some of her most influential mentors - George Taylor, Robert Lebowitz, and Carlo Buonomo.

Roni spent much of her career at TAMC in Honolulu where she served as the assistant residency program director, Chief of Pediatric Radiology, and Medical Director of Research Education of the Department of Clinical Investigation. In 2008, she deployed in service of Operation Iraqi Freedom as a trauma radiologist to Mosul, Iraq. Subsequently, she rose to the rank of colonel and became Chief of the Department of Radiology. She received the Army's "A" designator from the Surgeon General for academic excellence, and received the Outstanding Teacher of the Year Award from the Tripler Residency program in 2013. She was selected as a member of the elite Order of Military Medical Merit for excellence of service in the Army Medical Department and fostering fellowship and *esprit de corps* in 2013. After a distinguished 24-year career in the Army, Roni recently retired but will return to Tripler as a civilian pediatric radiologist.

During her time at Tripler and Walter Reed Army Medical Center before that, she taught in numerous RSNA Plenary Sessions on pediatric neuroradiology, child abuse, trauma radiology, teleradiology and remote radiology in austere settings, and countless hands-on ultrasound sessions. She served as consultant to the Armed Forces Center for Child Protection, providing expert witness testimony in 17 trials all over the world; provided teleradiology services to hospitals all over the Pacific Basin; provided onsite ultrasound expertise to medical missions in Nicaragua and Guatemala; served as radiology Officer-in-Charge for a military medical mission in Thailand; and taught pediatric radiology at the Armed Forces Institute of Pathology and in Fiji and Pago Pago, American Samoa, and Rwanda. Over the years, Roni had fostered mentoring relationships and collaborations with trainees and junior faculty members that have led to research projects and 32 publications in refereed journals and 39 abstracts/posters and exhibits. She has guided residents and junior faculty members in the study of whole-body MR for detection of anatomic changes in asymptomatic newborns, screening vitamin D deficiency in young children without suspected trauma, and, most importantly, demonstrating intracranial hemorrhage in over 100 asymptomatic newborns on MR. She is also working on clinical competency training for ultrasound guided foreign body removal in war and the use of finger-tip ultrasound in the evaluation of umbilical vascular catheter placement. Many of her trainees have gone on to train in pediatric radiology and to pursue their own research.

On a personal note, Roni met the love of her life and husband of 27 years, Bob Rooks, during graduate school at Duke University. Together they have raised three happy and successful daughters, Lexi, Tori, and Liza, born during medical school, residency, and fellowship, respectively. Their secret to success may have been implementation of weekly "forced family fun" nights, perhaps a side effect of years of military life. Following in her mother's footsteps, daughter Lexi is now a second lieutenant in the Army currently finishing her doctorate in Physical Therapy.

Throughout her long career as a pediatric radiologist in the US Army, Dr. Roni has accepted many unique challenges in the service of our country, yet she has always been able to maintain her focus on teaching and mentoring students, residents, and junior faculty. In this way, her career honors the tradition of Jack O. Haller, whose enthusiasm as a teacher and mentor inspired so many to achieve more than they thought possible.

Ellen M. Chung, MD

SPR 2018 JACK O. HALLER AWARD

Yukata Sato, MD, PhD

I am honored to write this biography for Yutaka Sato, MD, PhD, co-recipient of the Society for Pediatric Radiology, Jack O. Haller Award for Excellence in Teaching.

"All right, you win", he said as he handed me a $1.00 bill. As a fellow in pediatric radiology at the University of Iowa, it was a great feeling to have figured out a challenging case before the Chief of Pediatric Radiology. The incentive that this gave me, went far beyond the value of the dollar bill, and is just one of the many ways that Yutaka Sato makes learning fun in the reading room.

Yutaka asks questions of trainees and engages them by soliciting their opinions. He makes you feel like a peer whose opinion is truly valued in the reading room. The resulting atmosphere naturally stimulates the medical students, residents, fellows, and junior faculty to learn more about each case they encounter so that they can make a valuable contribution to the daily discussions.

Intelligent, inquisitive, funny, and humble are just a few words that can be used to describe Yutaka. He has mentored many medical students, residents, fellows and faculty members. The medical students and residents at the University of Iowa have awarded him "Faculty Teacher of the Year" on multiple occasions. Of his more than 150 publications, many are co-authored with trainees. Over the years, many University of Iowa radiology residents have chosen to stay there to do their fellowships in Pediatric Radiology.

Under Yutaka's mentorship, a very strong academic relationship has been built between the University Of Iowa Department Of Radiology and the Japanese society of Radiology resulting in a constant stream of visiting faculty members. Several of his former mentees now hold leadership positions in the Society of Pediatric Radiology, Japanese Society of Pediatric Radiology, and Asian and Oceanic Society for Pediatric Radiology. Hence, even while practicing and teaching in the small college town of Iowa City, Yutaka has helped further clinical and academic pediatric radiology in different parts of the world through his numerous mentees.

Finally, apart from all his academic successes, Yutaka is a genuinely warm, generous, and kind-hearted person. He tailgates with his son during Iowa football season with an open-invitation to everyone in the department: from technologists and film-room staff to residents and attendings. Yutaka has not only taught us radiology, he has also taught us the more important things in life: cherish time with family and friends, have a hobby, be a colleague/friend to the technical and administrative staff, and enjoy all that you do at the end of the day.

In summary, Yutaka is an excellent educator, mentor, and author. Through his excellent mentorship skills, he has influenced the careers of many pediatric radiologists who hope to carry the baton forward.

Geetika Khanna, MD, MS

HEIDI PATRIQUIN AWARD

In recognition of Dr. Patriquin's commitment to international education, this fellowship is designed to subsidize the expenses of one Pediatric Radiologist per year who practices outside of North America.

Bernadette Wambui Muthee, MD
Aga Khan University Hospital Nairobi, Kenya

JOHN P. CAFFEY AWARDS

John P. Caffey, MD 1895-1978

Dr. John P. Caffey was regarded throughout the world as the father of pediatric radiology. His classic textbook, "Pediatric X-Ray Diagnosis", which was first published in 1945, has become the recognized bible and authority in its field. The seventh edition of this book was completed several months before his death in 1978. It has been among the most successful books of its kind in the medical field.

Dr. Caffey was born in Castle Gate, Utah on March 30, 1895. It is interesting that he was born in the same year that Roentgen discovered the x-ray. Dr. Caffey was graduated from University of Michigan Medical School in 1919, following which he served an internship in internal medicine at Barnes Hospital in St. Louis. He spent three years in Eastern Europe with the American Red Cross and the American Relief Administration, and returned to the United States for additional training in medicine and in pediatrics at the Universities of Michigan and Columbia, respectively.

While in the private practice of pediatrics in New York City at the old Babies Hospital of Columbia University College of Physicians and Surgeons, he become interested in radiology and was charged with developing a department of pediatric radiology in 1929. He frequently expressed appreciation and admiration for Ross Golden, Chairman of Radiology at Columbia Presbyterian Hospital, who allowed him to develop a separate department of diagnostic radiology without undue interference, and who was always available to help and advise him.

Dr. Caffey's keen intelligence and inquiring mind quickly established him as the leader in the fields of pediatric x-ray diagnosis, which recognition became worldwide almost instantaneously with the publication of his book in 1945.

Dr. Caffey received many awards in recognition of his achievements. Outstanding among these were the Mackenzie Davidson Medical of the British Institute of Radiology in 1956, the Distinguished Service Award of the Columbia Presbyterian Medical Center in 1962, the Outstanding Achievemeng Award of the University of Michigan in 1965, the Howland Award of the American Pediatric Society in 1967, the Jacobi Award of the American Medical Association in 1972, and the Gold Medal Award of the American College of Radiology in 1975. He had been a member of the American Journal of Roentgenology. He was a counselor of The Society for Pediatric Radiology and was an honorary member of the European Society of Paediatric Radiology.

Dr. Caffey's contributions to the pediatric radiologic literature were many. He was instrumental in directing attention to the fact that a prominent thymic shadow was a sign of good health and not of disease, an observation that literally spelled the end to the practice of thymic irradiation in infancy. Infantile cortical hyperostosis was described by him and is called "Caffey's Disease". Dr. Caffey in 1946 first recognized the telltale radiographic changes that characterize the battered child, and his students helped disseminate his teachings about these findings. It was Dr. Caffey who first recognized and descried the characteristic bony changes in vitamin A poisoning. He recognized and described the findings associated with prenatal bowing of the skeleton.

In 1963, 3 years after his retirement from Babies Hospital, he joined the staff of the Children's Hospital of Pittsburgh as associate radiologist and as Visiting Professor of Radiology and Pediatrics at the University of Pittsburgh School of Medicine. Although Dr. Caffey came to Children's Hospital and the University of Pittsburgh in an emeritus position, he worked daily and on weekends throughout the years he was there. In Pittsburgh, he made four major new contributions to the medical literature. He described the entity, "idiopathic familial hyperphosphatasemia". He recognized and described the earliest radiological changes in Perthes' Disease. He called attention to the potentially serious effects of shaking children, and used this as a subject of his Jacobi Award lecture. He described, with the late Dr. Kenny, a hitherto unrecognized form of dwarfism which is now known as the Caffey-Kenny dwarf. The John Caffey Society, which includes as its members pediatric radiologists who have been intimately associated with Dr. Caffey, or who have been trained by his students, was established in 1961. This society is now among the most prestigious in the field of radiology. His book and the society named in his honor will live on as important memorials to this great man.

His greatness was obvious to all who worked with him. He was warm, kind, stimulating, argumentative, and above all, honest in his approach to medicine and to x-ray diagnoses. His dedication to the truth was expressed in his abiding interest in the limitations of x-ray signs in pediatric diagnosis and in his interest in normal variation in the growing skeleton. He was concerned with the written and spoken word and was a skilled semanticist. His book and his articles are masterpieces of language and construction. He stimulated and was stimulated and loved by all who had the privilege of working with him. Radiology and Pediatrics have lost a great man, but they shall ever have been enriched by his presence.

Bertram R. Girdany, MD

JOHN P. CAFFEY AWARD PAPERS (1969-1998)

1969- Pneumonia of Atypical Measles: Residual Nodular Lesions; Young LW, Smith DI, Glasgow LA.

1970- Plain Skull Roentgenograms in Children with Head Trauma; Roberts F, Shopfner CE.

1971- Vascular Thromboembolism Complicating Umbilical Artery Catheterization; Williams HJ, Jarvis CW, Neal WA, Reynolds JW.

1972- Hydrometrocolpos in Infancy; Reed MH, Griscom NT.

1973- Various Radionuclide Patterns of Cerebral Inflammation in Infants and Children; Gilday DL.

1974- The Tethered Filum; Fitz CR, Harwood-Nash DC.

1975- B-Mode Ultrasound and the Nonvisualizing Kidney in Pediatrics; Shkolnik A.

1976- The Pediatric Tracheostomy: Roentgen Signs of Normal Healing and Complications-The Value of Xerography; Scott JR, Kramer SS.

1977- A Prospective Study of Intraventricular Hemorrhage in Premature Newborns Using Computed Tomography; Burstein J, Papile L, Burstein R.

1978- Chemotherapy-Induced Inhibition of Compensatory Renal Growth in the Immature Mouse; Moskowitz PS, Donaldson SS.

1979- Lithiasis Due to Interruption of the Enterohepatic Circulation of Bile Salts; Kirks DR.

1980- Cranial Ultrasound Findings in Patients with Meningomyelocele; Babcock DS, Han BK.

1981- Effect of Contrast Agents in the Lungs of Animals; McAlister WH, Siegel MJ, Shackelford GD, Glasier CH, Askin FB.

1982- Real-Time Ultrasonographic Detection of Vesicoureteral Reflux in Children; Kessler RM, Altman DH.

1983- Ultrasonic Evaluation of Caudal Spine Anomalies in Children; Naidich TP, Fernbach SK, McLone DG, Shkolnik A.

1984- Experimental Neonatal Intraventricular Hemorrhage: Clinical Radiographic and Pathologic Features; Goske MJ, Morin FC, Eskin TA.

1985- The Metaphyseal Lesion in Abused Infants: A Radiologic? Histopathologic Study; Kleinman PK, Marks SC, Blackbourne BD.

1986- Magnetic Resonance Appearance of Blood and Blood Products; Cohen MD, Smith JA, Cory DA.

1987- Intussusception Reduction by Rectal Insufflation of Air; Gu L, Alton DJ, Daneman A, Stringer DA, Liu P, Wilmot DM, Reilly BJ.

1988- MR Imaging Determination of the Location of the Conus Medullaris in Normal Children and in Children with Tethered Cord Syndrome; Wilson DA, Prince JR.

1989- Early Avascular Necrosis: MRI and Histological Examination in an Animal Model; Brody AS, Strong M, Babikian G, Seidel FG, Kuhn JP.

1990- Determination of Functional Residual Capacity from Digital Radiography in an Animal Model of the Neonatal Chest; White KS, Muelenaer AA, Beam CA, Effmann EL.

1991- Juvenile Colonic Perforation: Experimental Results and Clinical Applications; Shiels II WE, Keller GL, Ryckman FR, Daugherty CC, Specker BL, Kirks DR, Summa DW.

1992- Pulmonary oxygen toxicity: Experimental assessment of capillary leakiness using contrast-enhanced MRI; Brasch RC, Berthezene Y, Vexler V, Shames DM, Jerome H, Clément O, Mühler AR, Kuwatsuru R.

1993- High Resolution CT Assessment of Bronchoconstriction: Differential Effects of Methacholine and Histamine; Kramer SS, Hoffman EA, Amirav I.

1994- Inhibition of Neutrophil Phagocytosis by Barium Sulfate; Hernanz-Schulman M, Hakim RM, Schulman G, Vanholder R.

1995- Evaluation of Perfusion of the Normal and Ischemic Cartilaginous Epiphysis by Using Gadolinium-enhanced MR Imaging; Jaramillo D, Shapiro F, Villegas OL, Mulkern RV, Doty D, Dwek J.

1996- The Detection of Pulmonary Metastases with Pathological Correlation: Effect of Breathing on the Accuracy of Spiral CT. Coakley FV, Cohen MD, Waters D, Davis MM.

1997- MR Imaging Microvessel Permeability Correlates with Pathologic Tumor Grade; Brasch RC, Daldrup HE, Shames DM, Rosenau W, Okuhata Y, Wendland, MF.

1998- Imaging Acute Heart and Lung Transplant Rejection in Rats by Using Tc-99m -radiolabeled Annexin V; Blankenberg FG, Vriens, P, Robbins RC, Ohtusuki K, Tait JF, Strauss HW.

JOHN P. CAFFEY AWARD FOR BEST BASIC SCIENCE RESEARCH PAPER

1999- Changes in Renal Blood Flow Depicted with Contrast-enhanced Harmonic Imaging During Acute Urinary Obstruction; Claudon, M, Barnewolt, CE, Taylor, GA, Dunning, PS, Gobet, R, MD; Badawy, A.

2000- Detection of Early Atherosclerosis with Radiolabeled Monocyte Chemoattractant Protein-1 in Prediabetic Zucker Rats; Blankenberg FG, Tait, JF, Strauss, HW, Valentine HA.

2001- Computer-Simulated Radiation Dose Reduction For Pediatric Abdominal Helical CT, Frush, D, Slack,CC, Hollingsworth, CL, Bisset III,GS, Donnelly, LF, Hsieh,Jl

2002- Understanding the Functional Angiogenic Process in an Antigen-Induced Arthritis Model: Correlative BOLD MR Imaging (fMRI) of the Stages of Synovitis along the Time Course of the Disease; A. S. Doria, MD , Diagnostic Imaging, Hospital for Sick Children, Ontario, P.S. Babyn, MD, A. Crawley, PhD, M. Noseworthy, PhD, K. Pritzker, MD, R. B. Salter, MD, et al

2003- A Novel Method for Non-Viral Gene-Therapy: Transcatheter Hydrodynamic Delivery Using Isolated Liver as a Depot Organ In a Rabbit Model; Kevin Baskin, MD, Children's Hospital of Philadelphia, PA, Simon J. Eastman, PhD; Ronald K. Scheule, PhD; Bradley L. Hodges, PhD; Qiuming Chu, MS; Richard B. Towbin, MD

2004- Site-Specific Induction of Lymphatic Malformations in a Rat Model for Image-Guided Therapy; Robert F. Short, MS, Department of Radiology, Children's Radiological Institute, Children's Hospital, Columbus, OH; William E. Shiels, DO; Thomas J. Sferra, MD; Katherine Nicol, MD; Minka Schofield, MD; Gregory Wiet, MD

2005- Quantitative Measurement of Microbubble Ultrasound Contrast Agent Flow To Assess the Efficacy of Angiogenesis Inhibitors In Vivo; Beth McCarville, MD, Dept of Rad Sciences, St. Jude Children's Research Hosp, Memphis, TN; Christian Streck, MD; Chin-Shang Li, PhD; Andrew Davidoff, MD

2006- 4Cu-Immuno-PET Imaging of Neuroblastoma with Bioengineered Anti-GD2 Antibodies; Stephan D Voss, MD, PhD, Radiology, Children's Hospital Boston, Harvard Medical School, Boston, MA; Suzanne V Smith, PhD; Nadine M Di Bartolo, PhD; Lacey J McIntosh; Erika M Cyr; Ali A Bonab, PhD, et. al.

2007- MR Imaging of Adenocarcinomas with Folate-Receptor Targeted Contrast Agents; Heike E Daldrup-Link, MD, PhD, Radiology, University of California San Francisco, San Francisco, CA; Zhen J Wang, MD; Reinhard Meier, MD; Claire Corot, PhD

2008- Evaluation of Quality Assurance Quality Control Phantom for Digital Neonatal Chest Projection Imaging; Steven Don, MD, Mallinckrodt Institute of Radiology, Washington University School of Medicine

2009- Faster Pediatric MRI Via Compressed Sensing - Shreyas Vasanawala, Stanford University, Marcus Alley, Richard Barth, Brian Hargreaves, John Pauly, Michael Lustig

2010- Clinical Evaluation of Readout-Segmented-EPI for Diffusion-Weighted Imaging – Roland Bammer, PhD, Stanford University, Palo Alto, CA, Samantha J Holdsworth, PhD;Stefan Skare, PhD; Kristen Yeom, MD; Patrick D Barnes, MD

2010- High-Resolution Motion-Corrected Diffusion-Tensor Imaging (DTI) in Infants – Stefan T Skare, PhD, Stanford University, Stanford, CA; Samantha J Holdsworth, PhD; Kirsten Yeom, MD; Patrick D Barnes, MD; Roland Bammer, PhD

2010- 3D SAP-EPI in Motion-Corrected Fast Susceptibility Weighted Imaging (SWI) – Roland Bammer, PhD, Stanford University, Palo Alto, CA, Samantha J Holdsworth, PhD; Stefan Skare, PhD; Kristen Yeom, MD; Patrick D Barnes, MD

2010- T1-Weighted 3D SAP-EPI for Use in Pediatric Imaging – Roland Bammer, PhD, Stanford University, Palo Alto, CA, Samantha J Holdsworth, PhD; Stefan Skare, PhD; Kristen Yeom, MD; Patrick D Barnes, MD

2011- An MR System for Imaging Neonates in the NICU, Jean Tkach, Randy Giaquinto, Wolfgang Loew, Ronald Pratt, Barret Daniels, Blaise Jones, Lane Donnelly, Charles Dumoulin, Cincinnati Children's Hospital Medical Center

2012- Advantages of a Nanoparticle Blood Pool Contrast Agent Over Conventional Intravascular Glomerular-Filtered Contrast Agents for Pulmonary Vascular Imaging; Ananth Annapragada, Texas Children's Hospital, R. Paul Guillerman, Eric Hoffman, David Kaczka, Ketan Ghaghada, Cristian Badea

2013- Psychometric Function: A Novel Statistical Analysis Approach to Optimize CT Dose: Steven Don, MD, Mallinckrodt Institute of Radiology, St. Louis, MO,Bruce Whiting, David Politte, Parinaz Massoumzadeh, Charles Hildebolt

2014- No longer a holiday: Improving the pediatric radiology elective for medical students and pediatric housestaff Eddie Hyatt, Vanderbilt University, Department of Radiology and Radiological Sciences, Nashville, TN, Cody Penrod, Sudha Singh, Jayne Seekins, DO, Amy Fleming, Melissa Hilmes, MD

2015- Gonad Shields: Good or Bad for Patient Radiation Exposure?; Summer L. Kaplan, MD, Department of Radiology, The Children's Hospital of Philadelphia, Philadelphia, PA, Dennise Magill, MS, Marc A. Felice, MS, Sayed Ali, MD, Xiaowei Zhu, MS

2016- In vivo Profiling of Folate Receptor Expression in Rat Placenta Using MR Molecular Imaging; Ketan Ghaghada, PhD, Zbigniew Starosolski, PhD, Eric Tanifum, PhD, Haijun Gao, PhD, Igor Stupin, MD, PhD, Saakshi Bhayana, BS, Chandresh Patel, BS, Chandrasekhar Yallampalli, DVM, PhD, Ananth Annapragada, PhD, Texas Children's Hospital, Houston, TX

2017- Performance of a Deep Neural Network Learning Model in Assessing Skeletal Maturity on Pediatric Hand Radiographs; David B. Larson, MD, MBA, Matthew C. Chen, Matthew P. Lungren, MD, MPH, Safwan S. Halabi, MD, Nicholas V. Stence, MD, Curtis P. Langlotz, MD, PhD Radiology, Stanford University, Stanford, CA University of Colorado, Aurora, CO

JOHN P. CAFFEY AWARD FOR BEST CLINICAL RESEARCH OR EDUCATION PAPER

1999 - Triangular Cord Sign in Biliary Atresia: A Gold Standard for the Millennium? Tan Kendrick AP, Phua, KB, Subramaniam, R.

2000 - Cisterna Magna Thrombus and Subsequent Posthemorrhageic Hydrocephalus. Cramer BC, Walsh EA.

2001 - Aneurysmal Bone Cysts In Children: Percutaneous Sclerosing Therapy, An Alternative To Surgery. Dubois J, Garel LA, Rypens FF, Grimard G, Isler, M, Mercier C

2002 - MR Imaging of Kidneys: Functional Evaluation Using F-15 Perfusion Imaging, Grattan-Smith D, Jones RA; Little S, Perez M, Kirsch A

2003 - Differential Regurgitation in Branch Pulmonary Arteries after TOF Repair. Yoo SJ, Kang IS, Redington A, Benson LN; Macgowan CK; Valsangiacomo ER

2004 - Feasibility of a Free-Breathing SSFP Sequence for Dymanic Cardiac Imaging in Pediatric Patients. Krishnamurthy, R, Muthupillai R, Vick G, Su J, Kovalchin J, Chung T; Diagnostic Imaging, Texas Children's Hospital, Houston, TX

2005 - Evaluation of High Resolution Cervical Spine CT In 529 Cases of Pediatric Trauma: Value Versus Radiation Exposure. Shiran, D, Jimenez, R, Altman, D, DuBose, M, Lorenzo, R

2006 - Alterations in Regional O2 Saturation (StO2) and Capillary Blood Volume (HbT) with Brain Injuries and ECMO. P Ellen Grant, MD, Pediatric Radiology, Massachusetts General Hospital, Boston, MA; George Themelis; Kara Arvin, MD; Sonal Thaker; Kalpathy K Krishnamoorthy, MD; Maria Angela Franceschini, PhD

2007 - Evaluation of Single Functioning Kidneys Using MR Urography. Damien Grattan-Smith, MBBS, Department of Radiology, Children's Healthcare of Atlanta, Atlanta, GA; Richard Jones, PhD; Stephen Little, MD; Andrew Kirsch, MD; Adina Alazraki, MD

2008 - Evaluating the Effects of Childhood Lead Exposure with Proton MR Spectroscopy & Diffusion Tensor Imaging Neuroradiology; Kim M Cecil PhD, Cincinnati Children's Hospital Medical Center

2009 - Improving Patient Safety: Effects of a Safety Program on Performance and Culture in a Department of Radiology at a Children's Hospital - Lane Donnelly, Cincinnati Children's Hospital Medical Center, Julie Dickerson, Martha Goodfriend, Stephen Muething

2010 - Juvenile Osteochondritis Dissecans (JOCD): Is It a Growth Disturbance of the Secondary Physis of the Epiphysis? Tal Laor, MD, Cincinnati Children's Hospital Medical Center, Cincinnati, OH, Eric J Wall, MD; Andrew M Zbojniewicz, MD

2011 - Quantitative Assessment of Blood Flow with 4D Phase-Contrast MRI and Autocalibrating Parallel Imaging Compressed Sensing, Albert Hsiao, Stanford University, Micheal Lustig, Marcus Alley, Mark Murphy, Shreyas Vasanawala

2012 - Multidetector CT Pulmonary Angiography in Children with Suspected Pulmonary Embolism: Thromboembolic Risk Factors and Implications for Appropriate Use; Edward Lee, MD, MPH, Children's Hospital, Boston, Sunny K. Tse, David Zurakowski , Victor M. Johnson, Tracy A. Donald, Phillip M. Boiselle

2013 - Prospective Comparison of MRI and Ultrasound for the Diagnosis of Pediatric Appendicitis; Robert Orth, MD, PhD, Texas Children's Hospital, Houston, TX, R. Paul Guillerman, Prakash Masand, MD, Wei Zhang, George Bisset

2014 - Ultrasound-Derived Shear Wave Speed Correlates with Liver Fibrosis in Children; Jonathan Dillman, M.D., Department of Radiology, Section of Pediatric Radiology, University of Michigan C.S. Mott Children's Hospital, Ann Arbor, MI, Ethan Smith, Amer Heider, Nahid Keshavarzi, Jacob Bilhartz, Jonathan Rubin

2015 - Contrast Enhanced Ultrasound in the Assessment of Pediatric Solid Tumor Response to Anti-Angiogenic Therapy; Beth McCarville, MD, Department of Radiological Sciences, Division of Diagnostic Imaging, St. Jude Children's Research Hospital, Memphis, TN, Jamie Coleman, MD, Junyu Guo, PhD, Yimei Li, PhD, Xingyu Li, PhD, Fariba Navid, MD

2016 - Intra-operative MRI guided, laparoscopic-assisted anorectoplasty in the treatment for imperforate anus; Damien Grattan-Smith, MBBS, Children's Healthcare of Atlanta, Atlanta, GA, George Raschbaum, John Bleacher, Joseph Williams, Edwin Smith, Stephen Little, Richard Jones

2017 - CXR Reduction Protocol in the Neonatal Intensive Care Unit (NICU) – Lessons Learned; Michelande Ridore, MS, Dorothy Bulas, MD, William Pastor, MS, MPH, Sarah McKenney, PhD, Lamia Soghier, MD, Billie Lou Short, MD, CNMC, Washington DC

JOHN P. CAFFEY AWARD FOR POSTERS

1994- Wilms Tumor: Unusual Manifestations. Navoy JF, Royal SA, Vaid YN, Mroczek EC.

1995- Evaluation of Suspected Air Trapping with Dynamic CT Densitometry. Johnson JL, Kramer SS, Mahboubi S.

1996- MR Imaging in the Diagnosis of Experimental Pyelonephritis in Piglets. Pennington, Lonergan GJ, Flack CE, Waguespack L, Jackson CB.

1997- Sensorineural Hearing Loss in Children. Lowe LH, Vezina GL.

1998- Primary Immunodeficiencies: An Immunology Primer for Radiologists. Manson DE, Sikka BS, Cohen S, Reid B, Roifman CM.

1999- Retinoblastoma: US Findings with Pathologic Correlation Kaste, SC, Jenkins, III, JJ, Pratt, CB; Langston, JW, Haik, BG

2001- Mitochondrial Disorders Of Oxidative Phosphorylation In Children: Patterns Of Disease Palasis S, Grattan-Smith JD, Shoffner JM, Neish AS, Stewart S.

2002- Volumetric Localization of Somatosensory Cortex in Children Using Synthetic Aperture Magnetrometry. Xiang J, MD, PhD, The Hospital for Sick Children, Toronto, ON, Canada Chuang S., MD; Holowka S; Babyn P, Otsubo H, Sharma R

2003- Assessing the Use of Magnetic Resonance Imaging in Determining the Age of Closure of Growth Plates. Rajwani T, Huang EM, Secretan C, Bhargava R, Lambert R, Bagnall K

2004- Outstanding Basic Science Research Poster - Imaging of the Diaphragm in Neonates and Young Infants, with Special Emphasis on Diaphragmatic Motion. Epelman M, Navarro O, Miller S Department of Diagnostic Imaging, Hospital for Sick Children, Toronto, ON, Canada

2004- Outstanding Clinical Research Poster - The Spectrum of Renal Cystic Disease in Children. Restrepo R, Ranson M, Sookman J, Jacobson E, Daneman A, Fontalvo L, Department of Radiology, Miami Children's Hospital, Miami, FL

2005- 3D MRI and CT in the Evaluation of Congenital Anomalies of the Aortic Arch. Dehkharghani S, Olson K, Richardson, R

2006- Diffusion Weighted Imaging in Pediatric Neuroradiology: A Primer. Pallavi Sagar, MD, Pediatric Radiology, Massachusetts General Hospital, Boston, MA; P Ellen Grant, MD

2006- Imaging of Suprarenal Fossa in Children: Radiological Approach and Clinico-Pathological Correlation. Kamlesh Kukreja, MD, Radiology, Miami Children's Hospital, Miami, FL; Ricardo Restrepo, MD; Maria D'almeida, MD

2007- Neuroimaging of Nonaccidental Trauma: Pitfalls and Controversies. Lisa H Lowe, MD, Radiology, Children's Mercy Hospitals and Clinics and The University of Missouri-Kansas City, Kansas City, MO; Ruby E Obaldo, MD; Kristin A Fickenscher, MD; Irene Walsh, MD

2008- Estimation of Cumulative Effective Doses from Diagnostic and Interventional Radiological Examinations in Pediatric Oncology Patients. KE Thomas, BA Ahmed, P Shroff, B Connolly, A Lee Chong, C Gordon, The Hospital for Sick Children – Toronto

2009- Case Report: Multi-Modality Imaging Manifestations of the Meckel's Diverticulum in Pediatric Patients. Manish K Kotecha, MD, Richard D Bellah, MD, Andres H Pena, MD, Peter Mattei, MD

2009- Educational: MR Urography: Functional Analysis – Made Simple! Dmitry Khrichenko, BSc, Kassa Darge, MD, PhD

2009- Scientific: MRI Findings in the Term Infant with Neonatal Seizures. An Etiologic Approach - Monica Rebollo Polo,Julie Hurteau-Miller, Eoghan Laffan, Hazar Tabban, Husein Naser, Khaldoun Koujok

2010- Scientific: Dual Phase Intravenous Contrast Injection in Pediatric Body CT Erika Mann, MD, Hospital for Sick Children,Toronto, ON, CA, Amin Alzahrani; Nancy Padfield; Liane Farrell; Guila BenDavid; Karen Thomas, MD

2010- Educational: Hemangiomas Revisited: The Useful, the Unusual and the New Ricardo Restrepo, MD, Miami Children's Hospital, Miami, FL, Rajaneeshankar Palani, MD; Umamahesh Matapathi, MD; Nolan Altman, MD; Luisa Cervantes, MD; Ana-Margarita Duarte, MD; Ibrahim Amjad, MD

2010- Case Report: MRI of Congenital Urethroperineal Fistula Maryam Ghadimi Mahani, MD, University of Michigan Health System, C.S. Mott Children's Hospital, Ann Arbor, MI, Jonathan R Dillman, MD; Deepa Pai, MD; John M Park, MD; Michael A Dipietro, MD; Maria F Ladino Torres, MD

2011- Scientific: Updated Estimated Radiation Dose for Pediatric Nuclear Medicine Studies, Frederick Grant, Children's Hospital, Boston, Laura Drubach, S. Ted Treves, Fred Fahey

2011- Educational: Button Battery Ingestion in Children: What the Radiologist Must Know, Mariam Kappil, Children's Memorial Hospital, Chicago, Cynthia Rigsby, Martha Saker, Emma Boylan

2011- Case Report: MR Imaging Features of Fetal Mediastinal and Intrapericardial Teratomas, Eva Rubio, Children's National Medical Center, Washington, DC, Beth Kline-Fath, Maria Calvo-Garcia, Carolina Guimaraes

2012- Case Report: Neuroimaging in Hemiplegic Migraine: Cases and Review of the Literature, Nicholas V. Stence, Children's Hospital Colorado, Sita Kedia, John A. Maloney, Jennifer Armstrong-Wells, Timothy Bernard

2012- Educational: Primary and Secondary Amenorrhea in Pediatric Patients: From the Beginning to the End, Cesar Cortes, Miami Children's Hospital, Yanerys Ramos, Ricardo Restrepo, Alejandro Diaz, Lorena Sequeira, Edward Lee

2012- Scientific: Prenatal Evaluation of Limb Body Wall Complex with Emphasis on MRI, Elisa Aguirre-Pascual, Hospital Universitario de Getafe, Teresa Victoria, Ann Johnson, Nancy Chauvin, Beverly Coleman, Monica Epelman

2013- Case Report: Percutaneous trans-splenic embolization of Roux limb varices in children with chronic portal vein occlusion (PVO) post orthotopic liver transplant (OLT) Sheena Pimpalwar,MD, Texas Children's Hospital- Interventional radiology, Houston, TX; Aparna Annam, Ponraj Chinnadurai, Alberto Hernandez

2013- Educational: MR imaging of coronary arteries in children: Case Based Teaching File, Roy Jacob, MD, Children's Medical center, Dallas, TX; Shannon Blalock, Jeanne Dillenbeck

2013- Scientific Exhibit: Phantom Iterative Reconstruction Technique (PIRT)-a quantitative ALARA method to test iterative reconstructions effect on image quality and dose in the pediatric population Anne McLellan, DO, Medical, Radiology, Phoenix Children's Hospital, Phoenix, AZ; James Owen, MS, Robyn Augustyn, BSRT (R)(CT), John Egelhoff, DO, John Curran, MD Jeffrey Miller, MD, Richard Southard, MD William Pavlicek, PhD, Richard Towbin, MD

2013- Scientific Exhibit: Morbidity associated with delayed treatment of cholelithiasis in pediatric patients with sickle cell disease Heather Imsande, MD, Boston Medical Center, Boston, MA

2014- Case Report: Contrast-enhanced Ultrasound of Pediatric Abdominal Visceral Trauma: Initial Data; Beatrice Dionigi, Carol Barnewolt, Jill Zalieckas, David Mooney, Harriet Paltiel, MD, Department of Surgery, Boston Children's Hospital, Boston, MA

2014- Educational Poster: The Pediatric Breast: What to do with Lumps and Bumps; Natalie Burns, University of Washington Medical Center, Seattle, WA, Habib Rahbar, Teresa Chapman

2014- Scientific Poster: Towards radiation dose reduction in MDCT with iterative reconstruction for the prenatal diagnosis of skeletal dysplasia: the minimum radiation dose required to evaluate the normal fetal bones?; Chihiro Tani, Hiroshima University Hospital, Hiroshima, Japan, Yoshinori Funama, Chikako Fujioka, Kazuo Awai

2015- Case Report: Congenital Portocaval Shunt: A Rare Entity, Arash Zandieh, MD, Georgetown University Hospital, Washington, DC, Christabel Lee, Frank Volberg

2015- Educational Poster: Pediatric Radiology Economics and Politics in Jeopardy: A Primer, David Swenson, MD, The Alpert Medical School of Brown University, Providence, RI, Cassandra Sams

2015- Scientific Poster: Infant Bone Age Estimation Based on Fibular Shaft Length: A Validation Study, Andy Tsai, MD, PhD, Boston Children's Hospital, Boston, MA, Catherine Stamoulis, Sarah Bixby, Michael Breen, Susan Connolly, Paul Kleinman

2016- Case Report: Imaging Appearances of Crayons; Aaron McAllister, MD, MS, Radiology, Cincinnati Children's Hospital, Cincinnati, OH, Neil Lall, MD, Radiology, Cincinnati Children's Hospital, Cincinnati, OH

2016- Educational Poster: Pediatric Thyroid Cancer: Common Sonographic Appearances and Pitfalls; Claudia Martinez-Rios, MD, Diagnostic Imaging, The Hospital for Sick Children, Toronto, ON, Canada, Lydia Bajno, Alan Daneman, Rahim Moineddin, Danielle CM van der Kaay, Jonathan Wasserman

2016- Scientific Poster: Ultrasound Diagnosis of Median Arcuate Ligament Syndrome (MALS): A Single Institutional Experience; Anjum Bandarkar, Children's National Health System, Washington, DC, Hansel Otero, MD

2017- Case Report: Cutaneous Metastases of Infantile Choriocarcinoma can Mimic Infantile Hemangioma both Clinically and Radiographically; Logan Dance, MD; Patricia Cornejo, MD; Mittun Patel, MD, Phoenix Children's Hospital, Phoenix, AZ

2017- Educational Poster: Sonographic Evaluation of Diaphragmatic Motion: A Practical Guide to Performance and Interpretation; Benjamin D. Smith, MD, Hansel Otero, MD, Tara Cielma, Anjum Bandarkar, MD, Children’s National Medical Center, Washington, DC

2017- Educational Poster: Nuts and Bolts: A Radiologist’s Guide to Orthopedic Hardware Utilized in the Lower Extremities of Children; Hailey Allen, MD, Radiology University of Wisconsin, Madison, WI, Kirkland Davis, MD, Kenneth Noonan, MD, Jie Nguyen, MD

2017- Scientific Poster: Sinusoidal Obstruction Syndrome Causes Increased Liver Stiffness; Naresh Reddivalla, MD, Erin Opfer, DO, Amie Robinson, BSRT(R)(MR) CCRP, Kimberly J Reid, MS, Mohamed Radhi, MD, & Sherwin Chan, MD, PhD, The Children’s Mercy Hospital, Kansas City, MO

The top candidates being considered for a Caffey Poster Award from the Scientific and Educational categories will present their work during one of the scheduled breaks in the exhibit hall.

2018 EDWARD B. D. NEUHAUSER LECTURE

Curious Bones: Sustaining Discovery in the Face of Doubt

Paul K. Kleinman, MD, FAAP

Dr. Paul Kleinman is an extraordinary radiologist, researcher and teacher. His thorough and meticulous study of the imaging of child abuse has shaped the understanding of not only generations of radiologists but also of pediatricians, other health care providers, lawyers and law enforcement officials who deal with this terrible problem on a daily basis.

Paul Kleinman grew up in upstate New York. He earned his medical degree from SUNY Downstate and completed residencies in both pediatrics and radiology at Cornell's New York Hospital. Paul spent 23 years as the Director of Pediatric Radiology at the University of Massachusetts Medical School. In 2002, Paul joined Boston Children's Hospital as Chief of Musculoskeletal Imaging, a position that he held until his retirement from clinical practice in 2017. He remains a member of the Associate Scientific Research Staff at Boston Children's Hospital and is Professor Emeritus of Radiology at Harvard Medical School.

Paul's research interest in child abuse developed at UMass after he was asked to consult on cases of infant death. The collaboration with forensic pathologist Brian Blackbourne, the Chief Medical Examiner for the Commonwealth of Massachusetts, and Sandy Marks, a UMass Professor of Anatomy, led to a multidisciplinary study of the various fractures seen in infant fatalities. The radiologic and pathologic description of the classic metaphyseal lesion (CML) earned Paul the Society for Pediatric Radiology's Caffey Award in 1985.

Paul's research led to the classification of fractures by their specificity for abuse. His work helped establish the American Academy of Pediatrics and SPR-ACR guidelines for imaging children suspected of abuse. Even today, with years of experience and an almost intuitive sense for diagnosing cases of child maltreatment, Paul remains careful to rule out every reasonable differential consideration. His consistent example of "rigorous methodology" and rational approach to clinical evaluation teaches exactitude and specificity. Over his career, Paul has authored more than 175 original papers, manuscripts and chapters. Beyond his seminal contribution to the imaging of child abuse, he has provided valuable insights into many other areas of musculoskeletal imaging. He still considers himself a pediatric generalist at heart.

Paul's book Diagnostic Imaging of Child Abuse, now in its 3rd edition, has left an indelible mark on its field and has defined our current understanding of the imaging findings of child abuse. It is the bible for radiologists and pediatricians caring for suspected victims of child maltreatment.

Among his weighty professional achievements, perhaps Paul's greatest legacy is his role as mentor, motivating and inspiring many colleagues and trainees. Radiology trainees at Boston Children's Hospital have honored him with the John A. Kirkpatrick Teacher of the Year Award in 2006 and 2007, and the Robert L. Lebowitz Mentoring Award in 2007 and 2009. He received the Jack O. Haller Award for Excellence in Teaching from the Society for Pediatric Radiology in 2011, the SPR Presidential Recognition Award in 2000 and the Gold Medal from the Society for Pediatric Radiology in 2017 for his lifetime contributions. In 2018, an Endowed Chair of Musculoskeletal Radiology was created in his name at Boston Children's Hospital.

Jeannette M. Pérez-Rosselló, MD
Diego Jaramillo, MD, MPH

2018 SOCIAL EVENTS

SPR RESEARCH AND EDUCATION FOUNDATION FUN RUN

Underwritten by Texas Children's Hospital
Wednesday, May 16, 2018
6:00 a.m.
Join us for a three-mile run through Downtown Nashville and get your day off to a great start! Runners and walkers are all welcome. Entrance fee is $25 and includes a Tshirt. Runners/ walkers should meet in the Hotel lobby at 5:45 a.m.

WELCOME RECEPTION

Wednesday, May 16, 2018
7:00-8:15 p.m.
Omni Nashville Hotel
Hors d'oeuvres and Refreshments
Business Casual Attire

RECEPTION AND ANNUAL BANQUET

Friday, May 18, 2018
7:00-10:30 p.m.
Omni Nashville Hotel
Reception, Dinner and Dancing
Business Casual Attire

ACTIVITIES

The Omni Nashville Hotel employs concierge staff who are happy to share their detailed knowledge of Nashville, Tennessee and the surrounding area. You may contact them by telephone at (615) 782-5300.

Additional information is included on the SPR website.

2018 61st SPR Annual Meeting & Postgraduate Course

"Value-added Pediatric Radiology"

TUESDAY – MAY 15, 2018

7:00 AM	**8:00 AM**	**Continental Breakfast**
7:00 AM	**5:30 PM**	**Registration**
8:00 AM	**5:00 PM**	**SPR Online Cases of the Day Activity**
8:00 AM	**8:20 AM**	**General Postgraduate Course Welcome**
8:00 AM	**8:20 AM**	**Body Imaging Postgraduate Course Welcome**
8:20 AM	**10:00 AM**	**General Postgraduate Course: Neuroradiology (SAM Session)** *Janet R. Reid, MD, FRCPC, Moderator*
	8:20-8:45 a.m.	**Newborn Hypoxic Ischemic Injury** Hisham M. Dahmoush, MBBCh, FRCR Alexis B. R. Maddocks, MD
	8:45-9:05 a.m.	**Imaging of Sinusitis/Mastoiditis and Complications** Jill V. Hunter, MBBS Sumit Pruthi, MD
	9:05-9:35 a.m.	**Imaging of Spinal Trauma** Karuna V. Shekdar, MD Judith Gadde, DO
	9:35-10:00 a.m.	**TORCH and Zika CNS Infections** Dorothy I. Bulas, MD, FACR, FAAP Jason N. Wright, MD
8:20 AM	**10:00 AM**	**Body Imaging Postgraduate Course: Liver Imaging (SAM Session)** *Jonathan R. Dillman, MD, MSc, Moderator*
	8:20-8:45 a.m.	**Liver Masses – PRETEXT Staging** Alexander J. Towbin, MD Judy H. Squires, MD
	8:45-9:05 a.m.	**Budd-Chiari/Veno-Occlusive Disease** M. Beth McCarville, MD Martha M. Munden, MD
	9:05-9:35 a.m.	**Iron and Fat Deposition** Shreyas S. Vasanawala, MD, PhD Robert C. Orth, MD, PhD
	9:35-10:00 a.m.	**Transplant Complications – US/Doppler (Early and Late)** Rama S. Ayyala, MD Michael R. Acord, MD
10:00 AM	**10:20 AM**	**Break**

COLOR KEY

Scientific Session
General Postgraduate Course
Body Imaging Postgraduate Course
General Session
Sunrise/Midday Session
Technologist Program

TUESDAY – MAY 15, 2018 *(Continued)*

10:20 AM – 12:00 PM **General Postgraduate Course: Musculoskeletal (SAM Session)**
Jonathan R. Dillman, MD, MSc, Moderator

10:20-10:45 a.m. **Adolescent Hip Imaging**
Sarah D. Bixby, MD
Nancy A. Chauvin, MD

10:45-11:10 a.m. **Imaging of Knee Cartilage**
Matthew R. Hammer, MD
Jerry R. Dwek, MD

11:10-11:35 a.m. **Ultrasound of Painful Joints**
Andrew M. Zbojniewicz, MD
Mahesh M. Thapa, MD

11:35-12:00 p.m. **Throwing Adolescent Athlete**
Arthur B. Meyers, MD
Victor M. Ho-Fung, MD

10:20 AM – 12:00 PM **Body Imaging Postgraduate Course: Pancreatobiliary (SAM Session)**
Janet R. Reid, MD, FRCPC, Moderator

10:20-10:45 a.m. **Neonatal Cholestasis**
Sara M. O'Hara MD
Janet R. Reid, MD, FRCPC

10:45-11:10 a.m. **Acute Recurrent and Chronic Pancreatitis**
Sudha A. Anupindi, MD
Andrew T. Trout, MD

11:10-11:35 a.m. **Pancreatic Trauma**
Michael Aquino, MD
Michael J. Callahan, MD

11:35-12:00 p.m. **Evaluation of Pediatric CBD Dilation**
Sudha A. Anupindi, MD
Ruth Lim, MD

12:00 PM – 1:30 PM **Lunch On Your Own**

12:00 PM – 1:30 PM **jSPR Luncheon** *(pre-registration required)*

1:30 PM – 3:10 PM **General Postgraduate Course: Fetal (SAM Session)**
Janet R. Reid, MD, FRCPC, Moderator

1:30-1:55 p.m. **Myelomeningocele Imaging**
Deborah Zarnow, MD
Davis M. Mirsky, MD

1:55-2:20 p.m. **Fetal Neck Masses**
Beth M. Kline-Fath, MD
Christopher I. Cassady, MD, FAAP

2:20-2:45 p.m. **Congenital Diaphragmatic Hernia Update**
Teresa Victoria, MD, PhD
Erika Rubesova, MD

2:45-3:10 p.m. **Placental Imaging**
Brandon P. Brown, MD
Maria F. Ladino-Torres, MD

COLOR KEY

Scientific Session
General Postgraduate Course
Body Imaging Postgraduate Course
General Session
Sunrise/Midday Session
Technologist Program

TUESDAY – MAY 15, 2018 *(Continued)*

1:30 PM	**3:10 PM**	**Body Imaging Postgraduate Course: Vascular (SAM Session)** *Jonathan R. Dillman, MD, MSc, Moderator*
	1:30-1:55 p.m.	**Vasculitis, including Vessel Wall Imaging** Geetika Khanna, MD, MS Eric J. Crotty, MD
	1:55-2:20 p.m.	**Imaging of Vasculopathy/Aortopathy** Prakash M. Masand, MD Eric J. Crotty, MD
	2:20-2:45 p.m.	**Venography in the Post-Ablavar Era** Cynthia K. Rigsby, MD, FACR Arnold Carl Merrow, MD
	2:45-3:10 p.m.	**Lymphatic MR Imaging** David M. Biko, MD Rajesh Krishnamurthy, MD
3:10 PM	**3:30 PM**	**Break**
3:30 PM	**5:10 PM**	**General Postgraduate Course: Patient Safety & Technique (SAM Session)** *Jonathan R. Dillman, MD, MSc, Moderator*
	3:30-3:45 p.m.	**Post-Contrast Acute Kidney Disorder** Matthew S. Davenport, MD
	3:45-4:00 p.m.	**Gadolinium Update** Daniel J. Podberesky, MD
	4:00-4:15 p.m.	**Sedation/Anesthesia Update** Joshua Nickerson, MD
	4:15-4:30 p.m.	**What kVp Should I Use?** Samuel L. Brady, MS, PhD
	4:30-4:45 p.m.	**Contrast Reaction Management** Jonathan R. Dillman, MD, MSc
	4:45-5:00 p.m.	**MRI Device Safety Update** Suraj D. Serai, PhD
	5:00-5:10 p.m.	**Q&A**
3:30 PM	**5:10 PM**	**Body Imaging Postgraduate Course: Gastrointestinal Radiology (SAM Session)** *Janet R. Reid, MD, FRCPC, Moderator*
	3:30-3:55 p.m.	**Perineal/Perianal Crohn's Disease** Govind B. Chavhan, MD Ethan A. Smith, MD
	3:55-4:20 p.m.	**Crohn's Disease Standardized Nomenclature/Reporting** Kassa Darge, MD, PhD Michael S. Gee, MD, PhD
	4:20-4:45 p.m.	**Median Arcuate Ligament Syndrome** James S. Donaldson, MD, FACR Seng H. Ong, MBBS
	4:45-5:10 p.m.	**Small Bowel Tumors** Jesse Courtier, MD Ellen M. Chung, MD
5:10 PM		**Adjourn**

COLOR KEY

Scientific Session
General Postgraduate Course
Body Imaging Postgraduate Course
General Session
Sunrise/Midday Session
Technologist Program

WEDNESDAY – MAY 16, 2018

6:00 AM		**SPR REF Fun Run**
7:00 AM	**8:00 AM**	**Continental Breakfast & Exhibits**
7:00 AM	**5:45 PM**	**Registration**
8:00 AM	**5:00 PM**	**SPR Online Cases of the Day Activity**
8:00 AM	**9:40 AM**	**General Postgraduate Course: Radiation Dose Monitoring – Watching Ourselves as We Watch Our Kids Part I** *Donald P. Frush, MD, FACR, Moderator*
	8:00-8:15 a.m.	**Into Oz: Follow the Yellow Brick Rad** Donald P. Frush, MD, FACR
	8:15-8:55 a.m.	**ABCs of Dose Metrics for Dose Monitoring** Samuel L. Brady, MD, PhD Keith J. Strauss, MSc, FACR
	8:55-9:25 a.m.	**A Walk Through the Market** Sarah McKenney, PhD, DABR
	9:25-9:40 a.m.	**Dose Metrics in the Patient Report: Myopic or Foresighted?** Beverley Newman, MD, FACR
8:00 AM	**9:40 AM**	**Body Imaging Postgraduate Course: Chest (SAM Session)** *Jonathan R. Dillman, MD, MSc, Moderator*
	8:00-8:25 a.m.	**Congenital Lung Lesions** Andrew Schapiro, MD Maryam Ghadimi Mahani, MD
	8:25-8:50 a.m.	**Dynamic Airway Imaging (Non-Sleep Apnea)** Edward Y. Lee, MD, MPH Robert J. Fleck, MD
	8:50-9:15 a.m.	**Ultrasound of the Lung and Pleura** Harriet J. Paltiel, MD Monica Epelman, MD
	9:15-9:40 a.m.	**Childhood Interstitial Lung Disease** R. Paul Guillerman, MD David A. Mong, MD
9:40 AM	**10:10 AM**	**Break & Exhibits**
10:10 AM	**11:50 AM**	**General Postgraduate Course: Radiation Dose Monitoring – Watching Ourselves as We Watch Our Kids Part II** *Donald P. Frush, MD, FACR, Moderator*
	10:10-10:50 a.m.	**Navigating Dose Monitoring: Panel Discussion** **Panelists:** Donald P. Frush, MD, FACR R. Paul Guillermann, MD Ehsan Samei, PhD, DABR, FAAPM, FSPIE Keith J. Strauss, MSc, FACR Beverley Newman, MD, FACR Samuel L. Brady, MS, PhD Sarah McKenney, PhD, DABR
	10:50-11:20 a.m.	**Into the Mist? Future Opportunities and Challenges** Paul Guillerman, MD Ehsan Samei, PhD, DABR, FAAPM, FSPIE
	11:20-11:50 a.m.	**Concluding Statements and Audience Q&A**

COLOR KEY

Scientific Session
General Postgraduate Course
Body Imaging Postgraduate Course
General Session
Sunrise/Midday Session
Technologist Program

WEDNESDAY – MAY 16, 2018 *(Continued)*

10:10 AM – 11:50 AM **Body Imaging Postgraduate Course: Neonatal (SAM Session)**
Jonathan R. Dillman, MD, MSc and Janet R. Reid, MD, FRCP, Moderators

10:10-10:35 a.m. **High Intestinal Obstruction**
Boaz Karmazyn, MD
David A. Bloom, MD, FACR

10:35-11:00 a.m. **Newborn Low Intestinal Obstruction**
Laura Z. Fenton, MD
R. Pinar Karakas, MD

11:00-11:25 a.m. **Newborn Lines and Tubes – Normal and Abnormal**
Pallavi Sagar, MD
David Saul, MD

11:25-11:50 a.m. **Anorectal Malformations**
Steven J. Kraus, MD, MS, FAAP
D. Gregory Bates, MD

11:50 AM – 1:20 PM **Lunch on Your Own**

11:50 AM – 1:20 PM **3D Read with the Experts** *(Non-CME Session)*
Dianna M. E. Bardo, MD, FSCCT, FNASCI and Mark R. Ferguson, MD, Moderators
Speaker: Sherwin S. Chan, MD
Experts: Eric Hoggard, MD, Luis Goncalves, MD and Prakash M. Masand, MD

11:50 AM – 1:20 PM **MR Protocol Session** *(Non-CME Session)*
Shreyas S. Vasanawala, MD, PhD, Michael S. Gee, MD, PhD and Taylor Chung, MD, Moderators
Topic 1: Update on last year's topics
Topic 2: Coils – Scanner vendor options, 3rd party options and beyond
Topic 3: Acoustic Noise – Options and Tradeoffs

ANNUAL MEETING

1:20 PM – 1:30 PM **Annual Meeting Welcome & Dedication**
Peter J. Strouse, MD, FACR

1:30 PM – 2:00 PM **The Power of Diversity: Meeting Today's (and Tomorrow's) Greatest Healthcare Challenges**
Stephanie E. Spottswood, MD, MSPH

2:05 PM – 3:05 PM **Edward B. Neuhauser Lecture**
Curious Bones: Sustaining Discovery in the Face of Doubt
Paul K. Kleinman, MD, FAAP

3:15 PM – 4:15 PM **Pediatric Radiology Jeopardy**
George S. Bisset, III, MD, FACR, Host

Team E:
Josée Dubois, MD
Tal Laor, MD
Cynthia K. Rigsby, MD, FACR
Nancy K. Rollins, MD

Team T:
Ashok Panigrahy, MD
Daniel J. Podberesky, MD
Stephen F. Simoneaux, MD
Andrew T. Trout, MD

4:15 PM – 4:45 PM **Break & Exhibits**

WEDNESDAY – MAY 16, 2018 *(Continued)*

4:45 PM 5:45 PM **Scientific Session I-A: Gastrointestinal Radiology**
Jonathan R. Dillman, MD, MSc and Mary-Louise Greer, MBBS, Moderators

P001	4:45	4:55	Rees, Mitchell	Inter-radiologist Agreement Using Society of Abdominal Radiology-Society for Pediatric Radiology-American Gastroenterological Association Consensus Nomenclature for Reporting CT and MR Enterography in Pediatric Small Bowel Crohn Disease
P002	4:55	5:05	Karpewycz, John	Accuracy of Magnetic Resonance Enterography in the Assessment of Pediatric Inflammatory Bowel Disease of the Colon in Patients Undergoing Colectomy
P003	5:05	5:15	Gottumukkala, Ravi	Comparison of Three Oral Contrast Preparations for Magnetic Resonance Enterography in Pediatric Crohn's Disease Patients: A Randomized Trial
P004	5:15	5:25	Dillman, Jonathan	Breeza vs. VoLumen for Pediatric CT and MR Enterography: a Prospective, Randomized, Blinded Patient Acceptability Study
P005	5:25	5:35	Choi, Jungwhan	Use of Small Bowel Ultrasound to Predict Response to Infliximab Induction
P006	5:35	5:45	Gokli, Ami	Contrast Enhanced Ultrasound of the Bowel in Children with Suspected Inflammatory Bowel Disease (IBD).

4:45 PM 5:45 PM **Scientific Session I-B: Musculoskeletal Imaging**
Lauren W. Averill, MD and Sarah D. Bixby, MD, Moderators

P007	4:45	4:55	Panwar, Jyoti	Inter-reader Reliability Study of a New MRI Scoring System for TMJ Evaluation in JIA with the Use of Measurement Aids: Special Interest Group from the MRI in JIA in OMERACT
P008	4:55	5:05	Ditzler, Matthew	Modified Friedman Technique: A New Proposed Method of Measuring Glenoid Version in the Setting of Glenohumeral Dysplasia
P009	5:05	5:15	Milks, Kathryn	Advancements in Pediatric Wrist and Thumb Imaging: Sonography in Normal Infants
P010	5:15	5:25	Nicholas, Jennifer	Lulun II: Ultrasound Evaluation of Bone Age in Rural Ecuadorian Children
P011	5:25	5:35	Sánchez, Mariana	Digital X-ray Metacarpal Radiogrammetry and Dual X-ray Absorptiometry in Mexican Children and Adolescents.
P012	5:35	5:45	Amarneh, Mohammad	Fibro-Adipose Vascular Anomaly (FAVA): A review of imaging features.

4:45 PM 5:45 PM **Scientific Session I-C: Interventional Radiology**
John M. Racadio, MD and Leah E. Braswell, MD

P013	4:45	4:55	Robinson, Amie	The Utility of Percutaneous Image Guided Tumor Ablation in the Treatment of Solid and Vascular Tumors in the Pediatric Population
P014	4:55	5:05	Roebuck, Derek	Cryoablation of benign soft tissue lesions in children: initial experience
P015	5:05	5:15	Srinivasan, Abhay	A combined retrospective and prospective single-institution review of image-guided needle biopsy of relapsed or refractory neuroblastoma with a focus on the use of pre-biopsy MIBG imaging to predict tumor characteristics
P016	5:15	5:25	Srinivasan, Abhay	Comparison of MR guided joint injection with a fluoroscopic approach for pediatric MR arthrography
P017	5:25	5:35	Acord, Michael	Surveillance Cerebral Angiography in Children with Arteriovenous Malformations: How many vessels should be interrogated?
P018	5:35	5:45	Bhavane, Rohan	A novel approach to deep tissue intra-operative imaging using indocyanine green fluorescence

5:45 PM **Adjourn**

5:50 PM 7:00 PM **Awards Ceremony**

7:00 PM 8:15 PM **Welcome Reception**

THURSDAY, MAY 17, 2018

6:30 AM	**8:30 AM**	**Continental Breakfast & Exhibits**
6:30 AM	**5:30 PM**	**Registration**
7:00 AM	**5:30 PM**	**SPR Online Case of the Day Activity**
7:00 AM	**8:20 AM**	**Sunrise Workshop – Evidence for Child Abuse Fractures** *Jeannette M. Perez-Rossello, MD, Moderator*
	7:00-7:20 a.m.	**Evidence Base for Fractures in Child Abuse** Megan B. Marine, MD
	7:20-7:40 a.m.	**Differential Diagnosis for Findings on Skeletal Survey vs. Child Abuse** Jeannie K. Kwon, MD
	7:40-7:50 a.m.	**Entities Provided in Defense Cases (Rickets & Ehlers Danlos)** Daniel M. Schwartz, MD
	7:50-8:20 a.m.	**Using the Literature to Assess What is Child Abuse or Not** Jeannette M. Perez-Rossello, MD
7:00 AM	**8:20 AM**	**Sunrise Workshop – Cardiac CT** *Prakash M. Masand, MD and Lorna P. Browne, MBBS, Moderators*
	7:00-7:02 a.m.	**Introduction & Overview**
	7:02-7:15 a.m.	**Cardiac CT Techniques in Neonates** Siddarth P. Jadhav, MD
	7:15-7:28 a.m.	**Common Indications for Cardiac CT in Neonates and Infants** Ladonna J. Malone, MD
	7:28-7:41 a.m.	**Coronary CT in Neonates and Infants: How I Do It?** Prakash M. Masand, MD
	7:41-7:54 a.m.	**Interpreting Heterotaxy in Neonates and Infants** Andrada R. Popescu, MD
	7:54-8:07 a.m.	**Vascular Rings and Slings in Infants** Mark R. Ferguson, MD
	8:07-8:20 a.m.	**Craziest Cases** Lorna P. Browne, MBBS
7:00 AM	**8:20 AM**	**Sunrise Workshop – Evolving Practice Models: Future/Present** *Richard E. Heller, III, MD, MBA, Moderator*
	7:00-7:20 a.m.	**Changing Reimbursement Systems in (Pediatric) Radiology: Value-Based Payment Reform** Richard E. Heller, III, MD, MBA
	7:20-7:40 a.m.	**Health Care Now…Results of the 2017 Annual Trust Survey** Brandon Edwards, CEO, ReviveHealth
	7:40-8:00 a.m.	**The Children's Hospital as Part of a Large Private Practice** Peter G. Kruk, MD
	8:00-8:20 a.m.	**The Pediatric Radiologist in the General Private Practice** Kimberly A. Garver, MD

COLOR KEY

Scientific Session
General Postgraduate Course
Body Imaging Postgraduate Course
General Session
Sunrise/Midday Session
Technologist Program

THURSDAY, MAY 17, 2018 *(continued)*

7:00 AM – 8:20 AM **Sunrise Workshop – MR Techniques for Imaging Children**
Michael S. Gee, MD, PhD and Jesse Courtier, MD, Moderators

7:00-7:15 a.m. **Non-scanner Related Techniques for MR Imaging of Awake Children**
Michael S. Gee, MD, PhD

7:15-7:30 a.m. **Essential Neuroradiology Sequences for Evaluating Children**
Mai-Lan Ho, MD

7:30-7:45 a.m. **Essential Body Sequences for Evaluation of Children**
Jesse Courtier, MD

7:45-8:00 a.m. **Considerations for Pediatric MSK Imaging**
Delma Y. Jarrett, MD

8:00-8:10 a.m. **Cardiac and Vascular MR Imaging: Tips and Tricks**
Sherwin S. Chan, MD

8:10-8:20 a.m. **MR Protocols in the Pediatric ER**
Unmi K. Udayasankar, MD

7:00 AM – 8:20 AM **Sunrise Workshop – Update on Contrast Media:**
New Agents, New Concerns and Strategies for Safe Use
R. Paul Guillerman, MD, Moderator

7:00-7:20 a.m. **Strategies for Optimizing Enteric Contrast for Fluoroscopy, CT and MRI**
Michael J. Callahan, MD

7:20-7:40 a.m. **Approach to Imaging Patients with Renal Impairment or Heighted Risk of Adverse Contrast Reaction**
Matthew S. Davenport, MD

7:40-8:00 a.m. **Safety Considerations for Ultrasound Contrast Agents**
Kassa Darge, MD, PhD

8:00-8:20 a.m. **Gadolinium-Based Contrast Agents: Time to Image Gently?**
R. Paul Guillerman, MD

7:00 AM – 8:20 AM **Sunrise Workshop – Pediatric Nuclear Medicine: Learn to Read Like an Expert**
Marguerite T. Parisi, MD, MS, Moderator

7:00-7:15 a.m. **CNS Imaging in Nuclear Medicine**
Adina L. Alazraki, MD, FAAP

7:15-7:30 a.m. **Australian Perspectives on Nuclear Renography**
Monica A. Rossleigh, MD

7:30-7:45 a.m. **Musculoskeletal Scintigraphy**
Susan E. Sharp, MD

7:45-8:00 a.m. **Gastrointestinal Scintigraphy**
Helen R. Nadel, MD, FRCPC

8:00-8:20 a.m. **Challenging Cases in NM Oncologic Imaging**
Marguerite T. Parisi, MD, MS

COLOR KEY

Scientific Session
General Postgraduate Course
Body Imaging Postgraduate Course
General Session
Sunrise/Midday Session
Technologist Program

THURSDAY, MAY 17, 2018 *(continued)*

8:30 AM 10:10 AM **Scientific Session II-A: Neuroradiology**

Maura E. Ryan, MD and Ashok Panigrahy, MD, Moderators

8:30-8:50 a.m. **Keynote Presentation Challenges in Pediatric Obstructive Sleep Apnea**

Amy Whigham, MD

P019	8:50	9:00	Altinok, Deniz	Analysis of diffusion restriction in the corpus callosum in children with abusive head trauma
P020	9:00	9:10	Mata-Mbemba, Daddy	Pediatric pituitary adenoma: imaging features and clinical outcome.
P021	9:10	9:20	Sabin, Noah	Potential Imaging and Neurosurgical Correlates of Molecular Subgroups of Posterior Fossa Ependymoma in Children
P022	9:20	9:30	Harreld, Julie	Analyzing Misdiagnosed Metastasis on Imaging Studies
P023	9:30	9:40	Alves Rosa, Joao	Normal head and neck lymph nodes in the healthy paediatric population
P024	9:40	9:50	Eid, Hadeel	Magnetic resonance (MR) assessment of optic nerve thickness and tortuosity for recognition of optic glioma in children with NF1
P025	9:50	10:00	Hsu, Ariel	The Unwound Cochlea: a Specific Marker of Branchio-oto-renal Syndrome
P026	10:00	10:10	Whitehead, Matthew	Pseudo-color Perceptual Enhancement for Detection of Cochlear Signal Alterations in Pediatric Patients with Sensorineural Hearing Loss

8:30 AM 10:10 AM **Scientific Session II-B: Musculoskeletal Imaging**

Jeannette M. Perez-Rossello, MD and Aparna Joshi, MD, Moderators

8:30-8:50 a.m. **Keynote Presentation**

Deborah Lowen, MD

P027	8:50	9:00	Pomeranz, Christy	Accuracy of Skeletal Survey in Evaluation of Rib Fractures Compared to CT in the Setting of Accidental and Non Accidental Trauma.
P028	9:00	9:10	Tsai, Andy	How Often is Subperiosteal New Bone Formation Noted with the Distal Tibial Classic Metaphyseal Lesion?
P029	9:10	9:20	Kriss, Spencer	Radiographic characteristics that delineate abusive from accidental skull fractures, including the significance of fracture extension to sutures.
P030	9:20	9:30	Starosolski, Zbigniew	Gaussian noise simulating reduced X-ray dose does not affect sensitivity of a Neural Network trained to detect tibial fractures in X-ray images
P031	9:30	9:40	Starosolski, Zbigniew	Toddler tibial fractures computer-aided diagnosis by convolutional neural network and transfer learning
P032	9:40	9:50	Alsharief, Alaa	Can combined diffusion-weighted imaging/conventional MRI replace post gadolinium-based contrast-enhanced MRI in the assessment of pediatric osseous sarcomas?
P033	9:50	10:00	Ecklund, Kirsten	Bone Marrow MR and MRS Evidence of Adrenal and Gonadal Hormone Replacement Therapy Efficacy in girls with Anorexia Nervosa
P034	10:00	10:10	Eutsler, Eric	Metal artifact reduction in pediatric dual energy CT using monoenergetic extrapolation

8:30 AM 10:10 AM **Scientific Session II-C: Thoracic Imaging**

David M. Biko, MD and Beverly Newman, MD, Moderators

8:30-8:50 a.m. **Keynote Presentation**

Lisa Young, MD

P035	8:50	9:00	Ma, Grace	Comparison of Prenatal Ultrasound, Prenatal MRI, and Postnatal CTA for Evaluation of Congenital Lung Malformations: Can Postnatal CTA Provide Additional Information?
P036	9:00	9:10	Biko, David	Magnetic Resonance Imaging of Central Lymphatics in Noonan's Syndrome
P037	9:10	9:20	Handly, Brian	Initial Clinical Evaluation of Stationary Digital Chest Tomosynthesis in Patients with Cystic Fibrosis
P038	9:20	9:30	Fenlon, Edward	Trending Use and Results of Computed Tomographic Angiography for Diagnosing Pulmonary Embolism in the Pediatric Emergency Department: A 13-Year Retrospective Study.
P039	9:30	9:40	Krishnamurthy, Rajesh	Target mode prospective EKG gated volumetric CT reduces the need for sedation for chest CT in young children

P040	9:40	9:50	Averill, Lauren	Tracheal Narrowing in Children and Young Adults with Mucopolysaccharidosis IVA: Evaluation with CT Angiography
P041	9:50	10:00	May, Lauren	A Novel Approach Using Volumetric Dynamic Airway CT to Determine Optimal Positive End Expiratory Pressure (PEEP) Settings in Neonates Requiring Long-Term Ventilator Support
P042	10:00	10:10	Rozovsky, Katya	Imaging patterns in pediatric pulmonary blastomycosis

8:30 AM 10:10 AM **Technologist Opening Session**

Laura Gruber, MBA, RT(R), RDMS, RVT, Moderator

8:30-9:00 a.m. **Ice Breaker**
Laura Gruber, MBA, RT(R), RDMS, RVT

9:00-9:30 a.m. **Recruiting Talent – Career Models**
Merima Karastanovic, MS, RT(R)(MR)

9:30-10:10 a.m. **Generational Differences in the Workplace**
Melissa Goehner, BA RT(R)(CT)

10:10 AM 10:40 AM **Break & Exhibits**

10:40 AM 12:00 PM **Midday Workshop – Evidence Base for Abusive Head Trauma**

Arabinda K. Choudhary, MBBS, FACHE, MBA, Moderator

10:40-11:00 a.m. **Evidence Base for Abusive Head Trauma**
Laura L. Hayes, MD

11:00-11:20 a.m. **Evidence Base for Spine Trauma**
Arabinda K. Choudhary, MBBS, FACHE, MBA

11:20-11:40 a.m. **Abusive Head Trauma: Diagnostic Challenges**
Gary L. Hedlund, DO

11:40-12:00 p.m. **Addressing Issues**
Dawn E. Saunders, MD

10:40 AM 12:00 PM **Midday Workshop – IR Lite – Unleaded and Photon Free!**

Eric J. Monroe, MD, Moderator

10:40-11:00 a.m. **Mobile Strike: Lean Lessons Learned from a Sprawling Service**
Eric J. Monroe, MD

11:00-11:15 a.m. **Ultrasound-guided Tunneled Line Placement**
C. Matthew Hawkins, MD

11:15-11:30 a.m. **Ultrasound-guided Lumbar Punctures**
Ann Gill, MD

11:30-11:45 a.m. **Ultrasound-guided Drainage Procedures**
Sheryl A. Tulin-Silver, MD

11:45-12:00 p.m. **Ultrasound-guided MSK Procedures: Beyond the Big Joints**
Jeffrey P. Otjen, MD

10:40 AM 12:00 PM **Midday Workshop – Novel Use of Musculoskeletal Ultrasound**

Monica Epelman, MD and Mahesh M. Thapa, MD, Moderators

Introductions and Overview
Monica Epelman, MD

10:40-10:50 a.m. **Role of Ultrasound in the Evaluation of Musculoskeletal Neoplasms**
Diego Jaramillo, MD, MPH

10:50-11:00 a.m. **Ultrasound Evaluation of Magnetic Growing Roots**
Arthur B. Meyers, MD

11:00-11:10 a.m. **Ultrasound of the Joints in Pediatric Sport Injuries**
Nancy A. Chauvin, MD

11:10-11:20 a.m. **Ultrasound Imaging of Vascular Anomalies: Pearls an Pitfalls**
Oscar M. Navarro, MD

11:20-11:30 a.m. **Ultrasound Imaging of Brachial Plexus Injuries**
Ramesh S. Iyer, MD

	11:30-11:40 a.m.	**Stress Sonography of the Ulnar Collateral Ligament in Baseball Pitchers** Lauren W. Averill, MD
	11:40-11:50 a.m.	**Ultrasound Imaging of Carpal Tunnel Syndrome** Mahesh M. Thapa, MD
	11:50-12:00 p.m.	**Panel/Audience Discussion - Question & Answers**
10:40 AM	**12:00 PM**	**Midday Workshop – Thoracic Imaging** *Robert J. Fleck, MD, Moderator*
	10:40-10:55 a.m.	**Diffuse Lung Disease in the Infant** Jason P. Weinman, MD
	10:55-11:10 a.m.	**Strategies for Optimizing Thoracic CT and MRI in Children** Sarah Desoky, MD
	11:10-11:25 a.m.	**Noninfectious Complications of Stem Cell Transplant** Matthew Cooper, MD
	11:25-11:45 a.m.	**Innovated Imaging of the Pediatric Airway** Robert J. Fleck, MD
	11:45-12:00 p.m.	**Interesting/Challenge Cases in Chest Imaging** Maryam Ghadimi Mahani, MD
10:40 AM	**12:00 PM**	**Midday Workshop – Professionalism** *Brandon P. Brown, MD, MA, Moderator*
	10:40-11:00 a.m.	**The Value of Mentorship in Professionalism** Richard B. Gunderman MD, PhD
	11:00-11:20 a.m.	**Communication and the Pediatric Radiologist** Sarah S. Milla, MD, FAAP
	11:20-11:40 a.m.	**Imaging 3.0: Building a Culture of Professionalism** Brandon P. Brown, MD
	11:40-12:00 p.m.	**Discussion questions and Q/A Panel**
10:40 AM	**12:00 PM**	**Midday Workshop – World Federation of Pediatric Imaging (WFPI) – Updates in Outreach** *Dorothy I. Bulas, MD, FAAP and Cicero T. Silva, MD, Moderators*
	10:40-10:45 a.m.	**Introductions and Overview**
	10:45-11:00 a.m.	**World TB Day Summit Update** Bernard F. Laya, DO
	11:00-11:15 a.m.	**Facilitating a Radiology Curriculum in Haiti Using Tablet PCs: Progress and Challenges** Jennifer L. Nicholas, MD
	11:15-11:30 a.m.	**POCUS Updates - A Key to Radiology Outreach** Kara-Lee Pool, MD
	11:30-11:40 a.m.	**WFPI Project - Pediatric MRI Protocols for Low Resource Settings** Michael S. Gee, MD, PhD
	11:40-11:55 a.m.	**Outreach Experiences - Issues to Consider** Panelists: Veronica J. Rooks, MD & Ramdas Senasi, MBBS
	11:55-12:00 p.m.	**Questions and Answers**
12:00 PM	**1:30 PM**	**Lunch On Your Own**

COLOR KEY

Scientific Session
General Postgraduate Course
Body Imaging Postgraduate Course
General Session
Sunrise/Midday Session
Technologist Program

THURSDAY, MAY 17, 2018 *(continued)*

12:00 PM 1:30 PM **CT Protocol Session: State of the Art in CT: Let's Cut to the Chase!**
(Non-CME Session)
Michael J. Callahan, MD, and Prakash M. Masand, MD, Moderators

12:05-12:13 p.m. **"Post-64" Era in CT Scanning with Emphasis on Faster Acquisition Techniques**
Robert MacDougall, MSc

12:13-12:21 p.m. **Fast Pitch Pediatric Head CT: "Mission Impossible?"**
Christina Dodge, MS

12:21-12:29 p.m. **Dynamic CT of the Pediatric Airway: "Take My Breath Away"**
Abbey Winant, MD

12:29-12:37 p.m. **Pediatric CT Angiography: "Injection Perfection"**
Karen Lyons, MD

12:37-12:45 p.m. **Pediatric CTA in the Acute Setting: "Practical Tips for Success"**
Tushar Chandra, MD

12:45-12:53 p.m. **CT Imaging in Pediatric Oncology: Do I Sedate or Radiate?**
Kara G. Gill, MD

12:53-1:01 p.m. **Dose Optimization for High Pitch Imaging: "Image Gently and Rapidly"**
Grace S. Phillips, MD

1:01-1:30 p.m. **Questions and Answers with Panel Discussion**

12:00 PM 1:30 PM **SPR Research and Education Foundation Symposium (Non-CME Session)**

12:00-12:10 p.m. **Welcome and Introduction** - Peter J. Strouse, MD, FACR and J. Damien Grattan-Smith, MBBS

12:10-12:20 p.m. **2016 Multi-Institute Pilot Award: Single Ventricle Reconstruction III: Brain Connectome and Neurodevelopmental Outcomes - Part II**
Ashok Panigrahy, MD

12:20-12:25 p.m. **2016 Seed Grant: Study for the Detection of Gadolinium Deposition in Resected Bowel Specimens of Patients with Inflammatory Bowel Disease**
Shannon G. Farmakis, MD

12:25-12:35 p.m. **2016 Education Project Grant: MOOC-based Repetitive Image Quizzes for Learning Concepts in Pediatric Radiology**
Cara E. Morin, MD, PhD

12:35-12:45 p.m. **2016 Young Investigator: Accurate assessment of kidney function through Motionrobust DCEM**
Sila Kurugol, PhD, MS

12:45-1:30 p.m. **REF Updates and Announcement of the 2018 Grant Recipients**
J. Damien Grattan-Smith, MBBS

1:30 PM 3:30 PM **Scientific Session III-A: Genitourinary Radiology**
Harriet J. Paltiel, MD and Monica Epelman, MD, Moderators

1:30-1:50 p.m. **Keynote Presentation**
Stacy Tanaka, MD

P043	1:50	2:00	Stanescu, A. Luana	Gadolinium bone tissue retention in pediatric patients after contrast-enhanced MR exams: pathologic confirmation.
P044	2:00	2:10	Tao, Ting	Safety and efficacy of gadoterate meglumine in children <2 years of age
P045	2:10	2:20	Zucker, Evan	Free-Breathing Ferumoxytol-Enhanced MRI for Preoperative Renal Transplant Vascular Mapping in Infants and Children
P046	2:20	2:30	Kurugol, Sila	Feed and Wrap MRU
P047	2:30	2:40	Otero, Hansel	Morphologic and Functional Evaluation of Duplicated Renal Collecting Systems with MR Urography: A Descriptive Analysis
P048	2:40	2:50	Acharya, Patricia	Evaluation of the Urinary Tract Dilation Classification System for postnatal hydronephrosis in the prediction of clinical outcomes
P049	2:50	3:00	Back, Susan	Preliminary experience with Contrast Enhanced Ultrasound (CEUS) of the Pediatric Kidney
P050	3:00	3:10	Chow, Jeanne	Contrast enhanced ultrasound for the evaluation of complex anorectal and genitourinary anomalies
P051	3:10	3:20	Pai, Vinay	Infant Female Urethral Catheterization: A New Simulator from Special Effects
P052	3:20	3:30	Dao, Kimberly	Pediatric Ovarian Volumes Measured at Ultrasound After Contralateral Unilateral Oophorectomy

COLOR KEY

Scientific Session
General Postgraduate Course
Body Imaging Postgraduate Course
General Session
Sunrise/Midday Session
Technologist Program

THURSDAY, MAY 17, 2018 *(continued)*

1:30 PM 3:30 PM **Scientific Session III-B: Fetal/Neonatal Imaging**

Brandon P. Brown, MD and Erika Rubesova, MD, Moderators

1:30-1:50 p.m. **Keynote Presentation**

Jill Kilkelly, MD

P053	1:50	2:00	Dong, Su-Zhen	Feasibility of fetal MRI in the evaluation of fetal cardiovascular anomalies.
P054	2:00	2:10	Dong, Su-Zhen	Fetal cardiac MRI in the evaluation of congenital aortic arch anomalies
P055	2:10	2:20	Oliver, Edward	Two's Company – Multiple Thoracic Anomalies on Prenatal Ultrasound and MRI
P056	2:20	2:30	Wise, Rachel	A Multifactorial Severity Score for Congenital Diaphragmatic Hernia (CDH) using Fetal MRI
P057	2:30	2:40	Smitthimedhin, Anilawan	Normal size of the fetal adrenal gland on prenatal MR Imaging
P058	2:40	2:50	Didier, Ryne	Novel Computerized Analytic Technique for Quantification of Amniotic Fluid Volu in Fetal MRI
P059	2:50	3:00	Norris, Carrie	Using Quantitative MRI to Identify Abnormal Perfusion in Invasive Placental Disease
P060	3:00	3:10	Tsai, Andy	Congenital Skeletal Anomalies with Lower Limb-Length Discrepancy: Does Constant Inhibition Occur In Utero?
P061	3:10	3:20	Victoria, Teresa	Ultra-Low Dose Fetal CTL How to Further Decrease Radiation Dose While Main Diagnostic Accuracy
P062	3:20	3:30	Deaver, Pamela	Perinatal imaging autopsy: Value and comparison with conventional autopsy

1:30 PM 3:30 PM **Scientific Session III-C: Informatics, QI, Education & Healthcare Policy**

Richard E. Heller, III, MD, MBA and Ramesh S. Iyer, MD, Moderators

1:30-1:50 p.m. **Keynote Presentation - Technologist Skill: Moving from Built-in Mediocrity to Built-in Excellence Using a Coaching Model**

David B. Larson, MD, MBA

P063	1:50	2:00	Snyder, Elizabeth	Gaging Potential Risk to Patients in Pediatric Radiology by Review of Over 2,000 Incident Reports
P064	2:00	2:10	Hingsbergen, Elizabeth	Identifying the primary cause of safety events and complaints in the routine operations of a pediatric radiology department
P065	2:10	2:20	Porterfield, Ronna	Analysis of Quick Hits at a Daily Readiness Huddle at a Large Free-Standing Children's Hospital
P066	2:20	2:30	Iyer, Ramesh	Survey of Peer Review Programs Amongst Pediatric Radiologists: Report from the SPR Quality and Safety Committee
P067	2:30	2:40	Gates, Erica	Potential Risk of Hypothyroidism in Infants Receiving Iodinated Contrast: Are Pediatric Radiology Practitioners Aware of the Food and Drug Administration (FDA) Drug Safety Communication?
P068	2:40	2:50	Frush, Daniel	Utilization of computed tomography imaging in the pediatric emergency department
P069	2:50	3:00	Hagedorn, Kelly	Cost comparison of ultrasound versus MRI for adolescent female patients with suspected appendicitis using time-driven activity-based costing
P070	3:00	3:10	Aquino, Michael	Survey of after-hours radiology coverage in children's hospitals.
P071	3:10	3:20	Ayyala, Rama	Evaluation of Stressors that Contribute to Burnout Amongst Pediatric Radiologists: A Survey of the Society for Pediatric Radiology
P072	3:20	3:30	Pfeifer, Cory	Assessing the Pediatric Radiology Job Market: Winter is Coming for Employers

THURSDAY, MAY 17, 2018 *(continued)*

1:30 PM – 3:30 PM **Technologist Session**
Lorraine Chisari, RDMS, RVT, Moderator

1:30-1:50 p.m. **Common Pediatric Fluoroscopy Exams**
Ciji N. Gilley, RT(R)

1:50-2:10 p.m. **MRE (Enterography)**
Gina Roberts, ARRT (R)(CT)(MRI)

2:10-2:30 p.m. **Happy Spitter or Surgical Referral?: Sonographic Approach to the Vomiting Infant**
Jason Hooper, BS, RDMS, RVT

2:30-2:50 p.m. **US Contrast**
Trudy Morgan, RDMS

2:50-3:10 p.m. **Transplant US Imaging**
Lacy Gandor, RDMS

3:10-3:30 p.m. **3D Post Processing and Printing**
Gabe Linke, BSRT (R)(MR)

3:30 PM – 4:00 PM **Break & Exhibits**

4:00 PM – 5:30 PM **Scientific Session IV-A: Gastrointestinal Radiology**
Govind B. Chavhan, MD and Hansel J. Otero, MD, Moderators

4:00-4:20 p.m. **Keynote Presentation**
Dedrick Moulton, MD

P073	4:20	4:30	Dillman, Jonathan	Diagnostic Performance of Magnetic Resonance Cholangiopancreatography (MRCP) versus Endoscopic Retrograde Cholangiopancreatography (ERCP) in the Pediatric Population: A Clinical Effectiveness Study
P074	4:30	4:40	Trout, Andrew	Normal Pancreatic Secretion in Children Measured by MRI with Secretin
P075	4:40	4:50	Dillman, Jonathan	Diagnostic performance of quantitative MRI parameters for predicting radiologic portal hypertension in autoimmune liver diseases
P076	4:50	5:00	Stefek, Heather	Relationship between 2D phase contrast MRI Rex shunt blood flow, Rex shunt diameter, and clinical indicators of portal hypertension
P077	5:00	5:10	Romberg, Erin	Validation of LI-RADS in Evaluation of Pediatric Liver Masses
P078	5:10	5:20	Lipsich, Jose	Congenital portosystemic shunts (CPSS): clinical outcome after treatment. Experience in a tertiary hospital in Argentina
P079	5:20	5:30	Back, Susan	Preliminary experience with Contrast Enhanced Ultrasound (CEUS) of the Pediatric Liver

4:00 PM – 5:30 PM **Scientific Session IV-B: Cardiovascular Imaging**
Randolph K. Otto, MD and Prakash M. Masand, MD, Moderators

4:00-4:20 p.m. **Keynote Presentation**
Jason Christensen, MD

P080	4:20	4:30	Malone, LaDonna	Coronary artery assessment in pediatric patients using ultrafast ECG gated CT: Is this a viable alternative to prospectively gated technique?
P081	4:30	4:40	Barrera, Christian	Depiction of the Native Coronary Arteries during ECG-triggered high-pitch spiral Dual-Source Cardiac CTA in Children: Determinants of Image Quality
P082	4:40	4:50	Masand, Prakash	Myocardial bridging in a cohort of pediatric patients with anomalous aortic origin of coronary artery (AAOCA): “Double whammy”!
P083	4:50	5:00	Ortiz-Neira, Clara L	Coronary artery imaging in Kawasaki disease with Computed Tomography Angiography and Echocardiography, a comparative analysis
P084	5:00	5:10	Markush, Dor	Delayed Myocardial Enhancement in Children: Comparison of Conventional Technique to a Free Breathing Single-Shot Technique in Duchenne Muscular Dystrophy
P085	5:10	5:20	Biko, David	Association of T2 Lymphatic Imaging in Single Ventricle Patients After Superior Cavopulmonary Connection with Acute Post-Fontan Outcomes
P086	5:20	5:30	Davis, Joseph	Aortic Disease in Patients with Mucopolysaccharidosis

COLOR KEY

Scientific Session
General Postgraduate Course
Body Imaging Postgraduate Course
General Session
Sunrise/Midday Session
Technologist Program

THURSDAY, MAY 17, 2018 *(Continued)*/ FRIDAY, MAY 18, 2018

4:00 PM – 5:30 PM **Scientific Session IV-C: ALARA**
Steven Don, MD and Robert MacDougall, MSc, Moderators

4:00-4:20 p.m. **Keynote Presentation**
Marta Hernanz-Schulman, MD, FACR

P087	4:20	4:30	Sharma, Priya	Assessing Pediatric Fluoroscopy Radiation Dose Awareness amongst Clinicians
P088	4:30	4:40	Kaplan, Summer	Reduced-Dose Radiography Protocol for Focused Assessment of Feeding Tube Position
P089	4:40	4:50	Don, Steven	Stochastic Noise Tolerance in Pediatric Appendicitis CT
P090	4:50	5:00	Southard, Richard	Knowledge-Based Iterative Reconstruction verses Filtered-Back Reconstruction Head CT in Children Referred from the Emergency Department: Dose Reduction, Image Quality, and Image Reconstruction Time
P091	5:00	5:10	Ngo, Jennifer	Development and Testing of an Innovative Simulation Paradigm for Subtle Liver Lesion Detection in Pediatric CT
P092	5:10	5:20	Ngo, Jennifer	An Innovative Simulation Paradigm for Evaluation of Subtle Liver lesions in Pediatric CT: Performance and Confidence
P093	5:20	5:30	MacDougall, Robert	Development of a tool to aid the radiologic technologist using augmented reality and computer vision

4:00 PM – 5:00 PM **Technologist Family Feud**
Christine Harris, RT (R) (MR), Moderator

4:00-5:00 p.m. **Family Feud**
Nikki D. Butler, BMSc, RT(R)(QM)

5:00 PM – 5:30 PM **Technologist Session: Global Health Panel**
Christine Harris, RT (R) (MR)
Laura Poznick, AAS, RDMS
Lacy Gandor, RDMS

5:30 PM **Adjourn**

FRIDAY, MAY 18, 2018

6:30 AM – 8:30 AM **Continental Breakfast & Exhibits**

6:30 AM – 6:00 PM **Registration**

7:00 AM – 5:20 PM **SPR Online Case of the Day Activity**

7:00 AM – 8:20 AM **Sunrise Workshop – Child Abuse Trial Perspectives**
Joëlle A. Moreno, JD, Moderator

7:00-7:20 a.m. **10 Points for the Radiologist to Know About Trials**
Joëlle A. Moreno, JD

7:20-7:40 a.m. **Testimony: The Do's and Don't's**
Jerry R. Dwek, MD

7:40-8:00 a.m. **Putting It All Together**
Superior Court Judge Kevin C. Doyle

8:00-8:20 a.m. **Questions and Answers**

COLOR KEY

Scientific Session
General Postgraduate Course
Body Imaging Postgraduate Course
General Session
Sunrise/Midday Session
Technologist Program

FRIDAY, MAY 18, 2018 (continued)

7:00 AM – 8:20 AM **Sunrise Workshop – Advanced Body Imaging**
Jonathan R. Dillman, MD, MSc, Moderator

7:00-7:15 a.m. **MR Elastography Update**
Jonathan R. Dillman, MD, MSc

7:15-7:30 a.m. **Dixon MRI Applications**
Andrew T. Trout, MD

7:30-7:45 a.m. **Free Breathing Body MRI**
Michael S. Gee, MD, PhD

7:45-8:00 a.m. **Update on Dual-Energy CT in Children**
Sarah D. Bixby, MD

8:00-8:15 a.m. **CT Iterative Reconstruction: Where Do We Stand?**
Samuel L. Brady, MS, PhD

8:15-8:20 a.m. **Questions and Answers**

7:00 AM – 8:20 AM **Sunrise Workshop – Pearls in Fetal Imaging**
Teresa Victoria, MD, PhD, Moderator

7:00-7:15 a.m. **How to Approach Abnormal Placentation**
Mariana Meyers, MD

7:15-7:30 a.m. **Motion Correction in Fetal MRI**
Camilo Jaimes, MD

7:30-7:45 a.m. **Prenatal Evaluation of Lymphatic Disorders with Postnatal Correlation**
David M. Biko, MD

7:45-8:00 a.m. **How to Start a Fetal Program**
Beth M. Kline-Fath, MD

8:00-8:15 a.m. **How the Radiologist Adds Value to Patient Care with Emphasis in Fetal MRI**
Brandon P. Brown, MD

8:15-8:20 a.m. **The Unusual Lung Lesions**
Teresa Victoria, MD, PhD

7:00 AM – 8:20 AM **Sunrise Workshop – Physics**
Robert MacDougall, MS, Moderator

7:00-7:15 a.m. **Pediatric Digital Radiography: From EI to IQ**
Robert MacDougall, MS

7:15-7:30 a.m. **Using Informatics Tools to Drive Quality Improvement**
Cristina Dodge, MS

7:30-7:45 a.m. **Contrast Ultrasound Primer**
Samuel L. Brady, MS, PhD

7:45-8:00 a.m. **Radiation Management and Dosimetric QA in Interventional Radiology**
Nicholas Shkumat, MSc

8:00-8:20 a.m. **MRI Safety: Physics and Practice**
Jie Deng, PhD

7:00 AM – 8:20 AM **Sunrise Workshop – Diversity**
Ashok Panigrahy, MD and Stephanie E. Spottswood, MD, MSPH, Moderators

7:00-7:20 a.m. **Diversity and Unconscious Bias in Healthcare**
Stephanie E. Spottswood, MD, MSPH

7:20-7:40 a.m. **Supporting LGTBTQ Patients and Families**
Jesse M. Ehrenfeld, MD, MPH

7:40-8:00 a.m. **"Disability - Its Name and Faces"**
Cindy R. Miller, MD

8:00-8:20 a.m. **Diversity, Discrimination, and Mitigation** Panel Discussion with:
Johnathan Dallas, BS, Jesse M. Ehrenfeld, MD, MPH, Cindy R. Miller, MD and Stephanie E. Spottswood, MD, MSPH

COLOR KEY

Scientific Session
General Postgraduate Course
Body Imaging Postgraduate Course
General Session
Sunrise/Midday Session
Technologist Program

FRIDAY, MAY 18, 2018 (continued)

8:30 AM 10:10 AM **Technologist Session**
David A. Bloom, MD, FACR, Moderator

8:30-8:50 a.m. **Child Life Services in Pediatric Radiology**
Sarah Beth Gray, CCLS

8:50-9:10 a.m. **The Role of Nursing in Preparing Patients for Imaging**
Leslie Mintz, BSN

9:10-9:30 a.m. **Interactive VR on IV Sticks**
Gabe Linke, BSRT (R)(MR) and Nicole Hardin, MS, RT, (R)(M)(CIIP)

9:30-9:50 a.m. **PAWS (Patient Awake While Scanning) MRI Program**
Sarah Beth Gray, CCLS

9:50-10:10 a.m. **"Try Without" Program**
Leslie Mintz, BSN

8:30 AM 10:10 AM **Scientific Session V-A: Gastrointestinal Radiology**
Michael S. Gee, MD, PhD and Gary R. Schooler, MD, Moderators

8:30-8:50 a.m. **Keynote Presentation**
Lea Matsuoka, MD

P094	8:50	9:00	Dillman, Jonathan	Multiparametric Liver MRI in Children and Young Adults with Autoimmune Liver Disease: Correlation between Quantitative Imaging Methods
P095	9:00	9:10	Trout, Andrew	Predictive Performance of MR Elastography in Children and Young Adults with Suspected Liver Disease
P096	9:10	9:20	Davis, James	Assessment of pediatric liver allografts with shear wave elastography
P097	9:20	9:30	Goette, Matthew	Shear Wave Elastography Ultrasound for Hepatic Veno-occlusive Disease in a Pediatric Population undergoing Hematopoietic Stem Cell Transplantation
P098	9:30	9:40	Diaz, Eric	Can MRI Liver Stiffness Predict be used to Predict Focal Liver Lesions in Fontan Patients?
P099	9:40	9:50	Thompson, Benjamin	Magnetic resonance elastography of the liver in children: variations in regional stiffness
P100	9:50	10:00	Robinson, Amie	Methotrexate Therapy Increases Hepatic Stiffness in Patients with Inflammatory Bowel Disease
P101	10:00	10:10	Hunte, David	Abdominal Fat Distribution and its Relationship with Liver and Pancreatic Fat Fraction, Liver Stiffness and Diabetic Status

8:30 A 10:10 AM **Scientific Session V-B: Fetal/Neonatal Imaging**
Beth M. Kline-Fath, MD and Marianna Meyers, MD, Moderators

8:30-8:50 a.m. **Keynote Presentation - Fetal Diagnosis of Surgical Anomalies: Effect on Pre and Postnatal Therapy**
John Pietsch, MD

P102	8:50	9:00	Didier, Ryne	Contrast-Enhanced Brain Ultrasound on Extreme Premature Twin Fetal Lambs Maintained by the EXTra-uterine Environment for Neonatal Support (EXTEND): A Promising Imaging Technique
P103	9:00	9:10	Bulas, Dorothy	Fetal and Postnatal Brain Imaging for the Detection of ZIKV Encephalopathy in the Fetus/Newborn
P104	9:10	9:20	Snyder, Elizabeth	Fetal MRI Findings in Diencephalosynapsis
P105	9:20	9:30	Guimaraes, Carolina	Posterior Fossa Findings in Prenatal Diagnosis of Dystroglycanopathy – Extending Beyond Brainstem Kinking
P106	9:30	9:40	Zare, Megan	Establishment of normative values for the fetal posterior fossa by MRI.
P107	9:40	9:50	Rubio, Eva	Predictive Value of Prenatal Alveolar Cleft Size in Determining the Likelihood of Secondary Palatal Defects
P108	9:50	10:00	Guimaraes, Carolina	The Use of Echo Planar Imaging in the Identification of the Upper Spinal Bony Defect Level During Prenatal Evaluation of Open Neural Tube Defect - A Pilot Study
P109	10:00	10:10	Nagaraj, Usha	Decreased Rectal Meconium Signal on MRI in Fetuses with Open Spinal Dysraphism

COLOR KEY

Scientific Session
General Postgraduate Course
Body Imaging Postgraduate Course
General Session
Sunrise/Midday Session
Technologist Program

FRIDAY, MAY 18, 2018 *(continued)*

8:30 AM **10:10 AM** **Scientific Session V-C: Neuroradiology**
Susan Palasis, MD and Hisham Dahmoush, MD, Moderators

8:30-8:50 a.m. **Keynote Presentation – Economically Motivated Patient Steerage: The Pediatric Perspective**
Richard E. Heller III, MD, MBA

P110	8:50	9:00	Bhargava, Ravi	Globus pallidus and Dentate nuclei signal on T1-weighted MRI does not change after multiple exposures to Gadobutrol in pediatric patients
P111	9:00	9:10	Kwong, Yin Yee	Commonly Encountered Intracranial Calcifications: Prevalence In Pediatric And Young Adult Patients.
P112	9:10	9:20	Retrouvey, Michele	Sonographic Fronto-Occipital Ratio (FOR) in Evaluation of Hydrocephalus
P113	9:20	9:30	Ndolo, Josephine	Ferumoxytol whole body vascular imaging including the central nervous system in pediatric patients: a single center's initial experience
P114	9:30	9:40	Chukus, Anjeza	Arterial Spin Labeling and Ferumoxytol-based Spoiled Gradient Recalled Acquisition Magnetic Resonance Imaging Versus Digital Subtraction Angiography for Surveillance of Residual Brain Arteriovenous Malformations in Children: A Single-Institution Analysis of Inter-Modality Reliability
P115	9:40	9:50	Starosolski, Zbigniew	Gender-dependent cerebrovascular alterations in Moyamoya mice model correlate with the prevalence in pediatric population
P116	9:50	10:00	Hu, Houchun	Motion Insensitive 3D T1-Weighted Post-Contrast Brain MRI Using a Golden Angle Radial Acquisition

10:10 AM **10:40 AM** **Break & Exhibits**

10:40 AM **12:00 PM** **Midday Workshop – Critical Skills in Pediatric Radiology**
Lane F. Donnelly, MD, Moderator

10:40-11:00 a.m. **Communication - Listening Skills - A Key to Effective Leadership**
Lane F. Donnelly, MD

11:00-11:20 a.m. **Daily Readiness - Managing Today's Work**
Craig M. Johnson, DO

11:20-11:40 a.m. **Improvement - Systems to Promote Problem Solving Accountability**
David B. Larson, MD, MBA

11:40-12:00 p.m. **People - Faculty Development & Engagement**
Brian D. Coley, MD, FACR, FAIUM

10:40 AM **12:00 PM** **Midday Workshop – Dynamic Airway and Pulmonary Imaging**
S. Bruce Greenberg, MD, Moderator

10:40-10:54 a.m. **Technical Aspects of Dynamic Airway Imaging**
Karen Lyons, MB, BCh, BAO

10:54-11:12 a.m. **Upper Airway Dynamic Imaging by MR and CT**
Robert J. Fleck, MD

11:12-11:30 a.m. **Anatomic and Functional Evaluation of the Thoracic Trachea, Airways and Lungs**
Prakash M. Masand, MD

11:30-11:42 a.m. **Cardiopulmonary Abnormalities**
S. Bruce Greenberg, MD

11:42-12:00 p.m. **Case Review**

10:40 AM **12:00 PM** **Midday Workshop – Pediatric Contrast Ultrasound – How to Do Session**
Kassa Darge, MD, PhD, Moderator

10:40-10:50 a.m. **Contrast US: How to Start**
Kassa Darge, MD, PhD

10:50-11:00 a.m. **Contrast US: Challenges and Solutions as We Began**
Patricia T. Acharya, MD

11:00-11:10 a.m. **Intravenous Contrast US: How to Do**
Susan J. Back, MD

11:10-11:20 a.m. **Intravesical Contrast US: How to Do**
Jeanne Chow, MD

COLOR KEY
Scientific Session
General Postgraduate Course
Body Imaging Postgraduate Course
General Session
Sunrise/Midday Session
Technologist Program

11:20-11:30 a.m.	**Liver Contrast US: How to Interpret** Judy H. Squires, MD
11:30-11:40 a.m.	**Kidney Contrast US: How to Interpret** Susan J. Back, MD
11:40-11:50 a.m.	**Interventional Contrast US: Where to Apply** Abhay Srinivasan, MD
11:50-12:00 p.m.	**Contrast US: Questions and Answers**

10:40 AM 12:00 PM **Midday Workshop – Balancing Efficiency and Accuracy in Pediatric Neuroimaging**
Susan Palasis, MD, Moderator

10:40-11:05 a.m.	**Minimizing MR Scan Time in Pediatric Neuroimaging** Arastoo Vossough, MD, PhD
11:05-11:30 a.m.	**Maximizing Diagnostic Yield in Pediatric Neuroimaging** Mai Lan Ho, MD
11:30-11:55 a.m.	**Targeted Pediatric Neuroimaging** Susan Palasis, MD
11:55-12:00 p.m.	**Question and Answers**

10:40 AM 12:00 PM **Midday Workshop – MR Arthography**
Mahesh M. Thapa, MD, Moderator

10:40-10:55 a.m.	**How to Perform Ultrasound Guided Arthrograms of the Shoulder and Hip** Mahesh M. Thapa, MD
10:55-11:10 a.m.	**Shoulder Arthogram Interpretation** Bamidele F. Kammen, MD
11:10-11:25 a.m.	**Elbow Arthogram Injection and Interpretation** Jeffrey P. Otjen
11:25-11:40 a.m.	**Wrist Arthogram Injection and Interpretation** Anh-Vu H. Ngo, MD
11:40-11:55 a.m.	**Hip Arthogram Interpretation** Arnold Carl Merrow, MD
11:55-12:00 p.m.	**Questions and Answers**

10:40 AM 12:00 PM **Midday Workshop – Appendicitis**
Andrew T. Trout, MD, Moderator

10:40-10:55 a.m.	**Appendicitis - Why Are We Still Talking About This?** Andrew T. Trout, MD
10:55-11:05 a.m.	**Work-up of Appendicitis - The Private Practice Perspective** Kimberly A. Garver, MD
11:05-11:15 a.m.	**Work-up of Appendicitis - The Academic Perspective** Michael Aquino, MD
11:15-11:20 a.m.	**Discussion**
11:20-11:40 a.m.	**Appendicitis - What If? Decision Making and Problem Solving** Robert C. Orth, MD, PhD, MPH
11:40-12:00 p.m.	**Appendicitis - Lessons Learned, Mimics and Other Causes of RLQ Pain** Martha M. Munden, MD

12:00 PM 1:30 PM **Lunch On Your Own**

12:00 PM 1:30 PM **SPR Members' Business Meeting**

COLOR KEY

Scientific Session
General Postgraduate Course
Body Imaging Postgraduate Course
General Session
Sunrise/Midday Session
Technologist Program

FRIDAY, MAY 18, 2018

1:30 PM 3:20 PM **Scientific Session VI-A: Musculoskeletal Imaging**
Arthur B. Meyers, MD and Delma Y. Jarrett, MD, Moderators
1:30-1:50 p.m. **Keynote Presentation**
Jeffrey Martus, MD

P118	1:50	2:00	Artunduaga, Maddy	MR correlation of spica hip arthrographic sliver sign during closed reduction of developmental hip dysplasia of the hip
P119	2:00	2:10	Artunduaga, Maddy	Correlation of arthrographic inverted limbus sign and spica MRI in developmental dysplasia of the hip
P120	2:10	2:20	Bedoya, Maria	Diffusion-Tensor Imaging of the femoral physes: Can we predict future growth?
P121	2:20	2:30	Delgado, Jorge	Diffusion Tensor Imaging for the Evaluation of Physeal Microstructural Changes in Children Treated with High Dose Cis-Retinoic Acid (Cis-RA) for High Risk Neuroblastoma
P122	2:30	2:40	Rapp, Jordan	Morel-Lavellée lesions: MRI characteristics in the pediatric patient
P123	2:40	2:50	Tsai, Andy	Children with Unilateral Fibular Hemimelia Have Normal Lower Extremity Growth Trajectory and Skeletal Maturation
P124	2:50	3:00	Thompson, Benjamin	MRI of stress fractures: Relationship between Fredericson classification and time to recovery in children.
P125	3:00	3:10	Ditzler, Matthew	Pediatric Posterior Ankle Impingement: An Underdiagnosed Cause of Posterior Ankle Pain
P126	3:10	3:20	Ditzler, Matthew	MRI Findings of Pediatric Posterior Ankle Impingement and Associated Entities

1:30 PM 3:20 PM **Scientific Session VI-B: Oncology/Nuclear Medicine**
Geetika Khanna, MD, MS and Andrew T. Trout, MD, Moderators
1:30-1:50 p.m. **Keynote Presentation – Oncology is a Team Sport: How Radiologists Help Provide Optimal Cancer Care**
Scott C. Borinstein, MD

P127	1:50	2:00	Cain, Timothy	Introduction of a clinical MR PET service into a dedicated children's hospital; lessons learned from the first 550 patients
P128	2:00	2:10	Kaste, Sue	The role of routine imaging in childhood melanoma (MM)
P129	2:10	2:20	Ranginwala, Saad	MR Imaging Features of Subtypes of Hepatocellular Adenomas in Children
P130	2:20	2:30	Kaste, Sue	Long-term Outcomes of Large Femoral Head Osteonecrotic (ON) Lesions in Pediatric Patients Treated for Leukemia or Lymphoma
P131	2:30	2:40	Ghaghada, Ketan	High-Resolution In Vivo Imaging of Tumor Angiogenesis in Orthotopic Xenograft and Transgenic Mouse Models of Neuroblastoma
P132	2:40	2:50	Lim-Dunham, Jennifer	Malignancy risk stratification of pediatric thyroid nodules using ACR Thyroid Imaging, Reporting and Data System (ACR TI-RADS)
P133	2:50	3:00	Low, Samantha	Streamlining primary care referrals for ultrasound assessment of paediatric cervical nodes in a NHS (UK) District General Hospital: Preliminary results from an ongoing study
P134	3:00	3:10	Shah, Summit	Hepatobiliary scintigraphy vs. ultrasound for assessment of gallbladder ejection fraction in pediatric patients with suspected biliary dyskinesia
P135	3:10	3:20	Sharp, Susan	Solid gastric emptying: does the 4 hour examination add value in children?

1:30 PM 3:20 PM **Scientific Session VI-C: Informatics, QI, Education & Healthcare Policy**
Paula N. Dickson, MD and Janet R. Reid, MD, FRCPC, Moderators
1:30-1:50 p.m. **Keynote Presentation - What does Value-added mean for education and radiology?**
Melissa A. Hilmes, MD

P136	1:50	2:00	Reid, Janet	Building a Comprehensive Learning Management System for Pediatric Radiology: How We Got There
P137	2:00	2:10	Shaikh, Raja	Simulation in Pediatric Interventional Radiology Environment: What lessons are we learning?
P138	2:10	2:20	D'Alessandro, Michael	Is Social Media a Growing or Declining Educational Method in Pediatric Radiology?
P139	2:20	2:30	Kaplan, Summer	Feasibility and Impact of Intensive Hands-On Sonography Training for Pediatric Radiology Fellows
P140	2:30	2:40	Hailu, Tigist	Body MRI Training During Pediatric Radiology Fellowship: Defining the Needs

P141	2:40	2:50	Miller, Elise	Radiology Resident Preparedness in Counseling Patients for MRI During Pregnancy
P142	2:50	3:00	Heller, Richard	Pediatric Radiology Support and Education for Radiologists in a Large, Multicentric Group Practice
P143	3:00	3:10	Francavilla, Michael	The Pediatric Normal Studies Database: First Years' Experience and Utilization Patterns
P144	3:10	3:20	Buskirk, Tricia	Reducing the sedation rates in MRI for pediatric patients utilizing an MRI simulator preparation session facilitated by a child life specialist.

1:30 PM **3:20 PM** **Technologist Scientific Session**

Stephen F. Simoneaux, MD, Moderator

P001 (T)	1:30	1:40	Morales, Gabriel	Evaluation of Meso-Rex Bypass with Ferumoxytol Contrast Enhanced MRI
P002 (T)	1:40	1:50	Brondell, Ashley	Implementation of a Pediatric MRI Lymphangiography Programs
P003 (T)	1:50	2:00	Stenger, Kristina	Conjoined Twins: A Life Together - A Case Report on Prenatal and Postnatal Imaging of Parapagus Dicephalus Twins
P004 (T)	2:00	2:10	Curran, David	Paediatric lower limb lymphoscintigraphy: A retrospective review of practice and dose optimization
P005 (T)	2:10	2:20	Patel, Falguni	Role of Ultrasound with Atypical Spitz tumor
P006 (T)	2:20	2:30	Thorkelson, Marrit	Advanced MRI Scan Techniques and 3D Post-Processing in Pediatric Patients
P007 (T)	2:30	2:40	Augustyn, Robyn	CT Iterative Reconstruction Increases Efficiency of 3D Image Post-Processing
P008 (T)	2:40	2:50	Pazienza, Rocco	The Diagnosis of Accidental and Non-Accidental Trauma Through Medical Imaging
P009 (T)	2:50	3:00	Hidalgo, Khristina	MRI Safety Screening Clearance Process
P010 (T)	3:00	3:10	Goehner, Melissa	Generational Differences in the Workplace
	3:10	3:20		Open Discussion

3:50 PM **5:20 PM** **Scientific Session VII-A: Gastrointestinal Radiology**

David A. Bloom, MD, FACR and Summer Kaplan, MD, Moderators

3:50-4:10 p.m. **Keynote Presentation - Pediatric Surgery and Radiology: How a Critical Partnership Developed and its Future Goals**

James A. O'Neill, MD

P145	4:10	4:20	Pomeranz, Christy	Intraabdominal soft tissue injuries on computed tomography (CT) in accidental versus non accidental trauma
P146	4:20	4:30	Blumfield, Einat	Perforated appendicitis vs Non-perforated Appendicitis: A Validation Study of a Score System Based on Sonographic, Clinical and Laboratory Findings
P147	4:30	4:40	Naz, Fozia	Rapid non-contrast MR protocol for evaluation of abdominal and pelvic abscesses in children
P148	4:40	4:50	Royall, Ivey	Does Prolongation of Time Between Intussusception Diagnosis and Therapeutic Enema Result In Increased Patient Morbidity: a Retrospective Review
P149	4:50	5:00	Goldman-Yassen, Adam	Non-emergent outpatient pediatric UGI series: can clinical parameters improve diagnostic yield?
P150	5:00	5:10	Wong, Kevin	Does prior CT or MRI obviate the need for Upper GI examination to rule out malrotation?
P151	5:10	5:20	Wong, Kevin	Making the Diagnosis of Mid Gut Volvulus: Limited Abdominal Ultrasound has changed our Clinical Practice

3:50 PM **5:20 PM** **Scientific Session VII-B: Cardiovascular Imaging/Gastrointestinal Radiology**

Cynthia K. Rigsby, MD, FACR and Mark R. Ferguson, MD, Moderators

3:50-4:10 p.m. **Keynote Presentation**

Eric Hoggard, MD

P152	4:10	4:20	Pednekar, Amol	Clinical Evaluation of Free Breathing CArdioREspiratory Synchronized (CARESync) Balanced Steady-State Free Precession (bSSFP) Cine Imaging in Pediatric Population
P153	4:20	4:30	Pednekar, Amol	Numerical Simulations of Geometric Markers for Left Ventricular Hypertrabeculation: Fractal Dimension and Isoperimetic Ratio
P154	4:30	4:40	Pednekar, Amol	Automatic Quantification of Left Ventricular Non-compaction using Fractal Analysis and Perimetric Ratio
P155	4:40	4:50	Li, Arleen	Comparison of MR Tissue Phase Mapping and MR Feature Tracking in Children with Hypertrophic Cardiomyopathy

P156	4:50	5:00	Krishnamurthy, Ramkumar	Quantitative Regional Fibrosis Burden in Duchenne Muscular Dystrophy Patients by Cardiac Magnetic Resonance Imaging
P157	5:00	5:10	Jones, Richard	Demonstration of linear correlation between R2* and liver iron concentration across multiple MR acquisition parameters at 1.5T and 3T.
P158	5:10	5:20	Tipirneni-Sajja, Aaryani	Automated Vessel Exclusion on Free-Breathing Ultrashort Echo Time Imaging For Assessment of Hepatic Iron Overload by R2*-MRI

3:50 PM **5:20 PM** **Scientific Session VII-C: Interventional Radiology**

Josée Dubois, MD and C. Matthew Hawkins, MD, Moderators

3:50-4:10 p.m. **Keynote Presentation**

Richard B. Towbin, MD, FACR

P159	4:10	4:20	Kukreja, Kamlesh	Developing an inpatient consult service at a large tertiary Children's hospital: process and lessons learned
P160	4:20	4:30	Hayatghaibi, Shireen	Reliability of an Updated Classification System for Adverse Events in Pediatric Interventional Radiology
P161	4:30	4:40	Cleveland, Heather	Portal Vein Recanalizations in Pediatric Liver Transplant Patients: Single Center Experience
P162	4:40	4:50	Toso, Seema	Diagnostic accuracy of ultrasound, computed tomography and wedge portography in the work-up for mesenterico-rex bypass in children with extrahepatic portal hypertension: a preliminary study
P163	4:50	5:00	Cronan, Julie	Endovascular stenting in adolescents with nutcracker syndrome
P164	5:00	5:10	Mayercik, Vera	Optimizing Pediatric Gastrojejunostomy Tube Maintenance
P165	5:10	5:20	Variyam, Darshan	Internal jugular vein tunneled central lines: To cuff or not to cuff?

3:50 PM **5:20 PM** **Technologist Session**

Lorraine Chisari, RDMS, RVT, Moderator

3:50-4:10 p.m. **Quality Roles in Imaging**
Nikki D. Butler, BMSc, RT(R)(QM)

4:10-4:30 p.m. **Creating Educational Videos**
Dana Brinson, BHA RT(R) and Jesse Green, RT(R)

4:30-4:50 p.m. **Panel Workflows for Image Quality Review**
Michelle Garza, (RTR) and Nikki D. Butler, BMSc, RT(R), (QM)

4:50-5:20 p.m. **Questions and Answers**

5:20 PM **Adjourn**

7:00 PM **10:30 PM** **Reception and Annual Banquet** (*separate registration fee applies)*

COLOR KEY

Scientific Session
General Postgraduate Course
Body Imaging Postgraduate Course
General Session
Sunrise/Midday Session
Technologist Program

SATURDAY – MAY 19, 2018

6:45 AM – 8:00 AM **Continental Breakfast**

6:30 AM – 12:00 PM **Registration**

7:00 AM – 7:50 AM **US Protocol Session (Non-CME Session)**
Monica Epelman, MD and Cicero T. Silva, MD, Moderators

7:00-7:01 a.m. **Introduction & Welcome**
7:01-7:30 a.m. **Ultrasound of Necrotizing Enterocolitis: Protocol, Pearls and Pitfalls**
Alan Daneman, MD
7:30-7:45 a.m. **Ultrasound of Vascular Anomalies: What the Interventionalist Want to Know**
Craig M. Johnson, DO
7:45-7:50 a.m. **US Protocol Session**

8:00 AM – 12:00 PM **Education Session – Creating a Teaching Portfolio: Getting Promoted on The Teaching Track**
Mahesh M. Thapa, MD and Janet R. Reid, MD, FRCPC, *Moderators*
Joe Otjen, MD, Michael Francavilla, MD and Brian R. Hopely, Proctors

8:00-8:10 a.m. **Introductions and Overview**
Mahesh M. Thapa, MD
8:10-8:20 a.m. **What is the Teaching Portfolio?**
Mahesh M. Thapa, MD
8:20-8:30 a.m. **Teaching Portfolio for Trainees**
Paula N. Dickson, MD
8:30-9:00 a.m. **Hands-on Exercise**
9:00-9:20 a.m. **What Makes a Good Teaching Philosophy?**
Janet R. Reid, MD, FRCPC
9:20-9:50 a.m. **Hands-on Exercise**
9 50-10:00 a.m. **Questions and Answers**
10:00-10:10 a.m. **Break**
10:10-10:20 a.m. **What Counts as Teaching**
Janet R. Reid, MD, FRCPC
10:20-10:50 a.m. **Hands-on Exercise**
10:50-11:10 a.m. **How to Digitally Keep Track of Your Teaching Activities and Productivity**
Anh-Vu H. Ngo, MD
11:10-11:40 a.m. **Hands-on Exercise**
11:40-12:00 p.m. **Wrap-up**

8:00 AM – 12:00 PM **Young Practitioners: The Future of Pediatric Interventional Radiology (SAM Session)**
Leah E. Braswell, MD and Manish N. Patel, DO, Moderators

8:00-8:30 a.m. **Transplant Interventions**
Jared R. Green, MD
8:30-9:00 a.m. **GI Interventions**
Anne Gill, MD
9:00-9:30 a.m. **GU Interventions**
Seth E. Vatsky, DO
9:30-9:45 a.m. **Discussion**
9:45-10:00 a.m. **Break**
10:00-10:30 a.m. **Aneurysmal Bone Cysts**
Leah E. Braswell, MD
10:30-11:00 a.m. **Venous Access**
Craig M. Johnson, DO
11:00-11:30 a.m. **Program Growth and Leadership**
C. Matthew Hawkins, MD
Nghia “Jack” Vo, MD
11:30-12:00 p.m. **Discussion**

SATURDAY – MAY 19, 2018 *(continued)*

8:00 AM 12:00 PM **Pediatric Neuroradiology Session (SAM Session)**

Laura L. Hayes, MD and Judith Gadde, DO, Moderators

8:00-8:25 a.m. **Eye(s) Have a Clue**
Timothy N. Booth, MD

8:25-8:50 a.m. **Imaging Approach of Congenital Ear Anomalies**
Caroline D. Robson, MBChB

8:50-9:15 a.m. **Current Concepts of Autoimmune Encephalitis**
Manohar Shroff, MD

9:15-9:40 a.m. **Emergent Neuroimaging for Suspected Acute Pediatric Stroke**
Susan Palasis, MD

9:40-10:05 a.m. **The Child with Intractable Seizures**
Erin S. Schwartz, MD

10:05-10:20 a.m. **Break**

10:20-10:45 a.m. **The New Molecular Classification of Pediatric Brain Tumors: Implications for the Radiologist**
Zoltan Patay, MD, PhD

10:45-11:10 a.m. **Treatment Related Complications in Pediatric Brain Tumors**
Dennis W. W. Shaw, MD

11:10-11:35 a.m. **Neuroimaging Evaluation of Hydrocephalus and Increased Intracranial Pressure**
Asim F. Choudhri, MD

11:35-12:00 p.m. **Update on Posterior Fossa Malformations**
Thierry A. G. M. Huisman, MD

8:00 AM 12:00 PM **Oncology Session (SAM Session)**

Adina L. Alazraki, MD, FAAP and Stephan D. Voss, MD, PhD, Moderators

8:00-9:50 a.m. **General Oncology**

8:00-8:05 a.m. **Introduction**
Adina L. Alazraki, MD, FAAP

8:05-8:25 a.m. **Bone Tumor Update**
Kelley W. Marshall, MD

8:25-8:50 a.m. **Whole Body Imaging in Cancer Predisposition Syndrome**
Stephan D. Voss, MD, PhD

8:50-9:10 a.m. **CNS Manifestations in Cancer Predisposition Syndromes**
Sarah S. Milla, MD, FAAP

9:10-9:35 a.m. **Pros and Cons of PET-CT and PET-MRI in Pediatric Oncology**
Michael S. Gee, MD, PhD and Lisa J. States, MD

Novel Radiotracers for Oncologic Imaging

9:35-9:50 a.m. Scott E. Snyder, PhD

9:50-10:05 a.m. **Break**

10:05-12:00 p.m. **Rare Tumors**

10:05-10:30 a.m. **Thyroid Cancer: From Diagnosis to Treatment**
Marguerite T. Parisi, MD, MS

10:30-10:55 a.m. **Neuroendocrine Tumors: What's New in Imaging?**
Andrew T. Trout, MD

10:55-11:20 a.m. **Zebras in Pediatric Oncology**
Sue C. Kaste, DO

11:20-11:40 a.m. **Update on RECIST**
M. Beth McCarville, MD

11:40-12:00 p.m. **Cases in Oncology: Audience Response**
Adina L. Alazraki, MD, FAAP
Helen R. Nadel, MD, FRCPC

COLOR KEY

Scientific Session
General Postgraduate Course
Body Imaging Postgraduate Course
General Session
Sunrise/Midday Session
Technologist Program

SATURDAY – MAY 19, 2018 *(continued)*

8:00 AM 12:00 PM **Hands-On Ultrasound Session: How to Do It Right!**
Kassa Darge, MD, PhD, Monica Epelman, MD and Marta Hernanz-Schulman, MD, FACR, Moderators

8:00-8:30 a.m. **Session 1: Ultrasound of the Vomiting Infant**
8:00-8:15 a.m. **US of the Vomiting Infant**
Marta Hernanz-Schulman, MD, FACR

8:*15-8:30 a.m.* **Hands-on Session**
Station 1: Marta Hernanz-Schulman, MD, FACR
Station 2: Monica Epelman, MD & Edward Arroyo, RDMS
Station 3: Lamont Hill, RDMS
Station 4: Jason Hooper, BS, RDMS, RVT
Station 5: Maria Smith, BS, RDMS, RVT

8:30-8:40 a.m. **Transition – Intro to Session 2**

8:40-9:55 a.m. **Session 2: Contrast Ultrasound**
8:40-8:55 a.m. **Intravenous Contrast Enhanced US**
Susan J. Back, MD
8:55-9:10 a.m. **Intravesical Contrast Enhanced US**
Jeanne Chow, MD
9:10-9:55 a.m. **Hands-on Session**
Station 1: **Preparation of Ultrasound Contrast Agents**
Laura Poznick, AAS, RDMS and Brandi Kozak, RDMS
Station 2: **Imaging of Microbubbles: A Teach Yourself Session**
Kassa Darge, MD, PhD
Station 3: **Imaging of Microbubbles: A Teach Yourself Session**
Jeanne Chow, MD and Trudy Morgan, RDMS
Station 4: **Simulation of Contrast Enhanced Voiding Urosonography**
Susan J. Back, MD and Sphoorti Shellikeri, MSc

9:55-10:10 a.m. **Break**

10:10-10:40 a.m. **Session 3: Ultrasound Elastography**
10:10-10:25 a.m. **US Elastography**
Jonathan R. Dillman, MD, MSc

10:25-10:40 a.m. **Hands-on Session**
Station 1: Monica Epelman, MD and Edward Arroyo, RDMS
Station 2: Jonathan R. Dillman, MD, MSc
Station 3: Trudy Morgan, RDMS
Station 4: Brandi Kozak, RDMS
Station 5: Maria Smith, RDMS, RVT

10:40-10:50 a.m. **Transition – Intro to Session 4**

10:50-11:20 a.m. **Session 4: Ultrasound of the Lungs**
10:50-11:05 a.m. **US of the Lung Parenchyma - Technique**
Monica Epelman, MD
11:05-11:20 a.m. **Hands-on Session**
Station 1: Monica Epelman, MD
Station 2: Maria Smith, RDMS, RVT
Station 3: Edward Arroyo, RDMS
Station 4: Brandi Kozak, RDMS
Station 5: Cicero T. Silva, MD

11:20-11:30 a.m. **Transition – Intro to Session 5**

11:30-12:00 p.m. **Session 5: Ultrasound of the Orbits**

11:30-11:45 a.m. **US of the Orbits**
Cicero T. Silva, MD

11:45-12:00 p.m. **Hands-on Session**
Station 1: Cicero T. Silva, MD
Station 2: Kassa Darge, MD, PhD
Station 3: Lamont Hill, RDMS
Station 4: Monica Epelman, MD
Station 5: Ricardo Faingold, MD
Station 6: Edward Arroyo, RDMS and Maria Smith, BS, RDMS, RVT

8:00 AM 12:00 PM **Technologist Session**
Laura Gruber, MBA, RT(R), RDMS, RVT, Michelle Garza, (RTR), Moderators

8:00-8:30 a.m. **Ultrasound Research**
Brandi Kozak, RDMS

8:30-8:50 a.m. **MR Fetal**
Kimberly Ritze, BS, RT(R), CT, MR

8:50-9:10 a.m. **Tiny Transjugular Intrahepatic Portosystemic Shunts (TIPS) for Kids**
Ray Ramoso, ARRT (r) (vi)

9:10-9:30 a.m. **MR Cardiac**
Marty Jones, MHA, RT (R)(MR)

9:30-9:50 a.m. **CT to Shield or Not to Shield**
Georgiena Prevett, MS, RT(R)(N) (CT)(MR), CNMT (CT)

9:50-10:10 a.m. **MR Safety**
Trista Raymer, RT (R)(CT)(MR)

10:10-10:20 a.m. **Questions and Answers**

10:20-10:35 a.m. **Break**

10:35-10:55 a.m. **NM Seizure Imaging**
Joseph MacLean, CNMT

10:55-11:15 a.m. **PET/MR Brain Imaging**
Elad Nevo MS, RT(MR)(N)(CT), CNMT

11:15-11:35 a.m. **IR (Boney Ablations)**
Michael Payne, RT

11:35-11:55 a.m. **Panel of Research in Imaging Overview of the Infrastructure of Research, Consenting, Protocols, Training**
Kimberly Ritze, BS, RT, CT, MR John Dell
Laura Gruber, MBA, RT(R), RDMS, RVT

11:55-12:00 p.m. **Questions and Answers**

12:00 PM **Meeting Adjourn**

COLOR KEY

Scientific Session
General Postgraduate Course
Body Imaging Postgraduate Course
General Session
Sunrise/Midday Session
Technologist Program

SCIENTIFIC PAPERS

Authors are listed in the order provided. An author listed in bold identifies the presenting author.

Paper #: 001

Inter-radiologist Agreement Using Society of Abdominal Radiology-Society for Pediatric Radiology-American Gastroenterological Association Consensus Nomenclature for Reporting CT and MR Enterography in Pediatric Small Bowel Crohn Disease

Mitchell Rees, MD[1], *mitchellrees@gmail.com*; Jonathan Dillman, MD, MSc[1], Alexander Towbin, MD[1], Ethan Smith, MD[1], Christopher Anton, MD[1], Mantosh Rattan, MD[1], Bin Zhang, PhD[1], Andrew Trout, MD[1]; [1]Radiology, Cincinnati Children's Hospital Medical Center, Cincinnati, OH

Disclosures: All authors have disclosed no financial interests, arrangements or affiliations in the context of this activity.

Purpose or Case Report: To assess inter-radiologist agreement using newly devised consensus recommendations for reporting CT/MR enterography exams in pediatric small bowel Crohn disease (CD), which were developed by the SAR-AGA and endorsed by several organizations including the Society for Pediatric Radiology.
Methods & Materials: A single investigator identified 25 CT and 25 MR pediatric enterography exams (January 2015 - April 2017) with the following distribution of ileal CD severity based on clinical interpretations: normal or chronic CD without active inflammation (40%), active inflammatory CD (20%), stricturing CD (20%), and penetrating CD (20%). 5 fellowship-trained pediatric radiologists, blinded to one another and imaging reports, documented major imaging findings and impressions based on SAR-AGA consensus recommendations. Inter-radiologist agreement was evaluated using Fleiss' multi-rater kappa.
Results: Inter-radiologist agreement (Table) was moderate for bowel wall enhancement pattern (0.41 [95% CI: 0.36-0.46]), degree of wall thickening (0.41 [95% CI: 0.35-0.47]), presence of intramural edema at MRI (0.47 [95% CI: 0.34-0.59]), presence of stricture (0.59 [95% CI: 0.52-0.65]), presence of penetrating disease (0.60 [95% CI: 0.51-0.68]) and presence of perianal disease (0.43 [95% CI: 0.34-0.52]); and was fair for presence of ulcerations (0.37 [95% CI: 0.28-0.46]) and presence of sacculations (0.31 [95% CI: 0.23-0.40]). Agreement for standardized impressions was substantial for stricturing disease (0.79 [95% CI: 0.70-0.87]); and moderate for degree of inflammation (0.49 [95% CI: 0.44-0.56]) and presence of penetrating disease (0.58 [95% CI: 0.49-0.67]).
Conclusions: Agreement was fair to moderate for major imaging findings of CD. Agreement was moderate to substantial for standardized impressions. Additional radiologist education is needed to decrease variability in standardized reporting of small bowel CD.

Paper #: 002

Accuracy of Magnetic Resonance Enterography in the Assessment of Pediatric Inflammatory Bowel Disease of the Colon in Patients Undergoing Colectomy

John Karpewycz. MBBS[1], *john.karpewycz@sickkids.ca*; Shilpa Radhakrishnan[1], Natashia Seemann[1], Sebastian King[2], Iram Siddiqui[1], Jacob Langer[1], Mary-Louise Greer[1]; [1]Hospital for Sick Children, Toronto, ON, Canada, [2]Royal Children's Hospital, Melbourne, VIC, Australia

Disclosures: All authors have disclosed no financial interests, arrangements or affiliations in the context of this activity.

Purpose or Case Report: Magnetic Resonance Enterography (MRE) is often performed in Pediatric Inflammatory Bowel Disease (PIBD), in accordance with the Porto Criteria. While primarily focused upon assessing small bowel, MRE also includes the colon. The purpose of this study was to obtain sensitivities and specificities of MRE findings in unprepared colon in comparison with post-colectomy histopathology. We aimed to determine whether MRE was an effective modality for assessing the colon in these patients.
Methods & Materials: This study has Ethics Board approval. A retrospective review was performed to identify all patients who underwent MRE < 2 years prior to colectomy for PIBD, between 2000 and 2014. Pre-colectomy MRE was independently reviewed in a segmental fashion by two pediatric radiologists, blinded to the initial radiology reports, clinical and pathology data. The five segments assessed were the cecum/ ascending colon, transverse, descending, sigmoid colon and rectum. Bowel wall MRE findings for review included thickening >3mm, T2 hyperintensity, gadolinium enhancement, diffusion restriction, ulceration, penetrating lesions and colonic stricturing (Fig. 1). Mesenteric MRE findings reviewed were 'comb sign', fibrofatty proliferation, T2 hyperintensity and gadolinium enhancement. This was reviewed with histopathology findings of acute or chronic inflammation or fibrosis. Frequency, sensitivity and specificity of MRE findings, relative to abnormal histopathology, were calculated per colonic segment. P-values were obtained using Fisher's exact test (P-value < 0.05 significant).
Results: Twenty patients (M:F = 8:12) met the inclusion criteria. The mean age was 11.8 years (SD 8.0 - 15.6 years) at clinical diagnosis of PIBD and 14.0 years (SD 11.3 - 16.7 years) at colectomy. An MRE diagnosis of Ulcerative Colitis (UC) was present in 15 patients (75%). Mean time from MRE to colectomy was 197 days (Table 1). Of 100 colonic segments evaluated,

71were considered abnormal on MRE, and 95 were abnormal on histopathology. No colonic segment considered abnormal on MRE was normal on histopathology. The finding of any abnormality on MRE had a statistically significant sensitivity of 0.75, with bowel wall thickening and bowel wall T2 hyperintensity being the most sensitive (Table 2).
Conclusions: MRE assessment of the colon is highly specific, with no colonic segment falsely considered abnormal. Overall, MRE is modestly sensitive, with bowel thickening and bowel wall T2 hyperintensity being the most sensitive individual findings.

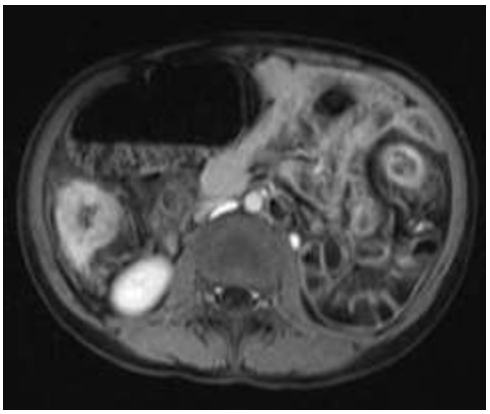

MRE Finding	Number of Segments affected, number (%)	Sensitivity	Specificity	p-Value
Any abnormal MRE finding	71 (71%)	0.75	1	0.0016
Bowel wall findings				
Bowel wall thickening (>3mm)	65 (65%)	0.68	1	0.0043
Bowel wall T2 hyperintensity	61 (61%)	0.64	1	0.0076
Bowel wall gadolinium enhancement	44 (44%)	0.46	1	0.065
Bowel wall Diffusion Restriction (85 segments assessed with DWI)	35 (42%)	0.42	1	0.14
Bowel wall ulceration	15 (15%)	0.16	1	1.0
Penetrating Lesion (Abscess or Fistula)	1 (1%)	0.01	1	1.0
Stricture	11 (11%)	0.12	1	1.0
Mesentery findings				
Comb sign	33 (46%)	0.35	1	0.17
Fibrofatty Proliferation	21 (30%)	0.22	1	0.58
T2 hyperintensity	7 (10%)	0.07	1	1.0
Mesenteric gadolinium enhancement	8 (11%)	0.08	1	1.0

Table 2: Frequency, sensitivity, specificity and p-Value of MRE imaging findings of the colon in patients pre-colectomy versus histopathology findings

Patient Demographics	
Gender, M/F, Number (%)	8 (40%) / 12 (60%)
Age at Diagnosis (years), Average (Range)	11.8 (3 – 17)
Age at Surgery (years), Average (Range)	14 (7 – 17)
Time between last pre-operative MRE and Colectomy (days), Average (Range)	197 (4 – 612)
MRE Diagnosis, Number (%)	
Ulcerative Colitis	15 (75%)
Crohn`s Disease	3 (15%)
IBD-U	1 (5%)
Normal MRE	1 (5%)
Pathology Diagnosis, Number (%)	
Ulcerative Colitis	16 (80%)
Crohn`s Disease	2 (10%)
IBD-U	2 (10%)

Table 1: Patient Demographics, MRE diagnosis following blinded consensus double read and pathology diagnosis.

Paper #: 003

Comparison of Three Oral Contrast Preparations for Magnetic Resonance Enterography in Pediatric Crohn's Disease Patients: A Randomized Trial

Ravi Gottumukkala, MD[1], *ravig3@gmail.com*; Annette LaPointe[1], Donna Sargent[1], Michael Gee, MD, PhD[1]; [1]Radiology, Massachusetts General Hospital, Boston, MA

Disclosures: All authors have disclosed no financial interests, arrangements or affiliations in the context of this activity.

Purpose or Case Report: To compare three magnetic resonance enterography (MRE) oral preparations in pediatric Crohn's disease patients with respect to patient-reported metrics of tolerability and radiologist-determined exam quality.
Methods & Materials: 47 pediatric patients (mean age 14.9 yrs, 57% female) with known Crohn's disease referred for MRE were randomized to an oral preparation with a sugar alcohol-based flavored beverage (Breeza, n = 15), polyethylene glycol preparation (Miralax, n = 14), or low-density barium sulfate suspension (VoLumen, n = 18). Patients were instructed to consume up to 1080 ml of oral contrast (360 ml every 15 min) beginning 50-60 min prior to MRE imaging and offered the opportunity to switch preparations. Following MRE, patients completed a questionnaire regarding their oral prep including: taste (1-5 scale), feeling of well-being (1-5 scale), and willingness to consume again (y/n). Two radiologists reviewed all MRE exams and rated exams for global features (active disease, overall small bowel distention [1-4 scale]) and features specific to individual small bowel segments (length of distention, maximal luminal diameter, opacification, and susceptibility artifact). Statistical methods included one-way ANOVA with Tukey's honest difference and Fisher's exact test.
Results: Crossover to a different preparation occurred in 7 patients (15%) and was significantly more frequent when the initial preparation was VoLumen versus one of the other two agents (33% vs. 3%, $p = 0.009$). Mean subjective taste ratings for both Miralax (3.6, $p < 0.0001$) and Breeza (2.8, $p = 0.035$) were superior to VoLumen (1.9), which persisted regardless of MRE evidence of active Crohn's disease. A trend toward increased patient willingness to drink Miralax again (83%) compared with VoLumen (57%) did not reach significance ($p = 0.13$). Ratings of well-being were similar among groups ($p = 0.16$). Overall small bowel distention and bowel segment-specific metrics (distention, maximal diameter, opacification, and susceptibility) did not significantly differ among groups.
Conclusions: In pediatric Crohn's disease patients, Miralax and Breeza are rated as more palatable than VoLumen, and all three preparations achieve a similar degree of small bowel distension and opacification on MRE. These results suggest that patients should be given a choice of oral contrast preparations, as a sizable proportion may need to switch to a different agent in order to ingest the requisite oral contrast volume.

Paper #: 004

Breeza vs. VoLumen for Pediatric CT and MR Enterography: a Prospective, Randomized, Blinded Patient Acceptability Study

Jonathan Dillman, MD, MSc[1], *jonathan.dillman@cchmc.org*; Alexander Towbin, MD[1], Rebecca Imbus, BA[1], Erica Gates, Associates Degree of Applied Science[1], Julie Young, AAS[1], Andrew Trout[1]; [1]Department of Radiology, Cincinnati Children's Hospital Medical Center, Cincinnati, OH

Disclosures: All authors have disclosed no financial interests, arrangements or affiliations in the context of this activity.

Purpose or Case Report: To prospectively compare patient acceptance of two neutral (negative) oral contrast materials used for pediatric CT and MR enterography using a randomized, blinded approach.
Methods & Materials: IRB approval was obtained for this prospective, HIPAA-compliant study; informed consent and assent were obtained. 65 pediatric patients (<18 years-old) undergoing clinically-indicated CT or MR enterography examinations where enrolled and randomized to receive one of two different neutral oral contrast materials (Breeza Flavored Beverage for Neutral Abdominal/Pelvic Imaging; Beekley Medical or VoLumen Barium Sulfate Suspension; Bracco Diagnostics). Patients and investigators (other than the CT or MRI technologist and clinical research coordinator) were blinded to the oral contrast material administered. For each subject, the following were documented: age, sex, if the prescribed weight-based oral prep was completed, and if the patient vomited during or after drinking the oral prep. After oral prep completion, subjects were asked to rate the taste and texture of the oral contrast material they received on a scale from 0 to 10, with 0=very bad and 10=very good. Patients also were asked to rate how they felt about their overall health state on that day of imaging, with 0=poor and 10=great. Taste, texture, and overall health state were compared between the two contrast material cohorts using unpaired t-tests. Proportions were compared using Fisher's exact tests.
Results: 33 subjects received Breeza, while 32 subjects received VoLumen. There was no difference in mean age (p=0.59) or sex distribution (p>0.99) for patients receiving Breeza (13.5 ± 2.6 years, 15 females [45%]) versus VoLumen (13.8 ± 2.8 years, 14 females [44%]). There was no difference in overall health state between the two contrast material cohorts (p=0.28). 28/33 (85%) subjects completed the prescribed oral prep when consuming Breeza, while 17/32 (53%) subjects completed the prescribed prep when consuming VoLumen (p=0.007). Breeza received higher mean taste (6.1 ± 2.5 vs. 2.8 ± 2.6; p<0.0001) and texture scores (7.3 ± 2.3 vs. 3.6 ± 3.0; p<0.0001) than VoLumen. No subject consuming Breeza vomited during or after the oral prep, while 1/32 (3%) subjects consuming VoLumen vomited (p=0.49).
Conclusions: Pediatric patients undergoing CT and MR enterography tolerate Breeza better than VoLumen, with Breeza more likely to result in oral prep completion. This is likely in part due to Breeza having a preferred taste and texture.

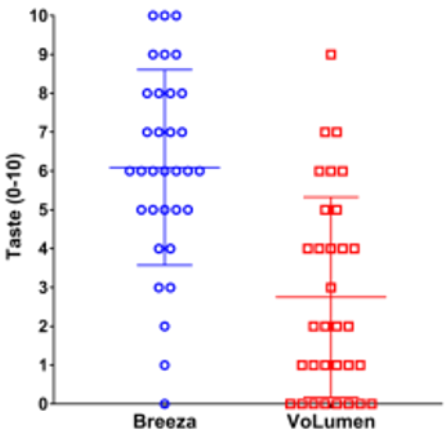

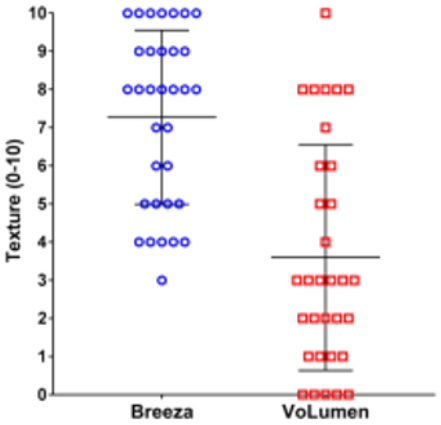

Paper #: 005

Use of Small Bowel Ultrasound to Predict Response to Infliximab Induction

Jungwhan Choi, MD[1], *jungwhan.choi@mountsinai.org*; Becky Phan, BSc[1], Marla Dubinsky, MD[1], Henrietta Rosenberg, MD[1]; [1]Kravis Children's Hospital at Mount Sinai, New York, NY

Disclosures: All authors have disclosed no financial interests, arrangements or affiliations in the context of this activity.

Purpose or Case Report: Small bowel ultrasound (SBUS) is emerging as first line imaging for Crohn's disease given its wide availability, low cost, lack of radiation and ability for dynamic imaging. The purpose of this study is to evaluate the use of SBUS in pediatric Crohn's disease to assess response to infliximab therapy in conjunction with inflammatory markers and markers of mucosal healing.
Methods & Materials: Children with Crohn's disease requiring infliximab therapy were prospectively enrolled. Clinical activity, laboratory tests (ESR, CRP and fecal calprotectin) and SBUS were evaluated at baseline (T0) and following 14 weeks of therapy (T1). Quantitative and qualitative ultrasound parameters were evaluated: disease extension (cm); bowel wall thickness (mm); presence of bowel wall hyperemia, strictures, creeping fat, free fluid, abscess, and / or obstruction; and degree of bowel dilatation, peristalsis, and stool burden.
Results: 13 patients were included. All patients achieved clinical remission at T1 ($p < 0.01$) as well as statistically significant decrease in ESR and CRP ($p < 0.01$). Patients with decreased fecal calprotectin (69%) showed a decrease in bowel wall thickness and disease extension at T1 (4.9 ± 1.5 mm and 6.8 ± 3.8 cm versus 5.5 ± 1.0 mm and 11.3 ± 1.4 cm at baseline, respectively). In patients with increased fecal calprotectin (31%) there was an increase in bowel wall thickness and disease extension at T1 (3.9 ± 0.7 mm and 4.6 ± 2.3 cm versus 2.6 ± 1.0 mm and 3.2 ± 3.2 cm at baseline, respectively), despite clinical remission. The number of patients with bowel wall hyperemia, free pelvic fluid and creeping fat decreased at T1. The presence of stricture and degree of bowel dilatation, stool burden and peristalsis did not change at T1.
Conclusions: Although caution is needed due to the small sample size, data suggests that SBUS in conjunction with fecal calprotectin can predict response to therapy with infliximab, despite clinical remission.

Paper #: 006

Contrast Enhanced Ultrasound of the Bowel in Children with Suspected Inflammatory Bowel Disease (IBD).

Ami Gokli[1], *aag298@nyu.edu*; David Biko, MD[1], Anush Sridharan, PhD[1], Carolina Maya, MD[1], Máire Conrad[1], Sudha Anupindi, MD[1]; [1]Children's Hospital of Philadelphia, Philadelphia, PA

Disclosures: All authors have disclosed no financial interests, arrangements or affiliations in the context of this activity.

Purpose or Case Report: Contrast enhanced ultrasound (CEUS) is a promising technique which has been well established and FDA approved for the characterization of liver lesions in children; however, CEUS has several other pediatric applications. In this study we describe our initial experience with CEUS for evaluation of inflammatory bowel disease (IBD), including feasibility, safety, technical imaging factors, dosing and qualitative/quantitative assessment.
Methods & Materials: A total of 12 subjects (mean age 8, range 3-13) had CEUS of the bowel for suspected or confirmed diagnosis of IBD over a 16-month period. In all studies, an initial baseline gray-scale bowel US was performed followed by a focused CEUS exam of abnormal loops of bowel with intravenous Lumason®. Baseline gray-scale images were evaluated for bowel wall thickening, degree of hyperemia, and extraluminal findings. Initially qualitative assessment of the bowel wall enhancement was made. Quantitatively, peak enhancement and wash-out curves were calculated (Figs. 1,2). Imaging results were correlated with colonoscopy, histopathology, genetics and inflammatory markers. Imaging protocols were also evaluated to optimize study quality. Safety profile and dosing for each patient were recorded.
Results: For our cohort, diagnoses were Crohn disease (n=8) and indeterminate colitis (n=3). One (n=1) was too early in the disease process for definitive diagnosis. We identified a total of 23 diseased bowel segments. CEUS qualitatively identified at least one segment of active bowel inflammation in all subjects correlating with clinical and gray-scale evaluation. Quantitative analysis was performed in all subjects. In four patients, time to peak confirmed active inflammation, which correlated with gray-scale features of bowel wall thickening, hyperemia, with pathology performed within 0-10 months of sonogram, and with positive inflammatory markers (CRP, ESR, fecal calprotectin). Adaptations of our protocol were made throughout the study in response to reassessment of image quality with our average contrast dose per injection being 1.07 mL/ 0.044 mL/kg (range 0.016-0.078mL/kg). The average number of injections performed per exam was three. No adverse events occurred with contrast injection.
Conclusions: Our pilot study shows CEUS is feasible and can easily and safely identify actively inflamed bowel in IBD patients. With technique optimization, CEUS can be a promising alternative to conventional MRE, obviating the need for sedation or gadolinium.

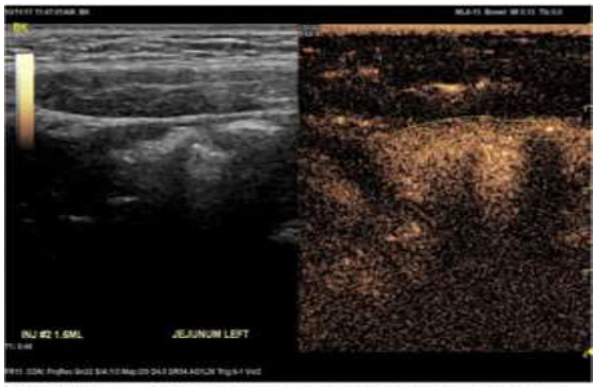

(a) Dual-screen ultrasound representation of abnormal segment of bowel with grey scale (left) and contrast enhanced (right) image of matching segment. CEUS image demonstrates transmural enhancement, two ROIs within the most enhancing region of the anterior bowel wall have been manually drawn. The calculated time to peak is 5.8 sec.

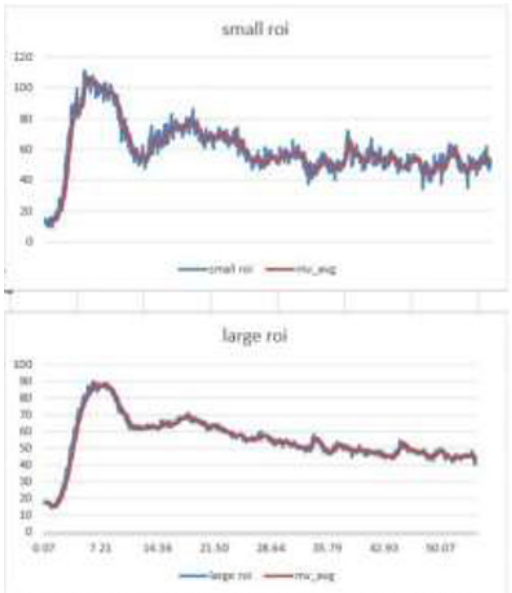

(b) Post-processing results obtained from raw data. Time intensity curves are generated from the manually drawn ROIs on the CEUS portion of the dual image; a curve is created for both ROIs separately. Curves demonstrate fast wash-in indicative of active inflammation.

Paper #: 007

Inter-reader Reliability Study of a New MRI Scoring System for TMJ Evaluation in JIA with the Use of Measurement Aids: Special Interest Group from the MRI in JIA in OMERACT

Mirkamal Tolend[15], *mirkamal.tolend@sickkids.ca*; Christian Kellenberger, MD[2], Thitiporn Junhasavasdikul, MD[3], Shelly Abramowicz, DMD, MPH[4], Julien Aguet, MD[2], Simone Appenzeller, MD, PhD[6], Linda Arvidsson, DDS, PhD[5], Emilio Inarejos Clemente[7], Saurabh Guleria, MD[8], Jacob Jaremko, MD, PhD[9], Thekla von Kalle, MD[10], Eva Kirkhus, MD, PhD[11], Bernd Koos, DMD[12], Tore Larheim, DDS, PhD[5], Arthur Meyers, MD[13], Elka Miller, MD[14], **Jyoti Panwar, MD[15]**, Zachary Peacock, DMD, MD[16], Cory Resnick, DMD, MD[17], Jennifer Stimec[1], Nikolay Tzaribachev, MD[18], George Tomlinson, PhD[15], Brian Feldman, MD, MSc[1], Andrea Doria, MD, PhD, MSc[1]; [1]The Hospital for Sick Children, Toronto, ON, Canada, [2]University Children's Hospital Zürich, Zürich, Switzerland, [3]Ramathibodi Hospital, Bangkok, Thailand, [4]Children's Healthcare of Atlanta, Atlanta, GA, [5]University of Oslo, Oslo, Norway, [6]University of Campinas, Campinas, Brazil, [7]Hospital Sant Joan de Deu, Barcelona, Spain, [8]Austin Radiological Association, Austin, TX, [9]University of Alberta, Edmonton, AB, Canada, [10]Radiologisches Institut, Olgahospital Klinikum,

Stuttgart, Germany, [11]Oslo University Hospital, Oslo, Norway, [12]University Hospital Tübingen, Tübingen, Germany, [13]Nemours Children's Hospital, Orlando, FL, [14]Children's Hospital of Eastern Ontario, Ottawa, ON, Canada, [15]University of Toronto, Toronto, ON, Canada, [16]Massachusetts General Hospital, Boston, MA, [17]Boston Children's Hospital, Boston, MA, [18]Pediatric Rheumatology Research Institute, Bad Bramstedt, Germany

Disclosures: Arthur Meyers has indicated a relationship with Amirsys and Elsevier for receiving royalties. All other authors have disclosed no financial interests, arrangements or affiliations in the context of this activity.

Purpose or Case Report: Contrast-enhanced MRI remains the best available modality to detect and monitor juvenile idiopathic arthritis (JIA)-related inflammation and damage in the temporomandibular joint (TMJ). A multi-institution, multi-disciplinary group recently drafted a new MRI scoring system for TMJ in JIA for standardizing diagnostic assessment and for use as an outcome measure.
Objectives: 1) To test the inter-reader reliability of the new consensus scoring system, 2) to compare its reliability to previous independently-developed scoring systems, 3) to assess the effect of measurement aids (atlas and tutorial) on improving inter-reader reliability among radiologists and non-radiologists.
Methods & Materials: Thirty-one MRI exams of bilateral TMJs were scored independently using the new scoring system by 15 radiologists, 2 oral-maxillofacial surgeons, 2 pediatric rheumatologists, and 1 orthodontist. Thirteen readers were randomized into two groups: group 1 read without, and then with a pictorial grading atlas; group 2 read twice using the atlas, but with a calibration tutorial between readings. Group 3, consisting of 7 readers who participated in a previous study testing existing scoring systems, read once post-tutorial with the atlas. Single-measure, absolute agreement intraclass correlation coefficients of domain and total scores were calculated within the 5 radiologists in each group, and within the non-radiologists.
Results: Among radiologists, 5-reader reliabilities ranged from .60-.73 across reading methods for the inflammatory domain, .79-.82 for the damage domain, and .76-.86 for total score. Inflammatory domain reliability of initial reading improved with atlas between groups 1 and 2 (.60 vs .73, p<.01), though this was not observed within group 1 before and after using atlas. Among non-radiologists, 2- or 3-reader reliabilities ranged from .40-.69 for inflammatory, .49-.70 for damage, and .51-.76 for total scores. Inflammatory score improved after using atlas (.40 vs .68, p<0.001). When tested using the same readers (group 3) and subset of cases as the previous study, the inter-reader reliability of inflammatory domain improved compared to 3 existing scoring systems (.66 vs .34-.53, p<0.016). Reliability of radiologists in group 3 (long-term involvement in development), and group 2B (newer members) did not differ.
Conclusions: The new consensus scoring system showed good-to-excellent levels of inter-reader reliability, with improved reliability in the inflammatory domain compared to 3 previous scoring systems.

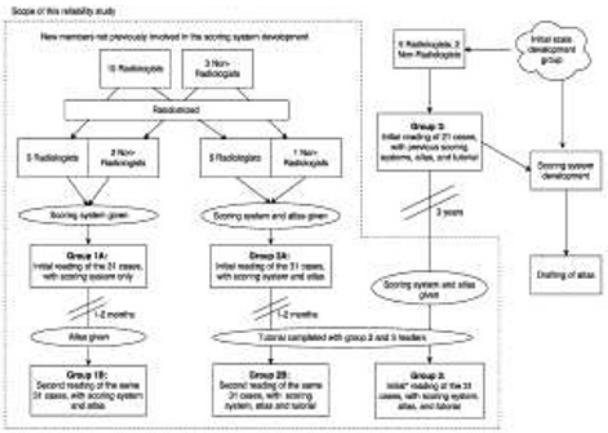

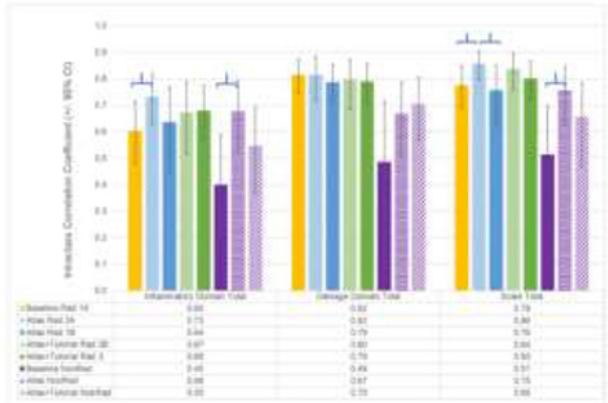

Figure 2: Inter-reader reliability of domain and total scores. Inflammatory domain is rated 0-8, the damage domain 0-5, total score 0-13. Grades are ordinal, but due to the high number of categories and for comparability, ICC coefficients were used. Error bars represent 95% confidence intervals (CI). Abbreviations: 1A, initial reading of group 1; 1B, second reading of group 1, with atlas; 2A, initial reading of group 2, with atlas; 2B, second reading of group 2, with atlas and post-tutorial; 3, initial reading of group 3, with atlas and post-tutorial; NonRad, non-radiologists; Rad, radiologists. "[" indicates statistical significance (p<0.01).

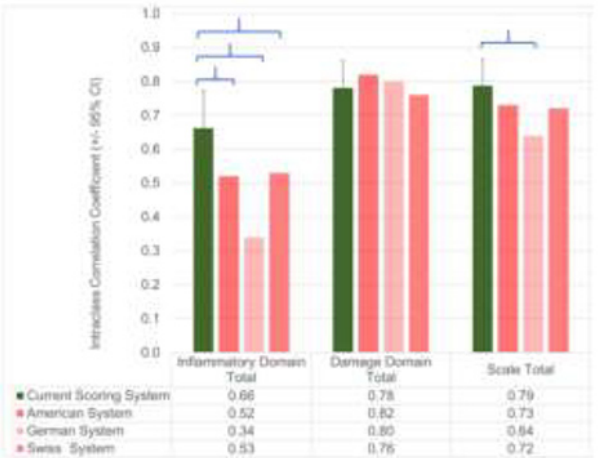

Figure 3: Inter-reader reliability of the current scoring system compared with existing systems, using the same group of readers and cases as a previous reliability exercise. Red bars represent point values of domain and scale total scores from the previous scoring systems. "[" indicates statistical significance (p<0.016).

Paper #: 008

Modified Friedman Technique: A New Proposed Method of Measuring Glenoid Version in the Setting of Glenohumeral Dysplasia

Matthew Ditzler, MD[1], *mgditzle@texaschildrens.org*; J. Kan, MD[1], Maddy Artunduaga, MD[1], Siddharth Jadhav, MD[1], Bryce Bell, MD[2], Wei Zhang, PhD[1], Robert Orth, MD, PhD[1]; [1]Pediatric Radiology, Texas Children's Hospital, Houston, TX, [2]Texas Children's Hospital, Houston, TX

Disclosures: All authors have disclosed no financial interests, arrangements or affiliations in the context of this activity.

Purpose or Case Report: Glenoid version angles (GVAs) are routinely measured to objectively follow changes related to glenohumeral dysplasia (GHD) in the setting of brachial plexus birth palsy. The technique for measuring GVA based on cross sectional imaging was initially described by Friedman et al. Recent literature for non-dysplastic shoulders advocates the use of more time-consuming reconstruction and reformation techniques for an accurate assessment of the GVA. The purpose of this study was to investigate the validity of Friedman's method compared with true-axial reformations (TARs) produced on a 3D workstation, and a new, proposed modified Friedman technique we developed.
Methods & Materials: 60 shoulders from 30 bilateral shoulder MRIs performed in patients 6-48 months to evaluate GHD from 2013-17 were reviewed. Five pediatric radiologists performed GVA measurements using Friedman's method, a modified Friedman's method, and a previously described TAR method. The modified Friedman's method generates a GVA with two lines: 1) along the glenoid articulating margin, and 2) between the glenoid midpoint and the anteromedial scapula at the most cephalad axial image with the acromion (Figs. A,B). Readers were blinded to their own and others' measurements. Inter-rater agreement and angle comparisons were assessed using intraclass correlation (ICC) and linear mixed model analysis.
Results: ICC measured 0.56-0.62 in normal shoulders and 0.81-0.83 in dysplastic shoulders. GVA measurements were significantly different when comparing Friedman's method to TARs in normal shoulders (-9.9±6.1° vs -8.1±5.4°; P<0.0001) and dysplastic shoulders (-33.4±17.7° vs -27.9±16.9°; P<0.0001). GVA measurements were significantly different when comparing the modified Friedman's method to TARs in normal shoulders (-5.4±6.4° vs -8.1±5.4°; P<0.0001) but were not significantly different in dysplastic shoulders (-27.7±18.2° vs -27.9±16.9°; P=0.45).
Conclusions: The original Friedman method overestimated the degree of glenoid retroversion compared to the TAR method in both normal and dysplastic shoulders. In contrast, GVAs measured using the modified Friedman method were not statistically different than those generated using TARs in dysplastic shoulders. The modified Friedman technique is less time consuming because 3D post-processing is not necessary compared with TARs. Future studies employing a non-inferiority design will be necessary to determine whether the modified Friedman technique can replace TARs for measuring GVA in children with GHD.

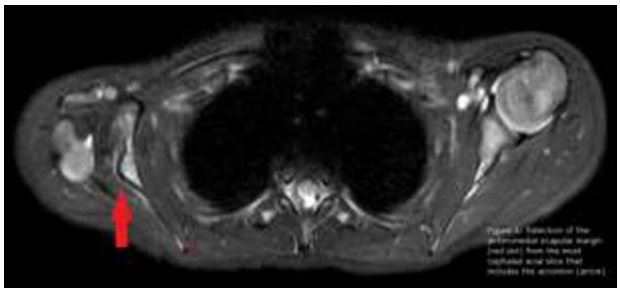

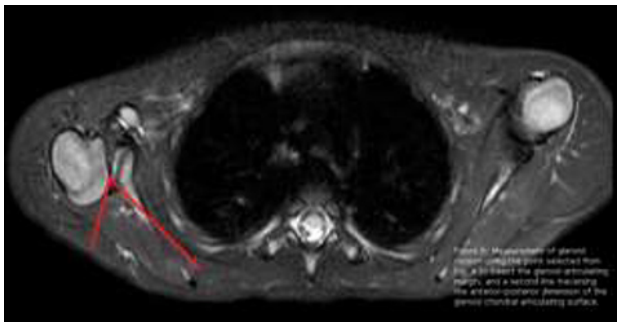

Paper #: 009

Advancements in Pediatric Wrist and Thumb Imaging: Sonography in Normal Infants

Kathryn Milks, MD[1], *ks.mueller@gmail.com*; Patrick Warren[1], James Popp, MD[1], Julie Samora, MD[1]; [1]Radiology, Nationwide Children's Hospital, Columbus, OH

Disclosures: All authors have disclosed no financial interests, arrangements or affiliations in the context of this activity.

Purpose or Case Report: We described the normal appearance and anatomy of the lateral carpus and base of the thumb by ultrasound in infants, to establish normative references based on age and body surface area (BSA). We hypothesize that characterization of the normal sonographic appearance of the pediatric base of the thumb and carpus will aid in preoperative assessment of infants with thumb hypoplasia.
Methods & Materials: Institutional review board (IRB) approval was obtained for this single-center pilot study. Healthy infants less than 12 months of age were enrolled. Infants with a known syndrome or musculoskeletal disorder were excluded. All enrolled participants underwent an ultrasound exam of the base of the thumb from the distal radial epiphysis through the first metacarpal was performed using a high frequency linear transducer. A pediatric radiologist acquired images. Longitudinal and transverse images as well as still and cine clips were obtained. Tissue contact was enhanced with the use of either a waterbath or standoff pad.
Results: Ultrasonographic evaluation of the base of the thumb was performed in 9 healthy infants (aged 8.9 ± 4.5 weeks, BSA 0.27 ± 0.032 m^2, 56% female). Our protocol measured craniocaudal (CC) and anterior-posterior (AP) dimensions in the scaphoid (triangle), trapezium (plus), and first metacarpal epiphysis (diamond); measurement were successful among all participants (Fig.1&2). The first metacarpal epiphysis was measured in three planes (CC, AP, and transverse). Assuming an elliptical shape, the areas of the scaphoid, trapezium, and first metacarpal epiphysis measured (mean ± SD) 0.23 ± 0.042 cm^2, 0.19 ± 0.066 cm^2, 0.11 ± 0.021 cm^2, respectively. Area of the trapezium correlated well with age (by ordinary least squares regression, $r^2 = 0.592$) and BSA ($r^2 = 0.602$). Areas of the scaphoid and first metacarpal epiphysis demonstrated fair

correlation with age (r^2 = 0.389 and 0.178, respectively) and relatively poorer correlation with BSA (r^2 = 0.326 and 0.116, respectively). The area ratio of the scaphoid/trapezius (mean ± SD, 1.31 ± 0.34) exhibited the least variability.
Conclusions: Our data suggest that ultrasound is well suited for the evaluation of the carpus and base of thumb in infants. Data serves as a reference against which wrist and thumb abnormalities can be compared. To our knowledge, this is a novel acquisition protocol and the first description of ultrasonographically-derived normative data of this sort, which represent the study's primary strengths.

Paper #: 010

Lulun II: Ultrasound Evaluation of Bone Age in Rural Ecuadorian Children

Jennifer Nicholas, MD, MHA[1], *jenniferlynn444@gmail.com*; Katherine Douglas, BA[1], Sarah True[2], David Habif, MD[2], Melissa Chapnick, RD, MPH[2], Carlos Andres Gallegos Riofrio[2], William Waters, PhD[3], Lora Iannotti, PhD[2]; [1]Washington University School of Medicine, Saint Louis, MO, [2]Washington University Brown School of Social Work and Public Health, Saint Louis, MO, [3]Universidad de San Francisco de Quito, Quito, Ecuador

Disclosures: All authors have disclosed no financial interests, arrangements or affiliations in the context of this activity.

Purpose or Case Report: Stunted growth (height-for-age Z < -2) is an indicator of chronic undernutrition. Worldwide, over 155 million children under five years are stunted. Undernutrition contributes to almost half of all deaths in young children. This project aimed to test the use of portable ultrasound technology in the field to determine bone age in rural Ecuadorian children and investigate the association of the ultrasound measures with nutritional status of the children.
Methods & Materials: Ecuadorian children (n=129) from Cotopaxi Province in Ecuador participated in the Lulun II study which was a cohort follow-up to Lulun I, a randomized controlled study that evaluated the impact of eggs in early complementary feeding. Targeted ultrasounds of the hand and wrist were performed by a pediatric radiologist, a medical student, or a graduate student in public health within the children's homes and schools.
Unique search pattern algorithms were developed for girls and boys based upon to the expected ossification centers at each interval defined by Greulich and Pyle. A Philips Lumify L12-4 broadband linear array transducer connected to a Samsung Galaxy tablet with an Android platform was used to perform the ultrasounds. Images were stored on the hard drive of the Samsung tablet and were evaluated by a pediatric radiologist who was blinded to the age of the child at the time of the interpretation.
Results: Children (boys, n=70; girls, n=59) were on average 33.9 mo (±1.78). Mean Z score for bone age in this population was -1.32 (±1.1), while for girls it was -1.01 (±0.95) and boys, -1.57 (±1.2). The overall Z score for height in boys and girls combined was -2.06 (±0.90) and -0.78 (±0.73) for weight. Mean height-for-age Z (HAZ) scores for girls was -1.88 (±0.88), and for boys -2.22 (±0.89) Weight-for-age Z score (WAZ) for girls was -0.78 (±0.73), and for boys -0.76 (±0.73). Bone age Z scores were positively correlated with HAZ (r=0.27), but not other anthropometric measures (r=0.04 for WAZ and -0.19 for BMIZ). Linear regression modeling demonstrated that HAZ, female sex of the child, and frequency of intake for milk and eggs significantly and positively predicted bone age Z for children (R^2=0.17; p<0.001).
Conclusions: Bone age in children around 3 years of age determined using a portable ultrasound device correlates to height-for-age in children with stunted growth and may prove to be an important tool in the evaluation of children's nutritional status and response to nutrition intervention in the field.


ULTRASOUND BONE AGE SCANNING ALGORITHM

1. radius and ulna (trans)
2. radial epiphysis (long)
3. distal and proximal carpal rows (trans/long)
4. 2nd metacarpal-phalangeal joint (long)

Age in months	BOY	GIRL
48	• trapezium • all phalanges	• scaphoid • trapezoid (five carpal centers)
42	• 2nd distal • 5th distal	• trapezium (by thumb)
36	• lunate	• lunate
30 girl 32 boy	• thumb metacarpal • thumb proximal • triquetral • 2nd middle • 2nd distal • 5th distal •	• 2nd distal • 5th middle
24	• 5th metacarpal • 5th proximal • 3rd middle and distal • 4th middle and distal	• triquetral • thumb metacarpal • thumb proximal
18	• 2nd metacarpal • 2nd proximal • 3rd metacarpal • 3rd proximal • 4th metacarpal • 4th proximal • thumb distal	• 5th metacarpal • 5th proximal
15	• radial head epiphysis	• 4th metacarpal • thumb distal
12	• nothing new	• distal radial epiphysis • 2nd metacarpal • 2nd proximal • 3rd metacarpal • 3rd proximal • 4th proximal
3	• capitate • hamate	• capitate • hamate

Paper #: 011

Digital X-ray Metacarpal Radiogrammetry and Dual X-ray Absorptiometry in Mexican Children and Adolescents

Mariana Sánchez Curiel Loyo[1] *marianascl@hotmail.com*; [1]Radiology, Children's Hospital of Mexico Federico Gómez, Mexico City, Mexico

Disclosures: All authors have disclosed no financial interests, arrangements or affiliations in the context of this activity.

Purpose or Case Report: Dual X-ray absorptiometry (DXA) is the most widely accepted and used technique to asses bone mineral density. However, in our country its use is limited by the high costs and lack of equipment with pediatric software. The BoneXpert software provides an automated radiogrammatic method to assess skeletal age. The program calculates the Bone Health Index (BHI), a measure of cortical thickness and mineralization, which is obtained from indices of three metacarpal bones. The purpose is to evaluate the correlation and concordance between BHI and DXA in healthy Mexican children and adolescents.
Methods & Materials: A cross-sectional study was conducted. We included 409 participants between 5 to 18 years, recruited from public and private schools in Mexico City. We obtained an anteroposterior radiography of the non-dominant hand for all participants. The images were analyzed using the BoneXpert® to obtain the BHI. In addition, we obtained a DXA readings of total body and lumbar vertebrae using a pediatric iDXA GE/V.15. We analyzed the correlations (Pearson correlation coefficients) and the concordance (Bland-Altman plots) between BHI and DXA. Local Committee approval HIM2015-055 / HIM2017-058.
Results: The BHI showed a positive correlations with the DXA readings for bone mineral density (r=0.658 to r=0.803; p<0.001); with similar results between boys (r= 0.614 to r=0.817; p<0.001)

and girls (r=0.711 to 0.815; p<0.001). We also observe positive correlations between BHI and bone mineral content by DXA, although with less magnitude (r=0.657 to r=0.753; p<0.001). The Bland-Altman plots showed good agreement between BHI Z-score and bone mineral density Z-score by DXA in boys (mean difference of -0.414, limits of agreement -2.683 to 1.855, Pitman test p=0.338) and girls (mean difference 0.126, limits of agreement -2.190 to 2.442, Pitman test p=0.455).
Conclusions: The digital X-ray metacarpal radiogrammetry measured by BoneXpert has a good correlation and adequate concordance with DXA in healthy children. However, it's necessary to evaluate their utility in diseases that affect bone density before considering it as a diagnostic method of bone health in children.

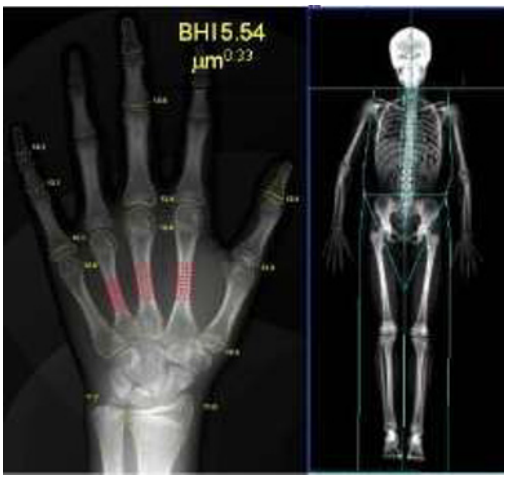

Paper #: 012

Fibro-Adipose Vascular Anomaly (FAVA): A review of imaging features

Mohammad Amarneh, MD[1], *dr.amarneh@gmail.com*; Murali Surnedi, MD[1], Raja Shaikh, MD[1]; [1]Boston Children's Hospital/ Harvard Medical School, Boston, MA

Disclosures: All authors have disclosed no financial interests, arrangements or affiliations in the context of this activity.

Purpose or Case Report: FAVA is a newly delineated complex vascular anomaly with unique clinical, radiologic and histopathologic features, first described by Alomari in 2014. Since its first description, there is still confusion, under recognition, and lack of awareness of the clinical and imaging features of this anomaly, which have led to incorrect diagnosis and improper treatment. The purpose of this presentation is to describe the clinical and imaging features of FAVA and how to distinguish it from other vascular anomalies and soft tissue tumors.
Methods & Materials: We conducted a retrospective study on all the FAVA cases diagnosed by our vascular anomaly center. We reviewed the medical records, and radiological studies including MRI, ultrasound, plain radiography, and angiography.
Results: We had a total of 46 FAVA lesions in 36 patients. The majority of the lesions were in the extremity. Up to this date, this is by far the largest series of FAVA in the literature. Pathologic diagnosis was confirmed in 17 patients. Three different patterns were noticed: focal, focal infiltrative and diffuse patterns.
Conclusions: FAVA has clinical and radiological features distinct from other common vascular anomalies and soft tissue tumors. Early recognition of this entity is crucial to direct proper management and avoid significant morbidity.

Paper #: 013

The Utility of Percutaneous Image Guided Tumor Ablation in the Treatment of Solid and Vascular Tumors in the Pediatric Population

Amie Robinson, BSRT(R)(MR)[1], *alrobinson@cmh.edu*; Travis Brown, DO[2], Hasnain Hasham, MD[3], Neil Maitra[2], Brent Cully, MD[1], Brenton Reading, MD[1], Stephanie Theut[1], Katherine Chastain, MD[1], Richard Hendrickson, MD[1], Kimberly Reid, MS[1], Douglas Rivard, DO[1]; [1]The Children's Mercy Hospital, Kansas City, MO, [2]University of Missouri - Kansas City, Kansas City, MO, [3]University of Kansas Medical Center, Kansas City, KS
Disclosures: All authors have disclosed no financial interests, arrangements or affiliations in the context of this activity.

Purpose or Case Report: Percutaneous image guided tumor ablation (PTA) is a minimally invasive image guided technique that utilizes thermal energy to treat a variety of lesions. The development of procedures like PTA for the treatment of solid and vascular tumors has been studied extensively in adults and found to have increased survival, decreased morbidity, and improved quality of life. This innovation in adult interventional radiology provides the template for new minimally invasive therapies in the pediatric population. The goal of this study is to evaluate improvement in patient quality of life, pre-and post-procedure pain, and imaging response to treatment. Our study aims to lay the groundwork for incorporating minimally invasive IR procedures/techniques to pediatric oncology protocols.
Methods & Materials: We conducted a single site retrospective cohort study evaluating patients 0-21, whom underwent PTA from January 2008 to July 2017. Clinical information about the patients underlying condition, surgical and treatment history, pre- and post-pain scales and imaging data were evaluated. Local institutional review board approval was obtained for this study.
Results: A total of 46 PTA procedures were performed on 38 pediatric patients. A little over half of the patients were female (n=22, 57.9%) and the average age was 11.3 ± 4.7 years. Majority were solid tumors (n=33, 86.8%) and five (13.2%) were vascular malformations. Over half were treated with radiofrequency ablation (n=26, 61.9%), 13 (31%) with cryoablation and three (7.1%) with microwave ablation. Three-fourths of PTA procedures were performed due to lack of response to prior therapies (n=35, 76.1%), followed by pain control (n=29, 63%). In evaluation of pre- and post-procedural pain, 25 (65.8%) reported moderate pain and three (7.9%) severe pain pre-procedure. During follow-up clinic visits, six patients (15.8%) reported mild pain at one-month, two (5.3%) at six-months and four (10.5%) at one-year post-PTA. Evaluation of tumor burden pre- and six-month post-PTA showed a 22.5% (± 49.2) mean decrease in tumor volume and 26.8% (± 35.7) decrease in CC dimension, 10.1% (± 42.2) in transverse and 16.5% (± 41.5) in AP measurements.
Conclusions: The use of percutaneous image guided tumor ablation is safe for pediatric patients with vascular or solid tumors refractory or not amendable to traditional therapies with a majority experiencing decreased pain and improved quality of life post procedure.

Paper #: 014

Cryoablation of benign soft tissue lesions in children: initial experience

Derek Roebuck[1], *Derek.Roebuck@gosh.nhs.uk*; Alex Barnacle, BM[1], Premal Patel, BM[1], Samantha Chippington, BM[1]; [1]Radiology, Great Ormond Street Hospital for Children, London, United Kingdom

Disclosures: All authors have disclosed no financial interests, arrangements or affiliations in the context of this activity.
Purpose or Case Report: Cryoablation is used increasingly commonly for treatment of benign soft tissue lesions in adults. There is little experience of cryoablation in children. Our aim was to evaluate the feasibility of cryoablation for benign soft tissue lesions in children.
Methods & Materials: Cases were retrospectively reviewed. Data was obtained from a prospectively maintained IR procedural database, RIS records and case-note review. This service was approved by the institution's New Procedures Panel. Institutional review board approval was not required by our institution for this retrospective review.
5 procedures were performed in 4 children (3 male). Median age was 4.5 years (range 1.4 - 11.1) and weight 17.3 kg (range 6.9 - 40). The anatomical location and biopsy-proven diagnoses were: calf fibroadipose vascular anomaly, thigh venous malformation, shoulder microcystic lymphatic malformation and chest wall hamartoma. Treatment indications included pain (n=3), lesion size (n=3), failure to thrive (n=1).
Results: Procedures were performed under anaesthesia with ultrasound (n=5) and/or cone-beam CT guidance (n=3), using the SeedNet Gold™ (Galil Medical Inc. MN, USA) ablation system (each time with 3 probes and 2 standard freeze-thaw cycles). Technical success was 100%. In-patient stay was 1-5 days. One patient required intravenous analgesia, fluids and nutrition for 3 days. Pain was resolved in 2/3 and significantly reduced in 1/3. Lesion volume reduced by 69-94% (measured in 2 patients). The patient failing to thrive has gained weight and improved her developmental milestones.
Conclusions: Cryoablation is technically feasible for benign soft tissue lesions in children. Initial experience suggests it is well-tolerated and effective.

Paper #: 015

A combined retrospective and prospective single-institution review of image-guided needle biopsy of relapsed or refractory neuroblastoma with a focus on the use of pre-biopsy MIBG imaging to predict tumor characteristics

Abhay Srinivasan[1], *srinivasaa@email.chop.edu*; Andrew Samoyedny[2], Lisa States, MD[1], Sphoorti Shellikeri, Master's in Biomedical Engineering[1], John Maris, MD[1], Yael Mosse, MD[1], Seth Vatsky, DO[1], Michael Acord, MD[1], Fernando Escobar[1], Christopher Edgar[1], Anne Marie Cahill[1];[1]The Children's Hospital of Philadelphia, Philadelphia, PA, [2]Drexel University College of Medicine, Philadelphia, PA

Disclosures: Anne Marie Cahill has indicated a relationship with All other authors have disclosed no financial interests, arrangements or affiliations in the context of this activity.

Purpose or Case Report: Relapsed neuroblastoma (NBL) that is refractory to conventional chemotherapy may be amenable to therapies specific to mutations. Eligibility for such therapies demands adequate biopsy for genetic profiling. We describe our experience with image-guided core biopsy of NBL for genetic profiling, with additional assessment of the potential value of pre-biopsy ^{123}I-methyliodobenzylguanidine (MIBG) scan for predicting tumor characteristics.
Methods & Materials: Metrics in this combined retrospective and prospective study include biopsy technique, complications, adequacy for tumor genetic analysis, and pre-biopsy MIBG measurements that may predict a sample's positivity, tumor cell percent, and mutational status.
Results: Tissue cores were successfully obtained from 100% of the 64 biopsies (27 soft tissue; 37 bone) performed on 45 children (M=26; F=19; mean age=102 months). 51/64 biopsies were deemed NBL-positive by pathology.
In 54/64 cases submitted for genetic profiling, adequacy for tumor genetic profiling (i.e. next-generation sequencing or specific mutational analysis) was achieved in 35/54 biopsies (65%). One of 64 biopsies (2%) resulted in a major complication. Four of 64 biopsies (6%) resulted in minor complications.
Lesion intensity on MIBG was qualitatively determined in comparison to liver uptake. MIBG-avidity was seen in 56 lesions, of which 47 were tumor-positive (PPV=84%). Compared against lesions with MIBG=liver, lesions with MIBG>liver had a significantly higher incidence of: tumor positivity upon biopsy (91% vs. 56%, P=0.049), biopsy tumor cell percentage (32% vs 20%, P=0.034), and presence of at least one NBL mutation of interest to our study (*N-Myc* amplification; ALK, CDK 4/6, and Ras/MAPK pathway mutations) (75% vs 17%, P=0.012). No such differences were found with lesions with MIBG<liver, although the number of this subset was small.
Conclusions: Image-guided core needle biopsy is a feasible procedure with moderate utility for obtaining relapsed or refractory NBL tumor samples for genetic analysis. MIBG uptake had a good predictive value for tumor-positivity upon biopsy. Lesions with a high MIBG uptake relative to liver may have a higher incidence of tumor-positivity, tumor cell %, and mutations of interest than less MIBG-avid lesions. Further study on quantitation of MIBG uptake for predicting NBL biopsy yield and tumor characteristics may be useful.

Biopsy NBL positivity by anatomical location

Lesion General Location	N	NBL+ Biopsies	% NBL +	% Marrow-Confined Lesions	% Bone Destruction Lesions	% Soft Tissue Lesions
Pelvic	25	20	80%	64%	16%	20%
Abdominal	10	6	60%	0%	0%	100%
Spinal	10	9	90%	80%	0%	20%
Lower limb	8	6	75%	88%	0%	12%
Thoracic	6	5	83%	33%	17%	50%
Upper limb	3	3	100%	67%	0%	33%
Cervical	1	1	100%	100%	0%	0%
Skull	1	1	100%	0%	100%	0%

MIBG signal intensity relative to liver vs. Biopsy NBL positivity

	Number of lesions	NBL + Lesions	% NBL +
MIBG Intensity > liver	35	32	91%
MIBG Intensity = liver	9	5	56%
MIBG intensity < liver	15	11	73%

MIBG intensity relative to liver vs. Biopsy tumor cell %

	Number of lesions	% Tumor Cells in Biopsy	Std Dev
MIBG Intensity > liver	30	36%	32%
MIBG Intensity = liver	8	13%	20%
MIBG intensity < liver	15	23%	29%

Paper #: 016

Comparison of MR guided joint injection with a fluoroscopic approach for pediatric MR arthrography

Abhay Srinivasan[1], *srinivasaa@email.chop.edu*; Sphoorti Shellikeri, Master's in Biomedical Engineering[1], Anne Marie Cahill[1], Victor Ho-Fung, MD[1], Randolph Setser[2], Michael Acord, MD[1], Seth Vatsky, DO[1], Fernando Escobar[1]; [1]Radiology, Children's Hospital of Philadelphia, Philadelphia, PA, [2]Siemens Medical Solutions Inc., Hoffman Estates, IL

Disclosures: Randolph Setser has indicated a relationship with Siemens Healthineers for having a salary. All other authors have disclosed no financial interests, arrangements or affiliations in the context of this activity.

Purpose or Case Report: We report our initial experience with combined MR-interventional and diagnostic shoulder MR arthrography (MRA) and study the efficacy of MR-guided (MRG) injection, comparing technical success, diagnostic quality, and procedure times to fluoroscopic-guided (FG) injection and subsequent MRA.

Methods & Materials: MRG injection of the shoulder performed on pediatric patients from Jan-Oct 2017 were included, as were age-matched FG injections from Jan 2016-Feb 2017. Technical success, complications and procedure times were compared. Diagnostic scans were evaluated by a musculoskeletal radiologist, using a Likert score for joint distension (1: optimal; 0: suboptimal), and contrast extravasation (grades 0 to 3).

Results: 39 patients (mean age 16 y) underwent MRG injection on a 3 Tesla scanner and 42 patients underwent FG injections (mean age 17 y). Procedure technique was similar between groups, with an anterior approach in all cases.

Technical success rates were 97.4% in MRG and 100% in FG procedures, with one MRG procedure aborted due to sedation reaction. There were no immediate procedure-related complications for either modality. The mean interventional procedure time for FG arthrograms was significantly lower than for MRG (16±10 min vs. 23±13 min, $p=0.01$), but the total interventional and diagnostic MRI procedure time was significantly lower for MRG cases (57±14 min vs. 78±21 min, $p<0.05$). Mean transition time from the procedure to diagnostic MR scan was significantly lower in MRG cases compared to FG cases (8±6 min vs. 31±17 min, $p<0.05$).

In all MRG and FG cases, the joint distension was optimal. Gadolinium extravasation rates were also similar between the groups: grade 0 in one FG case (2%); grade 1 in 24 MRG (63%) and 28 FG cases (67%); grade 2 in 9 MRG (24%) and 10 FG cases (24%), grade 3 in 5 MRG (13%) and 3 FG cases (7%). The diagnoses were: Normal: 4 (MRG), 7 (FG); labral tear: 23 (MRG) and 20 (FG); and other lesions (shoulder impingement/ dislocation, torn ligament, etc.): 11 (MRG) and 15 (FG). On follow-up, one MRG arthrogram patient reported new pain attributable to the procedure.

Conclusions: MRG injection of the shoulder can be successfully performed with low complications, real-time visualization of the needle and contrast, no ionizing radiation, and potential increased workflow efficiency. Technical success and diagnostic adequacy was similar among both modalities. Procedure times suggest MRG joint injections may be a feasible entry procedure in instituting an interventional MRI service.

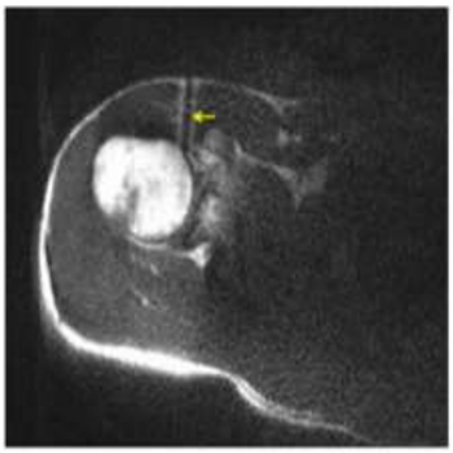

Figure 1a. MR-guided shoulder arthrogram of a 17 year-old male patient with a history of right anterior shoulder dislocation. The PD-weighted image demonstrates the needle introduced into the glenohumeral joint space

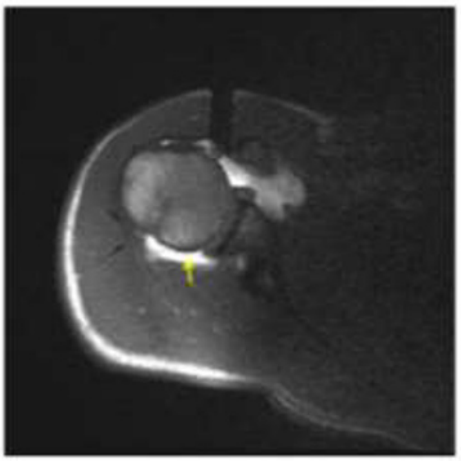

Figure 1b. Real-time T1-weighted image demonstrates the injected gadolinium

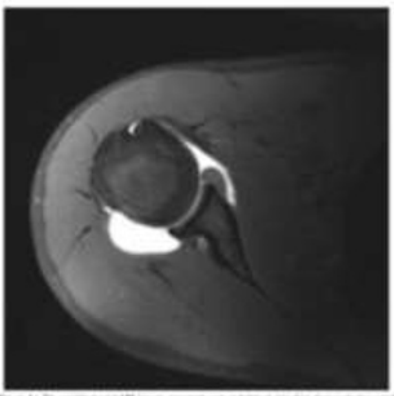

Figure 1c. T1-weighted axial MR image acquired post gadolinium injection demonstrates good distention of the joint capsule. Diagnosis: Hill-Sachs lesion with associated extensive anterior labral tear and SLAP component, and torn/absent middle glenohumeral ligament

Paper #: 017

Surveillance Cerebral Angiography in Children with Arteriovenous Malformations: How many vessels should be interrogated?

Michael Acord, MD[1], *acordm@email.chop.edu*; Anne Marie Cahill[1], Fernando Escobar[1], Seth Vatsky, DO[1], Abhay Srinivasan[1]; [1]The Children's Hospital of Philadelphia, Philadelphia, PA

Disclosures: All authors have disclosed no financial interests, arrangements or affiliations in the context of this activity.

Purpose or Case Report: Surveillance cerebral angiography following arteriovenous malformation (AVM) intervention in children includes interrogation of the bilateral internal or common carotid arteries and a single vertebral artery. The purpose of this study was to assess whether additional clinical information is gained from imaging all major intracranial vessels. In the absence of such data, surveillance angiography may be limited to the vascular territory of the prior AVM, thereby potentially decreasing the risks associated with arterial catheterization as well as radiation and contrast exposure.
Methods & Materials: A retrospective study of all surveillance cerebral angiograms was performed at a single tertiary pediatric hospital from January 1, 2007 through April 17, 2017 in patients with a history of an AVM. Patients with hereditary hemorrhagic telangiectasia were excluded. Basic demographic and AVM characteristics-- including the feeding vessel(s), Spetzler-Martin grade and subsequent intervention performed--were recorded. Data abstracted from the subsequent surveillance angiograms included vessels injected, number of angiographic runs, radiation dose, findings, and complications occurring up to 30 days post-procedure.
Results: 55 patients (30 males, 54.5%) underwent 105 surveillance angiograms during the study period (mean age, 13.8±4.2 years). Recurrence was found in 24 studies (22.9%), all in the territory of the initial AVM. Additional runs ranged from 1-8 (median 2) adding additional radiation exposure of 4356.4±4019.5 μGy-m^2 (n=64). No findings prompting changes in clinical management were discovered when examining other vascular territories. There were 2 (0.02%) non-permanent complications, 1 flow limiting spasm and 1 small air embolus, which occurred when catheterizing a non-territorial vessel.
Conclusions: In this single center study, no clinically relevant data were gained from catheterizing additional vessels during surveillance angiography. This suggests these exams may be tailored to interrogating the vascular territory relevant to the initial AVM.

Paper #: 018

A novel approach to deep tissue intra-operative imaging using indocyanine green fluorescence

Rohan Bhavane[1], *rcbhavan@texaschildrens.org*; Zbigniew Starosolski, PhD[1], Ketan Ghaghada, PhD[1], Ananth Annapragada, PhD[1]; [1]Pediatric Radiology, Texas Children's Hospital, Houston, TX

Disclosures: Rohan Bhavane has indicated a relationship with Sensulin, LLC for receiving stock options and royalty. Ananth Annapragada has indicated a relationship with Alzeca Inc. and Sensulin, LLC for receiving stock options as well as intellectual property rights, and receives research grants with the NIH and Alzeca, Inc. All other authors have disclosed no financial interests, arrangements or affiliations in the context of this activity.

Purpose or Case Report: Indocyanine green (ICG) near-infrared (NIR) fluorescence angiography provides a safe and rapid method for intraoperative evaluation of vessel and anastomotic patency in pediatric cardiac surgical reconstructions, and more recently, has shown utility in guiding tumor resection for hepatoblastoma patients. However, ICG fluorescence imaging, currently performed in NIR-I window (700-900 nm), is limited by tissue scattering to visualization of structures less than 3 mm below the surface. Fluorescence imaging in NIR-II window (1000-1700 nm wavelength) could greatly improve the penetration depth. In this work, we investigated the suitability of FDA-approved ICG as a NIR-II imaging agent for deep tissue imaging.
Methods & Materials: Fluorescence emission spectra (900-1500 nm) of ICG were collected in saline, plasma and ethanol. In vitro and in vivo imaging studies were performed using a novel fluorescent-imaging prototype that enabled simultaneous imaging in NIR-I and NIR-II windows. Liver tissue phantom inserted with ICG-filled capillary tubes were imaged in NIR-I and NIR-II window for visualization of deep vascular mimicking structures. *In vivo* studies of ICG fluorescence angiography were performed in hind limb and abdominal region of nude mice (n=6) to compare visualization of deep vascular structures in NIR-I and NIR-II imaging. Dynamic images were acquired before, during and after intravenous bolus administration of ICG (2 mg/kg). Contrast-to-noise ratio (CNR) were calculated.
Results: ICG demonstrated NIR-II fluorescence emission that strongly depended on the media. ICG fluorescence imaging in liver tissue phantom demonstrated visualization of structures at 3mm and 6mm depth in NIR-II window; the 6 mm structure was not visible in the clinically-used NIR-I window (Fig 1). CNR values were significantly ($p < 0.05$) higher in NIR-II window (18.4 +/- 0.6 at 3 mm depth and 5.6 +/- 0.4 at 6 mm depth) compared to NIR-I window (11.2 +/- 0.7 at 3 mm depth). *In vivo* vascular imaging in nude mouse demonstrated higher vessel conspicuity in NIR-II window compared to NIR-I window (Fig 2). Delayed abdominal imaging (~ 1 h post-administration of ICG) demonstrated higher CNR and improved edge conspicuity of bowel and intestines in NIR-II (Fig 3).
Conclusions: Strong ICG fluorescence in the NIR-II window permits visualization of deep structures with improved contrast-to-noise ratio when compared to clinically used NIR-I imaging. Translation of NIR-II imaging to the clinic is indicated.

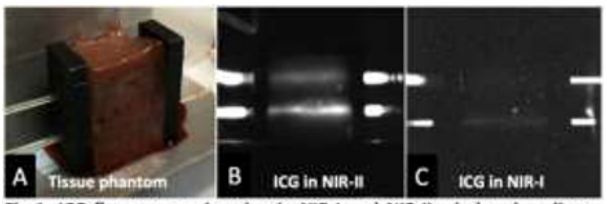

Fig 1. ICG fluorescence imaging in NIR-I and NIR-II window in a liver tissue phantom. (A) Colored photo showing liver tissue phantom containing ICG-filled capillary tubes mimicking vascular structures at depth of 3 mm (bottom tube) and 6 mm (upper tube). (B) NIR-II imaging demonstrates visualization of both 3 mm and 6 mm tubes; (C) NIR-I imaging only demonstrates visualization of 3 mm deep tube.

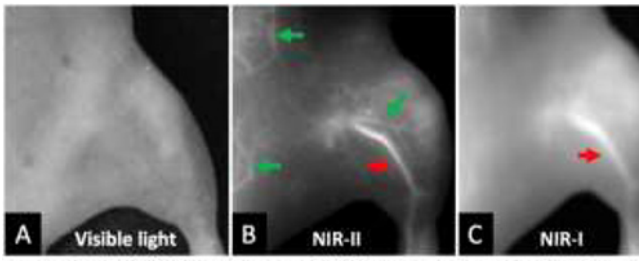

Fig 2. *In vivo* ICG fluorescence angiography in hind limb region of mouse. ICG fluoresce imaging in NIR-II window demonstrated improved visualization of vascular structures compa to imaging in NIR-I window. Vessel conspicuity for femoral vein (red arrow) is be demonstrated in NIR-II window. Several small vessels (green arrows) are only visible in N window. NIR-I and NIR-II images were simultaneously acquired 5 minutes after intraver administration of ICG.

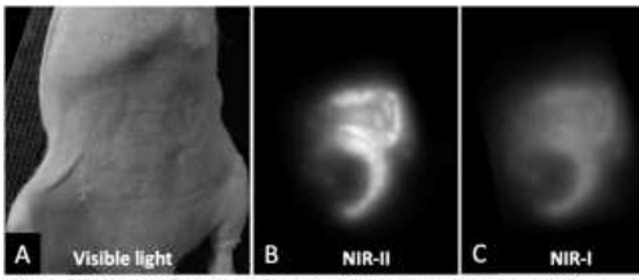

Fig 3. *In vivo* ICG fluorescence imaging of gastrointestinal structures. IC fluorescence imaging demonstrated improved visualization gastrointestinal track in NIR-II window compared to NIR-I window. NIR-I a NIR-II images were simultaneously acquired 60 minutes after intraveno administration of ICG.

Paper #: 019

Analysis of diffusion restriction in the corpus callosum in children with abusive head trauma

Deniz Altinok, MD[1], *altinokd@yahoo.com*; Aravind Mohandas, MD[1], Maera Haider, MD[1]; [1]Diagnostic Radiology, Detroit Medical Center, Royal Oak, MI

Disclosures: All authors have disclosed no financial interests, arrangements or affiliations in the context of this activity.

Purpose or Case Report: Abusive head trauma (AHT) in the pediatric age group has high morbidity and mortality, with several characteristic features on magnetic resonance imaging (MRI). This includes diffusion restriction within the brain, thought to be related to hypoxic injury. We aim to identify diffusion restriction specifically within the corpus callosum and study its association with other features on MRI.

Methods & Materials: A retrospective study was conducted including all consecutive cases with a confirmed diagnosis of AHT, based on clinical information and imaging findings, who underwent MRI examination between January 2010 and December 2016. Image acquisition was performed according to the routine protocol for suspected AHT and all cases were reviewed by an experienced pediatric neuroradiologist. Diffusion restriction in the corpus callosum, diffusion restriction in the remaining brain parenchyma, bridging vein thrombosis, subdural hemorrhage, retinal hemorrhage and cervical spinal ligament injury were tabulated. All statistical analysis was performed on SPSS.

Results: 80 children with a confirmed diagnosis of AHT underwent MRI at our institution, with an age range of 7 - 1462 days, of which 41 were boys (51.3%). Subdural hemorrhage was seen in 98.8% of cases, retinal haemorrhage in 80%, bridging vein thrombosis in 81.3% and cervical spinal ligament injury in 47.5%. 42.5% and 40% of the cases had diffusion restriction in the corpus callosum and rest of the brain parenchyma respectively. Correlation analysis using Pearson Chi square test showed a significant association between the findings of diffusion restriction in the corpus callosum with diffusion restriction in the rest of the brain parenchyma and cervical spinal ligament injury (p - 0.000002 & p - 0.008 respectively). No significant association was found between diffusion restriction in the rest of the brain parenchyma and cervical spinal ligament injury.

Conclusions: Diffusion restriction within the brain is well-documented in relation to AHT and is thought to result from hypoxic ischemic injury. However our results suggest that diffusion restriction within the corpus callosum shares a common mechanism of trauma with cervical spinal ligament injury.

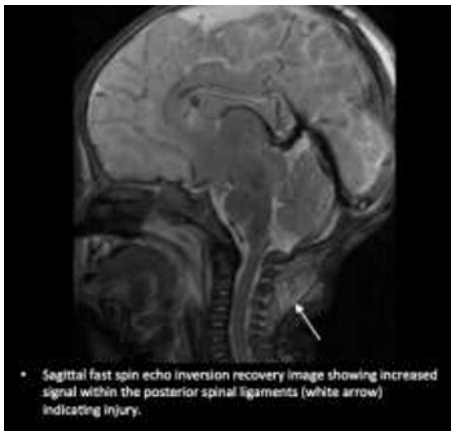

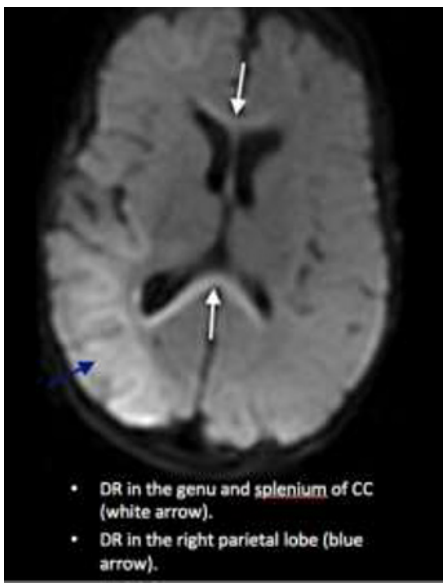

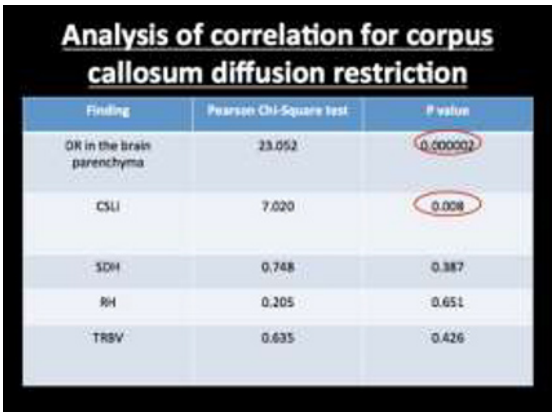

Paper #: 020

Pediatric pituitary adenoma: imaging features and clinical outcome

Daddy Mata-Mbemba, MD, PhD[1], *matadaddy@yahoo.fr*; Charles Raybaud, MD[1]; [1]The Hospital For Sick Children, University of Toronto, Toronto, ON, Canada

Disclosures: All authors have disclosed no financial interests, arrangements or affiliations in the context of this activity.

Purpose or Case Report: Pediatric pituitary adenomas are rarely reported in the literature. We aimed at identifying specific imaging features and clinical outcomes of pediatric pituitary adenomas with regard to their subtypes in this era of advanced MRI techniques.
Methods & Materials: We retrospectively reviewed the medical records of 73 consecutive pediatric (≤ 18 years) patients [age: 14.6 ± 2.4 years, Female = 54 (74%)] with radiological findings and endocrine testing consistent of pituitary adenoma who visit our institution between January 1999 and December 2016 (17-years period). On MRI, the following features of adenomas were examined: the size, demarcation (discrete or diffuse), signals patterns, presence of cystic necrosis, fluid-fluid level, hypointense rim on T2, location, mass effect and invasion of cavernous sinuses. The outcome (cured or not) was determined at 1 year after either conservative or surgical treatment. Patients were divided in prolactinomas and non-prolactinomas groups. Univariate analyses and multiple logistic regression were used accordingly.
Results: The most common pituitary adenomas was prolactinoma (79.4%). Patient with prolactinomas were older than those with non-prolactinomas (p=0.01). Prolactinomas were significantly larger and likely to bleed, to show a cystic change or fluid-fluid level, to demonstrate signal change in the follow-up studies, to extend in suprasellar fossa and to be treated conservatively ($p<0.05$, all) than non-prolactinomas. There was significant positive correlation between the size of prolactinomas and the level of prolactinemia ($\rho = 0.44$; $p<0.004$). On univariate analysis, larger size (p=0.01), diffuse adenoma with no visualisation of the normal parenchyma (p=0.01) and cavernous sinus invasion (p=0.003) were associated with worse outcome. However, on multivariate analysis, cavernous invasion was the only independent predictor of worse outcome (odd ratio= 5, p =0.01). There was no statistically significant difference in outcome between prolactinomas and non-prolactinomas.
Conclusions: Pediatric pituitary adenomas have some specific features with respects to subtypes. Some of their features could predict the worse outcome after treatment. Our result supports the current practice of first treating conservatively prolactinomas, as these patients overall yield similar outcome than non-prolactinomas which are usually treated surgically.

Paper #: 021

Potential Imaging and Neurosurgical Correlates of Molecular Subgroups of Posterior Fossa Ependymoma in Children

Noah Sabin[1], *noah.sabin@stjude.org*; Paul Klimo Jr[1], Frederick Boop[1], Thomas Merchant[1], David Ellison[1], Robert Ogg[1]; [1]St. Jude Children's Research Hospital, Memphis, TN

Disclosures: All authors have disclosed no financial interests, arrangements or affiliations in the context of this activity.

Purpose or Case Report: Recent research on pediatric ependymoma has established two distinct major molecular subgroups of posterior fossa tumors, PFA-1 and PFA-2. PFA-1 ependymomas have a genetic profile that suggest an origin in the lower brainstem while the molecular signature of PFA-2 lesions points to a source in the rostral posterior fossa. We examined whether brain imaging and reported location of tumor at surgery support distinct sites of origin for these subgroups of posterior fossa ependymoma.
Methods & Materials: A board certified pediatric neuroradiologist, without knowledge of molecular or neurosurgical findings, reviewed preoperative MRI examinations of the brain for 40 children with proven posterior fossa ependymoma. Tumor location was classified as central or lateral based on whether the mass was centered in the fourth ventricle or outside the fourth ventricle. Hydrocephalus was graded on a four-point scale: grade 0 - no evidence of hydrocephalus, grade 1 - mild ventricular enlargement, grade 2 - substantial ventricular enlargement, grade 3 - substantial ventricular enlargement with transependymal flow of cerebrospinal fluid. Operative records were reviewed by two pediatric neurosurgeons who were unaware of the molecular and neuroradiological findings. Putative tumor origin was classified as floor of the fourth ventricle, roof of the fourth ventricle, or lateral recess/cerebellopontine angle based on the operating surgeon's description in the neurosurgical record and the reviewing neurosurgeon's judgment of imaging and clinical data. Statistical analysis was performed for associations between the ependymoma subgroups and tumor location, origin, hydrocephalus, age at diagnosis, extent of resection and relapse.
Results: More PFA-1 ependymomas were located laterally than PFA-2 tumors (p=.012) and the tumor subgroups differed in site of origin (p=.049) and pattern of relapse (p=.032). The PFA-1 and PFA-2 ependymomas did not differ in age at diagnosis, the presence of hydrocephalus, or extent of resection.
Conclusions: Radiologic and neurosurgical criteria suggest that PFA-1 and PFA-2 ependymomas have distinct sites of origin. MRI findings indicate that the subgroups may have difference relapse patterns. Additional analysis with a larger cohort of patients is needed to truly establish these relationships.

Paper #: 022

Analyzing Misdiagnosed Metastasis on Imaging Studies

Julie Harreld, MD[1], *julie.harreld@stjude.org*; Jacqueline Angel, MD[1]; [1]Diagnostic Imaging, St. Jude Children's Research Hospital, Memphis, TN

Disclosures: All authors have disclosed no financial interests, arrangements or affiliations in the context of this activity.

Purpose or Case Report: Accurate detection of leptomeningeal metastasis is critical for appropriate risk stratification and treatment of childhood CNS tumors. MRI findings correlate better with survival than CSF analysis, but leptomeningeal metastases may be missed or misdiagnosed on examinations not optimized for pediatric cancer imaging. We investigated the association of missed metastases on outside MRI with technical imaging factors and radiologist qualifications to promote improvements in pediatric cancer imaging and metastasis detection.
Methods & Materials: We retrospectively reviewed reports for outside and in-house brain and spine MRIs performed within 35 days of each other for 86 children presenting to our institution between January 1, 2011 and December 31, 2012 with leptomeningeal-seeding (ependymoma or embryonal) brain tumors. Contemporaneous CSF and/or in-house MRI were considered gold standard for metastasis detection. Outside and in-house MRI techniques and radiologist qualifications were compared for cases of missed/misdiagnosed metastases.
Results: Thirty-one of 86 patients (36%) had leptomeningeal metastases (13 brain, 3 spine, 15 both) by initial in-house MRI ± CSF. Of these, 10 (32%) had metastases undiagnosed by OSH MRI of brain (n=3), spine (n=4), or both (n=3). Of these, 2/6 brain MRIs did not include DWI; 5/6 had no post-contrast FLAIR; and 1 had no IV contrast. Three of 7 missed spinal metastases were due to lack of OSH spine MRI; 1 OSH spine MRI had no post-contrast sequences. In-house and OSH false positive rates were identical (2/55 or 4%). Unlike in-house exams, all outside exams with missed metastases had gaps between slices on one or more sequences; four of 11 (36%) identifiable OSH radiologists had a CAQ in neuroradiology, compared to 3 out of 5 (60%) in-house neuroradiologists.
Conclusions: Standardization and optimization of MRI technique, and interpretation by subspecialty-trained neuroradiologists, could promote more accurate pediatric CNS cancer detection and risk assessment.
Figure: Post-contrast FLAIR for metastasis detection. (a) FLAIR images without contrast do not show leptomeningeal metastases, unlike (b) FLAIR with contrast. Metastases missed on initial outside imaging; confirmed by CSF.

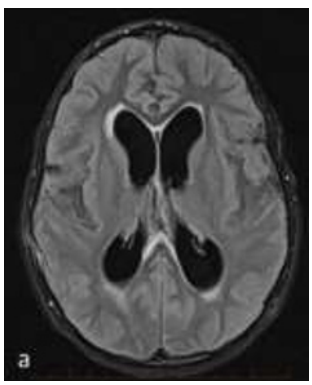

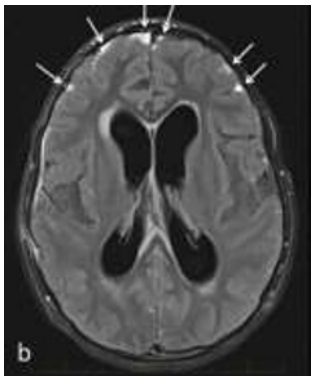

Paper #: 023

Normal head and neck lymph nodes in the healthy paediatric population

Joao Alves Rosa[1], *joaorosa4@hotmail.com*; Savvas Andronikou[2]; [1]University Hospital Bristol NHS Foundation Trust, Bristol, United Kingdom, [2]University of Bristol, Bristol, United Kingdom

Disclosures: All authors have disclosed no financial interests, arrangements or affiliations in the context of this activity.

Purpose or Case Report: Palpable lymph nodes are a normal finding in the healthy paediatric population, particularly in the head and neck, with authors quoting figures over 90%. Additionally, true lymphadenopathy (LN) is most often benign, infections the commonest cause. This is a common cause of concern, with numerous referrals for radiological investigations, namely ultrasound. Different sizes and a round nodal shape with a short to long axis ratio (ratio S/L) over 0.5 have been suggested to correlate with an ominous diagnosis. This has been demonstrated for supraclavicular LN but no such association between lymph node size or morphology was shown for nodes at other sites. Furthermore, measuring methods are often unclear. Our aim is to determine normal size range of head and neck lymph nodes in a healthy paediatric population.
Methods & Materials: Retrospective review of head and neck MRI studies of 200 patients aged between 5 months and 16 years. Exclusion criteria included fever, malignancy, surgery and other possible causes for LN. All studies were previously reported as normal. Eight different areas were assessed for the presence of lymph nodes (e.g. Image 1 and 2) and the short and long axis of the largest lymph node in each area was measured by two radiologists and the S/L ratio calculated.
Results: Lymph nodes were most commonly identified in the posterior and deep cervical, submandibular and occipital regions. Table 1 shows mean size and ratio for all regions. The largest nodes are located in the areas where they are also most frequently identified. Ratios differ according to location, with a rounder shape in the pre-auricular and occipital areas. Groups were created, according to NICHD Paediatric Terminology and statistically significant differences in size and shape were demonstrated between them. Namely, size differences in the deep and posterior cervical regions were found between the Infant/Toddler and Early Childhood groups and the remainder of the groups. Significant differences in shape were found in these same regions, with nodules showing a rounder morphology, represented by a higher S/L ratio, in the Infant/Toddler group.

Conclusions: This is the first study to characterize the normal distribution, size and shape of head and neck lymph nodes in a healthy paediatric population. While MRI is not the standard method of radiological assessment of lymphadenopathy, it allows for accurate and operator independent measurements and this will hopefully serve as a reference for future studies.

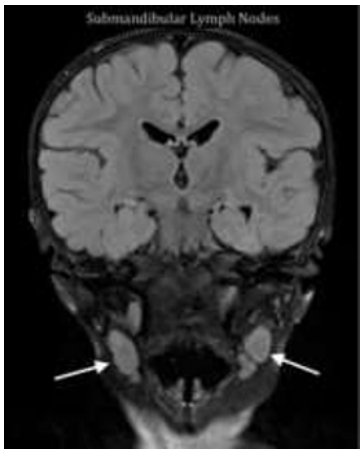

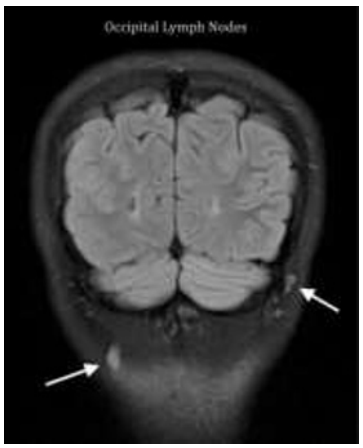

Location	Frequency (%)	Short Axis (mm)	Long Axis (mm)	Ratio (S/L)*
Superior Cervical	4	5,9	11,1	0,55
Deep Cervical	100	8,7	18,1	0,50
Posterior Cervical	92,5	7,9	15,4	0,53
Submandibular	99,5	10,5	19,7	0,55
Submental	12,4	6,3	10,0	0,68
Preauricular	33,5	6,0	7,8	0,64
Post-auricular	11,5	4,1	8,1	0,51
Occipital	67,5	5,0	8,1	0,63

Table 1 - Frequency of lymph nodes according to location with short and long axis measurements and short/long axis ratio (S/L ratio)
* S/L ratio: ratios closer to 1 indicate round nodes; ratios close to 0 indicate oval nodes

Paper #: 024

Magnetic resonance (MR) assessment of optic nerve thickness and tortuosity for recognition of optic glioma in children with NF1

Hadeel Eid, Fellow[1], *dr_hadeel_eid@yahoo.com*; Ahmed Aldraihem, MD[1], Flavia Menegotto, Paediatric Radiologist Consultant[2], Nagwa Wilson, M.D, PhD[1]; [1]Pediatric Radiology, The Montreal Children's Hospital, Montreal, QC, Canada, [2]Bristol Royal Hospital for Children- University Hospital Bristol-NHS Foundation Trust, Bristol, United Kingdom

Disclosures: All authors have disclosed no financial interests, arrangements or affiliations in the context of this activity.

Purpose or Case Report: To determine the ability of MR orbit to recognize early OPG in NF1 children by using OPN thickness & tortuosity as diagnostic parameters.
Methods & Materials: We retrospectively reviewed MR orbit of NF1 children from 2003 to 2016. Patients were divided into 2 groups; OPG group (n=71 nerves) & non-OPG group (n=151 nerves). We also assigned a control group of non-NF1 children with normal OPN (n=66 nerves). The OPN thickness was measured at 8 locations and mean thickness was calculated in axial & coronal planes. Moreover, 2 radiologists assessed OPN tortuosity using validated criteria including OPN interruption with & without return, deviation, lack of congruity & dilated subarachnoid space (SAS).
Results: The OPN mean thickness significantly varied between OPG & non-OPG groups ($p<0.0001$); cut-off value was ≥3 mm in axial plane (74.6% sensitivity & 90.1% specificity) and ≥3.5 mm in coronal plane (73.2% sensitivity & 94% specificity) ($p<0.0001$ for each). The OPN tortuosity criteria showed significant difference between OPG & non-OPG groups (p ranged between <0.0001_0.006). Interruption of the OPN with return showed the highest specificity (83.5%) while dilated SAS had the least specificity (61.2%). Combination of the 5 parameters increased the specificity up to 98.6%.
Conclusions: Objective assessment of the OPN thickness & tortuosity on MR based imaging is a good diagnostic parameter of an OPG in NF1 children older than 2 years.

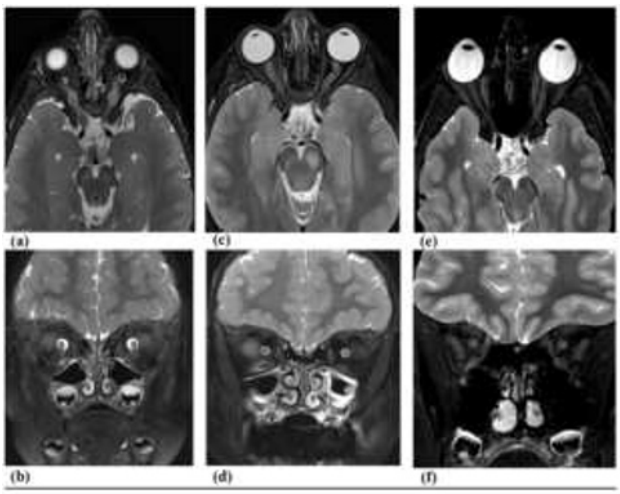

Fig. 1: MR orbit of children > 2 years old:
- (a & b): Axial & coronal T2WIs respectively of a 31 months old NF1 male with OPG. (a) Demonstrating thickening & hyperintense signal throughout the course of the right OPN and its left retroocular segment. The right OPN shows angular deviation and the left shows interruption with return. (b) Demonstrating lack of congruity of the optic nerves and bilaterally dilated SAS.
- (c & d): Axial & coronal T2WIs respectively of a 56 months old NF1 male without OPG. (a) Demonstrating thickening of both optic nerves with deviation of the left optic nerve. (b) Demonstrating mild chiral ectasia of the optic sheath.
- (e & f): Axial & coronal T2WIs respectively of a 72.4 months old female with nystagmus. (a) Demonstrating normal thickness and signal of the OPN on both sides with absence of the tortuosity criteria. (b) Demonstrating normal SAS bilaterally with proper congruity of the optic nerves.

Table 1: The maximum thickness of the OPN at every individual location in NF1children.

	OPN segment	Max. thickness (mm)	P value	Std. Error	AUC	Sensitivity	Specificity
Axial plane	Retro-ocular	3	<0.0001	0.03	0.772	57.7 %	80.8 %
	Mid-segment	2.5	<0.0001	0.03	0.817	57.7 %	82.1 %
	Intra-canalicular	2	<0.0001	0.03	0.809	73.2 %	70.9 %
	Pre-chiasmatic	4	<0.0001	0.03	0.844	74.6 %	74.8 %
	Of the whole OPN	3	<0.0001	0.022	0.910	74.6 %	90.1 %
Coronal plane	Retro-ocular	3.3	<0.0001	0.037	0.732	56.3 %	78.1 %
	Mid-segment	3	<0.0001	0.031	0.814	55 %	86.1 %
	Pre-chiasmatic	3.5	<0.0001	0.032	0.819	60.6 %	84.1 %
	Chiasmatic	4	<0.0001	0.036	0.777	69.6 %	80.1 %
	Of the whole OPN	3.5	<0.0001	0.027	0.902	73.2 %	94 %

Table 2: The sensitivity and specificity of each tortuosity parameter comparing OPG and non-OPG groups in children above 2 years.

	OPG group (n= 64)	Non-OPG group (n=139)	P-value	Sensitivity	Specificity	+ve predictive value	-ve predictive value
Interruption without return	27/64 42.2%	28/139 20.1%	< 0.0001	42.2 %	79.9 %	49.1 %	75 %
Interruption & return	24/64 37.5%	23/139 16.5%	< 0.0001	37.5 %	83.5 %	51.1 %	74.4 %
Axial deviation	33/64 51.6%	33/139 23.7%	< 0.0001	51.6 %	76.3 %	50 %	77.4 %
Dilated SAS	38/64 59.4%	54/139 38.8%	< 0.0001	59.4 %	61.2 %	41.3 %	76.6 %
Lack of congruity (COR)	30/64 46.9%	30/139 21.6%	< 0.0001	46.9 %	78.4 %	50 %	76.2 %
Increased SAG curvature	20/39 51.3%	28/109 25.7%	< 0.0001	51.3 %	74.3 %	41.7 %	81 %
Combined lack of congruity & dilated SAS	20/64 31.3%	18/139 12.9%	< 0.0001	31.3 %	87.1 %	52.6 %	73.3 %
Combined 5 parameters	5/64 7.8%	2/139 1.4%	< 0.0001	7.8 %	98.6%	71.4 %	69.9 %
All six parameters	5/39 12.8%	1/109 0.92%	< 0.0001	12.8%	99.1 %	83.3 %	76.1 %

Paper #: 025

The Unwound Cochlea: a Specific Marker of Branchio-oto-renal Syndrome

Ariel Hsu, MD[1], *afhsu@texaschildrens.org*; Michael Paldino, MD[1]; [1]Radiology, Texas Children's Hospital, Houston, TX

Disclosures: All authors have disclosed no financial interests, arrangements or affiliations in the context of this activity.

Purpose or Case Report: Cochlear malformations are common in children with branchio-oto-renal (BOR) syndrome. Yet the reported imaging findings do not generally contribute to the diagnosis of BOR. In our experience a specific type of dysmorphology - an unwound cochlea - is characteristic for this syndrome. The goal of this study is to determine the value of an unwound cochlea for the diagnosis of BOR.
Methods & Materials: Patients were identified retrospectively with a diagnosis of BOR and dedicated imaging of the temporal bone. Age-matched control patients with temporal bone imaging for hearing loss not related to BOR were also identified. A pediatric neuroradiologist reviewed all temporal bone imaging blinded to the diagnosis of BOR versus control for: qualitative assessment of unwound (or other) cochlear dysmorphology; and quantitative assessment of the basal-middle-turn (BMT) interval - maximal distance between the basal and middle turns of the cochlea. Fisher Exact and Wilcoxon Rank Sum tests were used to compare categorical and continuous variables respectively between groups.
Results: The study group comprised 8 patients with BOR (mean [SD] age: 8.0 [4.3] years; 6 males) and 50 controls with sensorineural hearing loss (mean [SD] age: 7.9 [4.1] years; 26 males). The cochlea was abnormal in all 8 BOR patients. In 7 patients (88%), imaging demonstrated an unwound cochlea bilaterally, with rotation and displacement of the middle turn away from the basal turn (Figure 1). In the other BOR patient (12%), CT demonstrated complete absence of the middle and apical turns bilaterally. None of the control patients demonstrated an unwound cochlea on either side. The unwound cochlea was significantly more frequent in the BOR population (p: 0.00002). Sensitivity, specificity and positive predictive value of an unwound cochlea for the diagnosis of BOR were 88%, 100%, and 100% respectively. Mean [SD] BMT interval for BOR patients was 2.7 [0.15] mm; 1.3 [0.19] mm in controls. The BMT interval was significantly larger in BOR patients than controls for both the right (p: 0.0003) and left (p: 0.00001) cochlea.
Conclusions: An unwound cochlea - characterized by rotation and displacement of the middle turn away from the basal turn - at temporal bone imaging was a specific marker of BOR.

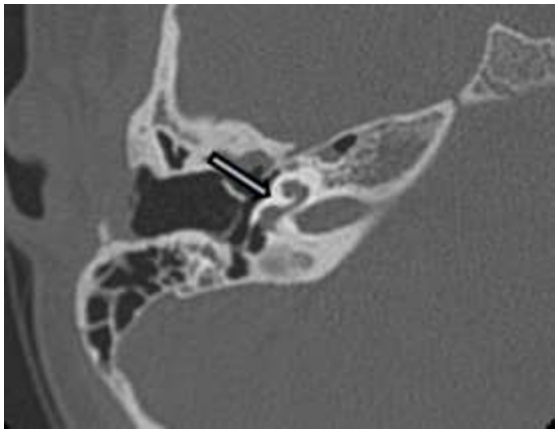

Paper #: 026

Pseudo-color Perceptual Enhancement for Detection of Cochlear Signal Alterations in Pediatric Patients with Sensorineural Hearing Loss

Matthew Whitehead, MD[1], *matthewthomaswhitehead@gmail.com*; Daniel Chung, MD[1], Lori Guillot, MD[1], Brian Reilly, MD[1]; [1]Neuroradiology, Children's National Medical Center, Washington, DC

Disclosures: All authors have disclosed no financial interests, arrangements or affiliations in the context of this activity.

Purpose or Case Report: The neuroimaging yield in defining the etiology of sensorineural hearing loss (SNHL) is relatively poor, somewhere between 20-50%. In patients without structural defects or cochlear signal changes, there could be differences in gray-scale data below the threshold of the human eye. Gray-scale images can be post-processed to enhance perception of tonal difference using pseudo-color schemes. We aim to retrospectively evaluate a series of unilateral SNHL patients and otherwise normal MR exams for labyrinthine color differences after pseudo-color post-processing.
Methods & Materials: The brain MR database at an academic children's hospital was queried for "hearing loss". Exams from patients with deficits other than unilateral SNHL were excluded. 68 exams were reviewed; 42 were excluded due to motion, asymmetric soft tissue signal, structural abnormalities, and/or lack of high-resolution T2WI or FIESTA labyrinthine images. Thirteen aged-matched normal MR exams from patients without hearing loss were chosen for comparison. Pseudo-color was applied with assignment of specific hues to each gray-scale intensity value using Functool software of ADW 4.3 workstation. Gray-scale and pseudo-color images were qualitatively evaluated for signal asymmetries by a board certified neuroradiologist blinded to the side of SNHL.
Results: 26 SNHL (mean 7.6+/-3 years old) and 13 normal control exams (mean 7.3+/-4 years old) met inclusion criteria. All SNHL and controls had normal gray-scale cochlear signal and all controls had symmetric pseudo-color signal. However, in 42% of the patients pseudo-color images revealed occult asymmetries localizing to the affected ear with "colder" hues (lower values), possibly reflecting complicated intralabyrinthine fluid in patients with SNHL. In the other 58%, no discernible cochlear color differences were present. No discordant findings were present.

Conclusions: Pseudo-color perceptual image enhancement reveals otherwise occult cochlear pathology on MR exams in patients with unilateral SNHL. Application of pseudo-color image enhancement techniques to gray-scale MR data can improve detection of cochlear pathology, and has therapeutic implications.

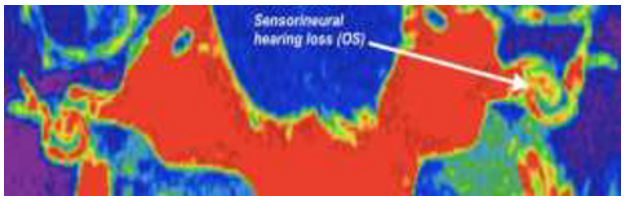

Paper #: 027

Accuracy of Skeletal Survey in Evaluation of Rib Fractures Compared to CT in the Setting of Accidental and Non Accidental Trauma.

Christy Pomeranz, MD[1], *christypomeranz@gmail.com*; Christian Barrera, MD[1], Xiaowei Zhu[1], Sabah Servaes[1]; [1]Radiology, Children's Hospital of Philadelphia, Philadelphia,PA

Disclosures: All authors have disclosed no financial interests, arrangements or affiliations in the context of this activity.

Purpose or Case Report: To evaluate the reliability of skeletal survey radiographs at detecting rib fractures compared to computed tomography (CT).
Methods & Materials: Following IRB approval, a retrospective review was performed on all patients who had experienced trauma and who had undergone both a skeletal survey and a CT of the chest and/or abdomen and pelvis within 30 days of one another from January 2009 - July 2017. All skeletal surveys were performed according to ACR-SPR guidelines using high resolution computed radiography. Images and reports were reviewed by a pediatric radiology fellow. Images were assessed for presence of rib fractures, location and evidence of healing in each modality.
Results: Data was collected on 57 patients who met inclusion criteria. Patients ranged in age from newborn to 8 years old. 25 (43%) of patients analyzed had a total of 225 rib fractures confirmed on CT. 49 (22%) of these rib fractures were acute. 62 (28%) of these rib fractures were anterior, 118 (52%) were posterior, and 45 (20%) were lateral.
10 of these 25 patients (40%) had 38 fractures not visualized on chest radiographs but demonstrated on CT, yielding a miss rate of 17%. 24 of the 38 missed fractures were acute (63%) and 14 were healing or chronic (27%). Acute rib fractures were much more likely to be missed on radiographs and this discrepancy was statistically significant ($p < 0.01$). 4 of the 38 missed fractures were anterior (11%), 24 were posterior (63%), and 10 were lateral (26%). Posterior rib fractures made up the majority of overall rib fractures as well as the majority of missed rib fractures. The ratios between these two groups was not statistically significant. All rib fractures were best see on the axial plane on CT. 8 patients had experienced accidental trauma; 35 cases were confirmed cases of non accidental trauma; and 14 cases were suspected non accidental trauma or unknown mechanism.
Conclusions: Skeletal survey radiographs in cases of accidental and non accidental trauma fail to demonstrate rib fractures in 17% of cases, compared to CT. Acute fractures are more likely to be missed than healing fractures and this difference is statistically significant. Location of rib fractures—anterior, posterior, lateral—did not affect the miss rate of rib fracture. Low-dose CT used in conjunction with radiography may be helpful.

TABLE 1. Patients data overview

Variable (N = 57)	Results (mean ± SD)
Age (years)	0.87 ± 1.46 (range 0 – 8)
Gender	35 male (61%), 22 girls (39%)
Weight (kg)	9.27 ± 5.53 (range 3 – 36)
Chest CT unenhanced radiation dose	
Children 2 – 4 years	
CTDI (mGy)	1.2 ± 0.4
DLP (mGycm)	23.3 ± 8.5
Radimetrics Estimate (mSv)	1.3 ± 1.2
AAPM 96 (mSv)	1.0 ± 0.5
Children 5 – 9 years	
CTDI (mGy)	1.4 ± 0.6
DLP (mGycm)	32.9 ± 14.3
Radimetrics Estimate (mSv)	1.5 ± 0.6
AAPM 96 (mSv)	1.2 ± 0.5
Radiation dose Skeletal Survey (mSv)*	0.3 ± 0
Trauma diagnosis	
Highly likely NAT	35 cases (61%)
Suspected NAT	14 cases (25%)
Accidental	8 cases (14%)

Note: * This parameter was set up according to our institutional protocol to all skeletal surveys, **CTDI** = Computed Tomography Dose Index, **DLP** = Dose Length Product, **NAT** = non accidental trauma, **AAPM** = The American Association of Physicists in Medicine.

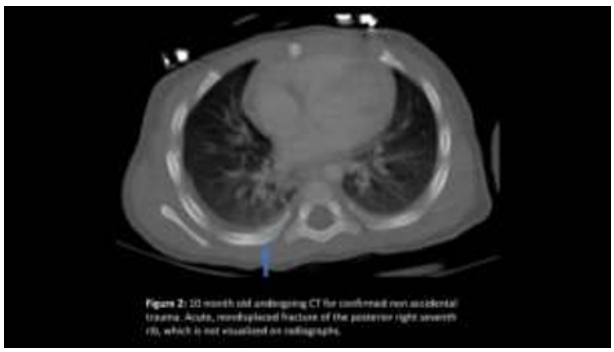

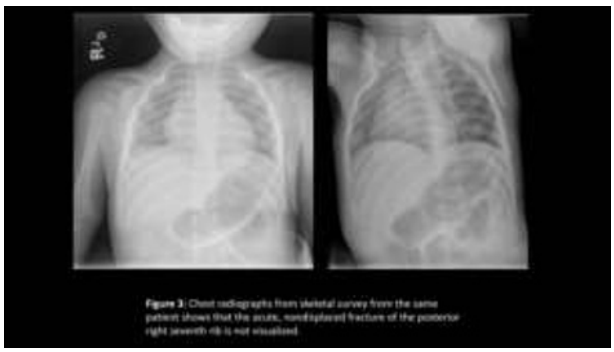

Paper #: 028

How often is Subperiosteal New Bone Formation Noted with the Distal Tibial Classic Metaphyseal Lesion?

Andy Tsai, MD, PhD[1], *andy.tsai@childrens.harvard.edu*; Paul Kleinman, MD[1]; [1]Radiology, Boston Children's Hospital, Boston, MA

Disclosures: All authors have disclosed no financial interests, arrangements or affiliations in the context of this activity.

Purpose or Case Report: The classic metaphyseal lesion (CML) is a strong indicator of infant abuse, and the distal tibia is one of the most common sites for this injury. Radiologic-histopathologic correlations in abused infants at the time of death suggest that subperiosteal new bone formation (SPNBF) is an uncommon concomitant of the CML. Despite these studies, the absence of SPNBF may be proffered in the medico-legal setting

to challenge the age or *even* the traumatic nature of the CML. The objective of this study is to determine the prevalence of SPNBF with distal tibial CMLs on serial skeletal surveys done for suspected infant abuse.
Methods & Materials: Reports of 1142 ACR-compliant skeletal surveys performed on infants (<1-year-old) for suspected abuse over a 12-year period (7/2005—8/2017) were reviewed to identify distal tibial CMLs. Inclusion criteria were: 1) Anteroposterior (AP) radiographic projections of a distal tibial CML on initial and/or two week follow-up skeletal survey, 2) additional fractures, 3) hospital child protection team consults and 4) mandated report filing for suspected abuse. Twenty-eight distal tibial CMLs were identified (14 unilateral, 7 bilateral) in 21 infants (mean age 2.4 months; SD=1.5 months; range=0.7—6.4 months). Fourteen of 21 infants also had rib fractures; 16/21 also had CMLs at other sites; and 16/21 also had non-CML long bone fractures. Randomly ordered initial and follow-up AP radiographs of distal tibial CMLs were shown simultaneously on PACS to two blinded pediatric radiologists (21- and 24-years' experience). Readers used a Likert scale to indicate the likelihood that SPNBF was present/absent on each of these radiographs.
Results: Inter-reader agreement for the presence/absence of SPNBF was moderate (19/28 CMLs; k=0.533). The readers agreed that distal tibial SPNBF was present on at least one of the two serial AP radiographs in 9 instances; they agreed that SPNBF was absent on both studies in 10 instances.
Conclusions: Two experienced pediatric radiologists agreed that SPNBF was present in a minority of distal tibial CMLs studied with serial radiography. This observation contrasts with the generally-accepted high prevalence of SPNBF with other types of long bone fractures. The lack of SPNBF should not be used to call into question the existence of CMLs, nor should the absence of SPNBF on a single exam be considered clear evidence that a CML is acute.

Paper #: 029

Radiographic characteristics that delineate abusive from accidental skull fractures, including the significance of fracture extension to sutures.

Spencer Kriss[1], *skriss2018@gmail.com*; Gina Bertocci, PhD[2], Melissa Currie[2], Angela Thompson[2], Vesna Kriss, MD[1]; [1]Norton Children's Hospital, Louisville, KY, [2]University of Louisville, Louisville, KY

S95

Abstract Paper #:029 withdrawn at author's request because the study lacked appropriate ethical oversight from a relevant ethics committee.

Paper #: 030

Gaussian noise simulating reduced X-ray dose does not affect sensitivity of a Neural Network trained to detect tibial fractures in X-ray images

Zbigniew Starosolski, PhD[1], *zastaros@texaschildrenshospital.org*; J. Kan, MD[1], Ananth Annapragada, PhD[1]; [1]Pediatric Radiology, Texas Children's Hospital, Houston, TX

Disclosures: Ananth Annapragada has indicated a relationship with Alzeca Inc. and Sensulin, LLC for receiving stock options as well as intellectual property rights, and receives research grants with the NIH and Alzeca, Inc. All other authors have disclosed no financial interests, arrangements or affiliations in the context of this activity.

Purpose or Case Report: We have previously shown that a Convolutional Neural Network (CNN) can correctly identify tibial fractures on radiographs. The purpose of this study was to determine if noise levels in the image, representing the effect of reduced X-ray dose, affect the accuracy of classification.
Methods & Materials: Using our electronic medical record system, a text word search was performed for all ankle radiographs performed between 2015 and 2017 to identify patients with distal tibia fractures. A normal control set without fractures was also generated from this time period. A total of 100 studies had tibial fractures, and 350 studies were normal. All images were cropped to a standard size of 299x299 pixels, and rotated to a standard orientation. A training set including 98 radiographs with fractures, and 98 radiographs without fractures was selected. A pre-trained CNN with 136 layers was augmented with an additional 2 fully convoluted reasoning layers and trained. Two sets of reasoning layers, one with 16 hidden units (CNN-16) and one with 64 hidden units (CNN-64), were tested. A test set containing 22 radiographs with fractures and 44 without fractures was identified from the parent set. Gaussian noise was then added to each test image, with relative standard deviations of 1, 2, 5, 10, and 20% respectively, resulting in a total of 6 superimposed noise levels (Figure 1). Each image was then classified by the two CNN's.

Results: CNN-16 returned a sensitivity of 81.8% and a specificity of 59.5%. CNN-64 returned an increased specificity of 79% but the sensitivity surprisingly dropped to 68.2%. When noise was superimposed on the images, CNN-16 showed no change in sensitivity, but the specificity steadily dropped from 59.5% to 43%. Similarly, CNN-64 showed practically no change in sensitivity, but the specificity dropped from 79% to 45%. (Figure 2)
Conclusions: Reducing X-ray dose leads to increased noise levels in images. Yet, CNN's trained on images with no superimposed noise, were capable of reading noisy images with no change in sensitivity, although the specificity dropped significantly. The drop in specificity could be associated with the lack of superimposed noise in the training sets. CNN's have the potential to dramatically reduce the required X-ray dose for the radiographic identification of fractures. The positive ramifications as CNN accuracy improves with time will be less radiation burden to patients when radiographs are optimized for computer learning and diagnosis rather than for the human eye.

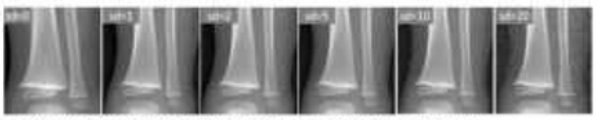

Figure 1. Pre-processing of radiograms. Superimposition of noise on image. Standard deviations of Gaussian noise from 0% to 20% are shown.

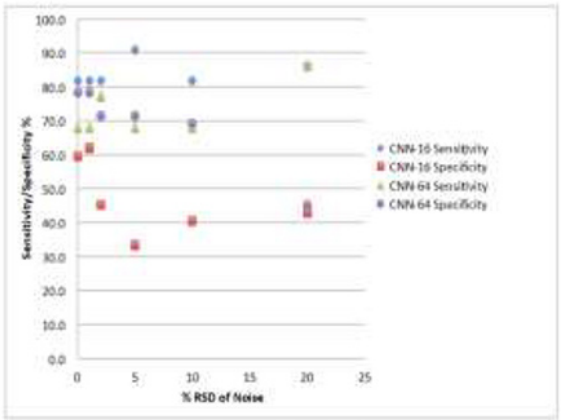

Figure 2. Effect of superimposed noise on the sensitivity and specificity of representative radiographs with classification by two CNN's.

Paper #: 031

Toddler tibial fractures computer-aided diagnosis by convolutional neural network and transfer learning

Zbigniew Starosolski,
PhD[1], *zastaros@texaschildrenshospital.org*; J. Kan, MD[1], Ananth Annapragada, PhD[1]; [1]Pediatric Radiology, Texas Children's Hospital, Houston, TX

Disclosures: Ananth Annapragada has indicated a relationship with Alzeca Inc. and Sensulin, LLC for receiving stock options as well as intellectual property rights, and receives research grants with the NIH and Alzeca, Inc. All other authors have disclosed no financial interests, arrangements or affiliations in the context of this activity.

Purpose or Case Report: Convolutional neural networks (CNN) show promise for automated radiologic imaging interpretation. Toddler's tibial fractures are a common cause of non-weightbearing in the preschool child diagnosed by radiography. The purpose of this study was to determine if CNN can be used for the computer aided diagnosis (CAD) of toddler's tibial fracture.
Methods & Materials: Through our radiology electronic medical records, a text word search was performed for all ankle radiographs performed between 2015 and 2017 to identify patients with distal tibia fractures. A normal control set without fractures was also generated from this time period. The formal report, follow-up, and re-evaluation of the radiographs by a pediatric musculoskeletal radiologist were used to confirm the presence or absence of a fracture. A total of 100 studies had tibial fractures, and 350 studies were normal. All images were cropped to a standard size of 299x299 pixels, and rotated to a standard orientation. A training set including 98 radiographs with fractures, and 98 radiographs without fractures was selected. A pre-trained CNN with 136 layers was augmented with an additional 2 fully convoluted reasoning layers and trained with this dataset. After training, a test set containing 22 radiographs with fractures and 44 without fractures was classified by the CNN.
Results: CNN automated radiologic interpretation correctly classified 18 of the 22 fracture cases and 27 of the 44 no-fracture cases, corresponding to sensitivity, specificity, and accuracy of 81.8%, 59.5% and 67.2%, respectively. In the 4/22 false negative exams the dominant feature was that fracture was very close or touching the edge of the image, a feature not well represented in the training set (Figure 3). The false positive exams were felt to be related to accentuated trabeculation which could mimic a nondisplaced fracture.
Conclusions: Our feasibility study on the use of CNN for CAD of tibial toddler's fractures has promise to automate and improve workflow for radiologists. Errors were primarily related to features not well represented in the training set. The training set in our study was relatively small, and we expect that with larger sets the overall accuracy will improve.

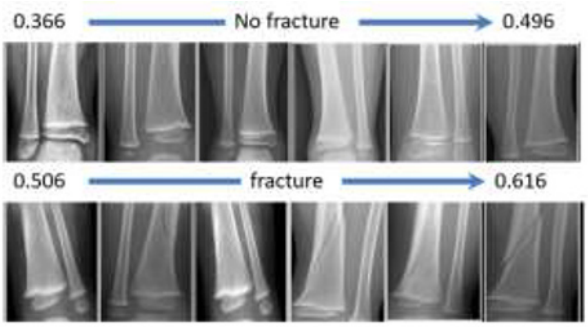

Figure 2. Representative radiographs with classification score. Top row: radiographs with no-fracture with score <0.5, bottom row: Radiographs with fracture with score ≥0.5

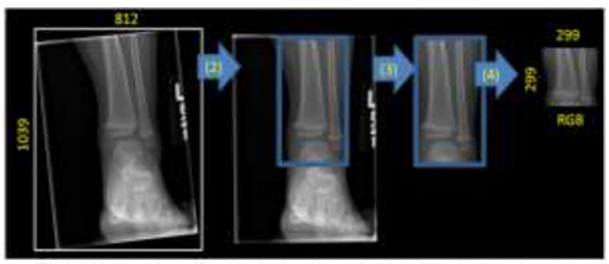

Figure 1. Pre-processing of radiographs. 1) Rotation 2) ROI selection 3) Cropping 4) Bilinear interpolation to matrix size 299x299pixels and conversion to RGB color.

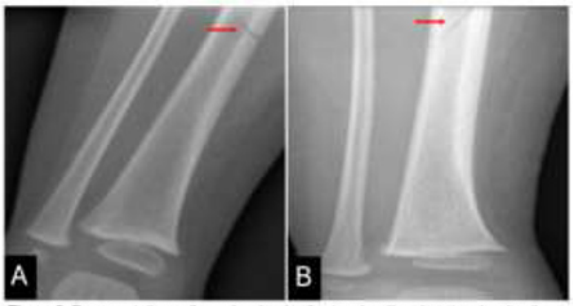

Figure 3. Representative radiographs showing fracture location close to edge, leading to reduced sensitivity and specificity.

Paper #: 032

Can combined diffusion-weighted imaging/conventional MRI replace post gadolinium-based contrast-enhanced MRI in the assessment of pediatric osseous sarcomas?

Alaa Alsharief, MBBS, SB-Rad[1], *a.alsharief@hotmail.com*; Claudia Martinez-Rios, MD[2], Sevan Hopyan[1], Afsaneh Amirabadi[3], Andrea Doria[1], Mary-Louise Greer, MBBS[1]; [1]University of Toronto, Toronto, ON, Canada, [2]University of Ottawa, Ottawa, ON, Canada, [3]Hospital for Sick Children, Toronto, ON, Canada

Disclosures: All authors have disclosed no financial interests, arrangements or affiliations in the context of this activity.

Purpose or Case Report: Because of rising concerns regarding gadolinium deposition in the brain after repeated intravenous administration of gadolinium-based contrast agents (GBCA), imaging alternatives decreasing or avoiding use of GBCA may be required in certain pathologies. The purpose of the study was to determine if diffusion-weighted imaging (DWI) in combination with conventional MRI can be used as an alternative technique to gadolinium-based contrast-enhanced (GBCE) MRI

Methods & Materials: MRI studies in children with histopathologically-proven osseous sarcomas were reviewed (blinded and then by consensus) if initial pre-treatment MRI included DWI and post-GBCA images. Patient demographic and clinical data were collected. Two radiologists captured tumor size, presence of skip lesions, necrosis, neurovascular invasion, lymph node enlargement, and diffusion restriction. Apparent diffusion coefficient (ADC) values were measured in non-necrotic osseous and soft tissue regions-of-interest (ROIs) with and without diffusion restriction and correlated with calculated relative enhancement values in areas with minimum ADC values. Descriptive statistics, paired T-test, Chi-square/ Fisher Exact test and Pearson correlation were performed.

Results: Twenty-one patients met the study criteria (mean age at presentation 11.3±4.2 years, 15 females); 14 with osteosarcomas and 7 with Ewing sarcomas; 6 in the axial and 15 in the appendicular skeleton with 11/21 in the femur. Qualitative comparison of features on conventional/DWI and GBCE MRI showed excellent correlation for tumor size $r = 0.873$, $p < 0.001$, and significant associations (Fisher Exact test) for skip lesions: $p < 0.001$; necrosis: $p = 0.021$; neurovascular involvement: $p < 0.001$; and enlarged lymph nodes: $p < 0.001$. Quantitative comparison between ADC values and relative enhancement in tumor (intra- and extra-cortical parts) performed in a subset lesion analysis showed moderate negative correlation between measurements in extracortical non-restricted tumor ROI ($r = -0.583$, $p = 0.014$); no correlations were noted in other ROIs.

Conclusions: Qualitatively combined DWI-conventional and GBCE MRI reveal substantial associations for several tumor features. Nevertheless, lack of association between quantitative ADC values (DWI) and relative enhancement (GBCE) MRI for most tumor ROIs reflects that quantitatively these techniques measure independent parameters, with DWI dependent upon tumor cellularity as well as perfusion.

12-year-old girl with distal right femoral osteosarcoma

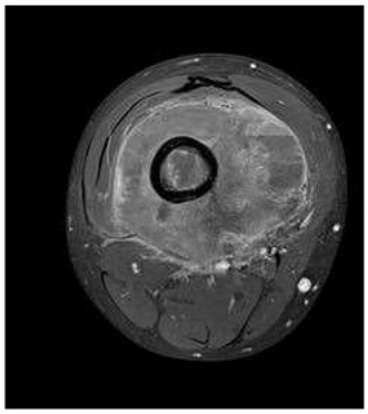

Axial T1 fat sat post GBCA showing heterogeneous enhancement of the tumor

12-year-old girl with distal right femoral osteosarcoma

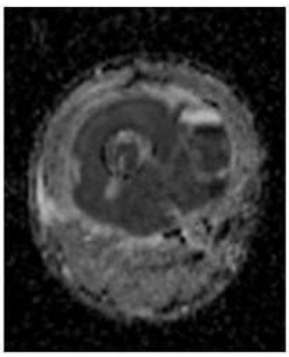

Axial ADC map demonstrates heterogeneous low value of the same tumor. Minimum ADC value is 0.8 and 0.5 in the intra and extra- cortical parts, respectively.

12-year-old girl with distal right femoral osteosarcoma

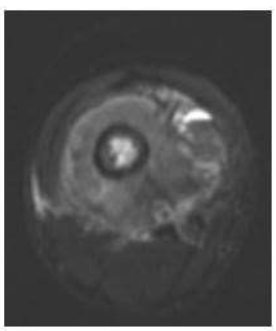

Axial DWI demonstrate heterogeneous high signal of the tumor in the intra-cortical and extra-cortical parts.

Paper #: 033

Bone Marrow MR and MRS Evidence of Adrenal and Gonadal Hormone Replacement Therapy Efficacy in girls with Anorexia Nervosa

Kirsten Ecklund, MD[1],*kirsten.ecklund@childrens.harvard.edu*; Sridhar Vajapeyam, PhD[1], Robert Mulkern, PhD[1], Henry Feldman[1], Jennifer O'Donnell[2], Amy DiVasta, MD[1], Clifford Rosen, MD[3], Catherine Gordon, MD[4]; [1]Radiology, Boston Children's Hospital, Boston, MA, [2]Robert Wood Johnson Medical School, New Brunswick, NJ, [3]Maine Medical Center Research Institute, Scarborough, ME, [4]Cincinnati Children's Hospital Medical Center, Cincinnati, OH

Disclosures: All authors have disclosed no financial interests, arrangements or affiliations in the context of this activity.

Purpose or Case Report: To prospectively utilize MR/MRS to assess the impact of hormone replacement therapy on marrow fat composition in girls with AN.
Methods & Materials: 70 adolescent girls with AN were randomized to DHEA +estrogen/progestin therapy vs placebo (35 per group). MR T1 relaxometry with variable TR and single voxel spectroscopy of the distal femoral metaphysis was performed at baseline and after 12 months of treatment/placebo. T1 maps and mean T1 values were recorded for ROIs in the metaphysis. Total lipid, unsaturation index (UI=unsaturated lipid/total lipid), T2 relaxation time of water, saturated fat, and unsaturated fat were calculated from the MR sprectra. Changes in MR variables were compared between active and placebo groups using repeated-measures analysis of variance, adjusted for age and BMI. Height, weight, and serum hormonal measures (estradiol, testosterone, leptin, DHEAS) were recorded at baseline and 12 months.
Results: There was no significant difference in age (11 - 18 yrs, mean 15.5 yrs), duration of amenorrhea (median 5 months), BMI (18.8 kg/m^2), or hormonal measures between the 2 groups at baseline. At 1 yr, mean T1 decreased by 2 ± 14 msec (estimate ± SE) in the active group, vs 25 ± 14 msec in the placebo group. The 12-month change in T1 and $T2_{unsat}$ increased with BMI in the active group but decreased in the placebo group (p=0.01 for interaction; figure). Decline in UI from baseline to 1 year was greater in the active group than in the placebo group (p=0.02). There was no significant difference in change in total lipid between the 2 groups. T2 water showed a greater decrease in the placebo group than in the active group (p=0.02).
Conclusions: In our study population of adolescent girls with mild to moderate AN, there was no significant difference in total marrow lipid content change between control and hormone therapy groups by MRS. However, greater decrease in the unsaturated fat index as well as a greater increase in the T1 measurements in the hormone therapy group indicating less fatty marrow were seen. Decrease in T2 water in the placebo group may indicate more restricted water mobility with less red marrow. Our results suggest that combined adrenal/gonadal hormone replacement therapy impacts marrow fat composition and seems to arrest increased conversion of red to yellow marrow known to occur in girls with AN.

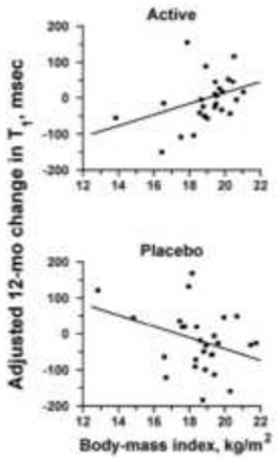

12-month change in T1 with body mass index: Marrow T1 increased (fat decreased) with BMI over 12 months in the hormonally treated group (top) but decreased (fat increased) in the placebo group (bottom) (p=0.01 for interaction).

Paper #: 034

Metal artifact reduction in pediatric dual energy CT using monoenergetic extrapolation

Eric Eutsler, MD[2], Irene Duba, B.A.[1], Marilyn Siegel, MD[2], Ahmed Halaweish[1]; [1]Siemens Healthineers, Malvern, PA, [2]Washington University School of Medicine, St. Louis, MO

Disclosures: Ahmed Halaweish has indicated a relationship with Siemens Healthineers for a salary. All other authors have disclosed no financial interests, arrangements or affiliations in the context of this activity.

Purpose or Case Report: To assess the performance of virtual monoenergetic in reducing metal artifacts from metallic spinal rods in pediatric dual-energy computed tomography (DECT).
Methods & Materials: Nine patients (aged 11-18 years) with spinal instrumentation were scanned using a 100kV/Sn140kV DECT technique on a Dual Source CT (Somatom Definition Flash). Virtual monoenergetic images from 90 - 170 keV were created using dedicated DE processing software (Monoenergetic+, Syngo.via). For each scan, an axial slice with metal artifacts was selected, and ROIs were drawn in three locations (anterior soft tissue, spinal cord, and posterior soft tissue) to measure noise and CT number (CT#) in Hounsfield units. Three measurements were taken at each site and averaged for each patient. The energies at which noise was lowest and CT# reached an "expected" value for soft tissue (between 30HU and 70HU) were recorded for each site in each patient. Optimal keV for noise reduction and contrast optimization was determined and compared to the standard image (mixed 100/140 kVp). Monoenergetic Images were also qualitatively assessed for maximum artifact reduction.
Results: Averaging across patients, noise was minimized and CT# was optimized at (mean ± std deviation) 128.5 ± 11.2 keV and 130.2 ± 14.6 keV respectively. Comparisons between average CT# in the mixed image and 130keV (optimal) monoenergetic images demonstrated a non-significant difference (p=0.57) for anterior ROIs, which were at a distance from the hardware and a significant difference (p<0.05) in both the posterior and spinal cord ROIs, both of which were closer to the hardware. Average CT# decreased from 88.3HU in the mixed image to 40.2 HU in the 130 keV image and from 251.21HU in the mixed image to 43.6HU in the 130 keV image for the posterior and spinal cord ROIs respectively. Differences in average image noise in the anterior ROI were not significant

(p=0.055). Average image noise in the posterior ROIs decreased significantly from 31.5HU to 24.4HU (p<0.05), and average image noise in the spinal cord changed significantly from 81.7HU to 41.9HU (p<0.05). In the qualitative assessment 130 to 150 keV was the optimal energy to maximize noise reduction in the spinal cord and posterior soft tissues close to the cord.
Conclusions: High keV Monoenegetic DECT reconstructions can significantly reduce metal artifacts and improve image quality. The data further show that this is best accomplished using 130 keV, with significant changes in CT values near the metal hardware.

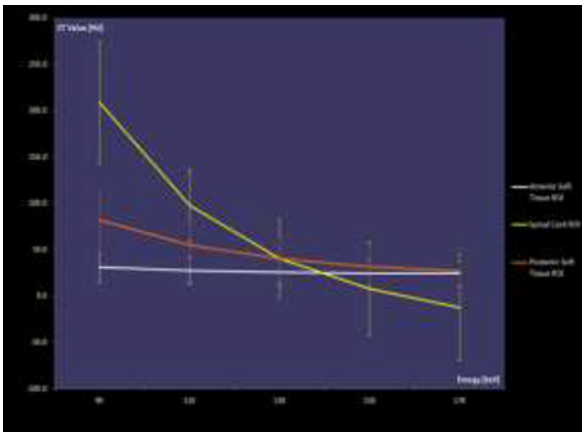

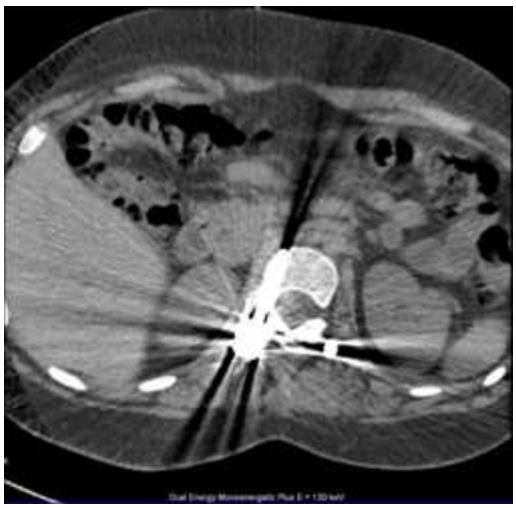

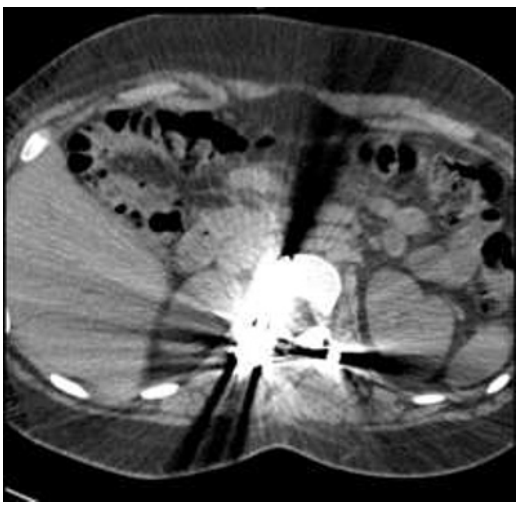

Paper #: 035

Comparison of Prenatal Ultrasound, Prenatal MRI, and Postnatal CTA for Evaluation of Congenital Lung Malformations: Can Postnatal CTA Provide Additional Information?

Grace Ma, MD[1], *grace.ma@childrens.harvard.edu*; Oren Johnson, MD[1], Amie McPherson, MD[1], Micheal Breen, MBBChBAO (Hons) BMedSc MRCPI FFRRCSI[1], Abbey Winant, MD[1], Edward Lee[1]; [1]Radiology, Boston Children's Hospital, Boston, MA

Disclosures: Abbey Winant has indicated a relationship with Bristol Myers Squibb for a research grant. All other authors have disclosed no financial interests, arrangements or affiliations in the context of this activity.

Purpose or Case Report: Prenatal ultrasound has become the standard of care for prenatal screening and assessment of fetal anomalies; while fetal MRI is often obtained for equivocal findings or for further characterization of fetal anomalies seen on ultrasound. Congenital lung malformations, including foregut duplication cysts, congenital pulmonary airway malformations, sequestrations and hybrid lesions, are usually discovered on prenatal ultrasound and further evaluated with prenatal MRI and postnatal CTA prior to surgical resection. The goal of our study is to assess the potential added diagnostic value of postnatal CTA in the evaluation of congenital lung malformations by comparing the imaging findings from prenatal US and MRI with postnatal CTA and correlating them to those found in surgery.
Methods & Materials: Retrospective evaluation of pediatric patients who have undergone postnatal CTA and prenatal US or MRI between July 2004 and 2017 for a prenatally diagnosed congenital lung malformation. Surgical and pathologic findings were obtained from the patient's medical records. Each pre- and post-natal diagnostic exam was reviewed for lesion size, appearance, margin, and presence of abnormal artery or vein. Patients without pre- or post-natal imaging preformed at our institution were excluded.
Results: The final study cohort consisted of 83 patients, 21 of which did not undergo surgical resection. Of the remaining 62 patients (22 females, 40 males; mean age at CTA, 5.0 ± 3 [SD] months; range, 1day - 13months), histopathologic diagnoses included congenital pulmonary airway malformations (n = 40, 64%), sequestrations (n = 11, 18%), hybrid lesions (n = 8, 13%) and foregut duplication cysts (n = 3, 5%). 21/62 (34%) and 12/62 (19%) were found to have an abnormal artery or vein, respectively, associated with the congenital lung malformation at surgery. For the detection of anomalous arterial feeder, CTA was found to have a higher diagnostic accuracy compared to prenatal imaging: 21/21(100%) for CTA, 11/18(61%) for US, and 9/18(50%) for MRI. Similarly, for the detection of anomalous veins, CTA was also found to be more sensitive: 10/12(83%) for CTA, 1/9(22%) for US and 0/10(0%) for MRI.
Conclusions: Prenatal US and MRI allows early detection and evaluation of congenital lung malformations but additional postnatal CTA adds diagnostic value in the detection of associated anomalous vessels, particularly in pre-surgical planning.

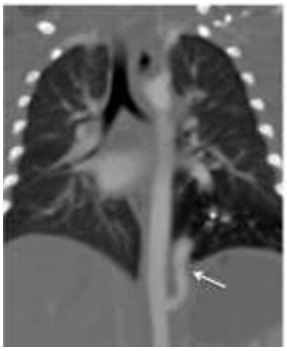

Figure 1. Coronal CTA of a 2 month old male with a prenatally diagnosed left lower lobe mass compatible with an intralobar sequestration on histopathology. A large arterial feeder from the upper abdominal aorta was found on surgical resection at 10 months of age. The anomalous artery (arrow) was seen on the preoperative postnatal CTA. The left lower lobe sequestration is partially visualized on this image(*).

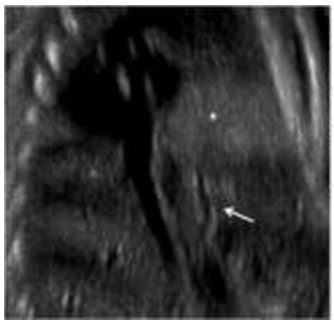

Figure 2. Gray-scale ultrasound of the same patient performed prenatally also demonstrates the anomalous arterial feeder originating from the upper abdominal aorta. The left lower lobe sequestration is partially visualized (*).

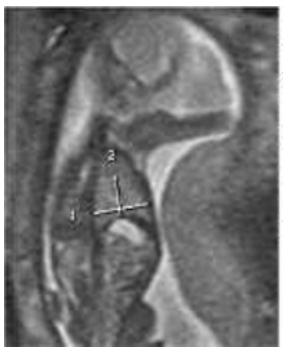

Figure 3. FSE T2 single shot MRI image of the same patient performed prenatally at 19 weeks and 2 days also demonstrates the left lower lobe mass (calipers). However, the anomalous artery was not visualized on MRI.

Paper #: 036

Magnetic Resonance Imaging of Central Lymphatics in Noonan's Syndrome

David Biko, MD[1], *bikod@email.chop.edu*; Maxim Itkin[1], Jordan Johnstone[1], Hansel Otero, MD[1], Teresa Victoria, MD, PhD[1], Yoav Dori[1]; [1]Department of Radiology, The Children's Hospital of Philadelphia, Philadelphia, PA

Disclosures: Maxim Itkin has indicated a relationship with Guerbet Group as a consultant, speaker and for receiving a research grant. All authors have disclosed no financial interests, arrangements or affiliations in the context of this activity.

Purpose or Case Report: Noonan's syndrome is a congenital multisystem disorder characterized by short stature, cardiac defects, and skeletal abnormalities. In 15-20% of patients, lymphatic abnormalities such as lymphedema, protein losing enteropathy, pulmonary lymphangiectasia, and chylothorax are described. In this study, we aim to demonstrate the central lymphatic imaging findings in Noonan's syndrome using both non-contrast T2 weighted imaging and dynamic contrast MR lymphangiography (DCMRL).
Methods & Materials: A retrospective review of children with a confirmed history of Noonan's syndrome who underwent DCMRL with a three-dimensional T2 weighted imaging between 1/2013 and 7/2017. Imaging was evaluated in consensus by a pediatric radiologist and pediatric interventional cardiologist who subspecialize in lymphatic imaging. T2 imaging was evaluated for pleural effusions and ascites along with increased signal in the soft tissues of the upper chest and neck, mediastinum, lungs in an interstitial distribution, periportal region, mesentery, and body wall. Anomalous lymphatic flow was identified on DCMRL and subjects were classified as central lymphatic flow disorder (CLFD) or pulmonary lymphatic perfusion syndrome (PLPS). The size and presence or absence of the thoracic duct (TD) was noted. The medical record was retrospectively reviewed. Medical management and lymphatic interventions along with outcomes including mortality were noted.
Results: A total of 5 subjects with a diagnosis of Noonan's syndrome underwent DCMRL with T2 weighted imaging. All subjects had some form of congenital heart disease. Subjects demonstrated abnormal T2 signal within the neck/axilla, mediastinum, interstitium of the lungs, and body wall. Pleural effusions were seen in all subjects and large volume ascites was seen in 2/5. An absent or hypoplastic TD was present in 3/5. 4 subjects with anomalous lymphatic flow to the lungs were classified as PLPS and 1 with multi-compartmental anomalous lymphatic flow as CLFD. All 4 subjects classified as PLPS improved, 2 were treated with lipiodol embolization and 2 were managed medically. The 1 CLFD subject expired following embolization.
Conclusions: Patients with Noonan's syndrome demonstrate central lymphatic flow disorders that can be successfully imaged with DCMRL. All patients imaged had anomalous lymphatic flow and half of the patients demonstrated an absent or hypoplastic central TD. Multi-compartmental anomalous lymphatic flow as seen in CLFD suggests a poor prognosis.

Paper #: 037

Initial Clinical Evaluation of Stationary Digital Chest Tomosynthesis in Patients with Cystic Fibrosis

Brian Handly, MD[1], *bhandly@med.unc.edu*; Elias Gunnell[1], Dora Franceschi[1], Christy Inscoe, MS[1], Alison Hartman[1], Jennifer Goralski, MD[1], Agathe Ceppe, MS[1], Cassandra Sams[1], Lynn Fordham, MD[1], Jianping Lu, PhD[1], Otto Zhou[1], Yueh Lee, MD/PhD[1]; [1]Radiology, University of North Carolina, Chapel Hill, NC

Disclosures: Yueh Lee has indicated a relationship with Xinray, Inc. for intellectual property rights. All other authors have disclosed no financial interests, arrangements or affiliations in the context of this activity.

Purpose or Case Report: Radiographic evaluation of cystic fibrosis currently relies on chest radiography or computed tomography. Recently, digital chest tomosynthesis has been proposed as an alternative. We have demonstrated the feasibility of a stationary digital chest tomosynthesis (s-DCT) system based on a carbon nanotube (CNT) linear x-ray source array. This system enables tomographic imaging without movement of the x-ray tube and allows for physiological gating. This is the first in-human study of s-DCT in cystic fibrosis patients.
Methods & Materials: CF patients undergoing chest radiography were also imaged on the s-DCT system Three board-certified pediatric radiologists reviewed both CXR and s-DCT images for technique and image quality. CF disease severity was assessed by Brasfield score on CXR and chest tomosynthesis score on s-DCT. Disease severity measures were also assessed against subject pulmonary function tests.
Results: Fourteen patients underwent s-DCT imaging following chest radiography. Readers scored the visualization of proximal bronchi, small airways and vascular pattern higher on s-DCT than CXR. Correlation between the averaged Brasfield score and averaged tomosynthesis disease severity score for CF was -0.73,

p=.0033. The CF disease severity score system for tomosynthesis had high correlation with FEV1 (-0.685), FEF 25-75% (-0.719), and good correlation with FVC (-0.582).
Conclusions: We demonstrate the potential of CNT x-ray based s-DCT for use in the evaluation of cystic fibrosis disease status, in the first clinical study of s-DCT.

Paper #: 038

Trending Use and Results of Computed Tomographic Angiography for Diagnosing Pulmonary Embolism in the Pediatric Emergency Department: A 13-Year Retrospective Study.

Edward Fenlon[1], *fenlone@email.chop.edu*; Summer Kaplan, MD MS[1], Christian Barrera, MD[1], Hansel Otero, MD[1], Michael Francavilla, MD[1]; [1]Radiology, Children's Hospital of Philadelphia, Philadelphia, PA

Disclosures: All authors have disclosed no financial interests, arrangements or affiliations in the context of this activity.

Purpose or Case Report: While pulmonary embolism (PE) is uncommon in children, quick and accurate diagnosis is crucial to ensure timely management. The rate of PE is reported to be approximately 16% among children with clinically suspected PE who underwent computed tomographic angiography (CTA). Studies on the prevalence of PE in children have not accounted for the point of clinical care. The pediatric emergency department (ED) is a common location where a child may present with symptoms concerning for PE. The purpose of this study is to evaluate the trends and results of CTAs ordered in the ED to evaluate for PE over a 13-year period in a tertiary care facility.
Methods & Materials: Institutional Review Board approval was obtained. Institutional electronic databases were used to search for study reports of patients who underwent CTA to evaluate for PE while in the ED. No image review was performed; all information and data was obtained from study reports. Exclusion criteria included age greater than 20 years and CTA ordered for reasons other than to evaluate for PE (e.g., aortic dissection, vascular trauma, etc.). Data recorded included: age, sex, presence of acute or chronic PE, presence of other findings in the impression, and presence of language indicating a suboptimal exam due to technical or patient related factors.
Results: A total of 308 CTAs performed between January 2005 and October 2017 met criteria, including 122 boys and 186 girls. The 13-year positive rate of acute or chronic PE was 16.2%. Mean and median age at time of CTA was 16.04 and 16.83 years respectively, with a standard deviation of 3.17 years. Age did not correlate with either the presence of PE (p=0.3109) or a limited CTA (p=0.4176). The yearly incidence of PE ranged from zero to seven while the number of CTAs increased from two studies in 2005 to 53 in 2016 (Fig 1). The rate of other important diagnostic findings in studies negative for PE was 39.9% and the overall rate of suboptimal exams was 14%.
Conclusions: Despite the tenfold increase in CTAs performed during 13 years, the incidence of PE has remained consistently low in the pediatric ED. While the prevalence of PE among children presenting to the ED would not be expected to vary significantly from year to year, there may be yearly trends in ordering practices by ED physicians that are affected by a multitude of factors including CT availability, changing perceptions of radiation risk, and the practice of "defensive medicine." More analysis may better elucidate the cause for this trend.

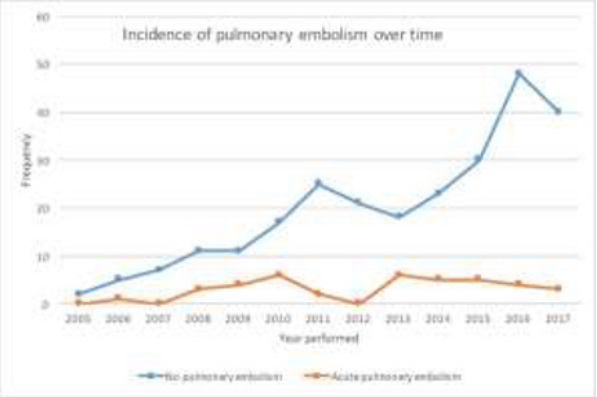

Paper #: 039

Target mode prospective EKG gated volumetric CT reduces the need for sedation for chest CT in young children

Rajesh Krishnamurthy[1], *Rajesh.Krishnamurthy@nationwidechildrens.org*; Jessica Morrison[1], Kevin Dolan[1], Jarred Lovelace[1], Akila Sankaran[1], Leah Dameron[1], Jennifer Yashko[1], Houchun Hu, PhD[1], David Hintenlang[2], Cody Young, DO[1]; [1]Nationwide Children's Hospital, Columbus, OH, [2]Ohio State University, Columbus, OH

Disclosures: All authors have disclosed no financial interests, arrangements or affiliations in the context of this activity.

Purpose or Case Report: We propose using the 'target mode' prospective EKG gating technique with volumetric 320-detector scanner for respiratory motion and gross motion compensation for routine lung and mediastinal CT in pediatric patients who cannot cooperate with volitional breath-holding, thereby avoiding the need for IV sedation or general anesthesia.
Methods & Materials: All chest and cardiovascular CT studies in patients ages 0-4 years performed at our institution between the period of January 2016 and September 2017 were included in the analysis. The target mode protocol was instituted in November 2016, with exposure time of 350ms, half-scan reconstruction, 80-100 kV and 30-150 mA (indication based). Heart rate was used to determine target phase and ImageExact (Toshiba, Tustin, CA) used to reconstruct a motionless phase of the cardiorespiratory cycle for the organ/s of interest (lung, mediastinum, vasculature). Rate of sedation for chest CT before and after the institution of the target mode protocol was compared using a test of proportions. Rate of call-back of patients for diagnostic inadequacy after an unsedated scan was monitored. Image quality grading by two radiologists on a 4-point scale, and quantitative image quality assessment by a physicist are pending.
Results: From Jan-Nov 2016, 232 out of 358 studies (65.3%) were performed with sedation/GA. From Dec 2016-Sep 2017, after the institution of the target mode protocol, 109 out of 310 patients (35.2%) were sedated. The 46% reduction in sedation rate was statistically significant (p<0.01) (Figure 1). All unsedated studies were done free-breathing and were diagnostic for the clinical indication, with no callbacks. From November 2016 to July of 2017, the unsedated target mode protocol was implemented for all chest indications, but allowing for radiologist/clinician preference for use of sedation, accounting for most of the remaining sedated cases. Starting in July 2017, unsedated CT protocol was made mandatory for all indications except high resolution CT, inspiratory-expiratory CT and coronary stenosis evaluation. Further data collection after this change and quantitative image quality assessment are ongoing.

Conclusions: Volumetric imaging with target mode prospective EKG gating provides diagnostic studies with adequate cardiac, respiratory and gross motion compensation for most chest and cardiovascular indications in awake, free-breathing children aged 0-4 years, and almost halved the sedation rate at our institution.

Figure 1: p-chart of rate of sedation for chest CTs in patients 0-4 years of age. The unsedated target mode protocol was instituted in end of November 2016. The ability of clinician/radiologist to override the unsedated protocol and request sedation was removed in July 2017.

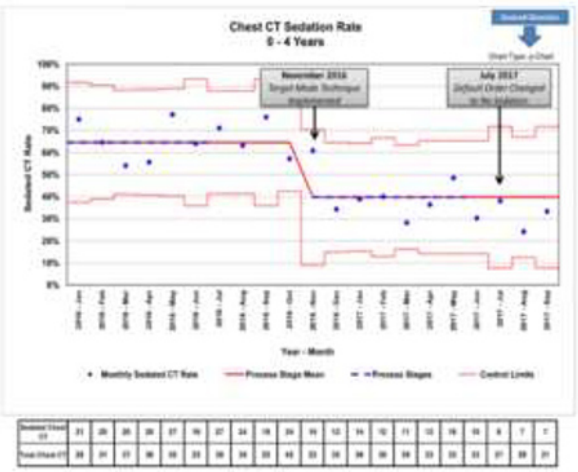

Paper #: 040

Tracheal Narrowing in Children and Young Adults with Mucopolysaccharidosis IVA: Evaluation with CT Angiography

Lauren Averill, MD[1], *laverill@nemours.org*; Mary Theroux[1], Christian Pizarro[1], Michael Bober, MD[1], William Mackenzie, MD[1], Colleen Ditro[1], Heidi Kecskemethy[1], Shunji Tomatsu[1]; [1]Nemours Children's Health System, Wilmington, DE

Disclosures: Michael Bober has indicated a relationship with Biomarin for a research grant. All other authors have disclosed no financial interests, arrangements or affiliations in the context of this activity.

Purpose or Case Report: Tracheal narrowing and tortuosity can cause respiratory distress and life-threatening anesthetic complications in mucopolysaccharidosis (MPS) IVA. Tracheostomy is difficult or impossible in these patients, with novel trachea reconstructive surgery being performed to reduce morbidity and mortality. We describe tracheal, vascular and bony anatomy of the thoracic inlet on CT angiography of the chest in children and young adults with MPS IVA.
Methods & Materials: The EMR of a tertiary care children's hospital was queried for all patients with MPS IVA and chest CTA. Images were analyzed using PACS and TeraRecon. The trachea shape at the thoracic inlet was described (C=round, D=mild flattening anterior-posterior (AP), U= mild flattening transversely, W=worm or ellipsoid, T=triangular). Direction of tracheal narrowing and deviation were recorded. The trachea cross sectional area (TCSA) was measured at level of greatest narrowing at the thoracic inlet, noting length and vertebral level. The largest cervical and thoracic TCSA were also measured. Other features described include: location of the brachiocephalic artery (BCA) in relation to tracheal narrowing, course of the BCA and aorta, sternum alignment, thyroid location, and AP diameter of the thoracic inlet from manubrium and clavicle heads to the spine.
Results: 27 patients (mean age 18 years, range 5-36 years) were included. Tracheal shape at the thoracic inlet was W in 18, T in 5, U in 3 and C in 1. All patients except one 6 year-old had tracheal narrowing at the thoracic inlet. Oblique narrowing (19/27) with rightward (23/27) and posterior (19/27) deviation was most commonly seen. Mean TCSA reduction from cervical to thoracic inlet was 74.9% (range 4-97.2%), and from thoracic to thoracic inlet was 66.5% (range -2.1-96%). Narrowing was centered from C6-T2, with mean length 2.6cm (range 1.1-5.2cm). The BCA was tortuous with a transverse course at the thoracic inlet in all patients, with aortic tortuosity in most (25/27). The BCA directly impinged upon the trachea in 18 patients. Pectus carinatum was present in 26/27 and excavatum in 1/27. Mean distance manubrium-spine was 2.8cm, and clavicle-spine was 2.5cm. Thyroid was located in the thoracic inlet in 21 patients.
Conclusions: Oblique tracheal narrowing at the thoracic inlet with rightward-posterior deviation is common in children and young adults with MPS IVA. BCA tortuosity, bony narrowing and soft tissue crowding are associated features, informing decisions regarding tracheal reconstructive surgery.

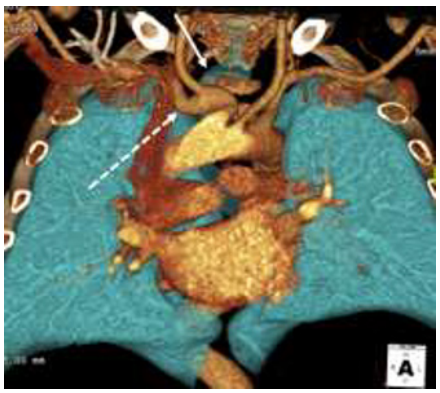

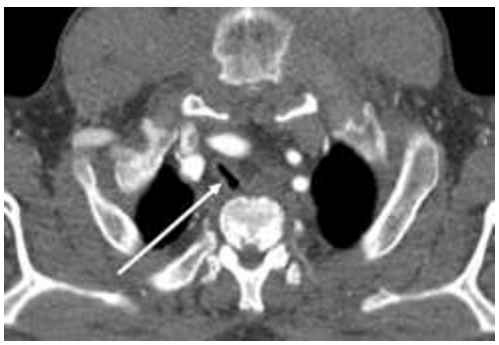

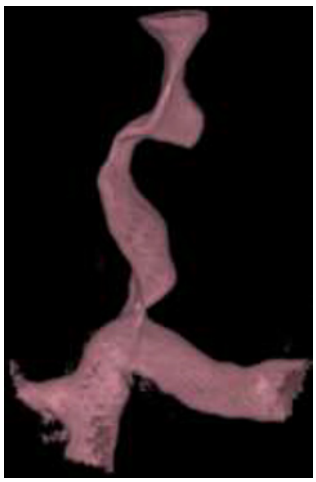

Paper #: 041

A Novel Approach Using Volumetric Dynamic Airway CT to Determine Optimal Positive End Expiratory Pressure (PEEP) Settings in Neonates Requiring Long-Term Ventilator Support

Lauren May, MD[1], *Lauren.a.may@gmail.com*; Siddharth Jadhav, MD[1], R. Guillerman[1], Pamela Ketwaroo[1], Prakash Masand, MD[1], Rajesh Krishnamurthy[2]; [1]Department of Radiology, Texas Children's Hospital, Houston, TX, [2]Nationwide Children's Hospital, Columbus, OH

Disclosures- The opinions expressed on this document are solely those of the authors and do not represent an endorsement by or the views of the United States Army, United States Air Force, the Department of Defense, or the U.S. Government. All other authors have disclosed no financial interests, arrangements or affiliations in the context of this activity.

Purpose or Case Report: Positive End Expiratory Pressure (PEEP) is a key mechanical ventilator setting in neonates with bronchopulmonary dysplasia (BPD). Excessive PEEP may result in insufficient CO_2 elimination and lung damage, while insufficient PEEP can result in impaired gas exchange secondary to airway and alveolar collapse. Determining PEEP settings based on clinical parameters alone is suboptimal due to the inability to titrate pressure with airway dimensions. The purpose of this study is to describe our experience using dynamic airway CT to determine the lowest PEEP setting sufficient to maintain airway patency in BPD patients requiring long-term ventilator support.

Methods & Materials: In this IRB approved study we retrospectively identified all neonatal patients with BPD that underwent volumetric CT with a dynamic airway protocol to optimize PEEP settings from December 2014 through February 2017. The goal was to identify the minimal PEEP necessary to maintain a cross-sectional area (CSA) of the trachea or mainstem bronchi of at least 50-60% of the maximal CSA and prevent atelectasis. Clinical data collected included history, age, sex, initial PEEP setting, PEEP settings trialed during CT, and PEEP setting used clinically after CT. Imaging data included the CSA of the trachea and mainstem bronchi at each setting, lung parenchymal findings, CTDI and DLP.

Results: Eight neonates with BPD underwent 9 CT exams. Mean age at time of CT was 173 days (74-334 days). Additional relevant diagnoses included tracheobronchomalacia in 3 patients and pulmonary hypertension in 3 patients. Patients underwent 1-4 airway volumes spanning the trachea and mainstem bronchi at different PEEP settings with a median of 3 volumetric scans per CT exam. Average CTDI and DLP per scan were 1.48 mGy (range: 0.5-2.6) and 11.63 mGy-cm (range: 3.3-24.6), respectively. Based on the minimal pressure necessary to maintain airway patency during PEEP trials on CT, PEEP was increased in 5 patients, decreased in 1 patient, and kept the same in 3 patients.

Conclusions: Dynamic airway CT is a promising adjunct to clinical assessment to optimize PEEP settings in neonatal BPD patients requiring long-term ventilator suppor

Age	Sex	Relevant Diagnoses	Trialed PEEP Settings*	Tracheal Collapse	Right Bronchus Collapse	Left Bronchus Collapse	PEEP Setting Used After CT	CTDI	DLP
2m 15d**	F	Bronchopulmonary Dysplasia Tracheobronchomalacia Pulmonary Hypertension	9 cm	< 20%	< 20%	< 20%	9 cm	1.8	19.9
			8 cm	40%	30-40%	30-40%		1.8	19.9
2m 25d	U	Bronchopulmonary Dysplasia	8 cm	50-60%	50-60%	50-60%	10 cm	1.9	11.4
			10 cm	50%	50%	50%		1.9	11.4
			9 cm	70-80%	70-80%	70-80%		1.9	11.4
			12 cm	40%	40%	40%		1.9	11.4
4m 25d	M	Bronchopulmonary Dysplasia Pulmonary Hypertension	14 cm	minimal	minimal	60 - 70 %	7 cm	0.6	5.3
			12 cm	minimal	minimal	60%		0.6	5.3
			10 cm	minimal	minimal	50%		0.6	5.3
			8 cm	minimal	minimal	70%		0.6	5.3
5m 11d**	F	Bronchopulmonary Dysplasia Tracheobronchomalaci Pulmonary Hypertension	11 cm	No expiration	No expiration	50-60%	11 cm	1.42	11.4
			13 cm	60%	50-60%	50-60%		1.42	11.4
			15 cm	50%	20-40%	20-40%		1.42	11.4
5m 22d	M	Bronchopulmonary Dysplasia Congenital Diaphragmatic Hernia	8 cm	70-80%	70-80%	70-80%	16 cm	0.94	7.5
			9 cm	50%	50%	50%		0.94	7.5
			12 cm	40-50%	40-50%	40-50%		0.94	7.5
			14 cm	40-50%	40-50%	40-50%		0.94	7.5
5m 23d	M	Bronchopulmonary Dysplasia Tracheobronchomalacia	12 cm	minimal	minimal	minimal	12 cm	1.4	11.2
6m 19d	F	Bronchopulmonary Dysplasia Pulmonary Hypertension	8 cm	40%	40%	<20%	8 cm	2.3	24.8
			5 cm	80%	80%	<20%		2.3	15.8
6m 25d	F	Bronchopulmonary Dysplasia	8 cm	30%	40-50%	30%	10 cm	1.8	18
			10 cm	30%	20-30%	30%		1.8	18
			11 cm	< 20%	< 20%	< 20%		1.8	18
11m 18d	M	Bronchopulmonary Dysplasia Tracheobronchomalacia	11 cm	60-70%	60-70%	60-70%	12 cm	1.7	17.1
			13 cm	50%	50%	50%		1.7	17.1
			12 cm	40%	40%	40%		1.7	17.1

*Initial PEEP Setting Varied Followed by PEEP settings trialed during CT
**Same patient

Paper #: 042

Imaging patterns in pediatric pulmonary blastomycosis

Katya Rozovsky, MD[1], *katro70@yahoo.com*; Martin Bunge[1], Richard Higgins, MD[1], Lina Alqublan[1], Raquel Consunji-Araneta[1], Sergio Fanella, MD[1]; [1]HSC, Children's Hospital of Winnipeg,University of Manitoba, Winnipeg, MB, Canada

Disclosures: All authors have disclosed no financial interests, arrangements or affiliations in the context of this activity.

Purpose or Case Report: To characterize the imaging patterns of pediatric pulmonary blastomycosis.

Methods & Materials: Retrospective study included patients aged 0-18 years with pulmonary blastomycosis, who underwent chest x-rays or chest CT from 2005 to 2016, divided by age: 0-1 year, 1-5 years, 5-12 years, and 12-18 years. The following data was collected: age, gender, clinical information, imaging findings during the first two weeks of admission, extrapulmonary involvement, and presence of scarring on follow-up exams. Concordance between chest x-rays and CT was analyzed.

Results: 36 patients were identified (28 males (78%)), age 3 month-17 years (mean 10.5 years). 0-1 year (2 patients, 1 male), 1-5 years (3 patients, 2 male), 5-12 years (12 patients, 12 male), 12-18 years (19 patients, 13 male). 35/36 patients had chest x-rays, 12/36 had x-rays and CT, 1 patient had CT. Air space consolidation was found in 94.4%, 76.5% unilateral (17 unilobar, 9 multilobar). Right lung was more frequently involved. The predominant distribution included upper and middle lobes. 76% had air bronchogram. In 55.9% consolidation was mass-like. 38.2% had cavitation measured more than1 cm. Cavitation was present in male patients exclusively. "Bubbly" pattern (multiple small cavities, distributed along the bronchial tree) was seen in 32.4%. In 69.5% consolidations were associated with other abnormal findings: pulmonary nodules (50%, (70.6% bilateral, 76.5% measured 0.3-1 cm in diameter)), diffuse patchy opacification (26.5%), interstitial reticulonodular pattern (41.2%), hilar lymphadenopathy (23.5%), pleural effusion (20.6%) and subsegmental or segmental atelectasis (5.9%). Extrapulmonary disease was present in 5/36 patients: ribs osteomyelitis (2 cases), multifocal osteomyelitis, skull lesion and brain mass-like lesion. Pulmonary scarring on follow-up exams was found in 70.4%. In two patients younger than 1 year no pulmonary nodules, hilar lymphadenopathy or extrapulmonary involvement was found. Concordance between x-rays and CT was excellent for location and extension of consolidation, diagnosis of cavitation, "bubbly" pattern and nodules; good for air bronchogram and pleural effusion, fair for atelectasis; and

poor for hilar lymphadenopathy and reticulonodular pattern.
Conclusions: We present the imaging features of pediatric pulmonary blastomycosis. In our series the most frequent pattern of lung involvement was the combination of consolidation with bilateral medium size lung nodules, accompanied by interstitial reticulonodular pattern.

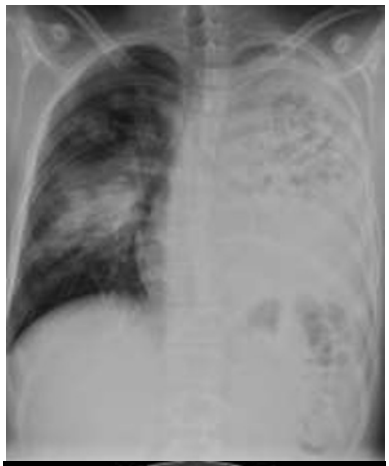

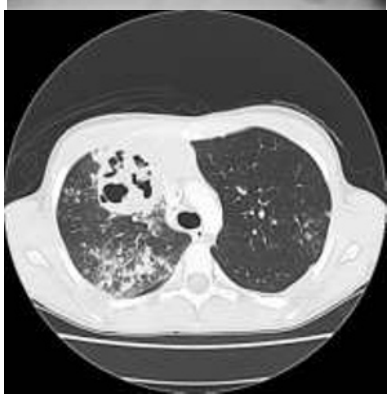

Table 1. Abnormal findings on chest x-rays in relation to age (calculated for 34 patients with lung consolidation)

Consolidation	Number of patients Total n=34	Age (years) 0-1 n=2 (5.9%)	1-5 n=3 (8.8%))	5-12 n=11 (32.4%)	12-18 n= 18 (52.9%))
Size of consolidation					
a) 3-6 cm	5/34 (14.7%)	0	1/3(33.3%)	2/11(18.2%)	2/18 (11.1%)
b) >6 cm	29/34 (85.3%	2/2(100%)	2/3(66.7%)	9/11(81.8%)	16/18(88.9%)
Air bronchogram	26/34(76.5%)	1/2(50%)	2/3(66.7%)	8/11(72.7%)	15/18(83.3%)
Mass-like appearance	19/34(55.9%)				
a)peripheral	2/19(10.5%)	0	1/3(33.3%)	0	1/18(5.6%)
b)central	8/19(42.1%)	0	1/3(33.3%)	3/11(27.3%)	4/18(22.2%)
c)peripheral and central	9/19(47.4%)	1/2(50%)	1/3(33.3%)	2/11(18.2%)	5/18(27.8%)
Cavitation	13/34(38.2%)	1/2(50%)	1/3(33%)	5/11(45.5%)	6/18(33.3%)
"Bubbly" pattern	11/34(32.4%)	1/2 (50%)	0	5/11(45.5%)	5/18(27.8%)
Mass effect	2/34(5.9%)	1/2 (50%)	0	1/11(9.1%)	0

Other chest x-rays abnormalities

Nodules	Number of patients	Age (years) 0-1	1-5	5-12	12-18
Nodules (total)	17/34 (50%)	0	2/3(66.7%)	7/11(63.6%)	8/18(44.4%)
Unilateral	5/17(29.4%)	0	0	1/11(9.1%)	4/18(22.2%)
Bilateral	12/17(70.6%)	0	2/3(66.7%)	6/11(54.5%)	4/18(22.2%)
0.3-1 cm in size	13/17(76.5%)	0	1/3(33.3%)	5/11(45.5%)	7/18(38.9%)
1-3 cm in size	4/17 (23.5%)	0	1/3(33.3%)	2/11(18.2%)	1/18(5.6%)
Diffuse patchy opacification	9/34(26.5%)	1/2(50%)	1/3(33.3%)	3/11(27.3%)	4/18(22.2%)
Reticular-nodular pattern	14/34(41.2%)	2/2(100%)	0	3/11(27.3%)	7/18(38.9%)
Atelectasis	2/34(5.9%)	0	1/3(33.3%)	0	1/18(5.6%)
Pleural effusion (total)	7/34(20.6%)	1/2(50%)	1/3(33.3%)	1/11(9.1%)	4/18(22.2%)
Small amount	4/7 (57.1%)	1/2(50%)	1/3(33.3%)	0	2/18(11.1%)
Large amount	3/7(42.9%)	0	0	1/11(9.1%)	2/18(11.1%)
Hilar lymphadenopathy	8/34(5.88%)	0	0	4/11(36.4%)	4/18(22.2%)
Extrapulmonary involvement (total)	5/34(14.7%)	0	1/3(33.3%)	2/11(18.2%)	2/18(11.1%)
Skull	1/5(20%)	0	0	0	1/18(5.6%)
Ribs	2/5(40%)	0	1/3(33.3%)	1/11(9.1%)	0
Brain	1/5(20%)	0	0	1/11(9.1%)	0
Multifocal bony osteomyelitis	1/5(20%)	0	0	0	1/18(5.6%)

Paper #: 043

Gadolinium bone tissue retention in pediatric patients after contrast-enhanced MR exams: pathologic confirmation.

A. Luana Stanescu, MD[1], *stanescu@u.washington.edu*; Dennis Shaw, MD[1], Seth Friedman, PhD[1], Kenneth Maravilla[2]; [1]Radiology, Seattle Children's Hospital, Seattle, WA, [2]University of Washington, Seattle, WA

Disclosures: All authors have disclosed no financial interests, arrangements or affiliations in the context of this activity.

Purpose or Case Report: Retained Gadolinium (Gd) in bone tissue has been demonstrated pathologically in adults from gadolinium based MRI contrast agents (GBCA). Bone Gd deposition has not been yet demonstrated pathologically in children. The long term effects of retained Gd are unknown, but may be of potentially greater concern in children given their expected longer period of exposure. Several factors may influence Gd retention. Generally, greater accumularion is suggested with linear agents compared with macrocyclic chelates, attributed to lower chelate affinity. The purpose of this study was to investigate whether Gd bone deposits are present in pediatric patients receiving GBCA and to quantify the amounts present.
Methods & Materials: Following IRB approval, bone fragments preserved in either formalin and/or saline solution from craniotomies in 17 pediatric patients between 6 months and 20 years of age were analyzed for elemental Gd using inductively coupled plasma-mass spectrometry (ICP-MS). Eleven subjects underwent at least one contrast-enhanced MR exam, with six subjects having no known exposure to GBCA serving as controls. Two subjects, one of each group, were excluded due to insufficient bone samples. Type and dose of contrast agent, number and timing of contrast-enhanced MR exams relative to the surgery and absence of evidence of renal failure were documented for patients with known GBCA exposure.
Results: Patient exposures ranged from 1 to >19 doses of GBCA including both macrocyclic and linear ionic agents. Gd was found to be present in bone tissue in all exposed patients, with concentrations ranging from <0.01 to 0.449 ng/g for saline preserved samples and 0.01 to 0.765 ng/g for formalin preserved

samples. Those who received only macrocyclic agents showed lower levels of Gd retention compared to patients who received both macrocyclic and linear GBCA.
Conclusions: This study demonstrates the first pathologic confirmation of Gd retention in bone tissue of pediatric patients exposed to GBCA including both macrocyclic and linear ionic agents. While the significance of these deposits remains unknown, at this point it would be prudent to avoid unnecessary use of GBCA in pediatric patients.

Paper #: 044

Safety and efficacy of gadoterate meglumine in children <2 years of age

Shannon Farmakis, MD[2], *shannon.farmakis@health.slu.edu*; Scott Wilson-Flewelling, MSIV[1], Vilaas Shetty, MD[1], **Ting Tao, MD**, PhD[2]; [1]Radiology, St. Louis University School of Medicine, St. Louis, MO, [2]SSM Health Cardinal Glennon Children's Hospital, St. Louis, MO

Disclosures: Shannon Farmakis has indicated a relationship with GE Healthcare for receiving a research grant. All other authors have disclosed no financial interests, arrangements or affiliations in the context of this activity.

Purpose or Case Report: To assess safety and efficacy of gadoterate meglumine (Dotarem®) in patients <2 years of age by evaluating adverse reactions and image quality following contrast administration.
Methods & Materials: Pediatric patients < 2 years of age undergoing MRI with and without contrast were prospectively enrolled and received a weight-based intravenous dose of Dotarem (0.1 mmol/kg). Almost all patients (96.3%) received sedation/anesthesia before MRI. The occurrence of adverse events (AE) was assessed at the time of injection, up to 2 hours after MRI, and by phone contact using a standard questionnaire 24 hours after MRI. AEs were documented including time of onset, duration of symptoms, intensity, causality, and subsequent outcome.Three radiologists blinded to the patients' clinical histories evaluated image quality by comparing pre-contrast images to combined pre- and post-contrast images in order to assess improvement in border delineation, internal morphology, and lesion enhancement following contrast administration.
Results: A total of 112 exams were completed in 111 patients (median 12 months; range 0.5 - 23 months; males 56%). There were no reactions at the injection site within the initial 2 hours. A total of 14 patients (12.5%), who had all received sedation/anesthesia, reported minor reactions within 24 hours (median age 11 months, range 5-23 months; male 78.6%). Six patients (5.4%) reported emesis during the 24-hour period with 1 case (0.9%) occurring within the initial 2 hours, likely related to drinking formula after anesthesia. Mild rashes were reported for 1 patient (0.9%) at the injection site and 3 patients (2.7%) at remote sites. Four patients (3.6%) reported a flushed face/warmth. No patient experienced anaphylaxis.
Image quality was evaluated in 110 exams, as no similar pre-contrast sequences were obtained in 2 exams. There was complete inter-reader agreement that post contrast images resulted in a 100% improvement in border delineation, internal morphology, and contrast enhancement.
Conclusions: No patient experienced AEs directly related to Dotarem, and the delayed onset of AEs was very limited. The higher reported rate of AEs in this study may be related to concomitant sedation/anesthesia as well as to over-reporting from parents due to 24-hour follow-up questionnaire. The study confirms a good safety profile for Dotarem in this very sensitive population. Use of Dotarem improved image quality and anatomic characterization compared to the pre-contrast images.

Paper #: 045

Free-Breathing Ferumoxytol-Enhanced MRI for Preoperative Renal Transplant Vascular Mapping in Infants and Children

Evan Zucker, MD[1], *zucker@post.harvard.edu*; Aya Kino, MD[1], Joseph Cheng[1], Richard Barth[1], Shreyas Vasanawala, MD, PhD[1]; [1]Stanford University, Stanford, CA

Disclosures: Joseph Cheng has indicated a relationship with HeartVista, Inc. as a consultant and receives royalty from GE Healthcare. All other authors have disclosed no financial interests, arrangements or affiliations in the context of this activity.

Purpose or Case Report: To evaluate the feasibility and image quality of free-breathing ferumoxytol-enhanced MRI for preoperative vascular mapping in infants and children with end-stage renal disease (ESRD) and contraindications to gadolinium, comparing motion-corrected 3D spoiled gradient echo (SPGR) and conical ultrashort echo time (UTE) acquisition strategies.
Methods & Materials: 25 consecutive children with ESRD who underwent post-ferumoxtyl MRI from 2013-17 were retrospectively identified (mean age: 4.1 years, range: 8.0 months-16.2 years; 16 male), including 11 (44.0%) under 2 years. 3 studies (12.0%) were performed awake, 6 (24.0%) with light anesthesia, and the rest with deep anesthesia. All exams included a 3D SPGR sequence; 19 (76.0%) also used conical UTE. On a 5-point scale (1-nondiagnostic, 5-excellent), two blinded radiologists independently scored image quality of selected vascular landmarks for each study/ acquisition. Scores were compared using Wilcoxon signed-ranks and rank-sum tests and interobserver agreement assessed with Cohen's kappa coefficient (k). To assess measurement precision of SPGR vs. UTE, AP and TRV diameters of selected vessels (aorta, IVC, common iliacs) were also obtained for each study/acquisition at matching anatomic levels and compared with Bland-Altman analysis.
Results: Individual and combined mean scores for all landmarks/acquisitions were ≥4.5, indicating good to excellent image quality (Figure 1), with moderate interobserver agreement (k=0.53). Both readers also scored all landmarks ≥3 (at least diagnostic) in every case, regardless of acquisition strategy. Right external and internal iliac vein scores were minimally greater for SPGR compared to UTE (5.0 +/- 0.2 vs. 4.8 +/- 0.5, P=0.046 and 5.0 +/- 0.0 vs. 4.8 +/- 0.6, P=0.008, respectively); there was no other significant difference by acquisition type. Mean composite landmark scores in infants under 2 were statistically equivalent to those of older children for SPGR (4.9 +/- 0.4 vs. 4.8 +/- 0.4, P=0.274) and slightly lower for UTE (4.6 +/- 0.7 vs. 4.9 +/- 0.3, P<0.001) (Figures 2-3). Vessel measurements were nearly equivalent for SPGR vs. UTE (mean difference: -0.01 mm, limits of agreement: -0.7 to +0.6 mm).
Conclusions: Free-breathing ferumoxytol-enhanced MR for pre-renal transplant vascular mapping is feasible in children across the age and sedation spectrum, with excellent diagnostic image quality. Both 3D SPGR and UTE are viable acquisition strategies with essentially equivalent delineation of arterial and venous structures.

Figure 1. Summary of Reader Image Quality Scores for Each Landmark and Acquisition Strategy

Anatomy	Reader 1 Mean Score (SD)		Reader 2 Mean Score (SD)		Combined Mean Score (SD)	
	3D SPGR (n = 23)	UTE (n = 18)	3D SPGR (n = 23)	UTE (n = 18)	3D SPGR (n = 23)	UTE (n = 18)
Abdominal aorta	5.0 (0.0)	4.9 (0.5)	5.0 (0.0)	4.8 (0.5)	5.0 (0.0)	4.9 (0.5)
Celiac axis	4.8 (0.4)	4.8 (0.3)	4.9 (0.3)	4.7 (0.8)	4.9 (0.3)	4.8 (0.5)
SMA	4.8 (0.4)	4.8 (0.5)	4.9 (0.3)	4.8 (0.5)	4.9 (0.4)	4.8 (0.5)
IMA	4.7 (0.5)	4.8 (0.5)	4.8 (0.4)	4.8 (0.5)	4.8 (0.4)	4.8 (0.5)
R renal artery	4.8 (0.4)	4.7 (0.8)	4.8 (0.4)	4.6 (0.8)	4.8 (0.4)	4.6 (0.8)
R common iliac art.	4.8 (0.4)	4.9 (0.3)	4.8 (0.4)	4.7 (0.8)	4.8 (0.4)	4.8 (0.5)
R external iliac art.	4.3 (0.5)	4.7 (0.8)	4.6 (0.5)	4.6 (0.8)	4.6 (0.5)	4.7 (0.8)
R internal iliac art.	4.6 (0.5)	4.8 (0.5)	4.7 (0.5)	4.7 (0.8)	4.7 (0.5)	4.6 (0.8)
Inferior vena cava	4.8 (0.4)	4.8 (0.5)	4.8 (0.4)	4.8 (0.5)	4.8 (0.4)	4.8 (0.5)
R renal vein	4.8 (0.4)	4.8 (0.5)	4.9 (0.3)	4.8 (0.5)	4.9 (0.4)	4.8 (0.5)
R common iliac vein	5.0 (0.0)	4.9 (0.3)	4.9 (0.3)	4.9 (0.5)	5.0 (0.2)	4.9 (0.5)
R external iliac vein	5.0 (0.0)	4.8 (0.5)	4.9 (0.3)	4.8 (0.5)	5.0 (0.2)	4.8 (0.5)
R internal iliac vein	5.0 (0.2)	4.9 (0.3)	5.0 (0.2)	4.6 (0.8)	5.0 (0.2)	4.8 (0.6)

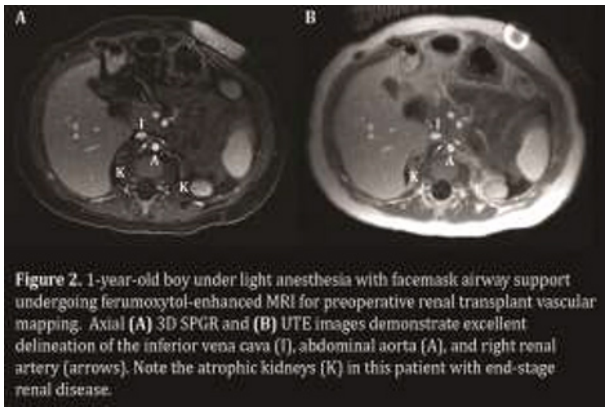

Figure 2. 1-year-old boy under light anesthesia with facemask airway support undergoing ferumoxytol-enhanced MRI for preoperative renal transplant vascular mapping. Axial **(A)** 3D SPGR and **(B)** UTE images demonstrate excellent delineation of the inferior vena cava (I), abdominal aorta (A), and right renal artery (arrows). Note the atrophic kidneys (K) in this patient with end-stage renal disease.

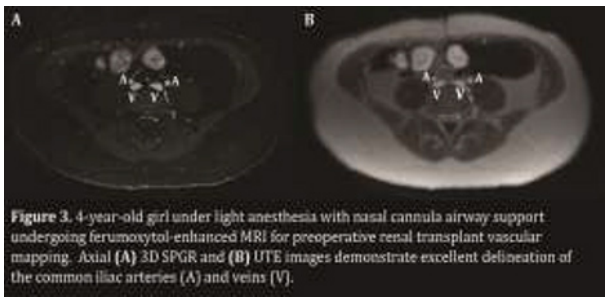

Figure 3. 4-year-old girl under light anesthesia with nasal cannula airway support undergoing ferumoxytol-enhanced MRI for preoperative renal transplant vascular mapping. Axial **(A)** 3D SPGR and **(B)** UTE images demonstrate excellent delineation of the common iliac arteries (A) and veins (V).

Paper #: 046

Feed and Wrap MRU

Sila Kurugol, PhD[1], *sila.kurugol@childrens.harvard.edu*; Onur Afacan, PhD[1], Catherine Seager[1], Reid Nichols[1], Richard Lee[1], Simon Warfield[1], Jeanne Chow, MD[1]; [1]Radiology, Boston Children's Hospital and Harvard Medical School, Boston, MA

Disclosures: All authors have disclosed no financial interests, arrangements or affiliations in the context of this activity.

Purpose or Case Report: One of the often described reasons against performing MR Urography (MRU) is the risk of sedation or anesthesia necessary to keep children motion-free. However, motion free imaging is crucial, especially during the dynamic contrast enhanced imaging. The purpose of our study was to perform MRU without sedation in infants using the feed-and-wrap technique (FW-MRU) and motion-robust dynamic radial VIBE (DRV) imaging to test if this method can be used as a successful alternative to MRU.

Methods & Materials: The departmental protocol for feed-and-wrap studies was used for infants undergoing MRU under 6 months of age. The protocol includes having the families arrive one hour prior to the scan timed to nap-times, 3 hours of fasting, feeding just prior to scanning, tightly swaddling and rocking the child to sleep. Patients were given IV hydration (10 ml/kg/hr NS) and Lasix (1mg/kg) prior to the start of scanning. MRU study included localizers, 3 plane T2FS, heavily T2 weighted 3D sequence, and dynamic contrast enhanced images using DRV and post contrast T1-FS axial images. DRV is used with compressed sensing image reconstruction to achieve motion-robust high spatiotemporal resolution imaging (3 secs/volume) with improved image quality, reducing streaking artifacts. The data was processed after the study using Sourbon's tracer kinetic model analysis to calculate differential renal function.

Results: 7 infants attempted FW-MRU on a 3T Siemens scanner between April 2016 to August 2017 with a mean age of 3.0 months (range 1.9 to 4.5). Sequence scan time was 45 minutes. In 6 of 7 patients, the infant was able to complete the study. In these patients, diagnostic anatomical and functional information could be obtained which led to useful data for medical/surgical management. Sample images showing different phases of contrast enhancement are shown in two patients (Figure 1&2). Sample Gadolinium concentration curve is shown in Figure 3. One patient was unable to fall-asleep and thus did not complete FW-MRU. 5/7 studies were performed for the indication of prenatal hydronephrosis. 2 studies were performed for complex genitourinary anomalies.

Conclusions: In all infants who were able to sleep, FW-MRU succeeded in obtaining anatomical and functional information useful for clinical decision-making. Initial experience with FW-MRU demonstrates it to be a safe and effective means of obtaining anatomic and functional imaging of the urinary tract in infants under 6 months of age without the use of sedation or anesthesia.

**Work supported by the SPR Research and Education Foundation*

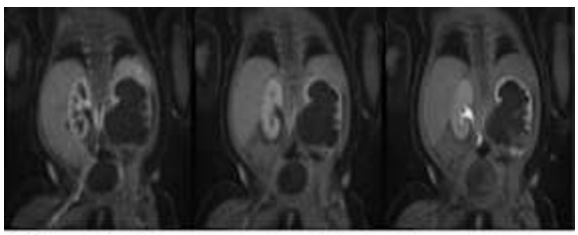

Figure 1. Dynamic contrast-enhanced images acquired using the motion-compensated dynamic radial VIBE (DRV) sequence. The contrast enhancement of kidney is shown at different time points for a 10 day old male with UPJ obstruction on the left side. Differential renal function was calculated as 46% for the left kidney and 54% for the right kidney.

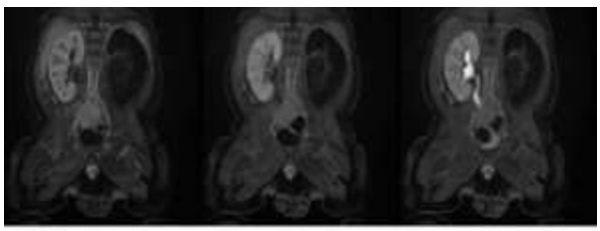

Figure 2. Dynamic contrast-enhanced images acquired using the high spatio-temporal resolution, motion-robust, dynamic radial VIBE (DRV) sequence. The contrast enhancement of kidneys are shown at different time points for a 9th day old male with left multicystic dysplastic kidney. Differential Renal Function was calculated to be 98% for the left kidney and 2% for the right kidney.

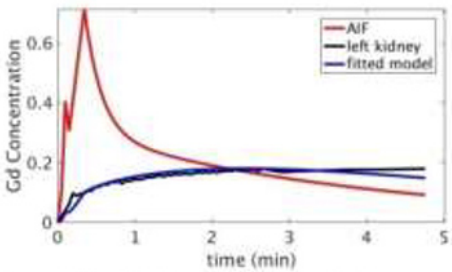

Figure 3. Gadolinium concentration versus time curve from the right kidney of the patient in Figure 2. Arterial input function is shown in red, the measured signal is shown in blue and the fitted model using Sourbron's tracer kinetic model is shown in black.

Paper #: 047

Morphologic and Functional Evaluation of Duplicated Renal Collecting Systems with MR Urography: A Descriptive Analysis

Hansel Otero, MD[1], *hanselotero@gmail.com*; Sally Emad-Eldin, MD[2], Carolina Maya, MD[1], Melkamu Adeb, MD[1], Susan Back, MD[1], Kassa Darge, MD, PhD[1]; [1]Children's Hospital of Philadelphia, Philadelphia, PA, [2]Cairo University, Cairo, Egypt
Disclosures: All authors have disclosed no financial interests, arrangements or affiliations in the context of this activity.

Purpose or Case Report: To describe the morphology and function of duplicated collecting systems in pediatric patients undergoing functional MR urography (fMRU).
Methods & Materials: This is a HIPPA compliant IRB approved retrospective study of all patients with duplicated collecting renal systems undergoing fMRU at our institution between 2010 and 2017. All studies were evaluated in consensus by two pediatric radiologists, blinded to clinical information and other urologic imaging. The reviewers determine the presence, morphology and function of duplicated collecting systems using both pre-contrast T2-weighted and dynamic post-contrast T1-weighted images with fat-saturation sequences. Morphologic features including pelvocaliceal dilatation, partial or complete ureteral duplication, ureteral dilatation, and the presence of ectopic ureteral insertion or ureteroceles were recorded. The functional analysis carried out per moiety was also documented.
Results: A total of 91 cases (67 girls; 24 boys), mean age 5.4 years (range 0-20 years) and 111 kidneys (41 right; 30 left and 20 bilateral), which yielded 222 evaluable moieties, were included in the final sample. One hundred and sixty-nine (76.1%) of the moieties had normal morphological features and normal functional results (average *contrast transit time* and *renal transit time* of 2 minutes 47 seconds and 3 minutes 21 seconds, respectively). The remaining 53 moieties (24.78%) were hypoplastic or dysplastic. Seventy-seven (34.68%) had pelvocaliceal dilatation. Slightly more than half (n=61; 54.95%) had completely duplicated ureters; 51 (45.95%) had ectopic ureters (24 intra- and 27 extra-vesical) and 9 (8.1%) had ureteroceles.
Conclusions: fMRU provides comprehensive information regarding the morphology and function of duplicated renal collecting systems, which encompass a heterogeneous group of urologic abnormalities.

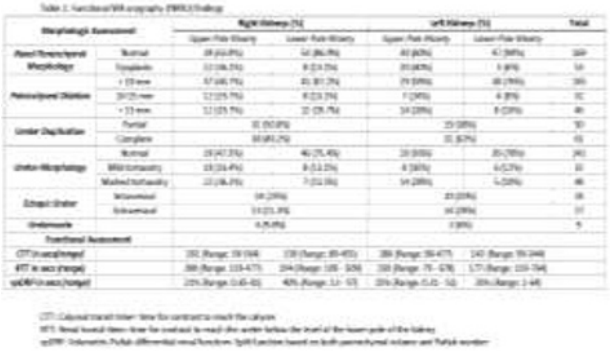

Paper #: 048

Evaluation of the Urinary Tract Dilation Classification System for postnatal hydronephrosis in the prediction of clinical outcomes

Patricia Acharya, MD[1] *patriciatacharya@gmail.com*; [1]Radiology, Loma Linda University, Loma Linda, CA

Disclosures: All authors have disclosed no financial interests, arrangements or affiliations in the context of this activity.

Purpose or Case Report: To assess the utility of the Urinary Tract Dilation (UTD) Classification System for grading postnatal hydronephrosis in predicting clinical outcomes.
Methods & Materials: We retrospectively reviewed charts of pediatric patients who presented with postnatal hydronephrosis from 2007 to 2017. We included patients diagnosed prenatally and those with urinary tract dilation discovered incidentally during the first year of life. Patients with neurogenic bladder and chromosomal anomalies, with extraurinary congenital malformations, or with followup of less than 24 months without resolution were excluded. Urinary tract dilation was graded using the UTD classification system followed by selection of a management protocol.
Results: Preliminary results show high reliability and validity of the UTD classification system in predicting the need for surgical intervention or assessment of renal function.
Conclusions: The UTD classification system can be used to accurately predict clinical outcomes in patients who need further assessment of renal function, antibiotic prophylaxis, or surgical intervention.

Paper #: 049

Preliminary experience with Contrast Enhanced Ultrasound (CEUS) of the Pediatric Kidney

Susan Back, MD[1], *susan.back@gmail.com*; Carolina Maya, MD[1], Aikaterini Ntoulia, MD, PhD[1], Hansel Otero, MD[1], Seth Vatsky, DO[1], Diana Bowen[1], Dana Weiss[1], Kassa Darge, MD, PhD[1], Richard Bellah, MD, FAAP[1]; [1]Children's Hospital of Philadelphia, Philadelphia, PA

Disclosures: All authors have disclosed no financial interests, arrangements or affiliations in the context of this activity.

Purpose or Case Report: CEUS is used to evaluate focal and traumatic renal lesions as a primary examination and assessment following baseline ultrasound (US), CT and MRI. CEUS in children is gaining momentum following the April 2016 United States Food and Drug Administration approval for intravenous administration of an US contrast agent for pediatric liver evaluation. This study describes our initial experience with CEUS of the pediatric kidney.

Methods & Materials: This is an IRB approved retrospective review of clinical and imaging findings of pediatric intravenous renal CEUS examinations over a 27-month period and relevant follow-up imaging.
Results: 61 CEUS exams were performed in 51 children with a median age of 9.2 years (range: 0- 21.7 y). Indications were: focal lesions (n = 31), trauma (n =13), renal perfusion (n = 11), UTI (n= 4), and hematuria (n= 2). A GE Logic E9 (n=30) or Philips Epiq 7 (n=31) US unit was used with either Lumason (n=46) or Optison (n=15) US contrast agent. For Lumason exams the contrast agent volume per injection ranged from 0.4- 2 mL (0.0071- 0.2 mL/kg). On average 2.3 injections/exam were done using a mean total dose of 1.85 mL (range: 0.6- 4.4mL) and mean total weight based dose of 0.01 mL/kg (range: 0.014- 0.46 mL/kg). For Optison exams the contrast agent volume per injection ranged from 0.2- 0.5 mL (0.004- 0.11 mL/kg). On average 3.4 injections/exam were done using a mean total dose of 1.25 mL (range: 0.3- 2.6 mL) and a mean total weight based dose of 0.06 mL/kg (range: 0.013- 0.45 mL/kg). The CEUS diagnosis was: normal or normal variant 46% (n=28); mass 16% (n=10); infection 15% (n=9); cyst 11% (n=7); trauma 6% (n=4); and abnormal perfusion 5% (n=3). 48 patients had available imaging prior to the CEUS: US (n=23), CT (n=16) and MRI (n=11). Follow up imaging was available for 29 exams in 21 children. The mean time between the CEUS and most recent imaging exam was 115 days (range: 1- 338 d). Review of the most recent study showed no lesion 23% (n=14), stable 18% (n=11) or decreased 6% (n=4) lesion size. There was concordance between CEUS and all 4 patients who had pathology: 1 malignant, 1 inflammation and 2 infections.
Conclusions: CEUS of the kidney can complement or supplant CT and MRI thereby reducing radiation exposure and need for sedation. Further experience will refine the role of CEUS in the imaging algorithm for the pediatric kidney.

Paper #: 050

Contrast enhanced ultrasound for the evaluation of complex anorectal and genitourinary anomalies

Jeanne Chow, MD[1], *jeanne.chow@childrens.harvard.edu*; Erin McNamara[1], Horacio Padua[1], Harriet Paltiel, MDCM[1], Belinda Dickie, MD[1]; [1]Children's Hospital Boston, Boston, MA

Disclosures: All authors have disclosed no financial interests, arrangements or affiliations in the context of this activity.

Purpose or Case Report: Children with complex anorectal and genitourinary malformations undergo a multitude of tests often involving radiation and sedation/anesthesia throughout their lifetime. Contrast enhanced ultrasound (CEUS) is a radiation and sedation/anesthetic- free imaging technique that has been used in evaluation of the genitourinary system. We compared the results of intracavitary CEUS to traditional fluoroscopic/cone beam CT tests and surgical results in patients with complex anorectal and genitourinary malformations.
Methods & Materials: Six children with complex congenital anorectal and genitourinary anomalies (3 cloacal malformations, 2 anorectal malformations, 1 urogenital sinus) had traditional fluoroscopic contrast studies or cone beam CT and CEUS studies performed sequentially often using the same catheters to introduce the contrast. For CEUS, 0.5 mL Lumason in 500mL NS was instilled and imaged using ultrasound contrast mode and transperineal, anterior and posterior sagittal techniques. Anatomical relationships and measurements based on fluoroscopic studies, CEUS and surgery/endoscopy were compared.
Results: In 5 of the 6 patients, the fistulous connections and anatomical relationships were identified both on CEUS and fluoroscopic or cone beam CT studies. In one male patient with imperforate anus, the rectourethral communication was only identified by fluoroscopic VCUG. However both CEUS and fluoroscopy revealed a urethral duplication. In the three patients with cloacal malformation, the length of the common channel, confluence of the vagina and rectum where they entered the common channel, and distance to the perineum were identified by both CEUS and contrast studies. All measurements and anatomical relationships were similar on fluoroscopic, CEUS and endoscopic/operative findings.
Conclusions: CEUS is a novel way to image the child with complex anorectal and genitourinary malformations. As many of these children undergo many radiologic procedures and interventions requiring radiation and sedation/anesthesia in their lifetime, CEUS represents an attractive, radiation-free and sedation/anesthesia-free alternative imaging technique. Our comparison study shows that this method provides an accurate means of imaging these children without the need for radiation or anesthesia.

Paper #: 051

Infant Female Urethral Catheterization: A New Simulator from Special Effects

Vinay Pai, MD[1], *vinay.pai@childrens.harvard.edu*; Maeve Geary, PhD[1], Maria Jorina[1], Michael Kurtz, MD[1], Rosemary Grant[1], Peter Weinstock, MD[1], Jeanne Chow, MD[1]; [1]Children's Hospital Boston, Boston, MA

Disclosures: All authors have disclosed no financial interests, arrangements or affiliations in the context of this activity.

Purpose or Case Report: The purpose of our project was to 1) design a life-like simulator for urinary catheterization in infant females 2) to evaluate clinician impressions of the currently available model (Fig 1) compared to the novel simulator (Figs 2a and 2b).
Methods & Materials: A silicone model for urinary catheterization (CATH-y) was created as a collaboration between the Departments of Radiology, Urology and Medical Simulation. The final product was made based on observing live human catheterization in the Radiology department during cystograms, observation in Urology clinics, and anatomic photographs and drawings. The CATH-y simulator was constructed and iterated using a combination of MRI-based models, 3D printing, material engineering, molding and hand sculpting to look and feel like human catheterization. The final model was compared to the current state of the art trainer using a survey.
A 41 question survey addressed the realism of the model in terms of the anatomic definition, the appearance, and the feeling during mock catheterization. Then the model was compared to the currently available trainer based on its appearance, feeling and function. Then questions were asked about the utility of the trainer. When possible, a Likert scale was used, as well as open-ended questions.
Results: 35 medical personnel answered the survey between 9/19 and 10/18/17. Most were young, with 62% between ages 25-34, and 53% reported female gender. 44% were trainees, with the remainder as staff members. 51% were physicians, 25% were nurses, and 22% were radiographers.
Whereas 0% of the respondents agreed strongly (7 or 8 out of a possible 8) that the commercially available simulator was useful in teaching catheterization, 97% of respondents agreed strongly that the novel simulator was useful. 82% responded that the new simulator would be extremely helpful for teaching students, and similarly extremely helpful for clinician practice and teaching families about catheterization (both 80%).
Conclusions: Radiologists can play a key role in creating useful simulation models, such as the CATH-y model for urinary catheterization. The collaboration of Radiology, Urology and

Simulation Departments created a life-like simulator which was shown to be superior to the currently available trainer based on the appearance, feeling and function. The novel simulator has the potential improve training for urinary catheterization not only for radiology tests but for other medical professionals and families and hopefully positively impact patient care.

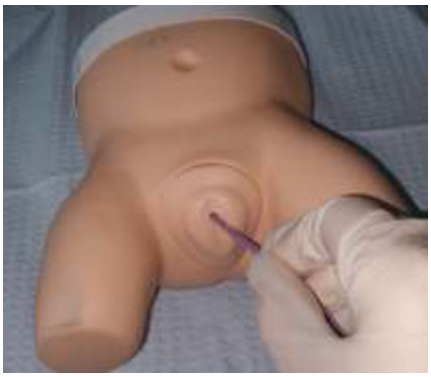

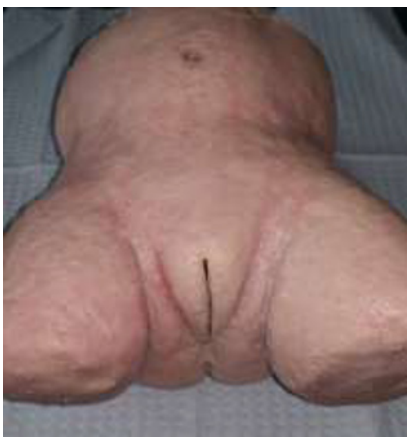

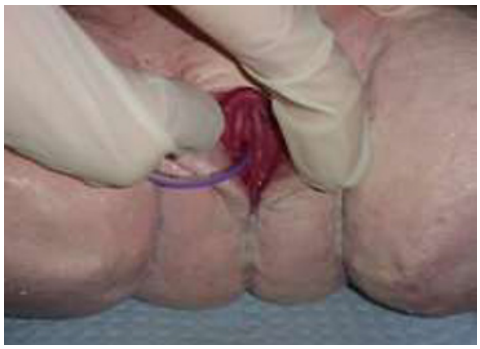

Paper #: 052

Pediatric Ovarian Volumes Measured at Ultrasound After Contralateral Unilateral Oophorectomy

Kimberly Dao, MD[1], *daoka@upmc.edu*; Pamela Poremski, RDMS[2], Sameh Tadros, MD[2], Judy Squires, MD[2]; [1]Department of Radiology at the University of Pittsburgh Medical Center, Pittsburgh, PA, [2]Department of Radiology at the Children's Hospital of Pittsburgh of UPMC, Pittsburgh, PA

Disclosures: All authors have disclosed no financial interests, arrangements or affiliations in the context of this activity.

Purpose or Case Report: In pediatric patients with prior unilateral oophorectomy, physiologic changes are known to occur in the remaining un-resected ovary. However, the effect on the imaging appearance of the remaining ovary is not well described. Normative pediatric measurements are needed in the setting of a remaining unilateral ovary because size is an important indication of ovarian torsion and 15% of cases of ovarian torsion occur in pediatric patients. If there is a concern for torsion in patients with prior unilateral oophorectomy, it is not possible to compare the remaining ovary size to the contralateral ovary. Our aim was to determine the average remaining ovarian volume in pediatric patients with prior oophorectomy categorized by decade of life in comparison to patients with two normal ovaries.
Methods & Materials: An IRB-approved retrospective review of ultrasounds and electronic medical records of patients aged 0 - 18 years with prior unilateral oophorectomies from 01/01/2000 and 08/01/2017 was performed. For comparison, pelvic ultrasounds of 80 consecutive normal female age-matched patients were evaluated from 9/26/2017 to 10/25/2017. Patients with possible ovarian size abnormality including those with cysts, mass, precocious or delayed puberty, or known syndrome (such as Turner) were excluded (n=22) yielding 116 normal ovaries for comparison. Ovaries from oophorectomy (n=65) and control groups were divided by patient decade of life (0-10 and ≥11-18 years), and mean ovarian volume was analyzed using the two-tailed Student's t-test.
Results: Higher mean ovary volume (mL) was observed in the 27 patients in the 1st decade of life with prior oophorectomy when compared to 48 normal ovaries (3.2 ± 3.62 vs 1.36 ± 0.76mL, , $p<0.002$) and in the 38 patients in the 2nd decade with prior oophorectomy when compared to 68 normal ovaries (10.2 ± 5.02 vs 6.87 ±3.80mL, $p<0.0003$).
Conclusions: Although the mean ovarian volume is higher in patients of all ages with prior unilateral oophorectomy, the average volume remains <20mL, which is the reported volume previously correlated with torsion. The provided normative volumes can be used if there is concern for ovarian torsion in pediatric patients with unilateral oophorectomy.

Paper #: 053

Feasibility of fetal MRI in the evaluation of fetal cardiovascular anomalies.

Su-Zhen Dong, Medical PhD[1], *dongsuzhen@126.com*; Ming Zhu[1]; [1]Radiology, Shanghai Children's Medical Center, Shanghai Jiaotong University School of Medicine, Shanghai, China

Disclosures: All authors have disclosed no financial interests, arrangements or affiliations in the context of this activity.

Purpose or Case Report: To evaluate the feasibility of cardiac magnetic resonance (CMR) in the assessment of fetal cardiovascular anomalies.
Methods & Materials: This retrospective review included 1476 pregnant women referred for a fetal cardiac MRI from January 2006 to June 2017 due to the finding of a cardiovascular anomaly by echocardiogram (echo) and/or technically limited echo. Screening obstetric ultrasound (US), echo by cardiologists and CMR data of all cases were compared with postnatal diagnoses (postnatal imaging, surgery and/or autopsy). Fetal CMR was performed at 1.5 T or 3.0 T. Sequences included steady state free precession (SSFP), non gated SSFP cine, single-shot turbo spin echo (SSTSE) and non-gated PC cine sequences. The CMR images were analyzed using an anatomic segmental approach by two radiologists and compared with fetal echo and postnatal findings when available.

Results: 1156 fetuses were referred for congenital cardiovascular anomalies noted on echo; 320 fetuses were referred for technically inadequate echocardiography but thought to likely be normal.
Of the 1156 fetuses referred for congenital cardiovascular anomalies, 518(44.8%) had no follow-up confirmation due to termination of pregnancy without autopsy. Comparing CMR to echo in cases with no follow up, CMR provided additional information (such as heterotaxy, extracardiac aortic arch and superior vena cava anomalies) in 179/518 (34.6%) but missed small VSD (4mm), abnormal mitral and /or tricuspid valves and abnormal pulmonary vein noted by echo.
There were 638 (55.2%) cases with anomalies confirmed by postnatal imaging, surgery and/or autopsy. Obstetric US were correct in 46.9% (299/638), fetal echos were correct in 83.2% (531/638), CMR were correct in 82.1% (524/638) when compared to postnatal findings. Fetal echoes had a higher specificity for evaluating ventricular size, septal defects and valve anomalies. CMR was more useful in evaluating extracardiac aortic arch, superior vena cava and malposition anomalies, heart diverticulum, pericardium cyst. CMR were technically limited in 9 cases due to polyhydramnios.
286 of 320 CMR cases performed due to technically inadequate echocardiography (maternal obesity, maternal abdominal wall edema, oligohydramnios, fetal position, twins, et al), had follow up. All of these cases were interpreted as normalby CMR and confirmed at FU.
Conclusions: Fetal CMR is a promising diagnostic tool for assessment of extracardiac vascular anomalies and can be a useful adjunct when fetal echocardiography is limited.

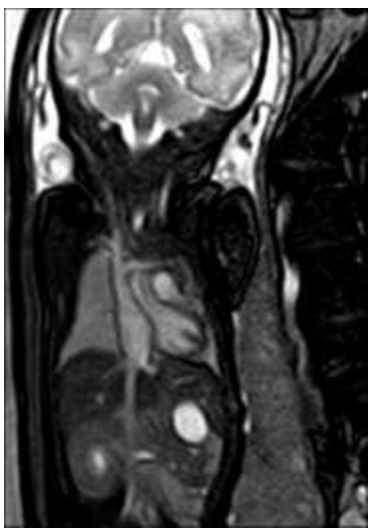

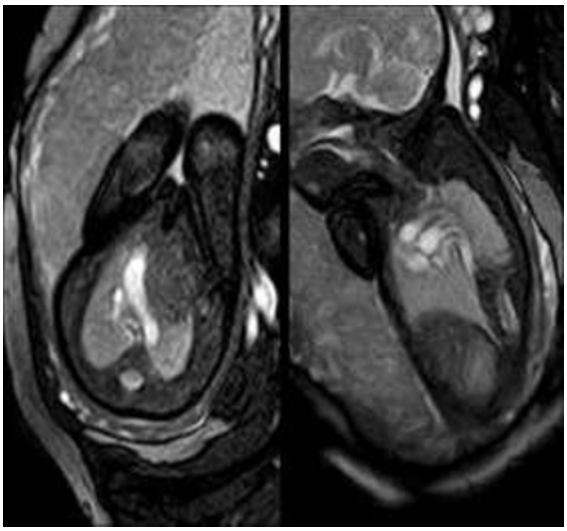

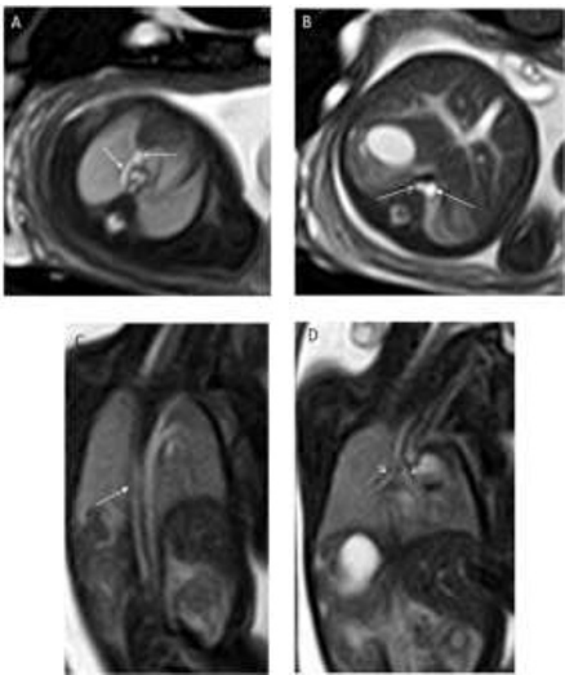

Paper #: 054

Fetal cardiac MRI in the evaluation of congenital aortic arch anomalies

Su-Zhen Dong, Medical PhD[1], *dongsuzhen@126.com*; Ming Zhu[1]; [1]Radiology, Shanghai Children's Medical Center, Shanghai Jiaotong University School of Medicine, Shanghai, China

Disclosures: All authors have disclosed no financial interests, arrangements or affiliations in the context of this activity.

Purpose or Case Report: Congenital aortic arch anomalies refer to a variety of abnormalities of the position and/or branching of the aortic arch. The aim of this study was to evaluate the feasibility of fetal cardiac magnetic resonance (CMR) in the assessment of fetal congenital aortic arch anomalies.
Methods & Materials: This retrospective review included 145 pregnant women (20-33 weeks gestation mean 24.5 weeks) referred to a children's hospital for a fetal cardiac MRI from

June 2005 to June 2017 due to the finding of a cardiovascular anomaly by fetal echocardiogram (echo) performed by a cardiologist or due to a technically limited echo. CMR was performed using 1.5T or 3.0 T unit. Sequences included steady-state free-precession (SSFP); non gated SSFP cine, single-shot turbo spin echo (SSTSE) and non-gated phase contrast (PC) cine sequences. Sequences included transverse fetal thorax, and four-chamber, short-axis, coronal and oblique sagittal planes of the fetal heart when possible. The radiologists were not blinded to the echo findings. Echo and CMR findings were compared with postnatal imaging and/or surgery.
Results: Anomalies identified by CMR included double aortic arch (n=35), right aortic arch with aberrant left subclavian artery (n=51), right aortic arch with mirror image branching (n=42), right aortic arch with right ductus arteriosus (n=6, 4 with other cardiovascular defects), right aortic arch with mirror image branching with retroesophageal ductus (n=6), left aortic arch with aberrant right subclavian artery (n=2) and cervical aortic arch (n=3). 95.2% (40/42) right aortic arch with mirror image branching had additional congenital intracardiac anomalies better seen by fetal echo. The remaining were not associated with additional congenital heart defect.
75.2% (109/145) arch anomalies were correctly diagnosed by fetal echo, while Fetal CMR was correct in 87.8% (127/145). 18 arch anomalies were missed by fetal echo but identified by MRI and confirmed postnatally, echos were technically limited in 6 cases due to maternal obesity, oligohydramnios, fetal position, twins. The cases echo missed/misdiagnosed included double aortic arch (n=7), right aortic arch with aberrant left subclavian artery (n=4), right aortic arch with right ductus arteriosus (n=3), right aortic arch with mirror image branching with retroesophageal ductus (n=3) and cervical aortic arch (n=1).
Conclusions: Fetal cardiac MRI can provide additional diagnostic information for fetal congenital aortic arch anomalies and can be a useful adjunct.

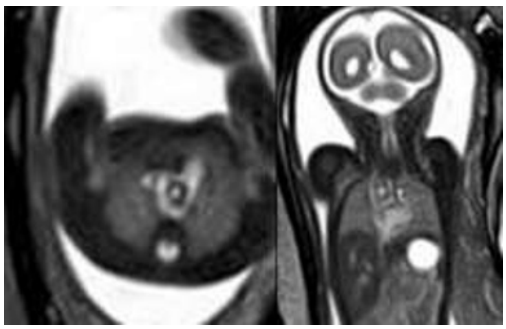

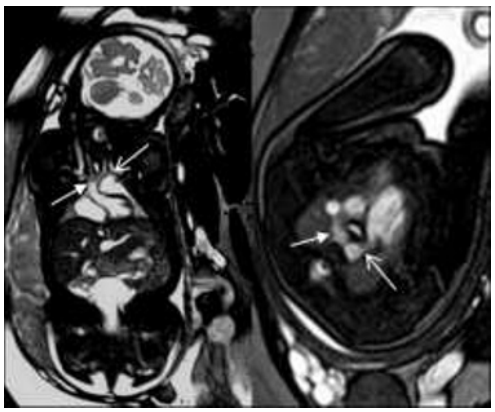

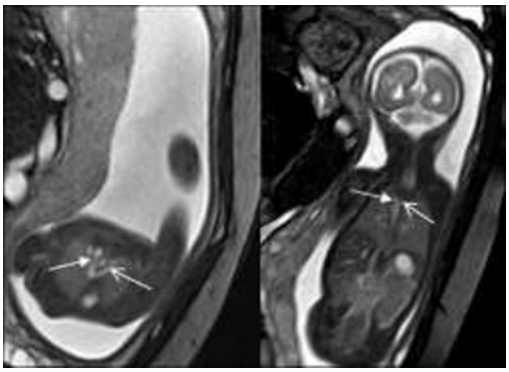

Paper #: 055

Two's Company – Multiple Thoracic Anomalies on Prenatal Ultrasound and MRI

Edward Oliver, MD, PhD[1], *olivere1@email.chop.edu*; Suzanne DeBari, BS, RDMS, RVT[1], Ryne Didier, MD[1], Ann Johnson[1], Nahla Khalek, MD, MPH[1], William Peranteau[1], Lori Howell, DNP, MS, RN[1], N Adzick[1], Beverly Coleman[1]; [1]The Children's Hospital of Philadelphia, Philadelphia, PA

Disclosures: All authors have disclosed no financial interests, arrangements or affiliations in the context of this activity.

Purpose or Case Report: To estimate the frequency of multiple congenital thoracic anomalies at our center; determine prenatal ultrasound (US) and magnetic resonance imaging (MRI) features of multifocal congenital lung lesions (congenital pulmonary airway malformation (CPAM), bronchopulmonary sequestration (BPS), and hybrid lesions); and determine the most common distribution or site of origin.
Methods & Materials: Single center, retrospective IRB-approved searches of radiology and clinical databases were performed from 2008-2017 for prenatally diagnosed thoracic anomalies that had multiple surgically-proven abnormalities, including congenital diaphragmatic hernia (CDH) with BPS, lung lesions with a final diagnosis of more than one congenital lung lesion, and lung lesions associated with foregut duplication cysts (FDC). Lesion location, size, echotexture and signal characteristics were assessed on prenatal imaging and correlated with postnatal surgical pathology.
Results: Of 410 CDH, 9 (2.2%) were associated with BPS. Of 817 lung lesion cases, 14 (1.7%) were multifocal with referral diagnoses indicating possible multifocality in 3/14 (21.4%). An additional 4 (2 CPAM and 2 BPS) were associated with FDC. Mean gestational age was 23 weeks (range, 19.2-36.6 weeks). All BPS were ipsilateral to the CDH (8 left and 1 right). Multifocal lung lesions were bilateral in 2 cases, unilateral multilobar in 7, and unilobar multisegmental in 5. Mean total CVR for multifocal lung lesions on US was 0.84 (range, 0.16-1.54). Lesion combinations were CPAM-CPAM in 9 cases, CPAM-hybrid in 3, CPAM-BPS in 1, and hybrid-hybrid in 1. Prenatal US and MRI both correctly identified multifocality in 7/14 cases (50%). Multifocality was identified postnatally in the remaining 7. Of the 5 unilateral lesions prospectively identified, multifocality was established through intrinsic differences in lesion imaging features in 1 case and through identification of a band of normal intervening lung in the remaining 4.
Conclusions: Multiple thoracic abnormalities were infrequently encountered but can be detected prenatally. Of multifocal lung lesions, the most common combination was CPAM-CPAM, with a unilateral multilobar distribution. Differences in intrinsic lesion imaging features and identification of normal intervening lung between lesions allowed for prospective prediction of

multifocality in almost half of the unilateral lesions. Prenatal recognition of multiple thoracic abnormalities is important for pregnancy counseling and postnatal surgical management.

Paper #: 056

A Multifactorial Severity Score for Congenital Diaphragmatic Hernia (CDH) using Fetal MRI

Rachel Wise[1], *rwise2011@gmail.com*; Thomas Reher[1], Brian Gray, MD[1], Monica Forbes-Amrhein, MD[1], Robert Vandewalle, MD[1], Brandon Brown, MD, MA[1]; [1]Indiana University School of Medicine, Indianapolis, IN

Disclosures: All authors have disclosed no financial interests, arrangements or affiliations in the context of this activity.

Purpose or Case Report: The prognostic value of multiple prenatal imaging biomarkers in the diagnosis and treatment of CDH has been well-established. Our purpose was to combine qualitative and volumetric analysis of the various fetal MR biomarkers within a single population and use weighted indices from these biomarkers to calculate a severity score in patients with CDH. This score might then be used to estimate risk of mortality in high-risk CDH patients and to assist in family counseling.
Methods & Materials: We retrospectively identified all cases of prenatally-diagnosed CDH at a single institution during 2004-2016. Factors identified on MRI included observed-to-expected total fetal lung volume (O/E TFLV), percent predicted lung volume (PPLV), and spleen, liver, and stomach position. Prenatal factors were compared with mortality. The ROC was optimized for O/E TFLV of 24% for mortality (sensitivity 64%, specificity 82%, AUC 0.72). Analysis was performed using bivariate and multivariate regression methods. Using weighted and normalized coefficients from the logistic regression of mortality, severity scores were calculated. The probability of mortality used to determine relative risk within this population was estimated using the method described in Figure 1.
Results: 41 patients were included in the study. Within our cohort of CDH patients, Mean (±SD) O/E TFLV was 32% ±22%, and survival was 41% (n=17). 48% had major comorbidities. Bivariate analysis identified O/E TFLV (p=0.007) and stomach position (p=0.049) as significantly associated with mortality. Multivariate regression revealed a relative weighting of prognostic factors as follows: O/E TFLV, stomach position, liver position, PPLV, and spleen position. These factors contributed to the probability of mortality results, as demonstrated in the Figure 2.
Conclusions: Using qualitative and volumetric assessment of various MRI biomarkers in patients with CDH, multiple of these biomarkers were found to be valuable collectively when assigned relative weighting, and multivariate analysis appears to stratify mortality. When combined into an algorithm after weighting, they can be used to estimate the probability of neonatal mortality and guide prenatal family counseling. Further studies are required for prospective validation.

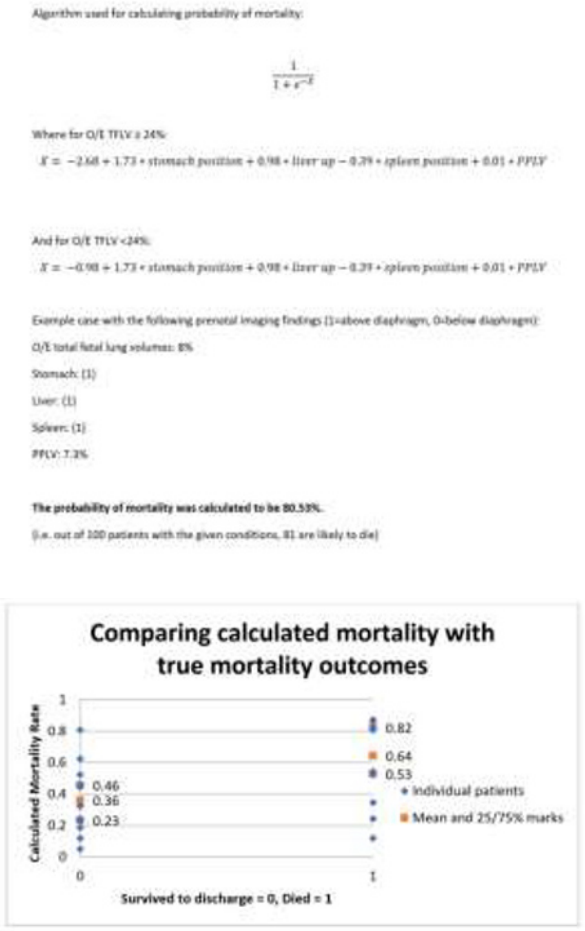

Paper #: 057

Normal size of the fetal adrenal gland on prenatal MR Imaging

Anilawan Smitthimedhin, MD[1], *fuuune@hotmail.com*; Eva Rubio, MD[1], Dorothy Bulas, MD[1], Anna Blask, MD[1], Judyta Loomis, MD[1]; [1]Radiology, Children's National Health System, Washington, DC

Disclosures: All authors have disclosed no financial interests, arrangements or affiliations in the context of this activity.

Purpose or Case Report: Previously reported ultrasound measurements of normal fetal adrenal gland sizes show a trend of increasing size with gestational age. Currently, there are no published reference standards of fetal adrenal size or imaging appearance on prenatal MRI.
The aim of this retrospective study is to establish the size and signal characteristics of the adrenal gland in normal fetuses from the mid-second trimester to the end of the third trimester.
Methods & Materials: In this HIPPA-compliant retrospective study, 207 MR examinations of fetuses with no signs of abdominal pathology from 1/1/2005 to 5/31/2017 were randomly selected. The adrenal glands were measured in coronal, sagittal or axial T2W planes. The length and thickness of the medial and lateral limbs of the right and left adrenal glands were measured. The signal characteristics of the adrenal glands on T1W and T2W sequences were also recorded.
Results: The gestational age ranged from 18-37 weeks. The adrenal glands were optimally seen in the coronal plane in the

majority of cases. The visibility of adrenal glands on T2W images was high (88.9-97.4%) up to 30 weeks, then declined (47.5-52.4% at 31-37 weeks). The ability to identify the adrenal gland on T1W images increased in later gestation, as follows: 18-22 weeks: 22.3%; 23-26 weeks: 33.3%; 27-30 weeks: 33.5%; 31-34 weeks: 41.1%; 35-37 weeks: 40%. The mean length of the adrenal limbs increased during gestation as follows: 18-22 weeks: 8.23 mm (SD 1.51); 23-26 weeks: 8.86 mm (SD 1.49); 27-30 weeks: 9.94 mm (SD 1.73); 31-34 weeks: 9.79 mm (SD 1.34); 35-37 weeks: 11 mm (SD 2.00). In the second trimester, the adrenal glands on T2W images were markedly hypointense and surrounded by bright perirenal fat. In the third trimester, the signal intensity on T2W images increased, the surrounding fat was obliterated and the glands became less conspicuous. They were bright on T1W images throughout the second and third trimester.

Conclusions: Normal adrenal gland sizes and signal intensities by prenatal MRI are reported. The ability to discretely identify adrenal glands on T2W images is high up to 30 weeks, but declines in the latter part of the third trimester. The visibility on T1W images increases with gestational age. The adrenal gland size increases with gestational age.

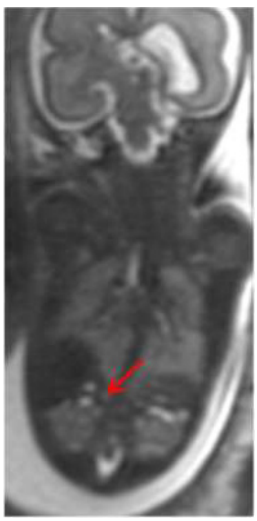

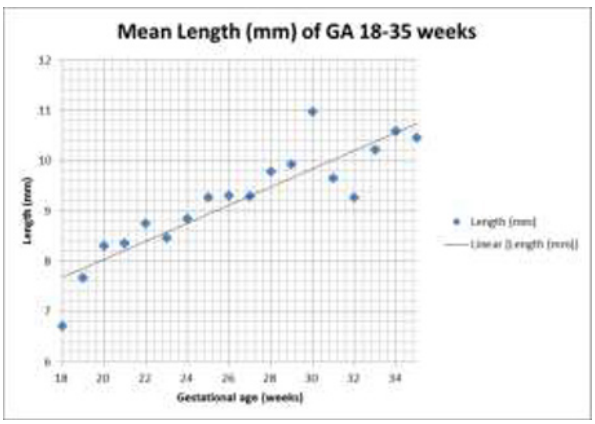

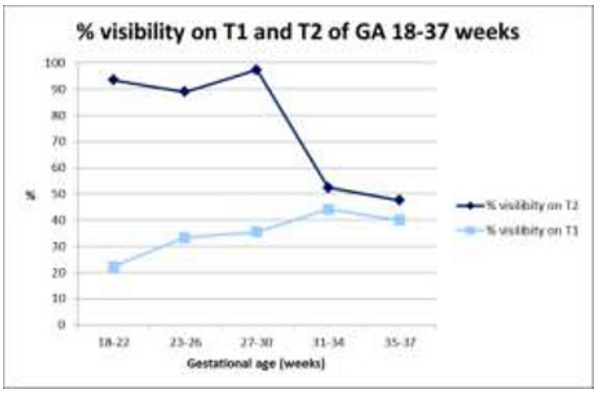

Paper #: 058

Novel Computerized Analytic Technique for Quantification of Amniotic Fluid Volume in Fetal MRI

Ryne Didier[1], *rdidier@gmail.com*; Dmitry Khrichenko[1], Christopher Edgar[1], Carolina Maya, MD[1], Julie Moldenhauer[1], Teresa Victoria, MD, PhD[1]; [1]Children's Hospital of Philadelphia, Philadelphia, PA

Disclosures: All authors have disclosed no financial interests, arrangements or affiliations in the context of this activity.

Purpose or Case Report: Fetal Magnetic Resonance Imaging (MRI) is increasingly utilized in the evaluation of suspected or confirmed congenital anomalies. Ultrasound assessment of amniotic fluid volume (AFV) is standardized and widely used, however concurrent results may not be available at the time of MRI interpretation. Assessment of AFV is crucial but no quantitative technique is currently available for MRI. We developed and evaluated the performance of a novel analytic technique to quantify AFV on fetal MRI.

Methods & Materials: This is a retrospective IRB-approved study. A 3D steady-state free precession (SSFP) sequence on a 1.5 Tesla MRI system (Siemens Medical Solutions, Erlangen, Germany) obtained clinically as part of the standard fetal MRI protocol was used for measurement of AFV. AFV-measuring software was developed in a Windows (Microsoft, Redmond, WA) environment using Interactive Data Language (IDL, Harris Geospatial, Broomfield, CO). The entire SSFP MRI sequence was loaded into the program in DICOM format. Several parameters such as minimum and maximum signal intensity were set empirically. After a satisfactory region of interest (ROI) was produced and confirmed visually, the calculated volumes were saved in a tabulated text format per slice. To evaluate the performance of the program, a pediatric radiologist, blinded to the results, used a hand-tracing method to calculate AFV per slice. To assess for agreement between the radiologist- and computer-generated measurements, Bland-Altman plots were created and intraclass correlation analysis was performed by slice and by total volume, respectively.

Results: AFV measurements were performed in six subjects in the late second and early third trimester (mean 25.6 weeks; range 23.0-28.6 weeks). Computer-analyzed AFV measurement is shown in Figure 1. Results of each volumetric assessment are shown in Table 1 and Figure 2. Bland-Altman plots for each subject by MRI slice demonstrated agreement between the radiologist and computer within normal variation. The intraclass correlation coefficient for total AFV was 0.883 where 0.75-0.90 represents "good reliability" (CI: 0.34-0.94; p=0.002)].

Conclusions: This novel computerized analysis quantifies AFV in fetal MRI and is concordant with radiologist-generated measurements thus offering a promising technique for objective MRI evaluation of AFV.

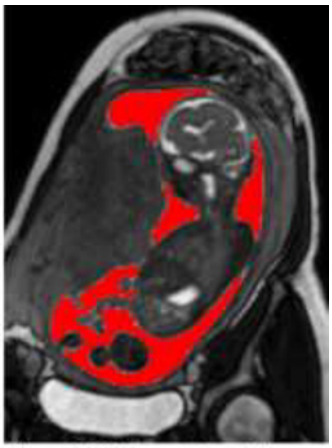

Figure 1: MRI image through the gravid uterus with computer-generated amniotic fluid volume (red) surrounding the fetus.

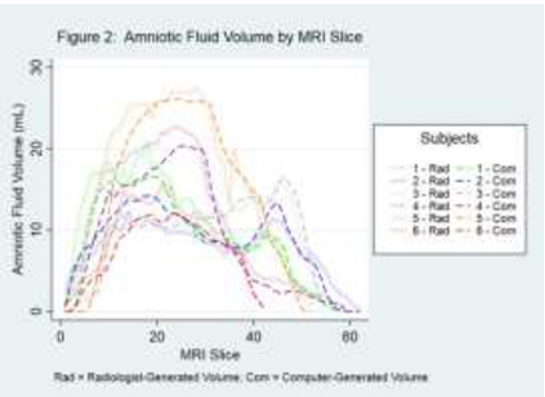

Table 1: Total Calculated Amniotic Fluid Volume

Subject	Rad (mL)	Com (mL)
1	603.58	521.87
2	484.82	532.59
3	527.54	529.06
4	649.10	539.34
5	860.36	766.66
6	383.24	312.58
Mean ± Std	**584.77 ± 163.90**	**533.68 ± 143.78**

Rad = Radiologist-Generated Volume

Com = Computer-Generated Volume

Std = standard deviation

Paper #: 059

Using Quantitative MRI to Identify Abnormal Perfusion in Invasive Placental Disease

Carrie Norris, MD[1], *norrisca@iupui.edu*; Scott Persohn, RT[1], Paul Territo[1], Brandon Brown, MD, MA[1]; [1]Indiana University School of Medicine, Indianapolis, IN

Disclosures: All authors have disclosed no financial interests, arrangements or affiliations in the context of this activity.

Purpose or Case Report: Invasive placental disease (IPD), is a growing cause of maternal and perinatal morbidity in the setting of increasing Cesarean section deliveries. Failure to accurately diagnose this condition can have devastating effects on both fetal and maternal health. Presently, prenatal ultrasound is used for initial evaluation, with selected high-risk patients undergoing additional MR imaging. However, studies have shown both US and MRI to be limited in their ability to accurately detect the morbidly adherent placenta. We evaluated whether multi-b-value diffusion weighted MR imaging (DWI) and quantitative intravoxel incoherent motion (IVIM) analysis techniques can accurately detect a difference in perfusion between normal and abnormally invasive placentae.
Methods & Materials: In our PACS database, all patients who received DWI MR imaging over the past 12 months for suspected IPD (based on prenatal US) were identified, yielding 11 cases, and 29 normal volunteers were recruited to serve as a control group. Patients underwent MR imaging between 14-30 weeks gestational age, with the mean at 25 weeks for the disease group and 26 weeks for the control group. Multi-b-value (0, 25, 50, 100, 150, 200, 300 and 400) DWI sequences were obtained for all patients, and intensity normalized to the b-0 image (nDWI). A subset of cases were used as model priors for a multi-spectral neural networking classification (MSNN) model, where regions of interest for placenta, fat, high intensity areas, and background were defined manually and nodal weights back-propagated and stored for future classification. Using the training weights, each nDWI case was voxel-wise classified yielding a 3D object map for placenta, fat, high intensity, and background regions. Post segmentation, average regional IVIM analysis was performed, using the following model: f(b) = Pf*exp(-Df*b)+(1-Pf)*exp(-Ds*b) for all normal and suspected cohorts, where Pf, Df, and Ds are the Perfusion Fraction, Fast, and Slow diffusion components of the nDWI signal.
Results: Of the 40 patients included in the study, average Pf were significantly elevated for the disease group, with an average Pf of 43% for the disease group, and 32% for the control (normal) group ($p < 0.001$, T-Test).
Conclusions: Quantitative DWI MR imaging of the placenta, using IVIM analysis coupled to a MSNN model, can provide valuable information regarding placental perfusion, and may be a useful adjunct to help distinguish those diagnostic dilemmas in which a morbidly adherent placenta is suspected.

Paper #: 060

Congenital Skeletal Anomalies with Lower Limb-Length Discrepancy: Does Constant Inhibition Occur *In Utero*?

Andy Tsai, MD, PhD[1], *andy.tsai@childrens.harvard.edu*; Tal Laor, MD[1], Judy Estroff, MD[1], James Kasser, MD[1]; [1]Radiology, Boston Children's Hospital, Boston, MA

Disclosures: All authors have disclosed no financial interests, arrangements or affiliations in the context of this activity.

Purpose or Case Report: Although the relative limb-length discrepancy (LLD) between unaffected and affected limbs in children with congenital skeletal anomalies is constant from birth to skeletal maturity (known as "constant inhibition"), the developmental pattern *in utero* is unknown. The widely used prenatal multiplier method to predict LLD at birth assumes constant inhibition *in utero* to be true. Verifying the *in utero* developmental pattern of LLD and thus, confirming the prenatal multiplier method for these fetuses is crucial for meaningful prenatal parental counseling. This study's objective is to elucidate the *in utero* developmental pattern in fetuses with lower limb congenital skeletal anomalies and LLD.
Methods & Materials: Clinical indications of 3605 lower extremity radiographs performed on infants (<1-year-old) at a large tertiary hospital over a 17 year period were reviewed. Inclusion criteria were: diagnosis of a lower limb congenital skeletal anomaly with LLD at birth, bilateral lower limb postnatal radiographs documenting the LLD, and mother's

prenatal ultrasound documenting the LLD. Available measurements of femur, tibia, and fibular lengths on prenatal ultrasounds and postnatal radiographs were collected, and ratios between unaffected and affected bones were calculated. Prenatal and postnatal length ratios for each bone and their aggregate were compared.

Results: Eighteen infants met inclusion criteria. Diagnoses were: posteromedial tibial bowing=6, proximal focal femoral deficiency=4, fibular hemimelia=3, tibial hemimelia=3, and congenital short femur=2. The postnatal and prenatal ratios between unaffected and affected tibias (n=17), fibulas (n=17), and femurs (n=13) were calculated. The correlation coefficients between the postnatal and prenatal length ratios were high for the tibia (R=0.987, p<0.0001, Fig. 1), fibula (R=0.982, p<0.0001, Fig. 2), femur (R=0.991, p<0.0001, Fig. 3), and their aggregate (0.984, p<0.0001). The relative differences in the postnatal and prenatal length ratios were small for the tibia (average=-0.026, SD=0.051), fibula (average=-0.025, SD=0.068), femur (average=0.012, SD=0.039), and their aggregate (average=-0.015, SD=0.057).

Conclusions: Our data indicate that the postnatal length ratios were equivalent to prenatal length ratios, supporting the constant inhibition pattern of LLD *in utero*. The constant inhibition pattern of LLD in congenital skeletal anomalies begins not at birth, but rather earlier *in utero* and validates the popular prenatal multiplier method for predicting LLD.

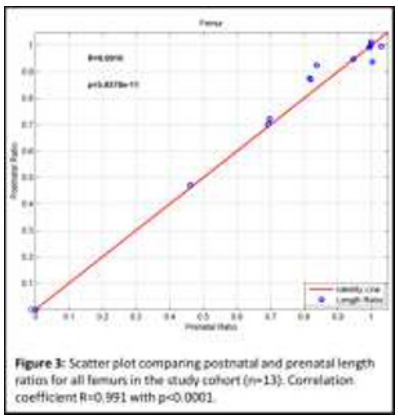

Figure 3: Scatter plot comparing postnatal and prenatal length ratios for all femurs in the study cohort (n=13). Correlation coefficient R=0.991 with p<0.0001.

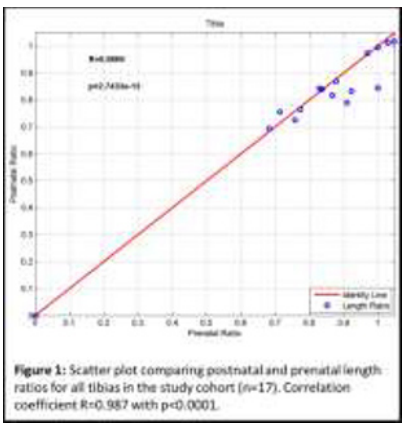

Figure 1: Scatter plot comparing postnatal and prenatal length ratios for all tibias in the study cohort (n=17). Correlation coefficient R=0.987 with p<0.0001.

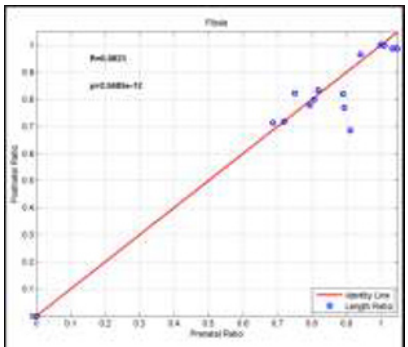

Figure 2: Scatter plot comparing postnatal and prenatal length ratios for all fibulas in the study cohort (n=17). Correlation coefficient R=0.982 with p<0.0001.

Paper #: 061

Ultra Low Dose Fetal CT: How to Further Decrease Radiation Dose While Maintaining Diagnostic

Teresa Victoria, MD, PhD[1], *victoria@email.chop.edu*; Sabah Servaes[1], Xiaowei Zhu[1], Christopher Edgar[1], Lisa States, MD[1], George Grigonis[2], Anna Dhody[2]; [1]Children's Hospital of Philadelphia, Philadelphia, PA, [2]Mütter Museum of the College of Physicians, Philadelphia, PA

Disclosures: All authors have disclosed no financial interests, arrangements or affiliations in the context of this activity.

Purpose or Case Report: Low-dose fetal CT is a helpful adjunct in evaluating prenatal skeletal dysplasias. Our current protocol aims at a fetal radiation dose of 5 mSv (threshold of fetal damage: 100 mSv). The goal of the study is to test different CT protocols to further reduce dose. The subject was a deceased fetal museum specimen of 5 months in GA scanned in an ethanol filled glass container

Methods & Materials: The fetal specimen was scanned as follows: 1.Current clinical protocol (100 Ref kVp, 95 Ref mAs, modulated mAs and kV), referred herein as Standard; 2. same as protocol 1 except 45 Ref mAs; Protocols 3 and 4: same as 1 and 2 except fixed 100 kVp; Protocols 5 and 6: same as 1 and 2 except fixed 80 kVp. Calculated radiation doses were set as 100% for Standard and estimated to be 100% for protocols 3, 5, and 50% of Standard for protocols 2,4, 6. Images were postprocessed using 3 different Seimens Safire iterative reconstruction (IR) algorithms (1, 3, 5). Contrast to noise ratio (CNR) was calculated. Visualization of different anatomical body parts (vertebral body, long bones, ribs, mandible, hand, clavicle, spine) was scored on scale of 1 (poor) to 5 (best). Non-parametric Friedman test examined visualization of anatomy among protocols. Repeated-measure ANOVA analysis assessed differences in CNR. Exploratory analyses examined CNR differences between Standard and all protocol Safire 5 images

Results: Friedman analysis showed significant difference in visualization of fetal anatomy between the Standard and other protocols ($p<0.001$), with simple effect Wilcoxon Signed Ranks tests showing that, except for Protocol 6, visualization for all other protocols differed from Standard (protocols 1,3, 5 > Standard; 2,4 < Standard; $ps < 0.05$). Exploratory analyses showed no significant differences in visualization of anatomy between Standard and Protocol 6 ($p = 0.29$) and Standard and Protocol 3 ($p = 0.18$), suggesting that these protocols could be interchanged, noting that Protocol 6 had 50% less radiation than Standard and Protocol 3.

When evaluating CNR IR across protocols, analysis showed a marginally significant effect, with Safire 5 tending to have higher CNR than Safire 1 ($p < 0.05$) and Safire 3 ($p = 0.09$)

Conclusions: Using Protocol 6, similar visualization of fetal body parts is attained while radiation dose is decreased by 50%. Across protocols, Safire 5 IR tended to provide highest contrast. When translated to actual patients, these findings can help achieve further dose reduction while maintaining diagnostic accuracy

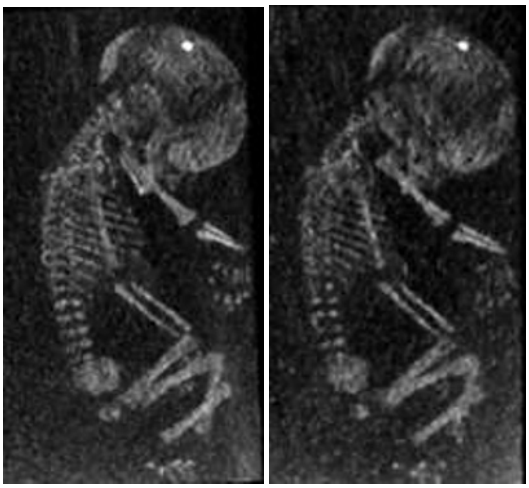

Paper #: 062

Perinatal imaging autopsy: Value and comparison with conventional autopsy

Pamela Deaver, MD[1], *pamela.deaver@gmail.com*; Christopher Cassady, MD[1], Debra Kearney, MD[1], Eumenia Castro, MD[1], Amy Mehollin-Ray, MD[1]; [1]Texas Children's Hospital, Houston, TX

Disclosures: All authors have disclosed no financial interests, arrangements or affiliations in the context of this activity.

Purpose or Case Report: Imaging autopsy (IA) in the perinatal period is an emerging service for providers and families, though little is known about how it compares with conventional autopsy (CA). Our purpose is to compare the two modalities using full unrestricted conventional autopsy (UCA) as the gold standard.
Methods & Materials: Following IRB approval, all patients who underwent imaging autopsy between May 2013 and September 2017 at our large tertiary children's hospital were enrolled. Review of the electronic medical record, including imaging and conventional autopsy findings, was performed. Findings at imaging autopsy, including suspected cause of death, were compared to those at conventional autopsy and subdivided by organ system.
Results: Eighty patients underwent IA between May 2013 and September 2017 at our institution. Of those, 62 (78%) also underwent conventional autopsy, including 30 (40%) unrestricted and 32 (38%) with restrictions. Mean gestational age of the IA/UCA combination cohort at birth was 31.6 ± 4 weeks. Twenty-two infants (73%) with IA/UCA were liveborn, with survival ranging from 5 minutes to 6 months. Causes of death related to structural abnormalities were well characterized by both IA and UCA (Figure 1). Seven (24%) discordant causes of death between IA and UCA were identified, with 6 accounted for by fulminant sepsis which was occult by IA (Figure 1). One case of hydranencephaly by UCA was thought to be severe acqueductal stenosis by IA. Surface anatomy and intracardiac anatomy were more fully detailed at UCA and often not well visualized by IA. Placental information was included at UCA but not IA.
Conclusions: Imaging autopsy may be a more palatable alternative to CA for some families, and determination of cause of death in the absence of perimortum infection is similar between the two modalities. In occasions in which CA is not authorized by the family, the combination of IA interpreted by an experienced reader, perimortum culture data, and external exam may be an alternative method to UCA.

Figure 1: Concordant IA/UCA findings in a 26 week 1 day intrauterine fetal demise with hypoplastic left heart syndrome and restrictive atrial septum who expired after unsuccessful attempted prenatal atrial septal stent placement. Two malpositioned stents (arrows), 1 in the right ventricle (A&B) and 1 partially extracardiac (C&D), are readily seen by both IA and UCA.

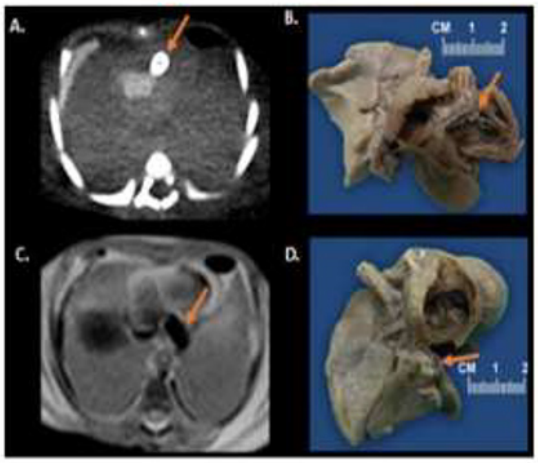

Figure 2: Discordant IA/UCA findings in a 27 week, 2 day liveborn infant with history of prenatally repaired open neural tube defect who expired at 6 days of life. Intraventricular T2 hypointense debris favored to reflect hemorrhage (A) corresponded to intraventricular pus at UCA (B). Parenchymal microabscess formation (arrows) was evident by UCA but occult by IA (C&D).

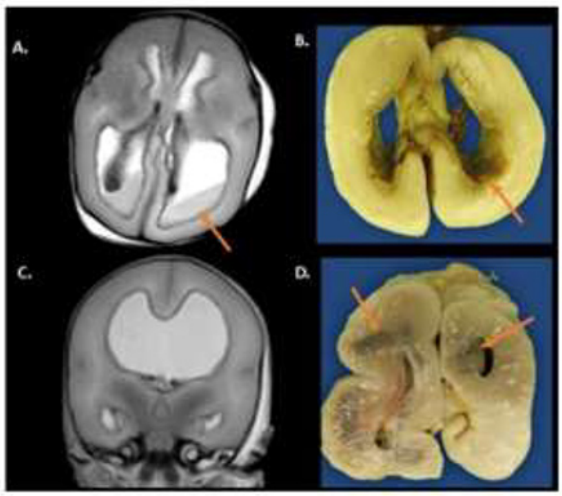

Paper #: 063

Gaging Potential Risk to Patients in Pediatric Radiology by Review of Over 2,000 Incident Reports

Elizabeth Snyder, MD[1], *elizabeth.j.snyder@gmail.com*; Wei Zhang, PhD[1], Kimberly Jasmin[1], Sam Thankachan[1], Lane Donnelly, MD[1]; [1]Texas Children's Hospital, Houston, TX

Disclosures: All authors have disclosed no financial interests, arrangements or affiliations in the context of this activity.

Purpose or Case Report: One way to study the potential risk for a patient entering a pediatric imaging department is to perform a common cause analysis of submitted incident reports.

We studied incident reports submitted over a 5-year period in a large pediatric imaging system to evaluate which imaging modalities and other factors were associated with a greater rate of filed incident reports.

Methods & Materials: During a 5-year period (2013-2017), all incident reports filed were reviewed and categorized by modality: X-ray (XR), CT, ultrasound (US), MRI, Nuclear Medicine (NM) and interventional radiology (IR). Other factors also noted included whether the patient was inpatient (IP), outpatient (OP), or Emergency Center (EC) patient as well as whether they were or were not under sedation/anesthesia. The number of incident reports was compared to the number of imaging studies performed during that time period to calculate an incident report rate for each factor. Statistical analysis of whether there were differences in these rates between modalities, sedation and non-sedation, and inpatient vs outpatient were performed using a chi-square test. For modalities, a pair-wise comparison with adjusted p-value for multiple comparison by Bonferrioni method was also performed.

Results: During the study period, there were 2,009 incident reports filed and 1,071,809 imaging studies performed for an incident report rate of 0.19%. Difference in rates by modality were statistically significant (p = 0.0001). There was a greater rate of incident reports in IR (1.54%) (p = 0.0001) and in MRI (p = 0.001) as compared to other imaging modalities (Table 1). There was a higher incident report rate for inpatients (0.34%) as compared to outpatient or EC (p = 0.0001) (Table 2). There was a higher rate of incident reports for patients under sedation (1.27%) as compared to non-sedated (0.12%) (p = 0.0001) (Table 3). Harm was perceived as being done in 1,302 of the incident reports although there were only 2 events during this 5-year period that were considered serious safety events by the institution, in which errors in radiology were primary contributing factors.

Conclusions: Using incident report rates as a proxy for potential patient harm, the areas of our pediatric radiology service that are associated with the greatest potential harm are IR, sedated patients, and inpatients. The areas associated with the least risk are US and XR. Safety improvement efforts should be focused on the high risk areas.

Table 1. Incident Report Rates Compared Between Imaging Modality

Modality	Number of Incident Reports	Imaging Studies	Incident Report Rate
IR	355	23,070	1.54%
MRI	572	91,579	0.62%
NM	73	13,075	0.53%
CT	252	66,326	0.38%
XR	595	686,757	0.09%
US	153	190,202	0.08%
N/A	9		
p = 0.0001			

Table 2. Incident Report Rate Compared Between Patient Type

Patient Type	Number of Incident Reports	Imaging Studies	Incident Report Rate
Inpatient	1037	303,050	0.34%
Outpatient	541	522,372	0.10%
EC	352	245,587	0.14%
N/A	74		
p = 0.0001			

Table 3. Incident Report Rate Compared Between Children who Underwent Sedation/Anesthesia Compared to those who Did Not

	Number of Incident Reports	Imaging Studies	Incident Report Rate
With Sedation	624	49,024	1.27%
Without Sedation	1294	1,022,785	0.12%
p = 0.0001			

Paper #: 064

Identifying the primary cause of safety events and complaints in the routine operations of a pediatric radiology department

Elizabeth Hingsbergen, MD[1], *Elizabeth.hingsbergen@nationwidechildrens.org*; Rajesh Krishnamurthy[1], Brent H. Adler, MD[1], Benjamin Thompson, MD[1], Houchun Hu, PhD[1], Erin Mesi, RT(R)[1], Tamara Viggiano[1], Nicholas Zumberge[1], Julee Eing[1]; [1]Radiology, Nationwide Children's Hospital, Columbus, OH

Disclosures: All authors have disclosed no financial interests, arrangements or affiliations in the context of this activity.

Purpose or Case Report: In order to facilitate transparency and improve quality across the enterprise, our pediatric hospital implemented an incident reporting system, named CS Stars, in 2011. The system is used to report, evaluate and track safety events and near misses regarding patients, visitors or employees, and to record customer feedback (complaints / grievances). The employee safety team within Radiology has benefited from this system by receiving a standardized detailed template of incidents. In this abstract, we analyze retrospectively data from CS Stars and identify the primary causes of errors and incidents reported for Radiology over one year.

Methods & Materials: CS Stars data were tracked for one year from October 2016 to October 2017. A total of 244 incidents were reported to involve Radiology. Each incident was reviewed by the safety team and categorized. The categories were evaluated for trends in order to facilitate quality improvement.

Results: A total of 244 CS stars events were reported. Of the 244 reported CS stars events, the largest category was communication failures (55%). Communication failures included subcategories of prescribing errors by clinicians, critical results reporting errors, communication errors between departments, and computer issues leading to delays and errors. The second largest category was failure to follow standard procedures, leading to safety events including wrong exam / wrong patient (27%).

Conclusions: Lack of communication is the root cause of the majority of untoward incidents involving radiology, and failure to follow standard procedures is the second largest cause. Knowledge of the root cause of these errors can guide quality improvement efforts, with improvement in professional-patient/family communication and inter-professional communication expected to produce the greatest res.

Event Type / Category	examples	#
Communications	Staff-to-staff miscommunication errors Electronic system delays and errors critical results errors lab specimen errors prescribing errors by clinicians	135
Failure to Follow Standard Operating Procedure	radiology wrong exam or wrong patient MRI screening failures radiation safety other policy breaches	65
Other	Equipment malfunction Aggressive patients Contrast agent reactions IV infiltrations staffing shortage miscellaneous	44

Paper #: 065

Analysis of Quick Hits at a Daily Readiness Huddle at a Large Free-Standing Children's Hospital

Ronna Porterfield, Bachelors[2], *ronna.porterfield@nationwidechildrens.org*; Benjamin Thompson[2], Kevin Dolan[1], Erin Mesi, RT(R)[2], Rajesh Krishnamurthy[2]; [1]Radiology Quality Improvement, Nationwide Children's Hospital, Columbus, OH, [2]Radiology, Nationwide Children's Hospital, Columbus, OH

Disclosures: All authors have disclosed no financial interests, arrangements or affiliations in the context of this activity.

Purpose or Case Report: Daily Readiness Huddle (DRH) is a common way of assessing a department's ongoing ability to care for patients in a safe and efficient manner. Issues that arise are classified as a quick hit or a complex issue based on the ability to use existing policies/protocols and specialist input. In this work, we prospectively analyze quick hits, complex issues, time to resolution, impact on department workflow and describe our DRH experience.

Methods & Materials: We implemented DRH to improve the communication, accountability and address concerns promptly using the "S-MESA" approach. We used a unique "dyad" based approach, with dyads composed of a radiologist combined with a modality manager on the operational side, and a specialty clinician on the clinical side. Dyads were created for all major endeavors of the department, had a strategic role in programmatic growth, and were owners of complex issues. Quick hits were managed by quality coordinators with expert input for dyad members. Issues were classified as a quick hit if they fell into one of the following categories:

Safety-including patient safety/employee safety

Methods-dealing with existing protocols, policies or standard of practice for imaging

Equipment-availability and functioning of equipment and technology

Supplies-availability based on daily need

Associates-staffing base on daily need

The quick hits were followed to resolution, with the type of issues and days to resolution being documented.

Results: Quick hits were tracked from Mar-Oct 2017. A total of 567 issues were classified as quick hits, with a majority (66.7%) involving methods and equipment (Fig1). Of the 220 method-related issues, the largest subcategories were care coordination, communication, unexpected high volume, scheduling errors, system errors and lack of policies or protocols for common situations (Fig2). The average days to resolution was 16.1 days (Fig3) with longer time to resolution noted in the early stages, and a progressive decline thereafter.

Conclusions: The DRH is a reliable format to discuss and resolve daily issues pertaining to safe and efficient patient care. A strategic approach to resolve quick hits is to empower quality coordinators to own the issues while seeking input from dyad specialists. This resulted in a progressive reduction in the time to resolution, a greater number of issues classified as quick hits rather than complex issues, and more efficient management of resources.

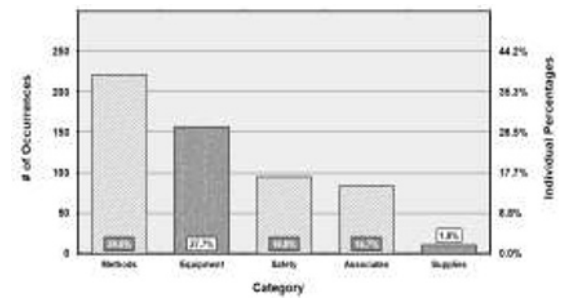

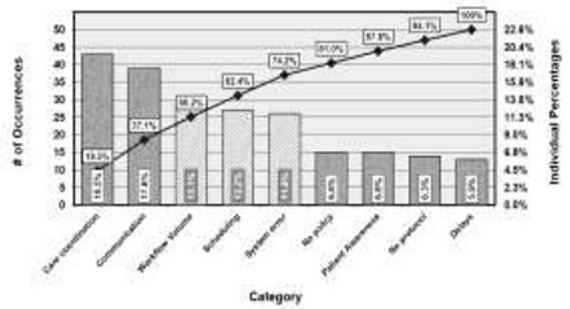

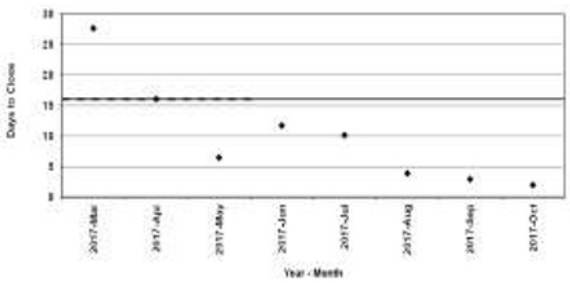

Paper #: 066

Survey of Peer Review Programs Amongst Pediatric Radiologists: Report from the SPR Quality and Safety Committee

Ramesh Iyer, MD[1], *rameshsiyer@gmail.com*; A. Luana Stanescu, MD[1]; [1]Radiology, Seattle Children's Hospital, Sammamish, WA

Disclosures: All authors have disclosed no financial interests, arrangements or affiliations in the context of this activity.

Purpose or Case Report: Since the 2002 introduction of RADPEER, radiology peer review has been central to quality improvement programs. Peer review programs may be implemented in a variety of formats with variable levels of acceptance by practitioners. Current implementations carry some concerns including fear that punitive action may follow subpar

performance, and the sense that the RADPEER process has little value beyond merely completing accreditation requirements. In an effort to understand concerns and opportunities to improve collaborative learning, the Society for Pediatric Radiology (SPR) Quality and Safety committee conducted a survey to aggregate member perspectives on peer review programs.
Objectives: To evaluate the current state of peer review programs in pediatric radiology practices, including implementation methods, perceived functions, strengths and weaknesses, and potential opportunities for improvement.
Methods & Materials: An online 16-question survey was distributed to SPR members. Survey questions pertained to type of peer review system, the use of numerical scores and review comments with perceptions on the utility of each, how feedback on interpretive discordances is given, and the use of peer learning conferences. Ample opportunity for free-entry responses was provided.
Results: A total of 219 responses were collected (15.3% of survey invitations), 80.2% of these from children's hospitals. 50% of respondents use a PACS-integrated system. 35.3% report that departmental quality conferences are held every month, while 19.3% report that they do not occur. 85.6% report that comment-enhanced feedback for interpretive discordances is either very important or somewhat important to performance improvement. 67.7% of respondents either rarely or never check their numerical scores. 81.73% either strongly or somewhat agree that comments are more effective feedback than numerical scores. 93.3% either strongly or somewhat agree that peer learning conferences would be beneficial to their practice. 47.7% feel that their current peer review system should be modified.
Conclusions: Conclusions: Survey results demonstrate that peer review systems in pediatric radiology practices are implemented in a wide variety of ways, and a large fraction of respondents think that their systems should be modified. Most respondents feel that feedback in form of comments and peer learning conferences are preferred over numerical scores, and are beneficial for performance improvement.

Paper #: 067

Potential Risk of Hypothyroidism in Infants Receiving Iodinated Contrast: Are Pediatric Radiology Practitioners Aware of the Food and Drug Administration (FDA) Drug Safety Communication?

Erica Gates, Associates Degree of Applied Science[1], *Erica.Kremer@cchmc.org*; Andrew Trout[1], Sparkle Netto[1], Jonathan Dillman, MD, MSc[1]; [1]Radiology, Cincinnati Children's Hospital Medical Center, Cincinnati, OH

Disclosures: All authors have disclosed no financial interests, arrangements or affiliations in the context of this activity.

Purpose or Case Report: On November 15, 2015 the United States FDA issued a drug safety communication describing rare cases of hypothyroidism in infants exposed to iodinated contrast material and required a package labeling change describing these cases. The purpose of this study was to understand awareness of this statement among the membership of the SPR and how the statement had changed clinical practice.
Methods & Materials: A six item survey regarding the FDA statement was distributed to active SPR members, including in-training and international members via email on August 16, 2017. The survey was administered via REDCap and was available for 50 days.
Results: 105 responses were received from 87 distinct sites. 16 sites had multiple respondents (≤3). 24 responses (23%) came from facilities outside of the continental United States. 96 responses were from practicing Pediatric Radiologists (6 trainees, 1 clinical trials executive, 2 not specified). 65 respondents (62%) were not aware of the FDA statement. Of the respondents aware of the FDA statement, 7 (18%) indicated the statement had changed their clinical practice. No respondent was aware of a case of hypothyroidism related to intravascular iodinated contrast at their institution. Based upon reported contrast material iodine content and per kg administered doses, per kg iodine load could be calculated for 66 respondents and ranged from 150 to 770 mg/kg. Only two respondents reported having maximum administered contrast doses relevant to infants. Only four respondents (4%) routinely discuss a risk of hypothyroidism with parents of children <1 year of age receiving intravascular iodinated contrast.
Conclusions: There is limited awareness among the SPR membership of an FDA statement regarding potential risk of hypothyroidism related to iodinated contrast administration in infants. Only a small minority of practitioners have changed practice related to the statement, and no respondent was aware of any documented case of hypothyroidism associated with intravascular iodinated contrast administration in an infant at their facility. Iodine doses administered vary widely across surveyed practices.

Paper #: 068

Utilization of computed tomography imaging in the pediatric emergency department

Daniel Frush[1], *jack.frush@gmail.com*; Clayton Commander[1], Terry Hartman[1], Aaron Cecil[1], Brian Handly[1], Daniel Park[1], Lynn Fordham[1]; [1]University of North Carolina, Durham, NC

Disclosures: All authors have disclosed no financial interests, arrangements or affiliations in the context of this activity.

Purpose or Case Report: In recent years, there has been a movement towards more judicious use of computed tomography (CT) imaging in an attempt to limit patient exposure to ionizing radiation. Pediatric patients are particularly vulnerable to the detrimental effects of cumulative radiation exposure, and many efforts to delineate thoughtful use have been developed with this specific population in mind. The Image Gently Alliance created a campaign in the late 2000s advocating for safe and high-quality pediatric imaging worldwide. The landmark study by the Pediatric Emergency Care Applied Research Network (PECARN) in 2009 validated prediction rules to identify children at low risk for clinically-important traumatic brain injuries and thus avoid head CTs altogether in such patients. It is in the context of these efforts that review the CT utilization rates in the pediatric emergency department (ED) at an academic medical center from 2008-2017 and compare them with utilization rates from 2000-2006.
Methods & Materials: We examined ED admission data and identified patients under 19 years of age who underwent imaging procedures within one day of ED admission. We analyzed five different categories of CT imaging—head, cervical spine, chest, abdomen (including abdominopelvic), and miscellaneous—as well as selected categories for magnetic resonance imaging (MRI) and ultrasound.
Results: Between July 2008 and June 2017, 4,955 pediatric patients underwent a total of 5,973 CT scans while in the ED; in comparison, 4,138 patients underwent 6,073 CT scans in the ED between 2000 and 2006. In comparing the first year of our study (July 2008 - June 2009) to the last (July 2016 - June 2017), we observed decreases in CT utilization across all categories, ranging from a 19% decrease in abdominal CT to a 66% decrease in chest CT. Relatively greater decreases in CT utilization were observed in infants (patients less than 3 years of age) than in children (3-12 years) or adolescents (greater than 12 years). Total utilization of abdominal and pelvic ultrasound increased, with the rise in abdominal ultrasound driven entirely

by a steep uptick in the number of limited abdominal studies. Brain MRI utilization also increased over the final two years of the study period.
Conclusions: Our results suggest that recent efforts have in fact played a role in decreasing utilization rates of several major categories of CT imaging.

Paper #: 069

Cost comparison of ultrasound versus MRI for adolescent female patients with suspected appendicitis using time-driven activity-based costing

Kelly Hagedorn, MD[1], *hagedorn.kelly@gmail.com*; Shireen Hayatghaibi, MPH[1], Matt Levine[1], Sam Thankachan[1], Mallory Caldwell[1], Robert Orth, MD, PhD[1]; [1]Texas Children's Hospital, Houston, TX

Disclosures: All authors have disclosed no financial interests, arrangements or affiliations in the context of this activity.

Purpose or Case Report: To establish the institutional cost of imaging adolescent female patients with suspected appendicitis, improve the ultrasound (US) workflow by identifying and correcting systematic inefficiencies, and compare the cost of US versus MRI for imaging this patient population.
Methods & Materials: Process maps were created using data from electronic medical record review and patient shadowing for adolescent female patients with suspected appendicitis ages 11-18 undergoing non-contrast US or MRI exams of the abdomen and pelvis. Our institutional protocol is to evaluate for ovarian torsion in all adolescent females with suspected appendicitis. Using time-driven activity based costing (TDABC), capacity cost rates for each resource in the process map were established from institutional accounting data incorporating personnel, equipment, and facility costs. The cost of each process step was determined by multiplying step-specific capacity costs by the average time required to complete the step. Total pathway costs for US and MRI were computed by summing the costs of all steps through each process pathway. Analyzing US technologist cycle time variation presented an opportunity to improve the US protocol. Through use of Plan-Do-Study-Act (PDSA) cycles, a revised, standardized ultrasound protocol was implemented and total US pathway costs recalculated.
Results: Process maps for US and MRI pathways were generated from 248 US and 52 MRI patient encounters (Figures 1 and 2). Mean total pathway time for patients undergoing US exams was 92 minutes longer than those undergoing evaluation with MRI. Total cost for US exams ranged from $171 to $367 (mean=$269), depending on whether the patient's bladder was full enough to perform the pelvic and appendix US exams concurrently. Following implementation of the revised appendix US protocol, average appendix scan times decreased by seven minutes (Figure 3). This resulted in a cost savings of $10 for all pathway routes, with total costs ranging from $161 to $357 (mean=$259). Total cost for MRI exams ranged from $159 to $167 (mean=$162), depending on whether MRI screening forms were completed prior to arrival at the MRI suite.
Conclusions: Our results show that MRI can be a faster and potentially less costly alternative to US for evaluating suspected appendicitis in adolescent female patients. While the cost of performing these exams will vary by institution, MRI may be a viable and in certain cases preferable alternative to US in this patient population.

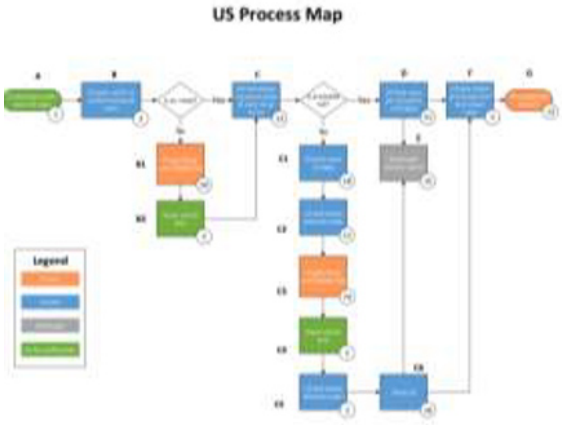

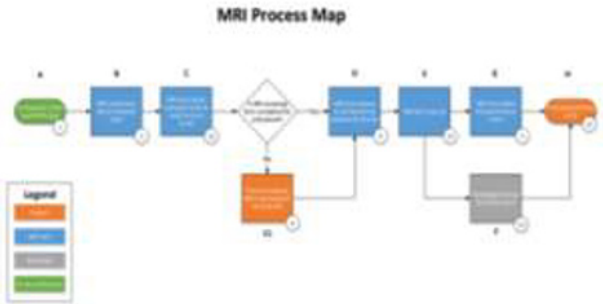

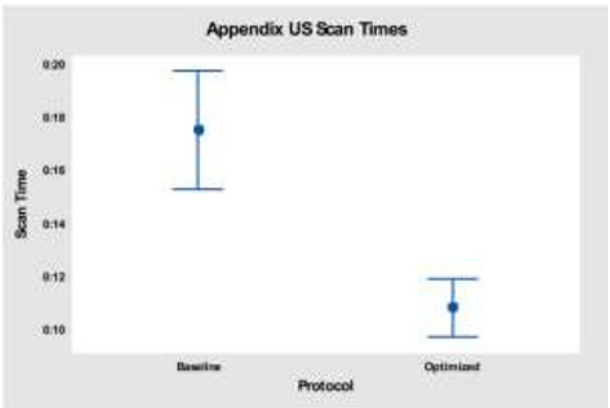

Paper #: 070

Survey of after-hours radiology coverage in children's hospitals.

Michael Aquino, MD[2], *mike.r.aquino@gmail.com*; David Dinan[4], George Koberlein, MD[1], Victor Ho-Fung, MD[5], Susan John, MD[3]; [1]Radiology, Cincinnati Children's Hospital Medical Center, Loveland, OH, [2]The Hospital for Sick Children, Toronto, ON, Canada, [3]University of Texas Health Sciences Center at Houston, Houston, TX, [4]Nemours Children's Hospital, Orlando, FL, [5]Children's Hospital of Philadelphia, Philadelphia, PA

Disclosures: All authors have disclosed no financial interests, arrangements or affiliations in the context of this activity.

Purpose or Case Report: The purpose of this study was to identify what radiology services are provided after-hours in children's hospitals and how radiology departments deliver this coverage.
Methods & Materials: A web-based survey was developed and asked respondents to provide detailed information on their after-hours radiology coverage. A delegate from each hospital represented in the Society of Chairs of Radiology at Children's Hospitals (SCORCH) was invited to complete the survey.
Results: Responses were submitted by 59% (47/79) of hospitals. Over 80% of respondents (39/47) indicated that their hospital provides contemporaneous interpretations of pediatric body radiology studies (radiographs, ultrasound, computed tomography) 24 hours a day, 7 days a week ("24/7"). The contemporaneous interpretations are provided by attending radiologists in 51% (20/39) of hospitals and 95% (19/20) of these interpretations are delivered in the form of final reports. The remaining 49% (19/39) of these hospitals rely on preliminary reports from radiology residents or fellows to provide contemporaneous interpretations.
Emergency radiology sections are used by 36% (14/47) of hospitals to staff the overnight duration of the "24/7" coverage. In 79% (11/14) of these hospitals, these sections are composed of pediatric radiologists. Teleradiology services are used by 8% (4/47) for overnight service. Overall, 55% (26/47) of hospitals described scheduling at least 1 attending pediatric radiologist on a late-shift that extends variable durations beyond 5 PM to provide contemporaneous interpretations after-hours. Only 4% (2/47) provide strictly beeper-call coverage after 5 PM.
The option to work remotely rather than in-house is offered to radiologists working after-hours in 21% (10/47) hospitals. Additional benefits such as increased income, more time off, or academic time is offered by (21/47) hospitals.
Conclusions: The majority of children's hospitals surveyed provide contemporaneous interpretations of pediatric body radiology studies with final or preliminary reports 24 hours a day, 7 days a week. Late-shifts staffed by attending radiologists are used by most surveyed hospitals to extend coverage for variable durations beyond 5 PM. Dedicated pediatric emergency radiology sections are commonly used to bridge late night and day shifts. Some hospitals provide additional incentive benefits for working after-hours including increased income, more time off, and the option to work remotely from home.

Paper #: 071

Evaluation of Stressors that Contribute to Burnout Amongst Pediatric Radiologists: A Survey of the Society for Pediatric Radiology

Rama Ayyala, MD[1], *rsa2121@columbia.edu*; Carrie Ruzal-Shapiro[1], Firas Ahmed[1], George Taylor[2]; [1]Columbia University Medical Center, New York, NY, [2]Boston Children's Hospital, Boston, MA

Disclosures: All authors have disclosed no financial interests, arrangements or affiliations in the context of this activity.

Purpose or Case Report: Burnout is a psychological syndrome that is characterized by three major components: emotional exhaustion, depersonalization, and perceived lack of accomplishment. There are multiple stressors that have been shown to play a role in the development of burnout in medicine. The purpose of this study is to evaluate the impact of various causes of stress on the prevalence of burnout in pediatric radiologists.
Methods & Materials: An anonymous survey was sent to Society for Pediatric Radiology members that included adapted questions from the Maslach Burnout Inventory (MBI) measuring aspects of burnout including emotional exhaustion, depersonalization and perception of low accomplishment. Data on demographics and questions regarding multiple stressors that contribute to development of burnout were included, which are based on previous studies regarding burnout in medicine. Topics evaluated include the call burden, financial stress, work-life balance, healthcare evolution and job market changes, and radiology overall as a career choice.
Results: The response rate was 460/1453 (32%). 50% of responding pediatric radiologists were female and 42% were practicing at academic institutions. Prevalence of emotional exhaustion was 66% (286/435), of depersonalization was 61% (265/433) and perceived lack of personal accomplishment was 15% (67/436). Work-life imbalance and stress related to caring for dependents were more prevalent among female radiologists (75%, p-value=0.019 and 45%, p-value=0.011). After hours call and competitive radiology job market were more prevalent stressors among female radiologists than male counterparts (53%, p-value=0.002 and 17%, p-value=0.030). In a multivariable logistic regression model predicting emotional exhaustion and depersonalization, after hours call and concerns about work-life balance were consistent and statistically significant predictors of burnout (ORs=2.3-7.6; p-value <0.001). Decreasing rates of reimbursement was an independent stressor associated with emotional exhaustion (OR=2.7; p-value=0.030) and financial strain was an independent stressor associated with depersonalization (OR=2.3; p-value=0.020).
Conclusions: Emotional exhaustion and depersonalization are prevalent among the community of pediatric radiology. On call responsibilities, work-life imbalance, and financial concerns were strong stressors contributing to the burnout. These stressors were more prevalent among female radiologists.

Paper #: 072

Assessing the Pediatric Radiology Job Market: Winter is Coming for Employers

Cory Pfeifer, MD[1] *cpfeifer2018@gmail.com*; ; [1]Diagnostic Radiology, University of Texas Southwestern Medical Center, Dallas, TX

Disclosures: All authors have disclosed no financial interests, arrangements or affiliations in the context of this activity.

Purpose or Case Report: The 2016-2017 academic year represented a significant recovery of the diagnostic radiology job market. As the available number of jobs has increased, however, the number of pediatric radiology fellows has declined. This study examines the recent supply and demand for pediatric radiologists as well as implications for fellows and employers moving forward.
Methods & Materials: The Society for Pediatric Radiology (SPR) and American College of Radiology (ACR) Career Centers were analyzed each day from July 1, 2016 through June 30, 2017. Job advertisements for fellowship positions were excluded. Fellowship occupation rates were derived from data reported by the Accreditation Council for Graduate Medical Education. Projected fellowship interest was assessed using chief-resident-derived survey data from the American Alliance of Academic Chief Residents in Radiology.
Results: There were 97 unique full-time attending-level jobs for pediatric radiologists advertised on the SPR Career Center during the 2016-2017 academic year. Of these openings, 72% were advertised by universities or free-standing children's hospitals. Distinct peaks in job openings in November 2016 and March 2017 were apparent. Positions were posted for a median

of 2 months and an average of 2.9 months. California and Texas were the states with the most openings. There were 96 jobs for pediatric radiologists posted on the ACR Career Center with a daily average of 16.2 pediatric radiology jobs, representing 3% of the average number of total diagnostic radiology jobs. The number of total jobs and pediatric radiology jobs have continued to increase in 2017. There were less than 2 pediatric radiology fellows for every 3 advertised positions in 2016-2017. Progressive declines in the number of pediatric fellows have been observed since 2013. Resident survey data forecasts continued decreases in the number of radiology graduates opting for pediatric radiology fellowships.
Conclusions: Progressive declines in the number of pediatric radiology fellows creates a favorable job market for current trainees, however, employers should expect significant declines in the number of new graduates over the coming years. Stakeholders should devote efforts to improving the appeal of pediatric radiology to current and future diagnostic radiology residents.

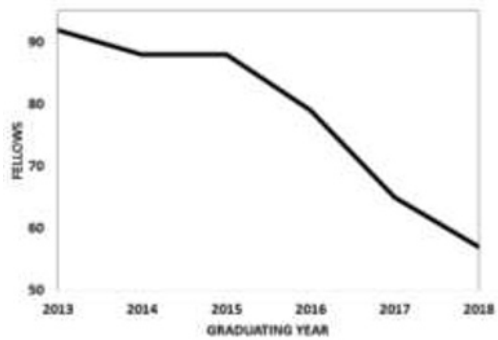

Paper #: 073

Diagnostic Performance of Magnetic Resonance Cholangiopancreatography (MRCP) versus Endoscopic Retrograde Cholangiopancreatography (ERCP) in the Pediatric Population: A Clinical Effectiveness Study

Jonathan Dillman, MD, MSc[1], *jonathan.dillman@cchmc.org*; Rakesh Patel, MD[1], Tom Lin[1], Alexander Towbin, MD[1], Andrew Trout[1]; [1]Cincinnati Children's Hospital Medical Center, Cincinnati, OH

Disclosures: All authors have disclosed no financial interests, arrangements or affiliations in the context of this activity.

Purpose or Case Report: Endoscopic retrograde cholangiopancreatography (ERCP) is considered the reference-standard for evaluation of biliary and pancreatic duct abnormalities. However, its use in children is limited by its invasive nature and small number of experienced providers. Magnetic resonance cholangiopancreatography (MRCP) is a well-recognized alternative that is able to provide high-quality images of the pancreatic and biliary system noninvasively. The purpose of this study was to determine the diagnostic performance of MRCP for detecting biliary and pancreatic abnormalities in a pediatric population, using ERCP as the reference standard.
Methods & Materials: Institutional review board approval with a waiver of informed consent was obtained for this retrospective, HIPAA-complaint investigation. Records from the Division of Gastroenterology and Department of Radiology were used to identify patients ≤18 years-old who had undergone both ERCP and MRCP within a four-week interval between January 1, 2013 and May 15, 2017. Biliary and pancreatic duct findings were documented for each modality to determine the diagnostic performance of MRCP (with 95% confidence intervals), using ERCP as the reference standard.
Results: 54 patients met inclusion criteria. Mean patient age at time of ERCP was 10.4±4.9 years, and 25 (46%) were boys. Mean interval between ERCP and MRCP was 11.2 ± 9.7 days. For detection of any abnormality (n=99), MRCP had a sensitivity of 76.8% (67.5-84.0%) and a positive predictive value (PPV) of 81.7% (72.7-88.3%) (Table 1). MRCP was 75.7% (59.9-86.6%) sensitive, with a PPV of 84.9% (69.1-93.4%) for biliary findings (n=37) and 73.5% (59.7-83.8%) sensitive, with a PPV of 78.3% (64.4-87.7%) for pancreatic findings (n=49). For detecting abnormalities that were both biliary and pancreatic (n=13), MRCP had a sensitivity of 92.3% (66.7-99.6%) and PPV of 85.7% (60.1-97.5%) (Table 2).
Conclusions: In clinical practice, MRCP is moderately sensitive for biliary and pancreatic abnormalities, with false negative and false positive exams being relatively common.

Table 1 – Diagnostic performance of MRCP for detecting biliary and pancreatic abnormalities, using ERCP as the reference standard (n=99 findings in 54 patients).

Analysis	Sensitivity (%) (95% CI) [N/D]	Positive Predictive Value (%) (95% CI) [N/D]
Overall patient population (n=99)	76.8 (67.5-84.0) [76/99]	81.7 (72.7-88.3) [76/93]
Biliary indication for MRCP (n=37)	75.7 (60.0-86.6) [28/37]	84.9 (69.1-93.4) [28/33]
Pancreatic indication for MRCP (n=49)	73.5 (59.7-83.8) [36/49]	78.3 (64.4-87.7) [36/46]
Both biliary & pancreatic indication for MRCP (n=13)	92.3 (66.7-99.6) [12/13]	85.7 (60.1-97.5) [12/14]
Biliary duct injection only (n=29)	79.3% (61.6-90.1%) [23/29]	85.2% (67.5-94.1%) [23/27]
Pancreatic duct injection only (n=5)	100% (56.6-100%) [5/5]	62.5% (30.6-86.3%) [5/8]
Biliary & pancreatic duct injection (n=65)	73.9% (62.1-83.0%) [48/65]	82.8% (71.1-90.4%) [48/58]

*MRCP = magnetic resonance cholangiopancreatography; ERCP = endoscopic retrograde cholangiopancreatography; CI = confidence interval; N/D = numerator/denominator.

Table 2 – False negative MRCP findings from overall patient population, using ERCP as the reference standard (n=23).

ERCP Findings	MRCP FN
Extra-hepatic biliary stricture	8
Pancreatic duct stone	4
Anomalous pancreatobiliary junction	2
Intra-hepatic biliary stricture(s)	2
Other (n=1)	7

* MRCP = magnetic resonance cholangiopancreatography; ERCP = endoscopic retrograde cholangiopancreatography; FN = False negative

Paper #: 074

Normal Pancreatic Secretion in Children Measured by MRI with Secretin

Andrew Trout[1], *andrew.trout@cchmc.org*; Maisam Abu-El-Haija[1], Suraj Serai, PhD[1], Lin Fei[1], Qin Sun[1]; [1]Radiology, Cincinnati Children's Hospital Medical Center, Cincinnati, OH

Disclosures: Andrew Trout has indicated a relationship with Guerbet Group as a consultant, Educational Symposium International as a speaker, Elsevier for receiving royalty and Toshiba America Medical systems for receiving a research grant. All other authors have disclosed no financial interests, arrangements or affiliations in the context of this activity.

Purpose or Case Report: Magnetic resonance cholangiopancreatography (MRCP) with secretin administration has been described as a non-invasive method of assessing pancreatic exocrine function. Normative data for pancreatic secretory response as measured by MRCP exist for adult patients but not for children. The purpose of this study was to prospectively determine normal secretory function as measured by MRCP for the pediatric population.
Methods & Materials: IRB approval was obtained for this prospective study of 50 pediatric volunteers ages a 6-16 years without a history of pancreatic disease. Volunteers underwent MRCP with secretin administration for calculation of normal pancreatic secretory function. Secretory function was quantified in terms of total secreted fluid volume through 15 minutes and in terms of secretion rate (mL/min) based on linear regression of the secretion curve from 0-15 minutes. Relationships between secretory function and size measures (age, height, weight, body mass index, body surface area [BSA]) were assessed with Spearman's rho and with step-wise multivariate regression.
Results: Total secreted fluid volume through 15 minutes ranged from 32 to 162 mL with a median of 79 mL (5^{th} percentile = 43 mL). Secretion rate ranged from 2 to 9.4 mL/min with a median of 5.1 mL/min. Secretory function correlated with subject age and all measures of subject size. The greatest correlation was to BSA (rho=0.54 for total volume and 0.59 for secretion rate, $p<0.0001$) [Figure] and BSA was the only predictor of secretory function in multivariate analysis. Effect size for BSA was a 38 mL increase in total secreted volume for every 1 m^2 increase in BSA.
Conclusions: Pancreatic secretory response as measured by MRCP with secretin is dependent on patient size, particularly BSA. Based on our population, total secreted fluid volume <43 mL (<5^{th} percentile) can likely be considered abnormal for a child. That said, normal secretory function in children <16 years of age is lower than previously described in adults suggesting the need for more granular age or size based normative cut-offs to asses pancreatic exocrine function in the pediatric population.

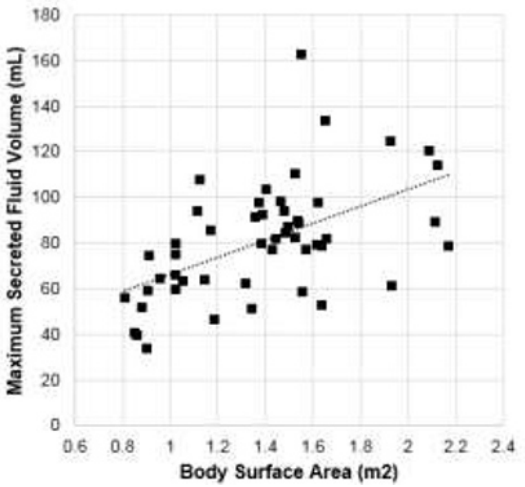

Paper #: 075

Diagnostic performance of quantitative MRI parameters for predicting radiologic portal hypertension in autoimmune liver diseases

Jonathan Dillman, MD, MSc[1], *jonathan.dillman@cchmc.org*; Andrew Trout[1], Suraj Serai, PhD[1], Alexander Miethke[1]; [1]Department of Radiology, Cincinnati Children's Hospital Medical Center, Cincinnati, OH

Disclosures: All authors have disclosed no financial interests, arrangements or affiliations in the context of this activity.

Purpose or Case Report: Accumulating fibrosis in chronic liver diseases increases the resistance to blood flow through the liver and results in portal hypertension. Portal hypertension is an important source of morbidity and mortality in children with chronic liver diseases, including autoimmune liver diseases (ALDs). The purpose of this study was to determine the diagnostic performance of multiple quantitative MRI parameters for predicting the presence of radiologic portal hypertension in ALD patients.

Methods & Materials: 29 patients with autoimmune liver disease (e.g., autoimmune hepatitis, primary sclerosing cholangitis) were enrolled in a prospective registry. Multiparametric MRI was performed on all subjects using a 1.5T imager (Ingenia; Philips Healthcare). Quantitative MRI sequences were performed through the mid liver, including iron-corrected T1 mapping (cT1), T2 mapping, T1rho mapping, and diffusion-weighted imaging (DWI, quantified as apparent diffusion coefficients [ADC]). MR elastography (60 Hz) of the liver and spleen was also performed. Anatomic MR imaging was reviewed by a single board-certified, fellowship-trained pediatric radiologist to document the presence of portal hypertension (based on the presence of at least 2 of the following 3 findings: ascites, splenomegaly, and portosystemic collateral vessels). Receiver operating characteristic curve analyses were used to determine the diagnostic performance of quantitative MRI parameters for predicting radiologic portal hypertension.
Results: Mean subject age was 15.3 ± 3.8 years; there were 15 male subjects. Splenic stiffness demonstrated the best diagnostic performance for distinguishing ALD patients without versus with portal hypertension (area under the ROC curve [AUROC]=0.97; p=0.0002) (Figure 1). Liver stiffness and cT1 also showed good ability to discriminate between these two patient groups (AUROC=0.93; p=0.0002 and AUROC=0.84; p=0.003, respectively). Liver T2, T1rho, and DWI ADC values showed poor diagnostic performance. Sensitivities, specificities, and cut-off values are presented in Table 1.
Conclusions: MRI splenic and liver stiffness measurements as well as cT1 values distinguish ALD patients without and with radiologic portal hypertension. It is conceivable that these noninvasive biomarkers can be used to identify pediatric patients at risk for developing portal hypertension and related complications, although confirmatory prospective studies are needed.

Table 1 – Diagnostic performance of quantitative MRI parameters for predicting radiologic portal hypertension* in autoimmune liver diseases.

	AUROC	Cut-off value**	Sensitivity (%)	Specificity (%)	p-value
Spleen stiffness (kPa)	0.97	>7.05	100	88.9	0.0002
Liver stiffness (kPa)	0.93	>4.48	80.0	94.7	0.0002
Iron-corrected T1 mapping (msec)	0.84	>904	80.0	89.5	0.003
T2 mapping (msec)	0.58	>68.0	70.0	47.4	0.51
T1rho mapping (msec)	0.56	>47.5	80.0	47.4	0.61
DWI ADC (x 10^{-3} mm^2)	0.63	<1.21	77.8	57.9	0.29
Age (years)	0.58	>16.5	60.0	63.2	>0.99

*Based on presence of at least 2 of the following 3 findings: ascites, varices, and splenomegaly.

**Cut-off values chosen using the Youden's J statistic.

AUROC = area under the receiver operating characteristic curve; DWI ADC = diffusion-weighted imaging apparent diffusion coefficient.

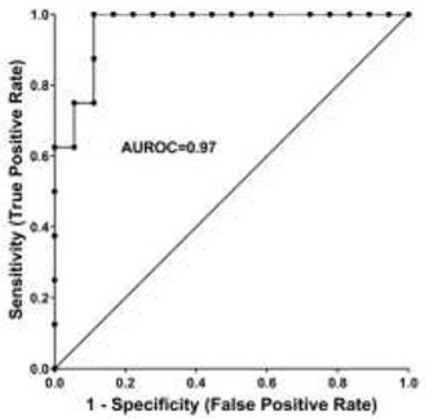

Paper #: 076

Relationship between 2D phase contrast MRI Rex shunt blood flow, Rex shunt diameter, and clinical indicators of portal hypertension

Heather Stefek, BS[1], *heather.stefek@northwestern.edu*; Haben Berhane[1], Andrada Popescu, MD[1], Shankar Rajeswaran[1], Riccardo Superina[2], Cynthia Rigsby, MD[1]; [1]Medical Imaging, Lurie Children's Hospital, Chicago, IL, [2]Division of Transplant Surgery - Lurie Children's Hospital, Chicago, IL

Disclosures: All authors have disclosed no financial interests, arrangements or affiliations in the context of this activity.

Purpose or Case Report: The meso-Rex bypass (Rex shunt) shunts blood from the superior mesenteric vein to the left portal vein and restores physiological blood flow to the liver in patients with extrahepatic portal vein thrombosis. While the majority of shunts remain patent for years, a subset develop stenoses and may require intervention to restore flow. Compromised shunt flow can cause coagulopathy and variceal bleeding, but complications occur on a spectrum, making it difficult to definitively assess shunt function and plan intervention timing. Our purpose is to determine the relationship between 2D phase-contrast MRI (PC-MR) measurement of Rex shunt blood flow and shunt diameter and compare shunt flow with platelet count, a clinical indicator of portal hypertension.
Methods & Materials: MR studies of all children with Rex shunts who underwent PC-MR (Siemens 1.5T Aera) from 2013-2017 were retrospectively analyzed. Minimum Rex shunt diameter was measured in 2 planes on contrast-enhanced MR angiography and was used to calculate cross-sectional area (π x r1 x r2) which was normalized to body surface area (BSA). Shunt flow (L/min) calculated from PC-MR (retrospectively ECG-triggered, 30 phases per heart beat, post-processed in QFlow, Medis) was divided by ascending aortic flow (L/min) to obtain the shunt to systemic blood flow ratio. Platelet counts drawn the same day as the MR were recorded. Correlations between minimum Rex shunt cross-sectional area, shunt to systemic flow, and platelet count were calculated. $P < 0.05$ was considered significant.
Results: 25 children (median age 9.5yrs, range 2.5-19yrs) with Rex shunts underwent MRI with PC-MR, most for routine Rex shunt surveillance. Median time between Rex shunt surgery and MR was 53 months (range 9-106 months). Median platelet count in 19 patients was 121 K/uL (range 42-232 K/uL). Significant relationships were seen between 1) minimum Rex shunt crosssectional area normalized to BSA and shunt to systemic flow and 2) between platelet count and shunt to systemic flow, with decreased flow corresponding to smaller shunt area ($p = 0.027$, $r = 0.44$) and lower platelet count ($p = 0.021$, $r = 0.52$).
Conclusions: Rex shunt blood flow correlates with shunt area and platelet count indicating a physiologic relationship between insufficient flow and development of complications related to portal hypertension such as thrombocytopenia. Rex shunt flow may represent a biomarker for shunt intervention need. Larger studies are needed to determine flow thresholds that will trigger intervention.

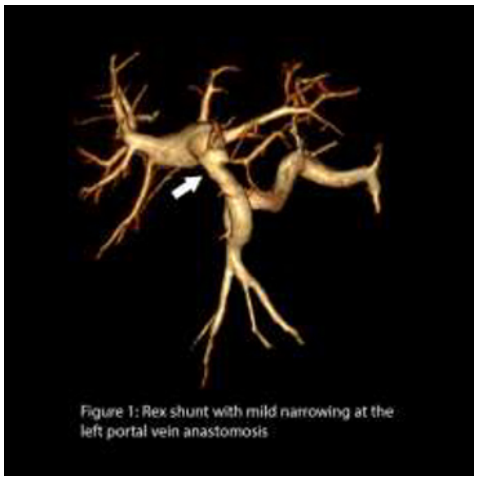

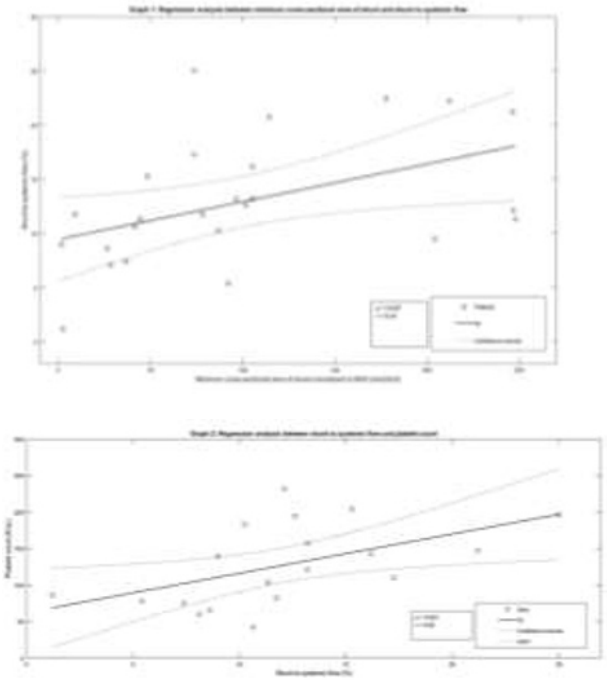

Paper #: 077

Validation of LI-RADS in Evaluation of Pediatric Liver Masses

Erin Romberg[1], *romberge@wustl.edu*; Tyler Fraum, MD[1], Eric Rohe[2], Kathryn Fowler, MD[1], Geetika Khanna[1]; [1]Mallinckrodt Institute of Radiology, Saint Louis, MO, [2]St. Louis University School of Medicine, St. Louis, MO

Disclosures: All authors have disclosed no financial interests, arrangements or affiliations in the context of this activity.

Purpose or Case Report: Liver Imaging Reporting and Data System (LI-RADS) has standardized the evaluation of hepatic lesions in adults at risk of developing hepatocellular carcinoma (HCC). No such standards exist to evaluate and stratify pediatric liver lesions. This study evaluates the applicability, diagnostic performance, and inter-rater reliability of LI-RADS v2017 in evaluation of pediatric liver masses, including children at risk for HCC.

Methods & Materials: Retrospective, IRB approved review of abdominal dynamic contrast enhanced (DCE) imaging over 10 years at a tertiary children's hospital yielded 151 liver lesions in children. Cases with known active extrahepatic malignancy or inadequate reference standard were excluded. Two blinded readers independently evaluated the remaining hepatic lesions and assigned LI-RADS categories. In patients with multiple lesions, only 1 randomly selected lesion was included in the analysis for a total of 41 lesions. Reference standard was pathology or stability on imaging > 1 year.

Results: 41 children (63% female) with median age of 12 years (range 0 - 17 years) formed the study cohort. Underlying liver disease predisposing to HCC was present in 11/41 patients. Of 41 included lesions: 6 were HCC, 8 were non-HCC malignancies, and 27 were benign by reference standard. With strict interpretation of the LI-RADS criteria, a LI-RADS 5 (LR-5) designation had a sensitivity of 67% [95% CI: 13-98%] and 100% [31-100%] for the two readers. Specificity of the LR-5 designation was 84% [68-93%] and 97% [85-100%] respectively. Inter-observer agreement was moderate (kappa 0.43) for LI-RADS 5 designation. LI-RADS performed even stronger in subset analysis of patients with underlying disease predisposing to HCC, with LR-5 designation demonstrating a sensitivity of 100% [5-100%] for both readers, and specificity of 80% [44-96%] and 100% [66-100%]. Of lesions designated by either reviewer as LR 1-3 (n=39), there was 1 instance of a malignant lesion incorrectly characterized as LR-2.

Conclusions: LI-RADS categorization demonstrates moderate to high sensitivity and specificity in differentiating hepatocellular carcinoma from other hepatic lesions in children, especially those at risk of developing HCC. Given the rarity of HCC in the pediatric population, further evaluation in a larger and perhaps multi-institutional cohort is necessary.

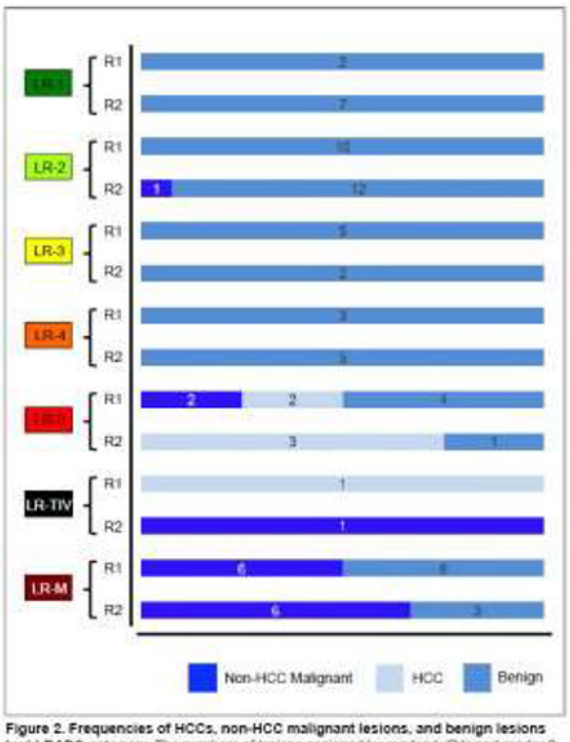

Figure 2. Frequencies of HCCs, non-HCC malignant lesions, and benign lesions by LI-RADS category. The numbers of lesions assigned by reader 1 (R1) and reader 2 (R2) to each LI-RADS category are shown. The horizontal bars, which are normalized to 100%, display the relative frequencies of hepatocellular carcinomas (HCCs), non-HCC malignant masses, and benign masses within each LI-RADS category.

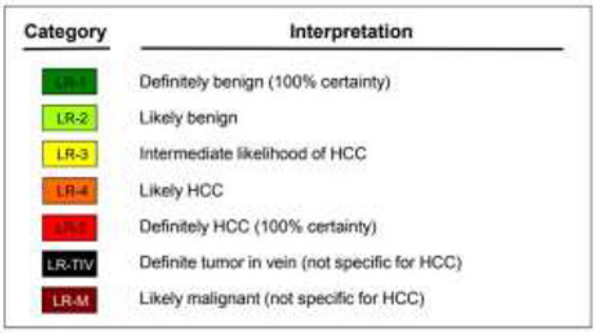

Figure 1. LI-RADS terminology.

Abbreviations: HCC = hepatocellular carcinoma

Paper #: 078

Congenital portosystemic shunts (CPSS): clinical outcome after treatment. Experience in a tertiary hospital in Argentina

Jose Lipsich, Radiology-in Jose Lipsich, Radiology in Chief[1], *joselipsich@gmail.com*; [1]Diagnóstico por Imágenes, Hospital Juan P. Garrahan, CABA, Argentina

Disclosures: All authors have disclosed no financial interests, arrangements or affiliations in the context of this activity.

Purpose or Case Report: To report our experience regarding treatment of CPSS, the clinical outcome and treatment response after treatment.
Methods & Materials: From 1995 to 2015, 33 children with CPSS were followed-up. Fourteen patients were treated, 8 by surgical means and 6 with endovascular occlusion. Clinical follow-up was available in 29 cases, with an average follow-up time of 86,7 months (range 24-203 month). Nine children had spontaneous closure of the shunt (all of them presented neonatal cholestasis as complication that resolved after shunt closure), 4 were lost of follow-up, 3 died and 3 are still being followed.
Results: Seven children presented with hepatopulmonary syndrome (HPS); 6 of them were treated and all of them resolved the HPS. Six children had pulmonary hypertension (PH) which was controlled in 3 (50%). Five hepatic tumors were diagnosed, and 3 (60%) disappeared after treatment. Four patients suffered encephalopathy that resolved in all children treated (100%). Five children had gastrointestinal bleeding. Two children were treated and none of them presented any bleeding episode in the follow-up.
Conclusions: Closure of CPSS lowers significantly the complications usually associated with this rare disease.

Paper #: 079

Preliminary experience with Contrast Enhanced Ultrasound (CEUS) of the Pediatric Liver

Susan Back, MD[1], *susan.back@gmail.com*; David Biko, MD[1], Carolina Maya, MD[1], Aikaterini Ntoulia, MD, PhD[1], Laura Poznick, AAS, ARDMS[1], Trudy Morgan[1], Kassa Darge, MD, PhD[1], Sudha Anupindi, MD[1]; [1]Radiology, Children's Hospital of Philadelphia, Penn Valley, PA

Disclosures: All authors have disclosed no financial interests, arrangements or affiliations in the context of this activity.

Purpose or Case Report: CEUS is used to evaluate focal and traumatic liver lesions as a primary examination and assessment following ultrasound (US), CT and MRI. CEUS in children is gaining momentum following the April 2016 United States Food and Drug Administration approval for intravenous administration of an US contrast agent for pediatric liver lesions. This study describes our initial experience with CEUS of the pediatric liver.
Methods & Materials: This is an IRB approved retrospective review of clinical and imaging findings of pediatric liver CEUS exams over a 27-month period and relevant follow-up imaging.
Results: There were 99 CEUS exams in 79 children with a median age of 8.6 years (range: 0.1- 25y). Indications were focal lesions (n=85) or trauma (n=14). A GE Logic E9 (n=42) or Philips Epiq 7 (n=57) US unit was used with either Lumason (n=72) or Optison (n=27) US contrast agent. For Lumason exams the volume per injection ranged from 0.2- 2 mL (0.006-0.58 mL/kg). On average 2.4 injections/exam were done using a mean total dose of 1.9 mL (range: 0.4- 5.4mL) and mean total weight based dose of 0.11 mL/kg (range: 0.007-0.6 mL/kg). For Optison exams the volume in each injection ranged from 0.1-0.5mL (0.002- 0.08 mL/kg). On average 3.3 injections/exam were done using a mean total dose of 1.1 mL (range: 0.3- 5.4mL) and mean total weight based dose of 0.09 mL/kg (range: 0.01-0.3 mL/kg). The CEUS diagnoses were: normal 18% (n=18), hemangioma 17% (n=17); regenerative nodule (RN) 12% (n=12); focal nodular hyperplasia (FNH) 12% (n=12); infection 11% (n=11); focal fat 9% (n=9); benign 9% (n=9); malignant 7% (n=7) and trauma 4% (n=4). 18/79 children had a contrast enhanced CT prior to or within 26 days of the CEUS. 36/79 children had previous MRI, 16 of which used a hepatocyte-specific contrast agent. Pathology was available for 9 patients: 3 malignant, 2 FNH, 2 inflammation, 1 granuloma, and 1 focal necrosis. Follow up imaging was available in 39% (n=39) of patients. The mean time between the CEUS and most recent imaging exam was 178 days (range: 3- 609d). Review of the most recent study showed no lesion 18% (n=7), stable 48% (n=19), increased 10% (n=4) or decreased 23% (n=9) lesion size. Lesions with increased size had enhancement patterns thought to be FNH and RN.
Conclusions: CEUS of the liver can complement or supplant CT and MRI thereby reducing radiation exposure and sedation. Further experience will refine the role of CEUS in the imaging algorithm for the pediatric liver.

Paper #: 080
Coronary artery assessment in pediatric patients using ultrafast ECG gated CT: Is this a viable alternative to prospectively gated technique?

LaDonna Malone, MD[1], *ladonnamalone@hotmail.com*; Andrew Mong, MD[1], Jason Weinman, MD[1], John Hughes[1], Andrew Olson[1], Lorna Browne[1]; [1]University of Colorado, Aurora, CO

Disclosures: All authors have disclosed no financial interests, arrangements or affiliations in the context of this activity.

Purpose or Case Report: Previous studies have demonstrated that pediatric coronary arteries can be adequately evaluated using a prospectively gated "step and shoot" technique. This technique acquires data during a fixed portion of the R-R interval over 3-5 heart beats with considerably lower radiation doses than the traditional retrospective method. Further advances in dual source CT, allow an ultrafast prospectively ECG triggered high pitch acquisition of the entire heart during a single heart beat with a sub-millisievert effective radiation dose. This technique has been shown to provide excellent coronary detail in adults with heart rates <65bpm, however its performance in children with higher heart rates is unknown. The purpose of this study was to evaluate if this gated ultrafast acquisition could be used to evaluate the proximal coronary arteries in children.

Methods & Materials: In this retrospective IRB approved study, the radiology database was searched for patients who underwent a clinically indicated prospectively ECG-triggered high-pitch dual-source CT between 2014 and 2016. Patients ≥18 years were excluded. The following data from the CT was recorded: age, sex, BSA, indication, average heart rate (HR), DLP, and CTDI vol. Images were then blindly assessed by two independent readers for overall image quality and quality of visualization of the proximal right and left coronary arteries using previously validated criteria. Interobserver variability and multivariate statistical analysis was performed.
Results: 100 scans were assessed (age range: 1 day to 18 y, median 0.26 y), 58 males and 42 females. Mean DLP: 18.6 mGy-cm, mean CTDIvol:0.61 mGy, mean effective radiation dose: 0.7 mSv. There was moderate interobserver agreement, Krippendorff's α= 0.49. When multivariate analysis was performed, only HR remained significant predictor of image quality ($p<0.001$). When HR ≤ 100bpm, image quality was adequate for coronary artery evaluation in 93% of cases compared to 66% for HR >100. Sub analysis of patients with HR >100bpm, showed when the BSA was ≥0.4 m2, coronary arteries were adequately visualized in 83% of cases.
Conclusions: In pediatric patients with heart rates < 100bpm, ultrafast prospective ECG-triggered high-pitch CT can routinely provide diagnostic quality imaging of the proximal coronary arteries with a sub-millisievert effective dose and may be considered in patients with even faster heart rates when the BSA ≥ 0.4m2.

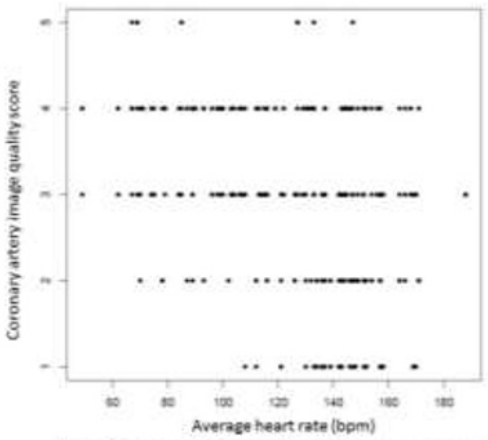

Figure 3: Scatter plot of average heart rate versus coronary artery image quality score.

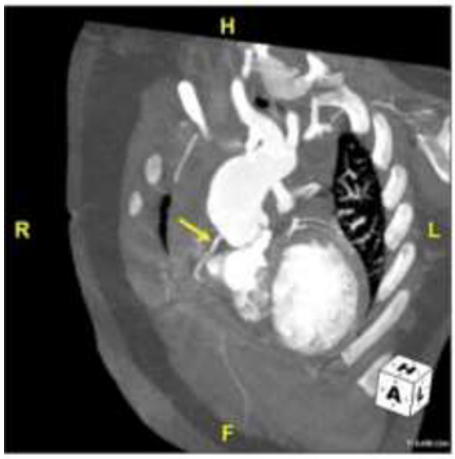

Figure 1: Sagittal oblique MIP image showing right coronary artery origin and proximal course (arrow) in a 20 month old male with HR 116 and BSA 0.54.

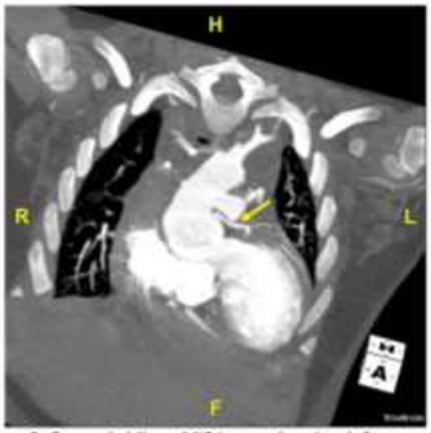

Figure 2: Coronal oblique MIP image showing left coronary artery origin and proximal course of LAD (arrow) in a 20 month old male with HR 116 and BSA 0.54.

Paper #: 081

Depiction of the Native Coronary Arteries during ECG-triggered high-pitch spiral Dual-Source Cardiac CTA in Children: Determinants of Image Quality

Christian Barrera, MD[1], *barreracac@email.chop.edu*; Hansel Otero, MD[1], Ammie White[1], David Saul, MD[1], David Biko, MD[1]; [1]Radiology, The Children's Hospital of Philadelphia, Philadelphia, PA

Disclosures: All authors have disclosed no financial interests, arrangements or affiliations in the context of this activity.

Purpose or Case Report: To determine the image quality and performance of Dual Source CT with ECG-triggered high-pitch spiral acquisition (Cardiac Flash) for the evaluation of native coronaries in children.
Methods & Materials: We identified all children with normal cardiac anatomy that underwent Cardiac Flash CTA between 8/2014 and 8/2017. Demographics, CT parameters, and medical history were obtained from the medical record. Two pediatric radiologist blinded to clinical data independently reviewed each case, determined coronary arteries origin and assigned a quality score for the origin and proximal segment of the right, left main, left anterior descending and proximal segment of the circumflex

coronary arteries (American Heart Association coronary segments 1, 2, 5, 6, and 11) following a four-point scale: 1-excellent, no artifact; 2-good, mild artifact; 3-acceptable, moderate artifact present but images still interpretable, 4-unevaluable, severe artifact renders interpretation not possible. The inter-observer agreement was evaluated with kappa. Scores of 0.41-0.60, 0.61-0.80 and ≥0.80 were regarded to be indicative of moderate, good, and excellent agreement, respectively. Analysis included Kruskal-Wallis test to examine whether our continuous variables predicted image quality.
Results: A total of 49 patients (26 boys) were selected. Patient data overview is summarized in Table 1. There were 43 (88%) patients with normal coronaries, 4 (8%) with anomalous, one (2%) with a normal variant and one (2%) indeterminate due to severe artifacts. 56 (23%) segments had excellent quality and 88 (36%) had mild artifact with overall worse scores in segments 1, 2 and 11. Out of all 245 segments, only 4.1% (10/245) were deemed unevaluable. Inter-observer agreement was moderate for all segments except for segment 1, which was excellent (Table 2). Worse quality scores were significantly associated with lower age, height, weight, BSA, and contrast injection rate as well as with higher heart rates in all segments ($ps<0.05$). The mean heart rate for excellent quality was 72.1 ± 23.7 (CI 95% 66.1-78.1), 99.2 ± 28.4 (CI 95% 93.5-104.9) for good,126.3 ± 40.1 (CI 95% 117.2-135.4) for acceptable, and 188.8 ± 66.1 (CI 95% 147.8-229.8) for poor quality.
Conclusions: ECG-triggered high-pitch spiral Dual-Source cardiac CTA allows for the evaluation of the origin of the coronaries in children with a low radiation dose. However, artifacts are common and more severe in smaller children and children with heart rates over 100 bpm.

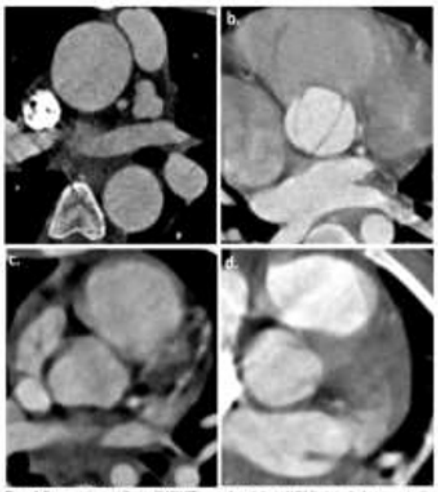

Figure 1. Representative axial Cardiac FLASH CT images through the mid-LCA illustrates the four image quality scores. 1 – Excellent, no artifacts (a); 2 – Good, mild artifact (b); 3 – Acceptable, moderate artifact present but images still interpretable (c); 4 – Unevaluable, severe artifact render interpretation, not possible (d)

Table 1. Patient data overview

Variable (N = 49)	Results (mean ± SD, range)
Age (years)	7.18 ± 7.02 (0 – 20)
Gender	Female 23, Male 26
Height (cm)	110.19 ± 47.71 (43.5 – 185.0)
Weight (kg)	29.86 ± 26.26 (2.3 – 82)
BMI (kg/m^2)	18.67 ± 4.56 (11.88 – 29.06)
BSA (m^2)	0.93 ± 0.62 (0.17 – 1.98)
Radiation dose (mSv)	1.82 ± 1.04 (0.3 – 4.7)
Heart rate at exam (bpm)	104.94 ± 42.38 (51 – 285)
Study indication	
Follow-up	21
Anatomy assessment	15
Hypoxemia or dyspnea	8
Preoperative evaluation	3
Chest pain	2

Table 2. Distribution of mean scores for overall image quality stratified by coronary segment

Segment (N = 245)	Results (median ± SD, 95% CI)	*Kappa* score†
Segment 1	2 ± 0.86, 2.02 – 2.23	0.81
Segment 2	2 ± 0.84, 2.30 – 2.51	0.73
Segment 5	2 ± 0.78, 1.72 – 1.91	0.66
Segment 6	2 ± 0.85, 1.91 – 2.13	0.72
Segment 11	2 ± 0.82, 2.10 – 2.31	0.71

Note: †Kappa with Linear Weighting

Paper #: 082

Myocardial bridging in a cohort of pediatric patients with anomalous aortic origin of coronary artery (AAOCA): "Double whammy"!

Prakash Masand, MD[2], *drmasand@gmail.com*; Siddharth Jadhav, MD[2], Hitesh Agrawal, MD[1], Cory Noel, MD[1], Carlos Mery[1], Silvana Molossi[1]; [1]Baylor College of Medicine, Houston, TX, [2]Texas Children's Hospital, Houston, TX

Disclosures: All authors have disclosed no financial interests, arrangements or affiliations in the context of this activity.

Purpose or Case Report: The incidence of myocardial bridging (MB) varies depending on the imaging modality utilized for coronary artery imaging. It is defined as a coronary artery coursing within the myocardium, completely surrounded by cardiac muscle fibres instead of along the epicardial surface. Computed Tomographic Angiography (CTA) is the most widely used non-invasive imaging test to diagnose this condition. Although usually silent, it can lead to myocardial ischemia, arrhythmias and even sudden cardiac death. We sought to determine the incidence of MB in a cohort of pediatric patients undergoing CTA for coronary anomaly evaluation.
Methods & Materials: The study was designed as a prospective evaluation following protocol IRB approval. We performed 184 CTAs for AAOCA using a uniform algorithm from 12/2012 to 02/2017. All the CTAs were performed without sedation, on a 320-detector volume CT scanner, with retrospective ECG gating. No pharmacologic agents were used to lower the heart rate. All exams were performed with iodinated contrast, administered via a peripheral extremity line. All exams were timed to the descending thoracic aorta, using a manual bolus track technique to achieve optimal left heart opacification. Dedicated 3-Dimensional post processing was performed on a separate workstation.
Results: A total of 184 patients underwent CTA with 27 (15 %) positive for MB (16 males, 59%): 17 with AAOCA and MB (63%) and 10 with MB (37%) only. The median age was 12.4 (4-16.6) yrs, with 13 (48%) presenting as an incidental finding, 6 (22%) with exertional symptoms (5 with syncope), 6 (22%) with non-exertional symptoms, and 2 (8%) with signs of myocardial ischemia . The median length for MB on CTA was 25 mm (range of 15-30 mm) with the left anterior descending coronary artery being the commonest affected vessel. 12 patients underwent cardiac catheterization with 6 exhibiting positive fractional flow reserve (FFR). Of these 5 have undergone surgery with 4 patients receiving unroofing of the MB segment and 1 undergoing bypass graft**.**
Conclusions: MB is often diagnosed in a pediatric patient undergoing coronary CTA for investigating an anomaly. In this prospective evaluation of pediatric patients, MB involving a coronary artery was diagnosed in 15% of patients. We saw a high co-incidence of AAOCA and MB (63%), which had a direct impact on patient management. As pediatric radiologists we need to be aware that AAOCA and MB often coexist.

Paper #: 083

Coronary artery imaging in Kawasaki disease with Computed Tomography Angiography and Echocardiography, a comparative analysis

Clara L Ortiz-Neira, MD[1], *claraneira@shaw.ca*; Siddharth Jadhav, MD[1], Snehal More, MD[2], Wei Zhang, PhD[1], Maddy Artunduaga[1], Pamela Ketwaroo[1], Prakash Masand, MD[1]; [1]Texas Children's Hospital, Houston, TX, [2]vRad, Eden Prairie, MN

Disclosures: All authors have disclosed no financial interests, arrangements or affiliations in the context of this activity.

Purpose or Case Report: Kawasaki disease (KD) is an acute febrile vasculitis of unknown origin. During the acute phase, patients can develop coronary artery aneurysms that need characterization and follow up to evaluate treatment response. Determination of location, size and complications is particularly important to guide treatment. Due to the need for imaging follow-up, non-invasive imaging modalities are preferred. This study compares coronary CT Angiography (CTA) and echocardiography in the evaluation of coronary artery disease in KD.

Methods & Materials: This was a retrospective evaluation of patients with clinical diagnosis of KD over a 5 year period beginning in January 2012. A total of 67 patients with both CTA and echocardiography were identified. Only patients that had CTA within 6 weeks of the echocardiogram were included. All CTA studies were performed on a 320 detector Toshiba Aquilion One volume scanner with retrospective EKG gating. Echocardiography was performed in the cardiology echo lab, and a pediatric cardiologist interpreted each exam. The echocardiographic coronary artery measurements were documented and compared with corresponding measurements on CTA. The presence and location of coronary artery aneurysms was recorded. To determine aneurysmal dilatation on CT, in addition to z-score (echocardiography based) extrapolation, we compared the size of the dilated segment to the native apparently normal coronary artery segment.

Results: 45 patients met the inclusion criteria. 30 patients were male (67%) with a mean age of 6.4 +/- 6 years and median age of 4.3 years at the time of imaging (Table 1). Wilcoxon signed rank test was applied to compare the echocardiographic and CTA measurements. Coronary artery measurements showed a statistical difference in the left main coronary artery, proximal left anterior descending (LAD) and distal right coronary artery (RCA) (Table 1, Figure 1). CTA detected a total of 63 aneurysms as compared to 53 on echocardiography. Echocardiography missed 2 aneurysms each in the proximal LAD, mid RCA and distal RCA, and one aneurysm each in the proximal RCA, proximal circumflex, mid LAD, and conal branch. The aneurysm missed in the proximal RCA was heavily calcified on CTA.

Conclusions: CTA is complementary to echocardiography in evaluation of coronary arteries in the setting of Kawasaki disease, especially the distal course. In patients with known distal coronary artery involvement CTA should be considered for follow-up.

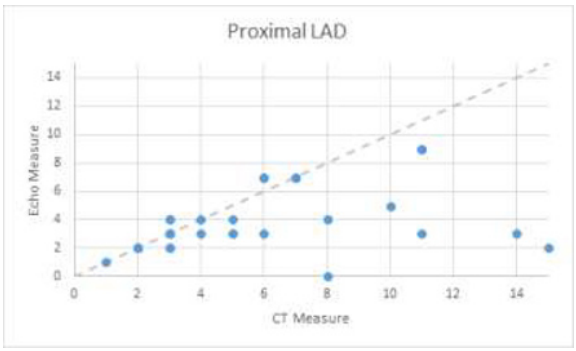

Table 1. Patient age (years) and coronary artery measurements (mm) on CTA and Echocardiography

	CT			ECHO			
Label	**N**	**Mean ± SD**	**Min/Median/Max**	**N**	**Mean ± SD**	**Min/Median/Max**	**P-Value**
Age at Exam (years)	45	6.41 ± 6.17	0.33/4.33/28.6	45	6.42 ± 6.17	0.10/4.31/28.4	0.7551
Left Main Coronary Artery	30	3.3 ± 1.26	2/3/6	30	3.83 ± 1.42	2/4/7	0.8306
Proximal LAD	31	5.1 ± 3.42	1/4/14	31	3.81 ± 2.14	1/3/9	0.0044
Mid LAD	21	3.86 ± 4.19	1/2/18	21	3.9 ± 3.33	1/3/14	0.8700
Proximal Circumflex	27	3.11 ± 1.83	1/2/9	27	2.89 ± 1.37	1/3/8	0.5562
Right Main Coronary Artery Origin	20	3.05 ± 1.23	1/3/6	20	3.2 ± 1.51	1/3/7	0.7512
Proximal Right Coronary Artery	29	3.03 ± 4.17	1/4/21	29	3.79 ± 2.14	1/4/12	0.1037
Mid Right Coronary Artery	13	5.62 ± 3.27	1/3/21	13	6 ± 5.51	1/4/20	0.8191
Distal Right Coronary Artery	21	3.38 ± 3.28	1/2/13	21	4.48 ± 3.18	1/4/14	0.0110

Paper #: 084

Delayed Myocardial Enhancement in Children: Comparison of Conventional Technique to a Free Breathing Single-Shot Technique in Duchenne Muscular Dystrophy

Dor Markush[1], *Dor.Markush@nationwidechildrens.org*; Sanmit Basu[1], Ramkumar Krishnamurthy, PhD[1], John Kovalchin[1], Lucy Hackman[1], Ross Edward[1], Kan Hor, MD[1], Rajesh Krishnamurthy[1]; [1]Nationwide Children's Hospital, Columbus, OH

Disclosures: Kan Hor has indicated a relationship with Medtronics and Capricor as a consultant/honoraria. All other authors have disclosed no financial interests, arrangements or affiliations in the context of this activity.

Purpose or Case Report: Delayed myocardial enhancement (DME) is a well-established method to assess myocardial fibrosis. In the pediatric population, utilization of the traditional segmented fast gradient echo inversion recovery technique (IR-GRE) is often limited by inability to breath-hold due to its long acquisition over several heartbeats. Single shot imaging (SS-GRE), wherein a slice is imaged in a single heartbeat, may overcome this limitation. However, establishment of utility and comparison to traditional DME methods is lacking in the pediatric population. We sought to evaluate the feasibility of using free-breathing (FB) SS-GRE for DME evaluation in a population with Duchenne muscular dystrophy (DMD), and to compare it with conventional breath-held (BH) IR-GRE technique.

Methods & Materials: Cardiovascular magnetic resonance imaging studies from fifteen consecutive patients with DMD imaged from August 2017 to October 2017 were retrospectively analyzed. All subjects were scanned with both BH IR-GRE and FB SS-GRE sequences in the short-axis plane, 6-10 minutes after Gadavist injection to assess for presence of DME. IR-GRE slices were acquired over 8-10 heart beats (~50 ms per heartbeat), while SS-GRE slices were acquired in one heartbeat (~250 ms). Both sequences had a spatial resolution of 1.8x1.8x8 mm^3. Image quality was evaluated in blinded fashion by two independent readers using a Likert scale scoring system of 1-5 (1= non-diagnostic, 5= excellent), and the presence of DME was

similarly assessed. Wilcoxon Rank-sum tests were used to compare the two sequences.
Results: Mean (±SD) age of our sample was 14.1 (±5) years, BSA 1.4 (±0.3) m^2, heart rate of 95 (±13) bpm, and left ventricular ejection fraction of 59 (±6) %. Compared to conventional IR-GRE technique, SS-GRE exhibited comparable image quality (reader 1: mean 3.8 vs. IR-GRE 3.8; p=0.76, reader 2: mean 4.0 vs IR-GRE 3.7; p = 0.29), and similar scar characterization ability (reader 1: mean 3.4 vs IR-GRE 3.5; p=0.59, reader 2: mean 3.9 vs IR-GRE 3.4; p = 0.16). Overall, between both readers, blinded analysis of the IR-GRE and SS-GRE sequences produced concordant results in 28/30 (93%) cases, and assessment of scarring was concordant in all 5/5 positive DME patients.
Conclusions: Free-breathing SS-GRE provides comparable imaging quality and scar detection ability when compared to IR-GRE. Benefits of SS-GRE include improved scan efficiency and respiratory motion compensation with FB acquisition compared to IR-GRE.

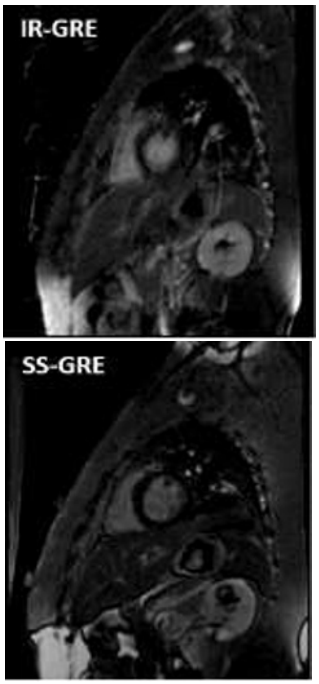

Paper #: 085

Association of T2 Lymphatic Imaging in Single Ventricle Patients After Superior Cavopulmonary Connection with Acute Post-Fontan Outcomes

David Biko, MD[1], *bikod@email.chop.edu*; Aaron Dewitt, MD[1], Erin Pinto, NP[1], Jordan Johnstone[1], Heather Griffis, PhD[1], Michael O'Byrne, MD[1], Mark Fogel, MD[1], Matthew Harris, MD[1], Sara Partington, MD[1], Kevin Whitehead, MD, PhD[1], David Saul, MD[1], David Goldberg[1], Jack Rychik[1], Andrew Glatz, MD[1], Matthew Gillespie, MD[1], Jonathan Rome, MD[1], Yoav Dori[1]; [1]Department of Radiology, The Children's Hospital of Philadelphia, Philadelphia, PA

Disclosures: All authors have disclosed no financial interests, arrangements or affiliations in the context of this activity.

Purpose or Case Report: Despite improved survival, many patients after total cavopulmonary connection (TCPC) will develop end organ dysfunction including the lymphatic system. In this study, we aim to demonstrate that lymphatic imaging using a highly T2 weighted sequence in patients post superior cavopulmonary connection (SCPC) is associated with post TCPC outcomes.
Methods & Materials: A retrospective review of all patients with history of surgical palliation with SCPC who underwent magnetic resonance (MR) imaging with a three-dimensional (3D) T2 weighted Sampling Perfection with Application optimized Contrasts using different flip angle Evolution (SPACE) sequence. Images were scored, blinded to clinical outcomes, based on the location of increased T2 signal on a scale of 1 to 4. Type 1 was interpreted as little or no increased T2 signal, type 2 as increased T2 signal within the supraclavicular region only, type 3 as supraclavicular T2 signal with extension into the mediastinum, and type 4 as supraclavicular T2 signal with extension into both the mediastinum and interstitium of the lung. The medical record was reviewed for the rate of TCPC completion, TCPC take-down, duration of post TCPC hospitalization and pleural effusion, postoperative diagnosis of plastic bronchitis, need for transplant, and mortality.
Results: A total of 83 subjects were identified. 64% of the subjects (n=53) were classified as type 1 or 2, 20% (n=17) were classified as type 3, and 16% (n=13) were classified as type 4. Failure of TCPC completion ($p<0.001$) was significantly higher in type 4, need for cardiac transplant (p=0.023), and mortality ($p<0.001$) were only present in type 4. Duration of effusions ($p<0.001$) and postoperative length of stay ($p<0.001$) were longer in type 4. When comparing type 3 and type 4 abnormalities, type 4 subjects demonstrated higher mortality (p=0.009) and lower rate of TCPC completion (p=0.009). The only 2 patients in the cohort to develop plastic bronchitis were type 4.
Conclusions: T2 weighted 3D SPACE imaging is a non-invasive tool for screening patients prior to TCPC which can be performed in conjunction with a cardiac MRI demonstrating a strong correlation with TCPC outcomes.

Paper #: 086

Aortic Disease in Patients with Mucopolysaccharidosis

Joseph Davis, MD[1], *joseph.davis@duke.edu*; Joseph Mammarappallil, MD, PhD[1], Gary Schooler, MD[1]; [1]Department of Radiology, Duke University, Durham, NC

Disclosures: All authors have disclosed no financial interests, arrangements or affiliations in the context of this activity.

Purpose or Case Report: Mucopolysaccharidosis (MPS) is a subset of lysosomal storage disease in which enzyme function necessary to break down glycosaminoglycans is insufficient to prevent these long chain carbohydrates from depositing in body tissues. The osseous, neurologic, and cardiac manifestations of MPS are well documented. Less well documented is deposition in large vessels, with only case reports and one series of eight cases reported in the literature. The purpose of this study is to determine the incidence of large vessel (specifically aortic) disease in patients with MPS.
Methods & Materials: An IRB-approved retrospective study was performed. A searchable electronic medical record database was used to identify all patients with MPS at our institution - a MPS referral and treatment center - within the timeframe of electronic record-keeping. All MPS patients on whom contrast enhanced CT (CECT) of the body (chest and/or abdomen/pelvis) was performed were identified and that imaging reviewed by two board certified radiologists for abnormal thickening (defined as > 1mm wall thickness) of the aortic wall. Demographic information including age at time of imaging, gender, and subtype of MPS was recorded.

Results: A total of 195 patients were identified, of which 69 (35%) had undergone CECT, with 30 (43%) demonstrating aortic wall thickness greater than 1 mm (see attached figures for representative examples). The average aortic wall thickness in these patients was 2.4 mm; 53% of those affected were male, 47% female (of those unaffected, 62% were male and 38% female). Median age at time of imaging for those with aortic disease is 1 year 2 months; median age at time of imaging for those without is 3 years 1 month. Twenty-eight (93%) of the patients with aortic disease had the Hurler subtype of MPS (MPS I). Thirteen (33%) of those unaffected had MPS I, 9 (23%) had Hunter (MPS II), 15 (38%) had Sanfilippo (MPS III), and 2 (5%) had Morquio (MPS IV).
Conclusions: In patients with MPS, deposition disease in the aorta is much less well documented than coronary involvement, but in this series (to the best of our knowledge the largest yet done) 43% of patients with CECT body imaging demonstrate some degree of aortic deposition disease. Those with large vessel involvement tend to be of the more severe MPS subtype, and demonstrate aortic changes at a young age. Attention to the aorta during routine cross sectional imaging of these patients may be helpful in early recognition of vascular disease and in direction of treatment.

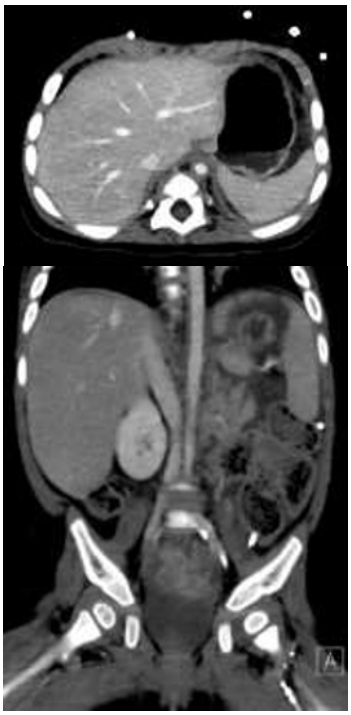

Paper #: 087

Assessing Pediatric Fluoroscopy Radiation Dose Awareness amongst Clinicians

Priya Sharma, MD[1], *priya.sharmamd@gmail.com*; Dhanashree Rajderkar, MD[1]; [1]University of Florida, Gainesville, FL

Disclosures: Priya Sharma has indicated a relationship with the Association for Medical Imaging Management and Toshiba Medical for receiving a research grant. Dhanashree Rajderkar has indicated a relationship with the Association for Medical Imaging Management and Toshiba Medical for receiving a research grant. All other authors have disclosed no financial interests, arrangements or affliliations in the context of this activity.

Purpose or Case Report: Although computed tomography and interventional procedures are known high dose radiological examinations, fluoroscopic exams are overlooked in their contribution to patient radiation dose. Fluoroscopic exams are often misperceived as being equivalent in dose to an x-ray. Clinicians are unaware that these exams consist of multiple images and are operator dependent in the amount of dose administered. Furthermore, clinicians are unaware of the doses administered and dose reduction campaigns.
The purpose of this study is to assess referring clinician knowledge before and after an educational session addressing pediatric radiation dose, dose awareness campaigns and the performance of fluoroscopic examinations.
Methods & Materials: A voluntary 12- question multiple-choice examination, covering topics of pediatric fluoroscopic examinations, radiation dose exposure, and dose awareness campaigns was given to pediatric residents, fellows and faculty from the Department of Pediatrics at our institution. The residents, fellows and attendings were then given a one-hour long education session. The same test was given to the subjects after the education session to assess knowledge gained. A student's independent sample t-test was used to compare the pre- and post-test scores.
Results: A total of 30 participants completed the pretest examination resulting in an average score of 5.67/12. The highest score achieved on the pre-test was 11/12. Only 23 participants completed the post-test examination resulting in an average score of 9.78/12. Of the 23 post -test participants, only 2 achieved a perfect score. Student t- test revealed a statistically significant increase in knowledge points after the educational session.
Conclusions: This project revealed clinical gaps of knowledge in regards to fluoroscopy in the pediatric population as well as pediatric dose awareness campaigns. In fact, only 8 out of 30 pediatric clinicians were aware of the "Imaging Gently" campaign. Lack of knowledge in set up of the fluoroscopic suite and amount of radiation administered during these exams also revealed that clinicians were not aware of how these exams are performed. However, it was determined that an educational session is effective in increasing overall awareness of radiation, dose administered and dose reduction campaigns amongst pediatric clinicians in regards to pediatric fluoroscopy. It is our hope that radiation dose awareness amongst clinicians will result in reduced overall radiation exposure in the pediatric population.

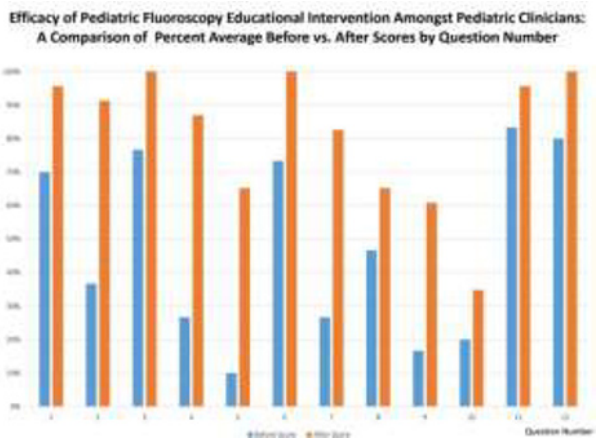

Paper #: 088

Reduced-Dose Radiography Protocol for Focused Assessment of Feeding Tube Position

Summer Kaplan, MD MS[1], *kaplans2@email.chop.edu*; Colleen Flowers[1], Sharon Irving[1], Jackie Crawford[1], Richard Lin[1], Laura Schleelein[1], Ann Johnson[1], Sudha Anupindi, MD[1], Ammie White, MD[1], Xiaowei Zhu[1]; [1]Radiology, The Children's Hospital of Philadelphia, Philadelphia, PA

Disclosures: All authors have disclosed no financial interests, arrangements or affiliations in the context of this activity.

Purpose or Case Report: Placement of a transesophageal feeding tube is a routine procedure for inpatients. Rarely, malpositioning in the airway may result in feeds being delivered into the lung, a critical adverse event. Radiography (XR) is the most accurate way to check feeding tube position, but its use is not standard. Care providers may be reluctant to order XR due to concern over radiation or uncertainly about which exam to order. Because the radiopaque tip of feeding tubes used at our institution is easily visualized under lower dose conditions, we developed a reduced dose and limited field of view XR protocol for focused evaluation of feeding tube placement.
Methods & Materials: This work was conducted as a quality improvement project. We identified the area of interest as being between the mid-chest and iliac crests. For each age group, we maintained standard kV and set mAs as low as possible. Three reviewers assessed visibility of a Corpak Viasys 6 French feeding tube at the lower limits of mAs in anthropomorphic phantoms. We then began 2 weeks of monitored clinical use in the pediatric intensive care unit. For each age-based XR protocol, we compared kV, mAs, and exposure index (EI) for the new protocol to the most recent abdomen XR in an index patient. Three radiologists assessed tip visibility, tip location, and image quality. Image quality was defined as routine diagnostic, somewhat limited, very limited, or non-diagnostic.
Results: Tip of the feeding tube was visible at the lowest mAs setting in all phantoms. During our 2-week monitoring period, 14 exams were performed. Age groups examined were 0 - 6-months (group 1), 6-months - 2-years (group 2), and 6 - 10-years (group 3), the majority in group 2. For an index patient in group 1, mAs was reduced by 66% and EI by 81%, while reviewers rated tip visible, location identifiable, and image quality "routine diagnostic". Group 2 results were the same as group 2, except image quality was "somewhat limited". In Group 3, mAs decreased by 71% and EI by 87%, while tube tip remained visible, location identifiable, and image quality "somewhat limited".
Conclusions: We show that focused evaluation of feeding tube tip location is possible using 66 - 71% lower mAs and EI reduction of 81 - 87%. Further protocol development will focus on statistical population doses, wider age range, and tabletop technique. Our preliminary work offers clinicians a simple, low-risk method for verifying tube placement, reducing barriers to safe feeding tube use.

Paper #: 089

Stochastic Noise Tolerance in Pediatric Appendicitis CT

Steven Don, MD[1], *dons@mir.wustl.edu*; David Politte, D.Sc.[1], Ruth Holdener, R.T.R. (CT)(M)[1], Ayan Mitra, PhD[1], Craig Abbey, PhD[2], Bruce Whiting, PhD[3]; [1]Washington University, St. Louis, MO, [2]University of California, Santa Barbara, Santa Barbara, CA, [3]University of Pittsburgh Medical Center, Pittsburgh, PA

Disclosures: Steven Don has indicated a relationship with Vantage Medical Imaging as a Co-founder. Craig Abbey has indicated a relationship with Toshiba Medical Research Corporation as a consultant. All other authors have disclosed no financial interests, arrangements or affiliations in the context of this activity.

Purpose or Case Report: To determine the magnitude of stochastic noise in CT images of the appendix and estimate how much dose reduction could be tolerated in such images.
Methods & Materials: Traditional method of measuring noise using a uniform region of interest does not work with non-uniform anatomical structures. An ensemble of reconstructed image simulations created a CT stochastic noise map. 136 CTs performed in children 18 years or younger, 74 cases without appendicitis and 62 non-perforated appendicitis cases, acquired on Siemens Sensation 16, AS 64, or Flash scanners, were used for image simulation based on 1 mm thick slices. 4 observers (2 pediatric radiologists, an abdominal fellow and attending) reviewed the images in the axial and coronal planes, and then marked the appendix on the best axial image. They rated the likelihood for appendicitis on a 6-point scale (1-definitely normal to 6-definitely appendicitis) and the visualization of the appendix (1-well-visualized to 6-obscured). ROC curves were created for the diagnostic accuracy. Then, using a sliding scale, they changed the amount of noise in the study, adjusting it until diagnostic confidence decreased (Fig 1). Marked appendix region stochastic noise was calculated at baseline and toleration level (Fig 2).
Results: ROC curves were high for all observers (0.95-0.96 AUC). Mean base noise for normal exams was 6.75 Hounsfield Units (HU) (0.19 [Standard Deviation HU]) and appendicitis was 6.94 HU (0.19) (Table 1). Noise tolerance for normal exams was 14.67 HU (0.18) and appendicitis was 13.91 HU (1.05), an increase of 2.17 and 2.00 respectively, or 75% dose reduction. The noise tolerance for cases ranked 1-2, definitely or probably normal, was 2.19, for 3-4, possibly normal or appendicitis was 1.80, and for 5-6, probably or definitely appendicitis was 2.01. The easy to visualize appendixes noise tolerance was 2.15, appendixes that needed coronal images to confirm was 1.85, and appendixes that were difficult or obscured was 1.80.
Conclusions: High ROC results are similar to published studies. Baseline appendix region stochastic noise was nominally 6.75 HU. The 2-fold noise tolerated by observers suggests a dose reduction potential of 75%. Easier to diagnose or visualize cases tolerated more noise than borderline diagnostic or difficult to visualize cases, indicating the need for challenging cases to avoid overestimating dose-reduction potential. These findings will be used to set the noise ranges to be tested in future dose simulation studies to achieve ALARA.

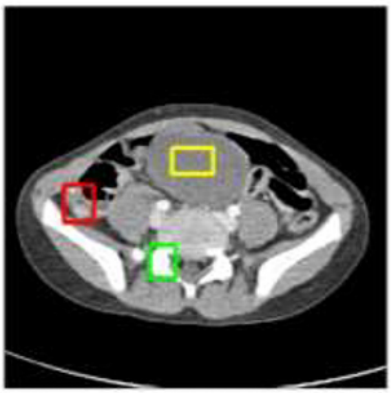

Fig 1. The image at the tolerated noise level of a 26 kg, 8 year-old male patient with appendicitis. The red box marks the appendix. Other regions of interest (ROI) include the bladder (yellow box) and pedicle (green box). In the uniform bladder region, where one typically measures noise in a CT image, the standard deviation (std) is 19 Hounsfield Units (HU), but anatomy in appendix and pedicle ROI's result in std's of 294 HU and 332 HU, respectively, overwhelming the stochastic noise component.

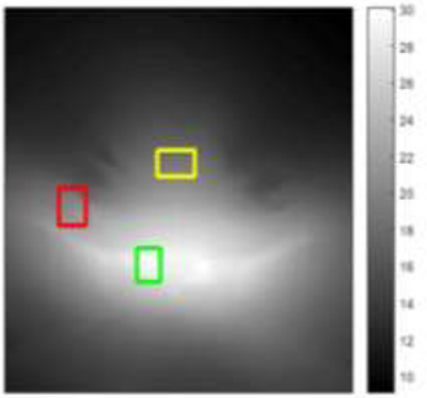

Fig 2. Stochastic noise map. The scale on the right indicates the magnitude of stochastic noise in HU at the tolerated level. In the uniform bladder (yellow box), the stochastic noise map measurement (19 HU) matches ROI std, as expected based on ergodicity. In the appendix region (red box), the stochastic noise map measurement is 20.4 HU (compared to Fig. 1 measured ROI std of 294 HU) while the pedicle region stochastic noise map measurement is 28 HU (compared to Fig. 1 measured ROI std of 332 HU). Thus, the stochastic noise in a local anatomic region can be estimated, rather than relying on noise estimates from a uniform region such as bladder or vessel, providing better estimates of noise toleration.

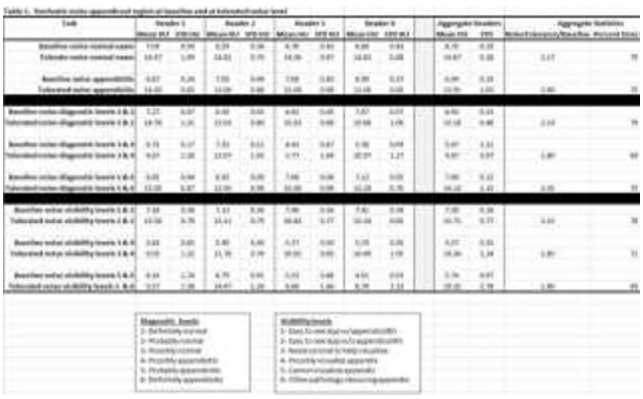

Paper #: 090

Knowledge-Based Iterative Reconstruction verses Filtered-Back Reconstruction Head CT in Children Referred from the Emergency Department: Dose Reduction, Image Quality, and Image Reconstruction Time

Richard Southard, MD[1], *rsouthard@phoenixchildrens.com*; Lingyun Chen, phD[1], Marrit Thorkelson[1], Robyn Augustyn[1], Dianna Bardo, MD[1]; [1]Department of Medical Imaging, Phoenix Children's Hospital, Phoenix, AZ

Disclosures: Richard Southard has indicated a relationship with Philips Healthcare for consultant/ honoraria, speaking and receiving a research grant. Robyn Augustyn has indicated a relationship with Koninklijke Philips, NV as a consultant and a speaker. All other authors have disclosed no financial interests, arrangements or affiliations in the context of this activity.

Purpose or Case Report: Iterative Reconstruction (IR) provides superior noise suppression when compared to standard filter-back projection (FBP) reconstructed images and allows the use of lower-dose protocols for pediatric CT exams while maintaining image quality and Radiologist diagnostic confidence. Some pure IR platforms have a lengthy image reconstruction time which limits use in the acute setting of trauma. Knowledge-based IR (IMR) was installed on our CT scanner (Brilliance iCT 256, Philips Healthcare, Cleveland, OH) situated in the main department of our hospital. A second CT scanner (Brilliance 64) that does not have IR capability is situated in the emergency department (ED). We compared brain CTs referred from the emergency room imaged on both scanners for reconstruction times, image quality, radiation dose, and physician diagnostic confidence.

Methods & Materials: This retrospective, HIPAA compliant and IRB approved study included 400 consecutive patients imaged with standard age-based protocols (<1.5 years, 1.5-6 years, 7-12 years, >13 years) using FBP image reconstruction (Brilliance 64), or using new low dose protocols designed for use with IMR image reconstruction (iCT 256). Patients with repeat studies, scans with excessive motion, metallic implants, or when the incorrect age-based protocol was used were excluded (n=27). Regions of interest (ROI) were drawn on the right thalamus and the right frontal white matter of each scan, and signal-to-noise (SNR) and contrast-to-noise (CNR) ratios were calculated. Patient age and estimated radiation dose (CTDI) were recorded. Study reconstruction times were determined by comparing the image creation times of the first image and the last image reconstructed.

Results: A total of 173 patients were imaged in the ED using FBP and 190 children were imaged in the main department using IMR reconstruction. The average reconstruction time of cases performed with FBP was 100 seconds, and with IMR was148 seconds. CTDI was reduced in all 4 age groups (14.5%, 20.3%, 28.0% and 34.1%) using IMR protocols, while SNR and CNR both improved two-fold.

Conclusions: IMR knowledge-based iterative reconstruction allowed us to reduce radiation dose an average of 24% for children undergoing emergency head CT exams, with only minimal increase of study reconstruction times, while improving image quality SNR and CNR two-fold.

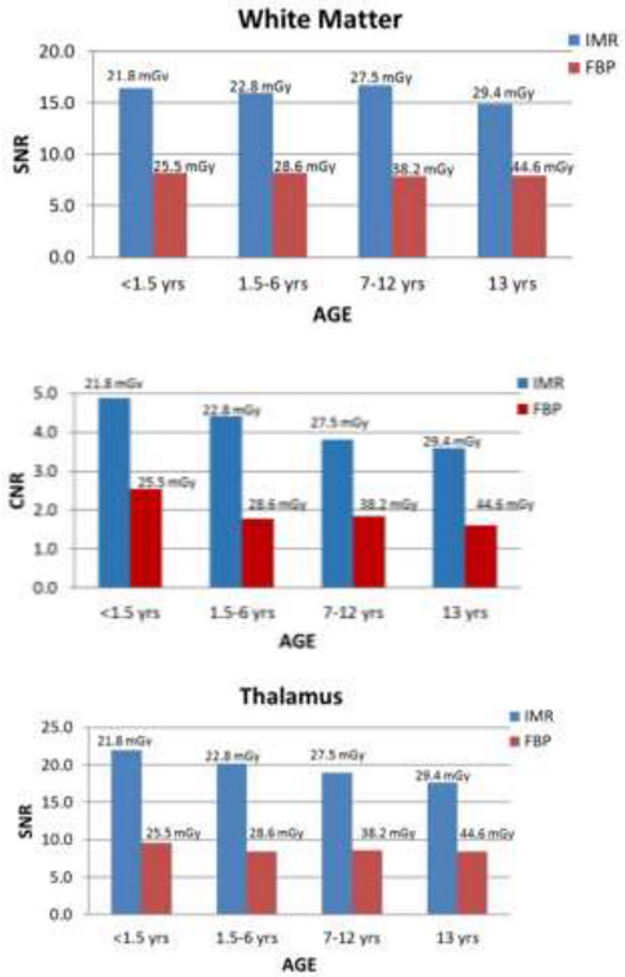

Paper #: 091

Development and Testing of an Innovative Simulation Paradigm for Subtle Liver Lesion Detection in Pediatric CT.

Jennifer Ngo, MD[1], *shafjl4@gmail.com*; Justin Solomon, PhD[1], Ehsan Samei[1], Taylor Richards[1], Lawrence Ngo, MD PhD[1], Brian Allen, MD[1], Joseph Davis, MD[1], Daniele Marin, MD[1], Charles Maxfield[1], Bhavik Patel, MD MBA[2], Gary Schooler, MD[1], Don Frush, MD[1]; [1]Radiology, Duke University Medical Center, Durham, NC, [2]Stanford Health Care, Stanford, CA

Disclosures: All authors have disclosed no financial interests, arrangements or affiliations in the context of this activity.

Purpose or Case Report: Investigations on impact of tube current (mA) reduction on detection of pediatric hepatic lesions have faced numerous obstacles including different phases of enhancement, lesion validity, exposure to additional radiation and the risk of a non-diagnostic exam. Our goal was to create a systematic, highly controlled observer performance paradigm for evaluation of simulated, subtle abnormalities (liver lesions) in pediatric CT affording creation of subtle lesions (truth), insertion of high fidelity noise (including texture) without additional radiation exposure, and an efficient and effective observer interface for study evaluation.

Methods & Materials: 30 normal pediatric (ages 0-10 yr) contrast-enhanced de-identified abdominal CT scans were retrospectively collected from the clinical database (IRB approved). 0-3 simulated anthropomorphic, low attenuation liver lesions (≤ 6mm) (Fig 1) were inserted into scans using proprietary LesionTool. Noise, validated as equivalent in magnitude and texture to reduced mA, was added to simulate reduced mA of 75% and 50% of the original scan. Three pediatric and three adult abdominal radiologists with 7-20 yrs of experience reviewed 90 data sets in 3 sessions spaced 2 weeks apart, e-marked the location of any lesions and rated their confidence using a scale of 0 to 100. Readers were surveyed after completion about the software interface.

Results: 83% (5/6) of readers felt the images were similar quality to diagnostic images and that the tools in the web interface were adequate. 100% of readers felt the interface was an efficient and effective method of recording lesion location and that the interface was easy to use. 67% of readers reported spending equal time per case compared to a reading room and 50% reported reviewing studies with an equal sensitivity as compared to their usual sensitivity. 33% felt that their sensitivity was higher and only 1 (16%) felt that sensitivity was lower than typical.

Conclusions: The existing validated simulation paradigm provides opportunity for evaluation of a wide variety (size, location, heterogeneity, attenuation; Fig 2) of lesions, risk-free dose reduction assessment and observer performance for pediatric CT. This paradigm allows a systematic, highly controlled evaluation of specific lesions with an efficient user interface. Tracking of response metrics, such as study review time, number of clicks and response location for accuracy, also allows for assessment of important performance metrics beyond simple detection.

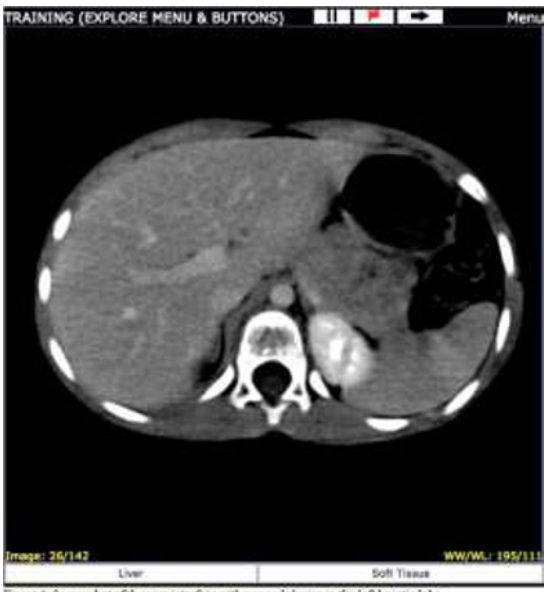

Figure 1: Screenshot of the user interface with a sample lesion in the left hepatic lobe.

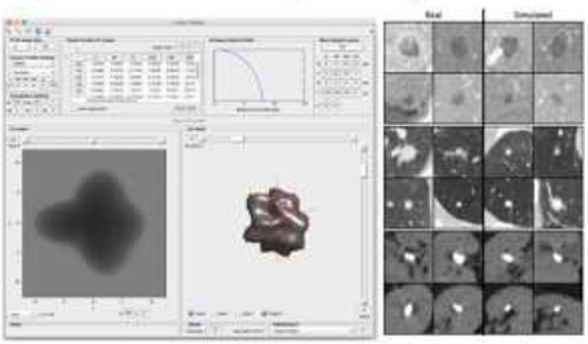

Figure 2: Screenshot of the lesion modeling tool (LesionTool, proprietary) and images of real versus simulated CT images of different lesion types (liver- top, lung- middle, and renal stones- bottom).

Paper #: 092

An Innovative Simulation Paradigm for Evaluation of Subtle Liver lesions in Pediatric CT: Performance and Confidence

Jennifer Ngo, MD[1], *shafjl4@gmail.com*; Justin Solomon, PhD[1], Ehsan Samei[1], Taylor Richards[1], Lawrence Ngo, MD PhD[1], Brian Allen, MD[1], Joseph Davis, MD[1], Daniele Marin, MD[1], Charles Maxfield[1], Bhavik Patel, MD MBA[2], Gary Schooler, MD[1], Don Frush, MD[1]; [1]Duke University Medical Center, Durham, NC, [2]Stanford Health Care, Stanford, CA

Disclosures: All authors have disclosed no financial interests, arrangements or affiliations in the context of this activity.

Purpose or Case Report: In the companion abstract, we described an innovative simulation paradigm and effective observer interface combining previously developed tools for systematic evaluation of CT dose reduction with subtle pediatric liver lesions. Our purpose was to test this paradigm to delineate the effect of dose reduction on diagnostic accuracy and reader confidence, the latter often minimized in importance.
Methods & Materials: 30 normal pediatric (ages 0-10 yr) contrast-enhanced de-identified abdominal CT scans were retrospectively collected from the clinical database (IRB approved). 0-3 simulated low-contrast liver lesions (≤ 6mm) were inserted using LesionTool (proprietary) and noise was added to simulate reduced tube current (mA) that was 75% and 50% that of the original scan. Three pediatric and three adult abdominal radiologists with 7-20 yrs of experience reviewed 90 data sets in 3 sessions and were asked to mark the location of lesions and rate their confidence on a scale of 0 to 100. Statistical analysis was performed using JMP Pro 13.
Results: Overall sensitivity was 38%, with significantly different sensitivities for 100%, 75% and 50% dose exams [52.8%, 35.5% and 24.7% respectively; $F(2,15)=26.92$, $p<0.0001$); Fig 1]. Sensitivity did not vary between pediatric and abdominal imagers ($p=0.34$). Average confidence per case significantly varied between the three dose levels [$F(2,415)=9.51$, $p=<0.0001$; Fig 2], with the mean confidence of the 100% and 75% dose exams varying significantly from the 50% dose exams ($p<0.001$), but not from one another ($p=0.994$). The number of clicks per study also varied significantly between the dose levels [$F(2,537) = 22.28$, $p=<0.0001$], with the number of clicks surprisingly decreasing as the noise level increased. There was no significant difference in the time to complete a case between the dose levels [$F(2,415) = 2.04$, $p=0.13$].
Conclusions: Academic pediatric and adult specialists did not differ in performance for subtle liver lesions. As expected, diagnostic accuracy significantly decreased as noise increased. However, confidence in the presence of a lesion did not change between the full dose and 75% dose scans. This suggests that readers are unaware of this decrease in performance, which should be accounted for in dose reduction efforts. Interestingly, higher noise studies did not take any longer to review, but the number of clicks decreased as noise increased, which may, in part, reflect less effort due to perceived decreased discrimination.

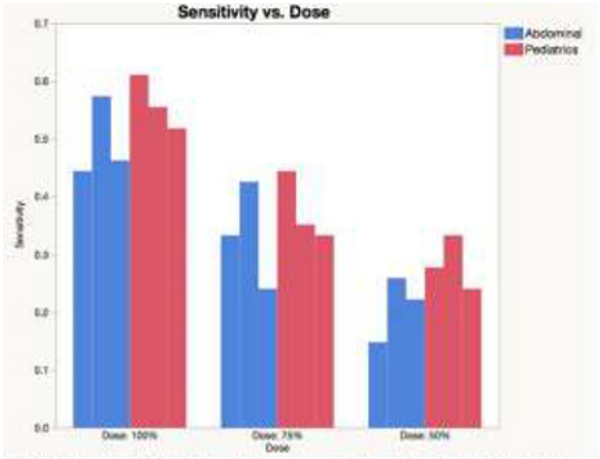

Fig 1: Reader sensitivity for liver lesions across all three dose levels with each bar representing a reader. The bars are color coded to denote pediatric versus abdominal imagers. As dose decreased, sensitivity also decreased.

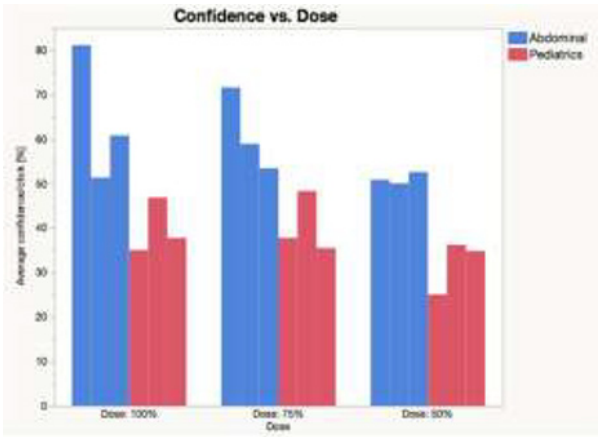

Fig 2: Confidence in the presence of liver lesions across all three dose levels with each bar representing a reader. The bars are color coded to denote pediatric versus abdominal imagers. Confidence was significantly lower in the 50% dose cases than the other dose levels, but was not different between the 75% and 100% dose levels.

Paper #: 093

Development of a tool to aid the radiologic technologist using augmented reality and computer vision

Robert MacDougall, MSc,
Robert.D.MacDougall@childrens.harvard.edu; Steven Don, MD[2], Benoit Scherrer, PhD[1]; [1]Radiology, Boston Children's Hospital, Boston, MA, [2]Mallinkrodt Institute of Radiology, St. Louis, MO

Disclosures: Steven Don has indicated a relationship with Vantage Medical Imaging as a Co-founder. All other authors have disclosed no financial interests, arrangements or affiliations in the context of this activity.

Purpose or Case Report: To describe the development of a novel device designed to aid the radiologic technologist in reducing exposure variation and repeat imaging in computed and digital radiography.

Methods & Materials: The device consists of four generic components: 1) a 3-D depth-sensing camera with high-resolution color video and infrared depth sensor, 2) a processing unit where all real-time computations are performed, 3) an application programming interface to communicate with the processing unit and 4) the user interface displayed on a control room monitor. A schematic of the system architecture and components is provided in Figure 1. Proprietary processing software was developed in C++ using the Qt, OpenCV and FFMPEG libraries to analyze, in real time, the color and depth video streams from the 3-D depth-sensing camera. The 3-D depth camera was mounted to the tube assembly housing of a Philips Digital Diagnost digital radiography system.
Results: The prototype device uses a Microsoft Kinect™ V2 consisting of a 1,080p color video and time-of-flight infrared depth sensor. An Intel NUC personal computer was used for the processing unit and the user interface was displayed on a 19.5″ HD touchscreen monitor. At start-up, the device requires calibration, which runs in less than 2 seconds and is fully automatic. A computer vision algorithm precisely localizes the imaging equipment via pattern matching of visual markers of the automatic exposure control chambers and image receptor. Once calibrated, the software calculates patient thickness and tracks in real time (15 fps) the patient positioning and patient motion. Motion estimation is achieved by assessing the position of the tracked body part or by using an optical flow algorithm. During the exam, the user interface displays real-time video of the patient along the central ray axis with overlays of automatic exposure control chambers, image receptor, body part thickness, patient skeleton tracking and motion tracer (Figure 2). The software is designed to alert the technologist when a problem arises, such as when the body part is not centered correctly on the detector or the patient has moved off the automatic exposure control chambers (Figure 3). Alerts can be visual, auditory, or both.
Conclusions: The device empowers the technologist by providing critical, real-time information to set the x-ray technique, enhance the workflow and to alert the technologist of issues that may result in repeat imaging before the patient is exposed.

**Work supported by the SPR Research and Education Foundation*

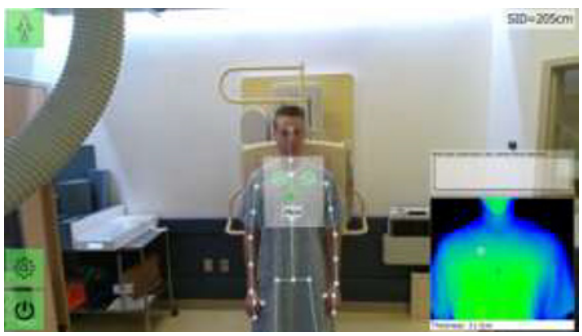

Paper #: 094

Multiparametric Liver MRI in Children and Young Adults with Autoimmune Liver Disease: Correlation between Quantitative Imaging Methods

Jonathan Dillman, MD, MSc[1], *jonathan.dillman@cchmc.org*; Suraj Serai, PhD[1], Andrew Trout[1], Alexander Miethke[1]; [1]Department of Radiology, Cincinnati Children's Hospital Medical Center, Cincinnati, OH

Disclosures: All authors have disclosed no financial interests, arrangements or affiliations in the context of this activity.

Purpose or Case Report: To assess correlations between quantitative MRI measures of chronic liver disease in a pediatric and young adult population.
Methods & Materials: 29 children and young adults with autoimmune liver disease (e.g., autoimmune hepatitis, sclerosing cholangitis) were enrolled in a prospective registry. Multiparametric MRI was performed on all subjects using a 1.5T imager (Ingenia; Philips Healthcare). Quantitative MRI sequences were performed through the mid liver, including MR elastography (MRE, 60 Hz), iron-corrected T1 mapping (cT1), T2 mapping, T1rho mapping, and diffusion-weighted imaging (DWI, quantified as apparent diffusion coefficients [ADC]). Liver and spleen volumes as well as splenic stiffness were also obtained. Spearman correlation was used to assess bivariate relationships. $P<0.05$ was considered statistically significant.
Results: Mean subject age was 15.3 years (range, 7-23 years); 15 individuals were male. 8 of 28 bivariate comparisons were significant. Liver stiffness correlated with splenic stiffness ($\rho=0.60$, $p=0.001$), cT1 ($\rho=0.39$, $p=0.038$), and DWI ADC ($\rho=-0.37$, $p=0.048$). Splenic volume correlated with liver stiffness ($\rho=0.67$, $p<0.0001$) and splenic stiffness ($\rho=0.73$, $p<0.0001$). Other significant correlations included: cT1 vs. T2 ($\rho=0.52$, $p=0.004$), T2 vs. T1 rho ($\rho=0.49$, $p=0.007$), and cT1 vs. splenic stiffness ($\rho=0.41$, $p=0.036$).
Conclusions: There were both significant and nonsignificant correlations between putative MRI biomarkers of chronic liver disease in our study population. This suggests that these quantitative imaging methods likely measure different components of the chronic liver disease process, and further research is needed to determine how these techniques predict liver inflammation and fibrosis when combined in a multiparametric manner.

Paper #: 095

Predictive Performance of MR Elastography in Children and Young Adults with Suspected Liver Disease

Andrew Trout[1], *andrew.trout@cchmc.org*; Rachel Sheridan[1], Suraj Serai, PhD[1], Stavra Xanthakos[1], Weizhe Su[2], Bin Zhang[1], Daniel Wallihan, MD[3]; [1]Radiology, Cincinnati Children's Hospital Medical Center, Cincinnati, OH, [2]University of Cincinnati, Department of Mathematics, Cincinnati, OH, [3]Levine Children's Hospital, Charlotte, NC

Disclosures: All authors have disclosed no financial interests, arrangements or affiliations in the context of this activity.

Purpose or Case Report: MR elastography (MRE) is being increasingly used in the pediatric population but data concerning diagnostic performance in this population is limited. The purpose of this study was to define the diagnostic performance of MRE in a population of children and young adults <21 years of age who underwent liver biopsy within three months of MRE.
Methods & Materials: This was a retrospective review of patients undergoing hepatic MRE and liver biopsy for any suspected liver disease other than prior liver transplantation or Fontan palliation of congenital heart disease. A single experienced observer processed all MRE exams and a single experienced pathologist reviewed all biopsy specimens. The diagnostic performance of MRE was expressed in terms of sensitivity, specificity and area under the receiver operating characteristic curve (AUROC).
Results: 89 patients, ages 0.3-20.6 years met inclusion criteria. Median interval between biopsy and MRE was 26 days. 44 patients (51.2%) had hepatic steatosis involving ≥5% of hepatocytes on histopathologic analysis. The population distribution of liver fibrosis stage and associated measured liver stiffness values by MRE are shown in the table. Overall AUROC for distinguishing stage 0-1 vs. ≥2 fibrosis was 0.699 (95%CI: 0.586-0.811) and was significantly lower for patients with steatosis than those without (AUROC=0.529 [95%CI: 0.350-0.708] vs. 0.818 [95%CI: 0.671-0.964], respectively; p=0.014). A stiffness cut-off of 2.27 kPa maximized sensitivity and specificity for distinction of stage 0-1 from ≥2 fibrosis in the entire population (68.6% [95%CI: 57.2-80.1%] and 74.3% [95%CI: 63.5-85.1%], respectively).
Conclusions: In the pediatric and young adult population, there appears to be a confounding effect of steatosis on the prediction of liver fibrosis based on MRE-derived liver stiffness. MRE performs significantly better for the distinction of stage 0-1 from ≥2 fibrosis in patients without hepatic steatosis than in patients with hepatic steatosis.

Population distribution of liver fibrosis stage with associated mean (±SD) liver stiffness values as measured by MR elastography

Fibrosis Stage	Mean Liver Stiffness
0	2.77 ± 0.63 kPa
1	2.85 ± 0.66 kPa
2	3.11 ± 0.97 kPa
3	5.03 ± 2.16 kPa
4	4.68 ± 1.32 kPa

Paper #: 096

Assessment of pediatric liver allografts with shear wave elastography

James Davis, MD[2], *davisjc2@upmc.edu*; James Squires[1], Allisin Drum[3], Patrick McKiernan[1], Wael Abdalla[3], George Mazariegos[4], Judy Squires, MD[3]; [1]Department of Gastroenterology, Children's Hospital of Pittsburgh of UPMC, Pittsburgh, PA, [2]Department of Radiology, University of Pittsburgh Medical Center, Pittsburgh, PA, [3]Department of Radiology, Children's Hospital of Pittsburgh of UPMC, Pittsburgh, PA, [4]Thomas E. Starzl Transplantation Institute, University of Pittsburgh Medical Center, Pittsburgh, PA

Disclosures: All authors have disclosed no financial interests, arrangements or affiliations in the context of this activity.

Purpose or Case Report: Pediatric liver transplant (LT) recipients are at risk for many transplant-related complications. A variety of histological changes has been reported in post-LT biopsies, with abnormalities more frequent in for-cause biopsies investigating allograft dysfunction. Importantly, abnormal graft histology is also seen in protocol biopsies from children who are clinically well with normal liver biochemistry. Shear-wave elastography (SWE) is a noninvasive, rapid method to assess liver tissue stiffness as a surrogate marker for fibrosis. Its utility has been validated in adults; however, data in pediatrics is lacking. Our aim was to assess the utility of SWE for the evaluation of liver fibrosis in hepatic allografts of pediatric patients and correlate with histology.
Methods & Materials: Median SWE velocity measurements (in m/s) were obtained in pediatric patients undergoing hepatic allograft biopsy for either surveillance, clinically suspected, or follow up of known graft dysfunction. SWE was performed using a GE Logiq E9 machine and C1-6 transducer within 3 days of biopsy. Histological reports were reviewed for the presence of fibrosis and/or rejection. When available, data was extracted from the medical record that correlated with testing. Continuous data were normally distributed. Mean was calculated and analyzed using two-tailed Student's t-test.
Results: From 10/1/2016 to 9/30/2017, 56 pediatric (mean age 11.7 yrs) LT recipients underwent allograft biopsies. Histological findings included fibrosis (17/56, 30%) and rejection (22/56, 39%). Higher median SWE velocity was seen in liver transplant patients with fibrosis than without (1.52 vs 1.40, $p<0.05$). No additional biochemical parameters distinguished fibrotic vs non-fibrotic subjects. (Table 1). Neither median SWE nor biochemical parameters could distinguish between subjects with rejection vs those without. (Table 2) Notably, in a sub-analysis of subjects with near-normal liver biochemistry (ALT, AST <1.5 ULN) and without markers of fibrosis (platelet >150, APRI < 0.7) SWE velocity was significantly higher (1.56 vs 1.34, $p<0.04$) in subjects with fibrosis (n=7) vs those without fibrosis (n=10).
Conclusions: Median SWE velocity values are higher in pediatric patients with allograft fibrosis, with and without biochemical markers of graft dysfunction and fibrosis. SWE may be able to detect clinical and sub-clinical fibrosis enabling non-invasive assessments of pediatric liver transplant recipients.

Table 1. Ultrasound elastography to determine fibrosis in pediatric liver allograft

Elastography	Fibrosis (n=17)	No Fibrosis (n=39)	P Value
Average Median Velocity (Q1-Q3)	1.52 (1.31 - 1.64)	1.40 (1.29 - 1.51)	<0.05
Biochemical Parameter			
INR, median, Q1-Q3	1.13 (1 - 1.2)	1.15 (1.1 - 1.2)	0.68
GGT (IU/L), median, Q1-Q3	106 (24 - 149.5)	147.3 (16.8 - 140.5)	0.62
Platelets (1000/mm^3), median, Q1-Q3	220.7 (195.8 - 274.8)	219.1 (178.5 - 253.5)	0.95
AST (IU/L), median, Q1-Q3	70 (25.3 - 65.5)	65.9 (22.5 - 60.3)	0.86
ALT (IU/L), median, Q1-Q3	111.3 (27.8 - 109)	96.4 (25.5 - 96.8)	0.74
Total Bilirubin (umol/L), median, Q1-Q3	1.87 (0.56 - 1.28)	0.7 (0.3 - 0.73)	0.07
Fibrosis Scoring			
APRI	1.33 (0.19 - 0.53)	0.48 (0.17 - 0.67)	0.14

INR, international normalized ratio; GGT, gamma-glutamyl transferase; AST, Aspartate aminotransferase; ALT, Alanine aminotransferase; APRI, AST to platelet ratio index

Table 2. Ultrasound elastography to determine acute cellular rejection in pediatric liver allograft

Elastography	Rejection (n=22)	No Rejection (n=34)	P Value
Average Median Velocity (Q1-Q3)	1.44 (1.34 - 1.52)	1.43 (1.26 - 1.57)	0.94
Biochemical Parameter			
INR, median, Q1-Q3	1.14 (1.1 - 1.2)	1.15 (1.1 - 1.2)	0.83
GGT (IU/L), median, Q1-Q3	171.9 (18 - 145)	111.5 (17 - 125)	0.41
Platelets (1000/mm^3), median, Q1-Q3	233.4 (183 - 281)	210.5 (176.3 - 249.3)	0.33
AST (IU/L), median, Q1-Q3	84.7 (23 - 112)	54.8 (21.5 - 65)	0.24
ALT (IU/L), median, Q1-Q3	121.3 (26 - 159.8)	86 (25 - 86.5)	0.38
Total Bilirubin (umol/L), median, Q1-Q3	0.7 (0.3 - 0.73)	1.28 (0.43 - 1.08)	0.3

INR, International normalized ratio; GGT, gamma-glutamyl transferase; AST, Aspartate aminotransferase; ALT, Alanine aminotransferase

Paper #: 097

Shear Wave Elastography Ultrasound for Hepatic Veno-occlusive Disease in a Pediatric Population undergoing Hematopoietic Stem Cell Transplantation

Matthew Goette, PhD[1], *mjgoette@texaschildrens.org*; Nicholas Dodd, BM[1], Robert Krance, MD[1], Prakash Masand, MD[1]; [1]Pediatric Radiology, Texas Children's Hospital, Houston, TX

Disclosures: All authors have disclosed no financial interests, arrangements or affiliations in the context of this activity.

Purpose or Case Report: To evaluate the feasibility of shear wave elastography (SWE) ultrasound as a potential complimentary non-invasive tool to facilitate early diagnosis of hepatic veno-occlusive disease (HVOD) in a pediatric population undergoing hematopoietic stem cell transplantation (HSCT).
Methods & Materials: Under IRB approval, HSCT patients with a clinical suspicion of HVOD were recruited for the study (N=14, age: 9.9 ± 6.3 y). Diagnosis of HVOD was made by fulfillment of the Revised Seattle Criteria as determined by a physician using the following clinical and ultrasonography criteria: right upper quadrant pain, total bilirubin, percent weight gain, and ascites, as well as the detection of portal venous flow reversal. All patients underwent serial ultrasound examinations, which included evaluation by grayscale, Doppler, and SWE. Ten exams were performed every other day using a GE Logic-E9 ultrasound unit with linear and curvilinear transducers. Four elastography measurements each were made in Couinaud's liver segments 5, 6, 7 and 8 (16 total for each patient). All exams were performed with the patient being NPO for 4 hours prior to the SWE evaluation.
Results: Of the 14 recruited patients, six completed fewer than 8 exams due to discharge or withdrawal of consent. Figure 1 displays each patient's average SWE velocity (m/s) over all exams obtained in liver segments 5 through 8 and the spleen. The average SWE velocity in the liver from all patients in this population was 1.77 ± 0.24 m/s (range: 1.39 to 2.40 m/s), which was higher than the vendor specified cut-off value for normal hepatic stiffness (1.35 m/s). The patient with the highest measured SWE velocity (2.18 ± 0.28 m/s), Pt. 10, was the only patient to die due to multi-organ failure as a fatal complication of HVOD. This patient's SWE measurements were significantly higher than the rest of the cohort with more than three exams (p=0.00085), with a mean SWE velocity greater than 2.10 m/s. Figure 2 displays the average SWE measurement in the entire liver for each patient over the course of the study.
Conclusions: This study demonstrated elevated liver stiffness values with SWE in pediatric patients undergoing HSCT with clinically suspected HVOD, and the potential ability to delineate severe disease in this population.

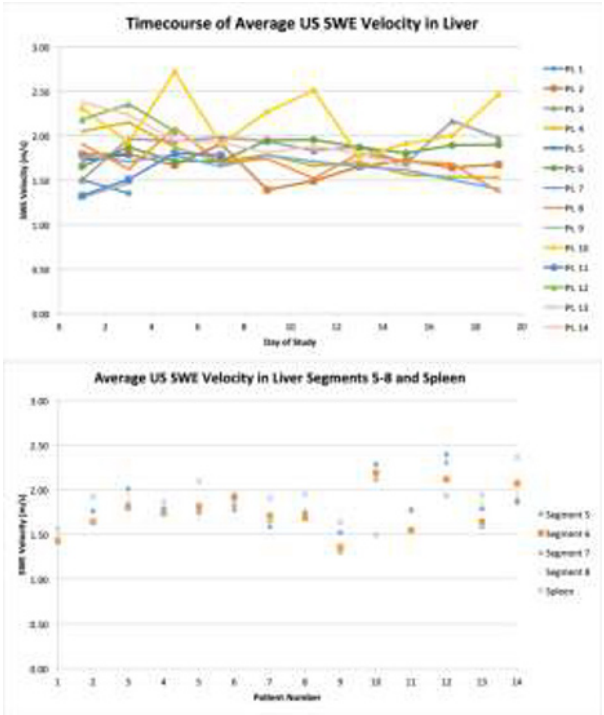

Paper #: 098

Can MRI Liver Stiffness Predict be used to Predict Focal Liver Lesions in Fontan Patients?

Eric Diaz, MD[1], *eric.diaz@gmail.com*; Andrew Trout[1], Jonathan Dillman, MD, MSc[1]; [1]CCHMC, Cincinnati, OH

Disclosures: All authors have disclosed no financial interests, arrangements or affiliations in the context of this activity.

Purpose or Case Report: The Fontan operation is used to palliate single ventricle physiology congenital heart disease. Although the operation restores essential blood flow and improves arterial oxygen saturations, resultant systemic venous hypertension and decreased cardiac output predispose to end-organ injury. Fontan-associated Liver Disease (FALD) is a major form of end-organ disease in this population. The purpose of this study was to define the relationship between two of the major components of FALD: liver stiffness (a surrogate for organ congestion and fibrosis) measured by MR elastography (MRE) and focal liver lesions.
Methods & Materials: In this retrospective study, medical records were searched for patients that had been previously palliated with the Fontan operation and had subsequently undergone MRI of the liver with and without intravenous contrast material as well as MRE on the same day between January 1, 2012 and May 31, 2017. Mean and maximum liver stiffness (kPa) measured by MRE and the presence of focal liver lesions were documented. Mann-Whitney U tests were used to compare medians (age, mean liver stiffness, and maximum liver stiffness) between patients without and with focal liver lesions.

Results: Of the 37 patients that met inclusion criteria, 26 (70%) had one or more focal liver lesions. Median age was 20.6 years (IQR [interquartile range]: 12.1-29.1 years) for patients without liver lesions versus 20.6 years (IQR: 17.0-28.9 years) for patients with liver lesions (p=0.81). There was no difference in mean liver stiffness between patients without liver lesions 5.1 kPa (IQR: 4.1-5.6 kPa) and patients with liver lesions 4.3 kPa (IQR: 3.6-5.5 kPa) (p=0.10). Patients without liver lesions had significantly higher maximum liver stiffness than patients with liver lesions (6.1 kPa [IQR: 4.7-6.6 kPa] versus 4.5 kPa [IQR: 4.0-6.0 kPa]) (p=0.04).
Conclusions: Our study suggests that neither age nor mean liver stiffness measured by MRE is associated with the presence of focal lesions in patients status post the Fontan operation. However, maximum liver stiffness was significantly higher in individuals *without* focal liver lesions, an unexpected finding. Our findings raise the possibility that liver stiffening and development of liver lesions may proceed independently in Fontan patients.

Paper #: 099

Magnetic resonance elastography of the liver in children: variations in regional stiffness

Benjamin Thompson[1], *benpthompson@hotmail.com*; Ramkumar Krishnamurthy, PhD[1], Rajesh Krishnamurthy[1], Mark Smith, MS[1], Cheryl Gariepy[1], Carol Potter[1], Houchun Hu, PhD[1]; [1]Radiology, Nationwide Children's Hospital, Columbus, OH

Disclosures: All authors have disclosed no financial interests, arrangements or affiliations in the context of this activity.

Purpose or Case Report: Magnetic resonance elastography (MRE) is a non-invasive and reliable method for measuring liver stiffness. In this work, we hypothesize that MRE is sensitive to variations in tissue stiffness across the organ. We believe that liver fibrosis is heterogenous due to differences in portal blood supply and that consequently the certain hepatic lobes have a higher propensity to develop fibrosis than others. We test our hypothesis in pediatric patients by measuring MRE using global and local region-of-interest (ROI) analyses.
Methods & Materials: MRE was performed on a GE Signa 3T platform using the commercial product "MR Touch". Eight axial slices were acquired, which were co-localized to anatomical DWI and Dixon water-fat sequences. We obtained data in 19 patients (avg: 14y, range: 1-22y) referred for clinical liver exam. Liver stiffness measurements were made via two approaches: (1) Global - one large ROI was drawn on each of the eight MRE slices encompassing all visible liver using co-registered DWI and Dixon images for guidance. The average stiffness across the eight slices was then computed; (2) Local - smaller ROIs were drawn on each of the eight slices corresponding to the Couinaud classification. The average of each of the eight segments was computed. With both approaches, care was taken to avoid vessels and non-liver structures.
Results: Table 1 summarizes the measurement results. A one-way ANOVA yielded liver stiffness values that were statistically different in segments VI and VII than in the other segments. In each individual, we further averaged measurements in segments II and III to represent the left lobe and segments V-VIII to represent the right lobe. We found three individuals (Patients #6, 18, and 19) who had statistically significant differences between the two lobes. Two individuals had stiffer right lobes; one had a stiffer left lobe. In comparing the global ROI to the local ROI approach for quantifying liver stiffness, we found average values in segments III, V, and VIII to most closely approximate the average stiffness across the entire organ.
Conclusions: Our preliminary results support literature findings of using MRE in children and show that the technique is sensitive to detecting variations in tissue stiffness across hepatic lobes. We believe the difference in right and left lobe portal vasculature and their respective drainage from the upper and lower gastrointestinal tracts is partly responsible for the observed difference in hepatic stiffness.

All Values in kPa				Couinaud Segments								
Patient	Age (y)	Left Lobe	Right Lobe	I	II	III	IV	V	VI	VII	VIII	Global
1	1.4	2.7	2.8	2.6	2.9	2.6	3.2	2.3	3.5	2.4	2.8	2.5
2	16.6	3.1	2.5	1.8	3.6	2.5	3.3	2.7	2.3	2.5	2.6	2.6
3	16.8	3.4	3.1	3.6	3.7	3	3.9	4	3	2.2	3.2	3.0
4	11.1	3.8	3.3	1.2	4.3	3.2	4.5	2.2	3.2	3	4.6	2.8
5	14.2	2.7	2.9	1.7	2.7	2.6	2.4	2.8	3.1	3.2	2.5	2.6
6	15.5	3.1	3.9	2.7	3	3.2	4.1	3.8	4	3.8	3.8	3.2
7	9.8	2.4	2.7	2.7	2.1	2.7	2.7	1.9	2.4	3.3	3.2	2.3
8	20.0	3.2	3.1	2.6	3.1	3.3	2.4	3.8	2.9	2.7	3	2.5
9	15.4	2.9	2.6	2.3	2.7	3.1	2.4	2.1	2.9	3.2	2.2	2.5
10	16.8	3.1	2.8	1.6	2.7	3.4	2.6	2.4	3.5	3.3	1.9	2.2
11	19.9	2.0	2.0	0.8	2.1	1.8	1.7	1.6	2.1	2.5	1.6	1.7
12	11.6	2.2	2.5	2.1	2.5	1.9	2.7	2.9	2.4	2.6	2.2	2.6
13	22.5	3.4	5.4	3.6	2	4.7	3.3	5.7	6.4	4.1	5.3	5.3
14	1.0	2.1	3.0	1.8	2.3	1.8	2.5	3.1	2.7	3.6	2.7	2.5
15	16.6	3.4	3.6	3.4	4.1	2.7	3.9	3.6	3.6	3.3	3.7	3.5
16	13.5	2.5	2.6	1.9	2.3	2.6	2.7	2.6	3.3	2.2	2.2	2.8
17	12.9	2.5	2.3	2.2	2.3	2.6	2.7	2.6	2.1	2.1	2.5	2.8
18	17.0	2.9	2.3	2.9	3	2.7	3.1	2.2	2.3	2.6	2.2	2.3
19	12.4	2.4	3.4	2.2	2.6	2.2	2.1	3.6	4.1	3.2	2.6	2.7

Paper #: 100

Methotrexate Therapy Increases Hepatic Stiffness in Patients with Inflammatory Bowel Disease

Amie Robinson, BSRT(R)(MR)[1], *alrobinson@cmh.edu*; Shweta Vadlamani[2], Alka Goyal, MD[1], Emily Kucera, MD[1], Sherwin Chan, MD PhD[1]; [1]Radiology, The Children's Mercy Hospital, Kansas City, MO, [2]University of Kansas School of Medicine, Kansas City, KS

Disclosures: All authors have disclosed no financial interests, arrangements or affiliations in the context of this activity.

Purpose or Case Report: The use of methotrexate as a first line immunomodulator and/or as an adjuvant to biologic therapy has been on the rise in pediatric inflammatory bowel disease (IBD). However, there is paucity of data for evaluation and monitoring of hepatic fibrosis associated with prolonged methotrexate usage in patients with IBD. Ultrasound elastography is a noninvasive technique that can assess liver stiffness, which has been show to correlate with pathologically diagnosed hepatic fibrosis. We wanted to test the hypothesis that hepatic stiffness increases in IBD patients with methotrexate exposure
Methods & Materials: This is a single site prospective cross-sectional study evaluating ultrasound elastography results on IBD patients between 1/2017 and 10/2017. We included subject's ages 2 through 22 years who have a diagnosis of IBD and different cumulative dose exposures to methotrexate. Local institutional review board approval was granted for this study and all included patients gave informed consent. Subjects underwent a single ultrasound elastography exam. Clinical, medications and laboratory data were collected out of the subject's medical record. All subjects with pre-existing liver disease were excluded. The patients were divided into two groups, controls with no methotrexate exposure and subjects with prior methotrexate exposure.
Results: A total of 42 (18 controls and 24 methotrexate exposure) subjects underwent ultrasound elastography. Two-thirds of the patients are male (n=28, 67%) and the median age was 15 (range 5-22) years. Majority of patients had a diagnosis of Crohn Disease (n=29, 69%). The median cumulative methotrexate dose was 517 mg (range 118mg-2973mg). Shear wave velocity was compared between the control and methotrexate groups. The mean shear wave velocity values were

significantly higher in patients with methotrexate exposure compared to the controls (1.37 vs. 1.23 m/s. p=0.04).
Conclusions: Ultrasound elastography may be useful in detecting early changes in hepatic stiffness in patients receiving methotrexate prior to liver enzyme changes or clinically apparent liver disease. This technique should be studied further as a monitoring tool for patients on methotrexate.

Paper #: 101

Abdominal Fat Distribution and its Relationship with Liver and Pancreatic Fat Fraction, Liver Stiffness and Diabetic Status

David Hunte[1], *David.Hunte@cchmc.org*; Andrew Trout[1], Marialena Mouzaki[1], Alexander Towbin, MD[1], Stavra Xanthakos[1], Jonathan Dillman, MD, MSc[1]; [1]Radiology, Cincinnati Children's Hospital Medical Center, Cincinnati, OH

Disclosures: All authors have disclosed no financial interests, arrangements or affiliations in the context of this activity.

Purpose or Case Report: Fatty liver disease is increasingly recognized as a multisystem disease. The purpose of this study was to assess the relationship between measures of anatomic fat depots, liver fat fraction, liver stiffness, pancreatic fat fraction, and diabetic status in pediatric patients.
Methods & Materials: This was a retrospective study of pediatric patients with fatty liver disease who had undergone liver MR elastography (MRE) and multi-point Dixon-based fat quantification between September 2015 and July 2017. A single observer measured liver and pancreatic proton density fat fraction, abdominal subcutaneous fat thickness, and visceral fat thickness (deep fascia of rectus muscle to anterior aspect of L2). Clinical records were reviewed to abstract demographic data (age, sex, body mass index [BMI]), liver stiffness, and type 2 diabetes status. Bivariate correlations were assessed with Spearman's rho, and multiple linear and multiple logistic regression models were used to assess relationships between outcome and predictor variables.
Results: 87 patients were included in this study (mean age: 14.3±3.4 years; 27 [31%] females; mean BMI: 36.1±7.8 kg/m^2). 7/87 (8%) patients were diabetic, and 45/87 (52%) were insulin resistant. Mean liver stiffness was 2.5±0.9 kPa, mean liver fat fraction was 18.7±10.3% and mean pancreatic fat fraction was 5.9±5%.
Liver fat fraction was significantly correlated only with visceral fat thickness at univariate analysis (ρ=0.31, p=0.004). Based on multivariate modeling, liver stiffness was significantly associated with liver fat fraction (-0.022kPa/+1%, p=0.018) and visceral fat thickness (+0.18kPa/1 cm, p=0.0007). At univariate analysis, pancreatic fat fraction was significantly correlated with age (ρ=0.28, p=0.012), BMI (ρ=0.34, p=0.002), subcutaneous fat thickness (ρ=0.23, p=0.04), and visceral fat thickness (ρ=0.24, p=0.03), but these relationships did not persist upon multivariate modeling. Diabetic status was not significantly associated with any measure of abdominal fat.
Conclusions: Liver and pancreatic fat fraction are both weakly but significantly correlated with visceral fat thickness suggesting a relationship between visceral, but not subcutaneous, adiposity and liver and pancreatic steatosis in children. Hepatic steatosis appears to have a softening effect on liver stiffness as measured by MRE, and increased visceral fat thickness appears to be associated with increased liver stiffness. None of our imaging findings could predict diabetic status.

Paper #: 102

Contrast-Enhanced Brain Ultrasound on Extreme Premature Twin Fetal Lambs Maintained by the EXTra-uterine Environment for Neonatal Support (EXTEND): A Promising Imaging Technique

Ryne Didier[1], *rdidier@gmail.com*; Anush Sridharan[1], Kendall Lawrence[1], Marcus Davey[1], Beverly Coleman[1], Alan Flake[1]; [1]Children's Hospital of Philadelphia, Philadelphia, PA

Disclosures: All authors have disclosed no financial interests, arrangements or affiliations in the context of this activity.

Purpose or Case Report: With recent progress in the development of an artificial environment to support the extreme premature infant, advanced imaging techniques are necessary to evaluate the brain parenchyma. We aimed to evaluate a) the feasibility of contrast-enhanced ultrasound (CEUS) and b) brain perfusion in fetal lambs maintained on the EXTEND system.
Methods & Materials: Following IACUC-approved protocols, twin premature fetal lambs [102 days gestational age (GA), Term = 145 days] were transferred from placental support to the EXTEND system[1]. Twin B was immediately subjected to a 12-hour period of sub-physiologic flow (152mL/kg/min) and oxygen delivery (15.9mL/kg/min). Twin A maintained physiologic flow (>233mL/kg/min) and oxygen delivery (>22mL/kg/min). Lumason® ultrasound (US) contrast boluses were administered into the pumpless umbilical arterial to umbilical venous oxygenator circuit. Serial CEUS examinations were performed using a GE Logiq E9 US system and C2-9 transducer. Time-to-peak (TTP) measurements were obtained and Parametric maps were created. Hemodynamic parameters and measurements across the oxygenator were recorded. Serum oxygen and lactate values were obtained pre- and post-examination. Post-mortem MRIs were performed.
[1]Partridge EA et al. An extra-uterine system to physiologically support the extreme premature lamb. Nat Commun. 2017;8:15112.
Results: To account for microbubble destruction within the support equipment, up to 0.59mL/kg contrast was required for optimal visualization. There were no statistically significant changes in measured variables (Table 1). On grayscale images, Twin B demonstrated ventriculomegaly and loss of grey-white differentiation with progressive loss of parenchymal white matter which was not observed in Twin A. With CEUS, Twin B demonstrated increased TTP enhancement and decreased parenchymal perfusion when compared to Twin A at 108 and 105 days, respectively (Figure 1). Twin B demonstrated progressively increased TTP enhancement within the brain and brainstem at 115 and 129 days GA and post-mortem MRI confirmed hydranencephaly.
Conclusions: CEUS of the brain is feasible in fetal lambs maintained on the EXTEND system and changes in perfusion can be quantified. These findings establish a foundation for further evaluation of this promising technique with potential applications in the setting of fetal hypoxia.

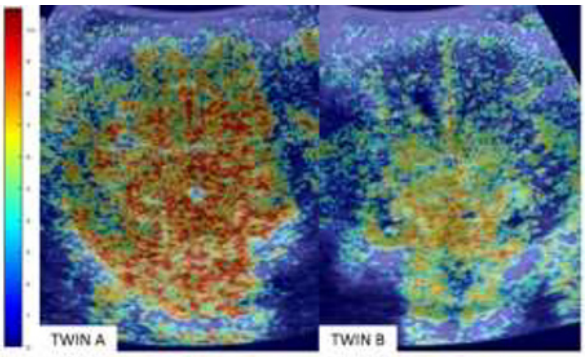

Figure 1: Coronal Parametric maps of the brain created from contrast-enhanced ultrasound performed in premature fetal lambs maintained on the EXTEND system demonstrating decreased parenchymal enhancement in Twin B concordant with known hypoxic injury when compared to Twin A.

Paper #: 103

Fetal and Postnatal Brain Imaging for the Detection of ZIKV Encephalopathy in the Fetus/Newborn

Dorothy Bulas, MD[1], *dbulas@cnmc.org*; Sarah Mulkey, MD[1], Gilbert Vezina, MD[1], Yamil Fourzali, MD[2], Margarita Arroyave-Wessel[1], Caitlin Cristante[1], Christopher Swisher[1], Youssef Kousa, MD[1], Carlos Cure, MD[3], Roberta DeBiasi, MD[3], Adre du Plessis[1]; [1]CNMC, Washington DC, DC, [2]Sabbag Radiologos, Baranquilla, Colombia, [3]BIOMELab, Baranquilla, Colombia

Disclosures: All authors have disclosed no financial interests, arrangements or affiliations in the context of this activity.

Purpose or Case Report: To compare the prenatal US/MRI (feUS/feMRI) and postnatal US/MRI findings of the fetus/newborn exposed to ZIKV in the first and second trimesters.
Methods & Materials: An IRB approved prospective longitudinal neuroimaging study of fetuses/newborns of pregnant women with clinical and/or lab confirmed (RT-PCR and/or IgM/PRNT) diagnosis of Zika infection was performed. Subjects were enrolled from Columbia (endemic) or United States (travel related). Gestational age (GA) at exposure and timing between ZIKV exposure/symptoms and imaging was documented. The feMRI/ feUS and postnatal US/MR protocols were standardized between sites. Subjects had 1 to 2 feMRI/ feUS, depending upon GA at enrollment. Postnatally, infants received an unsedated brain MRI and cranial US
Results: 48 ZIKV exposed/infected in first or second trimester pregnant women were enrolled (46 Colombia, 2 USA). Subjects had symptoms of ZIKV infection at mean of 8.4 ± 5.7 wks GA. The first feMRI and feUS were performed at 25.1 ± 6.3 wks GA. 36 had a second feMRI and feUS at 31.1 ± 4.2 wks GA. 3/48 (6%) cases had an abnormal feMRI: (1) heterotopias and abnormal cortical indent, (2) parietal encephalocele and Chiari II, (3) thin corpus callosum, dysplastic brainstem, temporal cysts, subependymal heterotopias, and generalized cerebral/cerebellar atrophy. FeUS in these 3 cases found (1) normal study, (2) parietal encephalocele and Chiari II, (3) significant ventriculomegaly with decreasing percentile of head circumference from 32 to 36 wks GA (38% to 3.6%). Postnatal head US revealed findings not seen on feUS or postnatal MRI: choroid plexus or germinal matrix cysts in 9 infants and lenticulostriate vasculopathy in 1 infant.
Conclusions: FeMRI and feUS provide complimentary information in the assessment of fetal brain changes in ZIKV. FeMRI can reveal more extensive brain changes than seen by feUS. Further studies are needed to determine if cystic changes on postnatal head US are related to ZIKV, or are incidental findings.

Paper #: 104

Fetal MRI Findings in Diencephalosynapsis

Elizabeth Snyder, MD[1], *elizabeth.j.snyder@gmail.com*; Michael Paldino, MD[1], Carolina Guimaraes[1], Wei Zhang, PhD[1], Lisa Emrick[1], Nilesh Desai[1]; [1]Texas Children's Hospital, Houston, TX

Disclosures: All authors have disclosed no financial interests, arrangements or affiliations in the context of this activity.

Purpose or Case Report: Diencephalosynapsis is a midline brain malformation characterized by partial or complete fusion of the thalami and/or hypothalamus. Yet little data exists regarding this entity in the prenatal literature, especially with regard to its occurrence in isolation from holoprosencephaly. The goal of this study is to describe and measure the diagnostic value of fetal MRI findings of diencephalosynapsis.
Methods & Materials: All cases of fetal ventriculomegaly with both prenatal and postnatal brain imaging from 2007-2017 were identified. Post-natal MRI was defined as the reference standard for the diagnosis of diencephalosynapsis. A pediatric neuroradiologist blinded to the diagnosis of diencephalosynapsis versus control reviewed the prenatal MRI of all patients with diencephalosynapsis as well as 29 control patients imaged for ventriculomegaly. Each case was scored for the presence of diencephalosynapsis and salient imaging findings were recorded. After a delay, re-review of the entire study cohort was undertaken by the same reader to measure reliability of the pre-natal diagnosis. Fisher exact test and Wilcoxon Rank Sum test were used to compare categorical and continuous imaging findings respectively between case and control groups. Cohen's kappa measured intra-rater reliability. Sensitivity and specificity of fetal MRI for the gold standard diagnosis of diencephalosynapsis were computed in standard fashion.
Results: 309 cases of prenatal ventriculomegaly with both prenatal and postnatal MRI were reviewed. Seventeen patients were confirmed to have diencephalosynapsis by postnatal MRI. Loss of interthalamic cleavage ($p<0.0001$) and effacement of the posterior recess of the third ventricle ($p<0.0001$) were both significantly associated with a diagnosis of diencephalosynapsis (Table 1). Patients with diencephalosynapsis tended to have a smaller third ventricle ($p<0.005$) and a fenestrated or absent septum pellucidum ($p<0.02$). Intra-rater agreement on the diagnosis of diencephalosynapsis was excellent (Kappa [95%CI]: 0.91 [0.80, 1.00]). Sensitivity and specificity of fetal MRI for the detection of diencephalosynapsis were 94% and 83% respectively (Table 2).
Conclusions: Absent interthalamic cleavage and effacement of the posterior recess of the third ventricle on fetal MRI suggest the diagnosis of diencephalosynapsis. Fetal MRI is sensitive, specific, and reliable for the diagnosis of diencephalosynapsis and may be useful for prenatal diagnosis and counseling.

Table 1. Comparison of MRI findings of diencephalosynapsis cases versus controls

	Overall (n = 46)	Control (n = 29)	Cases (n = 17)	P-Value
Finding	**n(% of n)**			
Macrocephaly on fetal US (>95% HC)	14 (30)	9(31)	5(29)	1.000
Microcephaly on fetal US (<5%)	12 (26)	6(21)	6(35)	.3142
Effacement of subarachnoid spaces	28 (61)	16(55)	12(71)	.3607
Fenestrated, absent septum pellucidum	13 (72)	17(59)	16(94)	.0158
Third ventriculomegaly	20 (43)	16(55)	4(24)	.0636
Loss of interthalamic cleavage	20 (43)	4(14)	16(94)	<.0001
Effacement of posterior recess of third ventricle	22 (48)	6(21)	16(94)	<.0001
Cortical dysplasia	13 (28)	5(17)	8(47)	.0441
Brainstem dysplasia	4/44 (9.1)	3(10)	1/15(6.7)	1.000
Vermian abnormality	12/45 (27)	7(24)	5/16(31)	.7284
Cerebellar abnormality	11/45 (24)	6(21)	5/16(31)	.4834
Ventricular diverticulum	13 (28)	7(24)	6(35)	.5048

Table 2. Diagnostic value of fetal MRI for diencephalosynapsis

Sen. (95% CI)	Spe. (95% CI)	PPV (95% CI)	NPV (95% CI)	Accuracy (95% CI)
0.94 (0.71, 1.00)	0.83 (0.64, 0.94)	0.76 (0.53, 0.92)	0.96 (0.80, 1.00)	0.87 (0.74, 0.95)

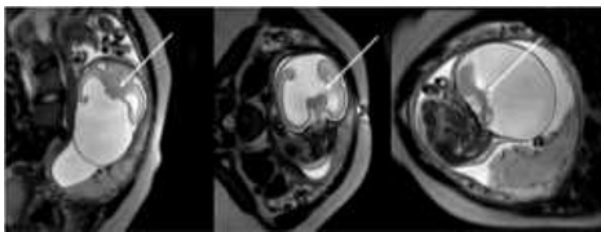

Paper #: 105

Posterior Fossa Findings in Prenatal Diagnosis of Dystroglycanopathy – Extending Beyond Brainstem Kinking

Carolina Guimaraes, Dr.[1], *caroguimaraes55@gmail.com*; Fernanda Braojos, MD[1], Christopher Cassady, MD[1], Amy Mehollin-Ray, MD[1], Wei Zhang, PhD[1], Nilesh Desai[1]; [1]Texas Children's Hospital, Houston, TX

Disclosures: All authors have disclosed no financial interests, arrangements or affiliations in the context of this activity.

Purpose or Case Report: Prenatal diagnosis of dystroglycanopathy relies strongly on the identification of a hypoplastic kinked brainstem, especially when evaluation of brain sulcation is limited by early gestational age. Although this finding is specific, it is not pathognomonic. Our purpose is to evaluate the predictive value of additional posterior fossa findings on prenatal MRI in patients diagnosed with dystroglycanopathy. We also access the reproducibility of prenatal detection and compare prenatal and postnatal MRI.
Methods & Materials: Fetuses with posterior fossa abnormalities were retrospectively identified from our referral database between January 2008 and August 2017. Only cases with both prenatal and postnatal MRI were included. The disease group included cases of dystroglycanopathy confirmed either by genotype or by postnatal phenotype. The control group included all remaining cases of prenatally diagnosed posterior fossa anomalies seen during the same period. Two fetal radiologists randomly reviewed all pre- and postnatal MRI studies, evaluating for the presence of selected posterior fossa findings common to dystroglycanopathies. Posterior fossa findings were analyzed first on axial plane, blinded to diagnosis and to any additional findings. Brainstem kinking was evaluated on the sagittal plane only after axial analysis was recorded. Sensitivity, specificity and negative and positive predictive values were calculated. The agreement between the two readers and between pre- and postnatal imaging was analyzed using Cohen's Kappa coefficient.
Results: A total of 37 patients were identified, of which 10 were diagnosed with dystroglycanopathy. All evaluated variables, except vermian hypoplasia, were statistically significant discriminators ($p < 0.0001$) between the study and control groups (Table 1). Findings of pontine cleft and cerebellar dysplasia (abnormal signal and irregular contours) were highly specific (Figure 1), similar to brainstem kinking (Table 2). There was excellent agreement between pre and post-natal MRI for all the evaluated variables and good to excellent agreement between the readers (Table 1).
Conclusions: Pontine cleft and cerebellar dysplasia are highly specific findings of dystroglycanopathy, especially when seen in conjunction. Identification of these findings adds diagnostic confidence when evaluating a fetus for suspected dystroglycanopathy and can be adequately identified on prenatal MRI.

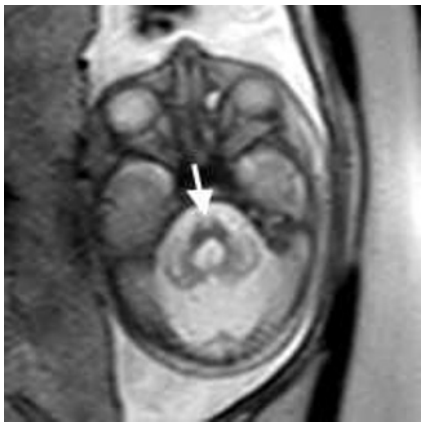

Table 1: Prevalence of Prenatal Imaging Findings and Agreement

	Reader 1 Prenatal MRI		Reader 2 Prenatal MRI		P- value	Readers Agreement	Pre vs Postnatal MRI Agreement
MRI Variables	Control (N = 27)	Study group (N = 10)	Control (N = 27)	Study group (N = 10)		Kappa Coefficient	Kappa Coefficient Reader 1 / 2
Abnormal cerebellar signal	3 (11%)	9 (90%)	1 (3.7%)	10 (100%)	<0.0001	0.86	0.87 / 0.85
Irregular cerebellar contour	2 (7.4%)	9 (90%)	0 (0%)	10 (100%)	<0.0001	0.82	0.79 / 0.82
Pontine cleft	3 (7.4 %)	10 (100%)	3 (11%)	10 (100%)	<0.0001	0.92	0.87 / 0.74
Above 3 findings in conjunction	1 (3.7%)	9 (90%)	0 (0%)	10 (100%)	<0.0001	0.86	0.85 / 1.00
Kinked brainstem	1 (3.7%)	10 (100%)	2 (7.4%)	10 (100%)	<0.0001	0.94	1.00 / 0.91
Midbrain dysplasia	8 (30%)	10 (100%)	3 (11%)	10 (100%)	<0.0001	0.73	0.77 / 0.69
Vermian hypoplasia	12 (44%)	9 (90%)	12 (44%)	10 (100%)	0.002	0.83	0.83 / 0.77

*Fleiss's equally arbitrary guidelines characterize Kappa over 0.75 as excellent, 0.40 to 0.75 as fair to good, and below 0.40 as poor.

Paper #: 106

Establishment of normative values for the fetal posterior fossa by MRI.

Megan Zare, MD[1], *meganmz@uw.edu*; Teresa Chapman, MD[1], Sarah Menashe, MD[1], Adam Alessio, PhD[1], Gisele Ishak, MD[1]; [1]Seattle Children's Hospital, Seattle, WA

Disclosures: Adam Alessio has indicated a relationship with GE Healthcare and Philips Healthcare for receiving research grants. All other authors have disclosed no financial interests, arrangements or affiliations in the context of this activity.

Purpose or Case Report: Fetal brain malformations suspected based on prenatal ultrasound may be further evaluated with fetal MRI in the second or third trimester. Suspected Dandy-Walker continuum anomalies constitute a significant percentage of prenatal cases evaluated by MRI. Diagnostic radiologists may struggle with a subjective assessment of posterior fossa size. In

order to help unify the description of posterior fossa malformations, we sought to establish objective measurements for the posterior fossa in normal fetuses between 18 and 36 weeks gestational age.
Methods & Materials: T2-weighted images of normal fetal brains in sagittal projection (Figure 1a) were obtained from fetal MR studies of normal brains performed for indications other than suspected posterior fossa anomalies from 2009 to 2017. For this initial assessment, 78 fetal brains were included in the retrospective analysis. Gestational age was determined by last menstrual period or earliest US measurements. Four radiologists reviewed images independently and recorded the following measurements for each case: the posterior fossa perimeter (Figure 1b), the tegmento-vermian angle (TVA - Figure 1c), and the superior posterior fossa angle (SPFA - Figure 1d).
Results: For each feature, the mean of the measurements, the percentage of absolute difference of the reader measurement compared to mean measurement, and the interclass correlation (ICC) were calculated. Values are reported as mean ± standard deviation (Table 1). Perimeter appears to be very linear with age (Figure 2, r^2 = 0.92, p<0.001), with the perimeter increasing by approximately 4.1 cm for each week of growth, whereas the SPFA and the TVA are independent of gestational age. For all included cases, the TVA averaged 2.6±1.5 degrees among all four readers.
Conclusions: The posterior fossa perimeter and superior posterior fossa angle are novel measurements that can be used for establishing the expected size of the posterior fossa in second- and third-trimester fetuses by MR imaging.

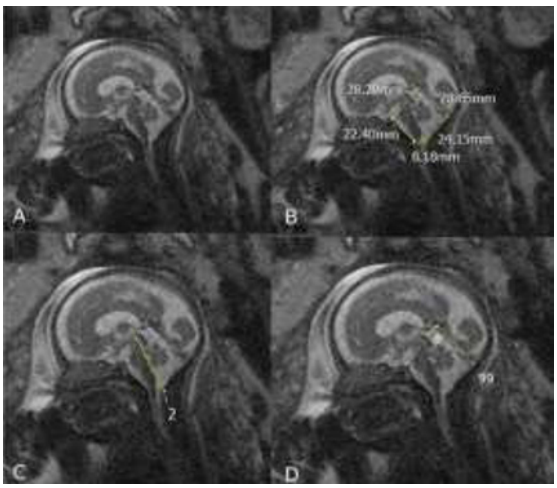

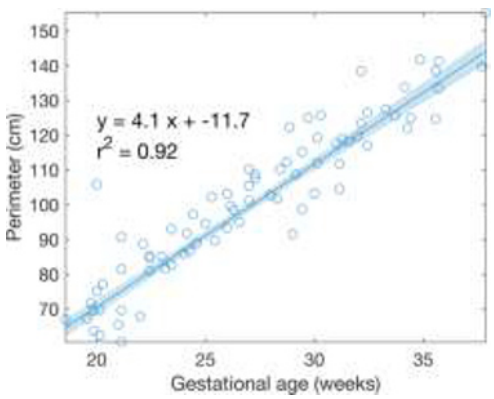

Age Category	Age (weeks)	N	PERIMETER Measurement (mm)	% Absolute Difference	ICC*	SPFA Measurement (mm)	% Absolute Difference	ICC*
GA <23 wks	20.9±1.2	21	75.8±11.4	6± 5%	0.73	102.3±7.7	7± 4%	0.33
23 – 27 wks	25.2±1.3	19	94.8±7.8	4± 1%	0.84	96.9±6.5	4± 2%	0.55
27 – 31 wks	29.1±1.1	17	110.7±9.5	4± 2%	0.77	100.3±5.4	5± 3%	0.25
GA >31 wks	33.8±2.1	21	128.0±11.8	4± 2%	0.88	99.7±4.9	4± 2%	0.48
All	27.2±5.2	78	102.1±22.5	4± 3%	0.95	99.9±6.4	5± 3%	0.38

Paper #: 107

Predictive Value of Prenatal Alveolar Cleft Size in Determining the Likelihood of Secondary Palatal Defects

Eva Rubio, MD[1], *rubioeva@yahoo.com*; Anna Blask, MD[1], Dorothy Bulas, MD[1]; [1]Children's National Medical Center, Washington, DC

Disclosures: All authors have disclosed no financial interests, arrangements or affiliations in the context of this activity.

Purpose or Case Report: Prenatal ultrasonography (US) remains a primary tool for fetal screening and connecting patients to craniofacial centers. While identification of cleft lip and accompanying cleft of the alveolar ridge is relatively simple, diagnosing clefts of the secondary palate remains challenging. The objective of this study is to review our experience and correlate prenatal alveolar cleft width with the likelihood of a cleft of the secondary palate.
Methods & Materials: With IRB approval, we retrospectively reviewed charts from January 2012 to February 2016. Exclusion criteria included incomplete postnatal follow up and bilateral complete cleft lip/palate. Prenatal and postnatal data were examined. Prenatal imaging findings of the alveolar ridge and any defects were compared with postnatal phenotype.
Results: Of 74 fetuses referred for cleft lip/palate evaluation, 42 had complete prenatal and postnatal data. Excluded were 6 with bilateral defects and 6 with inadequate alveolar visualization. Thirty patients with unilateral defects were analyzed. In 10 patients, the alveolar ridge was intact by prenatal US, all with postnatally confirmed intact secondary palate and cleft lip. Small alveolar defects <4 mm were noted prenatally in 3 patients, and postnatal examination documented complete or near complete cleft lip in all 3, and near complete secondary cleft palate in 1. The remaining 17 patients had alveolar defects of 5 mm or greater diameter on prenatal US; postnatally 15 had complete cleft lip and palate, and the remaining 2 had an intact secondary palate. Based on these measurements, a large alveolar defect on prenatal US indicates significantly greater odds of a secondary palate defect (OR=130.2, p=.0023, 95% CI 5.7-2995.7).
Conclusions: Our review demonstrates that prenatal defects of the alveolus measuring 5 mm or greater are highly predictive of the presence of a cleft of the secondary palate. Per contra, a normal alveolar ridge is associated with intact secondary palate.

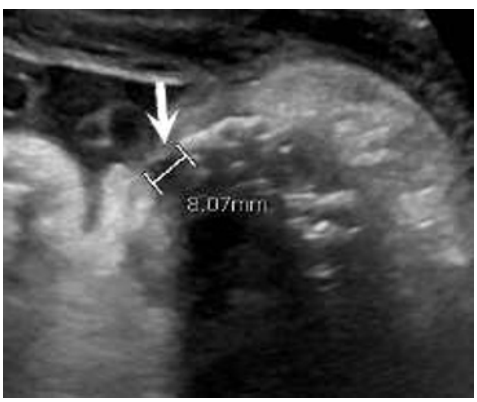

Paper #: 108

The Use of Echo Planar Imaging in the Identification of the Upper Spinal Bony Defect Level During Prenatal Evaluation of Open Neural Tube Defect - A Pilot Study

Carolina Guimaraes[1], *caroguimaraes55@gmail.com*; Fernanda Braojos, MD[1], HaiThuy Nguyen, MD[1]; [1]Texas Children's Hospital, Houston, TX

Disclosures: All authors have disclosed no financial interests, arrangements or affiliations in the context of this activity.

Purpose or Case Report: The upper level of spinal bony defect in cases of prenatally diagnosed open neural tube defect (ONTD) has significant prognostic implications and is one of the criteria used to identify potential candidates for *in-utero* repair. Ultrasound is the current gold standard method for prenatal diagnosis of the defect level but accurate determination can be challenging. The purpose of this pilot study is to evaluate the use of MR echo planar imaging (EPI) in the identification of the upper level of the bony defect in comparison with ultrasound. Optimal imaging acquisition planes will be discussed.
Methods & Materials: All fetuses referred to our institution with the diagnosis of ONTD from August through October 2017 had MR EPI sequence performed in the coronal and axial planes. Ultrasound was performed on the same date, utilizing standard methodology for the evaluation of spinal bony defect. Two fetal radiologists reviewed all the EPI sequences, evaluating for the upper level of spinal bony defect. The reviewers were blinded to any other MRI sequence and to the ultrasound results. After consensus was reached, the level of spinal defect identified on EPI sequence was compared to the level identified on ultrasound.
Results: A total of 11 ONTD patients were imaged during the studied period. EPI sequences were considered non-diagnostic in 2 patients. Of the 9 diagnostic studies, the reviewers' assessment of the upper level of spinal bony defect was identical to the level determined by ultrasound in 8 (88.8%) of 9 evaluated cases (Figures 1 and 2). The single misinterpreted case was in retrospect felt to be at least in part secondary to a technical error, as the coronal plane was centered at the thoracic spine rather than at the lumbosacral spine.
Conclusions: EPI sequence during fetal MRI may be a complimentary or an alternative tool to ultrasound in the assessment of the upper level of spinal defects in patients with ONTD seeking *in-utero* repair. Optimal technique includes the use of axial and coronal planes performed sequentially and perpendicular to each other. The coronal plane should be centered at the lumbosacral region. This ongoing pilot study may serve as the starting point for a collaborative prospective multi-center study. Future directions include comparison with post-natal imaging and assessment of functional levels.

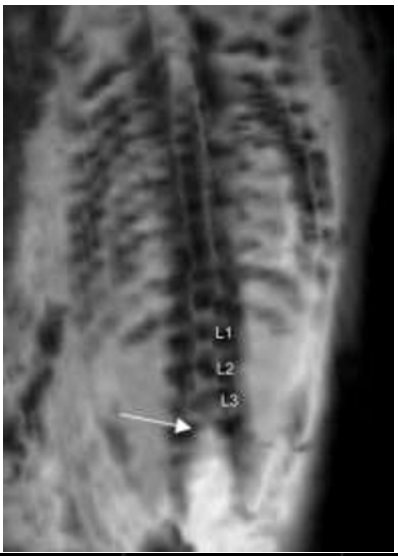

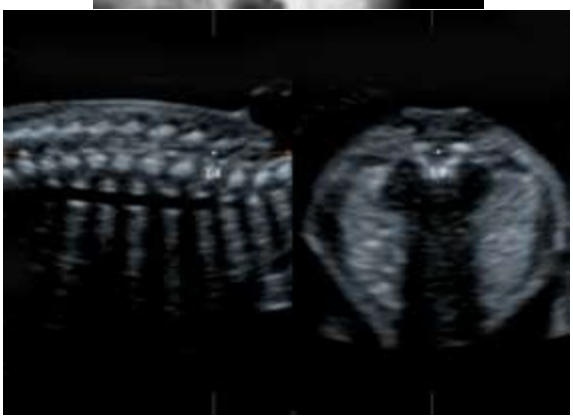

Paper #: 109

Decreased Rectal Meconium Signal on MRI in Fetuses with Open Spinal Dysraphism

Usha Nagaraj[1], *Usha.Nagaraj@cchmc.org*; Maria Calvo-Garcia, MD[1], Arnold Merrow, MD[1], Beth Kline-Fath, MD[1]; [1]Cincinnati Children's Hospital Medical Center, Cincinnati, OH

Disclosures: All authors have disclosed no financial interests, arrangements or affiliations in the context of this activity.
Purpose or Case Report: To evaluate for the presence or absence of meconium signal in fetuses with open spinal dysraphism and correlate findings with the postnatal exam.
Methods & Materials: This is an IRB approved HIPPA compliant retrospective analysis of fetal MRIs performed at our institution for open spinal dysraphism from 2004-2016. Only fetuses ≥20 weeks gestational age with diagnostic quality T1-weighted images on MRI and postnatal clinical and imaging follow-up at our institution were included in this study.
Results: A total of 110 fetuses (average gestational age of 24 ± 3.4 weeks) met inclusion criteria. Of these fetuses, 81.8% (90/110) had T1 hyperintense rectal meconium signal. The average height of the meconium column in fetuses ≥23 weeks with a measurable column was 11.1 ± 4.3 mm; however, all fetuses (n=17) except 1 at gestational age of 23 weeks had a meconium column that measured 9mm or less . 1/110 fetuses had imperforate anus on postnatal exam with rectovestibular fistula, but this fetus had a normal meconium column height on fetal MRI of 22 mm. The remaining 20/110 fetuses lacking normal rectal meconium signal were born without evidence of

anorectal malformation or bowel obstruction.
Conclusions: Decreased or absent T1 hyperintense rectal meconium signal in fetuses with open spinal dysraphisms does not correlate with postnatal anal atresia or bowel obstruction and may be a reflection of neurogenic bowel in this patient population.

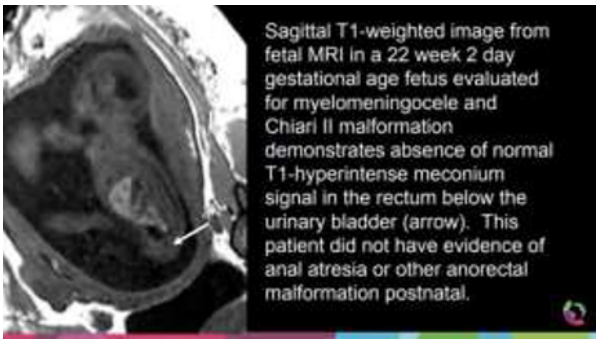

Paper #: 110

Globus pallidus and Dentate nuclei signal on T1-weighted MRI does not change after multiple exposures to Gadobutrol in pediatric patients

Ravi Bhargava, MD FRCPC FRCPC[1], Nikhilesh Bhargava[1], Michael Hawkes[1]; [1]Radiology & Diagnostic Imaging, University of Alberta, Edmonton, AB, Canada

Disclosures: All authors have disclosed no financial interests, arrangements or affiliations in the context of this activity.

Purpose or Case Report: Reports have shown increasing T1 signal of the globus pallidi (GP) and dentate nucleus (DN) post multiple doses of gadolinium based MRI contrast agents. To date, no studies have been performed in children who have solely received multiple doses of the contrast agent gadobutrol (GB). The purpose of our study was to see if patients (pts) who had received at least 5 doses of GB or greater than 14 doses had a change in the signal intensity of the GP or DN.
.**Methods & Materials:** After IRB approval, the brain tumor registry was queried to identify all pts less than 17 years of age seen at our hospital between January 1 2009 and December 31 2016. Pts who received contrast at another hospital, had renal dysfunction, a phakomatosis, had tumor or edema in structures to be measured, received a non-GB MR contrast agent, or did not have a sixth MRI scan were excluded. The remaining pts had the signal intensity of their GP, corpus callosum genu (CC), and DN prior to the administration of 0.1 mmol/ kg of GB measured on T1 non-enhanced axial images from their first 6 MRI's done on our Siemens 1.5 Tesla MRI. A pediatric neuroradiologist measured the signal intensities. Ratios of GP:CC & DN:CC were calculated. Similar measurements were made on all studies of the 6 pts who had received > than 14 doses of contrast.
Results: 91 pts were included. A subset of 46 pts underwent at least 6 GB exams, and 6 of these received > 14 doses. The median age at first exam was 5.4 yrs. (range 26 days-17 yrs) and 53% were male. The GP:CC prior to any GB increased with pt age at first exam (0.0052 per year). In contrast, there was no significant change in the DN:CC with increasing age (Fig. 1). In the subgroup of patients who underwent ≥6 exams and received a median cumulative GB dose of 11 mL (range 3.9-31 mL) between the 1st and 5th, there were no significant changes in signal intensity ratios: +0.018±0.087 (P=0.17) and -0.015±0.11 (P=0.44) for the GP and DN, respectively. Figure 2 compares the group average of ratios between the 1st and 5th GB exams. In the subgroup of patients who underwent ≥14 exams (Fig. 3) and received a median cumulative GB dose of 64 mL (range 40-91) mL by the time of their last exam, there was no statistically significant change in signal intensity ratio in the GP (p=0.15) or the DN (p=0.50) with increasing number of doses of GB.
Conclusions: There is no increase in T1-weighted signal in the globus pallidus or dentate nucleus following the administration of multiple doses of Gadobutrol.

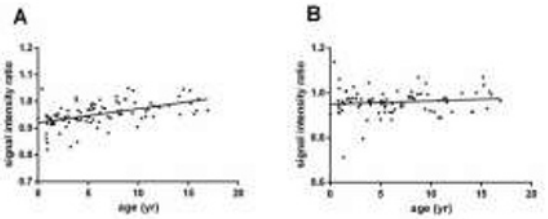

Figure 1. In 91 children undergoing their first MRI (no history of GB administration), signal intensity ratio in the globus pallidus increased with age (Panel A, P<0.0001). In contrast, signal intensity ratio in the dentate nucleus was similar at different ages (Panel B, P=0.30).

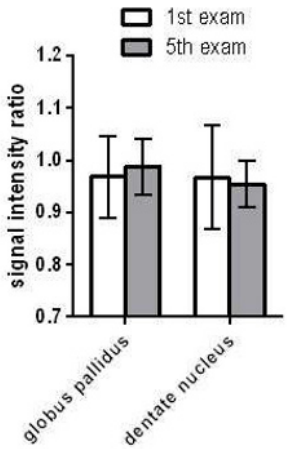

Figure 2. Bar plots of the average globus pallidus and dentate nucleus signal intensity ratios at the first and fifth gadolinium-based contrast agent exam. Error bars indicate standard deviation. No statistically significant differences were observed.

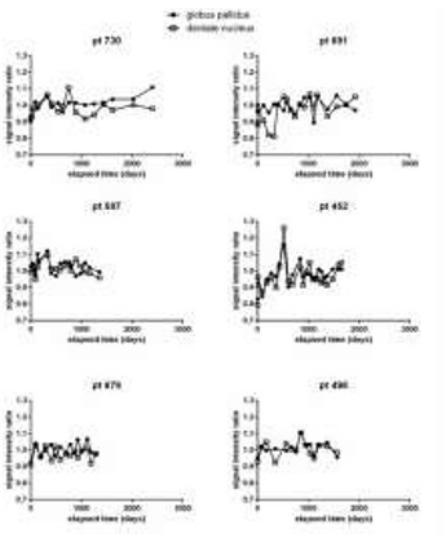

Figure 3. Longitudinal profile of signal intensity ratio in the globus pallidus (solid circles) and the dentate nucleus (open squares) among 6 patients who underwent ≥14 GBCA exams. Using LME models, no statistically significant change in signal intensity ratio was observed with increasing number of doses of gadobutrol.

Paper #: 111

Commonly Encountered Intracranial Calcifications: Prevalence In Pediatric And Young Adult Patients.

Yin Yee Kwong[1], *char.kwong@gmail.com*; Martin LAW[2], Elaine Kan[1]; [1]Department of Diagnostic and Interventional Radiology, Kwong Wah Hospital, Hong Kong, Hong Kong, [2]Department of Radiology, Queen Mary Hospital, Hong Kong

Disclosures: All authors have disclosed no financial interests, arrangements or affiliations in the context of this activity.

Purpose or Case Report: Our aim is to investigate the prevalence of calcification in pineal/ habenular region, choroid plexus and basal ganglia on Computed Tomography(CT) images in first two decades of life.
Methods & Materials: 443 consecutive CT brain plain exams performed for 371 patients age 0-20, in the period of Nov 2015 to Dec 2016, at a single regional hospital were retrospectively analyzed. Patients with pineal mass, history of intracranial haemorrhage, congenital intracranial infection and known metabolic disease were excluded. For patients with multiple scans in this period, only the first study was included. All CT brains were performed with a 64 multidetector CT and 5mm-thick axial images were analyzed on a Carestream workstation by a single radiologist with 7 years of experience.
Results: 363 patients were included in final analysis. The mean age of patient was 10.86 +/- 7.11. There were 167 patients under the age of 10. 205 patients were male.
Pineal/habenular calcifications were present in 35.8% (n=130; age range 6-20 years; median 17 years) (5.4% for Pt age 0-10). Choroid plexus calcifications were noted in 24.2% (n=88; range 3-20; median 17 years) (3.6% for Pt age 0-10). Only 1.1% patients had basal ganglia calcifications (n=4; range 14-20; median 16.5 years).
There was positive correlation between presence of pineal calcifications and choroid plexus calcifications ($P<0.0001$) as well as between presence of pineal calcifications and basal ganglia calcifications ($p<0.05$). No statistically significant difference was detected between the patients' sex and the presence of calcification in any of the region of interest.
Conclusions: Pineal/habenular calcifications are the most common
physiological intracranial calcifications in this age group while basal ganglia calcifications are the least common physiological intracranial calcifications**.** Pineal/habenular calcifications are not present in children younger than 6 years of age, hence if seen before the age of 6, pathological cause might need to be considered.

Paper #: 112

Sonographic Fronto-Occipital Ratio (FOR) in Evaluation of Hydrocephalus

Michele Retrouvey[1], *michele.retrouvey@gmail.com*; Susan Back, MD[1], Richard Bellah[1], Arastoo Vossough, PhD, MD[1], Gregory Heuer, MD[1], John Flibotte, MD[1], Summer Kaplan, MD MS[1]; [1]The Children's Hospital of Philadelphia, Philadelphia, PA

Disclosures: All authors have disclosed no financial interests, arrangements or affiliations in the context of this activity.

Purpose or Case Report: Neonatal hydrocephalus is a common problem and imaging is critical to guiding intervention, such as the timing of shunt placement. Measurement of the fronto-occipital ratio (FOR) has been validated on magnetic resonance imaging as an objective tool for tracking ventricular size. However, neonates are more routinely evaluated with head ultrasound (US). FOR relies on axial measurements and its use has not been validated in ultrasound. We have developed a modified FOR calculation based on landmarks in the coronal plane on US. We sought to evaluate inter-rater reliability of FOR measurements on US and MRI and to compare the measurements from these modalities.
Methods & Materials: We retrospectively reviewed images acquired between 01/01/2010 and 08/31/2017 on infants < 1 year old who had a FOR head US protocol and a brain MRI within a 24-hour time frame. Myelomeningocele patients were the predominant patient population, and therefore were exclusively considered for this study. Patients who had shunt placement between the US and MRI, or with excessive image motion degradation were excluded. Two reviewers independently measured FOR in the axial plane on MR (MR-FOR) and in the coronal plane on US (US-FOR). Inter-rater reliability for both US-FOR and MR-FOR was assessed using intraclass correlation coefficient with two-way mixed effects model for absolute agreement. Agreement between US-FOR and MR-FOR was assessed using Pearson correlation coefficient and Bland-Altman analysis. Systematic differences in US-FOR and MR-FOR measurements were assessed using paired two-way t-test on the mean of two measurements.
Results: We enrolled 18 exam pairs meeting our criteria. The inter-rater reliability for US-FOR was 0.979 ($p<0.001$), and for MR-FOR was 0.990 ($p<0.001$). Correlation between US-FOR and MR-FOR showed $r = 0.867$ ($p<0.001$) and the Bland-Altman plot showed substantial agreement. US-FOR overestimated size compared to axial MR-FOR as standard by an average of 0.077 ($p=0.0079$, 95% confidence interval: 0.053 to 0.100).
Conclusions: Our results show strong evidence for developing clinical use of US-FOR in management and monitoring for neonatal hydrocephalus. Inter-rater reliability is high and is comparable to accepted standard MR or CT measurement. There is good agreement between US-FOR and MR-FOR values. Current literature lacks objective guidelines for shunt placement, especially in children with myelomeningocele and US-FOR may provide a reliable and accessible tool for evaluation.

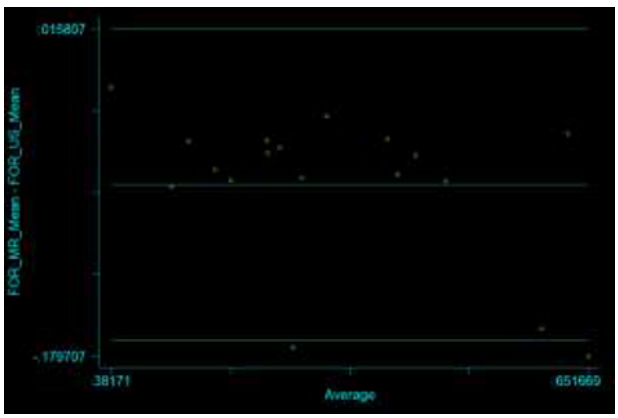

Paper #: 113

Ferumoxytol whole body vascular imaging including the central nervous system in pediatric patients: a single center's initial experience

Josephine Ndolo, MBChB[1], *josephine.m.ndolo@vanderbilt.edu*; Allen Newton[1], Jason Christensen, MD[1], Aashim Bhatia[1]; [1]Vanderbilt Children's Hospital, Nashville, TN

Disclosures: All authors have disclosed no financial interests, arrangements or affiliations in the context of this activity.

Purpose or Case Report: Ferumoxytol, an iron oxide nanoparticle coated by a carbohydrate shell, is increasingly reported as an off-label blood pool contrast agent for MR angiography (MRA). We explore its use in the central nervous system (CNS) and whole-body vascular imaging in pediatric patients.

Methods & Materials: Use of ferumoxytol for MRA was approved by the pharmacy and therapeutics committee. We retrospectively included patients from our initial three cases undergoing whole body and brain MRI for vascular abnormalities such as Takayasu's arteritis and Loeys-Dietz Syndrome in 2017.

Three children underwent MRA examinations at 3.0 T MRI after administration of diluted ferumoxytol at a dose of 3 mg/kg over 15 minutes. Whole body vascular imaging focused on the brain, chest, abdomen, and selected extremities based on clinical history. (fig 1, 2.)

Two blinded radiologists independently scored 11 named arteries on ferumoxytol-enhanced MRA according to a three-point subjective score where a score > 2 was considered diagnostic. The three-point scale was as follows: 1=Poor, precluding confident assessment; 2=Adequate for confident assessment of stenosis or occlusion, and 3=Excellent vascular definition sufficient for evaluation of fine detail. A total of 11 arteries in the head, neck, chest and abdomen were assessed for vessel caliber, tortuosity, stenosis and wall thickening.

Results: In all patients, the arteries were clearly visualized from the circle of Willis to the lower extremities with excellent signal-to-noise ratio. The average image quality scores for selected arteries was between 2.6 and 2.9. (fig 3.)

The radiologists were also able to confidently detect and characterize vascular abnormalities including tortuosity, stenosis, and wall thickening.

None of the patients had an adverse reaction to the ferumoxytol.

Conclusions: Ferumoxytol-enhanced MRA is a promising agent for the detection of vascular abnormalities in the brain or whole body. Additionally, the radiologist can interrogate multiple territories in one study, due to ferumoxytol's highly stable intravascular time. Therefore, from our early experience, ferumoxytol is a potential alternative to gadolinium-based contrast agents for high resolution neuro- and whole body MR angiography.

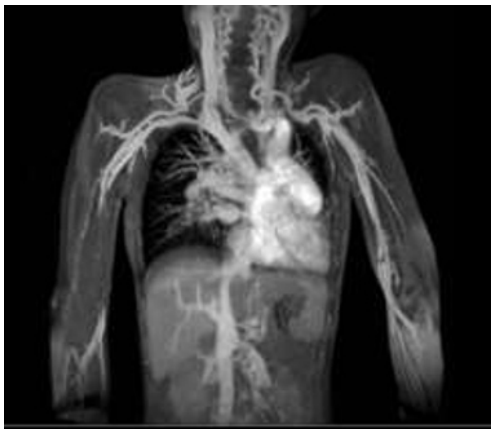

Figure 2. Arterial grading data

ARTERIES	Patient 1 average grading	Patient 2 average grading	Patient 3 average grading
ICA - cervical	3	2.5	3
ICA - petrous	3	2.5	3
ICA - cavernous	3	3.5	3.5
ICA - supraclinoid	2	3	3
Middle Cerebral	2	3	3
Vertebral (V4)	3	3	3
Basilar	3	3	3
Posterior cerebral	3	3	3
Subclavian	3	2	2
Brachiocephalic	3	3	3
Common carotid	3	3	3
Superior mesenteric	3	3	3
Celiac	2	3	3
Renal	3	3	2

Paper #: 114

Arterial Spin Labeling and Ferumoxytol-based Spoiled Gradient Recalled Acquisition Magnetic Resonance Imaging Versus Digital Subtraction Angiography for Surveillance of Residual Brain Arteriovenous Malformations in Children: A Single-Institution Analysis of Inter-Modality Reliability

Anjeza Chukus[1], *anjac18@gmail.com*; Michael Iv[1], Kristen Yeom, MD[1]; [1]Stanford University, Stanford, CA

Disclosures: All authors have disclosed no financial interests, arrangements or affiliations in the context of this activity.

Purpose or Case Report: Pediatric patients with brain arteriovenous malformations (AVMs) typically undergo a Digital Subtraction Angiography (DSA) at diagnosis and for surveillance following surgical intervention. To limit risk exposure from DSA, including radiation, we evaluated the sensitivity, specificity, and inter-modality agreement of DSA versus Magnetic Resonance with ferumoxytol contrast (Feraheme®, AMAG Pharmaceuticals Inc., Cambridge, MA, USA) using Arterial Spin Labeling (ASL) and Spoiled Gradient Recalled Acquisition (SPGR) series for surveillance of residual AVM.

Methods & Materials: A retrospective, single-center cohort of children treated for AVM from 2014 to 2016 who underwent surveillance by ASL, SPGR, and DSA was assembled. Comparing modalities, blinded raters assessed residual AVM, lesion evolution, and their diagnostic confidence using a Likert scale. Sensitivity, specificity, and inter-modality reliability were determined with DSA as the gold standard. Acute radiation exposure was compared to a safety threshold of 2Gy.
Results: Fifteen patients met criteria (mean 11 years, range 3 to 17). Average time between MR and DSA was 17 days (SD=98). Cohen's Kappa for ASL plus SPGR with DSA was 0.848 (p = <0.001), ASL only was 0.393 (p = 0.0139), and SPGR only was 0.848 (p = <0.001). Sensitivity and specificity of ASL plus SPGR and ASL and SPGR only were 92% and 100%, 72% and 100%, and 92% and 100% respectively. Raters reported greater diagnostic confidence with ferumoxytol MR series versus standard MR. On average, patients received two DSA studies for surveillance. Per study, radiation for Total Dose Area Product, Total Air Kerma, and Peak Air Kerma was 58,632 mGy.cm2 (95% CI: 38,570, 78693), 562 mGy (95% CI: 378, 747), 310 mGy (95% CI: 209, 411).
Two surveillance DSA studies constitute 56% (95% CI: 38-75%) of the 2Gy safety threshold.
Conclusions: Ferumoxytol-based MR performed excellently for AVM surveillance in children and should be considered to supplant Digital Subtraction Angiography.

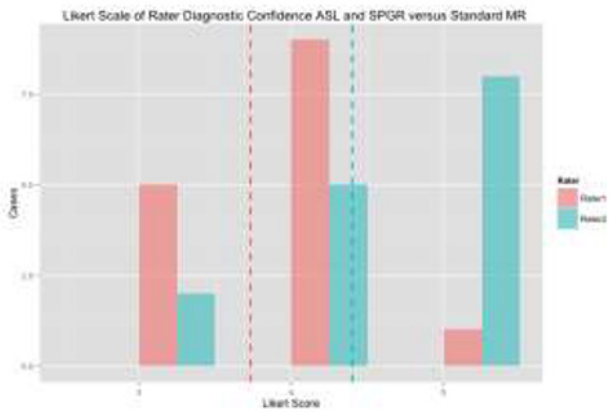

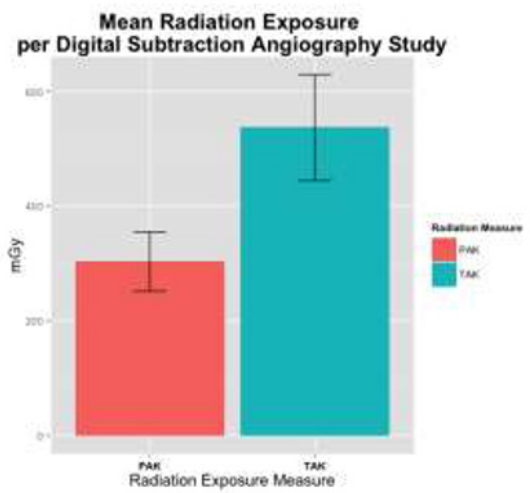

Paper #: 115

Gender-dependent cerebrovascular alterations in Moyamoya mice model correlate with the prevalence in pediatric population

Zbigniew Starosolski, PhD[1],
zastaros@texaschildrenshospital.org; Jamie Wright[2], Dianna Milewicz[2], Ananth Annapragada, PhD[1]; [1]Pediatric Radiology, Texas Children's Hospital, Houston, TX, [2]UT Health Medical School, Houston, TX

Disclosures: Ananth Annapragada has indicated. All other authors have disclosed no financial interests, arrangements or affiliations in the context of this activity.

Purpose or Case Report: Moyamoya disease (MMD) is a rare pediatric cerebrovascular disease characterized by abnormal straightening of cerebral arteries, progressive bilateral narrowing of Internal Carotid arteries and frequent occlusions in the Circle of Willis. The prevalence of MMD is higher in females than in males. ACTA2 mutations cause moyamoya-like arteriopathy. We assessed vessel morphology in the ACTA2-/- mouse model. This study was designed to evaluate morphological features in the ACTA2 -/- mouse model and to evaluate if the model follows the gender-distribution of human Moyamoya disease.
Methods & Materials: Animals (n=44) at 8-10 week age were i.v. injected with liposomal blood pool CT contrast agent and imaged with μCT. The animals were scanned while free breathing under anesthesia using 1.5 - 2.5% isoflurane. Images were reconstructed with 19 μm isotropic voxel size, insuring visualization of vessels > ~50 μm diameter. Only animals with a complete Circle of Willis were included in morphometric analysis (n=26). Image analysis of the CoW arteries was performed using a custom software and ImageJ.
Results: Wild type males and females do not show significant differences in morphometric features associated with MMD. Acta2-/- animals exhibit several morphometric changes compared to wild type. Fig1 shows a volume rendering of CoW area for representative animals. Fig1A-B, show normal, unaltered cerebral vasculature, while Fig1 C-D show straightening and reduced symmetry ib ACTA2 -/- animals. Acta2-/- females exhibit the greatest severity of cerebral malformation in the narrowing of L-SCA, curvature and mean circularity of L-ITCD and the lowest CoW area. Acta2-/- animals show straightening of large cerebral arteries, characteristic features of MMD. Acta2-/- females have more prominent malformations compared to males. Fig2A shows diagram of CoW arteries with only the morphometric features that are significantly different between tested groups. Fig2B is a box plot of vessel narrowing, ACTA2 -/- females have significantly greater narrowing (p<0.02) compared to the other groups, consistent with human disease. The ACTA2 -/- model therefore recapitulates the increased severity of disease in females as observed in humans.
Conclusions: The ACTA2 -/- model exhibits gender dependent MMD, consistent with the human condition. Morphometric analysis allows investigation of the alterations in cerebrovasculature of a MMD mouse model. ACTA2 -/-female mice show more severe arterial narrowing than ACTA2-/- male mice.

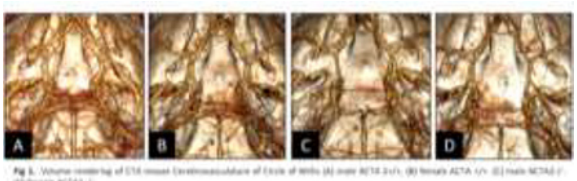

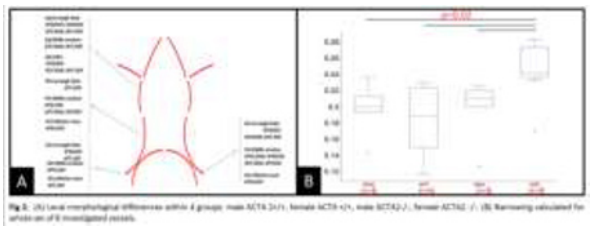

Paper #: 116

Motion Insensitive 3D T1-Weighted Post-Contrast Brain MRI Using a Golden Angle Radial Acquisition

Houchun Hu, PhD[3], *houchun.hu@nationwidechildrens.org*; Thomas Benkert, PhD[1], Jerome Rusin[3], Jeremy Jones, MD[3], Aaron McAllister, MD[3], Mark Smith, MS[3], Ramkumar Krishnamurthy, PhD[3], Rajesh Krishnamurthy, MD[3], Kai Tobias Block, PhD[2]; [1]Siemens Healthineers, Enlargen, Germany, [2]New York University Medical Center, New York, NY, [3]Radiology, Nationwide Children's Hospital, Columbus, OH

Disclosures: Thomas Benkert has indicated a relationship with Siemens Healthineers for receiving a salary. Aaron McAllister has indicated a relationship due to ownership with 3M, GE, JNJ and CHD. All other authors have disclosed no financial interests, arrangements or affiliations in the context of this activity.

Purpose or Case Report: With increasing interest in rapid MRIs aimed to reduce sedation in pediatric imaging, the purpose of this study was to evaluate a 3D golden-angle radial "stack of stars" gradient echo scan (i.e., RAVE - RAdial Volumetric Encoding) and to compare results with a conventional 3D inversion recovery sequence in post contrast brain imaging.
Methods & Materials: Studies were performed on a 3T Siemens Prisma system using either a 20 or 64-channel head array. Unlike traditional Cartesian acquisitions, MRI data in RAVE is acquired with consecutive k-space spokes that are rotated by the golden-angle (111.25 deg) to maximize k-space coverage efficiency. As a result of the radial trajectory, the center of k-space is oversampled and this feature affords RAVE's robustness to motion. When coupled with compressed sensing and parallel imaging, RAVE data can further yield time-resolved images during contrast passage. We evaluated RAVE in 20 patients (average age: 12.5y, range 2.2-21y) referred for brain MRI exams with contrast. Upon injection of standard dose contrast media (Gadavist), data from a RAVE acquisition and a conventional 3D IR-GRE (i.e., MPRAGE) were implemented (MPRAGE first). The two scans were matched in 1 mm native isotropic spatial resolution and volume coverage. On average, the MPRAGE acquisition took 5-6 minutes to complete, whereas the RAVE scan is ~25-30% faster. Three radiologists independently compared the data in terms of conspicuity of contrast-enhancing lesions and diagnostic image quality with respect to motion-related artifacts. A 3-point scale was used: -1=RAVE is superior, 0=RAVE and MPRAGE are equivalent, +1=MPRAGE is superior.
Results: All evaluators found the RAVE with MPRAGE reformats to be similar when presenting contrast-enhanced details in 15 cases (score= 0). In the remaining 5, RAVE was preferred (score= -1). RAVE was notably more resistant to subject motion and pulsation artifacts. No significant artifacts were noted in RAVE. Figures 1 and 2 show data in non-sedated 13y and 11y old patients, respectively, with significant head movements. Figure 3 illustrates time-resolved images from RAVE in a 7y old, 20s apart, showing an enhancing lesion (arrow).
Conclusions: Our study demonstrates the potential clinical utility of an accelerated 3D T1-weighted RAVE MRI sequence in unsedated pediatric brain imaging. The complementary technique is particularly useful in patients prone to head (and body) motion. Further evaluation in neonatal imaging and body and spine applications are warranted.

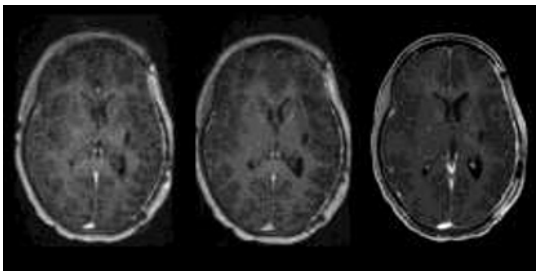

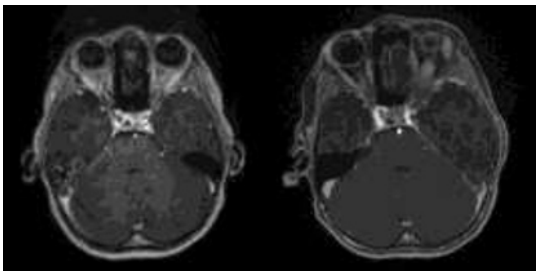

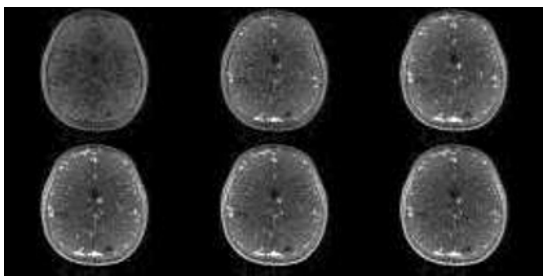

Paper #: 117

Quantitative Multi-Delay Arterial Spin Labeling MRI in Neonates and Children: Preliminary Experience

Houchun Hu, PhD[2], *houchun.hu@nationwidechildrens.org*; Mark Smith, MS[2], Jerome Rusin[2], Jeremy Jones, MD[2], Ramkumar Krishnamurthy, PhD[2], Bhavani Selvaraj[2], Rajesh Krishnamurthy[2], JJ Danny Wang, PhD[1]; [1]Laboratory of Neuro Imaging, University of Southern California, Los Angeles, CA, [2]Radiology, Nationwide Children's Hospital, Columbus, OH

Disclosures: Danny Wang has indicated a relationship with Transitional MRI, LLC for stock options. All other authors have disclosed no financial interests, arrangements or affiliations in the context of this activity.

Purpose or Case Report: With increasing concerns over intracranial Gd deposition, the purpose of this study was to evaluate a new quantitative 3D multi-phase arterial spin labeling (ASL) technique that yields cerebral blood flow, arterial transit time, and cerebral blood volume in neonates and children via a single acquisition. While the technique has been reported in adult populations, feasibility and application in pediatrics has not been previously demonstrated.
Methods & Materials: All studies were performed on a 3T Siemens Prisma platform and data were successfully reconstructed offline. We evaluated the technique in 3 neonates (5d-4mo) and 8 children (2.3y-17.8y). The multi-phase pseudo continuous ASL technique employed in this work consisted of a 5 post-labeling delay (PLD) scheme (300-2500ms with ~500ms intervals), with a label duration of 1500ms placed above the

carotid bifurcation. The sequence used a hybrid 3D gradient-spin-echo (i.e., GraSE) design to acquire data across the whole brain using a voxel size of 2.5mm in-plane and 3-4mm slices. We used a labeling distance of 75-90mm. Typical scan time was 6 minutes. Fitting of the multi-PLD signals subsequently yields cerebral blood flow (CBF), arterial transit time (ATT), and cerebral blood volume (CBV) maps. Three radiologists evaluated the ASL data in two categories: image quality (1-significant artifacts, 2-negligible artifacts, 3-no artifacts), and diagnostic utility in providing relevant information towards patient care (0-not useful, 1-useful).

Results: Figure 1 shows representative results in a normal 2y. Top row panes show individual images at the 5 PLDs. Note symmetry in the quantitative CBF, ATT, and CBV data that are shown in color in the lower row. Figure 2 shows select slices in a 10y with history of rhabdomyosarcoma, using the same color scale. Note asymmetry in the CBF map (thick arrow) and longer ATT (thin arrow), resulting in greater CBV posteriorly. Figure 3 shows a 17y patient with a history of stroke. There are two perfusion deficits (thick arrows) in the right anterior lateral frontal lobe, which corresponds to foci of cystic encephalomalacia seen on anatomical images. All radiologists found the ASL data to be clinically informative. One case had significant artifacts. Two cases had negligible artifacts. The remainder had no perceivable artifacts.

Conclusions: Our preliminary study demonstrates the feasibility of multi-phase ASL in pediatrics. Further evaluation in patients with seizures, strokes, tumors, and vascular malformations is warranted.

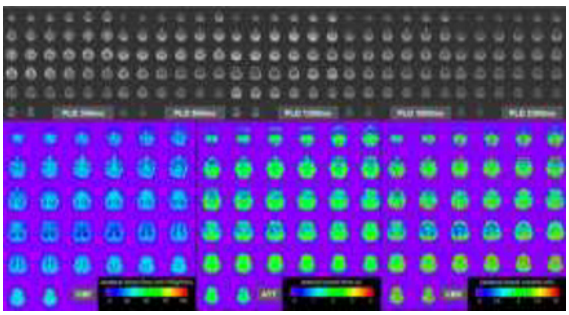

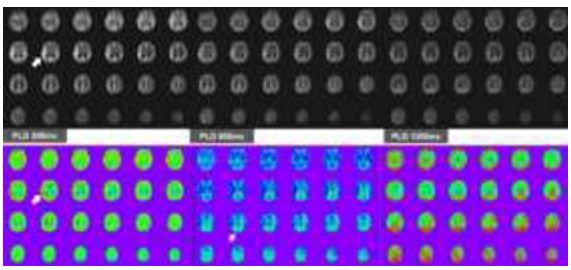

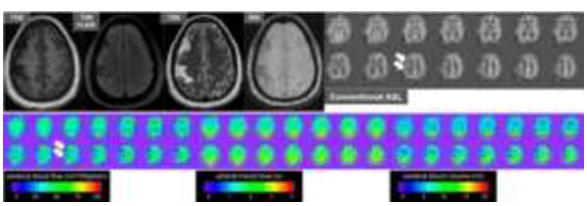

Paper #: 118

MR correlation of spica hip arthrographic sliver sign during closed reduction of developmental hip dysplasia of the hip

Maddy Artunduaga, MD[1], *maddyar@gmail.com*; J. Kan, MD[1], Matthew Ditzler, MD[1], Wei Zhang, PhD[1], Siddharth Jadhav, MD[1], Scott Rosenfeld[1]; [1]Texas Children's Hospital, Houston, TX

Disclosures: All authors have disclosed no financial interests, arrangements or affiliations in the context of this activity.

Purpose or Case Report: Intra-operative arthrography is commonly performed during closed hip reduction for the treatment of developmental dysplasia of the hip (DDH) to confirm hip location and identify potential intrinsic obstacles to reduction. While an arthrographic limbus sign has been described in the literature, in some cases, a "sliver" of contrast can be also identified extending along the superolateral recess of the femoroacetabular joint (figure). The aim of this study was to identify the prevalence and MR anatomic correlation of the spica hip arthrographic sliver sign after closed reduction for the treatment of DDH

Methods & Materials: A total of 51 hips in 42 patients, 37 females and 5 males less than 2 years of age who underwent closed reduction for DDH, were identified between 1/2011-9/2017. Syndromic and neuromuscular hip dysplasias were excluded. All patients had intra-operative arthrogram and subsequent spica MRI and were reviewed by a pediatric musculoskeletal radiologist. For intra-operative arthrography, the presence of sliver sign (figure), inverted limbus sign, or normal was determined. Findings were then correlated with spica MRI as reference and chondrolabral pathology was then categorized

Results: For the 51 hips, arthrographic sliver sign, inverted limbus sign, and normal were present in 10/51 (20%), 35/51 (69%), and 6/51 (12%), respectively. The prevalence of any labral pathology in the setting of a sliver sign, inverted limbus sign and normal arthrography were 6/10 (60%), 33/35 (94%) and 4/6 (67%), respectively (P=0.0136). For the sliver sign, 4 true positive studies represented a chondrolabral junction tear and 2 reflected a labral tear. In re-review of false positive intra-operative arthrograms for the sliver sign with correlation with spica MRI, this false positive finding was attributed to a normal labrocapsular recess projecting over the lateral column due to obliquity of the pelvis to the beam (N=4) rather than a chondrolabral junction or labral tear

Conclusions: We describe a new finding entitled the sliver sign, which is seen in approximately 20% of all arthrographic cases after closed hip reduction for the treatment of DDH. This sign corresponds to a chondrolabral junction tear in the majority of the cases although with a high false positive rate. It is important to obtain true AP views of the pelvis during arthrography as overlay of the normal labrocapsular recess along the lateral acetabular column can mimic the sliver sign.

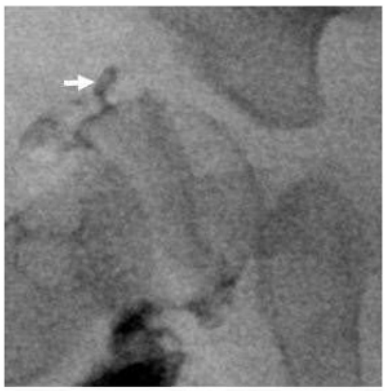

Figure A. Sliver sign in a 3-month-old girl with right DDH with intra-operative arthrography (arrow).

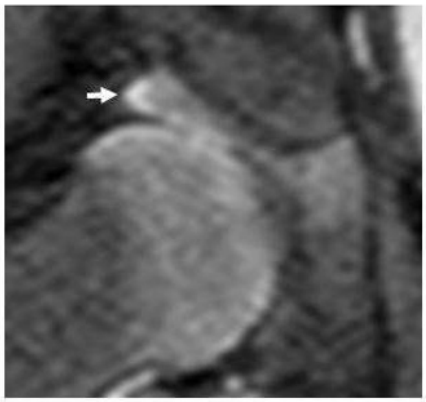

Figure B. MR T2 FS coronal performed immediately after arthrogram shows high-signal curvilinear extending along the chondrolabral junction reflecting a chondrolabral junction tear (arrow).

Paper #: 119

Correlation of arthrographic inverted limbus sign and spica MRI in developmental dysplasia of the hip

Maddy Artunduaga, MD[1], *maddyar@gmail.com*; J. Kan, MD[1], Matthew Ditzler, MD[1], Siddharth Jadhav, MD[1], Scott Rosenfeld[1]; [1]Texas Children's Hospital, Houston, TX

Disclosures: All authors have disclosed no financial interests, arrangements or affiliations in the context of this activity.

Purpose or Case Report: Intra-operative arthrography is routinely performed during closed reduction of developmental dysplasia of the hip (DDH). When present, an arthrographic inverted limbus sign (figure) is thought to represent interposed hypertrophied fibrocartilaginous labral tissue that may prevent concentric reduction of a dysplastic hip. The purpose of this study was to investigate the prevalence and anatomic MRI correlation of an inverted limbus sign identified by arthrography in children treated with closed hip reduction for DDH

Methods & Materials: This is a retrospective descriptive study. A total of 51 hips in 42 patients, 37 females and 5 males less than 2 years of age who underwent closed reduction for DDH, were identified between 1/2011-9/2017. Syndromic and neuromuscular hip dysplasias were excluded. All patients had intra-operative arthrogram and subsequent SPICA-MRI, which were reviewed by a pediatric musculoskeletal radiologist independently. For intra-operative arthrography, the presence or absence of an inverted limbus sign was documented. Afterward, MR findings of intrinsic superior femoroacetabular soft tissue interposition was evaluated and categorized based on pathology when present

Results: An arthrographic inverted limbus sign (figure) was identified in 35/51 hips (69%). When an inverted limbus sign was arthrographically found, an inverted labrum was present in 20 hips by MRI (57%). Alternative diagnoses on MRI (N=15) were a displaced or sheered-off superior labrum (N=2), a chondrolabral junction tear (N=11), and an entirely normal superior labrum (N=2). For the 16 hips that did not have an arthrographic inverted limbus sign, the range of MRI findings included a chondrolabral junction tear (N=7), an inverted labrum (N=2), a destroyed superior labrum (N=1), and an entirely normal superior labrum (N=6). The sensitivity and specificity of an arthrographic inverted limbus sign to detect labral pathology were 77% and 76%, respectively

Conclusions: An intra-operative arthrographic inverted limbus sign is a common arthrographic finding after closed reduction of DDH but is an unreliable indicator of an inverted superior labrum. Arthrography after closed hip reduction plays a valuable role in confirming concentric reduction of the hip intra-operatively. However, its role in identifying intrinsic obstacles to full reduction is limited when compared to post-reduction SPICA MRI

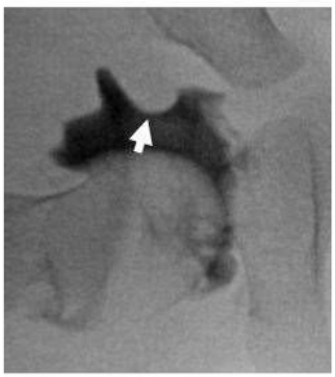

Figure A. Classic arthrographic inverted limbus sign in a 17-month-old female with right DDH (arrow).

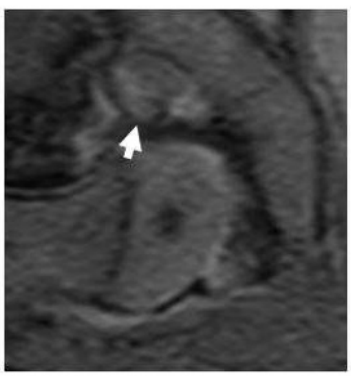

Figure B. MR T2 FS coronal performed immediately after arthrogram demonstrates an inverted labrum in the superior femoro-acetabular recess (arrow).

Paper #: 120

Diffusion-Tensor Imaging of the femoral physes: Can we predict future growth?

Maria Bedoya, MD[1], *bedoya3@gmail.com*; Christian Barrera, MD[1], Jorge Delgado[1], Nancy Chauvin, MD[1], Victor Ho-Fung, MD[1], Diego Jaramillo, MD, MPH[2]; [1]Radiology, The Children's Hospital of Philadelphia, Philadelphia, PA, [2]Nicklaus Children's Hospital, Miami, FL

Disclosures: All authors have disclosed no financial interests, arrangements or affiliations in the context of this activity.

Purpose or Case Report: Prior studies have shown that Diffusion-Tensor imaging (DTI) parameters (ADC, track length and volume) are higher in children who are at ages when the growth is fastest. Our purpose is to determine longitudinally the correlation between DTI tractography in the distal femur with growth rate and final height in children.

Methods & Materials: We identified retrospectively all children without physeal pathology and available DTI of the knee who were imaged at puberty age (girl ≥ 11 years, boys ≥ 13 years) according to their bone age. We recorded the heights at the moment of imaging and at maturity. Growth rate (cm/year) and height change from DTI to final height were calculated. We only included children who had reached their final height according to their growth chart and whose last measurement was at least 12 months after the MRI. On sagittal echo-planar DTI (20 directions, b values of 0 and 600 sec/mm^2), region of interest was placed in the femoral physis. Using a fractional anisotropy threshold of 0.15 and an angle threshold of 40°, we performed tractography and measured track number, length, volume and apparent diffusion coefficient (ADC). We used Mann-Whitney U test to compare DTI parameters with growth rate and Spearman Rho to assess correlation between DTI parameters and height change.

Results: We analyzed DTI images of 28 girls and 14 boys (42 subjects) with a mean age of 14.4 ± 1.5 (mean ± SD, range 11 - 17) and 15.1 ± 1.32 (range 12 - 17), respectively. The mean follow-up time was 28.4 ± 11.9 months between DTI and final height. Average growth rate and height change were 0.9 ± 1.5 cm/year and 2.4 ± 4.2 cm, respectively. Children with greater than the 50th percentile of growth rate had longer tracts, greater tract volumes and higher tract numbers compared to those below the 50th percentile of growth rate (Figure 1, *ps*<0.05). Mean diffusion parameters by groups are shown in Table 1. In addition, children with higher track number, longer tract length and greater tract volume have greater height change form DTI to final height (Figure 2, $r_s > .70$, $p < 0.01$).

Conclusions: This longitudinal study shows that during and after puberty, children grow more when their distal femoral physeal tracts are longer, more numerous, and have greater volume. The high correlation between DTI parameters and height change takes us closer to be able to predict potential of growth and possibly final height using DTI of the physes.

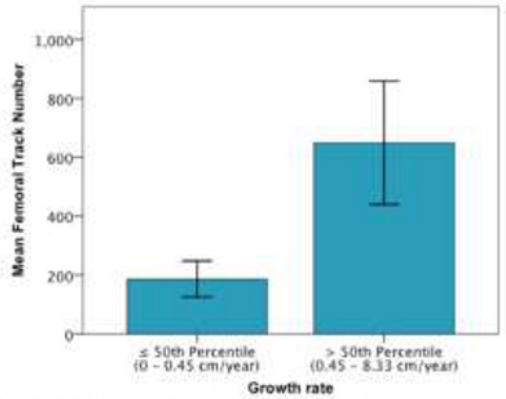

Figure 1. Bar chart shows the mean femoral track number in children with a growth rate over and below the 50th Percentile. Error Bars: 95% Confidence Interval

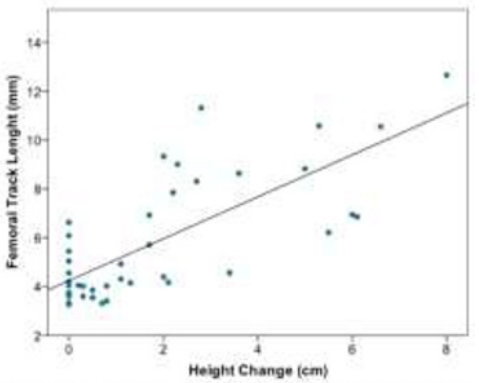

Figure 2. Scatterplot shows the correlation of the femoral track length with the height change between the initial and final height measurement

Table 1. Mean diffusion parameters of distal femoral physes according to growth rate percentile

DTI parameter (mean ± SD)	Growth rate percentile		p-value†
	≤ 50th Percentile	> 50th Percentile	
Track number	186.4 ± 134.8	649.5 ± 459.9	<.01
Track length (mm)	4.54 ± 1.44	7.25 ± 2.68	<.01
Track volume (cm^3)	4.15 ± 2.78	11.9 ± 7.55	<.01
ADC (mm^2/sec)	0.0011 ± 0.0002	0.0013 ± 0.0002	<.05

Note:† Mann-Whitney U test, DTI = Diffusion-Tensor Imaging, ADC = Apparent Diffusion Coefficient

Paper #: 121

Diffusion Tensor Imaging for the Evaluation of Physeal Microstructural Changes in Children Treated with High Dose *Cis*-Retinoic Acid (Cis-RA) for High Risk Neuroblastoma

Jorge Delgado[1], *delgadoj@email.chop.edu*; Hannah Sweeney, BS[1], Diego Jaramillo, MD, MPH[2], Nancy Chauvin, MD[1], Christian Barrera, MD[1], Sogol Mostoufi-Moab, MD[3]; [1]Radiology, Children's Hospital of Philadelphia, Philadelphia, PA, [2]Nicklaus Children's Hospital, Miami, FL, [3]Department of Pediatrics, Division of Oncology, The Children's Hospital of Philadelphia, Philadelphia, PA

Disclosures: All authors have disclosed no financial interests, arrangements or affiliations in the context of this activity.

Purpose or Case Report: Survival improvements in patients with high-risk neuroblastoma (HR-NBL) stem from increasingly intensive multi-modal therapy. The majority of HR-NBL survivors demonstrate striking growth failure and short stature even in the absence of treatment with total body irradiation. *Cis*-RA is a vitamin A derivative with numerous side effects, including osteoporosis and premature physeal plate closure. The goal of this study was to assess changes in physeal microstructure using diffusion-tensor imaging (DTI) of the distal

femoral physis in survivors of HR-NBL treated with high dose *cis*-RA.

Methods & Materials: We prospectively obtained and analyzed DTI of the distal femoral physis at 3.0T in 20 subjects (13 males, 7 females; mean age 12.4; range 9.5-16.3) diagnosed with HR-NBL and treated with high dose *cis*-RA. Survivors were compared with 40 sex- and age- (within 6 months) matched healthy controls that completed DTI at 3.0T, 26 males, 14 females (mean age 12.4; range 9.4 - 15.7). DTI were performed as sagittal echo-planar DTI (20 directions, b values of 0 and 600 sec/mm^2), and regions of interest (ROI) were placed in the femoral physis. For DTI post-processing, a fractional anisotropy (FA) threshold of 0.15 and an angle threshold of 40° were used. Parameters evaluated included: ROI based apparent diffusion coefficient (ADC) and FA, mean tract length, tract concentration (tract count/ROI area) and normalized track volume (track volume (cm^3)/ROI area(cm^2)). Mann-Whitney U test was used to analyze DTI parameters.

Results: Compared to healthy controls, the FA (P<0.001), normalized tract volume (P<0.01), and mean tract length (P=0.04) were lower in HR-NBL subjects. Tract concentration was half of normal (P<0.001). Difference of ADC values demonstrated a trend for statistical significance (P=0.06). Due to the presence of more random tracts in the impacted physes, the mean tract length underestimates the extent of disease. **Table 1** demonstrates median values and interquartile ranges of DTI parameters in HR-NBL survivors and controls.

Conclusions: DTI of the femoral physis demonstrated physeal disorganization with smaller and shorter physeal tracts in the femoral physis of HR-NBL survivors treated with high dose *cis*-RA compared to age- and sex-matched controls. Survivors demonstrated lower values for the concentration of tracts, normalized tract volume and the FA. These findings highlight the use of DTI of the femoral physis as an effective imaging modality to assess physeal damage due to antineoplastic treatment.

Figure 1. Femoral tractographic pattern overlaid on coronal reformation in an 11.3 year-old girl with history of high risk neuroblastoma treated with cis-Retinoic Acid (cumulative dose of 13,302 mg/m²). Short non-vertical tracts are visualized.

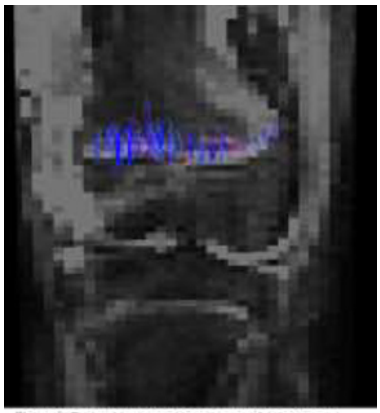

Figure 2. Femoral tractographic pattern overlaid on coronal reformation in a control 10.9-year-old girl. Note the presence of longer, more vertical tracts in the femoral physis compared to figure 1.

Median (interquartile range)	HR-NB (cases) (n=20)	Controls (n=40)	P-Value
Mean Age (years) (range)	12.5 (9.5-16.0)	12.4 (9.4-15.8)	-
Sex (M/F)	13/7	26/14	-
ROI FA	0.22 (0.18-0.26)	0.30 (0.26-0.35)	<0.001
Mean tract length (mm)	5.85 (4.77-7.18)	6.69 (5.66-8.59)	0.038
Tract concentration (tracts/cm²)	20.4 (10.7-31.1)	40.8 (26.0-54.2)	<0.001
Tract normalized volume (tract volume (cm^3)/physeal area (cm^2))	0.38 (0.25-0.59)	0.62 (0.48-0.91)	0.001
ROI ADC (mm^2/sec)	$1.55x10^{-3}$ ($1.46x10^{-3}$ - $1.64x10^{-3}$)	$1.45x10^{-3}$ ($1.38x10^{-3}$ - $1.57x10^{-3}$)	0.06

Table 1. Comparison of different DTI parameters between HR-NB and sex- age- (within 6 months) matched controls

Paper #: 122

Morel-Lavellée lesions: MRI characteristics in the pediatric patient

Jordan Rapp, MD[1], *jrapp24@gmail.com*; Victor Ho-Fung, MD[1]; [1]Children's Hospital of Philadelphia, Philadelphia, PA

Disclosures: All authors have disclosed no financial interests, arrangements or affiliations in the context of this activity.

Purpose or Case Report: A closed degloving injury is often referred to as a Morel-Lavellée injury regardless of location despite traditionally being associated with the hip in adult patients. Classically this has been described as a shearing type injury resulting in separation of fascial layers with fluid filling a potential space in the subcutaneous soft tissues. There is scant literature with descriptive findings in pediatric patients.

Methods & Materials: A retrospective analysis of the medical records was performed. All patients with a traumatic injury to the lower extremities and a subcutaneous fluid collection seen on MRI were evaluated. Patient demographics including age and gender, mechanism of injury and time delay from injury to imaging, and subsequent treatment was recorded. The fluid collections were assessed by two radiologists for location, size, shape, and signal characteristics including the presence of internal fat, blood, septations, and crossing vessels.

Results: 23 patients ranging in age from 7 to 19 years old were seen to have findings of degloving type injury on MRI. Patients were more often male (17/23, 73.9%) and had sports related injury (21/23, 91.3%), or less commonly related to motor vehicle collisions (2/23, 8.7%). The anterior knee was most often affected (19/23, 82.6%). Most lesions were ovoid and centered over the medial retinaculum 8/23 (34.8%) or lateral retinaculum 7/23 (30.3%), or horseshoe in shape, spanning the anterior knee draped over the patella. All lesions were located at the subcutaneous fat and fascial interface and contained internal fat lobules. The most common internal signal was simple fluid, and most commonly an incomplete capsule was observed. Several lesions had internal blood products and crossing vessels.

Conclusions: Morel-Lavellée injuries most commonly occur in pediatric patients in a location not classically described, the anterior knee, and most commonly occur after a sports related injury. The MRI findings are similar for all patients in that there is an ovoid or horseshoe shaped fluid collection at the fat/fascial interface containing internal fat droplets. Recognition of this entity with these specific imaging characteristics in a common location after a sports injury can allow for early identification. While most patients recover well with conservative management, patients may need additional intervention with aspiration or even debridement.

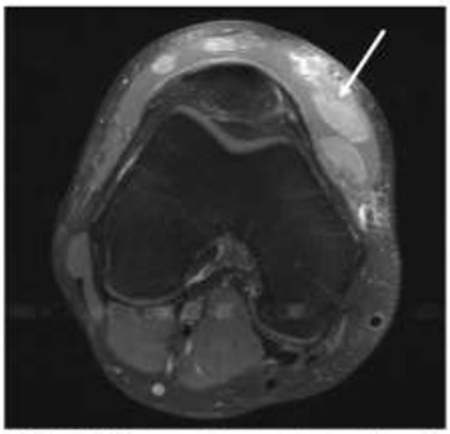

Fig 1. Axial T1 fat saturated sequence through the knee. A large horseshoe fluid collection is seen anteriorly draping over the patella. Note large fat globules internally (arrow).

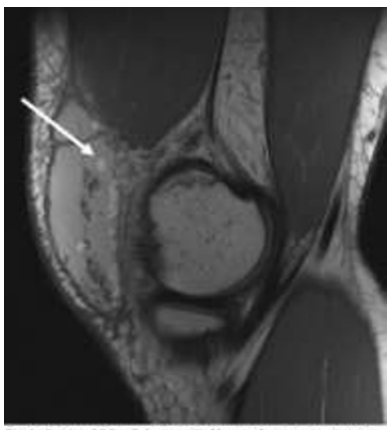

Fig 2. Sagittal PD of the medial knee demonstrating a large subcutaneous fluid collection with small internal fat droplets (arrow).

Paper #: 123

Children with Unilateral Fibular Hemimelia Have Normal Lower Extremity Growth Trajectory and Skeletal Maturation

Andy Tsai, MD, PhD[1], *andy.tsai@childrens.harvard.edu*; Paul Kleinman, MD[1], Tal Laor, MD[1], James Kasser, MD[1]; [1]Radiology, Boston Children's Hospital, Boston, MA

Disclosures: All authors have disclosed no financial interests, arrangements or affiliations in the context of this activity.

Purpose or Case Report: Fibular hemimelia (FH) is the most common congenital lower leg anomaly. It usually results in a limb-length discrepancy and often requires surgical correction. The literature generally ascribes to the concept of *constant inhibition*, a process by which length ratios between affected and unaffected limbs remain constant throughout growth, but rigorous scientific data supporting this concept are sparse. Also, some authors have recently suggested that children with FH have earlier skeletal maturation, potentially influencing management. The objective of this study is to elucidate the lower extremity growth patterns and skeletal maturation of children with unilateral FH.

Methods & Materials: Medical records of children with unilateral FH seen at a large pediatric hospital over a 17 year period were reviewed. Inclusion criteria were: at least 2 scanograms, no other confirmed or suspected metabolic/genetic disorders or acquired lower extremity insults. The study cohort's affected and unaffected femoral and tibial lengths were collected from scanogram reports, plotted against chronologic age and compared to published growth standards. If hand/wrist radiographs were available during the child's study interval, the estimated bone age (Greulich and Pyle) was plotted against chronologic age.

Results: Twenty-three children were included (15 boys, 8 girls) with a total of 115 scanograms (average 5, range 2-11, SD=2.7 scanograms). Average age at initial scanogram was 5.6 years (range 1.3-9.2 years). Average age at final scanogram was 10.4 years (range 5.2-18.3 years). At least 1 bone age assessment was performed in 19 children (total of 82 bone ages). All bone growth trajectories (affected and unaffected sides) paralleled normal growth standards for the femur and tibia (Figs. 1 & 2). Length ratios between affected and unaffected sides remained constant (Fig. 3), adhering to an upward slope pattern of differential limb growth. Individual average percent change in limb length ratio was 0.1-3.3% for the femur and 0.2-3.7% for the tibia. Skeletal maturation was within 2 SD of normal in 72/82 (88%) bone ages.

Conclusions: Lower extremity long bones of children with unilateral FH have a normal growth trajectory in keeping with *constant inhibition* and most children show normal skeletal maturation. These data contrast with the notion that children with unilateral FH have abnormal growth and earlier skeletal maturation. Recognition of this overall growth pattern can help predict ultimate limb length and guide management.

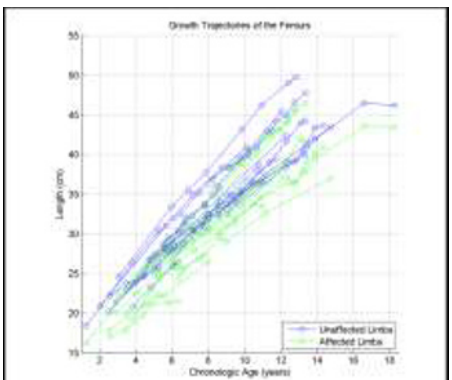

Figure 1: Growth trajectories for all unaffected and affected femurs in the study cohort (n=23).

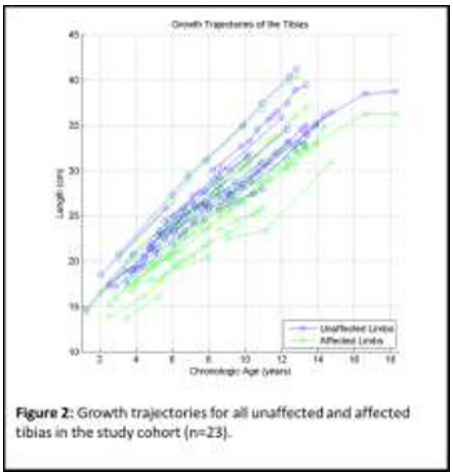

Figure 2: Growth trajectories for all unaffected and affected tibias in the study cohort (n=23).

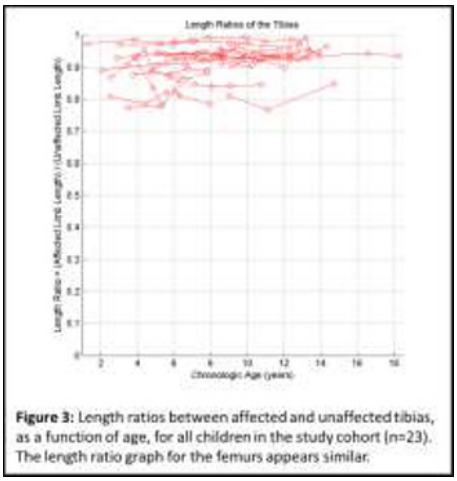

Figure 3: Length ratios between affected and unaffected tibias, as a function of age, for all children in the study cohort (n=23). The length ratio graph for the femurs appears similar.

Paper #: 124

MRI of stress fractures: Relationship between Fredericson classification and time to recovery in children.

Benjamin Thompson[1], *benpthompson@hotmail.com*; Frederick Ditmars[1], Houchun Hu[1], James MacDonald[1], Reno Ravindran, MD[1], Cody Young, DO[1]; [1]Radiology, Nationwide Children's Hospital, Columbus, OH

Disclosures: All authors have disclosed no financial interests, arrangements or affiliations in the context of this activity.

Purpose or Case Report: Stress fractures are a common injury making up 10% of treated injuries in sports medicine with the tibia being the most common injury location in pediatric patients. MRI is the gold standard for imaging evaluation of stress fractures with the Fredericson grading scale (I-IVb) as the most widely accepted grading system. The purpose of our study is to determine if there is a correlation between the grade of the fracture and time to recovery in children.
Methods & Materials: Two independent pediatric radiologists reviewed 106 consecutive tibial stress fractures using the Fredericson classification system (grade 1 = periosteal edema only, grade = bone marrow edema visible on T2-weighted images, grade 3 = bone marrow edema visible on T1-weighted and T2- weighted images, grade 4a = multiple focal areas of intracortical signal abnormality and grade 4b = linear areas of intracortical signal abnormality. Discrepancies were validated using radiologist consensus.
Two experienced sports medicine physicians independently examined and followed the patients to time of recovery. Time to recovery was defined as the date of the first appointment when the patient first reported symptoms to the date of the first appointment when the patient reported no symptoms.
Patients with comorbidities including obesity, osteoporosis, diabetes or failure to follow up were excluded. This resulted in 39 pediatric patients with MRI confirmed and clinically suspected fatigue fractures. The average age was 15 with an age range of 7-18.
Results: We found no statistically significant differences in time to recovery in subjects that were scored in the Fredericson classification grades of 2, 3, 4a, and 4b. The average time to recovery were: Grade 4b (n=54.63 days), grade 4a (n=54.40 days), grade 3 (n=48.54 days), grade 2 (n=59.36 days) and grade 1 (n=48 days). Our study only included one patient with a Fredericson grade of 1.
Conclusions: In our study, we found no statistical difference in time to recovery between stress fractures grade II-IVb. This suggests that as a predicted clinical outcome grades II-IVb can be combined to create an abbreviated Fredericson classification system. Our current study in children led to the similar findings as a previous report by Kijowski, et al. in adults.

Paper #: 125

Pediatric Posterior Ankle Impingement: An Underdiagnosed Cause of Posterior Ankle Pain

Matthew Ditzler, MD[1], *mgditzle@texaschildrens.org*; Siddharth Jadhav, MD[1], Snehal More, MD[2], Indranil Kushare[3]; [1]Pediatric Radiology, Texas Children's Hospital, Houston, TX, [2]vRad, Eden Prairie, MN, [3]Texas Children's Hospital, Houston, TX

Disclosures: All authors have disclosed no financial interests, arrangements or affiliations in the context of this activity.

Purpose or Case Report: Posterior ankle impingement (PAI) syndrome is a cause of ankle pain related to entrapment of soft tissue or osseous anatomical structures in the hindfoot and most commonly presents with plantar flexion predominant activities in athletes. The purpose of this study is to describe our experience with pediatric PAI as a clinically and radiologically underdiagnosed entity.
Methods & Materials: We prospectively followed all patients undergoing posterior ankle arthroscopy for suspected posterior ankle impingement since August 2016. Medical records were reviewed for demographics, presentation, physician referral history, initial diagnoses, imaging performed, and duration between presentation and diagnosis of posterior ankle impingement. Pre- and post-arthroscopy visual analog scale (VAS) pain scores and American Orthopedic Foot and Ankle Society (AOFAS) scores were also documented.
Results: 42 ankles in 32 patients underwent arthroscopic debridement for the treatment of PAI. The patients had previously been given several alternative diagnoses including peroneal subluxation/tendonitis, Achilles tendonitis, chronic regional pain syndrome, sural neuralgia, and chronic ankle sprain. Average patient age was 13.2 years (7.7-18.7 years) and 17 (53%) were male. The average delay in diagnosis from initial presentation was 20.2 months (range 24-60 months). 24 patients had a total of 27 pre-operative ankle MRIs (3 bilateral) and 20/24 had at least one normal pre-operative radiograph. The diagnosis of PAI was not specifically suggested on pre-operative imaging or initial clinical evaluation. All patients had arthroscopic confirmation of the diagnosis. They reported significant pain relief with debridement and showed improvement in average pre- to post-operative VAS pain scores (7.1 to 1.3) and AOFAS ankle scores (64.8 to 91.7) at average follow up of 3.0 months (range 1-6 months), further confirming the diagnosis.

Conclusions: PAI as a cause of posterior ankle pain in young athletes is a frequently overlooked diagnosis both clinically and radiologically. Patients with PAI are also often misdiagnosed, which leads to delays in care and associated morbidity. This condition is well described in the adult population, and although it presents similarly, is not as recognized in pediatric patients. Increased awareness about PAI is needed amongst orthopedic surgeons, primary care sports physicians, and radiologists involved in treating young athletes for timely diagnosis and management.

Paper #: 126

MRI Findings of Pediatric Posterior Ankle Impingement and Associated Entities

Matthew Ditzler, MD[1], *mgditzle@texaschildrens.org*; Siddharth Jadhav, MD[1], Snehal More, MD[2], Indranil Kushare[3]; [1]Pediatric Radiology, Texas Children's Hospital, Houston, TX, [2]vRad, Eden Prairie, MN, [3]Texas Children's Hospital, Houston, TX

Disclosures: All authors have disclosed no financial interests, arrangements or affiliations in the context of this activity.

Purpose or Case Report: Posterior ankle impingement (PAI) syndrome is a clinically and radiologically underdiagnosed cause of ankle pain in young athletes related to entrapment of soft tissue or osseous structures in the hindfoot. PAI most commonly presents with plantar flexion predominant activities in young athletes. The purpose of this study is to describe the most common and associated imaging findings on MRI in arthroscopically proven pediatric PAI.
Methods & Materials: We retrospectively reviewed imaging in all patients undergoing posterior ankle arthroscopy for suspected posterior ankle impingement since August 2016. Pre-operative ankle radiograph and MRI examinations were reviewed by two pediatric radiologists and findings were recorded independently. Recorded findings included the presence of an os trigonum or Stieda process, osseous edema, site of osseous edema, edema in fat adjacent to the posterior talus, effusion or synovitis in the posterior recesses of the tibiotalar and subtalar joints, flexor hallucis longus tendinopathy, posterior talofibular ligament pathology, and the presence of a posterior intermalleolar ligament. Ancillary findings not classically described with adult PAI were also recorded. Inter-reader discrepancies were settled by consensus review and frequency was calculated.
Results: 42 ankles in 32 patients underwent arthroscopic debridement for the treatment of PAI. Of these, 24 patients had a total of 27 ankle MRIs (3 bilateral). 20/24 (83%) patients had at least one normal pre-operative ankle radiograph. The most common MRI findings included the presence of an os trigonum or Stieda process (24/27, 89%) with associated osseous edema (17/27, 63%), joint effusion or synovitis in the posterior recess of the subtalar joint (20/27, 74%), a posterior intermalleolar ligament (18/27, 67%), and edema in the fat adjacent to the posterior talus (16/27, 59%).
Ancillary findings included the presence of a flat foot deformity (7/27, 26%), inflammation in the sinus tarsi (5/27, 19%), peroneal tendinopathy (3/27, 11%) and the presence of os naviculare (3/27, 11%).
All 24 patients demonstrated significant improvement in pain and function scores following arthroscopy, further confirming the diagnosis of PAI.
Conclusions: MRI findings in pediatric PAI are similar to those described in the adult population, but this condition remains underdiagnosed. Increased awareness about pediatric PAI, its MRI findings, and other associations is needed to prevent morbidity related to delayed or incorrect diagnoses.

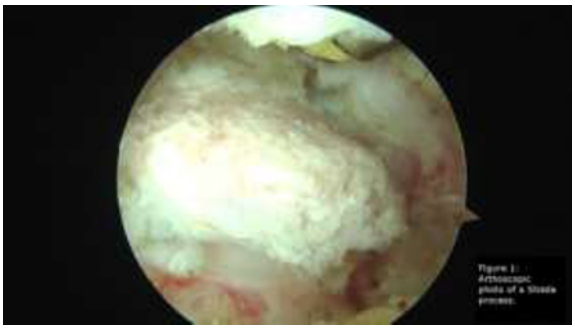

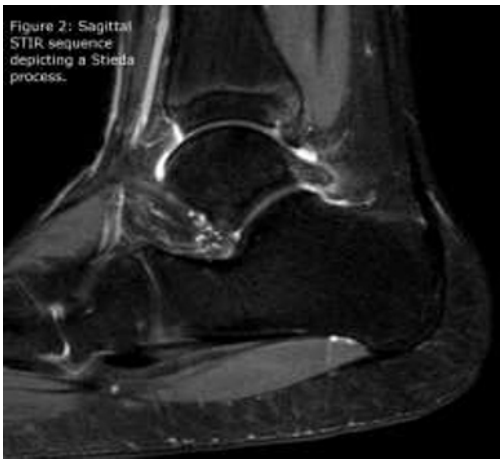

Paper #: 127

Introduction of a clinical MR PET service into a dedicated children's hospital; lessons learned from the first 550 patients

Timothy Cain, MBBS, MBA[1] *tim.cain@rch.org.au*; ; [1]Medical Imaging, The Royal Children's Hospital Melbourne, East Melbourne, VIC, Australia

Disclosures: All authors have disclosed no financial interests, arrangements or affiliations in the context of this activity.

Purpose or Case Report: MR PET is a relatively new technology with many theoretical advantages over PET/CT, especially in children. However, it is an expensive modality with reimbursement and workflow issues slowing its introduction into general paediatric imaging practice. The purpose of this paper is to document the successful introduction of a clinical MR PET scanner into a dedicated children's hospital, and report on the lessons learned during the first 18 months of operation.
Methods & Materials: The data comes from review of the hospital PACS files, and the RIS. Analysis is provided by critical Medical Imaging Specialist review of the images, feedback from referring clinicians and patients, and from MR PET team technologist and physician discussions.
Results: Oncology imaging was the most common indication with 22% of studies performed on patients with sarcomas, 21% on Lymphoma patients, 4% on patients with LCH and 3% on patients with other tumours. One third of studies were performed for the investigation of epilepsy, about 9% for the investigation of inflammation or infection, and 8% other indications. About 30% of studies were performed with a general anaesthetic. The radiation dose received by patients was usually about one half of that expected from a PET/CT offered off site at an adult hospital. Teamwork was considered important, with the interaction between the MR and Nuclear Medicine Technologists and their

discussions with the medical imaging specialists critical in performance of diagnostic studies. Nurses, anaesthetists and educational play therapists also played important roles. Taking time to optimise patient comfort in the scanner is considered an important investment and anxiolytics are now used more frequently in older children during awake scans.
MR generated attenuation correction maps were improved during the time period under review with better anatomical correlation observed, however a range of artefacts can be seen and must be dealt with in the same manner as accepted MR and PET/CT artefacts. The MR sequences must be chosen selectively to keep total imaging time within an acceptable range but still provide the required imaging information.
Conclusions: MR PET is a complex imaging technology that can be successfully introduced into a clinical paediatric imaging practice. Advances in technology and faster MR sequences will facilitate wider adoption, but teamwork, patient comfort and appropriate imaging protocol selection are likely to be ongoing requisites of any successful MR PET imaging service.

Paper #: 128

The role of routine imaging in childhood melanoma (MM)

Sue Kaste, DO[1], *sue.kaste@stjude.org*; Alberto Pappo[1], Hadeel Halalsheh, MD[1], Barry Shulkin[1], Fariba Navid, MD[2], Armita Bahrami, MD[1], Bhaskar Rao, MD[1], Michelle Wood, CRA II[1]; [1]Diagnostic Imaging, St. Jude Children's Research Hospital, Memphis, TN, [2]Children's Hospital of Los Angeles, Los Angeles, CA

Disclosures: All authors have disclosed no financial interests, arrangements or affiliations in the context of this activity.

Purpose or Case Report: We report our experience in children with MM treated uniformly on an institutional melanoma trial.
Methods & Materials: We retrospectively reviewed the clinical and imaging findings of patients with AJCC stage IIC-IV cutaneous MM treated on our institutional MEL06 protocol. Brain MRI/CT, PET/CT, CT chest, abdomen, and pelvis (CTCAP) were performed at diagnosis in all patients. On treatment, stratum A patients (PEG-interferon; AJCC IIC, IIIA, IIIB) (n=16) had the same imaging repeated every 6 months; stratum B1 (PEG-interferon and temozolomide; unresectable measurable disease metastatic, or recurrent) (n=2) had PETscans every 2 months and brain imaging every 4 months; those in stratum B2 (PEG-interferon and temozolomide; unresectable non-measurable , metastatic, or recurrent) (n=3) had the same imaging performed every 4 months. Off therapy all patients continued same imaging every 6 months for 3 years.
Results: There were 21 patients (11 female; median age 14years). Eleven had spitzoid and 10 conventional melanoma. Primary sites included head/neck (n=6), trunk (n=7), and extremities (n=8). Patients with spitzoid melanoma had 236 imaging studies (86 PET, 81 CTCAP, 11CT chest, 10 CT brain, and 48 MRI brain) with a median of 8, 7, 0, 4 and 0 studies/patient respectively. Median cost per patient was $32,718. Thirteen studies (5.8%) showed suspicious lesions with 28 additional scans and 2 diagnostic biopsies of which one only was positive stratum A with TERT promoter mutation and died from disease). For conventional MM, 162 studies (61 PET, 57 CTCAP, 8 CT chest, 7 CT brain, and 29 MRI brain) were performed with a median of 7, 6.5, 0, 1, 3 studies/patient respectively. Median cost per patient was $23,420. Twenty (14%) showed suspicious lesions with 19 additional scans and 6 diagnostic biopsies; four were positive (two at diagnosis, both died of disease). The other two recurred loco-regionally and were detected clinically; both are alive and disease free. One patient had diffuse metastases and died shortly after enrollment . After a median follow up of 6.3 years (range 0.4-9.2) 17 patients are alive and disease free.
Conclusions: Children with spitzoid melanoma should have minimal imaging at diagnosis and follow-up given the low risk of recurrence and low yield and high cost of aggressive imaging protocols. Patients with conventional MM should be imaged according to the adult guidelines.

Paper #: 129

MR Imaging Features of Subtypes of Hepatocellular Adenomas in Children

Saad Ranginwala, MD[1], *sranginwala@gmail.com*; Andrew Schapiro, MD[1], Andrew Trout[1], Alexander Towbin, MD[1], Anita Gupta[1], Jonathan Dillman, MD, MSc[1]; [1]Cincinnati Children's Hospital Medical Center, Cincinnati, OH

Disclosures: All authors have disclosed no financial interests, arrangements or affiliations in the context of this activity.

Purpose or Case Report: There are four defined subtypes of hepatocellular adenoma: inflammatory, HNF-1α inactivated, β-catenin activated, and mixed type. Specific MR imaging features have been described for three of the four subtypes in adults. However, to our knowledge, there has not been a description of the imaging features of adenoma subtypes in children. The purpose of this study was to define the typical MR imaging findings each of hepatocellular adenoma subtype in a pediatric population.
Methods & Materials: A pathology database was used to identify all patients with hepatocellular adenomas diagnosed and subtyped between 1/1/2000 and 5/15/2017. Patients were included if they had an MRI performed with the use of a hepatocyte specific contrast agent before biopsy/resection. MRI examinations were reviewed in consensus by two pediatric radiologists based with assessment of previously described imaging features. The frequency of imaging findings for each adenoma subtype was compared using a chi-squared test with a p-value of <0.05 considered to be significant.
Results: 20 hepatocellular adenomas in 16 patients (12 females [75%], mean age at MR imaging: 14.9 ± 6.1 years) were included in this study. There were 9 HNF-1α inactivated adenomas, 3 inflammatory adenomas, 4 β-catenin activated adenomas, and 4 mixed type adenomas. The imaging features of each adenoma subtype are detailed in Table 1. Of note, 6 adenomas (30%) were iso- or hyperintense in the hepatobiliary phase, including 1 inflammatory, 1 HNF-1α inactivated, 2 β-catenin activated, and 2 mixed type adenomas. Only the frequency of diffuse tumoral steatosis ($p=0.004$) and heterogenous hepatocyte phase appearance ($p=0.005$) significantly differed between adenoma subtypes. Diffuse tumoral steatosis was present in 89% (8/9) of HNF-1α inactivated adenomas, but in none of the inflammatory or β-catenin activated adenomas and in only 25% (1/4) of the mixed type adenomas. Hepatocyte phase heterogeneity was present in each (3/3) inflammatory adenoma, 50% (2/4) of the β-catenin activated adenomas, and 75% (3/4) of the mixed type adenomas, but in none (0/9) of the HNF-1α inactivated adenomas.
Conclusions: Of 20 molecularly subtyped hepatic adenomas, 30% were iso- or hyperintense in the hepatocyte phase, including 2 of 4 β-catenin activated adenomas which have the highest risk of malignant degeneration. HNF-1α inactivated adenomas can be distinguished from other adenoma subtypes by the presence of tumoral steatosis and a lack of hepatocyte phase heterogeneity.

	HNF-1α	Inflammatory	β-catenin	Mixed	p-value
T1w heterogeneity	2/9 (22%)	1/3 (33%)	1/4 (25%)	1/4 (25%)	0.99
T2w heterogeneity	6/9 (66%)	3/3 (100%)	2/4 (50%)	1/4 (25%)	0.22
Hemorrhage	1/9 (11%)	0/3 (0%)	0/4 (0%)	0/4 (0%)	0.73
Atoll Sign	0/9 (0%)	1/3 (33%)	0/4 (0%)	0/4 (0%)	0.11
Central Scar	1/9 (11%)	0/3 (0%)	1/4 (35%)	1/4 (25%)	0.74
Diffuse Steatosis	8/9 (89%)	0/3 (0%)	0/4 (0%)	1/4 (25%)	0.004*
Arterial Enhancement	3/9 (33%)	2/3 (66%)	4/4 (100%)	2/4 (50%)	0.16
Portal Venous Hyperenhancement	5/9 (56%)	0/3 (0%)	2/4 (50%)	1/4 (25%)	0.33
Hepatocyte Phase Hypointensity	8/9 (89%)	2/3 (66%)	2/4 (50%)	2/4 (50%)	0.38
Hepatocyte Phase Iso-/ Hyperintensity	1/9 (11%)	1/3 (33%)	2/4 (50%)	2/4 (50%)	0.14
Hepatocyte Phase Heterogeneity	0/9 (0%)	3/3 (100%)	2/4 (50%)	3/4 (75%)	0.005*

Paper #: 130

Long-term Outcomes of Large Femoral Head Osteonecrotic (ON) Lesions in Pediatric Patients Treated for Leukemia or Lymphoma

Sue Kaste, DO[1], *sue.kaste@stjude.org*; Michael Neel, MD[2], James Humphreys, BA[1], Sandra Murphy, RN[1]; [1]Diagnostic Imaging, St. Jude Children's Research Hospital, Memphis, TN, [2]OrthoMemphis, Memphis, TN

Disclosures: Michael Neel has indicated a relationship with Wright Medical Technology as a consultant/honoraria. All other authors have disclosed no financial interests, arrangements or affiliations in the context of this activity.

Purpose or Case Report: An estimated 1:750 Americans is a survivor of childhood cancer. Late toxicities, such as osteonecrosis (ON), can adversely effect quality of and functionality in life. We previously reported that 80% of femoral heads lesions involving ≥30% articular surface collapsed within 2 y of their diagnosis. We now report on long-term follow-up of such lesions, prospectively coded, to investigate characteristics that could inform development of imaging and intervention guidelines directed at ameliorating large ON lesions.
Methods & Materials: We retrospectively analyzed long-term outcomes of prospectively coded femoral head ON including patient demographics, primary malignancy, disease therapy, ON characteristics of the femoral head, ON therapy identified from a large electronic database of all ON MRs performed at a single institution since May, 1991.
Results: We identified 81 patients (43 girls) meeting eligibility criteria. Sixty-five patients were white, 11 black, 6 other. Sixty-seven patients had been diagnosed with acute lymphoblastic leukemia, 6 with acute myelogeneous leukemia, 8 with lymphoma. Median age at ON diagnosis was 15y (range, 3 - 22y). Median time to ON diagnosis from primary diagnosis of leukemia or lymphoma, 1.3y (range, 0.04 - 11.9y). Median follow-up from ON diagnosis was 5.8y (range, 0 -12.6y). Median age at last follow-up 21.2y (range, 4.1 - 34.2y). Over the follow-up period, ON lesion size remained stable in 51, regressed in 20,progressed in 10 from < to > 30% involvement articular surface femoral head; 1 patient died prior to follow-up. Surgical procedures comprised core decompression in 38 patients (26 unilateral), hemiarthroplasty in 12 (unilateral in 11), total hip arthroplasty in 30 (28 unilateral).
Conclusions: ON is a serious toxicity associated with added burden for medical and surgical care on survivors of childhood leukemia and lymphoma. Large lesions are typically associated with teenage and young adult patients. Surgical intervention to ameliorate pain and functional limitations are frequently necessary. Development of effective interventions to preserve joint integrity and function, short of invasive surgical procedures, are needed.

Paper #: 131

High-Resolution In Vivo Imaging of Tumor Angiogenesis in Orthotopic Xenograft and Transgenic Mouse Models of Neuroblastoma

Ketan Ghaghada, PhD[1], *kbghagha@texaschildrens.org*; Zbigniew Starosolski, PhD[1], Ananth Annapragada, PhD[1]; [1]Pediatric Radiology, Texas Children's Hospital, Houston, TX

Disclosures: Ananth Annapragada has indicated a relationship with Alzeca Inc. and Sensulin, LLC for receiving stock options as well as intellectual property rights, and receives research grants with the NIH and Alzeca, Inc. All other authors have disclosed no financial interests, arrangements or affiliations in the context of this activity.

Purpose or Case Report: A high degree of tumor vascularity in neuroblastoma (NB) has been correlated with disseminated disease, *MYCN* amplification and poor outcome. *In vivo* 3D visualization and quantification of tumor angiogenesis in pre-clinical studies could aid in the clinical translational of vascular targeted therapies. In this work, we studied tumor angiogenesis and evolution of tumor vasculature in mouse models of NB using contrast-enhanced CT(CECT) imaging.
Methods & Materials: Studies were performed in a SV40 transgenic and an orthotopic xenograft mouse model of NB. The transgenic NB model develops spontaneous bilateral adrenal tumors starting at 10 week age. For orthotopic xenograft model, MYCN-amplified human NGP cells were surgically implanted beneath the renal capsule of nude mice. High-resolution(35 μm) angiograms were acquired on a micro-CT scanner using long circulating blood pool contrast agent. Imaging was performed at 2, 3 and 4 week post-tumor implantation in xenograft group(n=6 per time point) and 15, 19 and 21 weeks of animal age in transgenic group(n=5 per time point) to capture angiograms at different stages of tumor age. CT images were analyzed to study evolving patterns of tumor angiogenesis and vascular development.
Results: The xenograft model showed a low degree of tumor angiogenesis regardless of tumor size(Fig 1). Spontaneous tumors in transgenic mice demonstrated a high degree of heterogenous vasculature throughout the tumor volume that was evident at all stages of tumor growth(Fig 2). Intratumoral vessel diameter progressively increased with tumor size and age; vessels as small as 70 μm were delineated on CT images. The density of large, highly tortuous venous structures(>500 μm) increased with tumor age. Unlike xenograft NB mice, transgenic NB mice demonstrated vessel occlusion, most likely due to tumor intrusion into nearby vessel(Fig 3). Old age tumors exhibited occlusion within tumor vasculature, suggestive of intravascular tumor thrombus. Vessel occlusion was observed in 40% of early age group(15 week), 80% of intermediate age group(19 week) and 100% of old age group(21 week). While distant metastases were not observed in xenograft mice, transgenic mice demonstrated lung and hepatic metastases in 20% of intermediate group and 50% of old age group.
Conclusions: CECT imaging using a long circulating blood pool contrast agent enabled the acquisition of high-resolution tumor angiograms, visualization of tumor-related vessel occlusion and distant metastases in mouse models of neuroblastoma.

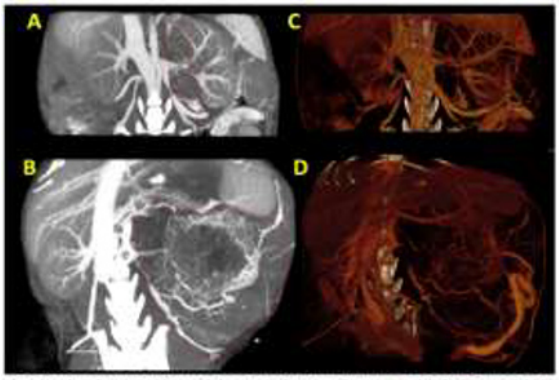

Fig 1. Imaging of tumor angiogenesis in orthotopic xenograft mouse model of NB. Coronal thick slab (left panel) and 3D volume rendered (right panel) images of intermediate age (3 weeks; top row) and old age (4 weeks; bottom row) xenograft tumors (red counters) demonstrating tumor vasculature at different stages of tumor growth.

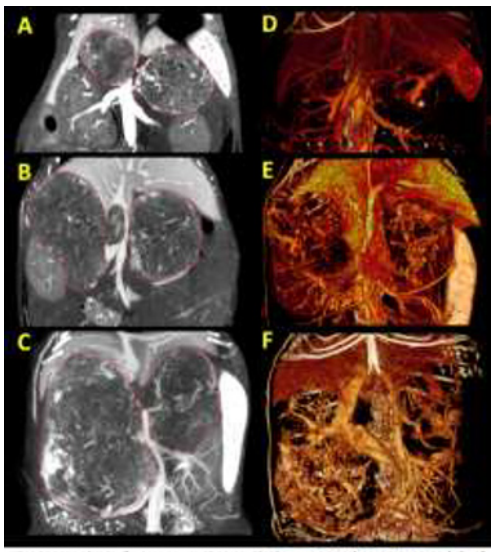

Fig 2. Imaging of tumor angiogenesis in transgenic mouse model of NB. Coronal thick slab (left panel) and 3D volume rendered (right panel) images of early age (15 week; top row); intermediate age (19 week; middle row) and old age (21 week; bottom row) spontaneous bilateral NB tumors (red counters) demonstrating high degree of intra-tumor vascularity.

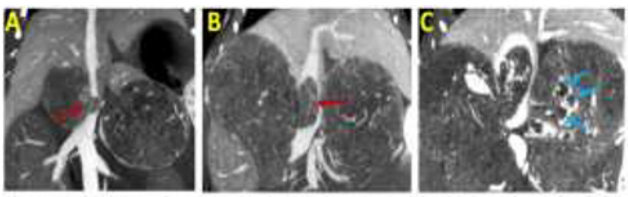

Fig 3. Visualization of vessel occlusion. Coronal thick slab of (A) early stage and (B) intermediate stage tumors demonstrate vessel occlusion (red arrows) due to intrusion of primary tumor into the inferior vena cava. (C) Occlusion of large intra-tumoral vessels was evident in late stage tumor (blue arrows).

Paper #: 132

Malignancy risk stratification of pediatric thyroid nodules using ACR Thyroid Imaging, Reporting and Data System (ACR TI-RADS)

Jennifer Lim-Dunham, MD[1], *jlim2@lumc.edu*; Iclal Erdem Toslak, MD[1], Michael Reiter, MD[1], Brendan Martin[2]; [1]Radiology, Loyola University Medical Center, Maywood, IL, [2]Loyola University Clinical Research Office, Maywood, IL

Disclosures: All authors have disclosed no financial interests, arrangements or affiliations in the context of this activity.

Purpose or Case Report: To assess the performance of the 2017 American College of Radiology Thyroid Imaging, Reporting and Data System (ACR TI-RADS) for categorization of malignancy in children with thyroid nodules.
Methods & Materials: Seventy-four thyroid nodules (median: 1.9 cm; IQR: 1.3-2.8) in 62 pediatric patients (56 female and 6 male) with histological diagnosis were retrospectively reviewed. Two radiologists independently rated the ultrasound images according to ACR TI-RADS lexicon for individual parameters (composition, echogenicity, shape, margins, and echogenic foci). Kappa coefficients were generated to assess intra- and inter-observer agreement and consensus was reached in cases where observers disagreed. Points were given for nodule features then added to determine TI-RADS level, ranging from 1 (benign) to 5 (high suspicion). Generalized linear mixed effects models were then used to evaluate performance of TI-RADS in predicting malignancy.
Results: Fifty-four nodules were benign and 20 malignant. 36 nodules (48.7%; 19 benign 17 malignant) were categorized as TI-RADS 5; 24 (32.4%; 22 benign 2 malignant) as TI-RADS 4; 6 (8.1%; 6 benign, 0 malignant) as TI-RADS 3; 4 (5.4%; 4 benign, 0 malignant) as TI-RADS 2; and 4 (5.4%; 3 benign, 1 malignant) as TI-RADS 1. There was moderate to almost perfect intra-observer agreement (Kappa range .46 to .94, $p<0.0001$) and fair to almost perfect inter-observer agreement (Kappa range .25 to .84, p .02 to <.0001) for all parameters. For every one unit increase on the ordinal TI-RADS scale, nodules were 2.63 times (95 CI: 1.08-6.41, $p=.03$) more likely to have a malignant diagnosis. For every one centimeter increase in size, nodules were 69% ($OR= 1.69$, 95 CI: 1.04-2.73, $p= .03$) more likely to have a malignant diagnosis. After adjusting for nodule size, ordinal TI-RADS scale ($OR= 2.27$, 95 CI: 0.93-5.54, $p = .07$) remained marginally associated with a malignant diagnosis but size was no longer associated. Except for one patient with a 0.8 cm malignant nodule rated as TI-RADS 1 who had another 2.5 cm malignant nodule, all malignant nodules (19/20; 95%) were rated as TI-RADS 4 or 5.
Conclusions: ACR TI-RADS allows for appropriate stratification of malignancy risk for thyroid nodules in children prior to tissue diagnosis. Subcentimeter nodules must be assessed with caution and additional nodules in patients with at least one other TI-RADS 4 or 5 nodule must be regarded with suspicion.

Paper #: 133

Streamlining primary care referrals for ultrasound assessment of paediatric cervical nodes in a NHS (UK) District General Hospital: Preliminary results from an ongoing study

Samantha Low[1], *samanthalowbl@gmail.com*; Aziekah Fiaz[1], Davina Pawaroo[1]; [1]Norfolk and Norwich University Hospital, Norwich, United Kingdom

Disclosures: All authors have disclosed no financial interests, arrangements or affiliations in the context of this activity.

Purpose or Case Report: Ever-increasing demand and limited resources are finely balanced in the publicly-funded British National Healthcare System (NHS). Inappropriate referrals are inefficient, expensive and must be minimised.
Palpable cervical nodes are common in the paediatric population. Subjectively, it is felt that too many unnecessary neck ultrasounds are performed due to poor clinical examination, poor understanding of aetiology and poor parent-clinician communication. Children are referred for ultrasounds to reassure the “worried-well parents”, with a normal study falsely de-meriting the utility of clinical follow-up. Ultrasound alone cannot be used to exclude malignancy and cannot supersede

prudent clinical follow-up.We want to review the quality of clinical requests, correlating this with the outcomes from individual ultrasound studies and recommend criteria to ensure that only appropriate patients are imaged.
Methods & Materials: Retrospective analysis of primary care referrals for ultrasound assessment of paediatric cervical nodes in the Norfolk and Norwich University hospital from April 2016 to 2017 was performed.
Results: There were 117 requests and 101 sonographic studies performed. 82 studies showed normal or reactive nodes, 11 were abnormal within which 2 necessitated invasive sampling and did not reveal underlying malignancy. 3 studies were cancelled due to patient distress.
We hypothesised whether the referral quality could be improved with the application of specific criteria.
The clinical criteria was produced with consensus from the paediatric medical and surgical team. If any response to the question(s) is "Yes", the ultrasound study would be performed.
- Is the lymph node >10mm in long axis or >5mm in short axis?
- Has the patient's symptoms been ongoing for >12 weeks/ 3 months?
- Is the node increasing in size?
- Are there new nodes appearing?
- Does the patient have systemic symptoms?
- Clinically, this is not a node i.e. not along the lymphatic drainage pathway?

Using these criteria on existing referrals, we found that the number of unnecessary ultrasound studies performed could be reduced by 21% (24 patients).
Conclusions: Ultrasound assessment for paediatric cervical nodes cannot replace clinical assessment and follow-up. We will be implementing the referral criteria into our online radiology requesting system. Results will be analysed in 6 to 12 months' time to assess if this would improve the quality of referrals and minimise the number of inappropriate and unnecessary ultrasound studies.

Paper #: 134

Hepatobiliary scintigraphy vs. ultrasound for assessment of gallbladder ejection fraction in pediatric patients with suspected biliary dyskinesia

Summit Shah, MD, MPH[1], *summitshah@gmail.com*; Matthew Robertson, MD[1], Adam Bobbey, MD[1]; [1]Radiology, Nationwide Children's Hospital, Columbus, OH

Disclosures: All authors have disclosed no financial interests, arrangements or affiliations in the context of this activity.

Purpose or Case Report: While sonography (US) has been compared to hepatobiliary scintigraphy (HIDA) for evaluation of gallbladder ejection fraction (GBEF), no data exists in the pediatric population. Previous work in pediatric patients (Cay 2006) was limited to showing that patients with biliary dyskinesia diagnosed on HIDA had lower GBEF on US compared to a normal control population. This prospective study compared GBEF via HIDA and US in pediatric patients following sincalide (CCK) infusion.
Methods & Materials: Patients who were referred for HIDA with CCK were consented and prospectively enrolled to also receive US before and after CCK administration. Standard of care HIDA scan was performed with weight based dosing of 99m-Tc Mibrofenin. Dynamic anterior imaging was performed until gallbladder was visualized, up to 1 hour. Intravenous CCK was administered over 45 minutes with dynamic imaging in the LAO position for 60 minutes. Gallbladder US was performed and volume calculated using the prolate ellipsoid formula immediately prior to CCK administration and following post-CCK nuclear medicine imaging.
Results: 20 patients were evaluated with demographic information listed in Figure 1. HIDA GBEF ranged from 37-98% while US GBEF ranged from (-12%)-84% (Figure 2). Graphical correlation of HIDA and US GBEF with fitted linear trendline is shown in Figure 3. Pearson correlation coefficient for HIDA and US EF was calculated at 0.19 (Figure 3). Pearson correlation coefficient for BMI and relative difference between NM and US GBEF was 0.35.
Conclusions: This is the first direct comparison of scintigraphy vs. sonography for sincalide augmented GBEF in pediatric patients. Our prospective study found a poor correlation between these two modalities with US GBEF both over and underestimating HIDA GBEF in various patients. There was a weak correlation with increasing BMI and increasing relative difference between GBEF measured on HIDA compared to US. Our study suggests US with ejection fraction may not be a suitable replacement for sincalide enhanced HIDA in the evaluation of biliary dyskinesia. When US is used as a screening examination, the potential for both false positive and negative exams exist and follow-up HIDA should be considered in clinically suspicious cases. Future investigation with an increased sample size including cases of abnormal EF on HIDA, and more accurate volumetric ultrasound measurements may better determine the optimal role of US as a radiation sparing alternative.

Age	Range: 9-18 years, median: 14 years
Sex	65% female, 35% male
BMI	Range: 18-36, mean 25

Figure 1. Patient Demographics

Pt Number	US GBEF (%)	HIDA GBEF (%)
1	45	39
2	67	57
3	74	52
4	76	92
5	68	80
6	66	57
7	-12	37
8	37	61
9	60	77
10	53	44
11	61	98
12	84	53
13	45	45
14	67	77
15	50	39
16	33	83
17	82	71
18	16	95
19	57	38
20	68	95

Figure 2. Ultrasound and HIDA scan gallbladder ejection fractions pre and post sincalide administration.

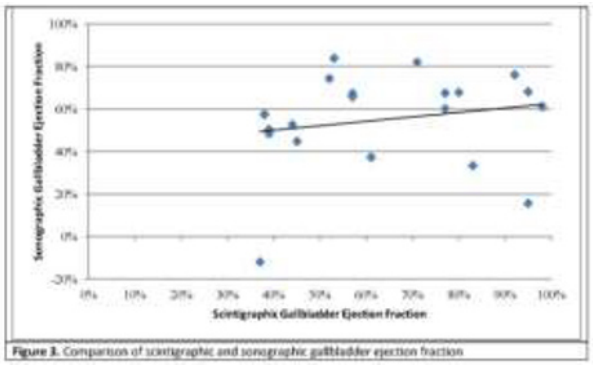

Figure 1. Comparison of scintigraphic and sonographic gallbladder ejection fraction

Paper #: 135

Solid gastric emptying: does the 4 hour examination add value in children?

Susan Sharp, MD[1], *susan.sharp@cchmc.org*; Andrew Trout[1]; [1]Department of Radiology, Cincinnati Children's Hospital, Cincinnati, OH

Disclosures: All authors have disclosed no financial interests, arrangements or affiliations in the context of this activity.

Purpose or Case Report: Adult procedure guidelines for solid meal gastric emptying examinations recommend imaging for up to 4 hours, as 4 hour exams detect abnormal emptying with greater sensitivity than 2 hour exams. The added diagnostic value of the additional 2 hours of imaging (which extends the visit duration for the patient/family and the exam duration for the technologist) has not yet been demonstrated in children. The purpose of this study was to determine the diagnostic differences between 4 hour and 2 hour gastric emptying exams in pediatric patients.
Methods & Materials: A retrospective review of solid and dual phase gastric emptying exams was performed in 165 pediatric patients (ages 2-18 years, mean 12.2 years, median 14 years; 63 male/102 female). Exams were assessed for percentage of solid gastric emptying at 1 hour, 2 hour, 3 hour, and 4 hour time points with comparison to published adult normal values. Data were analyzed to determine the added value of the 4 hour imaging time point.
Results: Solid gastric emptying was delayed in 39/165 (24%) patients at 2 hours and in 35/165 (21%) patients at 4 hours. Of those normal at 2 hours, 10/126 (8%) became abnormal at 4 hours. Of those abnormal at 2 hours, 14/39 (36%) normalized at 4 hours. Solid gastric emptying was delayed at both the 2 and 4 hour time points in 25/165 (15%) patients. With delayed emptying at either the 2 or 4 hour time point considered an abnormal result, 49/165 (30%) patients had abnormal solid gastric emptying. Importantly 10/49 (20%) abnormal exams showed delayed emptying only at the 4 hour time point.
Conclusions: Although most children (80%) with delayed gastric emptying of solids will be detected with 2 hours of imaging, extending the exam through 4 hours will detect a significant minority (20%) of patients with abnormal emptying.

Paper #: 136

Building a Comprehensive Learning Management System for Pediatric Radiology: How We Got There

Janet Reid, MD, FRCPC[1], *reidj@email.chop.edu*; Tigist Hailu, MPH[1], Michael Francavilla, MD[1], Lisa States, MD[1], Sudha Anupindi, MD[1], Hansel Otero, MD[1]; [1]Children's Hospital of Philadelphia, Philadelphia, PA

Disclosures: All authors have disclosed no financial interests, arrangements or affiliations in the context of this activity.

Purpose or Case Report: The excess of unfiltered information on the internet together with high volume workloads in radiology departments can adversely affect the quality of education in residency and fellowship. This LMS, a tool to help manage and increase timely access to educational and training content that also tracks utilization and progress overtime, could transform radiology education by identifying and consolidating valuable resources and incorporating them into daily practice.
Methods & Materials: Step 1: *Needs Assessment*- Identified and interviewed stakeholders within the department with a focus on students, residents, fellows, attendings, nurses, and technologists. Recognizing market forces shaping the demand for online radiology education (learning innovation, global engagement, health technologies, and health economics), a vision for our LMS and list of desired features was developed. **Step 2:** *Existing Resources Inventory*- All current learning content was identified: texts, online programs, conferences, articles, external links, etc. **Step 3:** *Choosing a Platform*- List of 95 system features was sent as a Request for Information to 10 North American LMS companies. A subset of superusers reviewed and scored detailed proposals from the top three companies, settling by consensus based on desired features, ease of use and self-governance opportunities. **Step 4:** *Implementation readiness assessment and roadmap*- Developed a plan for development, internal and external release of key system features including: curriculum management, content creation, tracking/notification, and network/collaboration. A timeline for staged rollout and scalability beyond our institution was also developed.
Results: In October 2017 we launched RADIAL (Radiology's Intelligent Adaptive Learning), an innovative LMS connected to our institutional Picture Archiving and Communication System (PACS) for easy navigation. Content is organized in tiles pointing to unique resources including: protocols, courses, links, teaching files, e-books, lectures, articles, interpretation tools, and question banks. Learning analytics assess navigation/use that when paired with learning profiles will assist in the development of adaptive learning.
Conclusions: Through a deliberate and thorough process, a full-service LMS was created with the future goal to transform learning and enable subject mastery.

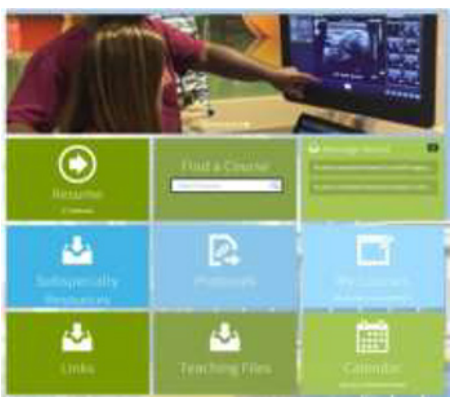

Paper #: 137

Simulation in Pediatric Interventional Radiology Environment: What lessons are we learning?

Raja Shaikh, MD[1], *drrajashaikh@yahoo.com*; Matthew Taylor, RN[1], Christopher Roussin, PhD[1]; [1]Boston Children's Hospital, Boston, MA

Disclosures: All authors have disclosed no financial interests, arrangements or affiliations in the context of this activity.

Purpose or Case Report: Interventional radiology (IR) space is a complex environment involving several personnel with different clinical and technical skills such as interventional radiologists, anesthesiologists, nurse practioners, nurses and technologists. In pediatric IR, there is an intricate parental/guardian involvement in the care of minors. The physical setting also requires a close integration of humans and technical hardware (digital subtraction angiography table, ultrasound machine, laser machine, anesthesia machine etc.). Most patients are also critically ill. These variables make it extremely important to create an environment which is synchronous and safe for patient care. A periodically occurring simulation was initiated in IR at our institution to bring together intelligent, improvement-oriented personnel to develop a team based practice in the interest of patient and employee safety.
Methods & Materials: Every simulation exercise involved real time enactment of an interventional procedural scenario coordinated by simulation facilitators. Scenarios were provided to a selected team consisting of an interventional radiologist (attending and fellow), anesthesiologist (attending and fellow), IR nurse, IR technologist. Interactive trainer mannequins were used as patients during the procedures. Participants were placed in a real life like situation. Scenario enactment was followed by debriefing session to the participants.
Results: Several important issues such as team communication, problem recognition and management, team integration were uncovered during these simulation sessions. Possible solutions were discussed. These recommendations were summarized and provided to divisional administration to affect policy changes.
Conclusions: IR simulation program is very essential in building a safe psychological and physical environment for patients and the IR personnel.

Paper #: 138

Is Social Media a Growing or Declining Educational Method in Pediatric Radiology?

Michael D'Alessandro, MD[1], *michael-dalessandro@uiowa.edu*; Donna D'Alessandro, MD[1]; [1]Radiology, University of Iowa, Iowa City, IA

Disclosures: All authors have disclosed no financial interests, arrangements or affiliations in the context of this activity.

Purpose or Case Report: Social media has become the dominant window for individuals into the Internet, supplanting the World Wide Web. Some medical educators have followed their learners from the Web to social media through the Free Open Access Medical Education (FOAM) movement which promotes and | or distributes free and openly accessible medical educational content through social media. FOAM also tries to bring order to the chaos of medical social media through the use of hashtags. The purpose of this study is to determine whether social media is a growing or declining educational method in pediatric radiology by measuring usage of common FOAM hashtags on social media platforms over time.
Methods & Materials: Monthly usage of five FOAM hashtags were studied on Twitter and Instagram over one year including those related to general medical education (#FOAMed, #MedEd), pediatric education (#FOAMPed), radiology education (#FOAMRad) and pediatric radiology education (#PedsRad). Data gathered included the number of participants and posts using the hashtags and the number of impressions generated by the posts. On Facebook, overall hashtag usage could not be measured.
Results: On Twitter, overall usage of the hashtags was significant and stable to slightly increased over the course of the study. #FOAMRad was used on average by 925 participants per month who made ~ 2,500 posts per month which led to an average of 5 million post impressions per month. #PedsRad was used on average by 90 participants per month who made ~ 200 posts per month which led to an average of 0.23 million post impressions per month. On Instagram, overall usage of the hashtags was minimal and stable over the course of the study. #FOAMRad was used on ~ 200 posts per month and #PedsRad was used on ~ 60 posts per month.
Conclusions: While social media use overall continues to increase rapidly, its use in pediatric radiology education does not appear to be increasing as rapidly. Indeed, its use as an educational method in pediatric radiology appears to have matured and reached a steady state. The reasons may include that both medical educators and learners are unaware of FOAM and thus do not tag and search for content with relevant hashtags, that Twitter, where the majority of FOAM occurs, is the only major social media platform that is not growing, and that individuals may not want to use, or are apprehensive to use, social media for work-related activities.

Paper #: 139

Feasibility and Impact of Intensive Hands-On Sonography Training for Pediatric Radiology Fellows

Summer Kaplan, MD MS[1], *kaplans2@email.chop.edu*; Michele Retrouvey[1], David Saul, MD[1], Tigist Hailu[1], Asef Khwaja[1], Michael Francavilla, MD[1], Ann Johnson[1], Richard Bellah[1], Victor Ho-Fung, MD[1], Sobia Mirza, MD[2], Michael Baad, MD[3], Judit Machnitz[1]; [1]The Children's Hospital of Philadelphia, Philadelphia, PA, [2]Children's National Hospital, Washington, DC, [3]Komansky's Children's Hospital, New York, NY

Disclosures: All authors have disclosed no financial interests, arrangements or affiliations in the context of this activity.

Purpose or Case Report: Radiology trainees today may get less hands-on scanning experience than peers in Emergency Medicine (EM) or Critical Care. However, it is critical that radiologists maintain scanning expertise to better care for patients and to consult for or supervise point of care US. To improve our pediatric radiology fellows' scanning skills, we developed a 5-hour hands-on US course to teach them to scan the 10 most commonly ordered EM exams. We assessed fellows' prior scanning experience and the impact of the course on fellows' confidence for performing US. We also summarized the time and financial resources needed for this course.
Methods & Materials: Fellows participating in the course completed surveys immediately before and after the course. Confidence for performing US in general and for specific exams was assessed using a 5-point scale. Neonatal brain protocol not in the course was used as a control. Changes in scanning confidence were assessed statistically with two-tailed t-tests. Radiologists participating in course organization were surveyed retrospectively for length of time spent on preparing handbook protocols, lectures, and in course organization. Costs for the course were itemized.

Results: Most fellows reported scanning 0 - 10 times during residency and 2 of 8 had no scanning experience prior to fellowship. Prior to the course, mean confidence for ultrasound scanning was: overall, 2.1/5; appendicitis, 2.0/5; pelvis, 1.7/5; neonatal brain, 2.1/5. After the course, fellow confidence for scanning was: overall, 3.3/5 ($p < 0.01$); appendicitis, 3.6/5 ($p < 0.005$); pelvis, 3.3/5 ($p < 0.005$); brain, 2.9/5.0 ($p = 0.13$). For the 5-hour course, 4 faculty spent a mean 2.6 hours each preparing lectures. Handbook materials for 10 protocols were compiled by 3 attendings and 4 fellows, with mean 2 hours spent per protocol. Course organization required 18 hours over 3 months. The largest amounts of time were spent formatting course book (7.5 hours) and setting up the room for scanning (2 hours). Cost for the course was $3040, with the largest sums for technologist overtime ($936) and food ($633). Cost for the course was covered by the Department of Radiology.
Conclusions: After a 5-hour hands-on US scanning course, pediatric radiology fellows were significantly more confident in their ability to scan. The cost and time burden is sustainable for our department, and the course will be continued in the future.

Paper #: 140

Body MRI Training During Pediatric Radiology Fellowship: Defining the Needs

Tigist Hailu, MPH[1], *hailut@email.chop.edu*; Susan Back, MD[1], Brian Hopely[1], Hansel Otero, MD[1], Victor Ho-Fung, MD[1], Janet Reid, MD, FRCPC[1]; [1]Radiology, Children's Hospital of Philadelphia, Philadelphia, PA

Disclosures: All authors have disclosed no financial interests, arrangements or affiliations in the context of this activity.
Purpose or Case Report: There is no comprehensive curriculum for pediatric body MRI during either residency or fellowship. Hence, fellows start their training with variable experience and expertise. To better serve patients, pediatric radiology fellows should gain a comprehensive understanding of body MRI that allows them to seamlessly transition into independent practitioners and future leaders. We conducted a needs assessment survey followed by a focus group interview to identify knowledge gaps and aid development of a curriculum resource for pediatric body MRI.
Methods & Materials: A comprehensive anonymous needs assessment survey was developed and distributed electronically in October 2016 to Society for Pediatric Radiology members who are current fellows and recent (<5 years) graduates from our ACGME accredited pediatric radiology fellowships. A follow up was sent in January 2017. We conducted a focus group with current fellows at our institution in October 2017 to help us better understand the survey findings.
Results: 81 pediatric radiologists (8 fellows and 73 attendings) completed the needs assessment survey and 5 current fellows participated in the focus group. The areas most commonly identified with limited or no instruction during training were technical including: setting up MR service, coil selection, and field inhomogeneity correction. The most commonly identified areas needing increased attention and inclusion within the curriculum were: coil choice and patient positioning (n=42, 52%); differences between contrast agents (n=40, 49%); field strength (n=33, 41%); and strategies for motion correction (n=33, 41%). Most fellows are uncomfortable with: setting up an MR service (n=57, 70%); correcting field inhomogeneity (n=56, 69%); and adjusting sequences to improve image quality (n=50, 62%). In the focus group, there was consensus about insufficient MR training in residency to prepare them for fellowship. The group preferred shorter lectures with ability to reference and watch repeatedly with an emphasis on learning via video education/tutorials.
Conclusions: While traditional instruction emphasizes image interpretation, this study shows that recent trainees of pediatric radiology fellowships need a curriculum with strong instruction in the technical and practical aspects of MRI.

Paper #: 141

Radiology Resident Preparedness in Counseling Patients for MRI During Pregnancy

Elise Miller[1], *milleeli@iupui.edu*; Jessica Smith[1], Brandon Brown, MD, MA[1]; [1]Indiana University, Indianapolis, IN

Disclosures: All authors have disclosed no financial interests, arrangements or affiliations in the context of this activity.

Purpose or Case Report: To evaluate the preparedness of radiology trainees in counseling pregnant patients for MRI and to create an educational video to fill identified gaps and standardize the information.
Methods & Materials: Pregnant patients undergoing MRI at our institution speak with residents prior to the exam. This study assesses trainee knowledge and ability to address concerns regarding MRI during pregnancy. We surveyed residents with an anonymous questionnaire.
Based on these data, we created a short gestational MRI educational video. The video will be shown to all radiology trainees and all pregnant women who receive MRI over a 6-month period from (November 2017-April 2018). The patient will then be given a brief survey to indicate how well informed she felt and how well the video prepared her for the exam. At the end of the study period, residents will be surveyed again to determine whether the use of the video was an effective educational tool.
Results: Initial results yielded 38 respondents. 55% felt only "somewhat comfortable" counseling pregnant women, and 11% felt "not comfortable at all." When asked about the current ACR stance on MRI safety, 79% answered incorrectly that "MRI should only be performed during certain trimesters," while only 21% answered correctly that MRI can be performed at any trimester. When asked about Gadolinium-based contrast use during pregnancy, 68% answered incorrectly "under no circumstances due to safety concerns," while only 29% answered correctly "only if critical." When asked "which of the following are known significant MRI-associated fetal risks," 24% of respondents chose "hearing loss," 5% chose "stillbirth/death," 0% chose "developmental" and "neoplasm," and 3% chose "all of the above." The remaining 71% of respondents correctly chose "none of the above." Finally, when asked if it would be helpful to have an MRI video for pregnant patients, 37 of 38 residents chose "yes." Results on the pregnant patient population are currently being collected.
Conclusions: The information pregnant women receive prior to MRI can be highly variable. Resident knowledge is frequently incorrect regarding MRI during pregnancy. Our solution has been to create a short video which will help to accurately educate pregnant patients in a consistent manner, and the video may also be used as an educational tool for radiology training. The video will be included as part of this presentation.

Paper #: 142

Pediatric Radiology Support and Education for Radiologists in a Large, Multicentric Group Practice

Richard Heller, MD, MBA[1]
Richard.Heller@radpartners.com; [1]Radiology, Radiology Partners, El Segundo, CA

Disclosures: All authors have disclosed no financial interests, arrangements or affiliations in the context of this activity.

Purpose or Case Report: Our practice is geographically dispersed and composed of radiologists in many sub-specialties, including pediatric. Since it is not feasible to have all pediatric imaging exams interpreted by a pediatric radiologist, we created a practice sub-group to develop ways to assist non-pediatric radiology colleagues when interpreting pediatric imaging exams. This presentation explains our process.
Methods & Materials: A Pediatric Radiology User Group (referred to as the Pediatric User Group, or "PUG") was created, composed of the fellowship-trained pediatric radiologists in our practice as well as several non-pediatric radiologists. The physicians in the PUG meet virtually on a regular basis, approximately every other month, to work on projects.
There are two categories of projects. In the first group, certain exams and conditions were identified as high-priority by radiologists in the practice, and dictation templates were created along with supporting documents intended to assist the interpreting radiologist. The second type of project is intended to support general education of pediatric radiology topics for physicians throughout the practice. This is accomplished through creation of PowerPoint presentations placed on our internal website.
Results: The PUG was started in July 2016. Through July 2017, the group has created 6 dictation templates and associated supporting documents. These include: neonatal renal ultrasound, cranial sonography, hip sonography, spine ultrasound, pyloric stenosis imaging and pediatric upper GI exam with an emphasis on malrotation. While the radiologists are not required to use the dictation templates, many say they do employ them. A 7th project on intussusception diagnosis and management was also completed. In addition, 3 PowerPoints were created and placed on our internal website. These are on pediatric musculoskeletal imaging, ultrasound and neck/chest imaging. Questions were written for these PowerPoints such that physicians may claim CME credit for their review time.
Conclusions: Within a large, geographically dispersed practice we created a pediatric sub-specialty virtual group for supportive and educational purposes. Feedback from non-pediatric radiologists about these resources has been uniformly positive. Based on the success of this model, other sub-specialties in the practice are now developing similar user groups.

Paper #: 143

The Pediatric Normal Studies Database: First Year's Experience and Utilization Patterns

Michael Francavilla, MD[1]
francavilm@email.chop.edu; [1]Radiology, Children's Hospital of Philadelphia, Philadelphia, PA

Disclosures: All authors have disclosed no financial interests, arrangements or affiliations in the context of this activity.
Purpose or Case Report: To evaluate the impact of an instantly searchable age- and gender-matched database of 30,000 normal radiographs, the Pediatric Normal Studies Database (NSDB), on clinical workflow and describe utilization patterns over the course of a year at an academic pediatric radiology department.
Methods & Materials: The NSDB was launched in August 2016 with 30,000 age- and gender matched normal radiographs available as a single-click resource from PACS at all workstations in our department. In August 2017, an anonymous survey was distributed to 35 pediatric body attendings and fellows in our institution. The survey included questions regarding whether they had heard about or used NSDB, alternatives to NSDB, and their opinion regarding speed, ease of use, and reliability compared to alternatives such as web search, reference textbooks, other web sites, and search of our institutional PACS using a 5-point Likert scale. Anonymous NSDB access analytic logs were reviewed for utilization patterns. The logs were de-anonymized for a period of 30 days for analysis of user roles. Descriptive statistical analysis and nonparametric tests for differences between the attending and fellow groups were performed.
Results: Thirty-one survey responses (24 attendings and 7 fellows) were received (89% response rate). Users agreed that the NSDB is clinically useful (weighted mean 4.6) and that it is faster, easier to use, and more reliable than alternatives (weighted means 3.8-4.4) with no significant difference between attendings and fellows. Reported alternative resources included bonepit.com, eanatomy.com, headneckbrainspine.com, Google, Elsevier STATdx, Greulich and Pyle, and Keats & Kahn's Atlas of Skeletal Maturation. Of 1,238 search sessions, the most commonly searched body parts were the ankle (n=144, 12% searches), knee (n=111, 9% searches), and elbow (n=101, 8% searches) followed by the hand, foot, chest, and femur. Thirty-two (3%) searches were initiated from skeletal surveys. Searches are becoming more frequent and are most common in infants and pre-teen-aged children. During the 30-day de-anonymized period, 17 attendings, 6 fellows, and 9 residents performed 115 (34%), 64 (21%), and 155 (45%) total searches, respectively.
Conclusions: The NSDB is an image database of normal radiographic anatomy and is regarded as being clinically useful and faster, easier to use, and more reliable than alternatives. Used by pediatric radiologists and trainees alike, it is most commonly used during the evaluation of the lower extremity.

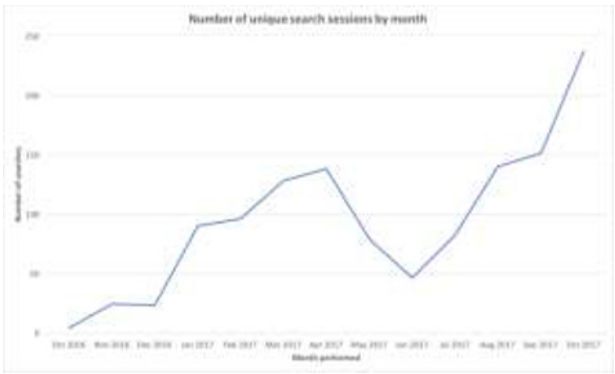

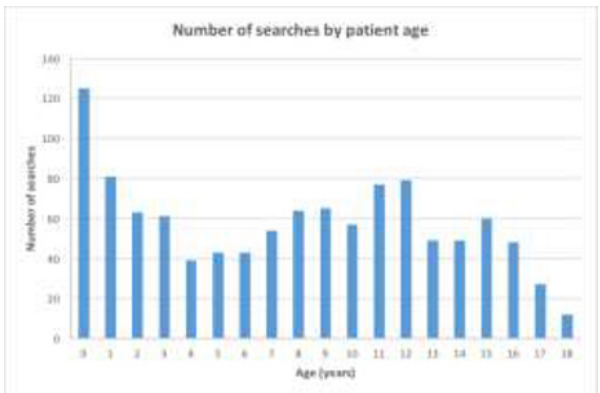

Example workflow of the user launching the NSDB from PACS and viewing a number of age- and gender-matched normal examples of the anatomy as thumbnails, larger images, and (optionally) in full resolution.

Paper #: 144

Reducing the sedation rates in MRI for pediatric patients utilizing an MRI simulator preparation session facilitated by a child life specialist.

Tricia Buskirk, Master of Science in Child and Family Studies[1], *Tricia.buskirk@nationwidechildrens.org*; Whitney Garrett, Bachelor of Science in Child and Family Studies[1], Arleen Karczewski, Bachelor of Science in Child Life Education[1];[1]Nationwide Children's Hospital, Columbus, OH

Disclosures: All authors have disclosed no financial interests, arrangements or affiliations in the context of this activity.

Purpose or Case Report: An MRI simulator was used to reduce the number of patients requiring sedation by allowing them the opportunity to have a realistic experience of an actual MRI prior to their MRI scan. A child life specialist engaged each patient in a simulator session to prepare them and allow them to become familiar with the MRI equipment and process.
Methods & Materials: Patients were identified by reviewing the MRI sedation schedule and the patient's chart. Simulator candidates were selected by assessing the type of scan, proximity to the hospital, age, and developmental or behavioral barriers. Each patient's parents were then consulted to make a final assessment of their child's potential for success in completing a non-sedated MRI. Parents showing interest were given the opportunity to have their child experience a simulator session. Prior to acquiring the MRI simulator, sedation was standard for patients under the age of 7 and whose chart showed past developmental or behavioral factors. Implementing the MRI simulator program decreased the number of patients requiring sedation. Practice time and education empowered patients to succeed without sedation due to being confident and aware of what an MRI entails.
Results: Since August of 2014, 416 patients have utilized the MRI simulator. Patients who utilized the MRI simulator were between the ages of 5-18. All of the patients chosen had scans that were scheduled to be one hour or less in length. Of the 416 patients that utilized the simulator, 354 of them were able to complete their scans without anesthesia which resulted in an 85% success rate. The 15% that were not able to complete their scans without sedation were unable to hold still or became too anxious during the actual scan. The success rate shows the benefit of allowing patients to practice and become familiar with the MRI before the actual scan. The MRI simulator reduced the number of patients requiring sedation and therefore increased patient safety, created a positive patient experience and reduced the cost for many families. Based on our current capacity for performing patient training on our MRI simulator and the observed rate of sedation required for these patients, we estimate an annual cost savings of approximately $200,000 for families.
Conclusions: Patients have a high success rate in completing their MRIs without sedation when it is paired with an MRI simulator session facilitated by a child life specialist.

Paper #: 145

Intraabdominal soft tissue injuries on computed tomography (CT) in accidental versus non accidental trauma

Disclosures: All authors have disclosed no financial interests, arrangements or affiliations in the context of this activity.

Christy Pomeranz, MD[1], *christypomeranz@gmail.com*; Christian Barrera, MD[1], Xiaowei Zhu[1], Sabah Servaes[1]; [1]Radiology, Children's Hospital of Philadelphia, Philadelphia, PA

Disclosures: All authors have disclosed no financial interests, arrangements or affiliations in the context of this activity.

Purpose or Case Report: To evaluate intraabdominal soft tissue injuries on computed tomography (CT) in accidental versus non accidental trauma (NAT).
Methods & Materials: Following IRB approval, a retrospective review was performed on all patients who had experienced trauma and who had undergone both a skeletal survey and a CT of the chest and/or abdomen and pelvis within 30 days of one another from January 2009 - July 2017. All CTs were performed at the Children's Hospital of Philadelphia with the exception of one study. Images and reports were reviewed by a pediatric radiology fellow.
Results: Data was collected on 57 patients who met inclusion criteria. Patients ranged in age from 0 to 8 years old. 35 cases were cases of NAT confirmed by the Suspected Child Abuse and Neglect Team; 8 cases were confirmed accidental trauma; and 14 cases were unknown mechanism. 53 CTs were performed with intravenous contrast and 4 CTs were performed without intravenous contrast.
30 patients had soft tissue injuries on CT while 27 patients had no evidence of injury on CT. Of the 35 confirmed cases of NAT, 21 patients had soft tissue injuries on CT (60%) and 14 did not. Of the 22 cases of accidental trauma or unknown mechanism, 9 patients had soft tissue injuries on CT (41%) and 13 did not. This difference was statistically significant ($p = 0.05$) with cases of NAT being more likely to have soft tissue injuries than accidental or unknown mechanisms. Soft tissue injuries included 17 cases of liver laceration, 5 cases of splenic laceration, 6 cases of bowel injury, 3 cases of kidney injury, 3 cases of adrenal hematoma, 2 cases of pancreatic laceration, 1 case of retroperitoneal hematoma, and 1 case of abdominal wall hematoma. There was no significant difference between NAT and accidental trauma for any of these injury types. Soft tissue injuries were statistically associated with rib fractures ($p = 0.02$) but not with other fractures, such as long bone fractures.
Conclusions: Although skeletal surveys are the mainstay of imaging in NAT, intraabdominal soft tissue injuries can also occur in NAT. These injuries occur at statistically significant higher rate than that of accidental trauma and may be missed on radiographs. The most common intraabdominal soft tissue injury to occur in both NAT and accidental trauma is liver laceration but a variety of other injuries can also be seen. Furthermore, the type of soft tissue injuries appear to be similar for NAT and accidental trauma without a difference injury profiles.

Table 1. Patient data overview

Variable (N = 57)	Results (mean ± SD)
Age (years)	0.87 ± 1.46 (range 0 – 8)
Gender	35 male (61%), 22 girls (39%)
Weight (kg)	9.27 ± 5.53 (range 3 – 36)
Computed Tomography Dose Index (vol*mGy)	2.51 ± 5.42 (range 0.11 – 41)
Dose Length Product (mGycm²)	64.5 ± 119.9 (range 3 – 903)
Radiation dose Skeletal Survey (mSv)†	0.3 ± 0
Radimetrics Estimated (mSv)	
Less than 1 year (N = 3)	1.0 ± 0.2
1 – 4 years old (N = 27)	2.0 ± 0.6
5 – 9 years old (N = 21)	3.2 ± 2.1
AAPM 96 Estimated (mSv)	
Less than 1 year (N = 3)	1.5 ± 0.5
1 – 4 years old (N = 27)	2.4 ± 0.8
5 – 9 years old (N = 21)	3.5 ± 2.3
Trauma diagnosis	
Highly likely NAT	35 cases (61%)
Unknown	14 cases (25%)
Accidental	8 cases (14%)

Note: †This radiation dose was set up according to our institutional protocol to all skeletal surveys. NAT = Non accidental trauma, AAPM = The American Association of Physicists in Medicine.

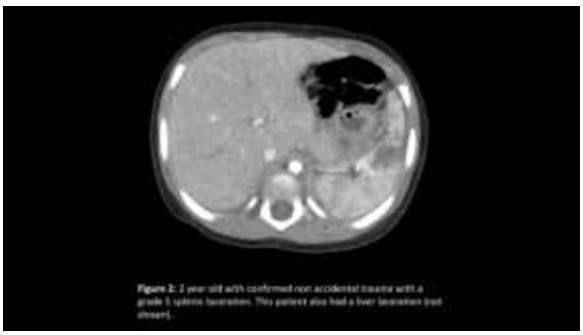

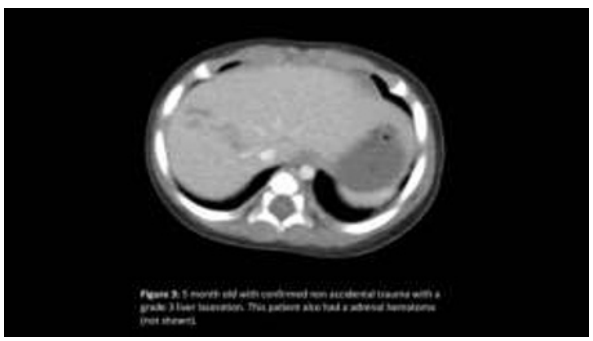

Paper #: 146

Perforated appendicitis vs Non-perforated Appendicitis: A Validation Study of a Score System Based on Sonographic, Clinical and Laboratory Findings

Einat Blumfield[1], Joel Wolf, MD[1], Benjamin Benson, MD[1], James Meltzer, MD[1], Adina Sperling, BS[3], Terry Levin, MD[2]; [1]Radiology, Albert Einstein College of Medicine/Jacobi Medical Center, Flushing, NY, [2]Montfiore Medical Center/ Albert Einstein College of Medicine, Bronx, NY, [3]New York Medical College, Valhalla, NY

Disclosures: All authors have disclosed no financial interests, arrangements or affiliations in the context of this activity.

Purpose or Case Report: The distinction between perforated and non-perforated appendicitis is beginning to be clinically relevant as a deciding factor of whether to surgically intervene on a pediatric patient or not. Perforation is treated in some institutions conservatively initially while non-perforated appendicitis would require an emergent surgery. While CT scans have proven to be a good imaging modality for differentiating perforated from non-perforated appendicitis, they expose pediatric patients to ionizing radiation. On a previous study performed in our institution a scoring system that incorporates clinical, laboratory, and ultrasound findings was developed (see attached table), with a high specificity (91%) and low-moderate sensitivity (29-61%, depending on the score cutoff value). We therefore performed a retrospective study from two institutions to validate this scoring system.

Methods & Materials: After receiving IRB approval (IRB# 2016-7083), we searched our data base for pediatric appendiceal ultrasound studies from June 2015 through June 2017 and the clinical (Tmax, days of fever, days of pain, age, presence of vomiting/diarrhea) laboratory (WBC, CRP, and ESR), and ultrasound findings (appendix size, loss of submucosal layer, complex free fluid, amount of echogenic fat, and abscess) were documented. This data was incorporated into the scoring system and compared to the gold standard, surgical and pathological evaluation. 149 cases were found, 44 patients with equivocal scores were missing data parameters that would possibly increase their score to be consistent with perforation. They were therefore excluded. The remaining 105 cases were scored. Sensitivity, specificity, positive predictive values (PPV), and negative predictive values (NPV) were calculated.

Results: The study population consisted of 70 males and 35 females ranging from 2 years to 18 years of age. 44 were deemed perforated by the scoring system with 43 actually perforated. When compared to surgical/pathological results the scoring system demonstrated the following results: Sensitivity=0.98, specificity= 0.73, PPV= 0.73, and NPV=0.98.

Conclusions: This study validates a scoring system based on clinical, laboratory and sonographic findings, for differentiation of perforated from non- perforated appendicitis in pediatric patients, with good results.

Scoring Values To Differentiate Perforated and Non-Perforated Appendicitis

History and Physical	Point
Age<8 years old	3
Fever≥2 days	5
Pain >2 days	3
Diarrhea	3
Vomiting	3
Maximum temperature ≥ 100.9° F	3
Laboratory Values	
WBC ≥ 17k	1
ESR ≥ 22 mm/h	5
CRP> 50 mg/L	3
US Findings	
Abscess	5
Large amount of echogenic fat	4
Complex free fluid	4
Appendix size ≥ 1.6cm	3
Loss of submucosal layer	3
Total	

Paper #: 147

Rapid non-contrast MR protocol for evaluation of abdominal and pelvic abscesses in children

Fozia Naz[1], *n_fozia@yahoo.com*; Nishard Abdeen, MD[1]; [1]Children Hospital Of Eastern Ontario, Ottawa, ON, Canada

Disclosures: All authors have disclosed no financial interests, arrangements or affiliations in the context of this activity.

Purpose or Case Report: To evaluate the clinical efficacy of a rapid non-contrast enhanced MR protocol for evaluation of abdominal and pelvic abscesses in children.

Methods & Materials: All patients having undergone clinically indicated MRI between June 1 2013 and July 30, 2017 for suspected abdominal and pelvic abscesses were identified through a keyword search of the radiology information system. The MR protocol comprised axial and coronal T2 weighted SSFSE, sagittal T2 with fat suppression and axial DWI of the abdomen and pelvis. Clinical chart and radiologic images were reviewed by a pediatric radiologist and fellow. Location of abscess or collection, presence of restricted diffusion (minimum ADC) and size were recorded. The route of drainage was also recorded if a drainage procedure was performed. Clinical out come and need for repeat procedures were also recorded.
Results: There were 53 patients with a mean age of 11 years. Three patients had tubo-ovarian abscesses, one had pelvic extension of a psoas abscess, and one had a post-operative abscess following ileoanal anastomosis. The remainder of the patients had perforated appendicitis or post appendectomy abscesses. The duration of the MRI study was 34 minutes. The average abscess volume was 120 cc with a mean ADC value of 1319 mm2/s.In 38 patients (72%), there was a collection in the pelvis, including 5 patients with both abdominal and pelvic collections. 35 patients underwent drainage by interventional radiology. Of these, 29 (82%) were drained transrectally, 3(9%) trans-abdominally and 3 (9%) had both transabdominal and transrectal drainages. All of the transrectally drained abscesses had a clear drainage path established on MRI, whereas ultrasound failed to demonstrate drainability in the 26 of these cases (89%). Of the 15 patients who had abscesses in the abdomen but not the pelvis, 12 (80%) underwent a percutaneous drainage while in 3 patients the collection was judged too small to drain. All patients had resolution of abscess although one patient required two drainage procedures for a recurrent abscess. In one patient the abscess collapsed during drainage and no catheter was left in place. None of the patients required CT.
Conclusions: Rapid non-contrast MRI is easy to perform, and can guide the appropriate treatment, particularly in the case of trans-rectal drainage where ultrasound is equivocal in most cases, with good clinical outcomes. The main advantage is avoidance of CT with concomitant radiation exposure and contrast administration.

Paper #: 148

Does Prolongation of Time Between Intussusception Diagnosis and Therapeutic Enema Result In Increased Patient Morbidity: a Retrospective Review

Ivey Royall, MD[1], *Ivey.Royall.MD@flhosp.org*; Aaron Lindsay, MD[1], Gregory Logsdon, MD[1], Matthew Swerdlow, MD[1], Julie Pepe, PhD[1], Jennifer Williams, MD[1]; [1]Florida Hospital, Orlando, FL

Disclosures: All authors have disclosed no financial interests, arrangements or affiliations in the context of this activity.

Purpose or Case Report: Ileocolic intussusception is an emergent condition with concern for bowel ischemia prompting rapid treatment. Therapeutic enema performed by a pediatric radiologist, with progression to surgery if reduction fails is standard of care. However, many hospitals do not have pediatric radiologists available and require transfer, delaying treatment. Despite increased concern for risk of bowel complication, there is limited data evaluating the effect of increased time to therapeutic enema and patient morbidity/mortality. Our purpose is to determine if there is increased patient morbidity/mortality associated with prolonged time between diagnosis and treatment of intussusception.
Methods & Materials: A retrospective evaluation of pediatric patients treated for intussusception at a children's hospital over a 10-year period was performed. Florida Hospital for Children is part of a multi-hospital system, and serves as a referral center for 12 community hospitals. Patient's records were reviewed for time of presentation, onset of symptoms, time of radiographic diagnosis, hospital transfer (if applicable), time of attempted enema reduction, success of reduction, and surgical outcomes (if applicable).
Results: A total of 147 presentations of intussusception occurred, of which 30 cases (20%) required surgery due to unsuccessful reduction. Nineteen cases (13%) resolved spontaneously. Ninety-five (65%) cases had enema attempts in up to 3 hours; of which 22 (23%) required surgery. Twenty-eight cases occurred greater than 3 and up to 6 hours (19%); of which 6 (21%) required surgery. Five (3.4%) had enema attempts over 6 hours from time of diagnosis; of which 2 (40%) required surgery. A chi square test of independence showed no statistically significant difference in surgical rates between the groups (p-value=0.660). Four (3%) patients required bowel resection secondary to ischemia. All 4 cases had reduction attempts in less than 3 hours and reported symptoms for over 24 hours.
Conclusions: There was no increase in morbidity as measured by need for surgical reduction of intussusception in patients treated in under 3 hours from time of diagnosis versus those treated between 3 and 6 hours from time of diagnosis. Additionally, risk for ischemic bowel injury was not associated with increased time between radiographic diagnosis and therapeutic enema attempt in our review. Further evaluation of patients treated greater than six hours from the time of diagnosis is needed given the low sample size of this group in this study.

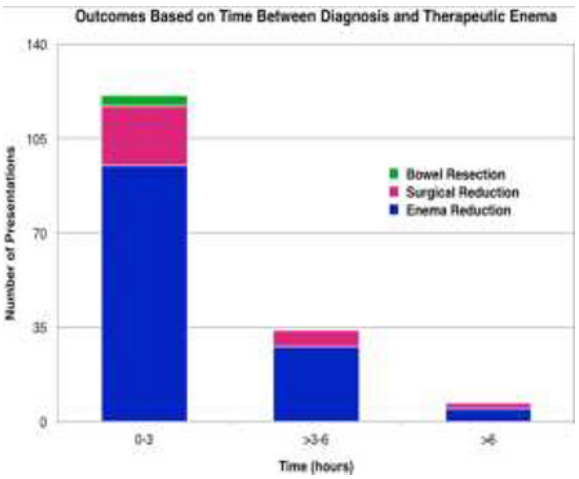

Paper #: 149

Non-emergent outpatient pediatric UGI series: can clinical parameters improve diagnostic yield?

Adam Goldman-Yassen[1], *adgoldmanyassen@gmail.com*; Jordana Gross[1], Inna Novak, MD[2], Terry Levin, MD[1]; [1]Montefiore Medical Center, Bronx, NY, [2]The Children's Hospital at Montefiore, Bronx, NY

Disclosures: All authors have disclosed no financial interests, arrangements or affiliations in the context of this activity.

Purpose or Case Report: Outpatient non-emergent upper gastrointestinal series (UGI) are frequently ordered in children with symptoms including abdominal pain, failure to thrive, and vomiting. In order to determine the utility of these studies, we evaluated the incidence of abnormal UGI findings in children without prior history of gastrointestinal (GI) pathology or abdominal surgery, and identified those clinical indications that improved diagnostic yield.

Methods & Materials: From October 2016-2017, UGI findings in children less than 18y were reviewed. Children with prior medical and surgical GI pathology were excluded. Exam indications and clinical history were obtained from the electronic medical record.
Results: Of 265 children with outpatient UGI, 191 had no prior GI history (mean 5.4 years, 51% female). Most common indications were non-bilious emesis (69%), abdominal pain (31%), and reflux (23%). Patients had normal studies in 164/191 cases (86%), including all 13 patients with reported bilious emesis. Of the 27 abnormal studies, 19 (70%) showed only gastroesophageal reflux (median age 2y). In the remaining 8 (30%), diagnoses included achalasia, small caliber esophagus with mucosal irregularity (diagnosis later confirmed as eosinophilic esophagitis), duodenum inversum, SMA syndrome, distal esophageal ring, wandering duodenum, gastroparesis and pylorospasm in an infant with known heart disease.
All abnormal cases occurred in older children/teens, except for one infant with congenital heart disease (median age 13.5y). Three had foreign body sensation/dysphagia while five described frequent vomiting with duration from 3-12 months.
Multivariable logistic regression (including weight loss, failure to thrive, bilious/non-bilious vomiting, foreign body sensation/dysphagia, adjusted for age and sex) found that failure to thrive (OR=18.2, p=0.02), foreign body sensation (OR=98, p=0.02), and increasing age in years (OR=1.3, p=0.01) were independent predictors of an abnormal UGI.
Conclusions: The yield of routine UGI in children with no GI history is low. In young children, most abnormal findings are related to gastroesophageal reflux. Diagnostic yield may be increased in those with failure to thrive or in older patients with prolonged symptoms of vomiting or foreign body sensation.

Paper #: 150

Does prior CT or MRI obviate the need for Upper GI examination to rule out malrotation?

Kevin Wong, DO[1], *kevinwong504@gmail.com*; Dane Van Tassel, MD[1], Deepa Biyyam, MD[1], Mostafa Youssfi, MD[1]; [1]Radiology, Phoenix Children's Hospital, Phoenix, AZ

Disclosures: All authors have disclosed no financial interests, arrangements or affiliations in the context of this activity.

Purpose or Case Report: To assess the diagnostic accuracy of CT and MRI in malrotation and to determine the most reliable cross-sectional criteria to exclude malrotation.
Methods & Materials: All patients who underwent an UGI during 2016-2017 were identified using keyword search tools in the radiology information system. 175 patients who underwent UGI also had relevant prior cross-sectional CT or MRI. These studies were blindly reviewed to determine superior mesenteric artery-vein relationship (SMA/SMV), the position of the 3rd portion of the duodenum (D3), the uncinate process of the pancreas and the location of the cecum, to diagnose malrotation. These results were compared to the UGI findings.
Results: 175 Patients who underwent UGI also had a relevant CT or MRI. Malrotation was found in 17 patients using cross-sectional imaging. All but one was confirmed on UGI. The remaining 158 cases were negative on cross-sectional imaging and confirmed on UGI. Using a combination of SMA/SMV relationship, the uncinate process of the pancreas, D3, and the location of the cecum, the sensitivity of cross-sectional imaging for malrotation was found to be 100% and the specificity was 97%.
Conclusions: Malrotation can be diagnosed on cross-sectional imaging based on the following 4 criteria: SMA/SMV relationship, the retroperitoneal position of D3, a normal uncinate process of the pancreas and the location of the cecum in the right lower quadrant; thus obviating the need for a subsequent upper GI examination.

Paper #: 151

Making the Diagnosis of Mid Gut Volvulus: Limited Abdominal Ultrasound has Changed our Clinical Practice

Disclosures: All authors have disclosed no financial interests, arrangements or affiliations in the context of this activity.

Kevin Wong, DO[1], *kevinwong504@gmail.com*; Dane Van Tassel, MD[1], Deepa Biyyam, MD[1], Monique Riemann, RDMS RVT[1], Justin Lee, MD[1], Craig Egan, MD[1], Dianna Bardo, MD[1], Mostafa Youssfi, MD[1]; [1]Radiology, Phoenix Children's Hospital, Phoenix, AZ

Purpose or Case Report: To assess the diagnostic accuracy of limited abdominal ultrasound (US) examination for mid-gut volvulus (MGV) and to evaluate how clinical practice has changed in a free-standing children's hospital leading to the near obsolescence of upper GI (UGI) studies for the diagnosis of MGV.
Methods & Materials: All patients with suspected MGV who underwent abdominal US during 2016-2017 were identified using keyword search tools in the radiology information system. Retrospective, blinded image review was performed by a certificate of added qualification (CAQ) pediatric radiologist. US were evaluated for the presence of the superior mesenteric artery (SMA) cutoff sign and twisting of the mesentery (whirlpool sign). Results were compared with the original radiology report and operative reports.
Results: 195 US studies were performed from 2016-2017. Most common presentations were vomiting (44%), abdominal pain (7%), and suspected mal-rotation (10%). 195 US were reviewed of which 16 were non-diagnostic. 179 diagnostic studies showed MGV in 14 patients. Those 14 patients were surgically explored and confirmed to have midgut volvulus. 10 of the 16 non-diagnostic US studies were further evaluated with UGI examination or CT with 1 patient demonstrating mal-rotation without volvulus. This 1 patient was explored surgically and was found to have mal-rotation without volvulus. The remaining 6 patients were followed clinically or found to have other etiologies of abdominal pain on surgical exploration. There were 164 negative US, none of whom went to surgery. The sensitivity and specificity of US was 100%.
Conclusions: Limited abdominal US is a highly accurate examination for the diagnosis of mid-gut volvulus. UGI exposes patients to ionizing radiation and should be reserved for patients in whom US is non-diagnostic or inconclusive.

Paper #: 152

Clinical Evaluation of Free Breathing CArdioREspiratory Synchronized (CARESync) Balanced Steady-State Free Precession (bSSFP) Cine Imaging in Pediatric Population

Amol Pednekar, PhD[1], *aspednek@texaschildrens.org*; Siddharth Jadhav, MD[1], Ivone Rodriguez[1], Connor Ho[1], Cory Noel, MD[1], Prakash Masand, MD[1]; [1]Radiology, Texas Children's Hospital, Houston, TX

Disclosures: All authors have disclosed no financial interests, arrangements or affiliations in the context of this activity.

Purpose or Case Report: Inability to perform breath-holds, an essential requirement for bulk motion minimization in cine balanced steady-state free precession (bSSFP) images, severely limits the image quality (IQ) in sedated pediatric patients. We evaluated IQ of fixed and adaptive CArdioREspiratory

Synchronized (CARESync) bSSFP sequence with prospective arrhythmia rejection and retrospective cardiac gating.
Methods & Materials: CARESync sequence described in Fig1 allows two free breathing modes: fixed - single R-R per respiration, and adaptive - multiple R-R per respiration with prospective rejection for inspiration during acquisition. Experienced CMR reader, blinded to CARESync mode, graded IQ for all sedated CMR scans (June-Sept 2017) performed on 1.5T clinical scanner, based on: blood to myocardial contrast, signal uniformity, and delineation of the endocardial contour throughout the cardiac cycle, on the scale of 1 to 5 where 5 corresponds to IQ equivalent to best possible with breath-hold sequence (Table1). Actual acquisition times and physiology events were retrieved from scanner log files.
Results: All 63 sedated patients (age 11.7±10.3, range 4mo-58yrs; 40 male; HR 85.2±18.1, range 48-140hbm; Resp 20.8±5.9, range 12-38 rpm) were scanned successfully with CARESync by two CMR experienced technologist without any supervision (41 fixed mode). The imaging parameters were: TR/TE/FA=2.5-2.7ms/1.25-1.35ms/60°; SENSE=1.3-2; temporal resolution 30-45ms. IQ scores ranked as excellent (26.5%), good (66%), to moderate (7.5%) from 253 sequences (63 SA, 63 VLA, 53 4CH, 25 LVOT, 30 RVOT, 19 AoRoot) (Fig2). The IQ scores for fixed and adaptive mode ($p=0.40$ two-sided Wilcoxon signed ranked test) were comparable. The acquisition duration per slice for adaptive mode (25.8±8.9s) was significantly shorter ($p<0.0017$) than for the fixed mode computed from logged cardiorespiratory rates (31.5±12.4s) (Fig2). The acquisition duration per slice for CARESync (26.0±8.5s) was significantly longer ($p<0.0001$) than the computed alternative of 4 NSA from logged R-Rs (21.7±6.2s). Fixed mode of CARESync has been previously reported to improve IQ significantly over multi-NSA and provide comparable ventricular volumes.
Conclusions: Cardio-respiratory synchronized, retrospectively cardiac-gated bSSFP sequence with prospective arrhythmia rejection provides consistently good image quality in sedated pediatric CMR studies, and adaptive mode allows further 18% reduction in scan time compared to fixed mode for favorable cardiorespiratory rates.

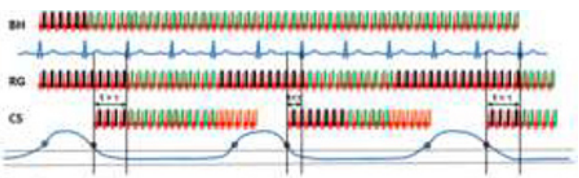

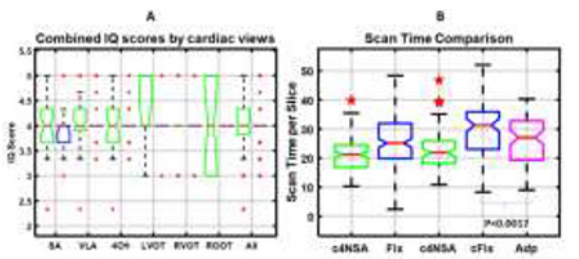

Figure 2: (A) Box plots of combined = (BMC + Edef + Art)/3 image quality scores for different cardiac views; green - fixed mode, blue - adaptive mode. (B) Box plots of scan times per slice for actual fixed (Fix in blue) and adaptive (Adp in magenta) mode acquisition and for corresponding calculated 4 number of signal averages (c4NSA in green) and calculated fixed mode (cFix in blue) acquisitions from logged cardiorespiratory rates. BMC, Edef, Art – refer to Table 1, SA – short-axis, VLA – vertical long-axis, 4CH – four chamber, LVOT – left ventricular outflow tract, RVOT – right ventricular outflow tract, ROOT – aortic root, All – for all views.

Table 1: Clinical score criteria

Score	BMC	Edef	Art
5	Excellent: Blood pool is hyperintense with excellent contrast against the myocardium; myocardium is uniformly bright throughout the cardiac cycle with little evidence of flashing.	Excellent: Papillary and endocardial trabeculae are clearly visible in the bright backdrop of the blood pool.	Excellent: Image is nearly artifact free.
4	Good: Blood pool is significantly brighter than the myocardium, as myocardial signal intensity is fairly uniform throughout the cardiac cycle.	Good: Papillary and endocardial trabeculae are visible but somewhat blurred during the cardiac cycle.	Good: Some motion artifact is present but does not affect overall image quality.
3	Moderate: Image is of diagnostic quality but features significant loss of blood to myocardial contrast or noticeable variation in myocardial signal throughout the cardiac cycle.	Moderate: Myocardial walls are barely distinguishable from endocardial trabeculae.	Moderate: Motion artifacts are visible, but image is still of diagnostic quality.
2	Poor: Blood-to-myocardial contrast is poor, but the image is still of diagnostic quality.	Poor: Myocardial walls and endocardial trabeculae are significantly blurred.	Poor: Images are nearly nondiagnostic with significant artifacts.
1	Nondiagnostic: Blood-to-myocardial contrast is poor; image was deemed nondiagnostic.	Nondiagnostic: Blood-to-myocardial edge definition is poor; image was deemed nondiagnostic.	Image is of nondiagnostic quality.

Art = motion artifact; BMC = blood-to-myocardial contrast; Edef = endocardial edge definition.

Paper #: 153

Numerical Simulations of Geometric Markers for Left Ventricular Hypertrabeculation: Fractal Dimension and Isoperimetic Ratio

Amol Pednekar, PhD[1], *aspednek@texaschildrens.org*; Carter Chu[2], Tobias Schlingmann[1], Zili Chu, PhD[1], Cory Noel, MD[1], Prakash Masand, MD[1]; [1]Radiology, Texas Children's Hospital, Houston, TX, [2]Clements High School, Houston, TX

Disclosures: All authors have disclosed no financial interests, arrangements or affiliations in the context of this activity.

Purpose or Case Report: The purpose of this numerical simulation is to evaluate the correlation and dynamic range of the isoperimetric ratio compared to the previously reported fractal dimension (FD) for the quantification of irregularity and complexity of the geometric structures associated with left ventricular trabeculation.
Methods & Materials: For the purpose of numerical simulations, the morphologic left ventricular endocardial boundary is represented in a binary image with a white circle of one pixel line width on a black background. In order to eliminate the influence of embedding space on FD calculation with the box counting method, square images centered at the circle and sides equal to the radius of the circle were created. The varying degrees of geometric irregularity of LV trabecular edge images is simulated using equations shown in Fig 1. Set of 10 simulated images were generated for each combination of amplitude (90% to 30% of original radius) and frequency (4 to 22 cycles over the entire perimeter) levels of variation in radius. FD were calculated using the box counting method. The perimetric ratio (PR) is calculated as the ratio of the perimeter length of the spatially variant radius to the perimeter of the constant radius circle. Short-axis stack of end-diastolic bright blood MR images from 30 LVNC positive patients (age 15±5.0, range 4-30 yrs, 22 m; NC/C 2.8±0.38, range 2.3-3.6) and 20 LVNC negative patients (age 16±7.4, range 8-39 yrs, 11 m) were analyzed retrospectively using a novel automated tool to compute FD and PR for each slice.

Results: Numerical solutions generated 1000 binary trabecular edge images for a FD ranging from 1.26 to 1.69 with corresponding values of PR varying from 1.01 to 5.8. Representative simulated images are shown in Fig 1. Representative clinical images are shown in Fig2. The relationship between FD and PR for simulated images can be expressed as $simPR = 0.005e^{4.21simFD}$. Fig 3 shows an overlay of FD and PR values of the 136 basal, 165 mid-ventricular, and 149 apical slices from 50 clinical cases on simulation derived values. The relationship between FD and PR for simulated images can be expressed as $cliPR = 0.005e^{3.41cliFD}$.
Conclusions: Numerical simulations estimate relationship between FD and PR to be exponential with estimated dynamic range for PR 11 times higher than the calculated FD range in clinical data. Observed dynamic range for PR in LVNC positive patients and negative controls, was 6 times higher than FD range.

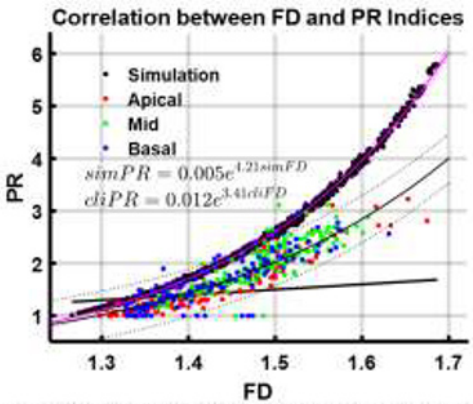

Figure 3: Scatter plot of simulated and clinical PR against FD with exponential fit and predication intervals; black – line of unity. FD - fractal dimension, PR - perimetric ratio.

$$x(\theta) = r(\theta)\cos(\theta), y(\theta) = r(\theta)\sin(\theta), where\ 0 \le \theta \le 2\pi,$$

$$r(\theta) = r_o - i.r_o.\sin(k_j\phi_j), where\ 0 \le \phi_j \le 2\pi$$

$$k_j = \frac{2\pi}{2\pi - \lambda_j}\ where\ \lambda_j = rand(0,1)\ such\ that\ \sum_{j=1}^{n} k_j = 2\pi\ with\ n\ cycles\ of\ \phi_j$$

$$i = 0.1, 0.1667, 0.233, \ldots, 0.7; j = 4, 6, \ldots, 22.$$

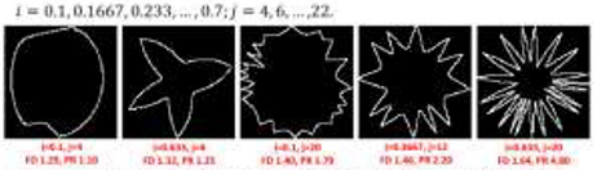

Figure 1: Representative simulated images with spatially varying radius spanning the spectrum of clinically observed FD range with corresponding PR. Delta change in radius is percentage (1-i) of original radius and frequency of varying radius is expressed as number of cycles (j) spanning the perimeter. Location of the peaks and valleys are determined by random number generator as expressed in equation above. FD - fractal dimension, PR - perimetric ratio.

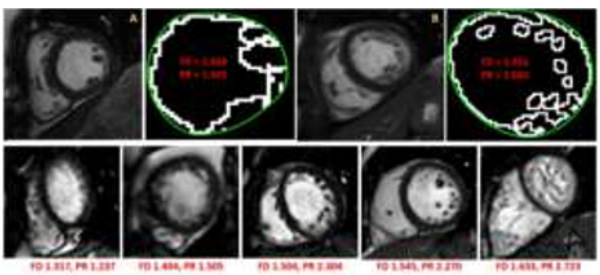

Figure 2: Top row depicts representative output images from the automatic tool for LVNC (A) negative and (B) positive subjects. Automatically thresholded trabecular edges are shown in white and automatically delineated endocardial contour is shown in green. Bottom row depicts the left ventricular images spanning the spectrum of FD values. FD – fractal dimension, PR – perimetric ratio, LVNC – left ventricular non-compaction.

Paper #: 154

Automatic Quantification of Left Ventricular Non-compaction using Fractal Analysis and Perimetric Ratio

Amol Pednekar, PhD[1], *aspednek@texaschildrens.org*; Tobias Schlingmann, MD, PhD[1], Siddharth Jadhav, MD[1], Cory Noel, MD[1], Prakash Masand, MD[1]; [1]Texas Children's Hospital, Houston, TX

Disclosures: All authors have disclosed no financial interests, arrangements or affiliations in the context of this activity.

Purpose or Case Report: Although MRI can reveal the non-compacted trabeculation (NC) distinctly from compacted myocardium (C), the current diagnostic criteria based on one dimensional measurements (NC/C>2.3) suffer from subjective variability and tend to over-diagnose left ventricular non-compaction (LVNC), especially in pediatric patients where LV trabeculation varies on a continuous spectrum. The purpose of this study is to clinically evaluate the automatic quantification of geometric irregularity and complexity associated with LVNC in bright blood MR images using fractal dimension (FD) and perimetric ratio (PR) in a pediatric cohort.
Methods & Materials: Short-axis stack of end-diastolic bright blood MR images from 30 LVNC positive patients (age 15±5.0, range 4-30 yrs, 22 m; NC/C 2.8±0.38, range 2.3-3.6) and 20 LVNC negative patients (age 16±7.4, range 8-39 yrs, 11 m) were analyzed retrospectively using a novel automated tool. The only user interaction required was to select the most basal and apical slice to be included in the analysis. The tool automatically tracks the LV size and shape. Otsu's thresholding algorithm delineates papillary and trabecular muscles. FD were computed on the resultant edge images using the box counting method. A piecewise closed Bézier curve of 2nd order geometric continuity was fitted through the salient points of the convex hull of these edges to obtain endocardial contours (Fig 1). The ratio of length of blood pool edges to endocardial contour perimeter (PR) was computed for each slice. Paired t-tests were performed between FD & PR and FD & FD*PR for all slices. Global LVNC index was calculated as the mean of the top half (MTH) of the slices sorted by particular index. Two sample t-tests were performed for FD, PR, and FD*PR between LVNC positive and negative patients.
Results: The analysis was performed successfully in all subjects (149 apical, 165 mid-ventricular, and 136 basal slices) with a computation time of 5±2 sec per subject. The mean±SD, p values and % change in median values with 95% confidence intervals are shown in Table 1.Figure 2 shows a one to one line plot and box plots for all indices along with a scatter plot for all slices.
Conclusions: In this study we described a novel tool as well as a novel index to automatically quantify LV trabecular complexity and irregularity. Both FD and PR indices distinguish LVNC patients from negative controls, while the PR and FD*PR respectively provide 6 and 11 times higher dynamic ranges.

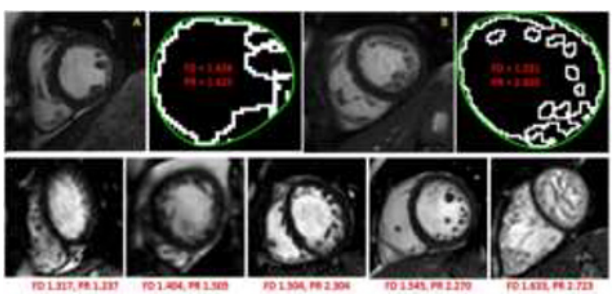

Figure 1: Top row depicts representative output images from the automatic tool for LVNC (A) negative and (B) positive subjects. Automatically thresholded trabecular edges are shown in white and automatically delineated endocardial contour is shown in green. Bottom row depicts the left ventricular images spanning the spectrum of FD values. FD – fractal dimension, PR – perimetric ratio, LVNC – left ventricular non-compaction.

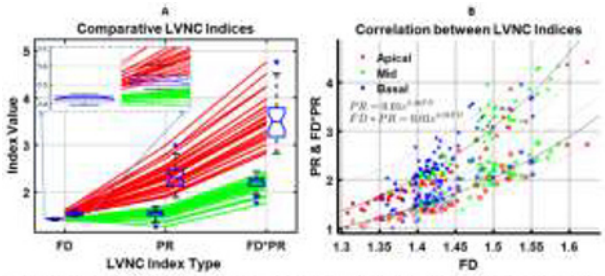

Figure 2: (A) One to one line and Box plot of MTH of FD, PR, and FD*PR; red: LVNC positive and green: LVNC negative. (B) Scatter plot of PR (hollow markers) and FD*PR (filled markers) against FD with exponential fit and predication intervals; circles: LVNC negative and stars: LVNC positive. FD - fractal dimension, MTH - mean of top half, PR - perimetric ratio, LVNC – left ventricular non-compaction.

	Apical	Mid-Ventricular	Basal	MTH
FD -	1.42±0.08	1.47±0.06	1.42±0.07	1.43±0.02
FD +	1.47±0.08	1.51±0.04	1.44±0.08	1.53±0.03
PR -	1.49±0.51	1.90±0.49	1.61±0.50	1.54±0.10
PR +	1.77±0.53	2.25±0.31	1.81±0.50	2.32±0.27
FD*PR -	2.15±0.90	2.82±0.83	2.32±0.83	2.19±0.17
FD*PR +	2.64±0.93	3.41±0.53	2.63±0.85	3.55±0.48
p FD +/-	< 0.0001	< 0.0001	< 0.0001	< 0.0001
p PR +/-	< 0.0001	< 0.0001	< 0.0001	< 0.0001
p FD*PR +/-	< 0.0001	< 0.0001	< 0.0001	< 0.0001
M% PR/FD -	-12(-15,-10)	10 (5, 14)	-5(-10, 1)	8 (4, 11)
M% PR/FD +	16 (10, 21)	47 (43, 51)	21 (15, 27)	51 (45, 57)
M% FD*PR/FD -	19 (15, 22)	57 (50, 65)	34 (25, 43)	53 (48, 59)
M% FD*PR/FD +	70 (60, 81)	123 (116, 129)	74 (64, 84)	131 (120, 140)

Table 1: Distribution of resultant FD, PR, and FD*PR values by morphological thirds of the LV and corresponding global LV indices calculated as mean value of the top half (MTH) of the LV slices sorted by each index. P-values from the two-sample t-tests between LVNC positive (+) and negative (-) patients. Percentage change in median values (M%) from paired t-tests of FD v/s PR and FD*PR. FD - fractal dimension, PR - perimetric ratio.

Paper #: 155

Comparison of MR Tissue Phase Mapping and MR Feature Tracking in Children with Hypertrophic Cardiomyopathy

Arleen Li[1], *arleen.li@northwestern.edu*; Alexander Ruh, PhD[1], Michael Markl, PhD[1], Joshua Robinson, MD[2], Cynthia Rigsby, MD[2]; [1]Northwestern University, Chicago, IL, [2]Ann & Robert H. Lurie Children's Hospital of Chicago, Chicago, IL

Disclosures: All authors have disclosed no financial interests, arrangements or affiliations in the context of this activity.

Purpose or Case Report: Hypertrophic cardiomyopathy (HCM) is a common genetic condition associated with increased risk of heart failure, atrial fibrillation, and sudden death. MR techniques have demonstrated reduced myocardial function in adults with HCM despite normal left ventricular (LV) ejection fraction. Changes in LV tissue structure, e.g. diffuse fibrosis, are also associated with elevated myocardial T1 and may be important outcome predictors. However, the performance of MR techniques assessing LV function (e.g. tissue phase mapping (TPM), feature tracking (FT)) and tissue abnormalities (e.g. T1-mapping) in children has not been systematically evaluated. We compared TPM and FT for assessment of global LV myocardial velocities in children with HCM relative to healthy controls, and assessed structure-function relationships between myocardial velocities, maximum LV wall thickness, and native myocardial T1.

Methods & Materials: 17 HCM patients and 21 age-matched controls (15.3±3.7yrs vs 15.6±4.0yrs, p=0.8) undergoing standard-of-care cardiac MRI were recruited to undergo TPM (black-blood prepared phase-contrast sequence with 3-directional velocity encoding). Global LV myocardial radial and longitudinal velocities were calculated from 1) TPM short axis images (in-house MATLAB tool) and 2) FT using short and long axis cine steady state free precession (SSFP) images (TomTec ImageArena). LV ejection fraction (EF) and maximum LV wall thickness were measured from short axis SSFP images. Native T1 was calculated from modified Look-Locker inversion recovery images.

Results: Mean HCM patient LVEF was 65±8% vs 57±3% in controls, p<0.01. Mean HCM patient maximum LV wall thickness was greater than controls (24±9mm vs 8±1mm, p<0.01). Mean LV T1 was higher in HCM patients than controls (1049±59ms vs 1000±33ms, p<0.01). Peak diastolic radial and longitudinal velocities in TPM and FT and peak systolic longitudinal velocity in TPM were reduced in HCM patients vs controls (Table 1). Among all subjects, peak global diastolic velocities using TPM and FT were correlated with mean LV T1 and maximum LV wall thickness (Table 2).

Conclusions: Both TPM and FT show decreased diastolic myocardial velocity in HCM patients, suggesting reduced myocardial relaxation despite normal LVEF. This may be an early indicator of disease and helpful in multiparametric HCM patient analysis. Significant associations between impaired diastolic LV velocities and elevated T1 indicate direct relationships between tissue structure abnormalities and LV function decline.

Table 1. Mean Global Radial and Longitudinal LV Velocities at Peak Systole and Peak Diastole, calculated using Tissue Phase Mapping (TPM) and Feature Tracking (FT)

	*p < 0.05	Radial Velocity (cm/s)		Longitudinal Velocity (cm/s)	
	**p < 0.01	Controls	HCM	Controls	HCM
TPM	Peak Systole	3.1 ± 0.7	3.3 ± 0.6	6.1 ± 1.8	4.8 ± 1.8*
	Peak Diastole	-4.9 ± 0.8	-3.7 ± 1.1**	-8.0 ± 1.5	-4.9 ± 2.1**
FT	Peak Systole	2.9 ± 0.5	3.0 ± 0.5	3.3 ± 0.7	2.8 ± 0.7
	Peak Diastole	-3.3 ± 0.4	-2.9 ± 0.8*	-4.0 ± 0.9	-3.0 ± 1.0*

Table 2. Correlation of Peak Diastolic Velocities calculated using Tissue Phase Mapping and Feature Tracking, with Native T1 Values and Maximum Left Ventricular Wall Thickness

		Peak Diastolic Radial Velocity		Peak Diastolic Longitudinal Velocity	
		r	p	r	p
Native T1 Values	Tissue Phase Mapping	0.67	<0.001	0.72	<0.001
	Feature Tracking	0.58	<0.001	0.57	0.005
Maximum LV Wall Thickness	Tissue Phase Mapping	0.56	<0.001	0.62	<0.001
	Feature Tracking	0.37	0.03	0.41	0.02

r, Pearson correlation coefficient; p<0.05 is considered significant

Paper #: 156

Quantitative Regional Fibrosis Burden in Duchenne Muscular Dystrophy Patients by Cardiac Magnetic Resonance Imaging

Ramkumar Krishnamurthy, PhD[1], *ramkumar.krishnamurthy@nationwidechildrens.org*; Sanjay Subramanian, B.S>[1], Alexander Long, Bachelors[1], Houchun Hu, PhD[1], Linda Cripe, MD[1], Rajesh Krishnamurthy[1], Kan Hor, MD[1]; [1]Radiology, Nationwide Children's Hospital, Columbus, OH

Disclosures: Kan Hor has indicated a relationship with Medtronics and Capricor as a consultant/honoraria. All other authors have disclosed no financial interests, arrangements or affiliations in the context of this activity.

Purpose or Case Report: Cardiac magnetic resonance imaging is used for assessment of ventricular function by ejection fraction (EF) and myocardial fibrosis by late gadolinium enhancement (LGE) for DMD patients. Earlier studies have shown that LGE precedes decline in EF[1-2]. However, there is limited data on quantitative regional fibrosis variability in DMD that might help disease monitoring. In this study, we sought to determine the regional variability between different slice locations, and hypothesize that apical LGE is associated with a later stage of the disease, when EF is abnormal.
Methods & Materials: LGE images of 87 DMD children acquired from November 2015 until June 2017 were analyzed. An observer drew contours on three short axis slices (basal, mid-level and apical), delineating the endocardium and epicardium, as well as a remote normal region (Figure 1) yielding mean and standard deviation. Area of fibrosis (scar) was defined as regions with signal intensity > 6X standard deviations from the remote normal mean. The scar burden (%) was defined as the ratio of area identified as scar within the slice to total area of the slice. This was calculated globally at the base, mid-ventricular and apical levels, as well as septal and lateral walls, and compared with EF.
Results: The age, ejection fraction and regional scar burden at three short axis levels are shown in table 1 and figure 2. It can be seen that
a. There is minimal scar present in the apical slices (8 /34 patients with scar). Patients with scar at apical slice always had scar at basal or mid-ventricular locations. Apical scar occurs at a later age.
b. The scar burden is high at the lateral walls when compared to the septal walls (17.1% in lateral vs 0.7 % in septal walls in patients >19 years old) (Figure 2).
c. Scar burden increases with age (Figure 2, table 1), while EF decreases with age and increasing scar burden.
Conclusions: Septal involvement occurred in older patients with reduced EF. LGE is more significant at the basal and mid-ventricular level and spares the apical level until older age, when EF is abnormal. Apical LGE only occurs in conjunction with basal and mid-ventricular LGE and never in isolation. Future studies are needed to assess the mechanism of this pattern of LGE.

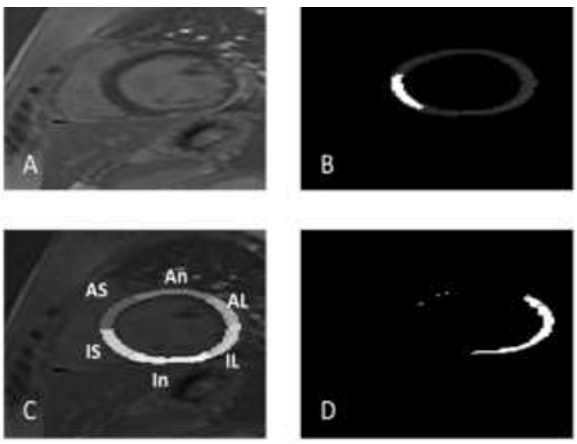

Figure 1: A late gadolinium enhanced (LGE) phase insensitive inversion recovery (PSIR) image obtained at the basal short axis level is shown (A). An observer manually drew contours delineating the endocardium as well as epicardium using a custom written Matlab program. Remote normal ROI was also drawn for each slice (B). The program semi-automatedly identified the six segments across the short axis slice (C), as well as the region of hyper-enhancement within the slice.

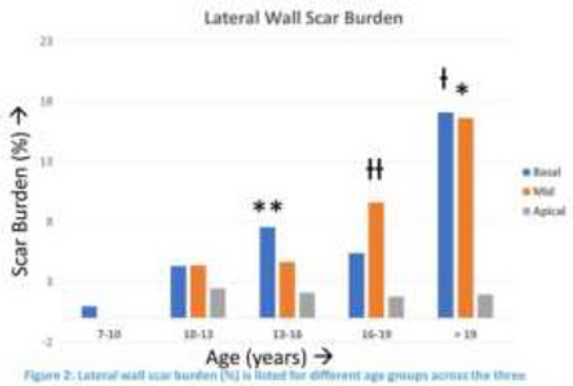

Figure 2: Lateral wall scar burden (%) is listed for different age groups across the three slices. † ℙ< 0.05 for SB at >19 years vs. all age groups * ℙ< 0.05 for SB at >19 years vs. all age groups except 16-19 years †† ℙ< 0.05 for SB at 16-19 years vs. all age lower groups ** ℙ< 0.05 for SB 13-16 years vs. all lower age groups

Age (years)	n	Ejection Fraction (%)	Total # scar	Scar burden (%) across age groups. Expressed as mean ± SD								
				Basal			Mid-Ventricle			Apical		
				# scar	Septal	Lateral	# scar	Septal	Lateral	# scar	Septal	Lateral
7 - 10	18	61.5 ± 3.6	2	2	0 ± 0	0.56 ± 3.6	1	0 ± 0	0 ± 0	0	0 ± 0	0 ± 0
10 - 13	19	60.2 ± 4.9	5	5	0 ± 0	8.3 ± 9.5	4	0 ± 0	8.4 ± 13	1	0 ± 0	2.5 ± 10.7
13 - 16	22	59 ± 11.8	9	9	0 ± 0	7.6 ± 12.6	9	0.3 ± 0.5	8.9 ± 12	3	0.2 ± 0.7	3.1 ± 9.3
16 - 19	16	52 ± 13.8	9	9	0 ± 0	5.4 ± 7.7	8	0.56 ± 0.5	9.6 ± 15.6	3	0 ± 0	1.8 ± 4.9
> 19	12	48 ± 11.1	8	7	0.7 ± 1.8	17.1 ± 17	8	1.0 ± 0.5	16.6 ± 19.5	2	0 ± 0	0 ± 5.3

Table 1: Information related to patients recruited for this study is shown. The patient group is divided into 5 sub groups based on the age. '# scar' denotes the number of patients with scar in that sub group of patients. As expected, the ejection fraction decreased with age, while the scar burden increased with age. More scar is seen in the lateral wall when compared to the septum. From

Paper #: 157

Demonstration of linear correlation between R2* and liver iron concentration across multiple MR acquisition parameters at 1.5T and 3T.

Richard Jones, MD[1], *rickyj@stanford.edu*; Jason Bentley, PhD[2],Valentina Taviani[3], Diego Hernando, PhD[4], Scott Reeder, MD, PhD[4], Shreyas Vasanawala, MD, PhD[1]; [1]Lucile Packard Children's Hospital, Stanford, CA, [2]Stanford University School of Medicine Quantitative Sciences Unit, Stanford, CA, [3]GE Healthcare, San Francisco, CA, [4]University of Wisconsin-Madison, Department of Radiology, Madison, WI

Disclosures: Valentina Taviani has indicated a relationship with GE Healthcare for having a salary. All other authors have disclosed no financial interests, arrangements or affiliations in the context of this activity.

Purpose or Case Report: Measure R2* in each liver segment, at different field strengths, image planes, and MR parameters; Determine the relationship between R2*, serum ferritin concentration, and liver iron concentration (LIC) as measured by Ferriscan and superconducting quantum interference device (SQUID) biosusceptometry.
Methods & Materials: R2* (the inverse of the T2* relaxation time) was measured at 1.5T and 3T on the same day using 10 different MR parameters including axial, sagittal, and coronal planes with varied echo spacing, flip angle, and slice thickness. The absolute agreement among R2* across liver regions and acquisition parameters was assessed using the intraclass correlation coefficient. Mean R2* values across 8 liver segments were calculated for each patient for comparison with LIC. The relationship between mean R2* and LIC for each reference method and MR acquisition parameter was summarized using the spearman rank correlation coefficient and normal linear regression.
Results: Thirty-three patients (mean 20 years, range 8 -70, 45% male) had 4696 total R2* MRI measurements at 1.5T and 3T. Thirty-two patients' ferritin (range 30-2728 ng/mL), 31 Ferriscan (range 0.9-25.2 mg/g dry tissue), and 14 SQUID (range 212-2625µg/g wet liver) measurements were obtained. There was high absolute agreement for R2* regardless of liver segment

(0.959-0.975 at 1.5T, 0.894-0.956 at 3T) and MR parameters (0.961-0.977 at 1.5T; 0.940-0.967 at 3T), Fig 1. There was no difference between average whole liver R2* and the right lobe average, Fig 2. Spearman correlation coefficients were high between R2* and LIC by Ferriscan (0.945-0.953 at 1.5T, 0.903-0.967 at 3T), SQUID (0.899-0.943 at 1.5T, 0.789-0.925 at 3T) and ferritin (0.814-0.846 at 1.5T, and 0.776-0.829 at 3T), regardless of MR acquisition parameters or liver segment (see Fig 3 for an example mean R2*/LIC linear regression analysis, using 1 of 10 acquisition parameters at 1.5T).

Conclusions: R2* is a consistent measure of liver iron concentration independent of liver segment, MR parameters, and magnet strength. As such, R2* may be considered a robust noninvasive biomarker of LIC, and represents an improvement over Ferriscan's greater cost, longer acquisition time, and longer post-processing time, and over SQUID, which has limited geographic availability.

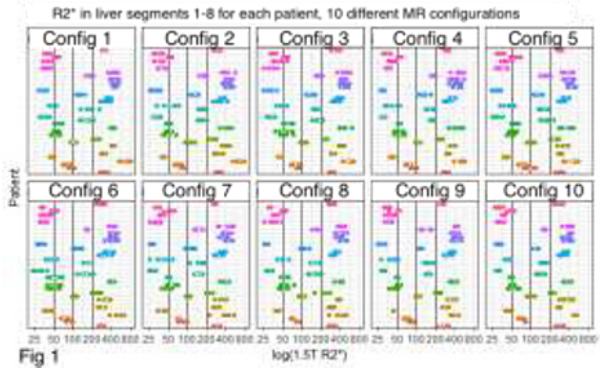

Fig 1

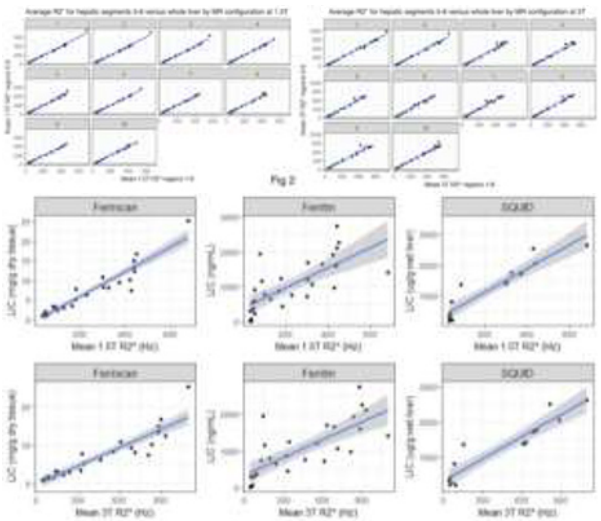

Fig 2

Paper #: 158

Automated Vessel Exclusion on Free-Breathing Ultrashort Echo Time Imaging For Assessment of Hepatic Iron Overload by R2*-MRI

Aaryani Tipirneni-Sajja[1], *aaryani.sajja@stjude.org*; Ruitian Song[1], Beth McCarville, MD[1], Ralf Loeffler[1], Jane Hankins[2], Claudia Hillenbrand[1]; [1]Diagnostic Imaging, St. Jude Children's Research Hospital, Memphis, TN, [2]Hematology, St. Jude Children's Research Hospital, Memphis, TN

Disclosures: All authors have disclosed no financial interests, arrangements or affiliations in the context of this activity.

Purpose or Case Report: Extraction of liver parenchyma is an important step in the evaluation of R2*-based hepatic iron content (HIC). Traditionally, this is performed on multiecho gradient echo (GRE) imaging by radiologists via T2*-thresholding, an iterative, time-consuming process susceptible to interrater variability. Automated vessel exclusion technique improves work flow by decreasing post-processing time and reducing human variability, however it has not been implemented on the new accurate MR-based technique, ultrashort echo time (UTE) imaging. UTE overcomes 2 critical limitations of GRE: (a) inaccuracy or failure in high iron overload (HIC >20 mg Fe/g), and (b) motion artifacts in patients unable to breath-hold (i.e., sedated children). This study evaluates an automated vessel exclusion technique for UTE imaging to accurately estimate mean liver R2*/HIC while optimizing the clinical workflow.

Methods & Materials: Free-breathing multiecho UTE data was collected from 139 patients with hepatic iron overload (58 male, 81 female; median age: 15±11 years). Quantitative T2*/R2* maps were calculated using non-linear least-squares fitting in MATLAB. A Frangi vesselness filter was applied to two different image inputs: T2* map and R2* map. The appropriate filter parameters (σ, spatial scale; β and c to suppress blob-like structures and background noise, respectively) were determined using simulations. Segmentation and R2* results obtained using the automated vesselness filter were compared to reference values recorded via manual T2* thresholding.

Results: The reference analysis based on T2*-thresholding did not completely exclude small vessels and pixels affected with partial volume effects at tissue and vessel boundaries and produced slightly lower R2* values compared to filter-based analysis (Fig1). Parenchyma areas extracted using the reference and automated methods had an average overlap area of 90-92% (Fig2). Mean liver R2* values estimated from filter-based methods showed a slope slightly over 1 and a small positive bias compared to reference R2* values (Fig3), likely because of incomplete vessel exclusion by reference method.

Conclusions: The excellent agreement between manual T2*-thresholding and automated liver parenchyma segmentation demonstrates the applicability, accuracy, and robustness of the vesselness filter for UTE imaging in the assessment of HIC. The filter improves the radiologist's workflow by reducing interactive input and interpretation time, potentially signifying the most efficient way to assess HIC.

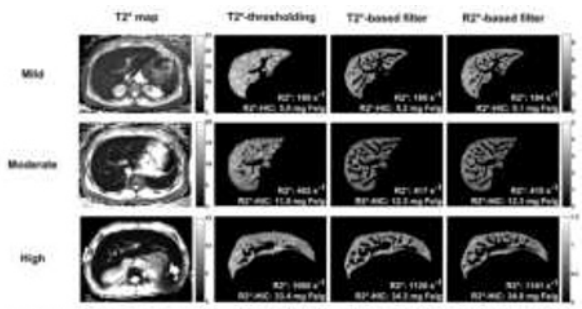

Figure 1. Quantitative T2* maps of the acquired slice (first column) and extracted parenchyma T2* maps obtained after vessel exclusion using manual, histogram-based T2*-thresholding performed by a radiologist (second column), and T2*-based (third column) and R2*-based (last column) filter methods in cases of mild (3 < HIC < 7 mg Fe/g, top row), moderate (7 < HIC < 15 mg Fe/g, middle row), and high (HIC > 15 mg Fe/g, bottom row) iron overload. Mean liver R2* and associated R2*-HIC values calculated using the R2*-biopsy HIC calibration curve for the extracted liver parenchyma for each technique are also given. Slight R2* underestimation was observed in T2*-thresholding analysis likely because of inclusion of small vessels and pixels affected by partial volume effects.
The free-breathing multiecho UTE sequence was applied at the location of the main portal vein with five interleaved echo trains (shifted by an echo time increment of ΔTEinc = 0.25 ms): TR/TE1/ΔTE = 52.5/0.1/1.0 ms, 12 echoes/interleave, radial lines = 192, α = 20°, slice thickness = 10 mm, number of averages = 3, and scan time = 5:08 min.

Paper #: 159

Developing an inpatient consult service at a large tertiary children's hospital: process and lessons learnt

Kamlesh Kukreja, MD[1], *drkamleshkukreja@yahoo.com*; Jose Hernandez, MD[1], Gregory Gardner, MD[1], Jessica Brown[1], Nicole Riccioni[1], Raphael Yoo, MD[1], Daniel Ashton[1]; [1]Radiology, Texas Children's Hospital, Bellaire, TX

Disclosures: All authors have disclosed no financial interests, arrangements or affiliations in the context of this activity.

Purpose or Case Report: Interventional radiology is becoming a clinical specialty by performing preprocedural consultation and also providing longitudinal care for patients to improve quality of care. The objective of this educational paper is to describe the process of establishing an inpatient consult service and aborting the old fashioned order based service for pediatric interventional radiology (PIR)
Methods & Materials: At our large tertiary care children's hospital, PIR service had been a order based service for 10 years since its establishment. We performed approximately 4200 procedures in 2015, approximately 60 % of which were inpatients. We created an inpatient consult service starting October 1, 2016 at our medical center campus by allowing referring providers to only place a consultation order for PIR. Every consultation would then result in patient being evaluated by PIR team { Physician Assistant (PA) /Nurse practitioner (NP) / Medical Doctor (MD)} followed by a consultation note and a procedure order (one of 6 generic imaging orders) if a procedure was indicated,
Results: Between 10/2016 to 09/2017, 1912 consults were performed resulting in total revenue of approximately 135,000. The consult service improved patient, IR staff and referring clinician satisfaction. Despite fears of significant delays in patient care, no delays were noticed in providing procedural care to the patients. We will describe the process as well as the lessons learnt such as omission of orders for feeding tubes (gastrojejunostomy and nasojejunal tubes), creation of consult notes in Epic and 6 generic IMG orders to improve efficiency of service, weekend consultation issues as well as introduction of consultation service at 2 other community hospitals since April 2017.
Conclusions: Providing inpatient consultation for pediatric IR procedures can be achieved. This service shifts the model of PIR from "procedural" to "clinical consultant" and generates additional revenue for the division.

Paper #: 160

Reliability of an Updated Classification System for Adverse Events in Pediatric Interventional Radiology

Shireen Hayatghaibi, MPH[1], *sehayatg@texaschildrens.org*; Daniel Ashton[1], Jose Hernandez, MD[1], Alex Chau, MD[1], Raphael Yoo, MD[1], Kamlesh Kukreja[1], Heather Cleveland, BSRS[1], Michael Paldino, MD[1]; [1]Radiology, Texas Children's Hospital, Houston, TX

Disclosures: All authors have disclosed no financial interests, arrangements or affiliations in the context of this activity.

Purpose or Case Report: The Society of Interventional Radiology's (SIR) classification grading system has been the standard for reporting adverse events in interventional radiology procedures since it was published in 2003. In response to concerns about inter-observer reliability, an updated grading system was developed by the SIR based on the Clavien-Dindo classification criteria used in surgery. The goal of this study was to measure the inter-observer reliability of the two SIR adverse event classification systems in a pediatric cohort.
Methods & Materials: From an existing departmental IR procedure database, 30 case scenarios were selected that reflected a broad spectrum of adverse event severity across a range of procedures. The case scenario topics included: central line placement as well as bone, liver, lung and renal biopsies. Four pediatric interventional radiologists scored all thirty pediatric clinical case scenarios according to both the standard and updated adverse event classification systems. Readers were provided with criteria for both classification systems at the time of their interpretation. Inter-observer agreement was assessed using Fleiss' kappa. The weighted degree of association of assessments by readers was measured using the Kendall's coefficient of concordance (KCC).
Results: Patient age from the case scenarios ranged from 2 months-20 years (mean 8.36 years). Fleiss' kappa statistic for inter-observer agreement in classification of adverse events according to the standard and updated SIR systems are presented in Table 1. The two systems were similar in terms of inter-observer agreement overall, demonstrating fair agreement. Agreement across the severity categories ranged widely for both systems. Perfect agreement was observed for patient death. Otherwise, kappa values for each severity category ranged from poor to substantial for the standard system and from poor to moderate for the updated system (Table 1). The KCC for the standard and updated classification systems were 0.77 and 0.55 respectively.
Conclusions: We observed overall fair inter-observer agreement for both the standard and updated SIR adverse event classification systems when applied in a pediatric cohort. Our findings support the need for a pediatric specific adverse event classification system.

Table 1: Inter-observer agreement for standard and updated AE classification systems

Standard Classification	Kappa	Updated Classification	Kappa
SIR A	0.27	Mild	0.29
SIR B	-0.05	Moderate	0.33
SIR C	0.35	Severe	0.50
SIR D	0.61	Life-Threatening	-0.02
SIR E	-0.008	Death	1.00
SIR F	1.00	None	0.16
None	0.14	**Overall**	**0.383**
Overall	**0.384**		

Paper #: 161

Portal Vein Recanalizations in Pediatric Liver Transplant Patients: Single Center Experience

Heather Cleveland, BSRS[1], *hxclevel@texaschildrens.org*; Aaditya Nagaraj, MD[1], Daniel Ashton[1], Jose Hernandez, MD[1], Alex Chau, MD[1]; [1]Radiology, Texas Children's Hospital, Houston, TX

Disclosures: All authors have disclosed no financial interests, arrangements or affiliations in the context of this activity.

Purpose or Case Report: Report the clinical outcome of successful portal vein recanalization in pediatric liver transplant patients with chronic portal vein thrombosis.

Methods & Materials: Retrospective IRB approved pediatric cohort study of 12 liver transplant patients (age at transplant range: 8-21 months, mean: 11) with chronic main portal vein thrombosis (PVT) who underwent portal vein (PV) recanalizations between August 2012 and September 2017. Three patients with failed PV recanalizations were excluded. Nine patients (4 male, 5 female) who underwent 23 PV interventions with successful recanalization were further evaluated for complications. Average clinic follow-up from last procedure performed was 441 days (range: 23-1120). Average duration of imaging follow-up from last procedure performed was 287 days (range: 1-1093). Patient demographics, technical details and follow up was recorded from time of transplant to most recent imaging and clinic visit. Complications were classified according to SIR standards.
Results: Transplant indication for all patients was biliary atresia. PVT with cavernous transformation was diagnosed by ultrasound or MRV. Average time to first PV intervention was 55 months (range: 19-149). Indications for intervention were: acute gastrointestinal bleeding (n=13); newly elevated liver enzymes with known PVT (n=3); new PV stenosis (n=3); scheduled follow-up splenoportogram (n=3); and hypersplenism (n=1). Interventions included PV recanalization, angioplasty, and stenting; varix embolization; and portosystemic shunt embolization. Three PV stents were placed.
A major complication was seen in one patient following trans-splenic access and post-tract embolization with gelfoam. Active bleeding was noted at the access site which required transfusion of blood products and ICU admission. No additional major complications were identified.
Conclusions: PV recanalizations in liver transplant patients with chronic PVT is low risk with excellent clinical outcome.

Paper #: 162

Diagnostic accuracy of ultrasound, computed tomography and wedge portography in the work-up for mesenterico-rex bypass in children with extrahepatic portal hypertension: a preliminary study

Seema Toso, Medical[1], *seema.toso@hcuge.ch*; Meryle Laurent[1], Romain Breguet[1], Merak Anooshiravani[1], Sylviane Hanquinet[1], Sylvain Terraz[1]; [1]Pediatric Radiology, Geneva University Hospital, Geneva, Switzerland

Disclosures: All authors have disclosed no financial interests, arrangements or affiliations in the context of this activity.

Purpose or Case Report: To identify the diagnostic accuracy of ultrasound (US), computed tomography (CT) scan and portography (wedge hepatic vein portography or direct portography) in the pre-operative work-up of mesenterico-rex bypass performed for extra-hepatic portal hypertension in children.
Methods & Materials: We conducted a retrospective analysis of pre-operative imaging for mesenterico-rex bypass in our tertiary hospital over the last 12 years. We analyzed all patients between the ages of 0-16 years, with extrahepatic portal hypertension necessitating surgical treatment that underwent US, CT and portography.
Two reviewers independently analysed the size of the left portal vein, the permeability of the mesenteric vein, the presence of communication between the left and right portal vein and the presence of liver disease on preoperative imaging with correlation to surgical findings. Statistical analysis of diagnostic accuracy was performed.
Results: Eleven patients underwent mesenterico-rex bypass for portal hypertension secondary to portal vein thrombosis. Two patients had partial liver transplant. Ultrasound with CT correlation was sufficient in responding to the preoperative criteria in 55% (6 /11) cases. Portography was useful in the 45% (5/11) cases where CT could not respond to preoperative criteria, in particular the presence of left-right communication.
Conclusions: In half of our cases, the use of ultrasound and CT is sufficient for preoperative planning for mesentrico-rex bypass. Diagnostic portography is mandatory in cases with large intra-hepatic cavernoma, where either the size of the left portal vein and/or the presence of left-right communication could not be confirmed.

Paper #: 163

Endovascular stenting in adolescents with nutcracker syndrome

Julie Cronan, MD[1], *jcronan@emory.edu*; Anne Gill, MD[1], C. Matthew Hawkins, MD[1]; [1]Radiology, Emory University School of Medicine, Atlanta, GA

Disclosures: All authors have disclosed no financial interests, arrangements or affiliations in the context of this activity.

Purpose or Case Report: Nutcracker syndrome (NCS) is defined as left renal vein (LRV) compression with concomitant clinical symptoms including flank pain, hematuria, and/or left-sided varicocele or pelvic congestion syndrome. While NCS most commonly presents in the 2nd and 3rddecade, the incidence of NCS in the pediatric population is not well documented. Historically in children, mild symptoms of NCS were observed. If symptoms were severe and persistent, patients often had renal vein surgical transposition. Endovascular stenting of the LRV is a potentially efficacious, less invasive, lower-risk alternative for NCS that has not been well studied in the adolescent population. The purpose of this study is to retrospectively evaluate the technical feasibility and efficacy of LRV stent placement in 6 adolescent patients with NCS.
Patients (mean age: 14.8 yrs; range: 12-18) presented with left flank pain (n=6) as well as gross hematuria (n=4), left-sided varicocele (n=1), and pelvic congestion syndrome (n=1). All patients were diagnosed via CT abd/pel with contrast in association with clinical exam and exclusion of all other causes of hematuria. Five patients had LRV compression between SMA and the aorta. One patient had LRV compression between the aorta and spine (retroaortic renal vein).
Venography demonstrated abnormal venous drainage in all patients: proximal blanching of contrast column in the LRV; complete occlusion with reflux of contrast into venous collaterals including lumbar (3), gonadal (2), and hemiazygos (1) systems. Intravascular ultrasound was used in all cases. Two patients required additional stent placement, as a single stent provided insufficient radial force to relieve compression. Endovascular stent placement [12mm x 60mm (n=3), 14mm x 60mm (n=5)] was technically successful in all patients with immediate improvement in venous drainage.
All patients were followed in the IR clinic. Mean follow-up = 2.2 months (range: 1-6 months). Improvement/resolution of hematuria = 100% (4/4). Resolution of pain = 67% (4/6). Improvement in pain = 33% (2/6). The patients with varicocele and pelvic congestion syndrome had resolution of symptoms. Major complications = 0. Minor complications = 3 (transient mild to moderate left flank or abdominal pain after stent placement).
Conclusions: In this small cohort, endovascular stenting appears to be a technically successful and efficacious therapeutic alternative for adolescent patients with NCS.

Paper #: 164

Optimizing Pediatric Gastrojejunostomy Tube Maintenance

Vera Mayercik, MD[1], Julia Rissmiller, MD[1], Anastasia Hryhorczuk[1], William Mehan, MD[1]; [1]Radiology, Tufts Medical Center, Boston, MA

Disclosures: All authors have disclosed no financial interests, arrangements or affiliations in the context of this activity.

Purpose or Case Report: For patients unable to maintain normal PO intake, gastrojejunostomy tubes represent a life-saving and life-prolonging intervention. Maintenance of these tubes, however, does not always adhere to a regimen. Lack of a structured exchange schedule for pediatric gastrojejunostomy tubes results in problematic exchanges, often scheduled only when the original tube becomes clogged or falls out. This results in more complex exchanges and delays in feeding which sometimes require interim hospitalization for parenteral nutrition. We developed a structured tube exchange program with the pediatric gastroenterology service to improve patient experiences and outcomes for children reliant on gastrojejunostomy feedings.
Methods & Materials: We introduced scheduled tube exchanges q3 months to preemptively change gastrojejunostomy tubes before problems developed. We measured fluoroscopy time of cases, wait time for tube exchange (measured from order date to case date), case time in the fluoroscopy suite (measured from KUB/scout time stamp to case completion), and number of de novo tube replacements (defined as a tube which had completely fallen out and could not be exchanged over a guidewire) before and after this intervention. The study was conducted over a period of 12 months with n = 9 cases pre intervetion and n = 10 cases post intervention.
Results: Before our intervention, mean fluoroscopy time was 48 seconds; mean case time was 82 minutes; mean wait time was 44.8 hours; and percentage of de novo replacements was 19%. After this intervention, mean fluoroscopy time was 34 seconds; mean case time was 29 minutes; mean wait time was 35 hours; and percentage of de novo replacements was 0%. Overall, fluoroscopy time was reduced by 29%. Case time was reduced by 65%. Wait time was reduced by 22%. De novo tube replacements were reduced by 100%.
Conclusions: Implementing scheduled gastrojejunostomy tube exchanges results in a better experience for patients with decreased radiation dose and wait time for tube replacement. Efficiency of the fluoroscopy suite was also improved, with shorter overall duration of cases and fewer de novo replacements.

Paper #: 165

Internal jugular vein tunneled central lines: To cuff or not to cuff?

Darshan Variyam, MD[1], *variyam@bcm.edu*; Daniel Ashton, MD[1], Heather Cleveland, BSRS[2], Shireen Hayatghaibi, MPH[2], Jose Hernandez, MD[2]; [1]Interventional Radiology, Texas Children's Hospital / Baylor College of Medicine, Houston, TX, [2]Texas Children's Hospital, Houston, TX

Disclosures: All authors have disclosed no financial interests, arrangements or affiliations in the context of this activity.

Purpose or Case Report: To measure early (≤30 days) and overall (per 1000 line days) complication rates for cuffed vs. non-cuffed tunneled central lines at a tertiary academic institution.

Methods & Materials: A total of 337 tunneled IJ lines were placed between January 2014 and December 2015. Patients were identified through PACS and EMR systems. Patient demographics, technical details of the procedure, and follow-up to line removal were recorded and documented in a HIPAA-compliant database. Complications were categorized as line malfunction, infection, malposition, bleeding, thrombosis. The early (≤ 30 days) complication rate was compared for cuffed vs. non-cuffed lines, as was the overall complication rate per 1000 line days. Early complications were compared between the two groups using the Fisher's exact test, and overall[b1] complications were evaluated with mid-p exact test for person times.
Results: Of the total tunneled internal jugular lines placed, 69 were cuffed and 268 were non-cuffed. Cuffed lines had a significantly higher early complication of line malfunction (7.2%, 5/69 vs. 1.9%, 5/268, p= 0.034) without a significant difference in the rate of infection (5.8%, 4/69 vs. 3%, 8/268, p=0.28) or total complications (18.8%, 13/69 vs. 11.2%, 30/268, p=0.11). Non-cuffed lines had an overall higher rate of malposition (2.4 vs. 1.1/1000 line days, p=0.048) and cuffed lines had a higher rate of catheter malfunction (2 vs 0.7/1000 line days, p=0.014). Differences in the remaining early and overall complications were not statistically significant.
Conclusions: There was no significant difference in the infection rate between cuffed and non-cuffed tunneled central lines. Non-cuffed lines had higher overall rates of malposition, while cuffed lines had a higher rate of early and overall line malfunction.

Alternate Paper

Enabling Free-Breathing Real-Time Cine in Pediatric Patients with Compressed Sensing

Ramkumar Krishnamurthy, PhD[1], *ramkumar.krishnamurthy@nationwidechildrens.org*; Yingmin Liu, PhD[2], Houchun Hu, PhD[1], Kan Hor, MD[1], Rajesh Krishnamurthy[1], Rizwan Ahmad, PhD[2]; [1]Radiology, Nationwide Children's Hospital, Columbus, OH, [2]Ohio State University, Columbus, OH

Disclosures: Kan Hor has indicated a relationship with Medtronics and Capricor as a consultant/honoraria. All other authors have disclosed no financial interests, arrangements or affiliations in the context of this activity.

Purpose or Case Report: Conventional cardiac MRI (CMR) acquisitions in children are limited by long acquisition time, need for sedation, and an inefficient workflow. A conventional cine SSFP short-axis stack typically takes 5-7 minutes to complete and is ineffective for subjects with arrhythmias. Available alternatives like free-breathing, real-time cine (RT-cine) SSFP have suboptimal temporal and spatial resolution. Recent advances in compressed sensing (CS) MRI techniques may overcome this limitation. We hypothesize that a CS-based approach will allow the scan time for a short axis RT-cine stack to be shortened to less than a minute without compromising spatial or temporal resolution.
Methods & Materials: Five patients (Age: 14-44 years ;4 males) underwent CMR study with both conventional breath-held cine SSFP (BH-cine) as well as CS-based free-breathing, cardiac-triggered RT-cine acquisitions (Ahmad and Schniter, DOI: 10.1109/TCI.2015.2485078). The short-axis of the ventricles was covered with 14 slices in each patient. The spatial resolution for both acquisitions was 1.8x1.8x8 mm^3; temporal resolution was 32 ms (BH-cine) and 32 ms (RT-cine) per cardiac phase. End-diastolic volume (EDV), end-systolic volume (ESV), ejection fraction (EF), and scan duration were computed using established methods, and compared between BH-cine and RT-

cine acquisitions using paired Student's t-test.
Results: Both BH-cine and RT-cine images were deemed of diagnostic quality by two expert readers. The EDV, ESV and EF showed good agreement (Mean EDV (BH-cine first): 144 ± 27 vs 137 ± 27 ml, p = 0.03; mean ESV: 58.8 ± 10.4 ml vs. 54.9 ± 6.4, p = 0.29; and mean EF = 58.8 ± 5% vs 54.9 ± 6.4 % ;p = 0.03); see figure 1. The scan times were significantly shorter for RT-cine (2 heart beats/slice; ~45 seconds for entire 14 slice acquisition) compared with BH-cine acquisition (6-8 beats/slice; ~5:38 minutes for 14-slice acquisition, p< 0.01). Figure 2 shows representative images acquired.
Conclusions: CS-based free-breathing RT-cine technique is feasible and provides images of comparable quality and diagnostic value when compared to conventional BH-cine SSFP, while significantly reducing scan time. It offers a potential solution to avoid the need for sedation for functional evaluation, improve diagnostic utility of MRI in arrhythmia, and improve CMR efficiency and workflow. Future reduction in reconstruction times, is needed prior to implementation of CS-based RT techniques into clinical practice.

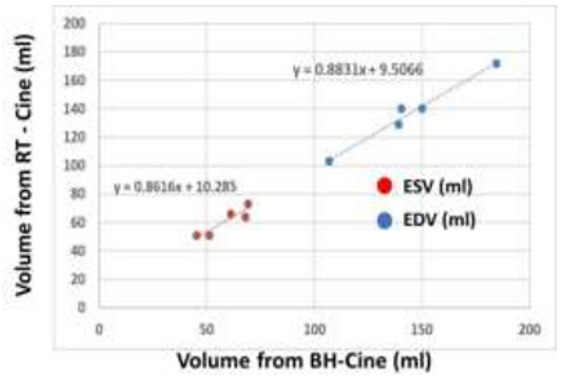

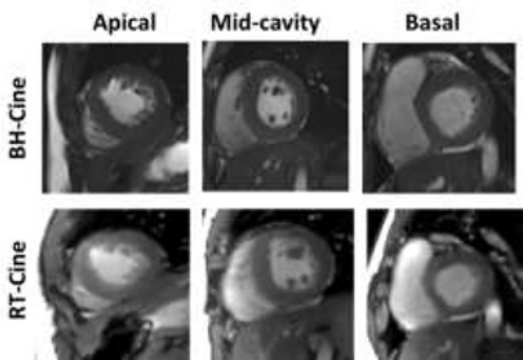

SCIENTIFIC PAPERS - TECHNOLOGISTS

(T) indicates an Imaging Technologist Program Submission

Paper #: 001 (T)

Evaluation of Meso-Rex Bypass with Ferumoxytol Contrast Enhanced MRI

Gabriel Morales, Bachelor[1], *gmorales@luriechildrens.org*; Christina Sammet, PhD, DABR[1], Riccardo Superina[1], Jie Deng, PhD[1], Cynthia Rigsby, MD[1]; [1]Medical Imaging, Ann & Robert H. Lurie Children's Hospital of Chicago, Chicago, IL

Disclosures: All authors have disclosed no financial interests, arrangements or affiliations in the context of this activity.

Purpose or Case Report: To evaluate the safety and effectiveness of ferumoxytol enhanced MRI to assess Meso-Rex bypass (Rex shunt). Rex shunt is a surgical procedure that restores blood flow to the liver in patients who have portal vein obstruction. This blockage causes high blood pressure in the veins in the abdomen (portal hypertension). Patients with this blockage may have enlargement of the spleen, intestinal bleeding, accumulation of fluid in the abdomen, and (ascites). The shunt acts to bypass the blockage by redirecting blood from a high pressure system to a low pressure system beyond the obstruction in the liver. Ferumoxytol is an iron contrast agent that has a long half-life and is excreted by the reticuloendothelial system. Kidney screening is not necessary for administration of ferumoxytol and it may be suitable for patients with impaired renal function.
Methods & Materials: Sixty Rex shunt MRI studies were performed at our institution using ferumoxytol as a contrast agent. Ferumoxytol was compared to gadobutrol and gadofosveset enhanced MRI for the evaluation of Rex shunt post-surgical appearance. A large gauge peripheral IV was placed in an upper extremity. A ferumoxytol and saline solution was loaded in the power injector with a total volume of 60mL. A radiologist and nurse were required to be present during infusion of ferumoxytol. The ferumoxytol was infused over 15 minutes (0.07 mL/s) followed by a saline flush. Blood pressure was recorded every two minutes during infusion and every five minutes post-infusion for 30 minutes. Post ferumoxytol MRI sequences included a coronal navigator-gated T1-weighted "Inversion Recovery Fast Low Angle Shot" (IR-FLASH) to include the abdominal vasculature. Sequence parameters TR/TE=502.44/1.47ms; TI=300ms; FA=16; FOV=32-40cm; Slice Thickness=1.33mm; Matrix=250x272; Bandwidth=497KHz. Flow was assessed in the Rex shunt using phase contrast imaging.
Results: The vasculature features of ferumoxytol improved MRI imaging quality compared to our experience with gadobutrol and were equivalent to or better than gadofosveset. While using ferumoxytol MRI imaging we were able to evaluate efficacy of the Rex shunts. One patient experienced nausea and transient mild hypotension following ferumoxytol infusion. No other side effects were seen in the other fifty nine cases that were conducted.
Conclusions: Ferumoxytol MRI is a promising tool to evaluate Meso-Rex bypass. Patients tolerated ferumoxytol well with no major side effects.

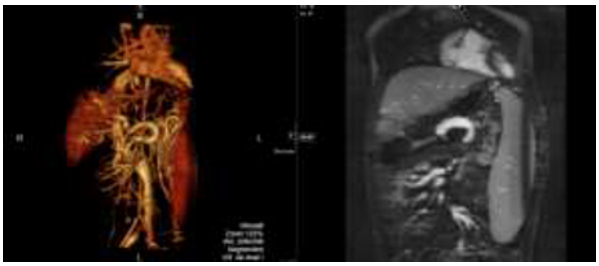

Paper #: 002 (T)

Implementation of a Pediatric MRI Lymphangiography Programs

Ashley Brondell[1], *brondlab02@gmail.com*; C. Matthew Hawkins, MD[1], Anne Gill, MD[1]; [1]Interventional Radiology, Children's Healthcare of Atlanta Egleston, Atlanta, GA

Disclosures: All authors have disclosed no financial interests, arrangements or affiliations in the context of this activity.

Purpose or Case Report:
To describe the logistical and technical aspects to implementing an MRI Lymphangiography program at a large, tertiary children's hospital.
Methods & Materials:
MRI Lymphangiography requires intra-nodal injection of gadolinium to allow for dynamic visualization of the central conducting lymphatics of the chest and abdomen. The most common indications include chylous leak (into a variety of body cavities) and plastic bronchitis. Because of the length of the procedure and need for breath holds, patients require general anesthesia. The patient is induced in the MR suite on a detachable MR scanner gantry. Once anesthetized, the patient and gantry are moved out of the MRI suite for ultrasound-guided, bilateral, inguinal lymph node access, which is performed by a pediatric interventional radiologist with 22 or 24-gauge angiocatheters. Once placed, the angiocatheters are connected to long tubing and a three way stopcock. A test injection of 1-2mL of saline is used to confirm intra-nodal access. The angiocatheters and tubing are stabilized, and the patient/gantry are wheeled back into the MR suite. MR imaging then ensues with injection of 0.1 mmol/kg of gadolinium based contrast at a dilution of one-part contrast to 2 parts normal saline. Rapid sequence, dynamic 3D gradient echo imaging is then performed of the abdomen and pelvis with a diagnostic radiologist performing the examination, while an interventional radiologist is in the suite injecting the diluted contrast.
Results: MR Lymphangiography examinations have been performed in 5 patients (mean age: 27 months (range: 2-89 months); mean weight: 13 kg (range: 3.1-26 kg) at Children's Healthcare of Atlanta. Presenting symptoms included: plastic bronchitis (2), chylous pleural effusion(s) (2), and chylous pericardial effusion (1). Four examinations successfully identified the lymphatic anatomic abnormality accounting for chylous leak; all of which were endovascularly or surgically repaired, subsequently. One MR lymphangiogram demonstrated normal central conducting lymphatics. (The child was later found to have plastic bronchitis from an aspirated foreign body.)
Conclusions: MR lymphangiography with intra-nodal gadolinium contrast injection is logistically and technically feasible in a pediatric hospital setting.

Paper #: 003 (T)

Conjoined Twins: A Life Together - A Case Report on Prenatal and Postnatal Imaging of Parapagus Dicephalus Twins

Kristina Stenger, Bachelors[1], *kristina.stenger@cchmc.org*; Paula Bennett[1]; [1]Radiology, Cincinnati Children's Hospital, Cinncinnati, IN

Disclosures: All authors have disclosed no financial interests, arrangements or affiliations in the context of this activity.

Purpose or Case Report: There are multiple variations of Conjoined twins. Prenatal and postnatal imaging is crucial in defining the shared structures, vascularity, and identifying any other significant anomalies. The determination of the shared organs is instrumental in helping the physicians and parents make the decision or potential for separation. In this specific case the twins were referred to our institution and had an MRI, and Ultrasound. At this time not only were the shared structures identified but also two rather significant anomalies were found, a congenital diaphragmatic hernia and an omphalocele. A specific plan for delivery and immediate postnatal care was made based on this imaging. Additionally extensive postnatal imaging was performed shortly after birth to help guide the physicians in their decisions for the management of the twins care.
Methods & Materials: The mother was first referred to our institution at 26 4/7wks gestation with having a monochorionic/monoamniotic conjoined twin pregnancy. A fetal MRI was performed. This showed that they were conjoined twins dicephalic parapagus. The fetus had separate brains which were normal, airways, spines, hearts (although small fusion difficult), Aortic roots with right twin's being small and a single descending thoracic aorta, stomachs, and gallbladders. Each fetus seemed to have two lungs however the more medial lungs possibly fused. Baby A was also found to have a diaphragmatic hernia containing liver, spleen and stomach.The twins shared an abdomen with a fused liver, two kidneys, single colon, single bladder, single 3 vessel umbilical cord, omphalocele containing bowel, and 4 extremities with hypogenetic limb central upper thoracic/lower neck.
She returned at 34 5/7wks gestation and a fetal ultrasound and another fetal MRI were performed. The MRI and ultrasound findings were the same except the ultrasound provided some additional vascular information. It showed there is a single 3VC with a single umbilical vein and single ductus venosus which connects to the IVC of Twin B and that the peak systolic velocities in the MCAs of both fetuses were elevated, which can be seen with fetal anemia.
Results: Dicephalic Parapagus Twins with a CDH and Omphalocele.
Conclusions: Based on the findings from all of the imaging it was decided that these particular twins would not be separated. The CDH and omphalocele were both repaired without complication. The twins are currently still inpatient receiving ongoing medical treatment.

Paper #: 004 (T)

Paediatric lower limb lymphoscintigraphy: A retrospective review of practice and dose optimisation

David Curran, BSc Radiography[1]
davecradiog@gmail.com; [1]Nuclear Medicine, Our Lady's Children's Hospital Crumlin, Dublin, Ireland

Disclosures: All authors have disclosed no financial interests, arrangements or affiliations in the context of this activity.

Purpose or Case Report: lower limb lymphoscintigraphy is a nuclear medicine examination of the lymphatics and their drainage pattern. It is an infrequently performed nuclear medicine examination in children. Due to its rarity, it is important to review its practice and have robust protocols in place. The aim of this study was to review the practice that was used for our previous examinations and gain an insight into areas that could be improved and optimised.
Methods & Materials: A retrospective review of all paediatric lower limb lymphoscintigrams between 2015 and 2017 (n=8) was performed. Data was extracted that included dose, injection technique, timing of imaging and scanning protocols.
Results: The information gained from reviewing our practice lead to a reduction in administered dose and a change to the scanning protocol.
Conclusions: On review of the previously performed examinations, an insight was gained into the different aspects of this infrequently performed examination. By optimising the different aspects of this examination, we were able to build a robust protocol to improve the imaging of paediatric patients that are referred to this imaging department for lower limb lymphoscintigraphy.

Paper #: 005 (T)

Role of Ultrasound with Atypical Spitz tumor

Falguni Patel, Associates[1] *fpatel0807@yahoo.com* ; [1]Medical Imaging (Ultrasound), Lurie Children's Hospital of Chicago, Chicago, IL

Disclosures: All authors have disclosed no financial interests, arrangements or affiliations in the context of this activity.

Purpose or Case Report: My purpose is to raise an awareness in the community regarding the Atypical Spitzoid tumor and how my facility is using ultrasound as a follow-up screening tool after the tumor excision to evaluate abnormal and enlarged lymph nodes in axilla region, inguinal region and popliteal fossa for reoccurrence of this disease instead of Sentinel lymph node biopsy in the pediatric patients.
Methods & Materials: I would like to do a power point presentation based on the following objectives:
Definitions and classifications of Spitzoid melanocytic lesions
Understanding of Atypical Spitz tumors (AST) and its treatment
Ultrasound imaging in follow up care for patients with AST at our organization
Case review from the very first patient with AST dx
Results: In 2015, My facility have initiated use of ultrasound as a screening tools for Atypical Spitz Tumor reoccurrence based on evaluating lymph nodes in the related area depending on where the tumor is removed, since than we have been following this group of patients every three months to check for Spitzoid tumor reoccurrence. I will present
Numbers of ultrasound exams we have performed at our facility within 3 years of timeframe
Protocols and Guidelines of what areas to be scanned for follow up exams
Consistency of measuring lymph nodes and ultrasound appearances of lymph nodes in three dimensions
I will also discuss our specific scanning protocols based on this diagnosis
Conclusions: In conclusion, I will discuss in my presentation the advantages of using frequent ultrasound to evaluate characteristics of lymph nodes verses unnecessary attempt of biopsies of these lymph nodes on pediatric patients. I will also go over some case studies that I have performed at my facility and a positive case study for reoccurrence of Atypical Spitz Tumor based on Ultrasound findings.
Performing a quick ultrasound every three months have definitely given a peace of mind for these patients and their worrisome care takers.
Thus, I would like an opportunity to present this interesting topic "Role of Ultrasound with Atypical Spitz tumor"

Paper #: 006 (T)

Advanced MRI Scan Techniques and 3D Post-Processing in Pediatric Patients

Marrit Thorkelson[1], *mthorkelson1@phoenixchildrens.com*; Robyn Augustyn, BSRT RT(R)(CT)[1], Amber Pokorney[1], Ryan Robison[1], Richard Southard, MD[1], Dianna Bardo, MD[1]; [1]3D Innovation Lab, Phoenix Children's Hospital, Phoenix, AZ

Disclosures: Robyn Augustyn has indicated a relationship with Koninklijke Philips, NV as a consultant and a speaker. Richard Southard has indicated a relationship with Philips Healthcare for consultant/ honoraria, speaking and receiving a research grant. All other authors have disclosed no financial interests, arrangements or affiliations in the context of this activity.

Purpose or Case Report: Three dimensional (3D) and two dimensional (2D) image post processing aids in radiological diagnosis and surgical procedure planning. Advances in MRI technology and sequence techniques enable 3D post processing for advanced image visualization a key component of diagnosis and patient care.
MRI generated volumetric data sets with high resolution isotropic pixels have stimulated dramatic developments in 2D and 3D image post processing techniques for clinical use and facilitate 3D print modeling. New or specialized sequences including non-contrast enhanced MR angiography **R**elaxation **E**nhanced **A**ngiography without **C**ontrast and **T**riggering (REACT), **PR**inciple **O**f **S**elective **E**xcitation **T**echniques-**W**ater **Selective** (PROSET) (WATS), navigator triggered and ECG-gated volumetric sequences, and T1 weighted 3D modified DIXON enable creation of 3D volumetric image segmentation, multiplanar and curved 2D reconstructions.
Each sequence may be employed for multiple anatomic purposes and are amenable to various reconstruction processes which enhance diagnosis in children.
Methods & Materials: MR imaging sequence diagrams are illustrated and sequence optimization parameters highlighted. Post-processing techniques will be explained in a step-by-step manner and examples of pathology from neuro, musculoskeletal, liver, bowel, renal, and vascular pathology will be shown.
Results: 3D post processed images help to visualize and give a better understanding and representation of the pediatric anatomy and pathology and expedites pre-surgical planning.
Conclusions: New advances in MRI pulse sequences enable 2D and 3D post-processing. 3D image post processing improves patient care.

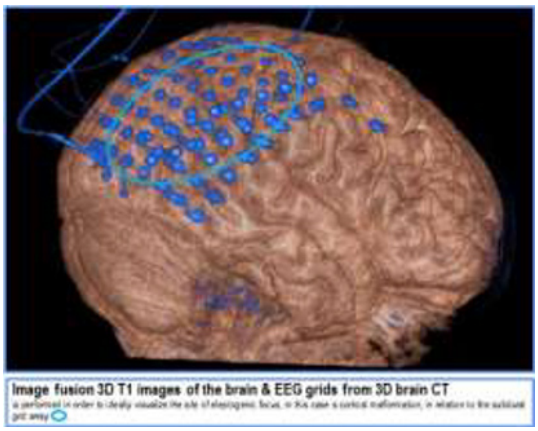

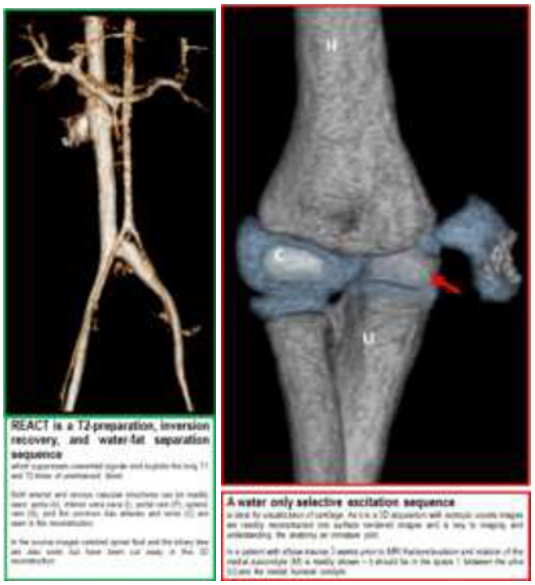

Paper #: 007 (T)

CT Iterative Reconstruction Increases Efficiency of 3D Image Post-Processing

Robyn Augustyn, BSRT RT(R)(CT)[1], *raugustyn@phoenixchildrens.com*; Marrit Thorkelson[1], Richard Southard, MD[1], Dianna Bardo, MD[1]; [1]3D Innovation Lab, Phoenix Children's Hospital, Phoenix, AZ

Disclosures: Robyn Augustyn has indicated a relationship with Koninklijke Philips, NV as a consultant and a speaker. Richard Southard has indicated a relationship with Philips Healthcare for consultant/ honoraria, speaking and receiving a research grant. All other authors have disclosed no financial interests, arrangements or affiliations in the context of this activity.

Purpose or Case Report: Utilization of low dose CT protocols is a universal goal throughout the Pediatric Radiology community. Iterative reconstruction (IR) techniques have been shown to be an effective in reducing image noise, therefore enabling dose reduction techniques. Increased edge detection and decreased image noise increases efficiency of 3D image post-processing.

Methods & Materials: All CT examinations performed at our institutions are reconstructed using 2 types of iterative reconstruction, hybrid or anatomic and knowledge or model based IR on 256 or a recently installed 128 multi-detector multi-energy spectral CT (Brilliance iCT and IQon CT, Philips Healthcare, Cleveland, OH).

Results: Noise suppression in IR techniques increases edge detection of anatomical structures and therefore increases efficiency of 3D image post-processing. This effect is superior when using model based IR compared to hybrid IR due to the greater degree of noise reduction.

In preliminary experience we have discovered features of multi energy CT which are advantageous for image post-processing. These include mitigation of beam-hardening artifact with high mono-energetic imaging and the use of low mono-energetic imaging to boost iodine density to improve angiographic images which may be limited by contrast or bolus timing.

Conclusions: IR and new spectral MECT imaging techniques are effective in improving image quality and therefore in increasing efficiency of 3D image post-processing.

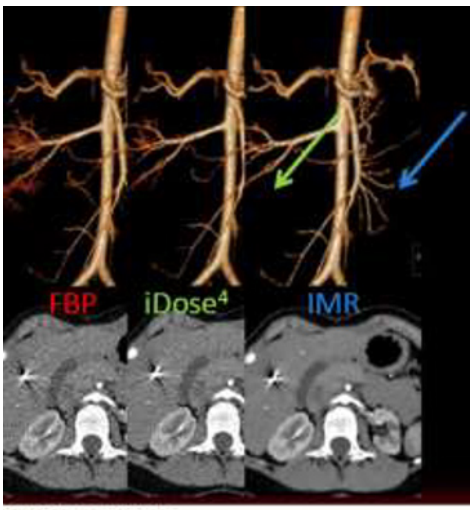

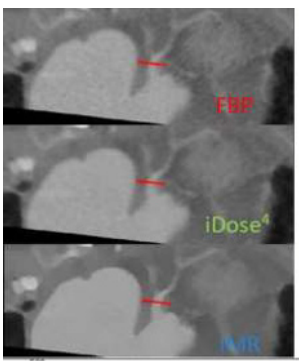

Cardiac ECG Gated CT
A histogram drawn through a coronary artery in a Filtered Back Projection (FBP), Hybrid Iterative Reconstruction (iDose), and Knowledge Based Reconstruction (IMR) demonstrates the IMR having a more dramatic edge slope, therefore increased spatial resolution.

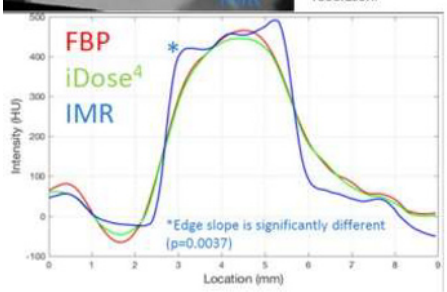

Paper #: 008 (T)

The Diagnosis of Accidental and Non-Accidental Trauma Through Medical Imaging

Rocco Pazienza[1] *rmpaz@sbcglobal.net*; [1]Medical Imaging, Lurie Children's Hospital, Chicago, IL

Disclosures: All authors have disclosed no financial interests, arrangements or affiliations in the context of this activity.

Purpose or Case Report: To explain the various imaging modalities and techniques used by both physicians and radiographers and to correlate them to both acute and chronic accidental and non-accidental traumas with the diagnostic modality that best demonstrates that particular injury. The author will show the importance and usage of various imaging modalities and techniques to both the novice radiographer to the most experienced physician.
Methods & Materials:
1. various textbooks
2. various internet articles
3. interviews with both physicians and radiographers specializing in their respective disciplines
Results: The author discovered that there are specific indications when selecting the proper imaging modality to be utilized to aid in the differentiation of accidental and non-accidental trauma. Some injuries require several imaging procedures to aid in the confirmation of a specific trauma. Some injuries may require follow-up examinations to be performed several weeks later to support a specific injury. But nearly all imaging modalities play a role -- large or small, chronic or acute, in the final identification and diagnosis of any accidental or non-accidental traumas.
Conclusions: Not all traumas can be diagnosed by any one imaging modality. Ultimately, it is the final decision of the physician to order the most appropriate imaging procedure. The decision may also lie with all of the imaging specialists involved in the final images to be used for specific traumas. We as imaging specialists have the responsibility and an obligation to speak for the pediatric population.

Paper #: 009 (T)

MRI Safety Screening Clearance Process

Khristina Hidalgo, BS, RT (R) (MR)[1], *Khristina.Hidalgo@stjude.org*; Carlos Gray, RT (R) (MR)[1]; [1]Diagnostic Imaging - MRI, St. Jude Children's Research Hospital, Memphis, TN

Disclosures: All authors have disclosed no financial interests, arrangements or affiliations in the context of this activity.

Purpose or Case Report: Ensuring patient safety is the first and foremost priority of any MRI department. It is imperative that the institution has established guidelines to achieve its MRI safety initiative. It is our objective to present a detailed MRI clearance procedure used in our institution, the different departments involved, and the essential resources required to ensure patients' safety.
Methods & Materials: The presentation is based upon our institution's actual process of screening and clearing a patient for MRI - from the arrival of the patient to the institution to the completion of the MRI scan, and the necessary post-documentation. The process will be supported by the use of our internal database with frequently encountered implants, MRI Safety websites, and the departmental staff - the MRI Safety Expert, Radiologists, Nursing Surgical Services Pre-screening Staff, and Program Coordinators.
This is a study of an actual patient arriving to our institution for an MRI procedure, which presents challenges involving unknown implants. Potential displacement and heating of these implants will cause a life threating situation.
To clear the patient for MRI, our screening and clearance forms and operative reports are necessary for identification of the implants in question. To work in conjunction with these documents, plain-film radiography will be done on the patient (if no previous imaging is available) to exclude potentially dangerous metallic foreign objects and devices.
The roles of the key players (the coordinators, MRI technologists, radiologists, and the MRI Safety Expert) on the screening and clearance of the patient will also be highlighted during the presentation.
Results: After facing the challenges of clearing the patient, and eliminating possible safety issues, the end result is a successful completion of MRI scan without any metal incidents or medical risk to the patient's health. In addition to our intended result, post documentation - such as the MRI Sharepoint Implant List, and updates to the patient's Power Chart - will be used as helpful tools to assist when the patient returns for a follow-up MRI appointment.
Conclusions: Comprehensive MRI safety clearance process is paramount for patient safety. Through a meticulous screening and clearing process, higher confidence in identifying implants, less cancelled exams which equates to higher efficiency, and the reduction or elimination of risks to patient health and safety are achieved.

Paper #: 010 (T)

Generational Differences in the Workplace

Melissa Goehner[1] *melissa.goehner@choa.org* ; [1]Diagnostic Radiology, Children's Healthcare of Atlanta, Stone Mountain, GA

Disclosures: All authors have disclosed no financial interests, arrangements or affiliations in the context of this activity.

Purpose or Case Report: With the changing of generations in the radiology workforce, there is increased importance for leadership to address the manner in which teams are managed and to foster the inter-relationships amongst staff.
Many times generations are stereotyped with certain characteristics that can present obstacles for leadership to overcome when creating unity. The purpose of this study was to survey radiology staff at a large children's hospital system to determine if generational differences existed and their effect in the workplace.
Methods & Materials: A survey was created and sent to the radiology department at Children's Healthcare of Atlanta, including technical, clinical and non-clinical staff in all modalities and support services. A total was 337 surveys were sent out. The survey questions include information on work-life balance, future career goals, communication of information, appropriate communication for praise, learning styles and department investment.
Results: A total of 119 surveys were received. The baby boomer generation (1946-1964) is 14% of our employee population. Generation X (1965-1976) is 36%. 48% are Millennials (1977-1995) and 1% is Generation Z(1996-present). However, when asked what generation each employee considers themselves to be, the results show 3% as Traditionalists, 14% as baby boomers, 59% as Generation X and 25% are Millennials. When asked how they like to receive information, 53% prefer to be communicated to by e-mail and 30% prefer to be communicated to by text message. The top 3 social media websites that the staff uses are e-mail (92%), Facebook (67%) and Instagram

(37%). The majority of staff take between 2-3 weeks of vacation a year (57%). Most people like to receive praise by email (37%), in private (28%) or in the department newsletter (24%). When looking into career advancement, 25% of staff want to stay in the same position that they are in currently, 12% want to be involved in leadership within their role, 14% want to be in leadership within the organization, 5% want to go into quality management, 24% want to return to school and further their education, 2% want to teach within the radiology field, 8% want to go into another industry and 10% hope to be retired.

Conclusions: Our study showed that there are generational differences and they do have an effect in the workplace. The differences effect the way that staff are communicated to, the amount of vacation that is taken, the way that staff likes to be recognized and career development and growth.

CASE REPORT, EDUCATIONAL AND SCIENTIFIC POSTERS

Authors are listed in the order provided. An author listed in bold identifies the presenting author.

Poster #: CR-001

Subdiaphragmatic pulmonary veins identified by ultrasound.

Josephine Ndolo,
MBChB[1], *josephine.m.ndolo@vanderbilt.edu*; Gabriella Crane[1], Marta Hernanz-Schulman, MD[1]; [1]Pediatric Radiology, Vanderbilt University, Nashville, TN

Disclosures: All authors have disclosed no financial interests, arrangements or affiliations in the context of this activity.

Purpose or Case Report: Scimitar syndrome and subdiaphragmatic total anomalous pulmonary venous connections (TAPVC) are congenital pulmonary vascular anomalies that are not typically diagnosed on routine abdominal sonography. We present three cases of ultrasound diagnosis of neonates with subdiaphragmatic pulmonary veins diagnosed on abdominal ultrasound; to the best of our knowledge, this is the first reported case of abdominal ultrasound diagnosis of previously unknown scimitar syndrome.

Case 1: 16 day old girl born at term with cardiac dextroposition and right lung hypoplasia. On abdominal ultrasound, a large vascular structure was seen draining into the inferior vena cava (IVC) near the hepatic confluence, arising in lung above the diaphragm. Doppler confirms venous flow into the IVC (Figure 1); an arterial aortic branch with pulmonary spectral Doppler signature, extended into the base of the right lung. The diagnosis of scimitar syndrome was made, confirmed several weeks later with CT angiography.

Case 2: One day old girl born at 29 weeks gestation had a prenatal diagnosis of complex congenital heart disease. Abdominal ultrasound demonstrated asplenia. As part of the complex, the examination demonstrated the common pulmonary vein draining into the left portal vein, decompressing into the heart via the ductus venosus, with color and spectral demonstration of flow direction and velocity. (Figure 2) Closure of the ductus venosus contributed to the demise of this child who was inoperable due to her extreme prematurity and her other congenital cardiac lesions.

Case 3: Eight day old term infant with multiple congenital anomalies. An abdominal ultrasound for heterotaxy evaluation demonstrated a large anomalous vessel arising in the chest between the descending aorta and esophagus posteriorly, and the atrium anteriorly, descending into the abdomen draining into the portal vein, with a partially obstructing membrane near the insertion point. (Figure 3). The TAPVC was repaired on day 9 of life with direct anastomosis to the left atrium.

Conclusion: In conclusion, subdiaphragmatic vascular components of thoracic anomalies should be recognized at abdominal sonography by pediatric radiologists, who may be the first to both recognize and diagnose these conditions.

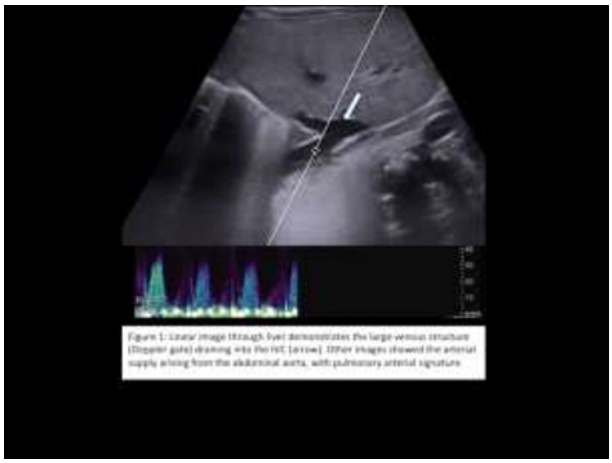

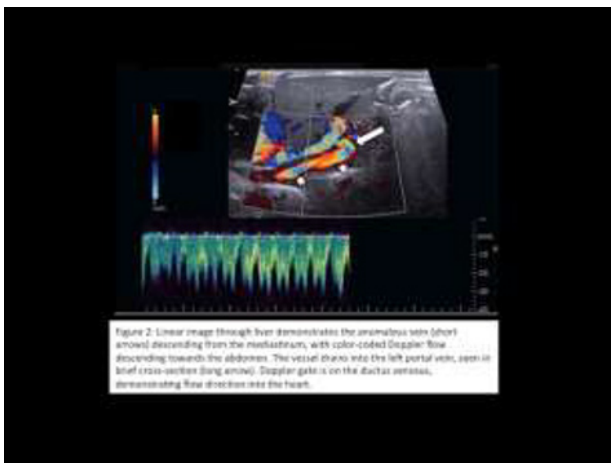

Poster #: CR-002

Multimodality Appearance of Congenital Gastric Immature Teratoma: Fetal MRI Reveals a Rare Radiographic Mimic of Meconium Pseudocyst

Cory Pfeifer, MD[1], *cpfeifer2018@gmail.com*; Angela Beavers, MD[2]; [1]Diagnostic Radiology, University of Texas Southwestern Medical Center, Dallas, TX, [2]University of Nebraska Medical Center, Omaha, NE

Disclosures: All authors have disclosed no financial interests, arrangements or affiliations in the context of this activity.

Purpose or Case Report: Teratomas uncommonly manifest in the gastrointestinal system, and most international literature cites the total number of gastric teratomas reported to be approximately 120. Of these, only 12-30 are of the immature variety. Reports of immature gastric teratoma in the United States are scant. Presented here are images from what appears to be the first known fetal MRI to demonstrate a gastric immature teratoma with follow-up radiographic, fluoroscopic, and CT imaging of the infant.
Methods & Materials: A 24-year-old G 5 P 2 gravid female presented for fetal MRI following an abnormal antenatal ultrasound which showed a complex abdominal mass. The MRI was obtained 34 weeks, 5 days. The child was later born at term, and serial radiographs were acquired followed by a CT of the abdomen and pelvis on the 4th day of life. Upper GI was performed on the 6th day of life.
Results: Fetal MRI revealed a lobulated, predominantly cystic mass occupying nearly the entire left hemiabdomen with internal septations and T2 hypointense nodules. The mass appeared to circumscribe the stomach. A normal distribution of meconium was present throughout the bowel. The patient was counselled by the radiologist at the time of the MRI who informed the patient that the most likely etiology for the mass was a meconium pseudocyst. Following delivery, an abdominal radiograph supported this diagnosis, as a large upper abdominal mass containing scattered internal calcifications was observed displacing multiple gas-filled bowel loops. The subsequent CT showed these central calcified components within both lobes of a bilobed upper abdominal mass. The left lobe of the mass was predominantly fluid attenuation, and the right lobe exhibited thickening and enhancement of the septations. Contrast flowed freely into the stomach and circumscribed the right lobe of the mass during an upper GI. The left lobe of the mass was not intraluminal. Contrast emptied into the duodenum and small bowel without evidence of obstruction. The mass was shown to represent an immature gastric teratoma following surgical resection.
Conclusions: Immature gastric teratoma is an exceedingly rare diagosis. Several imaging features suggested the much more common entity of meconium pseudocyst, and even CT failed to show macroscopic fat within the lesion. This case highlights the value of a multimodality approach to a case of an unusual pathology.

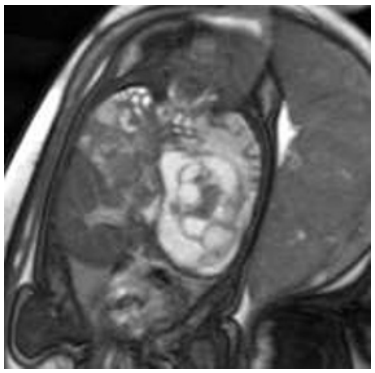

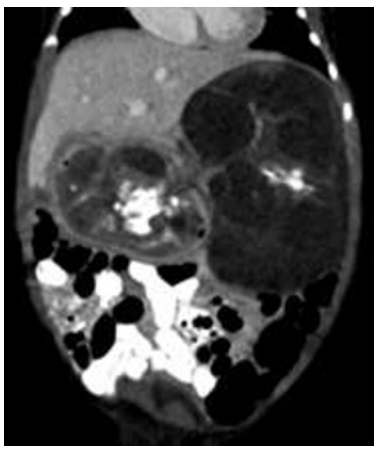

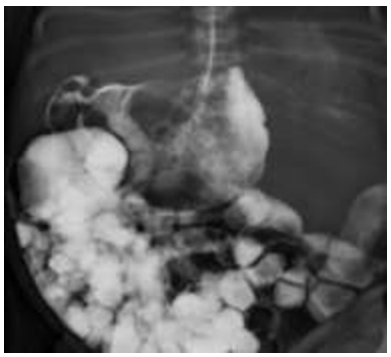

Poster #: CR-003

Colocolic Intussusception in Children with Colonic Polyp as the Lead Point

Laura Steinmeyer, MD[1], *lsteinmeyer@radiology.arizona.edu*; Sarah Desoky[1], Dorothy Gilbertson Dahdal, MD[1], Frank Morello[1], Unni Udayasankar, MD, FRCR[1]; [1]Medical Imaging, University of Arizona, Tucson, AZ

Disclosures: All authors have disclosed no financial interests, arrangements or affiliations in the context of this activity.

Purpose or Case Report: Acute colocolic intussusception is a rare in the pediatric population and generally involves a pathologic lead point, which usually necessitates surgical or endoscopic intervention. No prior published reports have demonstrated presurgical imaging findings of colonic polyp in cases of pediatric colocolic intussusceptions. We will present two pediatric cases from our institution that feature colocolic intussusception with an intestinal polyp as a lead point, with a goal to demonstrate specific sonographic and MR findings.

Methods & Materials:
Case 1 - A 2-year-old girl with recurrent "intussusceptions" (s/p multiple enema reductions as well as negative work-up with EGD and an elective exploratory laparotomy) was brought to the emergency department. An ultrasound and MRI abdomen/pelvis demonstrated a short segment colocolic intussusception at the hepatic flexure with suggestion of a polypoidal leadpoint. The ileocolic junction was normal. She was admitted to surgery for a second exploratory laparotomy, which revealed a colocolic intussusception involving the hepatic flexure with a polyp (3.4 x 2.2.cm) acting as a lead point which was resected. The patient did well after the procedure and was discharged to her home.
Case 2 - A 5-year-old boy initially presented to the emergency department with acute exacerbation of chronic abdominal pain and bloody diarrhea. An MRI abdomen/pelvis showed a short segment transient colo-colic intussusception with possibility of an intraluminal polypoidal mass. The patient returned a week later with worsening symptoms and an ultrasound study showed intussusception involving the transverse, descending and sigmoid colon as well as a pedunculated, well-defined heterogeneous intraluminal mass (measured 1.9 x 1.8 cm). An air enema successfully reduced the intussusception. Colonoscopy was performed the following day, which revealed a 2-cm transverse colonic polyp that was removed endoscopically. T
Conclusions: Colocolic intussusception is a rare subtype in the pediatric population, and when present can suggest the presence of a pathologic lead point. While colocolic intussusception is difficult to differentiate from ileocolic intussusception on ultrasound imaging alone, a mass acting as a lead point should make it a diagnostic consideration. MRI abdomen/pelvis may be helpful as a complementary examination to better delineate the colocolic nature of the intussusception as well as the mass acting as a lead point, thereby directing the appropriate treatment.

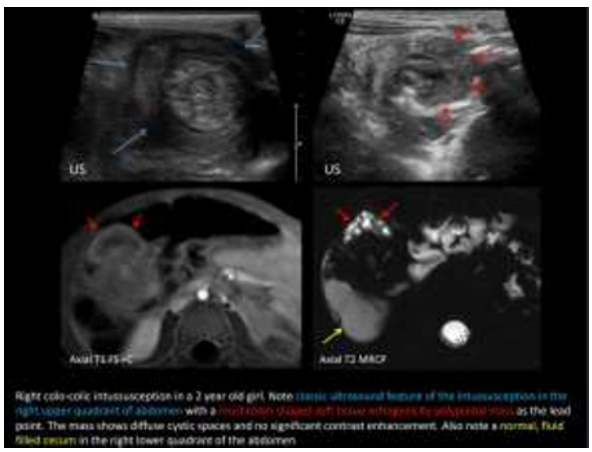

Right colo-colic intussusception in a 2 year old girl. Note classic ultrasound feature of the intussusception in the right upper quadrant of abdomen with a mushroom shaped soft tissue echogenicity/polypoidal mass as the lead point. The mass shows diffuse cystic spaces and no significant contrast enhancement. Also note a normal, fluid filled cecum in the right lower quadrant of the abdomen

Left colo-colic intussusception in a 2 year old girl. Note classic sonographic and MR features of the intussusception in the left mid abdomen with a pedunculated soft tissue echogenicity polypoid mass as the lead point. MRI clearly demonstrates a pedunculated exophytic mass with intraluminal mass in the distal transverse colon

Poster #: CR-004

Calcifying Nested Stromal Epithelial tumor of the liver: Case report of a rare primary liver tumor

Deepa Biyyam, MD[1], *dbiyyam@phoenixchildrens.com*; Mostafa Youssfi, MD[1], Gerald Mandell, MD[1], Steve Taylor, MHS, PA[1], Mittun Patel, MD[1]; [1]Radiology, Phoenix Children's Hospital, Phoenix, AZ

Disclosures: All authors have disclosed no financial interests, arrangements or affiliations in the context of this activity.

Purpose or Case Report: Calcifying nested stromal epithelial tumor (CNSET) is a very rare primary liver tumor in children. To our knowledge, about 30 cases have been reported in literature. We describe the imaging appearance and histopathologic features of this tumor detected in a 2 year old girl who presented with an incidentally detected calcified liver lesion on a chest x-ray which was obtained for cough. Computed tomography (CT) demonstrated a 5.5 centimeter sized heterogeneous mass with large coarse calcifications. MRI better demonstrated the margins of the lesion, which was predominantly hyper-intense on T2-weighted images. Large areas of signal void were seen in the superior aspect of the lesion, corresponding to the calcifications seen on CT. The lesion demonstrated restricted diffusion. Post-contrast, the lesion demonstrated enhancement in the portal venous phase with washout on the delayed phase. Initial diagnosis based on imaging findings and patient's age was hepatoblastoma. However, serum alpha- fetoprotein (AFP) was normal, which is unusual with hepatoblastoma. Patient underwent subsequent wedge biopsy, which was proven to represent calcifying nested stromal epithelial tumor of the liver. PET/CT, obtained to evaluate for metastatic disease, demonstrated increased FDG activity within the primary hepatic lesion, with SUV Max of 3.5, with no evidence of FDG avid metastatic disease. She then underwent right hepatectomy and cholecystectomy.
No sign of tumor recurrence has been noted to date on the follow up abdominal ultrasound examination in the past 2.5 years. Calcifying nested stromal epithelial tumor should be considered in the differential when a large heterogeneous liver tumor with coarse/ chunky calcifications is identified at imaging in the absence of elevated serum AFP in a child. Currently the standard treatment in complete surgical excision and liver transplantation if excision is not possible.

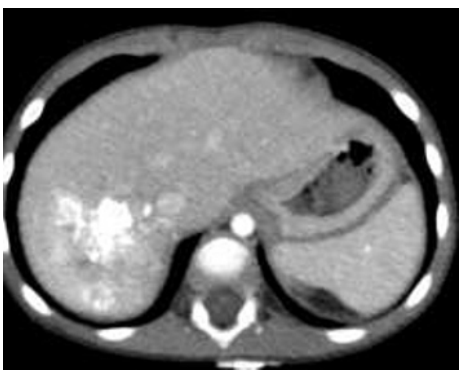

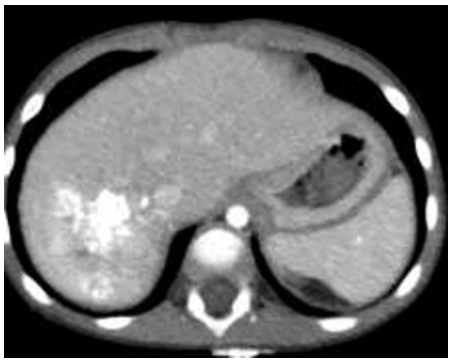

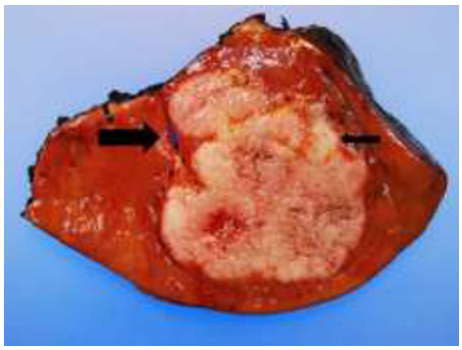

Poster #: CR-005

Pancreatic Heterotopia in a Neonatal Abdominopelvic Cyst

Shannon Farmakis, MD[1], *shannon.farmakis@health.slu.edu*; Noah Seymore, MD[2], Bachir Zoghbi, MD[2], Cirilo Sotelo-Avila, MD[1]; [1]Radiology, SSM Health Cardinal Glennon Children's Hospital, St. Louis, MO, [2]St. Louis University School of Medicine, St. Louis, MO

Disclosures: Shannon Farmakis has indicated a relationship with GE Healthcare for receiving a research grant. All other authors have disclosed no financial interests, arrangements or affiliations in the context of this activity.

Purpose or Case Report: Fetal abdominopelvic cystic lesions have various etiologies but are most commonly ovarian or gastrointestinal in origin. Congenital pancreatic cysts are rare entities that typically arise from the pancreatic body and tail, more often in females. In contrast, pancreatic heterotopia or an ectopic pancreas is defined as pancreatic tissue found outside the normal region of the pancreas without a vascular or anatomic connection to the pancreas. It is most commonly associated with the gastrointestinal tract, with >90% of cases located in the stomach, duodenum, or jejunum, and has been known to form cystic structures. We describe an unusual case of a term female neonate with a prenatal diagnosis of an abdominopelvic cyst. The patient had episodes of hypoglycemia secondary to hyperinsulinism requiring a continuous glucose infusion. On surgical resection, the cyst was found to extend from the retroperitoneum towards the left colon without connection to the pancreas or gastrointestinal tract. Histopathological evaluation showed components of pancreatic heterotopia including islets of Langerhans surrounded by acinar cells and dilated pancreatic ducts. The immunostain for Chromogranin showed numerous alpha and beta cells confirming pancreatic tissue. Hypoglycemic episodes improved following cyst resection.
This is the first reported case of retroperitoneal cystic pancreatic heterotopia in a neonate in the English literature. We will present the ultrasound findings as well as surgical and histopathologic images.

Methods & Materials: Our case is derived from the records from a tertiary children's care hospital.
Results: The etiologies and imaging findings of neonatal abdominopelvic cysts will be reviewed as well as relevant potential imaging techniques for workup of abdominopelvic cysts with an emphasis on the radiologic, surgical, and histopathologic findings of cystic pancreatic heterotopia.
Conclusions: Abdominopelvic cysts are commonly found on prenatal ultrasound and have a wide variety of etiologies. Pancreatic heterotopia is rare outside of the gastrointestinal tract but should be considered in the differential for abdominopelvic cysts, especially in the setting of hyperinsulinemia.

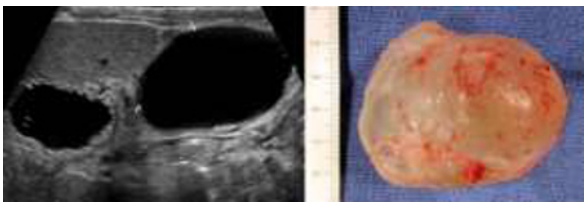

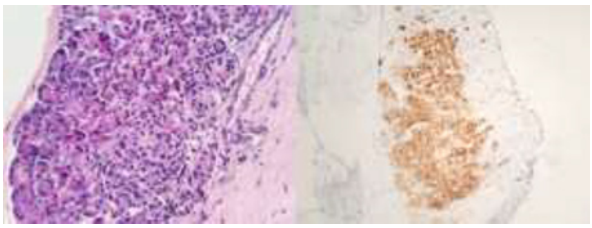

Poster #: CR-006

Small Bowel High Grade B-cell Lymphoma in an Adolescent Girl with Primary Intestinal Lymphangiectasia - Feared Association of a Rare Disease

Yi-ming Teo[1] *yi_ming_teo@nuhs.edu.sg*; ; [1]National University Hospital, Singapore

Disclosures: All authors have disclosed no financial interests, arrangements or affiliations in the context of this activity.

Purpose or Case Report: Intestinal lymphangiectasia is a rare disease characterised by dilated intestinal lacteals causing loss of lymph into the small bowel lumen and resultant hypoproteinemia, hypogammaglobulinemia, hypoalbuminemia and lymphopenia. The disease may occur as a primary / congenital form (primary idiopathic intestinal lymphangectasia / Waldmann disease) or as a secondary form resulting from causes of lymphatic obstruction, such as tumor or fibrosis.
Our case report describes the workup of an adolescent girl with known Primary Intestinal Lymphangiectasia (Waldmann disease) presenting with an acute history of abdominal pain and vomiting. We present her prior imaging leading to her initial diagnosis of Waldmann disease, as well as at the time of acute presentation, with imaging features raising suspicion for, and eventually leading to histo-pathologic confirmation of small bowel B-cell lymphoma.
Via this case report poster, we hope to create awareness of this rare disease, as well as its feared association of lymphoma. Typical imaging features are presented and discussed.

Poster #: CR-007

Wilm's tumor not in the kidney? Two case reports of extra-renal Willm's tumor and a review of the literature

Gregory Vorona, MD[1], *gregory.vorona@vcuhealth.org*; Akhil Kolluri[2], Stephen Smith[1], Madhu Gowda[1], Frances Austin[1], Charles Bagwell[1], Claudio Oiticica[1]; [1]The Children's Hospital of Richmond at Virginia Commonwealth University, Richmond, VA, [2]Virginia Commonwealth University, Richmond, VA

Disclosures: All authors have disclosed no financial interests, arrangements or affiliations in the context of this activity.

Purpose or Case Report: Wilm's tumor (nephroblastoma) is the most common pediatric renal mass, with rare reports of extra-renal Wilm's tumors which primarily arise elsewhere in the retroperitoneum. We present a small series of patients who have recently been treated at our institution with histologically-proven extra-renal Wilm's tumors. The first patient is a six year old female who initially presented to an outside hospital with a draining "perianal abscess", who on subsequent workup was found to have a large infiltrative pelvic mass and multiple pulmonary metastases (image 1). The second patient is a six year old female who initially presented with abrupt onset of right-sided abdominal pain which woke her from sleep, and who was found on imaging to have a large right-sided retroperitoneal hemorrhage originating from a hemorrhagic suprarenal mass (images 2 and 3).
We will review the pertinent imaging and histological findings from these patients, as well as briefly review what has been previously published about this rare rumor.
The imaging features of extra-renal Wilm's tumor are heterogeneous and not specific, making it important that the radiologist consider this etiology when presented with a retroperitoneal mass in a pediatric patient within the first decade of life.

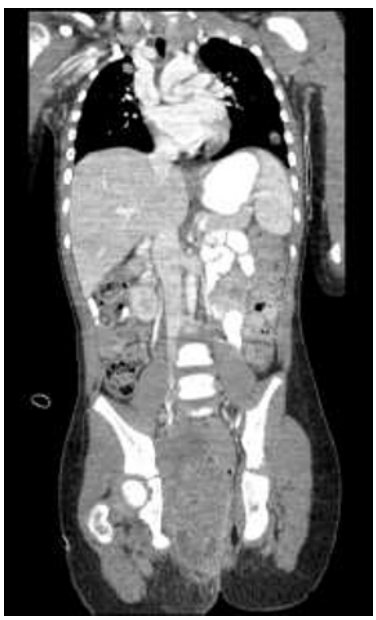

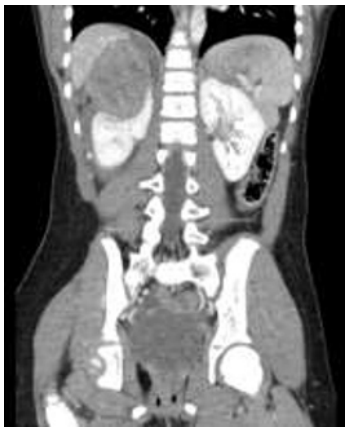

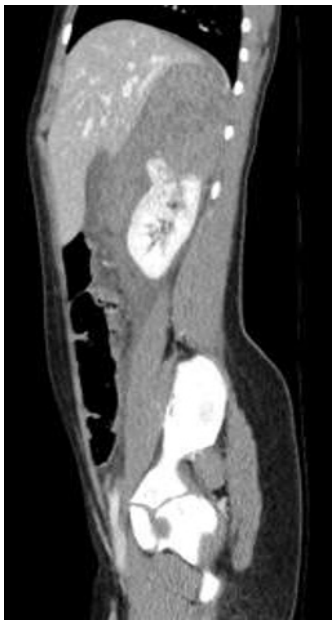

Poster #: CR-008

Short Rib Polydactyly Syndrome, Type III

Stephen Morgan, MD[1], *stephenmorgan13@gmail.com*; Deborah Conway, MD[1]; [1]Radiology, Memorial University Medical Center, Savannah, GA

Disclosures: All authors have disclosed no financial interests, arrangements or affiliations in the context of this activity.

Purpose or Case Report: An infant was born at 36 weeks, 3 days gestation with a known lethal skeletal dysplasia, diagnosed on prenatal ultrasound. The infant was born alive with APGARs of 5 and 3. Comfort care was initiated, and the infant expired one hour later. Plain films of the skeletal system were obtained, which showed short, horizontal ribs and a small thorax. They also showed hypoplastic iliac bones, flattened acetabula, and postaxial polydactyly. The metaphyses of the long bones had convex central areas with lateral metaphyseal spikes. The constellation of findings was consistent with Short Rib Polydactyly Syndrome type III (Verma-Naumoff).
Inherited in an autosomal recessive pattern, SRPS is a group of rare, lethal osteochondrodysplasias caused by mutations in the DYNC2H1 gene, a component of the cytoplasmic dynein complex, which is involved in the generation and maintenance of cilia. This mutation results in dyskinesia involving the

chondrocytes, leading to arrested maturation of cartilage and generalized loss of synchrony in cartilage removal and osteogenic differentiation.
Common anomalies that span all types of SRPS include a triad of micromelia, short horizontal ribs, and polydactyly. Four types of short-rib polydactyly syndrome have been described, which differ based on visceral involvement and the appearance of the metaphyses. Some have phenotypic overlap with various types of Short Rib-Thoracic Dysplasia. The four types of SRPS are: Saldino-Noonan (type I), Majewski (type II), Verma-Naumoff (type III), and Beemer-Langer (type IV). Type I (SN) is characterized by hypoplastic iliac bones, flattened acetabular roofs, rounded vertebrae with coronal clefts, and postaxial polydactyly. The long bones can have varied appearance of the metaphysis, including: pointed ends, convex central areas with lateral metaphyseal spikes, or ragged-appearing ends. A key distinguishing factor with type I is the absence of fibulae. Type III (VN) is very similar to type I, however, the fibulae are present. Visceral anomalies are less common with the Verma-Naumoff type. Type II (Majewski) presents with either pre- or postaxial polydactyly. The long bone metaphyses have smooth ends, the tibiae are ovoid and shorter than the fibulae, and the iliac bones are normal. Type IV (BL), like type II, can also have pre- or postaxial polydactyly and smooth metaphyses in the long bones. The distinguishing characteristics of the Beemer-Langer type include small iliac bones and bowed radii/ulnae.

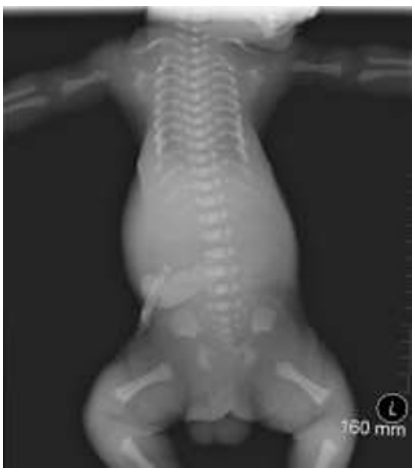

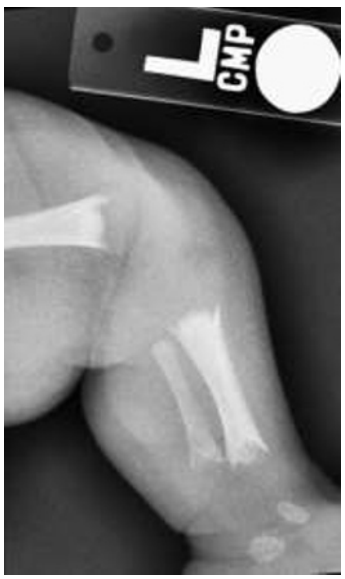

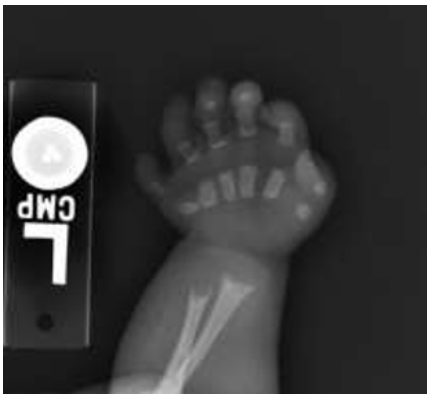

Poster #: CR-009

Lethal Heat Stroke Encephalopathy

Hales Skelton[2], *hskelton@pdx.edu*; Gary Hedlund, DO[1]; [1]Primary Children's Hospital, Salt Lake, UT, [2]Portland State University, Portland, OR

Disclosures: All authors have disclosed no financial interests, arrangements or affiliations in the context of this activity.

Purpose or Case Report: The purpose of this case report is to familiarize the radiologist with the MR imaging findings of fatal heat stroke.
Heat stroke is a severe illness characterized by a core temperature > 40 degrees Celsius, with clinical manifestations of delirium, seizures, and coma, resulting from environmental exposure or physical exertion. This report focuses upon environmental, or classical, fatal heat stroke in the case of a 4 year old male who was left alone for 30 minutes in a vehicle with ambient exterior temperatures of greater than 37.8 degrees Celsius.
As a form of hyperthermia, heat stroke ensues from thermoregulatory failure in addition to systemic inflammatory and coagulation phase responses, and conceivably, from modified manifestation of heat shock proteins. Infants and young children comprise a population specifically vulnerable to heat stroke due to their large surface area to volume ratio, underdeveloped thermoregulatory system with small blood volume relative to body size, and decreased sweat production. The CNS is especially susceptible to hyperthermia as cerebral edema and cerebrovascular congestion may lead to increased intracranial pressure, and ischemia or hemorrhage. The cerebellum is the area most sensitive to heat injury, with known direct injury to Purkinje cells, and resultant cerebellar atrophy, often leading to neuronal dysfunction, including ataxia.
MR imaging findings in heat stroke are typically multifocal reflecting the complex interplay of direct thermal injury, hypoxic ischemic injury, endothelial damage, cytokine mediated inflammation and coagulopathy.
MRI in our case of fatal heat stroke demonstrates diffuse signal abnormality within the peripheral cerebellar hemispheres (eg. Purkinje cell regions). MRI recapitulates the known pathology of fatal heat stroke with injury to Purkinge cells and adjacent Bergmann glia. Other reported heat stroke related MRI findings include T2 prolongation and restricted diffusion involving the paramedian thalamic nuclei, dentate nuclei, basal ganglia, hippocampii, and cerebral cortex particularly the vascular watershed zones.
If the health history for heat stroke is uncertain, the imaging differential diagnosis includes other cerebellar syndromes including: toxic - metabolic (eg. opiate toxicity), infectious-autoimmune (eg. Varicellar zoster cerebellitis), histiocytic

neoplastic-like (eg. histiocytoses) and neoplastic (eg. leptomeningeal PNET) should be considered in the imaging differential diagnosis.

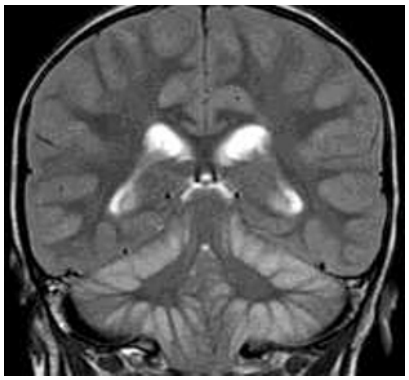

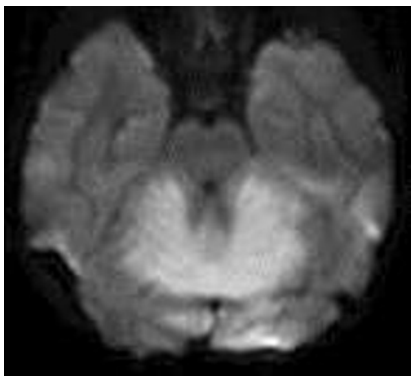

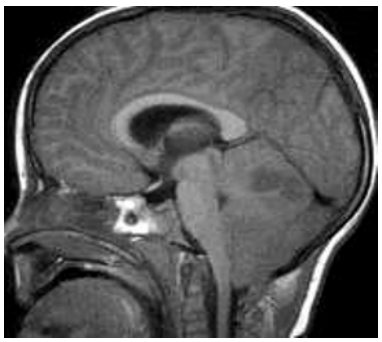

Poster #: CR-010

A neuroenteric cyst acting as a foreign body in the brainstem: imaging and clinical findings.

Juan Domingo Ly, MD[2], *lyliuj@upmc.edu*; Subramanian Subramanian, MD[1], Deepa Rajan, MD[4], Stephanie Greene, MD[3], Giulio Zuccoli[1]; [1]Neuroradiology, Children's Hospital of Pittsburgh of UPMC, Pittsburgh, PA, [2]Department of Radiology, University of Pittsburgh Medical Center, Pittsburgh, PA, [3]Department of Neurosurgery, Children's Hospital of Pittsburgh of UPMC, Pittsburgh, PA, [4]Department of Neurology, Children's Hospital of Pittsburgh of UPMC, Pittsburgh, PA

Disclosures: All authors have disclosed no financial interests, arrangements or affiliations in the context of this activity.

Purpose or Case Report: An 11-year-old female presented with 3-weeks history of intractable vomiting, nausea, blurred vision, vertical nystagmus and ataxia with gait instability. A CT scan revealed a small calcification at the left craniocervical junction (CJJ) and mild effacement of the fourth ventricle (Figure). MRI showed a partially-enhancing medulla oblongata lesion and a non-enhancing cystic exophytic lesion abutting the left pre-medullary cistern. There was avid thick enhancement along the ventrolateral surface of the medulla oblongata. No restricted diffusion was present. MR spectroscopy demonstrated decreased NAA and elevated lactates. Based on imaging findings, a brainstem glioma with exophytic component was suspected. The CBC, CMP, ESR and CRP were normal. The patient underwent suboccipital craniectomy with C1 laminectomy, and an exophytic pale gray mass was identified. Multiple specimens were taken, and frozen diagnosis showed only necrosis. The cyst wall was resected. Resection of the brainstem component was limited by neurophysiology. Histologically, the lesion consisted of a fibrous cyst wall lined by columnar to pseudostratified columnar epithelium, findings reflecting a neuroenteric cyst. No glial tissue was identified. Gram stain and Grocott stain were negative for bacterial and fungal specimens. An empiric treatment with wide spectrum antibiotic was started. Follow-up MRI demonstrated near complete resolution of edema in the medulla oblongata, and substantial decrease in enhancement in anterolateral exophytic component and patient has substantially improved clinically. In retrospect, a sinus tract extended from the cystic lesion at the craniocervical junction into the brainstem causing edema, inflammation and enhancement which resolved once the cyst was surgically decompressed.

Conclusion: This case shows a neuroenteric cyst connected to the brainstem, through a sinus tract leading to chronic inflammation and infection, resulting in imaging findings resembling a brainstem glioma. Surgical decompression of the cyst and antibiotic treatment resulted in resolution of the brainstem lesion.

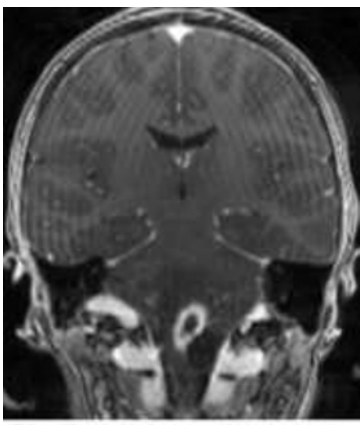

MRI Coronal T1w post contrast. Sinus tract connecting the neuroenteric cyst to the brainstem leading to chronic inflammation.

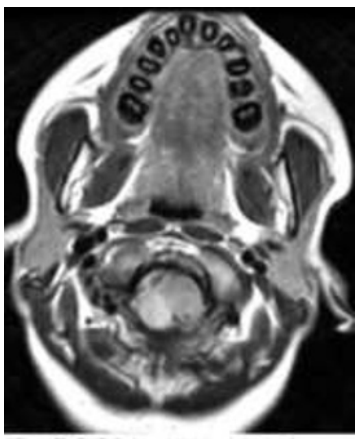

MR axial T2w FLAIR. Cystic exophytic lesion abutting the left premedullary cistern.

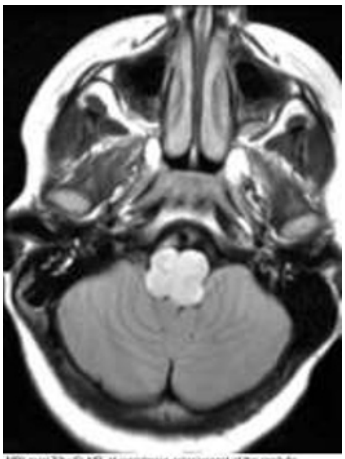

MRI axial T2w FLAIR. Hyperintense enlargement of the medulla oblongata mimicking a brain stem glioma.

Poster #: CR-011

Distinct Patterns of Reversible Diffusion Restriction in Propionic Acidemia

Cory Pfeifer, MD[1], *cpfeifer2018@gmail.com*; Keshav Menon, MD[1]; [1]Diagnostic Radiology, University of Texas Southwestern Medical Center, Dallas, TX

Disclosures: All authors have disclosed no financial interests, arrangements or affiliations in the context of this activity.

Purpose or Case Report: Propionic acidemia is a rare autosomal recessive disorder in which a genetic mutation results in the abnormal function of propionyl co-enzyme A (CoA) carboxylase, an enzyme involved in protein breakdown and lipid catabolsim. This results in the accumulation of metabolites which can have devastating neurologic consequences. The incidence in the United States has been reported as 1 in 100,000 births. The genetic and metabolic factors contributing to this disorder are discussed.
Methods & Materials: Brain MRI findings in propionic acidemia are described in 2 patients. The first patient is a 5-month-old male who was transferred from an outside hospital on respiratory support with severely elevated ammonia and metabolic acidosis. The second patient is a 15-year-old female who presented to the emergency department with a mild headache and increased sleepiness. Following admission, she decompensated significantly, and her serum ammonia level was shown to be three times the normal limit.
Results: MRI of the brain in the first child demonstrated diffusion restriction in a subcortical pattern evenly distributed throughout both cerebral hemispheres. In the second patient, MRI revealed cortical diffusion restriction throughout the entire left cerebral hemisphere, however, the right cerebral hemisphere was affected to a much lesser extent. Interestingly, parenchymal volume loss was prominent throughout the right cerebral hemisphere. The basal ganglia and thalami were not affected in either child. Follow-up MRI obtained in both children after appropriate therapy showed improvement in diffusion restriction. There was diffuse cerebral atrophy on follow-up of the first patient. Follow-up MRI of the second patient showed resolution of diffusion restriction and continued volume loss throughout the contralateral (right) cerebral hemisphere.
Conclusions: These cases illustrate unique and distinct patterns of diffusion restriction in propionic acidemia crises. Commonly reported findings in the literature include involvement of the basal ganglia and/or thalami which were not seen in these two children. The cases shown here further expand the differential diagnosis for nonspecific diffusion restriction and demonstrate uncommon presentations of an already rare disease entity.

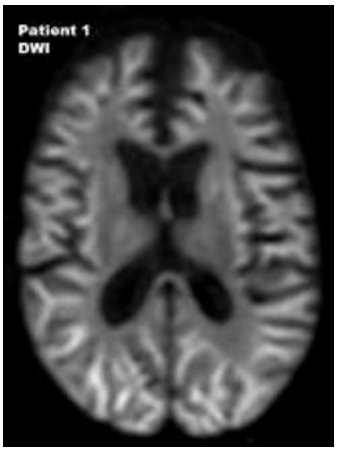

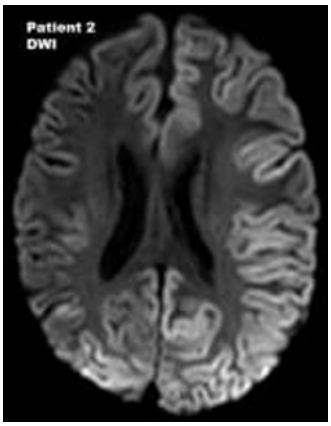

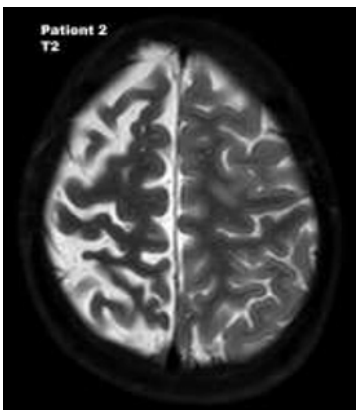

Poster #: CR-012

Segmental Spinal Dysgenesis: Case Series

Susan Taylor, DO[1], *sustaylor@augusta.edu*; Manish Bajaj, MBBS[1], Yutaka Sato, MD[2], Bruno Policeni, MD, MBA[2]; [1]Radiology, Augusta University Medical Center, Augusta, GA, [2]University of Iowa Hospitals and Clinics, Iowa City, IA

Disclosures: All authors have disclosed no financial interests, arrangements or affiliations in the context of this activity.

Purpose or Case Report: We will present imaging findings of segmental spinal dysgenesis in a series of 3 cases of this rare congenital abnormality. We will also describe the embryological basis and pertinent clinical features.

Case 1: 8-year-old female recently adopted from China with history of severe scoliosis, neurogenic bladder, and chronic kidney disease. Plain radiographs demonstrate severe destroscoliosis in thoracolumbar region with associated kyphosis. MRI reveals multiple segmentation/formation anomalies in the lumbosacral region. The coccyx was not identified, likely representing associated partial sacrococcygeal dysgenesis. The spinal cord was severely dysgenetic in the lower thoracic region (Figure 1, white outlined arrow). The superior segment of the spinal cord extends from the cervicomedullary junction to the level of T8, where it ends abruptly. No intervening cord tissue is seen between the T8 level and lumbar region. There is an enlarged spinal cord segment at the level of the sacrum in the spinal canal, separate from the superior segment (Figure 2, solid white arrow). CT with 3D reconstruction better demonstrated multiple segmentation/formation anomalies in the thoracic and lumbosacral region, including butterfly vertebrae, hemivertebrae, and block vertebrae. There were 10 ribs on the right noted with the superior 2 ribs fused.
Conclusions: Spinal segmental dysgenesis is a congenital developmental abnormality with severe hypoplasia/absence of variable length of the spine and spinal cord. The spinal cord in the involved portion may be severely hypoplastic to totally absent. There are no associated dorsal defects of meningomyelocele at the involved level

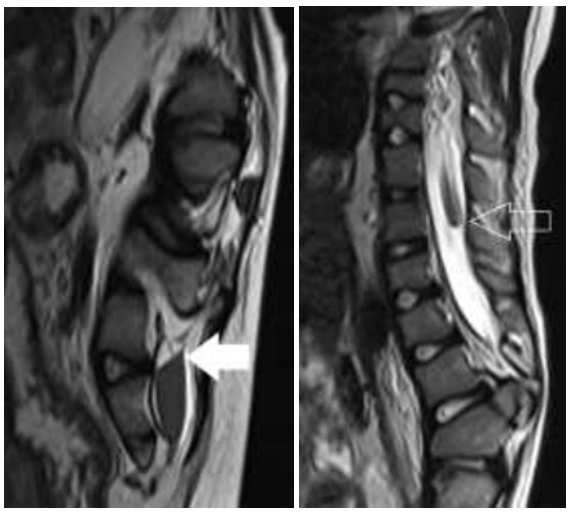

Poster #: CR-013

Metronidazole induced CNS toxicity.

Joseph Cao[2], *joseph.cao@phhs.org*; Cory Pfeifer, MD[1], Rebekah Clarke, MD[1], Daniel Veltkamp, MD[1]; [1]Children's Medical Center, Dallas, TX, [2]University of Texas Southwestern, Dallas, TX

Disclosures: All authors have disclosed no financial interests, arrangements or affiliations in the context of this activity.

Purpose or Case Report: Metronidazole is a commonly used and effective antimicrobial agent for gastrointestinal and genitourinary infections throughout the world. Common side effects of nausea, taste/appetite changes, and headache are well known, however, CNS side effects such as cerebellar dysfunction, dysarthria, and seizures have been reported even at therapeutic levels in rare instances. A previous review of the case literature concluded that resolution of symptoms was independent of age, however, evaluation of the pediatric population is limited.

Methods & Materials: The patient is a 17-year-old autistic male who presented with one day history of ataxia and leaning to the right during ambulation. He was afebrile, and lumbar puncture revealed no evidence of meningitis. There were no recent illnesses or sick contacts. Past medical history was significant for Hirschsprung's Disease.
Results: There is diffuse T2 signal abnormality throughout the cerebellar hemispheres with notable involvement of the cerebellar cortex and dentate nuclei. Symmetrical regions of abnormal FLAIR/T2 signal hyperintensity are also present within the dorsal pons and medulla. There is ill-defined T2 signal hyperintensity within the callosal splenium which demonstrates corresponding restricted diffusion. There is no associated contrast enhancement. Review of the patient's medical record showed long-term use of metronidazole. MRI changes and mental status improved following withdrawal of the medication.
Conclusions: Unexplained change in mental status often prompts imaging evaluation. The MR imaging findings of metronidazole induced CNS toxicity in this case expands on the limited literature of this condition in the pediatric population. Additionally, the unique imaging findings discussed will serve to initiate prompt cessation of therapy in an otherwise reversible disease course.

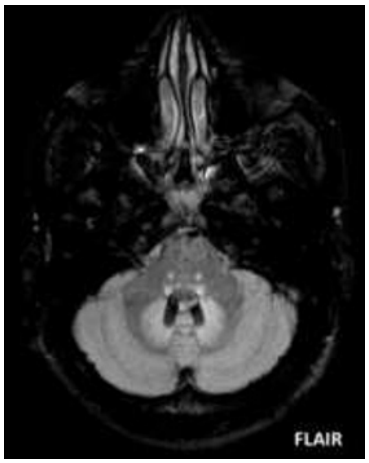

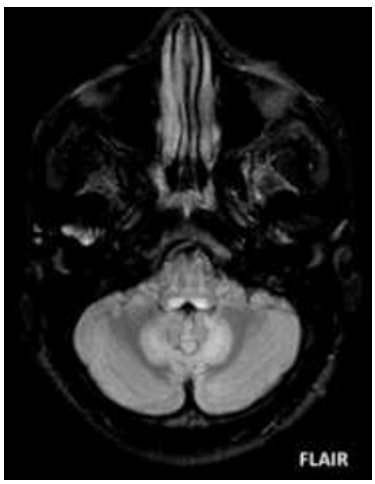

Poster #: CR-014

MRI Findings in a 13 year old with Massive Peritoneal Recurrent Wilms Tumor

Paul Grundlehner, MD[1], *Paul.Grundlehner@beaumont.org*; Donald Gibson, MD[2]; [1]Beaumont Health, Royal Oak, MI, [2]Beaumont Children's Hospital, Royal Oak, MI

Disclosures: All authors have disclosed no financial interests, arrangements or affiliations in the context of this activity.

Purpose or Case Report: Wilms tumor is a common malignant renal neoplasm in children and accounts for the vast majority of renal tumors in children. Modern treatment regimens have increased overall survival for Wilms tumor to over 90%[1]. Despite this, 10-15% of patients with favorable histology and up to 50% with anaplastic histology will experience primary progression or recurrence. The most common site of recurrence is to the lungs and the liver[2]. Peritoneal disease and recurrence has been described[3-4].

We present an interesting case of a 13-year-old female with extensive peritoneal recurrence of Wilms tumor. The patient initially presented at the age of 12 with a 3-day history of abdominal pain. CT revealed a 13 cm right renal mass with no other lesions in the chest, abdomen, or pelvis. She underwent right nephrectomy, during which she was upstaged to stage 3 when tumor rupture occured. Histology was favorable. She completed chemo and radiotherapy. CT CAP at 6 months follow-up showed no recurrent disease. Approximately 7 months later or 13 months after initial diagnosis the patient presented with constipation and abdominal pain. Initial non-contrast CT demonstrated filling of the abdomen and pelvis with a high density material(Figure 1). Given the patient's history and concern about some nodularity to the density, MRI was performed and demonstrated extensive heterogeneous mass-like peritoneal disease filling the abdomen and pelvis(Figure 2). There were additional areas of peritoneal caking and thickening(Figure 3). Ultrasound guided biopsy was performed and the pathology was identical to that of the excised Wilms. While unusual recurrent Wilms tumor should be included in the differetial diagnosis of massive intraperitoneal neoplasia

1. Metzger, M. L. (2005). Current Therapy for Wilms Tumor. *The Oncologist, 10*(10), 815-826. doi:10.1634/theoncologist.10-10-815

2. Dome, J. S., Rodriguez-Galindo, C., Spunt, S. L., & Santana, V. M. (2014). Pediatric Solid Tumors. In *Abeloff's Clinical Oncology* (5th ed.). Philadelphia: Churchill Livingstone/Elsevier.

3. Brisse, H. J., Schleiermacher, G., Sarnacki, S., Helfre, S., Philippe-Chomette, P., Boccon-Gibod, L., . . . Neuenschwander, S. (2008). Preoperative Wilms tumor rupture. *Cancer, 113*(1), 202-213. doi:10.1002/cncr.23535

4.Slasky, B. S., Bar-Ziv, J., Freeman, A. I., & Peylan-Ramu, N. (1997). CT appearances of involvement of the peritoneum, mesentery and omentum in Wilms tumor. *Pediatric Radiology, 27*(1), 14-17. doi:10.1007/s002470050053

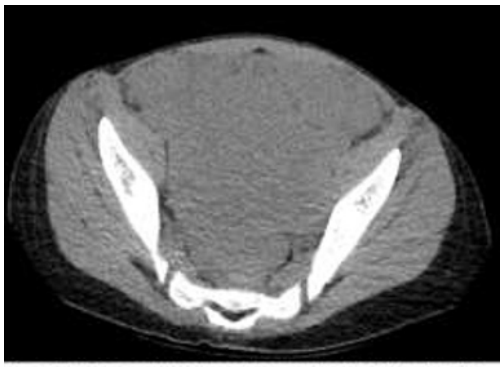

Figure 1. Initial non-contrast CT apperance suggests possible complex fluid or soft tissue mass in the abdomen and pelvis.

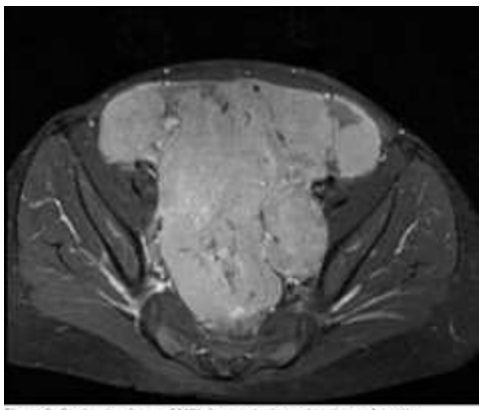

Figure 2. Contrast enhanced MRI demonstrates extensive enhancing peritoneal mass.

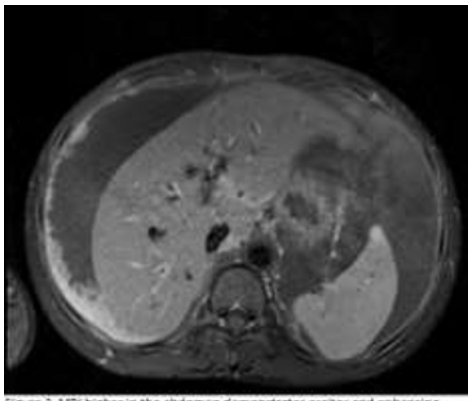

Figure 3. MRI higher in the abdomen demonstrates ascites and enhancing nodular peritoneal thickening.

Poster #: CR-015

A Fortuitous Balloon: Delayed Diagnosis of Tracheal Transection

James Lish, MD[1], Randy Richardson[1], Alice Lin[2]; [1]Radiology, St. Joseph's Hospital and Medical Center, Phoenix, AZ, [2]Creighton Medical School, Omaha, NE

Disclosures: All authors have disclosed no financial interests, arrangements or affiliations in the context of this activity.

Purpose or Case Report: Traumatic laryngotracheal transection is an uncommon occurrence most often secondary to blunt trauma to the neck. The most commonly described mechanism is a "clothesline" injury or strangulation, involving high speed impact of the neck across a chain, rope, chord, or strap, usually associated with the use of a motor or recreational vehicle. It is often instantaneously fatal, and those who survive may have

severe respiratory compromise requiring immediate advanced airway placement, or astonishingly, they may be asymptomatic. Tracheal transection may be identified when laryngoscopic intubation fails, during the placement of a surgical airway, or during initial CT or bronchoscopic evaluation.
We describe an 8-year-old male who experienced blunt neck trauma and was intubated successfully in the pre-hospital setting. Initial radiographic evaluation was significant for severe subcutaneous emphysema and pneumomediastinum. Bilateral thoracostomy tubes were placed. Initial CT evaluation again showed extensive pneumomediastinum without pneumothorax. Four days after initial hospitalization the patient was extubated without difficulty. Post-extubation chest x-ray showed irregular tracheal borders with focal hyperlucency adjacent the mid-cervical trachea in the former position of the endotracheal tube cuff. Repeat CT of the chest showed complete tracheal transection of the mid-cervical trachea. The patient subsequently underwent surgical repair and was discharged without complication. This is the first reported case of traumatic tracheal transection not identified on initial CT examination secondary to the position of the endotracheal balloon, with subsequent discovery of the complete transection on the post-extubation radiograph.
There is 1 reported case of tracheal transection identified on initial CT evaluation in the presence of a well-positioned endotracheal tube. Additionally, there is 1 reported case of tracheal transection not identified on initial CT evaluation, however the patient was not intubated and had minimal symptoms. Tracheal transection was confirmed via bronchoscopy in that case.
Tracheal transection is rare traumatic injury that can be difficult to identify. High clinical suspicion and careful examination with multiple modalities is often necessary to make a definitive diagnosis.

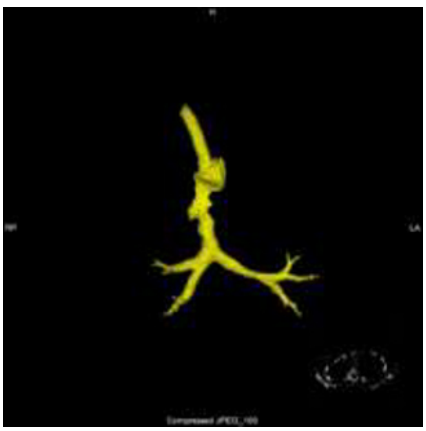

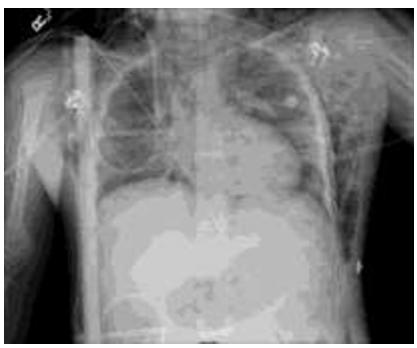

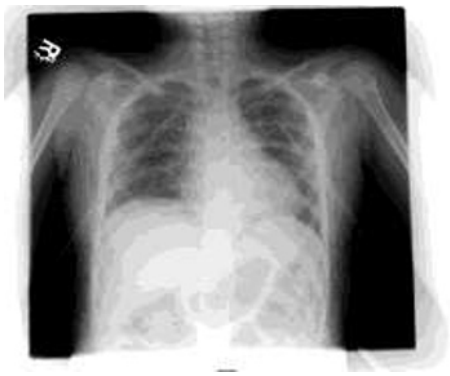

Poster #: CR-016

Diffuse Esophageal Leiomyomatosis: A case report
Jordan Rapp, MD[1], *jrapp24@gmail.com*; Mea Mallon[2]; [1]Children's Hospital of Philadelphia, Philadelphia, PA, [2]St. Christopher's Hospital for Children, Philadelphia, PA

Disclosures: All authors have disclosed no financial interests, arrangements or affiliations in the context of this activity.

Purpose or Case Report: A 15 year old female with no significant past medical history except for long standing dysphagia and intermittent chest pain presented for a frontal and lateral radiograph. The x-ray showed a long segment density along the right heart border concerning for mediastinal mass. The patient subsequently underwent a contrast enhanced CT. Diffuse circumferential thickening of the esophagus began just below the thoracic inlet and extending for approximately 17cm to the level of the esophageal hiatus.
Evaluation of the esophageal lumen was performed at our institution utilizing reduced pediatric dose pulsed fluoroscopy with a barium esophagram. While the cervical and upper 1/3 of the thoracic esophagus had a normal lumen diameter and contour, there was irregular contractility and motility throughout the upper esophagus. The lower 2/3 showed narrowing which did distend with barium passage.
At this juncture a biopsy of the lesion was performed with the resulting pathology consistent with a leiomyoma. Preoperative planning MRI was then undertaken. As seen with the CT, diffuse circumferential thickening of the esophagus began just below the thoracic inlet with progressive thickening continuing distally to a maximum thickness just above the GE junction.
The patient subsequently went on to have an Ivor-Lewis esophagectomy with gastric pull through. The diagnosis of diffuse esophageal leiomyomatosis was confirmed by pathology.
Diffuse esophageal leiomyomatosis (DEL) was probably first described by Hall in 1916 in a case report of a 17 year old female who died of starvation due to dysphagia, with the diagnosis subsequently made on autopsy. While some cases of DEL are sporadic, as in our case, there is a well-established association with the x-linked Alport Syndrome, especially in the pediatric population. Up to 5% of Alport patients are affected by DEL and as much as 2/3 of pediatric patients with DEL carry the diagnosis of Alport Syndrome. Esophageal-Vulvar syndrome, characterized by leiomyomata of both the vulva and esophagus, presents with findings of DEL on imaging in many cases, often in young adult females. While presentations may vary, the majority of patients present with long standing dysphagia. An Iver-Lewis esophagectomy with a gastric pull-through is the treatment of choice.

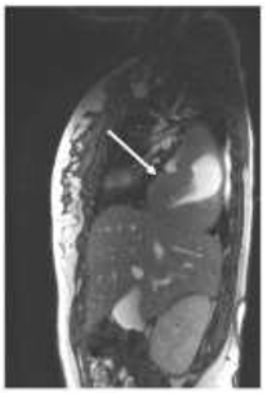

Fig 1. Sat T2 through the right hemithorax. Circumferential thickening of the distal esophagus is seen (arrow).

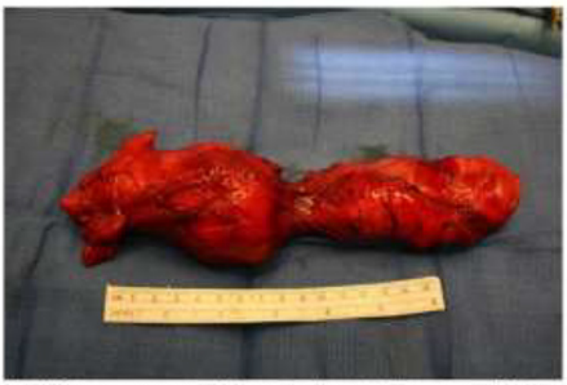

Fig 2. Gross appearance of the surgically resected esophagus. Diffuse thickening is due to leiomyomatosis

Poster #: EDU-001

Spetral Multi-Energy CT in Pediatrics: Physics Review and Clinical Applications

Richard Southard, MD[1], *rsouthard@phoenixchildrens.com*; Lingyun Chen, PhD[1], Carla Williams, RT[1], Dianna Bardo, MD[1]; [1]Department of Medical Imaging, Phoenix Children's Hospital, Phoenix, AZ

Disclosures: Richard Southard has indicated a relationship with Philips Healthcare for consultant/ honoraria, speaking and receiving a research grant. All other authors have disclosed no financial interests, arrangements or affiliations in the context of this activity.

Purpose or Case Report: Spectral or multi-energy CT (MECT), obtains raw data at more than one energy spectra which allows the decomposition of materials into their constituent elements. As opposed to conventional CT which yields data based on linear attenuation, MECT yields both structural and material-specific information. Only limited experience and literature are available regarding use and applications of MECT in the pediatric patient population. Our institution has recently installed a spectral MECT scanner which uses a single x-ray source modified multilayered detector CT, in our emergency department (ED). It is currently the only such scanner used for routine clinical pediatric imaging in the US, and 4th such unit in a children's hospital in the world. In this educational exhibit we will review the basic physics of MECT, the benefits and limitations of the single-source multi-layered detector geometry, and clinical applications of MECT and our experience to date in the pediatric population.

Methods & Materials: A Philips IQon Spectral MECT (Philips Healthcare, Cleveland, OH) was installed in our facility in October, 2017. Though positioned in the ED, routine inpatients and outpatients are also examined.

Results: We present cases in which MECT aided in diagnosis through use of spectral data and propose areas of further clinical diagnoses and research. Clinical cases thus far examined include children suffering acute trauma, abdominal pain, renal stones, congenital heart disease, headache, and tumor.

Features of MECT advantageous to pediatric patients include reconstruction of virtual non-contrast images, perfusion imaging, mitigation of beam-hardening artifact with high mono-energetic imaging, the use of low mono-energetic imaging to boost iodine density to improve angiographic images which may be limited by contrast or bolus timing, and urinary stone analysis and renal mass characterization.

Conclusions: The use of Spectral MECT at our institution has provided a significant advance in our ability to confidently diagnose various disease processes. As we gain more experience in the use of MECT in the pediatric population, we will be able to better define its role and uncover further areas of research.

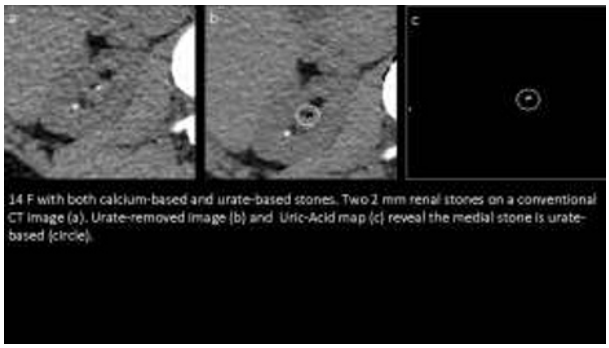

14 F with both calcium-based and urate-based stones. Two 2 mm renal stones on a conventional CT image (a). Urate-removed image (b) and Uric-Acid map (c) reveal the medial stone is urate-based (circle).

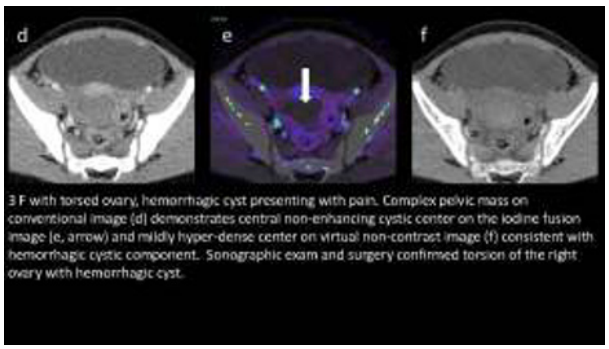

3 F with torsed ovary, hemorrhagic cyst presenting with pain. Complex pelvic mass on conventional image (d) demonstrates central non-enhancing cystic center on the iodine fusion image (e, arrow) and mildly hyper-dense center on virtual non-contrast image (f) consistent with hemorrhagic cystic component. Sonographic exam and surgery confirmed torsion of the right ovary with hemorrhagic cyst.

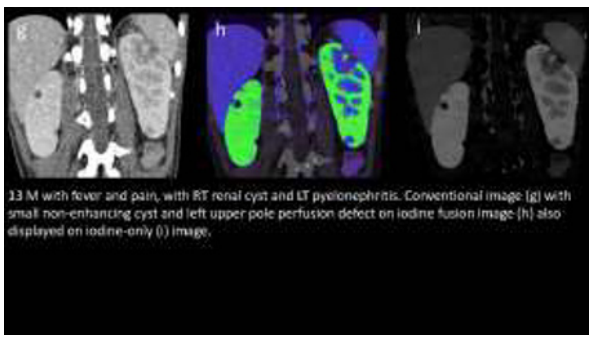

13 M with fever and pain, with RT renal cyst and LT pyelonephritis. Conventional image (g) with small non-enhancing cyst and left upper pole perfusion defect on iodine fusion image (h) also displayed on iodine-only (i) image.

Poster #: EDU-002

Unraveling the tangles: Ultrasound and Doppler in demystifying Congenital Hepatic Vascular Shunts

Komal Chughtai, MD[1], *komal_chughtai@urmc.rochester.edu*; David Saul[2], Apeksha Chaturvedi, MD[1]; [1]Imaging Sciences, University of Rochester Medical Center, Rochester, NY, [2]Children's Hospital of Philadelphia, Philadelphia, PA

Disclosures: All authors have disclosed no financial interests, arrangements or affiliations in the context of this activity.

Purpose or Case Report: Congenital hepatic vascular shunts occur secondary to abnormal formation and aberrant communication of blood vessels during fetal development. This spectrum of anomalies can be challenging to diagnose without a strong understanding of their embryology and clinical and imaging manifestations. Ultrasound is among the most widely used modalities in pediatric imaging, given its real-time nature, easy portability and lack of radiation exposure. This case-based exhibit reviews ultrasound and doppler imaging findings of congenital vascular shunts in the pediatric liver.
The broad categories of congenital hepatic vascular shunts include: arteriovenous (hepatic artery to hepatic vein), arterioportal (hepatic artery to portal vein), and portovenous (portal vein to hepatic vein). This exhibit starts by demonstrating the formation of normal hepatic vasculature during fetal development. This is followed by a discussion of embryological aberrations which lead to vascular shunts, clinical context of each anomaly (when to wait, worry or intervene), and the role of imaging in detection, quantification, prognostication and treatment of these anomalies.
There are case presentations and discussion of the following vascular anomalies: extrahepatic portosystemic shunt (also known as Abernethy Malformation), intrahepatic portosystemic shunt, arterioportal fistula, intrahepatic arteriovenous malformation, patent ductus venosus, infradiaphragmatic total anomalous pulmonary venous return, and hepatic hemangioma. Illustrations and ultrasound/Doppler images are included for most of these cases.
Besides providing a clinical and imaging review of anomalous hepatic vascular communications, this exhibit will reinforce an understanding of physiologic hepatic vascular shunts in fetal life and describe the sequence of successful transition to neonatal circulation. This understanding can be applied to clinical decision making.
Supplemental Files- legends:
1. File 1: Hepatic vascular shunts.
2. File 2: Portosystemic shunt. Turbulent flow within an aberrant vessel connecting left portal to left hepatic vein. Flow pulsatility/triphasicity within the portal vein.
3. File 3: Intrahepatic Arteriovenous Malformation. Tangle of enlarged vessels within left liver lobe. High velocity, low resistance arterial waveforms and pulsatile venous flow.

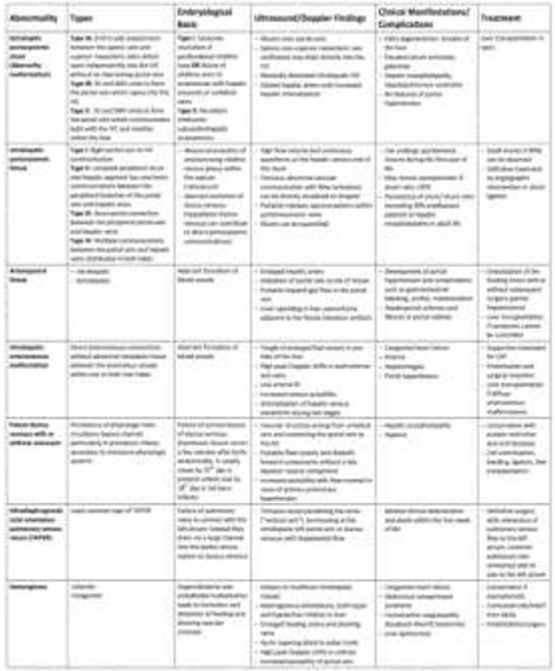

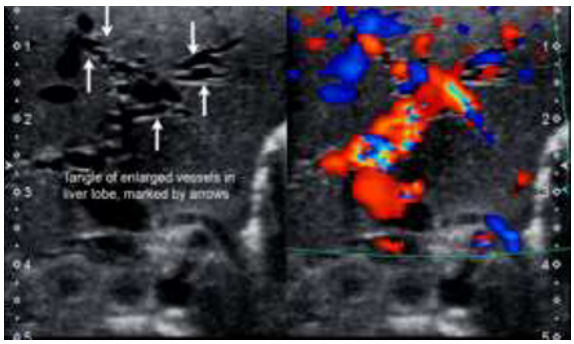

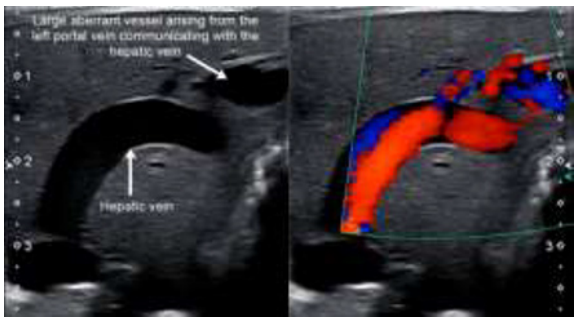

Poster #: EDU-003

Minimizing the Risk: Using the Feed and Wrap Method in Cardiac MR

Lindsay Griffin, MD[1], *lgriffin@uwhealth.org*; Christopher Francois, MD[1]; [1]Radiology, University of Wisconsin, Madison, WI

Disclosures: All authors have disclosed no financial interests, arrangements or affiliations in the context of this activity.

Purpose or Case Report: The purpose of this educational presentation is to review the feed and wrap method, also known as feed and sleep, swaddle, or bundle, as an alternative to deep sedation or general anesthesia through a pictorial review of

cardiac magnetic resonance (MR) studies performed using this method. The feed and wrap technique in which feeding and warmth are used to induce sleep and swaddling is used to reduce motion is described. Indications and contraindications as well risks and benefits of this method versus general anesthesia and deep sedation are discussed. Multiple examples of congenital heart disease including atrial and ventricular septal defects, atrioventricular canal defects, and double outlet right ventricle are provided, with sequences used, length of scan, and diagnostic quality also summarized. The example shown in Figures 1-3 is a 12-day-old female. The scan was completed in 12 minutes without intravenous contrast. Figure 1 is the scout image showing situs inversus. Figure 2 is a gated axial steady state free procession (SSFP) image showing a membranous ventricular septal defect (yellow arrow), an atrial septal defect (yellow arrowhead), and atrial inversion. Figure 3 is a 4D flow reconstruction showing the superior and inferior vena cava entering anatomic right atrium on the left, a right aortic arch with mirror branch pattern, and relationship to the main pulmonary artery (MPA).

Conclusions: After reviewing this educational exhibit, the reader will be able to implement the feed and wrap method as an alternative to general anesthesia or sedation in CT and MRI scans of infants. Examples are provided in cardiovascular imaging, of particular interest because the risk of adverse events under general anesthesia is higher in congenital heart disease patients and because of the complexity of disease being evaluated.

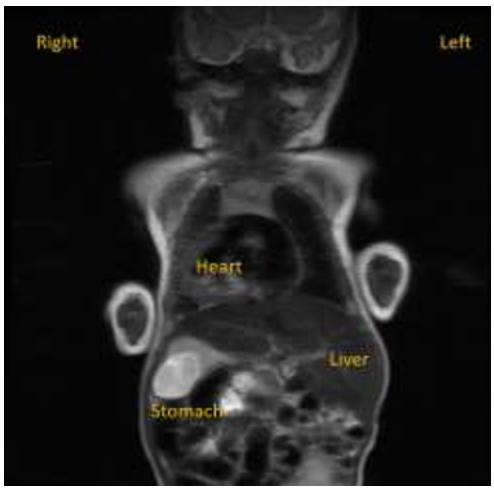

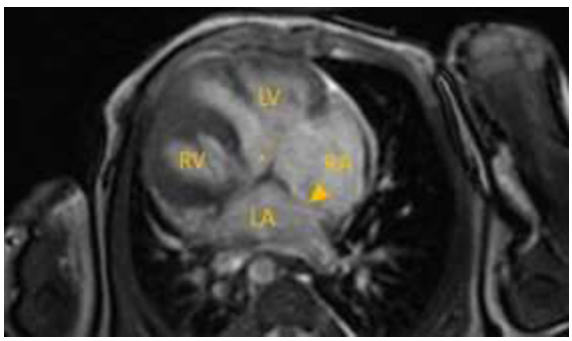

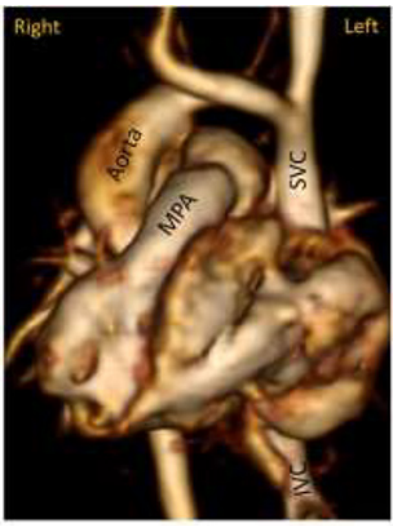

Poster #: EDU-004

Myocardial infarctions in young patients with congenital heart disease: Role of Cardiac MRI

Kathryn Henault, MD[1], *henaultk@gmail.com*; Shailendra Upadhyay, MD[2], Timothy Herbst[1], Michael O'Loughlin[1], Olga Toro-Salazar, MD[2]; [1]Hartford Hospital, Hartford, CT, [2]Connecticut Children's Hospital, Hartford, CT

Disclosures: All authors have disclosed no financial interests, arrangements or affiliations in the context of this activity.

Purpose or Case Report: CHD (congenital heart disease) occurs in approximately 1% of all live births with more than 90% survival into adulthood. Prevalence of coronary artery disease has been reported to be similar to general adult population. Patients with complex CHD may be subjected to non-atherosclerotic premature coronary artery disease due to anomalous coronaries, peri-coronary region interventions, or coronary re-implantation. Cardiac MRI (CMR) may provide valuable myocardium health information with pointers towards a coronary distribution in unsuspected chronic or acute cases. Acquisition of delayed enhancement sequences (LGE) and T1 mapping should be considered routine in CMR studies for assessment of interval ischemic events. Patients with complex CHD are also at risk for sudden cardiac arrest and LGE data may assist in further risk stratification of these patients. Three complex CHD patients who all suffered myocardial infarctions at a young age as a result of their multifaceted cardiac history are highlighted to illustrate the importance of this (see included table, Figure 1). Two CMR images (Figures 2,3) demonstrate delayed enhancement throughout the septum at the base to mid-cavity in a patient with truncus arteriosus type 1 who presented with a non-ST-elevation myocardial infarction (NSTEMI). Focal area of low-signal sub-endocaridum within the enhancement on Figure 3 favors microvascular obstruction.

CMR is a vital component of surgical planning and post-operative care of patients with CHD, providing accurate anatomical, functional, and flow information that assists in clinical management. Delayed enhancement sequences and post-gadolinium T1 mapping allow assessment of ischemic injury or infarct, and therefore should be considered part of routine follow up CMR studies in patients with complex CHD.

Patient	Diagnosis & Repair	Location of myocardial infarction/coronary distribution	Medical Context	Value added by cardiac MRI
1	**Tetralogy of Fallot:** s/p pulm. valve sparing repair in infancy	Thinning mural infarct at the basal inferior segment (posterior descending coronary artery distribution)	Transient hypotension on weaning off bypass at initial repair.	Potential for early recognition and intervention
2	**Tricuspid Atresia:** Palliated with mid-to-cardiac fontan	Severe systolic dysfunction, akinesis of mid-inferoseptal, inferior and lateral segments (corresponding transmural infarct on LGE)	Initial care in a foreign country	Myocardial scarring as evidenced by LGE for severe interval myocardial changes in complex CHD
3	**Truncus Arteriosus Type 1:** s/p right ventricle to pulmonary artery conduit repair/ replacements and mechanical aortic valve	Delayed enhancement in both the left anterior descending and posterior descending coronary artery distributions (likely embolic event from low INR)	Post sternotomy CT/Cerecyte requiring cardioversion - chest pain, troponin leak (NSTEMI)	Evaluation of acute intramural infarction in suspected low risk for CAD in CHD patients

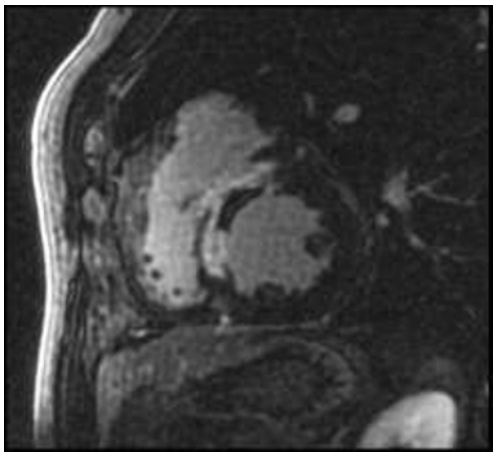

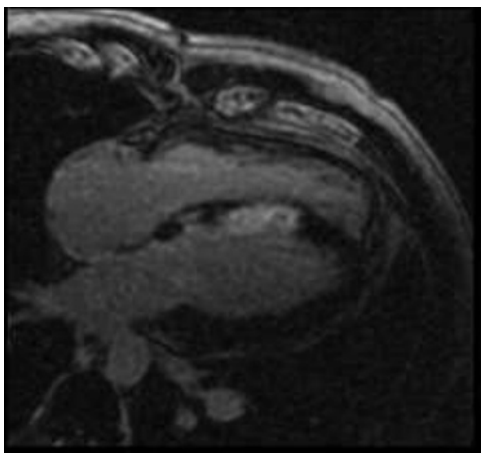

Poster #: EDU-005

Spectrum of imaging findings in Interruption of the Aortic Arch; what the Radiologist needs to know.

Signe Rebolledo, MD, MPH[1], *slrebolledo@uams.edu*; S Bruce Greenberg, MD[1], Karen Lyons, MB BCh BAO[1]; [1]Radiology, University of Arkansas for Medical Sciences, Little Rock, AR

Disclosures: All authors have disclosed no financial interests, arrangements or affiliations in the context of this activity.

Purpose or Case Report: The purpose of this educational presentation is to provide a pictorial review to promote recognition and understanding of the embryology, anatomy and spectrum of interruption of the aortic arch (IAA) in children.
Methods & Materials: Interruption of the aortic arch will be classified according to the the Celoria-Patton system. There are 3 main categories of IAA (A, B and C), which are defined by the location of the discontinuity. In addition to the three categories, there are 3 subtypes for each, for a total of nine types. Illustrative examples will be provided from clinical case material.
Results: Imaging findings will be reviewed, with an emphasis on CT/MR appearances, and discussion of important associated conditions and findings. Specific syndromes associated with IAA will be highlighted, and attention will be given to surgical intervention and post-operative imaging.
Conclusions: After reviewing this educational exhibit the reader will have a framework for recognizing and understanding IAA in the pediatric age group. They will have reviewed pre- and post-operative CT/MR imaging findings as well as the context and important associated findings.

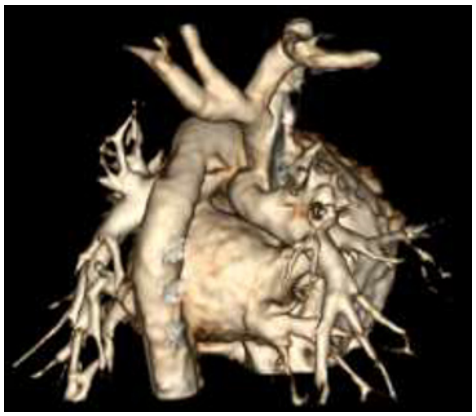

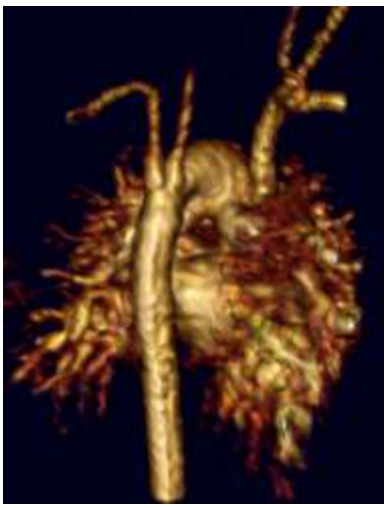

Poster #: EDU-006

Spectrum of abdominal aorta abnormalities in pediatric patients

Vandad Saadat, MD[1], *vandad.saadat@gmail.com*; Soni Chawla, MD[3], Johnathan Chen[2], Paul Iskander, MD[2], Shahnaz Ghahremani, MD[2]; [1]Internal Medicine, University of Miami, West Palm Beach, FL, [2]UCLA, Los Angeles, CA, [3]Olive View Medical Center, Los Angeles, CA

Disclosures: All authors have disclosed no financial interests, arrangements or affiliations in the context of this activity.

Purpose or Case Report: Awareness of abdominal aorta abnormalities in pediatric patients is essential for appropriate diagnosis and management of the patients suffering from these conditions. Due to a nonspecific presentation, and sometimes being asymptomatic earlier in life, imaging has an important role in diagnosis of these abnormalities. Aneurysm and dissection are excluded, as they are not specific to children and with few exceptions mostly present in older patients.
We review the clinical presentation and show imaging findings of mid aortic syndrome, Takayusu arteritis, rare entities such as idiopathic infantile arterial calcification. Also we show imaging of the anatomic variants of the distal aorta such as middle sacral artery, persistent sciatic artery, abdominal aorta coarctation and blind ending aorta, with a short review of embryologic development of abdominal aorta. These anomalies are not common, however if remain undiagnosed might have serious consequences.
-Midaortic syndrome is an uncommon disease with progressive narrowing of the abdominal aorta and its major branches, typically involving interrenal segment of the aorta; it affects mostly children and young adults, the cause is not clear, might be the result of an intrauterine insult to the intima and subintimal tissues. Aside from diagnosis, imaging has a major role in endovascular treatment of mid aortic syndrome.
-Takayusu arteritis, also predominantly involves aorta and its major branches of younger patients, with strong female predominance, and frequently found in Asian patients. Destruction of arterial medi leads to aneurysm formation and uncommonly rupture of the involved artery.
-Idiopathic infantile arterial calcification, a rare entity presenting with extensive calcification and stenosis of large and medium sized arteries, usually leads to early death from coronary artery occlusion.
-The aortoiliac variants are rare and not commonly discussed in the imaging literature. Some anomalies might be asymptomatic in young ages, but might complicate surgeries like heart, renal transplant, or hip surgery and increases the risk of morbidity and mortality. Some of these anomalies such as persistent sciatic artery need long term follow-up, given the possibility of aneurysmal degeneration.

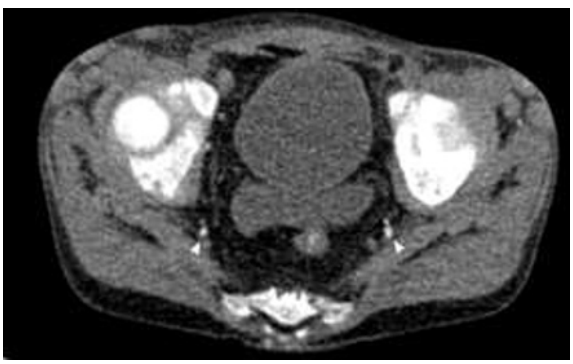

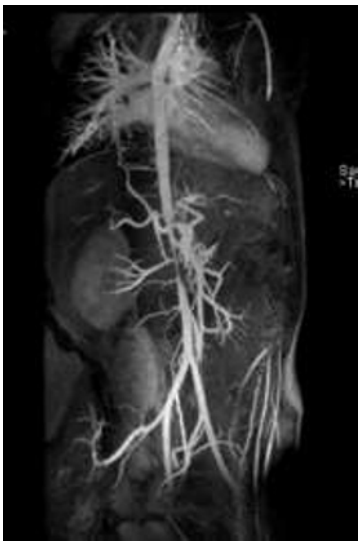

Poster #: EDU-007

Isolated unilateral absence of a pulmonary artery: imaging appearance from birth to adolescence

Jordan Rapp, MD[1], *jrapp24@gmail.com*; Erica Poletto, MD[2], Jaqueline Urbine[2], Archana Malik[2], Faaiza Kazmi[2], Mea Mallon[2]; [1]Children's Hospital of Philadelphia, Philadelphia, PA, [2]St. Christopher's Hospital for Children, Philadelphia, PA

Disclosures: All authors have disclosed no financial interests, arrangements or affiliations in the context of this activity.

Purpose or Case Report: The rare entity of an absent pulmonary artery has appeared in the literature since 1868, with most cases associated with congenital heart disease of various types. It has also long been observed that the absent pulmonary artery is contralateral to the aortic arch in almost every case. Isolated absence of a single pulmonary artery without associated congenital heart disease is less common, and these patients may present at any time from prenatal screening, neonatal period, early childhood, or even adolescence and adulthood. We will discuss the embryologic origins, clinical presentations, expected imaging findings, and treatment options based on patient ages from newborn to adolescence.
In neonates with an isolated absent pulmonary artery, a patent ductus arteriosus will allow for continued systemic blood supply. Even early on, narrowing of the PDA may be seen as involution is inevitable without intervention. The lung parenchyma is typically preserved, without yet evidence of hypoplasia or oligemia. Once the PDA has closed, robust collateral formation will occur. As patients age without repair, the lung parenchyma may become hypoplastic with diminished lung volumes and vascular markings. Findings suggestive of recurrent infection such as bronchiectasis may also be evident.
Early discovery and treatment is ideal as this will allow for prevention of long term sequelae and the greatest restoration of lung function as the options for repair are limited in the older

patient. There is no universal standard approach for repairing the underlying mechanism of providing blood flow to the intrapulmonary pulmonary artery. Early intervention in neonates included PDA stenting or anastomosing the main pulmonary artery with the intrapulmonary pulmonary artery using a synthetic graft. Patients that present after the neonatal period are not likely to be eligible for surgical repair. The most common long term effect of an absent pulmonary artery is pulmonary hypertension, seen in 40% of patients.
The entity of isolated unilateral absence of a pulmonary artery is rare, however demonstrates typical cardiothoracic findings depending on age at presentation. Understanding of embryology, specifically the 4th and 6th primitive aortic arches, allows one to understand why this malformation occurred and what findings to expect on imaging. The maintained PDA is vital for early lung blood supply and development and can aid in repair.

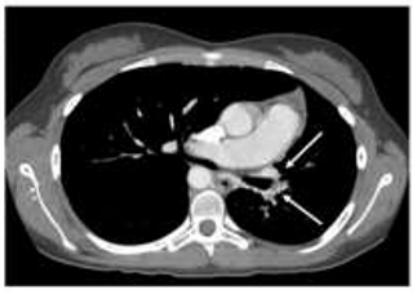

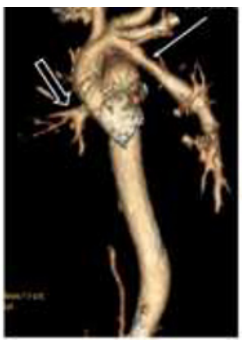

Poster #: EDU-008

Surgically Created Cardiac Shunts

Amy Farkas, MD[1], *afarkas@umc.edu*; Candace Howard-Claudio[1]; [1]Department of Radiology, University of Mississippi Medical Center, Jackson, MS

Disclosures: All authors have disclosed no financial interests, arrangements or affiliations in the context of this activity.

Purpose or Case Report: Congenital heart diseases alter the normal flow of blood through the heart. Conditions range in severity, from those that may simply require routine monitoring, to devastating lesions whose natural history is fatal. These complex conditions often require complicated surgically created cardiac shunts as treatment. Various diseases are often managed with the same procedure, with the goal of altering the abnormal hemodynamics. These surgeries may attempt to repair the lesion and restore normal physiology, or palliate the lesion as a bridge to future treatment including transplantation.
This electronic poster provides a case based review of surgically created cardiac shunts. Cases include patients who have undergone bidirectional Glenn, Fontan completion, Rastelli, and Norwood procedures and the Blalock-Taussig shunt. The poster will review the congenital heart abnormalities corrected by these procedures and the anatomy of the shunts on CT and MRI.

Poster #: EDU-009

Presurgical Evaluation of Congenital Heart Disease with CT Angiography: An Educational Guide for Pediatric Radiologists

Candace Scace[1] *candace.scace@gmail.com*; [1]Children's Hospital of Philadelphia, Philadelphia, PA

Disclosures: All authors have disclosed no financial interests, arrangements or affiliations in the context of this activity.

Purpose or Case Report: To provide a working knowledge of normal cardiac anatomy and a systematic guide to findings in common and uncommon congenital heart disease as seen on cardiac CTA.
Methods & Materials: A retrospective review of congenital cardiac anomalies was performed. A series of cardiac CT angiography cases with identified presurgical congenital heart disease was collected for review and presentation.
Results: Cardiac CTA findings and distinguishing imaging features of atrial and ventricular septal defect, coarctation of the aorta, transposition of the great vessels, double aortic arch, hypoplastic left heart, tetralogy of fallot, truncus arteriosus, anomalous coronary arteries and total anomalous pulmonary venous return are discussed.
Conclusions: This educational exhibit increases pediatric radiologists and trainees exposure to basic pediatric cardiovascular imaging and provides a basic framework for identification and interpretation of cardiac and extracardiac CT angiographic findings of congenital heart disease.

Poster #: EDU-010

Fetal cardiac MR imaging of congenital cardiovascular anomalies

Su-Zhen Dong, Medical PhD[1] *dongsuzhen@126.com*; [1]Radiology, Shanghai Children's Medical Center, Shanghai Jiaotong University School of Medicine, Shanghai, China

Disclosures: All authors have disclosed no financial interests, arrangements or affiliations in the context of this activity.

Purpose or Case Report: 1. Review the safety, limitations and advantages of fetal cardiac MR (CMR)
2. Discuss potentialindications of fetal CMR
3. Describe the technique of fetal CMR, including imaging sequences, imaging planes, the method of overcoming motion artifact
4. Illustrate the appearance of normal fetal cardiac structures and present a modified anatomic
segmental approach of congenital heart disease (CHD) at prenatal CMR
5. Demonstrate examples of fetal CMR in the evaluation of various cardiovascular anomalies
Methods & Materials: 924 pregnant women were referred to a children's hospital for a fetal CMR from January 2006 to June 2017, 638 due to the finding of a cardiovascular anomaly by echocardiogram (echo) and 286 due to technically limited echo, but thought to likely be normal. Studies were performed after 20 weeks gestation. Fetal CMR was performed at 1.5 T or 3.0 T (Discovery 750; GE Medical
Systems). Sequences included steady-state free-precession (SSFP), non gated SSFP cine, single-shot turbo spin echo (SSTSE) and non-gatedphase contrast (PC) cinesequences. Optimal imaging included transverse view of the fetal thorax, the

four-chamber, short-axis, coronal and oblique sagittal planes of the fetal heart. Follow up postnatal diagnoses were confirmed by postnatal imaging, surgery and/or autopsy.
Results: Examples of Fetal cardiac MRI cases will be presented. In 638 cases with anomalies, Obstetric US were correct in 46.9% (299/638), fetal echos were correct in 83.2% (531/638), CMR were correct in 82.1% (524/638) when compared to postnatal findings. Fetal echoes had a higher specificity for evaluating ventricular size, septal defects and valve anomalies. CMR was more useful in evaluating extracardiac aortic arch, superior vena cava and malposition anomalies,heart diverticulum, pericardium cyst. CMR was technically limited in 9 cases due to polyhydramnios.
In 286 cases, CMR performed due to technically inadequateechocardiography (maternal obesity, maternal abdominal wall edema, oligohydramnios, fetal position, twins, et al), had follow up. All of these cases were interpreted as normalby CMR and confirmed at FU.
Key point of scan technique includeSSFP sequence with overlapping slice, improving the artifacts is SSFP with radial k-space sampling.
Conclusions: While Fetal echo is the first choice in the evaluation of fetal cardiovascular anomalies; fetal CMR may be a useful adjunct particularly when echocardiography is limited.

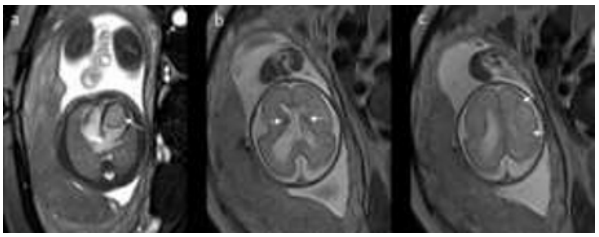

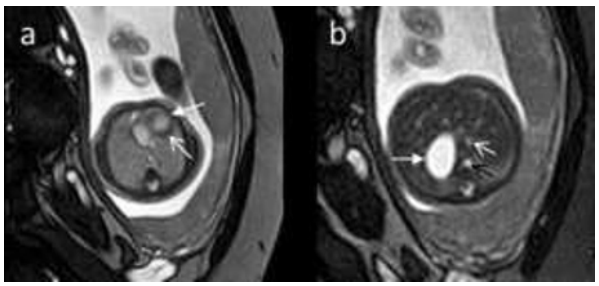

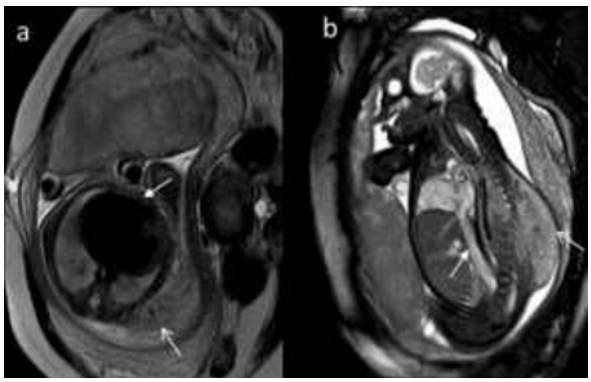

Poster #: EDU-011 - *Withdrawn*

Poster #: EDU-012

Below Deck: The Fetal Posterior fossa in Health and Disease

Matthew Whitehead, MD[1], *matthewthomaswhitehead@gmail.com*; Bonmyong Lee, MD[2]; [1]Neuroradiology, Children's National Medical Center, Washington, DC, [2]Johns Hopkins Medical Institute, Baltimore, MD

Disclosures: All authors have disclosed no financial interests, arrangements or affiliations in the context of this activity.

Purpose or Case Report: The posterior fossa houses the brainstem and cerebellum. These vital and complex parenchymal structures contain many important white matter tracts, nuclei, and neurons responsible for both basic fundamental and higher-level functions. A number of disease processes can interfere with rhombencephalic development, including genetic malformations and disruption such as hypoxia, toxins, infections, trauma, and vascular disorders. Structural changes associated with fetal imaging pathology that deviate from the normal gestational-age specific developmental patterns can define the etiology, improve our understanding of the disease, and help with prognostication. A comprehension of basic embryology and developmental anatomy is necessary to achieve a true understanding of posterior fossa anomalies and normal variants. In this exhibit, we aim to illustrate common and rare anomalies of the brainstem, cerebellum, meninges, and meningeal spaces visible on fetal MRI, presented in a temporal manner based on the embryologic development of the posterior fossa.
Methods & Materials: Fetal MRI and correlative fetal ultrasound and post-natal images with didactic value will be procured from the teaching file of a pediatric medical center in order to demonstrate developmental anatomy and posterior fossa pathology.
Results: Normal anatomy of the posterior fossa in various stages of developement will be shown and contrasted against the following entiites:
1. Cysts:
a. Blake pouch
b. Arachnoid duplication
c. Fibrous arachnoid
2. Insutls:
a. hemorrhage/infarction
b. Sinus thrombosis
c. Infection
3. Malformations:
a. Chiari II
b. Walker-Warburg syndrome
c. Diencephalic-mesencephalic junction malformation
d. Rhombencephalosynapsis
e. Dandy-Walker malformation
f. Joubert syndrome
g. Pontocerebellar hypoplasia
4. Tumor
Conclusions: Posterior fossa anomalies are common indications for fetal MRI. Most can be diagnosed and classified by appearance. Prognosis ultimately depends on type and presence or absence of additional abnormalities.

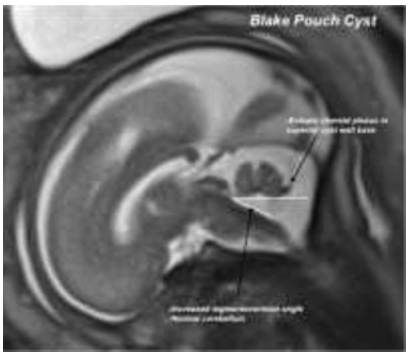

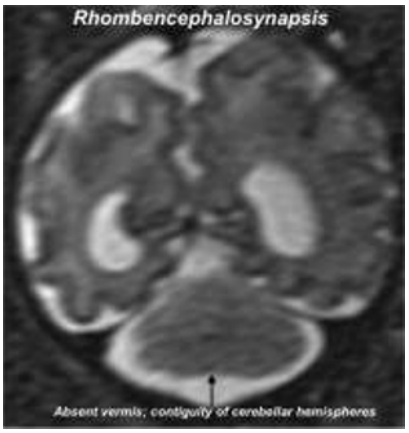

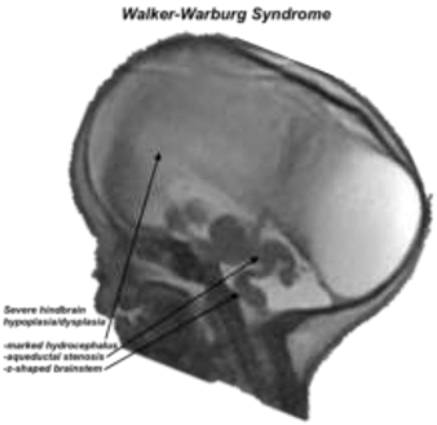

Poster #: EDU-013

Genitourinary Abnormalities on Fetal MRI: An Overview of Pathology, Embryology, and Clinical Implications

Amy Farkas, MD[1], *afarkas@umc.edu*; Manohar Roda[1]; [1]Department of Radiology, University of Mississippi Medical Center, Jackson, MS

Disclosures: All authors have disclosed no financial interests, arrangements or affiliations in the context of this activity.

Purpose or Case Report: Genitourinary abnormalities are frequently detected on prenatal ultrasound, with findings detected on 1 in 500 routine prenatal sonograms. Early detection of abnormalities of the genitourinary system is essential as it allows planning for further work-up and intervention and appropriate counseling of parents. Findings on prenatal ultrasound often trigger further evaluation with fetal MRI, as MRI can provide superior anatomic detail and better assess for associated findings. An understanding of the appearance of genitourinary abnormalities on fetal MRI is important to enable accurate diagnoses and effectively guide clinicians in patient management.

This educational poster highlights fetal MRI cases that demonstrate genitourinary abnormalities including bilateral renal agenesis with Potter sequence, crossed fused renal ectopia, multicystic dysplastic kidney, duplex collecting system, posterior urethral valves, patent urachus, allantoic cyst, prune belly syndrome, congenital megaureter, cloaca, bladder exstrophy, ureteropelvic junction obstruction, horseshoe kidney, and sirenomelia.

The goal of this exhibit is to provide familiarity with these findings and their clinical implications, which is particularly important for those with less fetal MRI experience. In addition, the exhibit will provide an overview of the embryology of the genitourinary system as it relates to the abnormalities to provide further context of the pathophysiology of these complex congenital conditions.

Poster #: EDU-014

Absence of the ductus venosus and the expected but abnormal course of umbilical venous lines.

Ryan Blagdon, MD, MSc[1], *ryanbla@gmail.com*; Deborah Thompson, MD[1], Pierre Schmit, MD[1]; [1]Dalhousie University and IWK Health Centre, Halifax, NS, Canada

Disclosures: All authors have disclosed no financial interests, arrangements or affiliations in the context of this activity.

Purpose or Case Report: The ductus venosus is a part of the fetal circulation that permits oxygenated blood in the umbilical vein to bypass the liver and provide oxygenated blood to the fetal brain and heart. Absence of the ductus venosus is a rare anomaly associated with a number of serious, life-threatening and often deadly conditions. Studies have evaluated the use of ultrasound for prenatal evaluation and detection of absent ductus venosus; however, no studies have reported non-ultrasound postnatal radiological findings of absent ductus venosus. Here, we describe the expected anatomy in those with absent ductus venosus and present abdominal x-rays of 3 infants to illustrate an expected but abnormal course of umbilical venous lines in these patients. As many as 15.6% of patients with absent ductus venosus have it in isolation and with 67-100% postnatal survival when occurring in isolation. Thus, the postnatal incidental identification of absent ductus venosus is a clinical possibility for pediatric radiologists that review abdominal x-rays to check catheter/line placement. Familiarity with this abnormal course of umbilical venous lines may assist in making this rare postnatal diagnosis and avoid potentially life-threatening complications secondary to line malposition/repositioning.

Poster #: EDU-015

Correlation of Congenital Cardiopulmonary Abnormalities on Fetal MRI with Prenatal Ultrasound

Amy Farkas, MD[1], *afarkas@umc.edu*; Manohar Roda[1]; [1]Department of Radiology, University of Mississippi Medical Center, Jackson, MS

Disclosures: All authors have disclosed no financial interests, arrangements or affiliations in the context of this activity.

Purpose or Case Report: As an inexpensive modality that does not require ionizing radiation, ultrasound is the preferred method for screening for fetal anomalies. When an abnormality is detected on ultrasound, the limitations of the modality often

elicit further evaluation with MRI, as MRI can provide more detail and information to the radiologist and clinician. Chest and cardiac pathologies are among the most common findings on prenatal ultrasound and often warrant additional imaging. Consequently, an understanding of these findings and how they appear on different modalities is essential to the pediatric imager. This electronic exhibit features fetal ultrasound and MRI of mediastinal lymphangioma, type I-III congenital pulmonary airway malformations, intralobar, extralobar, and subdiaphragmatic sequestrations, left and right sided congenital diaphragmatic hernias, hypoplastic left heart, heterotaxy, AV canal defect, and rhabdomyoma. In addition to reviewing the correlation of findings on ultrasound and MRI, prognosis as well as conditions and syndromes commonly associated with these chest and cardiac anomalies will be examined.
The goal of this exhibit is to provide an overview of common fetal cardiopulmonary abnormalities on different, complementary imaging modalities. Familiarity with these conditions is necessary for the radiologist to provide critical information to clinicians to allow prompt intervention in the postnatal period. These findings can additionally serve as an indication to the radiologist to search for associated findings, allowing prognostication and appropriate counseling of parents.

Poster #: EDU-016

The Many Faces of Omphalocele: A Practical Guide to Fetal MRI Evaluation

Katharyn Cassella, MS[2], *kdowns034@marian.edu*; Brandon Brown, MD, MA[1]; [1]Radiology and Imaging Sciences, Indiana University School of Medicine, Indianapolis, IN, [2]Marian University College of Osteopathic Medicine, Indianapolis, IN

Disclosures: All authors have disclosed no financial interests, arrangements or affiliations in the context of this activity.

Purpose or Case Report: With the increasing utilization of imaging in prenatal diagnosis, the fetal MR appearance of omphalocele has been well-described. However, as fetal MR plays a critical role not only for diagnosis but also for planning and family counseling, the radiologist is required to risk stratify the range of presentations of this anomaly. There is a broad spectrum of severity within this single diagnosis: ranging from a small and covered bowel-only defect, to a large and ruptured multi-organ hernia, to a complex omphalocele within a nonkaryotype fetal syndrome. Outcomes are highly variable, ranging from a simple hernia repaired with primary closure, to a protracted postnatal course with staged surgical repairs, to expected intrapartum demise. Further, neonatal pulmonary hypoplasia and hypertension often complicate more severe cases. Thus, accurate prognostication is essential to properly equip and prepare families, and thereby add value to perinatal care.
In this presentation, we outline a 7-point, systematic method for analyzing the varied presentations of omphalocele, as seen on both 1.5T and 3T MR field strengths. The approach we describe details the following diagnostic criteria: (1) the size of the defect, (2) type and volume of herniated organ contents, (3) presence/absence of an intact membrane, (4) presence/absence of hernia sac ascites, (5) associated pulmonary hypoplasia, (6) insertion of the umbilical cord, and (7) presence of irregular cord vessels. Finally, we demonstrate how this diagnosis can correlate with associated ischemic changes in the placenta, a finding which can further aid delivery planning and prognostication.

Poster #: EDU-017

Spectrum of IgG4 related diseases: A growing novel concept

Sarv Priya, MD[1], *sarv-priya@uiowa.edu*; Atsuhiko Handa[1], Renato Ferreira da Silva, MD[1], Lillian Lai, MD[2], Geetika Khanna[3], T. Shawn Sato[1]; [1]University of Iowa Hospitals & Clinics, Iowa City, IA, [2]Children's Hospital of Los Angeles, Los Angeles, CA, [3]Mallinckrodt Institute of Radiology, St. Louis, MO

Disclosures: All authors have disclosed no financial interests, arrangements or affiliations in the context of this activity.

Purpose or Case Report: Immunoglobulin4 related disease (IgG4RD) is an inflammatory condition involving multiple regions of the body resulting in fibrosis which can lead to eventual organ failure. This entity was originally described with autoimmune pancreatitis. Recently many other previously described lesions have been brought under the umbrella of IgG4RD. These include a spectrum of conditions involving the head and neck region (orbits, salivary and lacrimal glands), thyroid gland (Riedel's thyroiditis), vasculature (periaortitis), kidneys, lungs, retroperitoneum, mesentery, pituitary gland, biliary tract, pericardium, lymph nodes and pachymeninges. Reports of IgG4RD are quite rare in the pediatric literature, however this may be due to potential unawareness about the condition as well as the variable presentations and non-specific imaging features of IgG4RD. The prevalence in pediatric population is poorly described.
The exact pathophysiology of IgG4RD is yet to be completely elucidated. The imaging manifestations are non-specific, and primarily consist of tumefactive enlargement of involved organs and homogenous contrast enhancement and associated lymphadenopathy. IgG4RD may manifest in single organ or may present as widespread disease involving multiple organs. These features overlap with other mass forming conditions like malignancy or lymphoma. However, the presence of multifocal disease with more than one organ involvement may point towards possible IgG4 related disease. Other than IgG4 related autoimmune pancreatitis, there is no consensus on diagnostic criteria based upon imaging. Definitive diagnosis of IgG4RD is made with biopsy and the histology characterized by infiltration of lymphocytes and IgG4 plasma cells with storiform fibrosis and obliterative phlebitis. According to Boston consensus, the ratio of IgG4 /IgG in tissue should be more than 0.4 with more than 10 IgG4+ cells per high power field. Serum IgG4 levels range from normal to elevated. Steroids are effective as first line treatment in majority of patients.
Our aim in this presentation is to familiarize radiologists with the spectrum of imaging features, and areas of involvement in IgG4 related disease using cases of IgG4RD collected at three different pediatric hospitals. It is important for pediatric radiologists to be familiar with this relatively newly described disease entity and be aware of the spectrum of manifestations of IgG4RD, ensuring prompt recognition and early treatment.

Poster #: EDU-018

Taking "AIM" at bowel obstruction in children and infants: Not always the usual culprits

Adam Goldman-Yassen[1], *adgoldmanyassen@gmail.com*; Jessica Kurian, MD[1], Einat Blumfield[1], Terry Levin, MD[1]; [1]Montefiore Medical Center, Bronx, NY

Disclosures: All authors have disclosed no financial interests, arrangements or affiliations in the context of this activity.

Purpose or Case Report: Common causes of bowel obstruction (BO) in infants and children include appendicitis, adhesions, intussusception, inguinal hernia, midgut volvulus, and Meckel's diverticulum, for which the mnemonic "AIM" is used. We present uncommon causes of BO in infants and children and review the clinical presentation, imaging findings, and surgical diagnoses.
Methods & Materials: The hospital database was searched for cases of BO in infants and children under age 10 years during the years 2013-2017, excluding appendicitis, post-surgical adhesions, intussusception, inguinal hernia, midgut volvulus, and Meckel's diverticulum. Patient age, comorbidities, clinical presentation (including duration of symptoms), imaging findings, and surgical diagnoses were reviewed.
Results: Nine uncommon causes of BO were identified and included cecal volvulus (2 cases), primary midgut volvulus with normal bowel fixation (1 case), isolated ileal volvulus (1 case), congenital bands (2 cases), internal hernia (1 case), and radiolucent foreign bodies (2 cases). Patients ranged in age from 10 weeks to 11 years. Symptom duration was variable. Underlying comorbidities were present in 2 cases (Down's syndrome and Cornelia de Lange syndrome). Plain abdominal radiographs were available in all cases. Four patients underwent computed tomography, 2 patients underwent upper gastrointestinal series, and 1 underwent a contrast enema. Abdominal radiographs in cecal volvulus demonstrated right sided and midline colonic distension. In both the case of closed-loop obstruction with bands and primary volvulus, abdominal films demonstrated a midline mass containing air and displacing the colon laterally. The remainder of cases presented with dilated stacked small bowel loops indistinguishable from other causes of small bowel obstruction. Plain film findings of pneumatosis mimicking necrotizing enterocolitis (NEC) were present in an infant with isolated ileal volvulus. CT was the imaging modality most likely to aid in diagnosis but did not affect management. All patients underwent emergent surgery.
Conclusions: We discuss the unusual and often confusing imaging findings in uncommon causes of BO in infants and children. In some cases, radiographs mimic NEC, resulting in diagnostic delay. Awareness of characteristic plain films findings, such as those seen in cecal volvulus, may aid in diagnosis. In acutely ill patients, additional imaging may delay prompt surgical intervention.

Poster #: EDU-019

Stump Appendicitis

Alex Essenmacher, MD[1], *alex-essenmacher@uiowa.edu*; Simon Kao[1], T. Shawn Sato, MD[1]; [1]University of Iowa Hospitals and Clinics, Iowa City, IA

Disclosures: All authors have disclosed no financial interests, arrangements or affiliations in the context of this activity.

Purpose or Case Report: The management of acute appendicitis is most often surgical with appendectomy; the blind-ending, inflamed appendix is removed, usually laparoscopically. There is growing awareness of the potential for a delayed complication if only the tip or otherwise subtotal length is removed. A remnant portion of the base of the appendix, referred to as a stump, if long enough can become obstructed and symptomatic similar to the etiology of acute appendicitis. In cases of recurrent right lower quadrant pain in a patient with a surgical history of appendectomy, appendicitis remains on the differential diagnosis alongside non-appendiceal causes such a colitis and epiploic appendagitis. Imaging diagnosis by computed tomography or ultrasound of stump appendicitis is similar to acute appendicitis with right lower quadrant inflammation and stump distension and wall thickening. In this educational exhibit we will review the imaging features of stump appendicitis as well as developments in surgical techniques relevant to this delayed complication. Relevant anatomy and differential diagnosis for right lower quadrant pain will also be summarized.

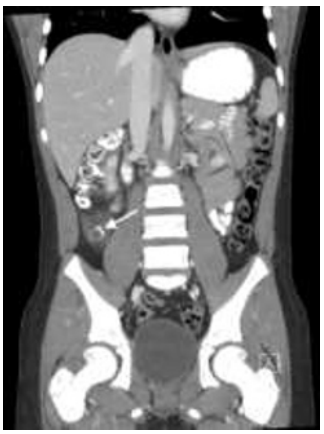

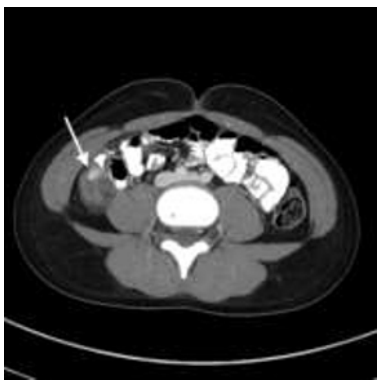

Poster #: EDU-020: ***Withdrawn***

Poster #: EDU-021

Disappearing Abdominal or Pelvic Masses in neonates, infants and young children: what a radiologist should know.

Daddy Mata-Mbemba, MD, PhD[1], *matadaddy@yahoo.fr*; Alan Daneman[1]; [1]Diagnostic Imaging, The Hospital For Sick Children, Toronto, ON, Canada

Disclosures: All authors have disclosed no financial interests, arrangements or affiliations in the context of this activity.

Purpose or Case Report: There are a variety of masses in neonates, infants and young children that may disappear spontaneously without active intervention. However, there has been no published review of what type of masses could disappear and what the spectrum of their imaging features is. It is essential for radiologists to understand imaging features of these entities in order to provide pediatrician and pediatric surgeons with critical information that will enable them to manage these patients expectantly without surgical intervention.
The entities that will be illustrate in this review include, among others: multicystic dysplastic kidneys, suprarenal masses (including intraabdominal sequestration, neuroblastoma and adrenal hemorrhage), ovarian cyst and torsion, duplication cyst of gastrointestinal tract, cyst of liver and kidneys.

We will:
1. Review the clinical and imaging features of these masses including their changes during follow-up imaging studies.
2. Emphasize the imaging features that are helpful in differentiating these entities from other entities that require active intervention
3. Describe an appropriate approach to deal with uncertain diagnoses.

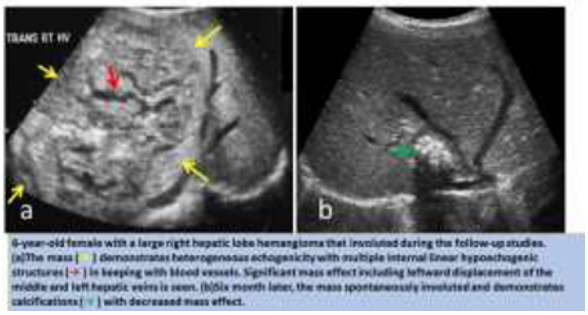

6-year-old female with a large right hepatic lobe hemangioma that involuted during the follow-up studies. (a)The mass ( ) demonstrates heterogeneous echogenicity with multiple internal linear hyperechogenic structures ( ) in keeping with blood vessels. Significant mass effect including leftward displacement of the middle and left hepatic veins is seen. (b)Six month later, the mass spontaneously involuted and demonstrates calcifications ( ) with decreased mass effect.

(a) 3-day-old female with complex solid/cystic right adnexal mass lesion ( ) in keeping with antenatal torsion of ovary. (b) At 3 month follow-up study, the mass ( ) which is seen adjacent to the bladder has spontaneously shrunken and calcified ( ).

Poster #: EDU-022

Blastomas- Head to Toe- A Comprehensive Review

Dhanashree Rajderkar, MD[1], *drdhana1@gmail.com*; Ameya Baxi[2], Carolyn Hanna[1], Priya Sharma, MD[1]; [1]University of Florida, Gainesville, FL, [2]UT Health, San Antonio, TX

Disclosures: Dhanashree Rajderkar has indicated a relationship with the Association for Medical Imaging Management and Toshiba Medical for receiving a research grant. Priya Sharma has indicated a relationship with the Association for Medical Imaging Management and Toshiba Medical for receiving a research grant. All other authors have disclosed no financial interests, arrangements or affiliations in the context of this activity.

Purpose or Case Report: In this educational exhibit we plan:
1. To identify and illustrate the spectrum of blastomas on various imaging modalities
2. To review the pathogenesis of these tumors
3. To describe and illustrate the typical and atypical imaging appearances and organ-wise differential diagnosis

Methods & Materials: Blastomas are rare childhood tumors that can affect any organ system in the body and at times can be devastating if left untreated. Controversy surrounds their nomenclature and there is no globally accepted classification. They are thought to arise from immature, primitive tissues with persistent embryonal elements on histology. These tumors affect a younger population and are usually malignant. Imaging is often non-specific but plays an important role in identification, management and follow-up. In this exhibit, we discuss the characteristic imaging features and pathogenesis of select blastomas.

Results: We will review the classification, pathogenesis and imaging features of the following lesions:
Ameloblastoma
Hamartoblastoma
Ganglioneuroblastoma
Neuroblastoma
Nephroblastoma
Hepatoblastoma
Medulloblastoma
Lipoblastoma
Osteoblastoma
Chondroblastoma
Hemangioblastoma
Gonadoblastoma
Sialoblastoma
Pleuropulmonary blastoma
Pancreatoblastoma
Pineoblastoma
Medullomyoblastoma

Conclusions: Blastomas are rare neoplasms and may have non-specific imaging appearances. They differ in epidemiology, clinical outcome, and prognosis. A high degree of clinical suspicion and familiarity with the various radiologic manifestations of blastomas allow early diagnosis and timely initiation of appropriate therapy, thereby reducing patient morbidity.

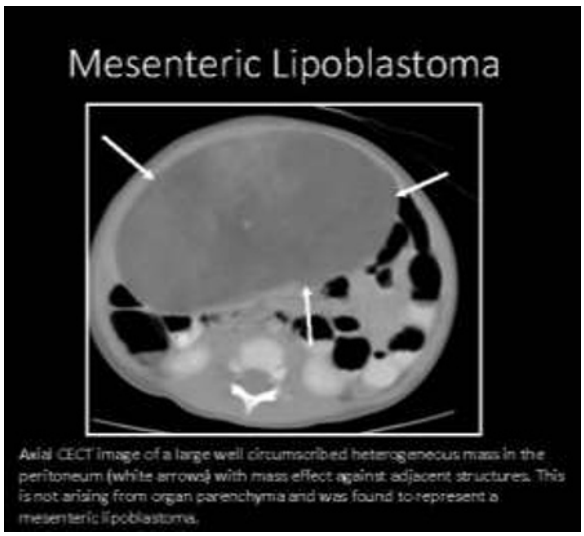

Axial CECT image of a large well circumscribed heterogeneous mass in the peritoneum (white arrows) with mass effect against adjacent structures. This is not arising from organ parenchyma and was found to represent a mesenteric lipoblastoma.

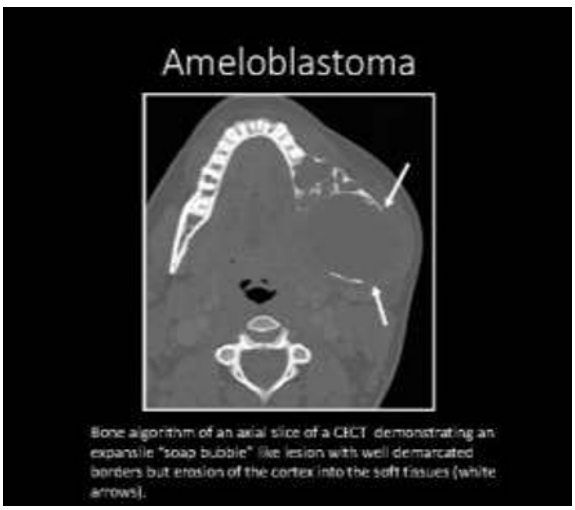

Bone algorithm of an axial slice of a CECT demonstrating an expansile "soap bubble" like lesion with well demarcated borders but erosion of the cortex into the soft tissues (white arrows).

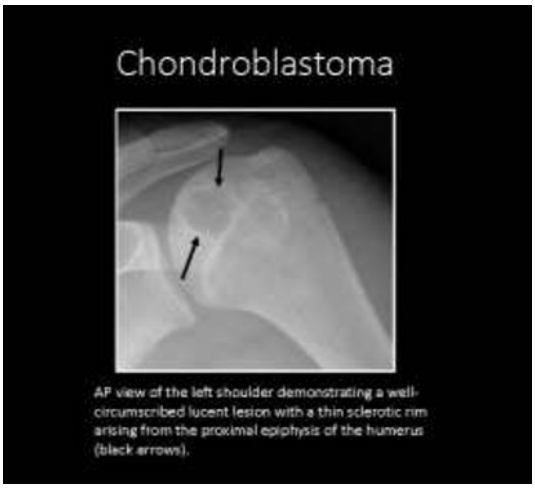

Poster #: EDU-023

Baby Bellies Gone Bad on Film: Imaging and Approach to Neonatal Gastrointestinal Emergencies.

Joseph Uricchio, MD[1], *joemuricchio@gmail.com*; Priya Sharma, MD[1], Dhanashree Rajderkar, MD[1]; [1]Radiology, University of Florida, Gainesville, FL

Disclosures: Priya Sharma has indicated a relationship with the Association for Medical Imaging Management and Toshiba Medical for receiving a research grant. Dhanashree Rajderkar has indicated a relationship with the Association for Medical Imaging Management and Toshiba Medical for receiving a research grant. All other authors have disclosed no financial interests, arrangements or affiliations in the context of this activity.

Purpose or Case Report: In this educational exhibit we will present a series of gastrointestinal (GI) emergencies encountered in the neonatal period. We will focus on typical presentations but will also include atypical cases and discuss multi-modality approach to imaging these patients.
Methods & Materials: GI emergencies are unfortunately a mainstay in the neonatal intensive care unit. Accurately diagnosing these potentially catastrophic disease processes is of paramount importance. Given that history and physical is extremely limited, accurately diagnosing neonatal GI emergencies can be quite the challenge often requiring the assistance of the radiology through x-rays and subsequent confirmatory fluoroscopic examinations, ultrasound or less commonly, computed tomography (CT) or magnetic resonance imaging (MRI). Since early diagnosis is associated with a substantially better outcome, imaging is essential in forming the proper management plan for these patients.
Results: We will use a case based approach to discuss the following neonatal emergencies of the gastrointestinal tract:
Malrotation
Duodenal atresia
Duodenal web
Jejunal or ilieal atresia
Meconium ileus
Meconium plug syndrome
Hirschsprung's disease
Necrotizing enterocolitis
Intestinal perforation
Meconium peritonitis and complications
Conclusions: Neonatal GI emergencies are all too common and remain associated with a high mortality and morbidity. Early diagnosis via knowledge of the classic as well as atypical radiographic findings combined with confirmatory tests can result in prompt diagnosis and management of these potential catastrophic events in the neonate.

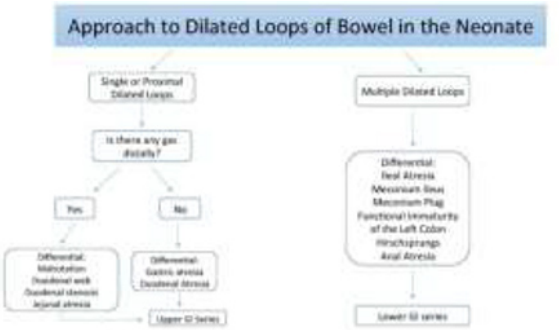

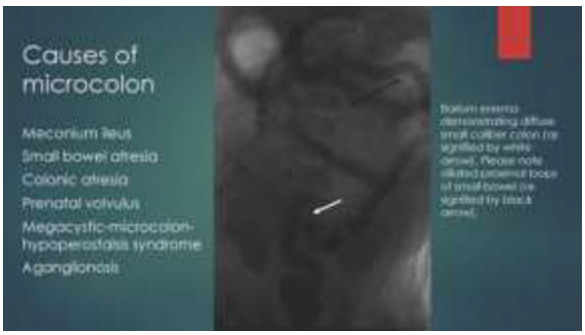

Poster #: EDU-024

Extra-intestinal Manifestations of Pediatric Inflammatory Bowel Disease

Hena Joshi[1], *hjoshi2@emory.edu*; Adina Alazraki, MD[1], Bradley Rostad, MD[1]; [1]Emory University, Atlanta, GA

Disclosures: All authors have disclosed no financial interests, arrangements or affiliations in the context of this activity.

Purpose or Case Report: Ulcerative colitis (UC) and Crohn disease are chronic, immune-mediated, inflammatory disorders of the gastrointestinal tract collectively referred to as inflammatory bowel disease (IBD). As many of 20-25% of patients with IBD initially present in childhood or adolescence, and the incidence of pediatric IBD is increasing. IBD primarily affects the bowel, but other organs can be involved. Nearly one-third of patients will have at least one extra-intestinal manifestation. Some extra-intestinal manifestations, such as that between UC and primary sclerosing cholangitis (PSC), are well-established. Others are less understood and may mimic more common pathology, particularly infection. Therefore, pediatric radiologists must become familiar with these extra-intestinal

manifestations and consider the diagnosis of IBD as the etiology for their pathology.
Methods & Materials: A case review of the imaging features of some common and uncommon extra-intestinal manifestations of pediatric IBD will be presented. A brief overview of pediatric IBD, its pathophysiology, clinical features, and the key imaging findings on various modalities will be provided. The role of imaging as a whole in making the diagnosis and guiding the management of IBD will also be described.
Results: In this educational exhibit, a series of cases will be presented to illustrate the imaging findings in pediatric IBD with emphasis on the extra-intestinal manifestations. We will review some well-known manifestations of IBD such as primary sclerosing cholangitis (PSC) and IBD related spondyloarthropathies, and highlight their key imaging characteristics. Additionally, we will also present cases of some uncommon extra-intestinal manifestations such as granulomatous hepatic abscesses and non-infectious lung parenchymal involvement, which may mimic other disease entities thus creating potential pitfalls for the radiologist.
Conclusions: Pediatric IBD is frequently associated with extra-intestinal involvement. These findings may be discovered when imaging the bowel or IBD may be suspected based on the combination of intestinal and extra-intestinal findings. It is therefore important for radiologists to consider these manifestations to provide an accurate assessment of the patient to the referring physician.

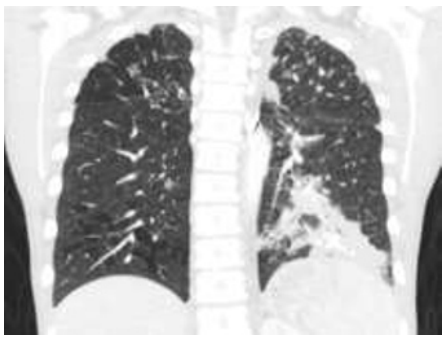

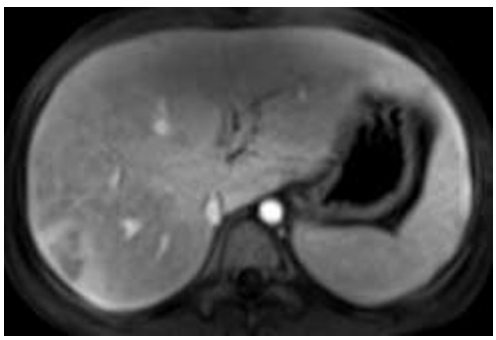

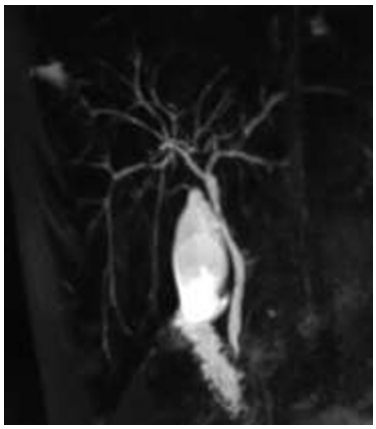

Poster #: EDU-025

Total Pancreatectomy and Islet Autotransplant: Preoperative imaging and post-surgical findings.

Jeff Ames, MD[1], *amesx042@umn.edu*; Tara Holm[1], Michael Murati, MD[1], Eric Hoggard[1], Kelly Dietz, MD[1]; [1]University of Minnesota Masonic Children's Hospital, Minneapolis, MN

Disclosures: All authors have disclosed no financial interests, arrangements or affiliations in the context of this activity.

Purpose or Case Report: Chronic pancreatitis (CP) is characterized by permanent damage to the pancreas resulting in endocrine and exocrine deficiencies. CP is often associated with a history of acute recurrent pancreatitis. Pediatric CP is most commonly linked to known genetic mutations, such as *PRSS1* or *CFTR*, and there is an increased risk of pancreatic adenocarcinoma in patients with hereditary pancreatitis. The mainstay of CP management involves controlling chronic pain and preserving quality of life.
Total pancreatectomy and islet auto-transplantation (TPIAT) is an option for managing pain in pediatric patients with uncontrollable pain or pancreatitis secondary to genetic causes. TPIAT was first performed at the University of Minnesota in 1971. Currently there are more than 15 academic institutions in the US performing TPIAT and that number continues to rise. TPIAT has been shown to be effective for pain relief as well as maintaining insulin independence in adults and young pediatric patients. The timing of TPIAT in a patient's disease course is critical because islet cell yield is inversely correlated with pancreatic fibrosis, and postoperative diabetes outcomes depend on islet yield.
Imaging prior to transplant is aimed at assessing changes of pancreatitis, vessel patency, and identifying vessel and pancreatic ductal anatomic variants. Preoperative imaging can also confirm adequate liver volume for the procedure and identify postoperative changes from previous procedures such as distal pancreatectomy or Puestow procedure (pancreaticojejunostomy).
Routine postoperative imaging consists of liver Doppler ultrasound screening because elevated infusion pressures during autotransplantation can result in endothelial injury and portal vein thrombosis. Delayed gastric emptying and small bowel ileus are common postsurgical complications, and targeted cross-sectional imaging, radiography, and fluoroscopy may be performed based on patient symptoms. Once bowel function has returned, enteral feeds are started via gastrojejunostomy tube and can sometimes be complicated by GJ tube-related intussusception. The largest retrospective review in pediatric patients showed a 20% surgical complication rate, with the most common complication being post-splenectomy thrombocytosis.

We present pertinent imaging findings for surgical planning in patients with CP prior to TPIAT, expected postoperative imaging findings, and imaging of postoperative complications.

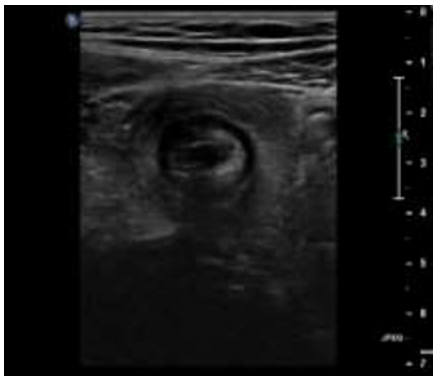

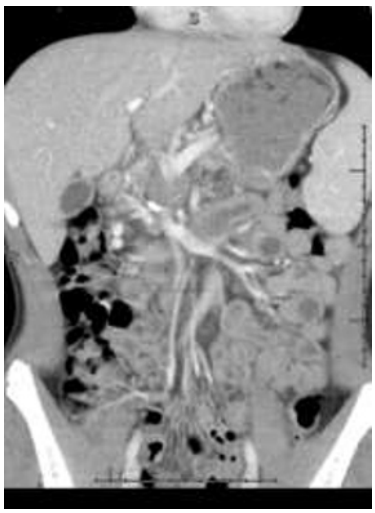

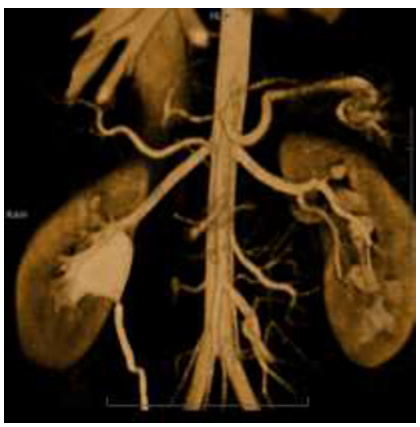

Poster #: EDU-026

Foreign body quiz

Joshua Finkle, MD[1], *Joshua.Finkle@uchospitals.edu*; Kate Feinstein[1]; [1]Radiology, University of Chicago, Chicago, IL

Disclosures: All authors have disclosed no financial interests, arrangements or affiliations in the context of this activity.

Purpose or Case Report: Kids put all sorts of things in their mouths. Foreign body ingestion is a common occurrence in children, and diagnostic imaging plays an important role in determining the nature of the foreign body and the need for emergent removal.
This presentation uses a question and answer format to provide high-yield clinically relevant information on the most commonly encountered foreign bodies including management guidelines for things like coins, batteries, and magnets. Both GI and airway foreign bodies are discussed. The presentation is catered mostly to trainees, but even experienced radiologists will enjoy challenging themselves to identify uncommon foreign bodies on imaging.

Poster #: EDU-027

Twists and Turns of Upper Abdominal Solid Viscera

Karthik Sundaram, MD, PhD[1], *karthik.m.sundaram@vanderbilt.edu*; Sudha Singh, MB BS, MD[1], Marta Hernanz-Schulman, MD[1]; [1]Department of Radiology, Vanderbilt University Medical Center, Nashville, TN
Disclosures: All authors have disclosed no financial interests, arrangements or affiliations in the context of this activity.

Purpose or Case Report: Introduction
Torsion or volvulus of upper abdominal viscera is rare and related to incomplete development and laxity of suspensory ligaments, or to poorly developed supernumerary accessory lobes. Clinical symptoms at presentation can be confusing and nonspecific, yet prompt recognition is essential to avoid life-threatening complications. Radiologists play an essential role in prompt recognition of these conditions. Our exhibit will review congenital anomalies of upper abdominal solid viscera that can lead to volvulus within an embryologic and anatomic framework. As examples, we include cases of mesenteroaxial gastric volvulus (Figure 1), torsion of an accessory hepatic lobe (Figure 2), and splenic torsion in the setting of polysplenia (Figure 3). Our cases include radiologic-pathologic correlations and therapeutic implications of solid visceral torsions.
Table of Contents/Outline:
Review of the embryology and anatomy of upper abdominal organs including a detailed pictorial of suspensory and anchoring ligaments.
Review and examples of types of gastric volvulus and treatment.
Review of variants of liver anatomy and of incidence and location of accessory hepatic lobes, with examples.
Review of splenic anatomy and normal variants, splenic torsion and gross malformations including variants seen in heterotaxy, with review of treatment options in splenic torsion, including observation, surgical pexy or resection.
Review of associated congenital anomalies (e.g. omphalocele, diaphragmatic hernia, and malrotation, etc.)

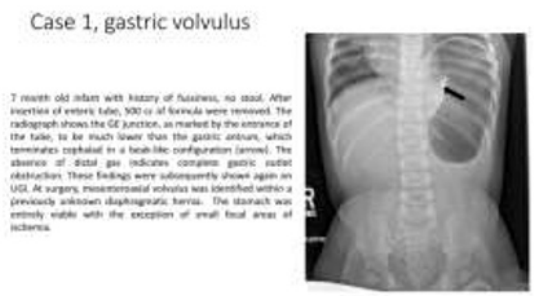

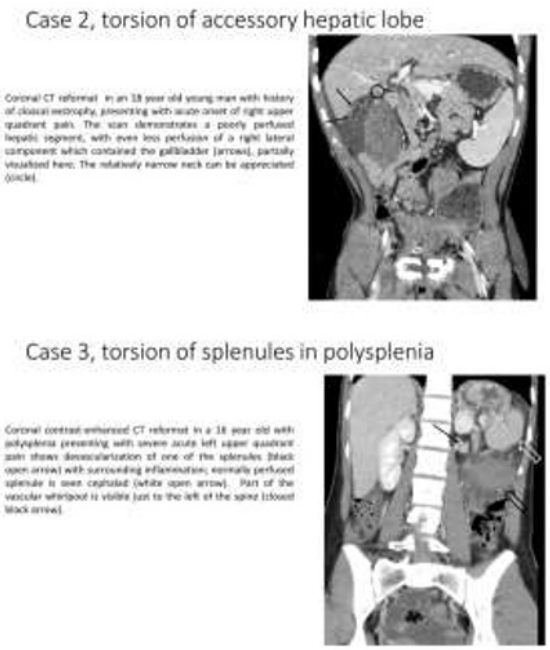

Poster #: EDU-028

It hurts when I swallow!

Albair Guirguis[1], *albairwilliam@yahoo.com*; Brooke Lampl, DO[1], Ellen Park[1], Ihsan Mamoun[1]; [1]Cleveland Clinic, Solon, OH

Disclosures: All authors have disclosed no financial interests, arrangements or affiliations in the context of this activity.

Purpose or Case Report: ***Background***: Esophageal disorders are relatively common in pediatric age group, clinically presenting with dysphagia, odynophagia, chest pain, cough, and aspiration. Etiologies may include infections and motility disorders, congenital disorders, and some traumatic (post foreign body or caustic ingestion)??? causes. Overlap exists in the appearance of esophageal pathology by fluoroscopy and cross-sectional evaluation. Recognition of the imaging features and how to differentiate various pathologies assist in diagnosis and further management.
***Purpose*:** To review the esophageal disorders that can manifest in children with specific attention to the imaging features of different pathologies.
Educational goal: To recognize and describe the different pathologies and to emphasize the key imaging features encountered in esophageal disorders.
***Technique and modalities of Imaging*:** Plain radiographs may be helpful in the newborn in the diagnosis of esophageal atresia, however esophagram is considered the primary tool for evaluation as it demonstrates both the anatomy and function of the esophagus. Cross sectional imaging such as CT and MRI may follow esophagram for further assessment of the extent of the diseases in some cases such as the wall involvement, extra-luminal extension, and extrinsic lesions.
Examples of cases (please refer to images)
Lymphoma involving the esophagus.
Ulcerating mass and irregular wall thickening of the lower esophagus.
Esophageal leimyomatosis (Alport syndrome).
Diffuse esophageal wall thickening and dilatation.
Congenital Esophageal stenosis.
Long segment of irregular concentric narrowing with mild proximal dilatation.

Listed below are some of the esophageal disorders included in the poster:
Congenital stenosis.
Achalasia.
Esophageal web.
Traumatic stricture (battery ingestion).
Esophageal perforation (post TOF repair).
Diffuse Esophageal Spasm.
Eosinophilic Esophagitis.
Tertiary contractions.
Hiatal hernia.
***Conclusion*:** Imaging is one of the main tools in the work up for esophageal disorders, allowing for appropriate management and treatment. Several cases will be presented, including clinical information, illustrated images and descriptions of the imaging findings. These cases will cover different pathologies, as a quick comprehensive review for esophageal disorders.

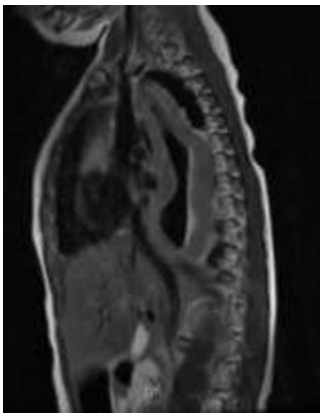

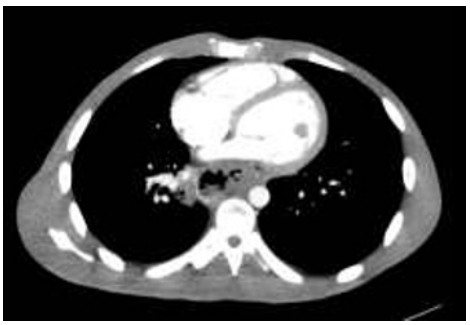

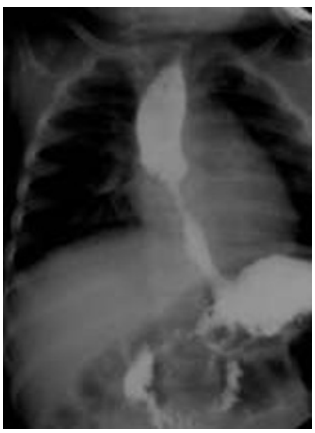

Poster #: EDU-029

Mimickers of malrotation in upper GI series

Anilawan Smitthimedhin, MD[1], *fuuune@hotmail.com*; Angela Suarez, MD[1], Ryan Webb[1], Hansel Otero, MD[1]; [1]Radiology, Children's National Health System, Washington, DC

Disclosures: All authors have disclosed no financial interests, arrangements or affiliations in the context of this activity.

Purpose or Case Report: The diagnosis of malrotation is heavily reliant on imaging. Upper GI series remain the gold standard with the normal position of the duodenojejunal junction lateral to the left-sided pedicles of the vertebral body, at the level of the duodenal bulb on frontal views and posterior (retroperitoneal) on lateral views. However, a variety of conditions might influence the position of the duodenojejunal junction, potentially leading to a misdiagnosis of malrotation. Such conditions include gastric over distension, splenomegaly, renal or retroperitoneal tumors, liver transplant, small bowel obstruction, the presence of properly or malpositioned enteric tubes and scoliosis. All of these may cause the duodenojejunal junction to be displaced. We present a series of cases highlighting conditions that mimic malrotation to increase the practicing radiologist awareness and help minimize interpretation errors.

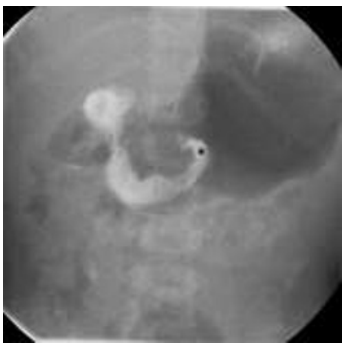

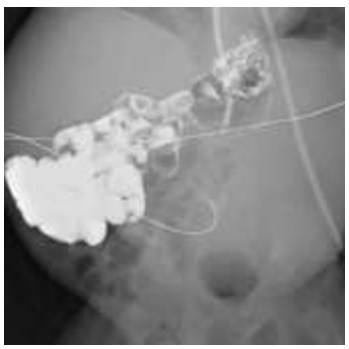

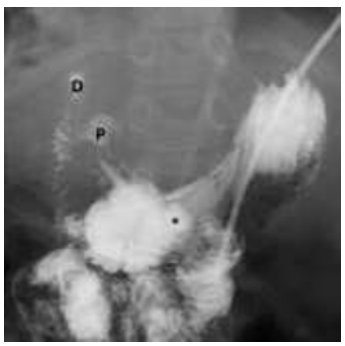

Poster #: EDU-030

MR Confidence with "IFFI" Findings: MRI appearance of Intraperitoneal Focal Fat Infarction in Children.

Meghan McClure, MD[2], *meghan.mcclure@unmc.edu*; Shahab Abdessalam, MD[1], Andria Powers, MD[1]; [1]Children's Hospital and Medical Center, Omaha, NE, [2]University of Nebraska Medical Center, Omaha, NE

Disclosures: All authors have disclosed no financial interests, arrangements or affiliations in the context of this activity.

Purpose or Case Report: Omental infarction and epiploic appendagitis are subtypes of a broader entity of abdominal fat necrosis known as intraperitoneal focal fat infarction (IFFI). IFFI is an uncommon cause of acute abdominal pain in children, and a known mimicker of acute appendicitis. The CT appearance of IFFI is well described, but the appearance is less familiar on MRI and is a potential imaging pitfall. Familiarity with the MRI appearance of IFFI is particularly timely, given the growing use of MRI in the evaluation of right lower quadrant pain in children. The purpose of this educational exhibit is to review the clinical history, pathologic appearance and treatment of IFFI, and describe MRI features that will allow the radiologist to make the correct diagnosis.

Methods & Materials: A retrospective case review was performed of the local PACS and electronic medical record at our institution on all MR examinations performed for appendicitis from December 2016 to October 2017. Available clinical history, laboratory results, imaging, pathology and follow-up were reviewed

Results: One hundred one appendicitis protocol MRIs were performed between December 2016 and October 2017. Of those, four patients were diagnosed with omental infarction or epiploic appendagitis based on surgical pathology or clinical features, which represented 4% of the cases clinically suspected to be acute appendicitis. Of these four cases ultimately diagnosed as IFFI, one MRI was initially interpreted as possible appendicitis, and one as Meckel's diverticulitis versus omental infarct. The third and fourth cases were diagnosed as omental infarction and epiploic appendagitis by MRI, with concordant clinical course and follow-up.

The four cases share the following common MRI features: localized T2 hyperintense inflammatory changes within the right lower hemiabdomen, interposed between the ascending colon and anterior abdominal wall; mild diffuse signal loss within the circumscribed changes from fat suppression on T2FS sequence compared to T2 sequence; noninflamed appendix identified distant from or near the inflammatory changes. Peripheral clefts of fluid around the localized inflammatory changes were noted in several cases.

Conclusions: IFFI is an uncommon cause of acute abdominal pain in children, and can clinically mimic acute appendicitis. Characteristic MR features described in this educational exhibit will aid the radiologist in making the correct diagnosis, leading to proper management and avoidance of unnecessary surgery

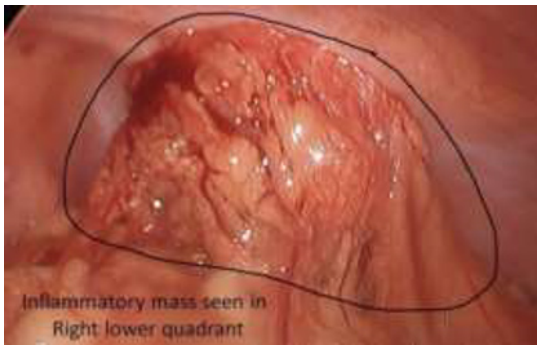

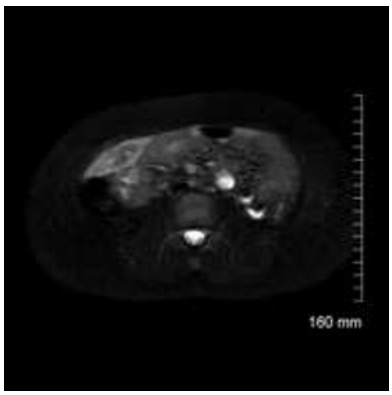

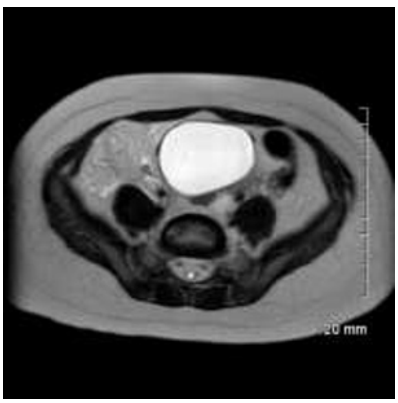

Poster #: EDU-031

Unusual Appendicitis Presentations

Janet Adams, RDMS (ABD, PS), RVT, CNMT, RT(N)[1], *janet.adams@cchmc.org*; Michelle Gramke, RDMS (ABD, PS), RT[1], Lindsey Hekler, MEd, RDMS (ABD, PS), RDCS[1]; [1]Cincinnati Children's Hospital Medical Center, Cincinnati, OH

Disclosures: All authors have disclosed no financial interests, arrangements or affiliations in the context of this activity.

Purpose or Case Report: Timely sonographic diagnosis of appendicitis can be critical for pediatric patients, as perforation rate is inversely related to the child's age, and atypical signs and symptoms can commonly obscure the clinical diagnosis.[1] In experienced hands, pediatric sonography for appendicitis has a high sensitivity and specificity and spares the child radiation.[2] Our educational poster entitled "Unusual Appendicitis Presentations" has been authored by experienced sonographers and will cover the following:

1. Scanning protocols and techniques used at our institution
2. Helpful tips that go beyond routine imaging to detect difficult appendicitis findings
3. Uncommon cases including neonatal, duplicated, mucinous, gangrenous, and disrupted appendicitis involving the bladder wall
4. Images from each case as well as patient symptoms, imaging findings and surgically confirmed diagnosis

1 McAbee G, Donn S, Mendelson R, McDonnell W, Gonzalez J, Ake J: Medical diagnoses commonly associated with pediatric malpractice lawsuits in the United States. J Amer Acad Pediatrics 2008;122(6):1282-1286.
2 Krishnamoorthi R, Ramarajan N, Wang N, et al. Effectiveness of a staged US and CT protocol for the diagnosis of pediatric appendicitis: reducing radiation exposure in the age of ALARA. Radiology 2011;259(1):231-239.

Poster #: EDU-032

Neonatal bowel obstruction in Cystic Fibrosis: Findings, Pitfalls and Mimickers

Nucharin Supakul, MD[1], *tanyasupakul@yahoo.com*; Matthew Wanner[1], Megan Marine, MD[1], Boaz Karmazyn, MD[1]; [1]Indiana University, Riley Hospital for Children, Indianapolis, IN

Disclosures: All authors have disclosed no financial interests, arrangements or affiliations in the context of this activity.

Purpose or Case Report: To summarize our experience in diagnosis neonatal bowel obstruction in cystic fibrosis (CF) patient using contrast enema study. This pictorial review will illustrate and discuss several aspects of imaging findings in non-complicated and complicated meconium ileus as well as the mimicker.
Key imaging findings, pearls and pitfalls in diagnosis and guided treatment will be made, emphasizing what radiologists need to know. Correlation with intraoperative findings and follow-up images will also be provided.
Methods & Materials: Using our radiology database, a retrospective review of barium enema studies in neonate with delayed pass meconium from 2010-2017 was obtained. Clinical data and imaging finding were reviewed. We will demonstrate imaging findings of non-complicated and complicated meconium ileus in CF neonate with delayed pass meconium, as microcolon secondary to meconium ileus, meconium plug, meconium peritonitis, colonic volvulus and ileal atresia. Imaging of the mimicker of meconium ileus will be discussed including microcolon secondary to very low birth weight and prematurity and total colonic Hirschsprung's disease.
Imaging checklists for diagnosis and guided either therapeutic enema or surgery will be demonstrated.
Results: Delayed pass meconium is the first sign of neonatal bowel obstruction. Approximately 20% of neonates with CF present with meconium ileus or meconium plug syndrome at birth due to abnormally thick and impacted meconium at the distal ileum or left-sided colon. However in some patients, it can present with complications such as meconium peritonitis or colonic volvulus which need immediate surgical intervention. Optimal imaging technique is important to generate a correct diagnosis and therapeutic treatment.
Conclusions: Contrast enema plays an important role in diagnosis and guided treatment in CF neonate with delayed pass meconium. Understanding imaging findings of non-complicated, complicated and mimicker of meconium ileus are crucial for radiologist to generate a correct diagnosis and guide treatment.

Figure 1: Classic meconium ileus in CF, complicated with ileal atresia later in her life.

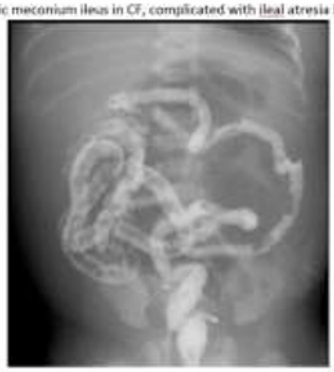

Figure 2: Meconium plug in CF.

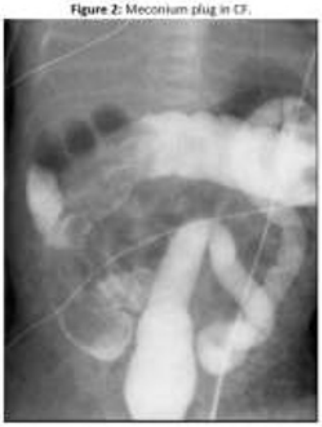

Figure 3: Microcolon in total colonic aganglionosis.

Poster #: EDU-033

The Journey of Infantile Hypertrophic Pyloric Stenosis (IHPS): from 1977 to 2017... A 40-year Review!

Soni Chawla, MD[1], *chawlasoni@gmail.com*; Raffi Ourfalian, DO[2]; [1]Olive View Hospital - UCLA Medical Center, Sylmar, CA, [2]Kaiser Permanente Los Angeles Medical Center, Los Angeles, CA

Disclosures: All authors have disclosed no financial interests, arrangements or affiliations in the context of this activity.

Purpose or Case Report: IHPS has a history that is intimately related to the evolution of Ultrasound(US). US was first used to diagnose IHPS as far back as 1977 (Teele and Smith), and as US technology advanced, the diagnosis of IHPS became more refined. We can make precise measurements for the pyloric muscle wall thickness (MWT), pyloric canal length (CL), and transverse pyloric diameter (TPD), and we have highly sensitive and specific signs (i.e. target, shoulder, double-track signs, etc) to aid us in the diagnosis of IHPS (Hernanz-Schulman 1998).

Why: IHPS is the most common cause of gastric outlet obstruction and one of the most common conditions requiring surgery in infants. The exact pathogenesis of IHPS is unknown, but it is an acquired, gradual and progressive disorder.
Who: The classic picture is 5 to 8-week old Caucasian male (4:1 M:F) who presents with non-bloody, non-bilious projectile vomiting. Classic physical exam findings including visible peristalsis and palpable pyloric olive are present in less than 50% cases. Delay in diagnosis can cause serious consequences.
When: We can typically do US at any age at the time of the next feed and as the baby is being bottle fed (ideally).
How: We use a linear 12-5 or curved 8-5 transducer, with 2D and cine imaging. The baby is placed in supine position, and we begin scanning at the epigastric region. We find the gastroesophageal junction and trace the lesser curvature of the stomach medially to find the pylorus.
What: Once we find it; we measure the MWT, CL, and TDP, and look for all the signs. One way to remember the normal limits is our "Rule of 4s". In IHPS, MWT is more than 4mm, CL is 4x4 = 16mm, and TDP is 4+4+4 = 12+mm. The signs include target sign (hypertrophied hypoechoic muscle surrounding echogenic mucosa), shoulder/nipple sign (bulging of hypertrophied pyloric muscle into the lumen of the antrum), and double-track sign (elongated pylorus with hypoechoic lumen, sandwiched between echogenic mucosa). If the measurements do not meet our "rule of 4s" and there are none of the signs, we can confidently rule out IHPS, or we may consider another differential diagnosis, like pylorospasm and mucosal hypertrophy due to other causes like prostaglandins. We've come a long way with refining and defining US diagnosis of IHPS until finally ultrasound is now the gold standard diagnostic modality for IHPS.

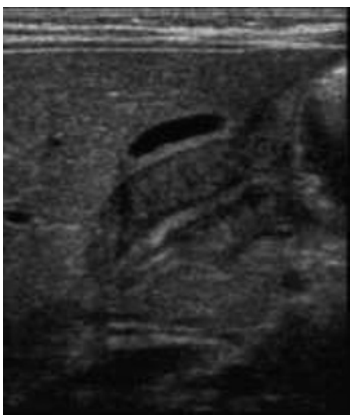

Reference	Pyloric muscle thickness: MWT	Pyloric canal length: CL	Transverse pyloric / AP diameter: TPD	Other Findings/ Conclusions
Ramsack 2nd Ed '78	+/- 3 mm	+/- 1.2 cm	—	No peristalsis through the pyloric
Grainger '78	> 2.5 mm	> 1.5 cm	> 11 mm	Pyloric canal does not open
Teele and Smith 1977	—	—	1.8 – 2.8 cm Avg (2.3)	Echolucent mass with central shallow collection of echoes
Hayden, Swischuk et al 1984	0.3 - 0.7cm (mean 0.42 cm)	1.4 - 2.2 cm (mean 1.81 cm)	0.9 - 1.7 cm (mean 1.27 cm)	Muscle thickness and Length are reliable***
Blumhagen et al 1986	4.6 +/- 0.6 mm	1.8 +/- 0.3 cm	—	Thickness of the muscle is the most discriminating and accurate criterion***
Swischuk, Hayden et al 1989	3 - 4 mm	+/- 1.5 cm	—	Pitfalls: Anesthesia affect & and if canal, hypertrophy, overdistended stomach
Neilson and Hellman 1993	> 2.5 mm	> 16 mm	> 11 mm	Mild bolus: canal does not open, Decreased gastric peristalsis, little passage of contents
Hernanz-Schulman, et al 1994	4.0 - 4.4 mm	1.1 - 1.5 cm	—	Highly sensitive and specific Signs: double-track, shoulder, nipple

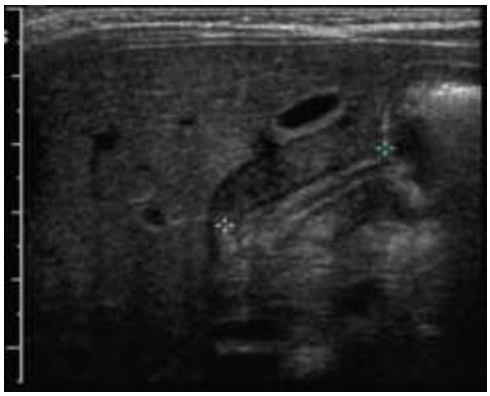

Poster #: EDU-034

Iatrogenic Upper GI Perforations in Neonates

Joel Wolf, MD[1], Juan Remon, MD[1], Eliza Myers, MD[1], Einat Blumfield[1]; [1]Albert Einstein College of Medicine/Jacobi Medical Center, Bronx, NY

Disclosures: All authors have disclosed no financial interests, arrangements or affiliations in the context of this activity.

Purpose or Case Report: Iatrogenic upper gastrointestinal (GI) injuries are rare occurrences with predisposition in premature births, low birth weight, multiple attempts at OGT placement. Medical literature on the topic consists of case reports and mostly has been from the perspective of management with very limited literature on diagnostic evaluation. As the clinical presentation of such iatrogenic injuries is nonspecific, the radiographic appearance may be the only clue for diagnosis and the typical findings should be recognized and diagnosed by radiologists and neonatologists. The purpose of this presentation is to describe the radiographic findings and a diagnostic approach to guide the radiologist. A retrospective case-review was performed from 2009-2017, of neonates with upper GI injuries associated with naso/orogastric tube placement or with pharyngeal auctioning at birth (a single case). Seven cases were found comprising of five females and two males. Six of seven neonates were premature with gestational ages ranging from 24 weeks and 2 days to 28 weeks, and birth weights spanning 515-1085 grams. The 38 week neonate weighed 3500 grams. We report three types of injury: 1) posterior pharyngeal rupture, 2) non-complicated esophageal rupture with formation of a false lumen, 3) complicated esophageal rupture with penetration into the right pleural space. Management has evolved over time from a primarily surgically oriented approach to a more conservative approach involving TPN and antibiotics.

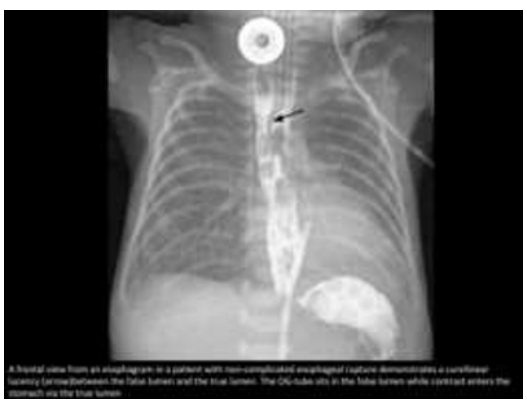

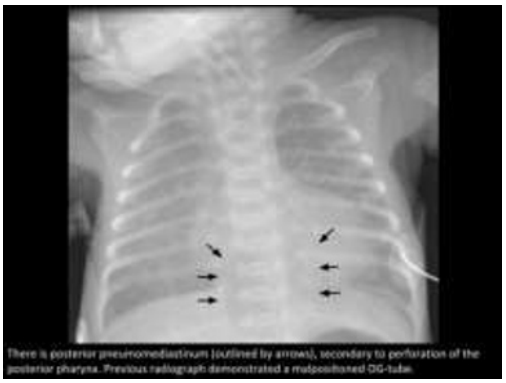

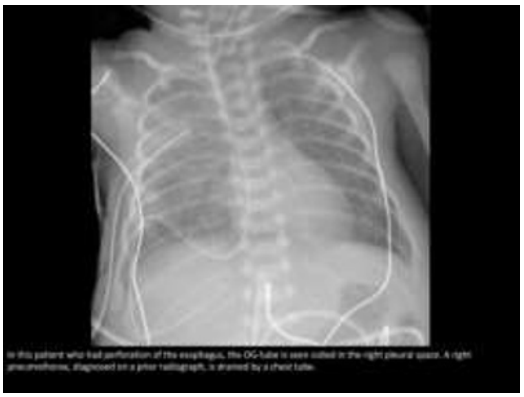

Poster #: EDU-035

Traumatic Injuries to the Pancreas in Children

Joseph McCrary, MD[1], *jmccrary@alumni.nd.edu*; Jennifer Talmadge, MD[1]; [1]Maine Medical Center, Department of Radiology, Portland, ME

Disclosures: All other authors have disclosed no financial interests, arrangements or affiliations in the context of this activity.

Purpose or Case Report: Accidental traumatic injuries of the pancreas are rare but dangerous. In children, blunt abdominal trauma is the most common mechanism.

The goal of this presentation is to review, through a series of cases, the diagnosis, imaging findings, classification, and management of accidental traumatic pancreatic injuries in children.

Our cases include an 18-year-old football player with traumatic pancreatitis and pseudocyst formation, a 12-year-old pinned between two vehicles who sustained a pancreatic laceration with full transection of the pancreatic duct, a 15-year-old soccer player with a pancreatic laceration and truncated duct on ERCP, and a 5-year-old boy who was run over by a car and developed shock pancreas.

Traumatic injuries, as graded by the guidelines of the American Association for the Surgery of Trauma, span a gamut including contusion, laceration, transection, duct injury, ampulla injury, and massive destruction of the pancreatic head. Complications include fistula, pancreatitis, and the development of pseudocysts. Through multiple imaging modalities - including CT, MR, MRCP, ERCP, and ultrasound - our cases illustrate many of these injuries and subsequent complications.

While nonoperative treatment of minor pancreatic injuries is widely accepted, the management of more severe pancreatic injuries, such as those involving the pancreatic duct, is more controversial. Duct injury, for example, has been reported to be

predictive of failure of non-operative management.
The radiologist, therefore, has the opportunity to play a pivotal role in patient care by characterizing the injury. Pancreatic organ and duct injuries can be subtle and correlation with multiple modalities as well as multidisciplinary discussion between the radiologist, surgeon, and gastroenterologist, are often required.

Poster #: EDU-036

Don't be fooled by the lateral view of the duodenum in suspected malrotation and midgut volvulus

Elena Lambert[1], *embhunter@doctors.org.uk*; Savvas Andronikou[1]; [1]Bristol Royal Hospital for Children, Taunton, United Kingdom

Disclosures: All authors have disclosed no financial interests, arrangements or affiliations in the context of this activity.

Purpose or Case Report: Background:
Malrotation is an important diagnosis that needs to be identified on routine imaging and in the emergency setting. In our institution it is always surgically corrected and therefore accurate diagnosis is essential. Current teaching, supported by research, states that a lateral view on an upper gastrointestinal contrast study (UGIS) can satisfactorily demonstrate normal anatomy and a diagnosis of malrotation. The diagnosis must be made with confidence in this position because any delay in turning the patient into the AP plane can result in contrast progressing into the jejunum with overlapping bowel loops compromising the diagnosis.
Methods & Materials: We present three cases saved from our regular clinical practice where the lateral component of the UGIS is misleading or confusing and diagnosis relied on adequate AP imaging.
Results: In the first patient we show that despite normal appearances on the lateral view, the AP imaging demonstrated malrotation which was referred for surgery.
The two other cases demonstrate 'duodenum redundum' on AP imaging, a normal variant. The lateral view in both cases demonstrates a meandering path of the second and third part of the duodenum as it courses towards the retroperitoneum. The lateral view was not diagnostic in these cases although we acknowledge that the appearances of a duodenum redundum on the lateral view may be a consistent finding.
Conclusions: We recognize that in the majority of circumstances the lateral view can be used for diagnosis but as cases of malrotation can be missed, AP imaging should remain as the standard for diagnosis.

Poster #: EDU-037

Multi-Modality Imaging Abnormalities of the Pediatric Spleen

Marci Handler[1], *marci.handler@gmail.com*; Scott Sosin, DO[1], Robyn Murphy[1]; [1]Radiology, Morristown Medical Center, Middlesex, NJ

Disclosures: All authors have disclosed no financial interests, arrangements or affiliations in the context of this activity.
Purpose or Case Report: Teaching Points
1. To review the normal imaging appearance of the spleen on ultrasound, CT and MRI.
2. Discuss the imaging characteristics of various pediatric splenic pathology.
3. Learn the epidemiology, appropriate imaging workup, and management of congenital pediatric splenic abnormalities.
Introduction
The spleen can be involved in a wide range of pathologies, yet can be frequently overlooked on imaging. Splenic disorders can be seen in isolation or may be secondary to a systemic disease. Different imaging modalities can be utilized to evaluate the spleen and include ultrasound, CT, and MRI. We will perform a case-based review of the imaging characteristics of various types of pediatric splenic pathologies. After completing this educational exhibit, the reader will be able to recognize the various causes and imaging characteristics of pediatric splenic diseases. The following topics will be discussed:
Congenital splenic anomalies - asplenia, polysplenia, accessory spleen
Splenomegaly
Trauma
Inflammation/infection
Infarction
Hemochromatosis
Splenic cysts
Hemangiomas
Hamartomas
Lymphoma
Splenic metastasis

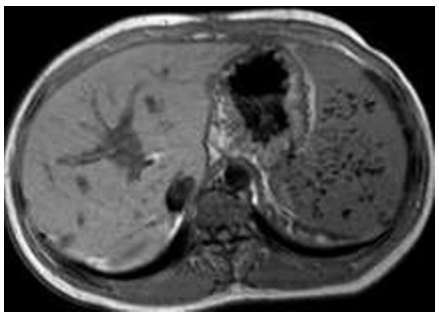

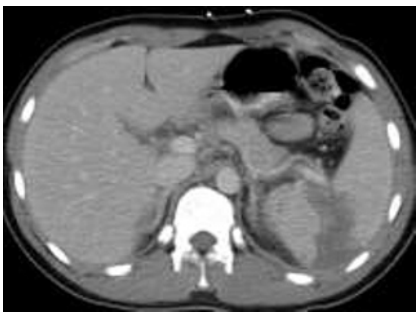

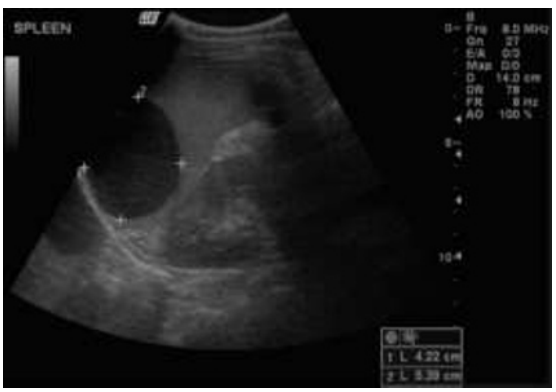

Poster #: EDU-038

Imaging Spectrum of Pediatric Intussusception

Akosua Sintim-Damoa, MD[1], *asintimd@uthsc.edu*; Benjamin Eovaldi, DO[1], Harris Cohen[1]; [1]Radiology, LeBonheur Children's Hospital, Memphis, TN

Disclosures: All authors have disclosed no financial interests, arrangements or affiliations in the context of this activity.

Purpose or Case Report: Intussusception is a common cause of bowel obstruction in the pediatric population that is important for the radiologist to recognize. A delay in diagnosis can lead to bowel obstruction and necrosis and ultimately bowel perforation. Radiographs and sonography are the primary modalities for diagnosis of the condition. Computed tomography use is of limited use due to radiation exposure but may be helpful when a pathologic lead point is suspected. The purpose of this educational review is to describe the clinical and characteristic radiographic and sonographic findings of intussusception in the pediatric population. Classic ileocolic intussusceptions will be discussed as well as imaging features that may predict failure to reduce with air enema. Small bowel small bowel intussusceptions and intussusceptions with lead points will also be reviewed. Finally, intussusceptions due to gastrojejunostomy tubes will be discussed.
Methods & Materials: A search of the radiology reports at our institution was performed from February 1, 2013 through October 1, 2017 for intussusception. Radiographs, ultrasounds, and, if applicable computed tomography and air contrast enema images were evaluated. Radiographs were evaluated for the presence of a soft tissue mass, absence of gas in the right lower quadrant on a decubitus image, and evidence of a small bowel obstruction. Additionally, in patients with gastrojejunostomy tubes, abnormal course of the tube was noted. Ultrasound images were evaluated for the size of the intussusception, the presence of color Doppler flow, trapped fluid within the intussusception, bowel wall edema, and free fluid. These findings were correlated with the ability to reduce with fluoroscopically assisted air enema.
Results: A variety of cases were obtained demonstrating:
a. Ileocolic intussusceptions reducible by air contrast enema
b. Ileocolic intussusceptions not reducible by air contrast enema
c. Small bowel small bowel intussusceptions
d. Ileocolic intussusceptions secondary to pathological lead points
e. Small bowel small bowel intussusceptions secondary to pathological lead points
f. Small bowel intussusceptions secondary to a gastrojejunostomy tubes
Conclusions: Accurate and timely diagnosis of intussusception is critical. The radiologist must maintain a high index of suspicion, particularly when reviewing emergency abdominal radiographs as classic findings may not be apparent. Knowledge of typical findings on radiographs and ultrasound will be helpful in making the diagnosis of intussusception.

Poster #: EDU-039

A to Z of Densities of a Myriad of Pediatric Foreign Bodies: "Rule of 3–5" Helps Us Prepare for the Triple Threat of Perforation, Small Bowel Obstruction (SBO) and Morbidity!

Jonathan Lin, BS[1], Alvin Chan, MD[2], Shahnaz Ghahremani, MD[3], Soni Chawla, MD[2]; [1]Penn State University College of Medicine, San Marino, CA, [2]OVMC, Sylmar, CA, [3]Ronald Reagan UCLA Medical Center, Los Angeles, CA

Disclosures: All authors have disclosed no financial interests, arrangements or affiliations in the context of this activity.

Purpose or Case Report: Children, especially toddlers, are the most frequent victims of foreign body (FB) ingestion because of their natural curiosity, tempting them to put everything into their mouths. Anything within arm's reach is fair game, from simple coins to the more dangerous button batteries and magnets. This study aims to provide a thorough review of plain radiographic findings of a myriad of foreign bodies (FBs) and associated complications. With the "Rule of 3-5", we aim to help radiologists and clinicians develop a rationale and systematic approach in managing FB ingestions.
Methods & Materials: A curated number of items were compiled to demonstrate the vast range of ingested objects. Items included categories such as food, wood, plastic, sand, chalk, crayon, playdough, glass, metal and magnets. The items were placed on cardboard in order of expected radiographic densities from radiolucent to radiopaque to radiodense and plain radiographic images were obtained. The images were post-processed to least contrast and maximum brightness to improve visualization and characterization of different FBs.
Results: On plain radiography, most FBs are visible to varying degrees depending on density. Lucent objects such as food, wood and plastic can be delineated by adjusting contrast and brightness. High-density, radiopaque items were readily visualized and better characterized by changing the contrast and brightness.
Although the majority of ingested FBs pass the gastrointestinal (GI) system spontaneously, some require emergent intervention due to the triple threat of perforation, SBO and morbidity. These emergencies can be remembered by the "Rule of 3-5": All long, linear or sharp objects measuring 3-5 cm in length; round, oval or polygonal objects measuring 3-5 cm in diameter; and multiple magnets or button batteries 3-5 in number require emergent attention.
Conclusions: Plain radiography from the level of the adenoid to anus is the best initial choice of imaging because of its easy availability, portability and ability to visualize objects of different densities. "Intelligent neglect" is suggested and uneventful expulsion is expected for all FBs, except those that fall within our "Rule of 3-5," which pose a triple threat and require emergent GI/surgical consultation. Further evaluation with upright/decubitus imaging to exclude free air and SBO or CT may be performed as clinically indicated.

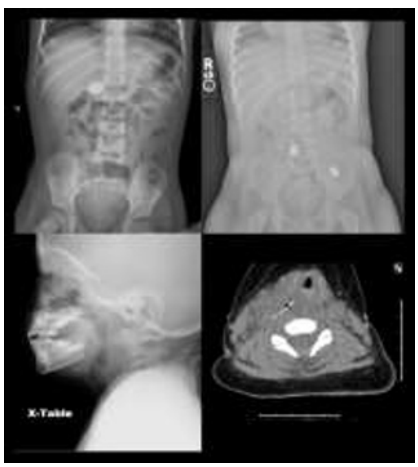

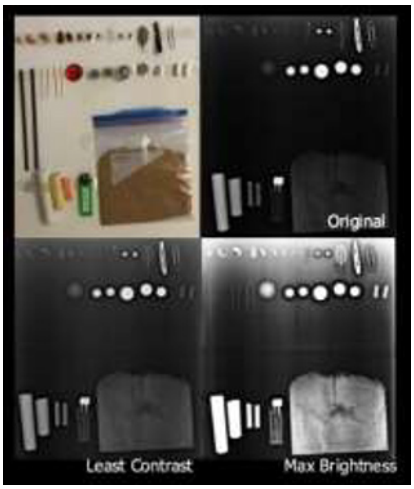

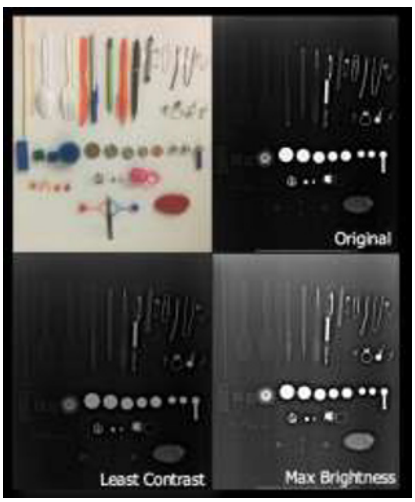

Poster #: EDU-040

"Fidgety Fingers, Spinner that Lingers": Recognizing the Imaging Characteristics of the Innumerable Types of the Most Exciting Toy of the Year.

Jonathan Lin, BS[1], Soni Chawla, MD[2]; [1]Penn State University College of Medicine, San Marino, CA, [2]Olive View Medical Center, Sylmar, CA

Disclosures: All authors have disclosed no financial interests, arrangements or affiliations in the context of this activity.

Purpose or Case Report: Fidget spinners (FS) have become an increasingly popular toy among children of all ages since April 2017. This toy comprises of a central bearing attached to two or more prongs made of plastic or metal and is designed to be spun between a user's fingers. With its popularity, FS have grown diverse in design, featuring additional components including light-emitting diode units, Bluetooth speakers, and button batteries. With its multiple small components, FS pose a risk of ingestion and aspiration among young children. This may be incidental or accidental due to the rapidly spinning nature of the toy. Since May 2017, there has been a growing number of cases of FS ingestions among young children internationally. Recognition of the different components of a FS on imaging, especially plain radiography, is important in the early diagnosis and prompt and accurate management of foreign body ingestion. To date, there is no available educational resource to aid and guide radiologists and clinical providers in identifying FS as a foreign body. The purpose of this educational exhibit is to assist radiologists and clinicians to identify the imaging findings associated with FS-related foreign body ingestions.

Methods & Materials: Radiographic images of twelve different FS were obtained. An internet search on case reports and news articles was performed and six cases of FS ingestion with radiographic imaging were compiled.

Results: On radiographic imaging, the internal components of different FS vary widely in shape, size and density. Adjusting contrast and brightness on plain radiography allows for better visualization of the different densities and components within the FS.

Conclusions: FS have become an increasingly popular toy among children this year and have been recognized as a foreign body internationally. FS comprise of small components that may lead to aspiration, small bowel obstruction and perforation, and caustic chemical injury due to the button batteries. The growing diversity among FS design may delay recognition and management. Along with obtaining a thorough clinical history, identification of FS on radiographic imaging is essential in early management and prevention of complications associated with foreign body ingestion.

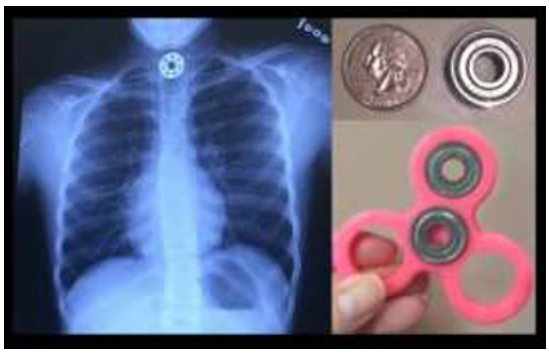

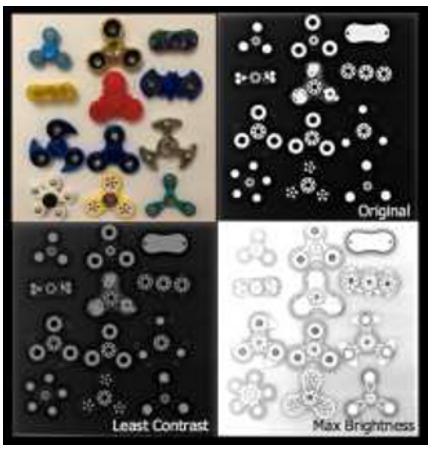

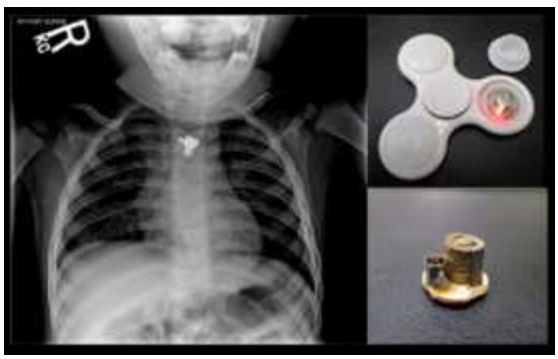

Poster #: EDU-041

Genitourinary Manifestations of Sickle Cell Disease in the Pediatric Patient: A Radiologic Overview

Erin Taylor, MD[1], *erin.taylor@yale.edu*; Brendon Graeber, MD[1]; Lauren Ehrlich, MD; [1]Radiology and Biomedical Imaging, Yale School of Medicine, New Haven, CT

Disclosures: All authors have disclosed no financial interests, arrangements or affiliations in the context of this activity.

Purpose or Case Report: Sickle cell disease (SCD) is characterized by repeated episodes of vaso-occlusion and hemolysis beginning in the pediatric period that result in serious multi-organ system complications. In particular, renal complications are often the cause of morbidity and reduced life expectancy of patients with SCD. Therefore, it is essential that radiologists be able to identify the imaging features early to help guide prompt and appropriate treatment.
Sequelae in pediatric patients include sickle cell nephropathy, infarction and papillary necrosis, and assorted glomerulopathies. These in turn can lead to altered hemodynamics, impaired urinary concentrating ability, hematuria, proteinuria, and acute and chronic kidney injury. Children with SCD are also at increased risk of asymptomatic bacteriuria and urinary tract infection. Even those children and young adults who only have sickle cell trait (SCT) rather than SCD may develop chronic kidney disease later in life and carry markedly increased risk for renal medullary carcinoma. Segmental testicular infarction can compromise fertility in patients with both SCD and SCT.
The genitourinary manifestations of SCD and SCT in the pediatric patient will be reviewed in this educational exhibit, with an emphasis on radiologic appearances. For each entity, the clinical presentation, pathophysiology, and differential diagnosis of the imaging findings will also be briefly reviewed.
The renal complications covered will include renal infarction, papillary necrosis, renal vein thrombosis (as a complication of nephrotic syndrome), urinary tract infection, hematuria, renal medullary carcinoma, and acute and chronic kidney disease. Testicular and penile sequelae of SCD including segmental testicular infarction and priapism will also be discussed. A variety of imaging modalities will be used to illustrate the various complications, including ultrasonography, computed tomography, and magnetic resonance imaging.

Poster #: EDU-042

Microbubbles made simple: The case for using contrast-enhanced ultrasound in pediatric radiology

Anush Sridharan, PhD[1], *sridharana@email.chop.edu*; Kassa Darge, MD, PhD[1]; [1]Radiology, Children's Hospital of Philadelphia, Philadelphia, PA

Disclosures: All authors have disclosed no financial interests, arrangements or affiliations in the context of this activity.

Purpose or Case Report: The ability to provide quick, real-time, easily accessible and radiation free diagnostic assessment makes ultrasound (US) imaging one of the most versatile imaging modalities. With the introduction and development of microbubble based ultrasound contrast agents (UCAs) in the early 90's the ability to detect and visualize complex vascular structures became a reality, overcoming some of the limitations that were existent with grayscale and Doppler imaging. UCA's are used extensively in the adult population for visualization of vasculature and evaluating vascular kinetics in solid organs and lesions. Although contrast-enhanced ultrasound (CEUS) can provide a powerful alternative approach to evaluate various pathologies in the pediatric population that would otherwise require radiation-based computed tomography (CT) or strenuous magnetic resonance imaging (MRI), it is important to understand the interaction between US and the microbubbles to optimize imaging and derive clinically relevant quantitative measures of vascularity.
Methods & Materials: This educational poster will outline the structural properties of microbubbles and the effects of various US imaging parameters on the behavior of these microbubbles. The various methods to perform dynamic CEUS in order to generate qualitative and quantitative measures will be introduced, including certain troubleshooting mechanisms. Finally, an overview of existing applications for CEUS in pediatrics based on experience at our institution will also be presented via cases, and the future of CEUS based on existing pre-clinical research will be briefly described.
Results: Through this educational poster, readers will be introduced to the basic concepts of CEUS including the physics of US interaction, generation of measures of vascular kinetics and some current clinical and research applications.
Conclusions: This poster should provide a good foundation for the reader to either develop on their existing experience with CEUS or be encouraged to use this novel technique for applications in pediatric radiology where CT and MRI can potentially be avoided.

Poster #: EDU-043

Imaging of the Gubernaculum – An Original Description of its Ultrasonographic Features.

Syeda Anum, BS[1], *syeda.anum@umassmed.edu*; E. Christine Wallace, MD[1]; [1]Umass Medical School, Boston, MA

Disclosures: All authors have disclosed no financial interests, arrangements or affiliations in the context of this activity.

Purpose or Case Report: To describe the ultrasonographic appearances of the gubernaculum in boys, review its utility in diagnosing cryptorchidism and provide a functional illustration of the gubernaculum as it conducts the testis into the scrotum. We will elucidate this process with a review of the relevant embryology.
Methods & Materials: This is a retrospective review of 26 imaging studies obtained as part of scrotal ultrasound evaluations of male patients for cryptorchidism, infection and masses, between 2007-2016. High-resolution linear ultrasound probes were used to demonstrate the scrotum, inguinal canal, pelvis and abdomen to evaluate the pathway of descent of the testis so that the undescended testis might be located. The gubernaculum was identified in this process. The patients were referred from NICU, maternity unit and outpatient settings.
Results: These 26 male patients ranged in age from 0 days to 59 months. We examined 4 preterm and 22 full term patients. 23/26 had undescended testes. Bilateral undescended testes were seen in 20/23 patients and a unilateral undescended testis in 3/23 patients. The gubernaculum was identified in 23/26 patients. It was seen bilaterally in 15/26 patients, of whom 12/15 were cryptorchid and 3/15 were descended. The gubernaculum was seen unilaterally in 8 cryptorchid boys. This provides a total of 38 gubernacula. It was not seen in 3 cryptorchid boys.
The gubernaculum is homogeneous in echogenicity and less echogenic than the adjacent testis. The echo-pattern is loosely aggregated. It is soft and compressible. It is not vascular on color Doppler evaluation. It has a slippery behavior and variable shape. In cross-section, it's size is similar to or slightly greater than the testis. It lies distal to and contiguous with the testis. It can be demonstrated passing to and through the internal (deep) ring, into the inguinal canal and to the base of the scrotum,

therefore it's length varies. It should not be confused with the testis as it does not have the characteristic testicular features of a mediastinum testis or strictly ovoid configuration.
Conclusions: The gubernaculum is a normal embryological structure not often described in the pediatric radiological literature. Confident demonstration of the gubernaculum can assist in locating the undescended testis and provides a more detailed diagnosis of cryptorchidism. Ultrasonographic demonstration of the arrested process of testicular descent also provides a beautiful illustration of the normal physiological mechanism of descent.

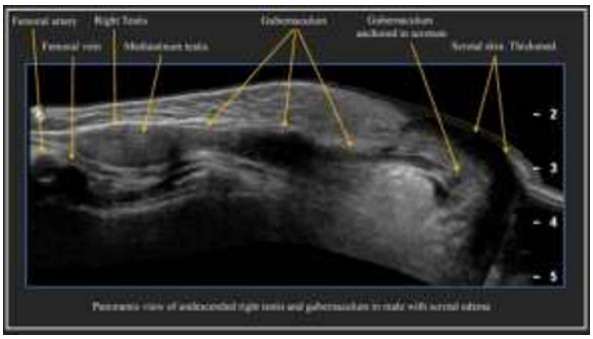

Poster #: EDU-044

Radiology of Unusual Pediatric Scrotal Anatomy and Pathology

Timothy Alves, MD[1], *talves@med.umich.edu*; Kathleen Gebarski, MD[1]; [1]Radiology, University of Michigan, Ann Arbor, MI

Disclosures: All authors have disclosed no financial interests, arrangements or affiliations in the context of this activity.

Purpose or Case Report: While hydroceles, patent processus vaginalis, inguinal hernias, varicoceles, epididymitis, orchitis, torsion of testes and appendages are common in pediatric radiological practice, other pathology and anatomical variants are unusual and may not be included in every day practice. We composed a pictorial guide of a wide variety of variants and diseases for education and reference.
Methods & Materials: Illustrative cases of ectasia of rete testes, testicular adrenal rests, tunica albuginea cyst, scrotal calcinosis, abdominoscrotal hydrocele, hematocele, meconium periorchitis, testicular epidermoid cyst, calcifying Sertoli cell tumor, lymphoma and paratesticular rhabdomyosarcoma were chosen from over ten years of imaging at our institution.
Results: Reviewing these cases provides an experience of a wide variety of unusual scrotal anatomy and pathology and improves the accuracy of interpretation.
Conclusions: A pictorial review of a wide variety of unusual scrotal anatomy and pathology improves the accuracy of interpretation.

Poster #: EDU-045

Pediatric Urinary Bladder Masses and Pseudo-masses: A Pictorial Review with Emphasis on Ultrasound Findings

Ami Gokli[1], *aag298@nyu.edu*; Christian Barrera, MD[1], Richard Bellah, MD, FAAP[1]; [1]Children's Hospital of Philadelphia, Philadelphia, PA

Disclosures: All authors have disclosed no financial interests, arrangements or affiliations in the context of this activity.

Purpose or Case Report: The complete ultrasound (US) evaluation of the urinary tract in a pediatric patient should include both the urinary bladder and kidneys. Evaluation of the bladder as part of that overall US examination, however, can be deemphasized or incomplete due a number of factors, such as one's neglecting to fully image the bladder from dome to bladder neck, suboptimal bladder distension, incomplete distension due to presence of an indwelling drainage catheter or vesicostomy, or in some instances, because the bladder is not included as part of the routine kidney ultrasound exam. True masses arising from the urinary bladder in children are generally rare, and at times, subtle and non-specific, and potentially mimicked by so-called pseudomasses, so we emphasize that correlation of findings with patient history is of paramount importance.
This pictorial review will illustrate and describe the US appearances (along with selective cross-sectional imaging), clinical manifestations, and tumor growth patterns of common and uncommon conditions arising from the pediatric urinary bladder, i.e. path-proven masses that include leiomyosarcoma, pheochromocytoma, nephrogenic adenoma, vascular malformation, low grade urothelial neoplasms, neurofibromatosis, fibroepithelial polyps, rhabdoid tumor, and rhabdomyosarcoma. Pseudomasses of the bladder that will also be illustrated and briefly discussed include hematomas, urachal remnants, complex ureteroceles, Deflux injection sites, foreign bodies, and cystitis (viral, eosinophilic, parasitic). In addition to emphasizing the importance of the complete bladder examination, the purpose of this review is to increase radiologist's awareness of the US appearances of the common and uncommon conditions which afflict the pediatric urinary bladder, as well as those conditions that can mimic bladder masses, in order to determine proper clinical management.

Poster #: EDU-046

Seeing double: One too many of an organ

Anne Misiura, MD[1], Faaiza Kazmi[1], Erica Poletto, MD[1], Mea Mallon[1], Archana Malik[1], Jaqueline Urbine[1]; [1]Radiology, St. Christopher's Hospital for Children, Philadelphia, PA

Disclosures: All authors have disclosed no financial interests, arrangements or affiliations in the context of this activity.

Purpose or Case Report: The duplication of structures in the body has been a curious topic to the field of medicine for centuries. It is rare to find a radiologist who has not seen at least one duplicated or partially duplicated organ, usually of the genitourinary system, and often incidentally. While implications of GU duplication have been study previously, often due to infertility or renal issues, other organ system duplications and their implications to the patient often remain a mystery.
Methods & Materials: A retrospective analysis of multimodality imaging in patients with duplicated structures presenting to an urban children's hospital since 2005. Imaging and clinical history are correlated with clinical, surgical, and pathologic findings where applicable. A variety of organ and structural duplications are selected for imaging review.
Results: An enthralling visual array of organ/structure duplication will include cases such as duplicated duodenum, gallbladder, vessels, urinary bladder/genitalia, among others. Clinical implications of each will be discussed as available on a case by case basis, as well as surgical and pathologic findings where applicable.
Conclusions: Organ/structure duplication is a spellbinding topic to the pediatric radiologist, as they are usually incidentally discovered, and the implications are often unknown. Each case is an opportunity for creation of mesmerizing reconstructed images and discussion with colleagues in other clinical areas.

Poster #: EDU-047

Pediatric Hydrosalpinx - making your differential diagnosis less fluid

Michael Lucin[1], *michael-lucin@uiowa.edu*; Robert Becker[1], T. Shawn Sato, MD[1]; [1]University of Iowa, Iowa City, IA

Disclosures: All authors have disclosed no financial interests, arrangements or affiliations in the context of this activity.

Purpose or Case Report: Hydrosalpinx can be difficult to differentiate from other cystic lesions in the pelvis - especially when large. However, there are imaging characteristics that may help narrow the differential diagnosis and initiate appropriate management earlier in the clinical course.
Methods & Materials: - Demonstrate the radiologic appearance of hydrosalpinx with a focus on anatomy and etiology.
- Illustrate the key imaging features in the differential diagnosis of hydrosalpinx.
- Discuss management options available to surgeons and gynecologists.
Results: We review cases of hydrosalpinx in pediatric patients with clinical course, illustrate the pertinent diagnostic findings with a focus on differential diagnosis, and discuss management.
Conclusions: A knowledgeable radiologist is critical in the expeditious and accurate diagnosis of hydrosalpinx in the pediatric population and bridges the gap between patient presentation and appropriate management while avoiding unnecessary or potentially harmful intervention.

Poster #: EDU-048

Cool Beans: Large Scale Renal Abnormalities in the Pediatric Patient

Bernard Goldwasser, MD[1], *bayruch@gmail.com*; Faaiza Kazmi, MD[1], Jacqueline Urbine, MD[1], Erica Poletto, MD[1], Archana Malik, MD[1], Mary Mallon, MD[1]; [1]St. Christopher's Hospital for Children, Philadelphia, PA

Disclosures: All authors have disclosed no financial interests, arrangements or affiliations in the context of this activity.

Purpose or Case Report: There is a wide array of pathologies which can cause diffuse changes in the pediatric kidney. The purpose of the presentation is to show a multimodality pictorial review of characteristic findings of a wide variety of diffuse renal abnormalities in the pediatric patient.
Methods & Materials: A search for diffuse renal lesions was performed by reviewing studies stored on the picture archiving and communication system of an urban children's hospital between 2006 and 2017. A literature search on current information related to the diagnoses was performed. The presented cases include: multicystic dysplastic kidney, renal vein thrombosis complicated by total parenteral nutrition infiltration, Wilm's tumor with a large subcapsular collection, autosomal dominant polycystic kidney disease, autosomal recessive polycystic kidney disease, multilocular cystic nephroma, multiple renal cysts in the setting of tuberous sclerosis, multiple angiomyolipomas in the setting of tuberous sclerosis, and clear cell sarcoma.
Results: A broad range of pathologies diffusely affect the pediatric kidney, including benign and malignant etiologies. By observing characteristics as described in the pictorial review, an appropriate differential diagnosis may be made, enabling appropriate and efficient clinical management.
Conclusions: Diffuse renal abnormalities sometimes demonstrate characteristic features that may help narrow the differential diagnosis affecting clinical decision making. This presentation will help the radiologist recognize these characteristic features. At times, a definitive diagnosis cannot be given and tissue sampling is required to make this determination.

Poster #: EDU-049

Ultrasound Appearance of Typical and Atypical Scrotal Abnormalities

Sean Kelleher[1], *skelleher09@gmail.com*; Brooke Lampl, DO[2], Ellen Park[2]; [1]MetroHealth, Cleveland, OH, [2]Cleveland Clinic, Cleveland, OH

Disclosures: All authors have disclosed no financial interests, arrangements or affiliations in the context of this activity.

Purpose or Case Report: Scrotal ultrasound is commonly performed in a pediatric practice with the nonspecific clinical presentation of pain, palpable abnormality, or enlargement of the scrotum. A wide variety of pathologies including congenital, neoplastic, infectious, and traumatic etiologies can occur within the scrotum due to its complex anatomy. A thorough understanding of the anatomy and spectrum of disease is necessary for diagnosis and potential treatment of these abnormalities. This educational exhibit will illustrate typical and atypical scrotal abnormalities, including testicular torsion, torsion of the testicular and epididymal appendix, and infectious processes associated with the clinical finding of pain. Additionally, we will provide a collection of testicular and extra-testicular masses, some demonstrating an unusual presentation.

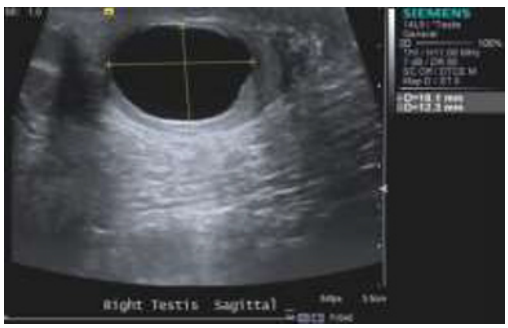

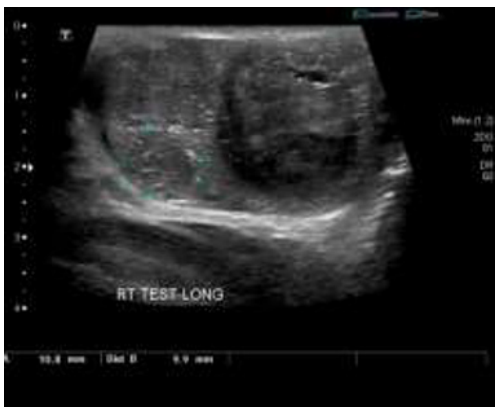

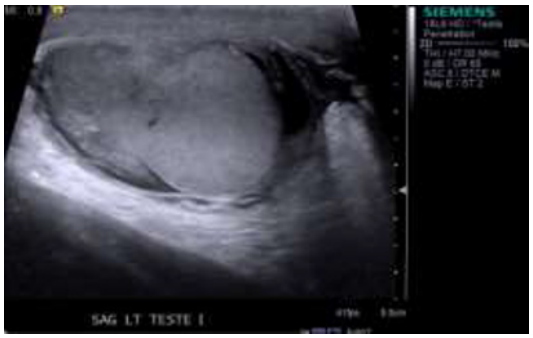

Poster #: EDU-050

Multi-Modality Imaging Findings in Pediatric Congenital Renal and Urinary Disorders

Scott Sosin, DO[1], *scott.sosin@gmail.com*; Marci Handler[1], Robyn Murphy[1]; [1]Morristown Medical Center, Middlesex, NJ

Disclosures: All authors have disclosed no financial interests, arrangements or affiliations in the context of this activity.

Purpose or Case Report: Teaching Points
1. Review normal renal anatomy and normal renal and urinary imaging findings in the pediatric population.
2. Discuss the imaging characteristics of the different causes of congenital pediatric renal and urinary disorders, predominantly utilizing ultrasonography and fluoroscopy.
3. Learn the epidemiology, appropriate workup, and management of congenital pediatric renal and urinary disorders.
Introduction
There is a large spectrum of frequently encountered congenital renal and urinary disorders, ranging from incidental findings to severe, life-threatening pathologies. Recognizing the multi-modality imaging characteristics of these anomalies is an important tool in any radiologists' arsenal. The purpose of this presentation is to perform a case-based imaging review of congenital renal and urinary disorders and discuss their etiologies and clinical importance. After completing this educational exhibit, the reader will be able to recognize the various causes and imaging features of congenital pediatric renal disorders. The following topics will be discussed:
Vesicoureteral reflux
Autosomal recessive polycystic disease (ARPKD)
Autosomal dominant polycystic disease (ADPKD)
Renal anomalies - agenesis/ectopia/horseshoe/duplicated
UPJ obstruction
Posterior urethral valves
Megaureter
Ureterocele
Multicystic dysplastic kidney
Mesoblastic nephroma

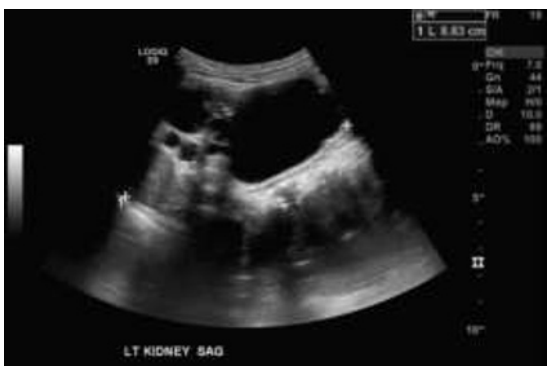

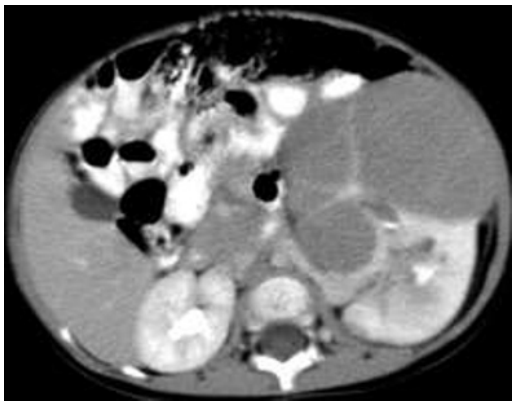

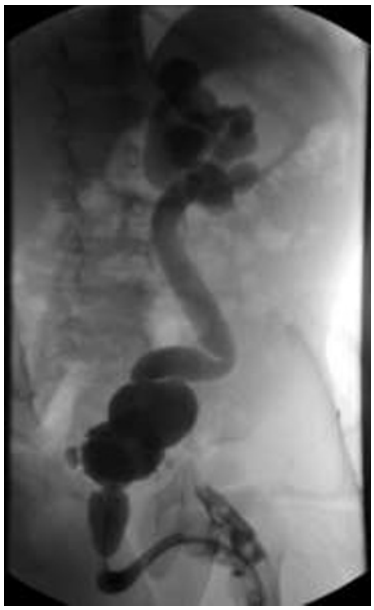

Poster #: EDU-051

Pediatric Radiology Fellowship Creation as an International Education Outreach in Ethiopia: the Experience of CHOP.

Jonathan Zember, MD[1], *jonathan.zember@gmail.com*; Daniel Zewdneh[2], Yocabel Gorfu[2], Janet Reid, MD, FRCPC[1], Andrew Steenhoff, MD[3], Kassa Darge, MD, PhD[1]; [1]Radiology, Children's Hospital of Philadelphia, Philadelphia, PA, [2]Addis Ababa University, Addis Ababa, Ethiopia, [3]Children's Hospital of Philadelphia, Philadelphia, PA

Disclosures: All authors have disclosed no financial interests, arrangements or affiliations in the context of this activity.

Purpose or Case Report: Since 2008, the Children's Hospital of Philadelphia (CHOP) Department of Radiology has conducted pediatric radiology international education outreach in Ethiopia. In 2008, there was not a single Ethiopian pediatric radiologist in a country of 100 million people, where 60% of the population is under the age of 20. As such, children are a major population for diagnostic imaging and the majority of radiologists are confronted with pediatric imaging. However, there was a lack of emphasis on much-needed training of pediatric imaging in radiology residencies. With an increasing number of pediatric subspecialties, the need for adequate pediatric imaging service had grown. This was particularly true at Black Lion Hospital (BLH), the country's main referral center, affiliated with Addis Ababa University (AAU). Radiology faculty at AAU saw value

in a pediatric radiology fellowship. The partnership goals between CHOP and AAU were to support and expand the pediatric radiology component in the BLH radiology residency and to carry out regular national pediatric radiology continuing medical education. The purpose of our project was to establish an accredited local pediatric radiology fellowship training in the Department of Radiology at BLH.
Methods & Materials: Core values were to ensure sustainability and self-sufficiency and included: 1- making the local radiology staff lead the curriculum design, 2- Formal accreditation from AAU, 3- Primary site of training in Ethiopia, and, 4- On-the-job-training of faculty in a format of "teaching the teachers".
Results: A two-year fellowship was successfully launched with its primary base in Addis Ababa, with components of distance learning, local instruction, a limited observership at CHOP, and pediatric radiology-focused research requirements. The training culminated in a final oral examination conducted by international visiting faculty. In 2017, Ethiopia graduated its first two pediatric radiologists after two years of fellowship. They are currently based at BLH, established a Pediatric Radiology Section with a director, and are actively recruiting the next fellow candidates.
Conclusions: Establishing a pediatric radiology fellowship through outreach is both doable and feasible. Our experience showed the request for a fellowship must arise from the host country. In order to optimize success, one must identify the needs of key stakeholders in the host country, engage them in the process, ensure accreditation, and base the fellowship there.

Poster #: EDU-052

3D Printed Training Simulator for Pediatric Upper GI Fluoroscopy

Jacob Wallace, MD[1], *wallacejacobc@gmail.com*; Debbie Desilet-Dobbs[1]; [1]Radiology, University of Kansas - Wichita, Wichita, KS

Disclosures: All authors have disclosed no financial interests, arrangements or affiliations in the context of this activity.

Purpose or Case Report: Learning the skills used to master pediatric fluoroscopic exams can be challenging. Hand-eye coordination and specific timing is required while at the same time being mindful of radiation dose and interpreting the images generated in real time. Training on live neonates will often mean less diagnostic exams and increased radiation dose for those exams.
An inexpensive reusable simulator model was devised to allow residents practice of upper GI fluoroscopic exams to increase efficiency using ALARA principles and utilizing 3D printing technology off-the-shelf dolls. Generic gastrografin provided a cost effective contrast medium as its concerns in real UGI studies are of no issue on the training models. A 30ml bottle of generic gastrografin can be purchased for less than $20, which would last for several simulated exams.
The 3D model was based on a computer generated imagery (CGI) mesh of a stomach which was modified in Blender™ to try to best replicate the full duodenum and effect of the ligament of Treitz. The final iteration of the model was printed in polylactic acid polymer (PLA) in a size that would fit inside the plastic doll, which already contained portions of the necessary tubing. The model was sealed to be watertight.
Testing under fluoroscopy showed that the model behaved similar enough to an infant when placed in various positions then filled with an appropriate volume contrast.
There are several limitations of this model including the lack of the distractions of a real pediatric patient. Also, the flow of contrast is purely gravity dependent without the effects of sphincters and peristalsis. Overlying skeletal structures and bowel gas are not represented, however these could also be simulated in various ways.
Future work on this and similar projects could include expansion into other organ systems such as the colon

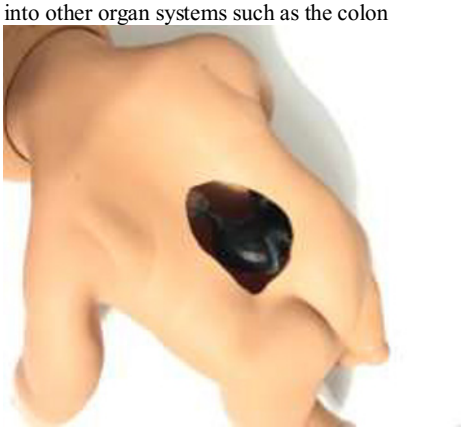

Poster #: EDU-053

Child Abuse in Sudan, Africa: Physician Awareness and Knowledge of Child Abuse Incidence, Child Abuse Imaging, and Management

Radya Osman, MD[1], *rgosman@iu.edu*; Megan Marine, MD[1], Boaz Karmazyn, MD[1], Richard Gunderman, MD, PHD[1], Darel Heitkamp, MD[1], Roberta Hibbard[1], Aaron Miller, MD, MPA[2], Alaaeldeen Mohammed, MD[3], Satti Satti, MD[4], Ilham Ahmed, MD[5], Shima Yagoub, MD[3], Mohamed Salih Bakeit, MBBS[3], Elrayah Mustafa, MD[6], Abdalla Gabir, MD, FRCR[6]; [1]Radiology, Indiana University, Indianapolis, IN, [2]Weill Cornell Medicine, New York, NY, [3]Sudan Medical Specialization Board, Khartoum, Sudan, [4]Sudan Association of Pediatricians, Khartoum, Sudan, [5]University of Khartoum, Khartoum, Sudan, [6]Sudanese Association of Radiologists, Khartoum, Sudan

Disclosures: All authors have disclosed no financial interests, arrangements or affiliations in the context of this activity.

Purpose or Case Report: To assess the awareness and knowledge of Radiologists, Pediatricians, Orthopedists and Emergency Physicians regarding child abuse incidence, imaging, and management in Sudan, Africa.
Methods & Materials: A descriptive cross-sectional survey study was performed. A 16-question paper and electronic survey were distributed to currently practicing resident and faculty Radiologists, Pediatricians, Orthopedists and Emergency Physicians in Sudan, Africa. 4 cases with radiographs were submitted as part of the survey to assess participants' knowledge regarding physical abuse findings. Answers were reported and statistical analysis comparing different specialties was performed using chi-square test.
Results: A total number of 400 physicians completed the survey, including 364 residents and 36 faculty physicians. 16.8% of physicians indicated there were no cases of child abuse in Sudan, Africa. 88.3% of physicians reported having seen at least 1 case, but less than 5 cases of physical abuse in their career. 46% of physicians indicated that they are not aware of existing child protection units in Sudan and 50.5 % admitted that they do not know how to contact child protection units. 77% of physicians reported that they have not received training regarding the identification of child abuse, and 53.8% indicated that there is no standard imaging protocol to evaluate cases of suspected physical abuse at their institution. 99% of the physicians who took the survey indicated that a training workshop would be helpful.

Conclusions: There is a gap in awareness and thus training of physicians regarding detection, evaluation, and management of child abuse in Sudan, Africa. While more research is needed to identify the causes and extent of the problem, there is an urgent need for educating physicians at different levels of training across different specialties regarding identification, imaging, and management of child abuse.

Table (3) Q 14. A 2 month old, not moving right leg well. The finding of the proximal tibia is most likely represents a...?

	Frequency	Percent
Normal variant, will resolve with age	55	13.8%
Classic metaphyseal which lesion fracture, which could be explained by an accidental cause	145	36.3%
Classic metaphyseal lesion fracture, highly specific for child abuse	200	50.0%
Total	400	100.0%

Table (2) Question (9) Have you received training regarding identification of child abuse cases?

	Frequency	Percent
yes	92	23.0%
no	308	77.0%
Total	400	100.0%

Figure (2). Question (9) Have you received training regarding identification of child abuse cases?

Poster #: EDU-054

Metal Artifacts in CT Imaging: Concepts and Initial Clinical Experience Using a Dual-Energy CT Scanner with Metal Artifact Reduction (MAR) Image Reconstruction

Nathan Artz, PhD[1], Richard Hornsby[1], Samuel Brady[2], Beth McCarville, MD[1], Elizabeth Nett[3], Franco Rupcich[3], Terry Blancq[1]; [1]Diagnostic Imaging, St. Jude Children's Research Hospital, Memphis, TN, [2]Cincinnati Children's Hospital Medical Center, Cincinnati, OH, [3]GE Healthcare, Waukesha, WI

Disclosures: All authors have disclosed no financial interests, arrangements or affiliations in the context of this activity.

Purpose or Case Report: This educational exhibit will review 1) challenges of CT imaging near metal, 2) current acquisition and reconstruction methods for reducing metallic artifacts, and 3) our initial experience using a GE Revolution CT system for Dual-energy scanning combined with metal artifact reduction (MAR) image reconstruction. Artifacts caused by metallic implants have limited clinical diagnoses for decades using single-energy CT (single kVp, polyenergetic beam) with standard image reconstruction. Low-energy photons in the beam are absorbed by metal, leaving only high-energy photons passing through (ie. beam hardening). Beam hardening due to metal, along with photon starvation and scatter, result in dark shading and bright/dark streaking, as well as lower signal-to-noise levels. Dual-energy CT (DECT) has demonstrated promise for beam hardening reduction because it enables reconstruction of a monoenergetic image, similar in theory to acquiring data with a monoenergetic beam. Recent developments in CT data reconstruction have also achieved better image quality near metal by mitigating shading and streaking artifacts. On our Revolution CT, MAR reconstruction is available solely in dual-energy mode. For our patients with metallic prostheses, we perform DECT and review monoenergetic images with and without MAR. MAR images typically show markedly reduced artifacts from metal and thereby improved image quality. Fig 1 displays 70 keV monoenergetic images both with and without MAR for a patient with a pacemaker. Streaking artifacts arising from the pacemaker were apparent throughout anatomy without MAR, while significantly reduced streaking and improved visualization of the aortic bifurcation is observed in the MAR reconstructed image. Images from a patient with pedicle screws and metallic rods in the spine are shown in Fig 2. Although present, shading and streaking was noticeably reduced with MAR allowing better visibility of the paraspinal soft-tissue structures and the main portal vein. On occasion, however, MAR yielded more severe artifacts for certain slices, such as in the thigh for a patient with a metallic femoral rod just above a total knee replacement (Fig 3). In summary, recent technical advancements incorporated into the Revolution CT system have improved image quality for many of our patients with metallic implants. Predicting a priori when MAR will be worse is not yet possible, so viewing monoenergetic images with and without MAR is recommended.

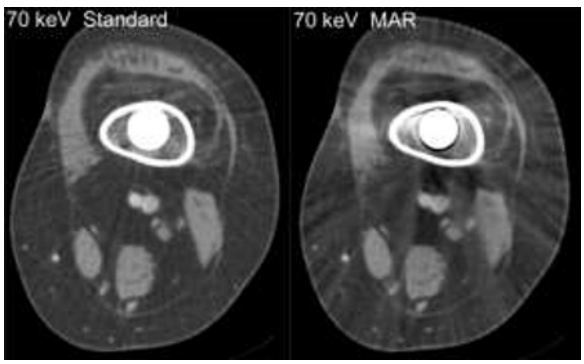

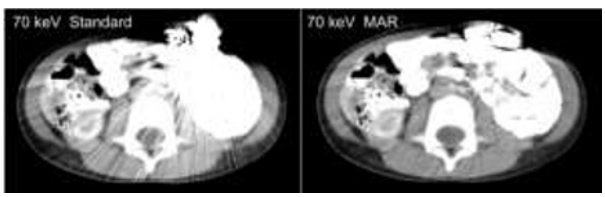

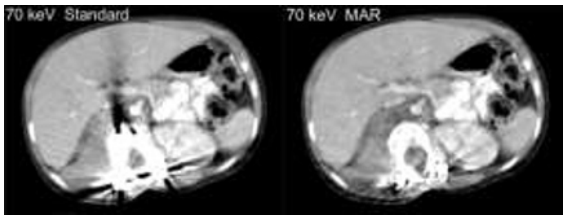

Poster #: EDU-055

From Imaging to Reimbursement: What the Pediatric Radiologist Needs to Know About Coding and Billing

Andrew Degnan, MD, MPhil[1], *degnan.andrew@gmail.com*; Chul Chung, MD[2], Richard Duszak, MD[3], Mark Alson, MD, FACR[4]; [1]Children's Hospital of Philadelphia, Philadelphia, PA, [2]University of Pittsburgh Medical Center, Pittsburgh, PA, [3]Emory School of Medicine, Atlanta, GA, [4]Sierra Imaging Associates, Clovis, CA

Disclosures: All authors have disclosed no financial interests, arrangements or affiliations in the context of this activity.

Purpose or Case Report: Coding and billing processes are complex, costly, and generally poorly understood by radiologists and other physicians. Despite the direct implications of radiology documentation on reimbursement, residents, fellows, and practicing radiologists receive little or no training in coding-related issues. It is thus important to understand the fundamentals of documentation, coding, billing, and reimbursement as they apply to the practice of pediatric radiology.
Methods & Materials: This presentation: (1) provides an overview of the unique payer structure within pediatric radiology including state-based CHIP programs, (2) discusses the essential processes by which radiologists request and receive reimbursement, (3) details the mechanisms of coding diagnoses using International Classification of Disease (ICD-10-CM) codes and imaging services using Current Procedural Terminology (CPT) and Healthcare Common Procedure Coding System (HCPCS) codes, and (4) explores reimbursement and coding-related issues specific to the practice of pediatric radiology.
Results: Radiologists can improve coding accuracy and enhance legitimate revenue through careful documentation of clinical necessity and detailed description of the services provided with an understanding of the components required for correct billing. Pediatric radiology presents unique challenges to reimbursement, including a unique study type distribution that favors lower cost studies and averts higher-valued cross-sectional imaging. In addition, no additional reimbursement is typically provided for the added complexity of interventional procedures and imaging studies in children. As such, many commonly-performed pediatric radiology services are undervalued.
Conclusions: Appropriate documentation, informed by knowledge of coding, billing, and reimbursement fundamentals, facilitates correct coding to ensure appropriate reimbursement for clinically-relevant services provided by pediatric radiologists. Understanding the payer and reimbursement environment specific to pediatric radiology can enhance advocacy efforts for pediatric radiology practices to provide economically sustainable access to high-quality care for children.

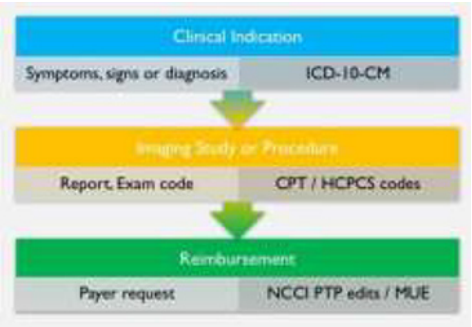

Poster #: EDU-056

Opportunities and Challenges in Teaching Radiology in a New Radiology Residency in Rwanda

Veronica Rooks, MD[4], *ronirooks@gmail.com*; David Rosman, MD[2], Sung Kim[3], Robert Harris, MD[1]; [1]University of Washington, Seattle, WA, [2]Massachusetts General Hospital, Boston, MA, [3]University of Pennsylvania, Philadelphia, PA, [4]Tripler Army Medical Center, Honolulu, HI

Disclosures: All authors have disclosed no financial interests, arrangements or affiliations in the context of this activity.

Purpose or Case Report: Review the experience teaching pediatric radiology to first year radiology residents in the first year of a new residency program in Rwanda.
One of the goals of the Human Resources for Health (HRH) program is to build a residency-trained physician workforce to create a sustainable health education infrastructure in Rwanda. Establishing a radiology residency program in a resource-poor African nation is a challenge being addressed by combining curricula from South Africa, Kenya, and United States and supplemented with ACGME materials. In Rwanda, the pediatric specialty is especially critical due to the high pediatric population as the country continues to recover from the 1994 genocide. Approximately 12 months of general radiology training, visiting faculty offered a two-month rotation in pediatric radiology. To assess efficacy, a pre- and post-rotation evaluation program was implemented. Objective, case-based tests consisting of 100 cases were implemented on the first and last day of the eight-week rotation, which comprised from nine to fifteen hours of formal lecture and case-based teaching each week. A paired t-test was used to compare pre- and post-rotation test results.View box examination scores for four first-year residents were recorded. Pretest mean: 27% (range 12-33% correct), Post-test mean 49% (range 27-62% correct), Average overall improvement: 22 percentage points (95% CI 12-32, p=0.005). Pediatric radiology knowledge did not increase as much as would be expected for developed world learners under the same curriculum. Complicating factors leading to complexity include basic medical knowledge, number of learning hours at view box vs didactic lecture, and the inconsistent caseload mix at local hospitals. Expected routine cases in the Western world are not commonplace in Africa; however, more challenging cases such as ischiopagus tetrapus, accessory limb, and extensive fat necrosis are seen. Language and cultural barriers impede teaching and uptake of new information. Diagnosis and communication must consider social, financial, and nutrition limitations. Equipment limitations, coupled with supply shortfalls, frequently influenced the exam recommendations. The challenges identified during this two-month experience should inform future efforts to teach medicine in low-resource countries. Curricula modifications may be needed to address language, social, financial and caseload challenges as well as equipment/resource shortages.

Poster #: EDU-057

Mastering Ultrasound through a Just-In-Time Mobile Application

Michele Retrouvey[1], *michele.retrouvey@gmail.com*; David Saul, MD[1], Susan Back, MD[1], Richard Bellah, MD, FAAP[1], Janet Reid, MD, FRCPC[1]; [1]Children's Hospital of Philadelphia, Philadelphia, PA

Disclosures: All authors have disclosed no financial interests, arrangements or affiliations in the context of this activity.

Purpose or Case Report: It is essential that budding pediatric radiologists have well-honed ultrasound (US) skills in order to provide correct image interpretation and excellent patient care. The lack of hands-on US experience is a critical gap in current radiology training. We sought to create an interactive, portable tool to remedy this issue.
Methods & Materials: A previously published needs assessment survey revealed a dearth of US hands-on skills amongst pediatric radiology fellows, where fewer than 45% had access to hands-on tutorials with sonographers, and only 23% had scanning responsibilities while on call. Most trainees reported their scanning skills has never been formally evaluated. To fill the learning gap, an electronic application (app) was designed with a user interface (UI) that optimized content delivery, through mobile or stationary devices using the principles of "just-in-time" (JIT) learning. A list of the requisite knowledge and skills for the top 10 emergency pediatric US scans was developed. All key resources and content were collected and assembled in the UI.
Results: The top ten emergency studies include-renal, RUQ, pylorus, intussusception, appendix, pelvis, hip, scrotum, spine, brain. A checklist-based UI was created in our LMS (Absorb, Calgary, Canada) including: protocols, image planes, images of normal and pathology, case log, links to previously created video-based micro-tutorials, "tips" for scan modification, evaluation by instructors, and transcripts. Through responsive design the app conforms to all mobile devices and desktop configuration and is operating system agnostic.
Conclusions: Our interactive mobile POC/JIT app is relatively simple to construct, with an appealing and easy-to-use interface and has potential to fill a gap in US skills during radiology training.

Poster #: EDU-058

Seeing Is Believing: The Value of Ultrasound-Guided Umbilical Catheter Placement

Michael Collard, MD[1], Cory Pfeifer, MD[1]; [1]Radiology, UT Southwestern, Coppell, TX

Disclosures: All authors have disclosed no financial interests, arrangements or affiliations in the context of this activity.

Purpose or Case Report: Umbilical catheters (UC) are ubiquitously utilized in neonatal intensive care units (NICU) during the early neonatal stage. Traditionally, these catheters are placed blindly, with the external length of the catheter being used to approximate catheter depth. This then requires subsequent radiographs to be obtained to assess for position, often in a sterile field, with considerable dead time. This exhibit will educate the viewer about the use of ultrasound guidance in the placement of these catheters.
Methods & Materials: Recent literature is reviewed. Approaches utilized with both abdominal ultrasound and echocardiography are discussed. Relevant neonatal anatomy is described. Complications related to malposition are reviewed, and measures related to efficiency and radiation dose are detailed.
Results: The traditional use of radiography to assess umbilical catheter placement in the neonatal population involves ionizing radiation and considerable lag time, yet the two-dimensional data included in this technique still results in only an approximate location for the catheter tip. Atypical vascular anatomy complicates this further, leading to the acquisition of additional radiographs before proper positioning is achieved. Furthermore, the sterile field created for catheter placement is typically maintained during the time of image acquisition and review, and the time lag in imaging interpretation may increase risk for procedure-related infection.
US-guided UC placement has been demonstrated to have equal or often better ability to identify accurate catheter tip positioning, with the added benefit of being performed real-time during the procedure, significantly limiting delays in care and radiation exposure. This has been shown to be particularly true in patients of increased birthweight. This represents an opportunity for radiologists to provide value in the care of these patients. Now that ultrasound resources are increasing in pediatric tertiary care centers, training and comfort with the procedure remain the only significant barrier to adoption.
Conclusions: The use of US guidance for UC placement has significant potential to improve catheter placement accuracy and clinical turnaround time from procedure beginning to final completion. This is an opportunity for radiologists to improve value via ultrasound-guided umbilical catheter placement while minimizing radiation dose to these young patients as consistent with the ALARA principle.

Poster #: EDU-059

Pediatric Interventional Radiology Biliary Procedures

Carlos Llorens, MD[1], *carlos.llorens@chp.edu*; Rakesh Sindhi[2], James Park, MD[1], John Crowley, MD[1]; [1]Department of Radiology, Children's Hospital of Pittsburgh of UPMC, Pittsburgh, PA, [2]Transplant Surgery, Children's Hospital of Pittsburgh of UPMC, Pittsburgh, PA

Disclosures: All authors have disclosed no financial interests, arrangements or affiliations in the context of this activity.

Purpose or Case Report: Pediatric Interventional Radiology biliary procedures are mainly performed on patients with liver transplant. Percutaneous transhepatic cholangiogram (PTC) is very useful for diagnosis of post-surgical development of strictures while at the same time allowing access for therapeutic measures such as biliary dilatation and diversion. Although post-surgical anatomy and non-dilated bile ducts may provide a challenge, biliary procedures have a high rate of success. The purpose of this exhibit is to review the biliary anatomy, discuss the available biliary procedures, including step-by-step explanation of the more common procedures and discussion of goal and outcomes of these procedures.
Methods & Materials: A single institution retrospective review was conducted to identify pediatric patients with prior biliary procedures. Selected patients were correlated with imaging findings and/or surgical findings, and/or clinical course.
Results: Review and discussion of biliary anatomy, PTC procedure with step-by-step explanation, discussion of other biliary procedures as well as discussion of goals and outcomes are presented. Sample cases from our institution are shown to illustrate our approach to biliary procedures. Cased-based examples are supplemented with a review of the current literature.

Conclusions: Interventional radiology biliary procedures are an essential part of pediatric liver transplant care. Knowledge of the how these procedures are done, empower not only the pediatric interventional radiologist performing the procedure, but also the pediatric radiologist who can aid in providing important information about post-surgical biliary anatomy as well as by identifying complications related to biliary procedures.

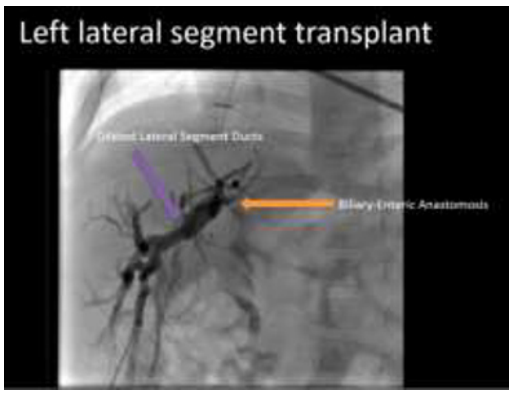

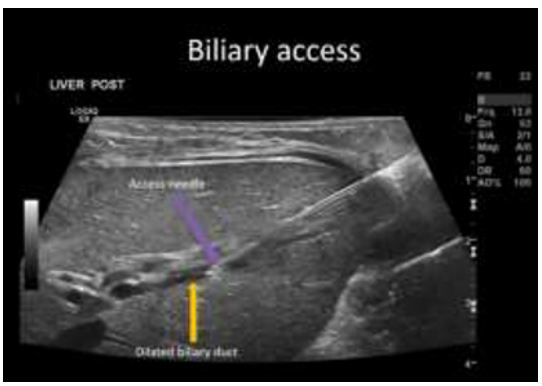

Poster #: EDU-060

Alternative Approaches to Nusinersen (Spinraza) Administration for Spinal Muscular Atrophy in Patients with Extensive Spinal Hardware

Scott Willard, MD[1], *mendocinos@yahoo.com*; Robin Kaye[1], Carrie Schaefer[1], David Aria, MD[1]; [1]Phoenix Children's Hospital, Phoenix, AZ

Disclosures: All authors have disclosed no financial interests, arrangements or affiliations in the context of this activity.

Purpose or Case Report: To describe alternative routes of Nusinersen administration in patients in whom traditional lumbar puncture is limited secondary to spinal hardware and bony fusion.
Methods & Materials: At our institution, we now have approximately 35 spinal muscular atrophy (SMA) patients receiving Nusinersen. Many type 2 and 3 SMA patients have severe scoliosis necessitating spinal fusion and rod placement. The associated new bone formation and bone grafts often preclude traditional lumbar puncture. In these patients, we order pre-procedure CT of the lumbar spine and MR of the cervical spine. Images are evaluated for possible trans-foraminal or cervical (C1-C2 or occiput-C1) puncture. Some institutions have reported the surgical creation of an access point for injection by drilling through the posterior bony mass. This places the patient at risk of surgery and the burr hole has a tendency to close up in time.
Results: In all patients with spinal fusion and hardware, a location for safe needle access was identified. Given our lack of comfort with transforaminal access initially, we began performing these with cone beam guidance. In time, we became comfortable with fluoroscopy alone. Additionally, we initially successfully performed three injections via cervical puncture. However, with the success of the transforaminal approach, these patients have now been converted to fluoroscopic transforaminal technique. In several patients, a small window in the otherwise fused posterior elements was identified by pre-procedure CT. Using 3D reconstructions, these windows were identified fluoroscopically and accessed via midline or interlaminar approach.
Conclusions: The presence of extensive bony fusion and spinal hardware should not preclude a patient from therapy or necessitate the surgical creation of an route for Nusinersen injection, given the available non-surgical alternative routes of administration. Cone beam CT is not generally needed, but may be reserved for difficult cases.

Poster #: EDU-061

Simplifying the Socket: A Guide to Creating Valuable Preoperative Hip CT Reports

Brittany Albers, MD[1] *brittany.albers@gmail.com*; ; [1]Pediatric Radiology, Mallinckrodt Institute of Radiology, St. Louis, MO

Disclosures: All authors have disclosed no financial interests, arrangements or affiliations in the context of this activity.

Purpose or Case Report: Femoroacetabular impingement (FAI) results from incongruence of the femoral head and acetabulum, and is a clinical diagnosis supported by imaging findings. Despite the traditional categorization of FAI into "pincer" and "cam" types in young and middle-aged adults, the etiology is often unclear with contributing factors from both sides of the hip joint, as well as the surrounding muscles and tendons. Many patients first become symptomatic during adolescence. Comprehensive early treatment, which includes both surgery and intensive physical therapy, both relieves symptoms and prevents the premature onset of osteoarthritis. Pediatric radiologists must provide relevant and actionable reporting on pre-operative imaging in order to maintain value. In addition to a descriptive assessment, the most commonly used quantitative measurements are acetabular version, α angle, and femoral version.
This image-rich exhibit reviews common acetabular and femoral morphologies associated with FAI , outlines our low-dose CT protocol, and simplifies obtaining proper reformations and measurements. At our institution, we utilize a low-dose CT protocol (equivalent to approximately 3-5 AP pelvis radiographs) for pre-operative planning, which allows for easy creation of the 2-D and 3-D reformatted images.

Normally, the acetabulum is anteverted 10-15 degrees to allow for physiologic movement. Decreased anteversion is correlated with pincer-type FAI. Measurement requires correction for pelvic tilt and is explained in Fig. 1. This method has been shown to be equivalent to the more complicated 3-D measurements.
The α angle is obtained from radial reformations. A normal α angle is 55-60 degrees or less, and an increased α angle is associated with cam-type FAI. Cam-type FAI most often results from deficient femoral head-neck offset in the anterosuperior quadrant, and α angles should be reported for each position in that quadrant. Creation of radial reformations and measurement of the α angle are explained in Fig. 2.
Assessing femoral version is important because many pediatric conditions that lead to FAI are associated with abnormal femoral version, including developmental hip dysplasia, Legg-Calve-Perthes disease, slipped capital femoral epiphyses, and septic arthritis/osteomyelitis. The femur is normally 10-20 degrees anteverted. Both decreased and increased femoral version are associated with FAI. The method for calculating femoral version is explained in Fig. 3.

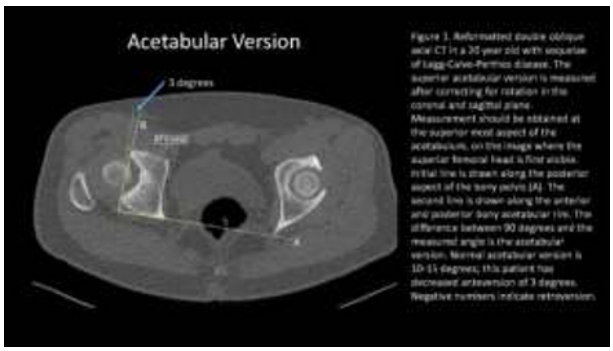

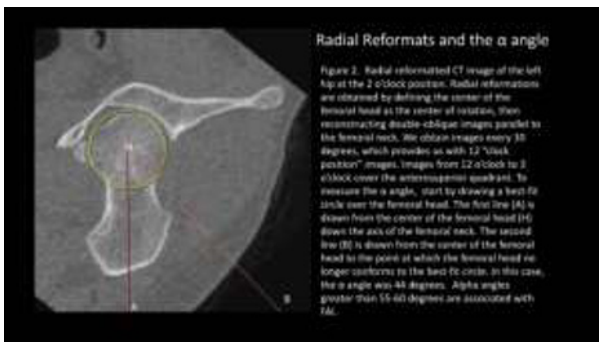

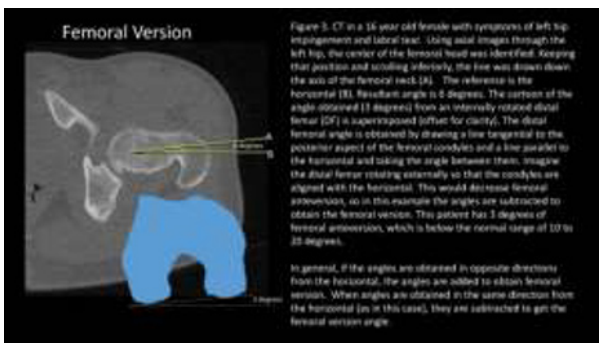

Poster #: EDU-062

ACL Reconstruction in the Pediatric Patient: What the Pediatric Radiologist Needs to Know

Aparna Joshi, MD[1], *ajoshi@dmc.org*; Kunal Kalra, MD[2]; [1]Pediatric Imaging, Children's Hospital of Michigan, Detroit, MI, [2]Pediatric Orthopedics, Children's Hospital of Michigan, Detroit, MI

Disclosures: All authors have disclosed no financial interests, arrangements or affiliations in the context of this activity.

Purpose or Case Report: The number of reconstruction surgeries of the anterior cruciate ligament (ACL) in pediatric patients has risen dramatically over the past two decades as a result of changes in treatment philosophy and perhaps frequency of injury. It is therefore important for pediatric radiologists to recognize the normal postoperative appearance of the different surgeries as well as their complications. This educational exhibit will review the types of reconstructive methods used in both skeletally immature and mature patients (physeal-sparing, partial transphyseal and transphyseal), complications (growth disturbances, graft failure, impingement, arthrofibrosis, intra-articular bodies) and relevant imaging findings on plain radiography and MRI.

Poster #: EDU-063

The Unique Patterns of Classic Metaphyseal Lesion Healing

Jared Shields, MD[1], *jarshie@iupui.edu*; Megan Marine, MD[1], Boaz Karmazyn, MD[1]; [1]Radiology, Indiana University School of Medicine, Brownsburg, IN

Disclosures: All authors have disclosed no financial interests, arrangements or affiliations in the context of this activity.

Purpose or Case Report: The Classic Metaphyseal Lesion (CML) is one of the most specific findings on skeletal surveys indicating child abuse. While there have been multiple studies to show the prevalence and specificity of the CML, very little has been published on the characteristic healing patterns.
The child protective team in our tertiary children's hospital reviews approximately 6,000 cases from all over the state every year. Many children with a positive skeletal survey will undergo a 14-day follow up survey.
The purpose of this study is to share our experience on patterns of CML healing by comparing the primary survey with its follow up. We have identified a few distinct patterns: Bone formation and sclerosis along the proximal metaphyseal zone, angular deformity of the metaphyseal corner, and subchondral metaphyseal lucencies. These patterns are represented by the accompanying supplemental figures and are described below.
Figure 1 is the 14-day follow up radiograph of an acute distal tibial CML diagnosed on the primary skeletal survey. This radiograph reveals increased sclerosis along the entire length of the metaphyseal zone, a common pattern of CML healing.
Figure 2 is 14-day follow up of a different patient who sustained a CML of the distal tibia. Healing in this case is denoted by the angular deformity and periosteal reaction along the metaphyseal corner.
Figure 3 is a radiograph of the left wrist from a patient's primary skeletal survey. The subchondral lucency identified along the lateral metaphysis is another common pattern indicative of a healing CML. Interestingly, the 14-day follow up skeletal survey of this patient demonstrated complete resolution of this finding with no signs of prior injury. In several other cases, the metaphysis on follow up exam appeared completely normal.
In summary, knowledge of the radiographic patterns of CML

healing can help to identify these lesions as their classic imaging characteristics change. It is also important to recognize that if the first radiograph demonstrates CML, a normal 14-day follow up radiograph does not exclude the diagnosis.

Figure 1

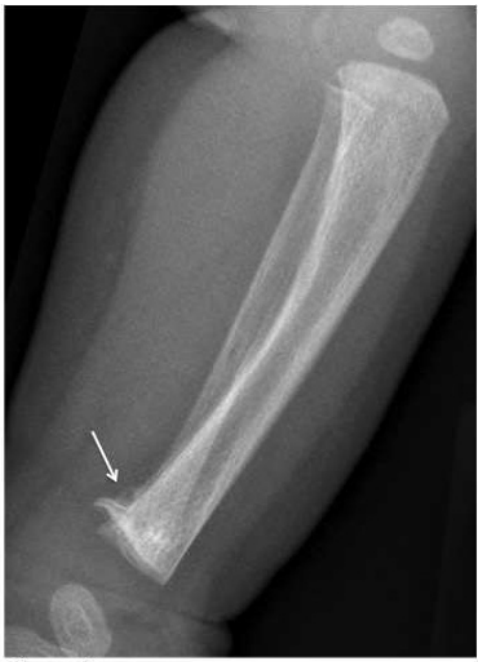

Figure 2

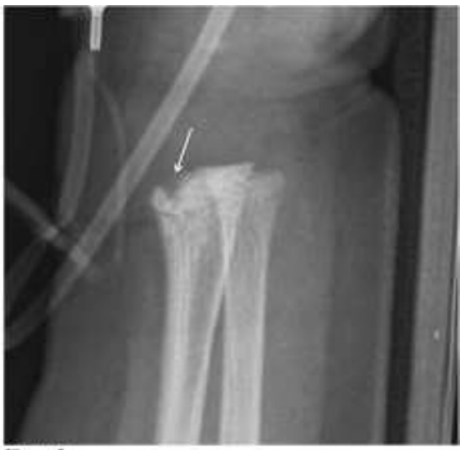

Figure 3

Poster #: EDU-064

Systematic Review on Diagnostic Accuracy of MRI for Assessment of Sacroiliac Joints in Children and Adults

Andrea Doria[1], *andrea.doria@sickkids.ca*; Vimarsha Swami, MD[1], Jacob Lester Jaremko, MD[2], Dax Rumsey, MD, FRCPC[2]; [1]Medical Imaging, University of Toronto, Toronto, ON, Canada, [2]University of Alberta, Edmonton, AB, Canada

Disclosures: All authors have disclosed no financial interests, arrangements or affiliations in the context of this activity.

Purpose or Case Report: Accurate and reproducible sacroiliac joint (SIJ) assessment on MRI in pediatric patients is challenging, often with high inter-observer variation. To facilitate consistent SIJ assessment, numerous scoring systems have been proposed. We sought to systematically review articles that evaluated diagnostic accuracy and reliability of existing MRI-based SIJ scoring systems for the evaluation of spondyloarthropathy in children and adults, and assess their applicability to pediatric patients.
Methods & Materials: Relevant studies were identified through a systematic literature search that included MEDLINE, EMBASE, and Cochrane Library Database. Studies reporting an element of diagnostic accuracy of an MRI-based SIJ scoring system were included: 1) reliability, 2) construct validity comparing MRI with other clinimetric measures, 3) criterion validity comparing MRI with a gold standard, and 4) ability of MRI to depict responsiveness to treatment. Canadian Task Force on Preventive Health guidelines were used to determine overall strength of recommendation (A-E) for scoring system utilization.
Results: From 38 eligible studies, 5 scoring systems were identified: the Spondyloarthritis Research Consortium of Canada (SPARCC) inflammation and structural scores, and the Leeds, Aarhus, and Berlin scoring systems. No scoring systems dedicated to pediatric patients were found, with none taking into account age-related changes of bone marrow. Only 1 study on the SPARCC scoring systems included pediatric patients, and was not dedicated to solely pediatric patients. Together the SPARCC scores had the highest number of studies reporting reliability (N=13), construct validity (N=10), and responsiveness (N=13). Good inter-observer reliability with intra-class correlation coefficients (ICCs) >0.8 was reported in 9/13 (69%) SPARCC inflammation, structural, 5/6 (83%) Berlin, 1/1 (100%) Leeds, and 0 Aarhus studies examining reliability. Seven (70%) studies demonstrated correlation between SPARCC scores and ESR, CRP, and standardized clinical severity indices. Twelve (92%) studies demonstrated decreases in SPARCC scores (lower scores = less severe disease) with treatment.
Conclusions: Currently no MRI scoring systems are available in the literature focusing on pediatric SIJ assessment. There is fair (grade B) evidence to recommend the use of the SPARCC method use, however adjustments are needed in this scale (e.g. grading for bone marrow changes over time) before routine use can be considered in pediatric patients.

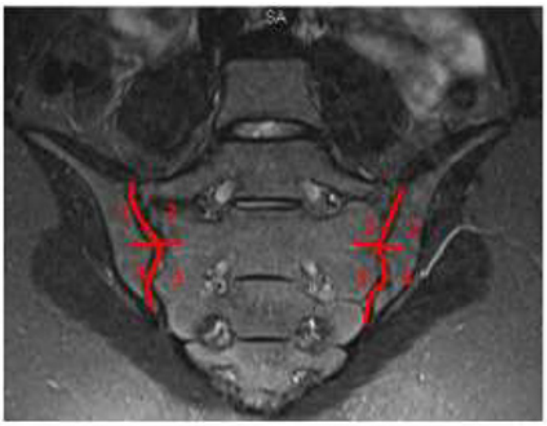

Conceptual framework of SIJ MRI standardized assessment tools. The SPARCC, Aarhus, Leeds, and Berlin methods all divide each SIJ into 4 quadrants (upper/lower iliac, upper/lower sacral). In the SPARCC method, BME and structural features (erosions, ankylosis, sclerosis, fat metaplasia) are scored in a binary fashion with 1 point = present, 0 points = absent. BME is also given additional points for high intensity (1 point) and increased depth >1cm (1 point) per slice. Maximum score per patient with SPARCC = 72, with 12 maximum points per coronal slice assessed on 6 consecutive slices. Berlin, Aarhus, and Leeds employ categorical assessment with increasing points given for mild, moderate, and severe features (both structural and inflammatory), with minor differences in point allocation between methods. Thresholds for what constitutes a positive examination for each scoring system have been described in the literature. SIJ = sacroiliac joint, BME = bone marrow edema

Poster #: EDU-065

Ultrasound Evaluation of Cervical Lymphadenopathy in Children

Lara Mrak[1], *lmrak@uwhealth.org*; Erica Riedesel, MD[2], Bradley Maxfield[1], Kara Gill, MD[1]; [1]University of Wisconsin, Madison, WI, [2]Emory University, Atlanta, GA

Disclosures: All authors have disclosed no financial interests, arrangements or affiliations in the context of this activity.

Purpose or Case Report: 1. Cervical lymphadenopathy is common in the pediatric population and is associated with a wide range of pathologies.
2. Ultrasound evaluation plays a critical role in distinguishing benign versus malignant etiologies.
3. Ultrasound characteristics can guide further management and potential interventions.
Case Discussion:
1. Normal cervical lymph nodes
2. Primary lymphoproliferative disorders
3. Metastatic disease
4. Granulomatous lymphadenitis
5. Reactive lymphadenopathy

Poster #: EDU-066

Coracoid Curiosities

Paige Sharp, MD[1], *pesharp@emory.edu*; Kiery Braithwaite, MD[1], Kelley Marshall, MD[1]; [1]Radiology, Emory University, Atlanta, GA

Disclosures: All authors have disclosed no financial interests, arrangements or affiliations in the context of this activity.

Purpose or Case Report: The coracoid process serves as a crucial anchor for multiple tendon and ligamentous attachments in the shoulder. While glenohumeral and labral pathology are more commonly implicated in shoulder injuries, the coracoid process can also be a primary pain generator within the shoulder. This educational poster will address normal coracoid anatomy and development, as well as pathologic conditions affecting the coracoid in the pediatric population, including fractures, infection, and neoplasm.
The coracoid is a beak-like projection that extends anteriorly from the ventral scapula. It serves as the origin for the pectoralis minor, coracobrachialis, and short head of the biceps. Ligamentous attachments extend from the coracoid to the clavicle (coracoclavicular ligaments), acromion (coracoacromial ligament), and humerus (coracohumeral ligament). Additionally, the transverse scapular ligament attaches to the coracoid base. The growth plate at the coracoid base is considered a “bipolar growth plate” and is made up of the primary ossification centers of the coracoid and the adjacent ventral scapula, similar to the tri-radiate cartilage of the acetabulum. The coracoid appears within the first year of life with fusion of the coracoid base growth plate occurring by age 14 to 15.
Physeal injuries occur at the base of the coracoid with imaging characteristics similar to other more typical locations (i.e. the proximal humerus in Little Leaguer’s shoulder). Key features include physeal widening with irregular bony margins, thought to be secondary to chronic repetitive pull from the attached musculature. Additionally, coracoid fractures occur in acute trauma and can be easily overlooked as they are frequently associated with other fractures. Direct blunt trauma by either an external object or the humeral head are associated with fractures of the base of the coracoid. Avulsions of the coracoid tip are seen with acromioclavicular separations with injury to the cocacoclavicular ligaments, more commonly seen in the pediatric population as the ligaments are relatively stronger than their osseous attachments.
While tumors of the coracoid are rare and more commonly occur in adults, primary tumors of the coracoid are seen in the pediatric population with case reports of osteoid osteomas, osteoblastomas, giant cell tumors, and aneurysmal bone cysts. Awareness of pathology affecting the coracoid process is helpful to the radiologist and clinician caring for the child with shoulder pain.

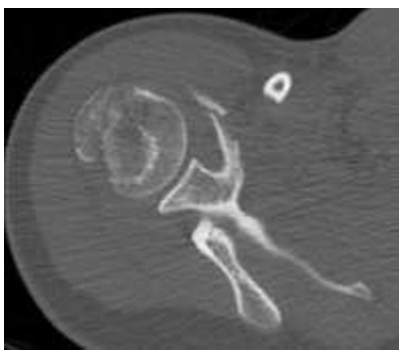

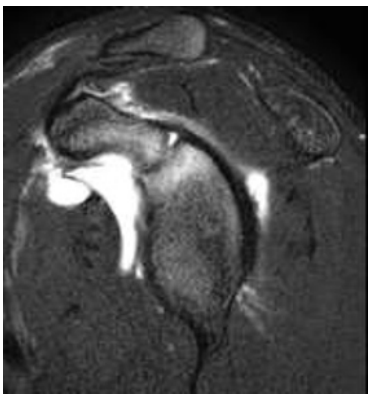

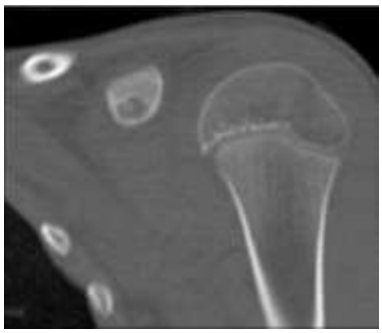

Poster #: EDU-067

Pediatric Fibrosing Diseases

Sarv Priya, MD[1], *sarv-priya@uiowa.edu*; Pankaj Watal[1], T. Shawn Sato[1], Yutaka Sato, MD[1]; [1]Pediatric Radiology, University of Iowa Hospitals & Clinics, Iowa City, IA

Disclosures: All authors have disclosed no financial interests, arrangements or affiliations in the context of this activity.

Purpose or Case Report: The prevalence of fibrosing diseases is uncommon in adult patients, and significantly more rare in the pediatric population. The spectrum of fibrosing diseases may be subdivided into two sub-categories: Inflammatory pseudotumors (IMT) and multifocal fibrosclerotic diseases. IMT has a predilection for visceral soft tissues and the most common sites of involvement include lung, abdominopelvic region, but virtually any site may be involved, including the somatic soft tissues, bone, larynx, uterus and CNS. Multifocal fibrosclerotic diseases encompasses retroperitoneal fibrosis, mediastinal fibrosis, reidel's thyroiditis, orbital pseudotumor, and sclerosing cholangitis to name a few. IMT's are predominantly neoplastic but may be post-traumatic or post-infectious. Fibrosclerosing diseases may be associated with inflammatory diseases (inflammatory bowel disease), autoimmune conditions (juvenile rheumatoid arthritis, systemic lupus erythematosus), malignant tumors (lymphoma), vasculitis and may arise secondary to drugs, toxins, trauma or radiation. Some may be idiopathic with no underlying cause.
The clinical presentation can be quite variable and often depends upon the site of involvement as well which adjacent structures are affected by the fibrosis.
Initial diagnosis can be suggested by imaging, but imaging findings are often non-specific. They can appear as mass forming and may be mistaken for more aggressive malignancy. Tissue is often needed for confirmation. Histopathology shows evidence of lymphocytic infiltration, activated fibroblasts, spindle shaped cells and granulation tissue.
The key issue for the pediatric radiologist is to be aware of these rare conditions and thus include them in their differential diagnosis. This diagnosis should be considered to avoid over aggressive biopsy, operation and chemotherapy. In addition, it may warrant work up for other associated fibrosing diseases in the appropriate clinical scenario.
In this presentation, we will provide a case based review of the features of pediatric inflammatory pseudotumors and fibrosclerotic diseases including myofibroblastic tumors, fibromatosis, fibrosarcomas, nodular and cranial fascitis as well as fibrotic conditions involving mediastinum, retroperitoneum, biliary tract and thyroid gland with their appropriate diagnostic work-up.
Our aim is to make people aware of these rare presentations, so that they are not lost in the long differential!

Poster #: EDU-068

Ultrasound for problem solving in pediatric musculoskeletal emergencies

Timothy Alves, MD[1], *talves@med.umich.edu*; Ramon Sanchez[1]; [1]Radiology, University of Michigan, Ann Arbor, MI

Disclosures: All authors have disclosed no financial interests, arrangements or affiliations in the context of this activity.

Purpose or Case Report: While radiographs, and to a lesser extent MRI, remain the mainstay imaging techniques for the evaluation of pediatric musculoskeletal emergencies, ultrasound can be a useful modality for problem solving. The purpose of this educational exhibit is to provide several illustrative cases in which ultrasound was helpful in clinical/diagnostic problem-solving in order to emphasize the importance of ultrasound in these scenarios and to ultimately improve diagnostic accuracy and efficiency.
Methods & Materials: Illustrative cases demonstrating the utility of ultrasound in problem-solving pediatric musculoskeletal emergencies were chosen from those seen in clinical practice at a tertiary care academic medical center. Examples include the use of ultrasound to differentiate shoulder and elbow dislocation from epiphysiolysis, for the detection of radiographically occult fractures, for the detection of osteomyelitis/brodie's abscess and subperiosteal abscess, for the evaluation of nursemaid's elbow, for the detection of classic metaphyseal lesions, and for the detection of pelvic apophyseal avulsion injury.
Results: Review of these illustrative cases highlights the important role of ultrasound in the evaluation of pediatric musculoskeletal emergencies and can improve the accuracy and efficiency of diagnosis.
Conclusions: A pictorial review of illustrative cases in which ultrasound was instrumental in problem-solving pediatric musculoskeletal emergency cases can improve the accuracy of interpretation and efficiency of diagnostic work-up.

Poster #: EDU-069

Clinical-Genetic-Imaging Review of Autoinflammatory Diseases in Children: Single-Center Experience

Alaa Alsharief, MBBS, SB-Rad[1], *a.alsharief@hotmail.com*; Ronald Laxer[1], Jennifer Stimec[1], Paul Babyn[2], Carina Man[3], Andrea Doria[1]; [1]University of Toronto, Toronto, ON, Canada, [2]University of Saskatoon, Saskatoon, SK, Canada, [3]Hospital for Sick Children, Toronto, ON, Canada

Disclosures: Ronald Laxer has indicated a relationship with Novartis, Sobi, Sanofi and Lilly as a consultant/honoraria. All other authors have disclosed no financial interests, arrangements or affiliations in the context of this activity.

Purpose or Case Report: 1. To review the contemporary literature and present an updated list of musculoskeletal and non-musculoskeletal imaging findings of patients with autoinflammatory diseases in our hospital. Most of these patients are found to have a genetic mutation that is responsible for their disease.
2. To present follow-up imaging findings, when available, and correlate those with patients' symptoms and type of treatment administered in approximately 40 patients with autoinflammatory diseases such as Cryopyrin-associated autoinflammatory syndrome, familial Mediterranean fever, PAPA (pyogenic arthritis, pyoderma gangrenousum, and acne) syndrome and much more. These findings can be related to

disease progression, treatment response or treatment-induced changes.

6-year-old male, known case of Muckle-Wells syndrome, presented with right scrotal palpable mass

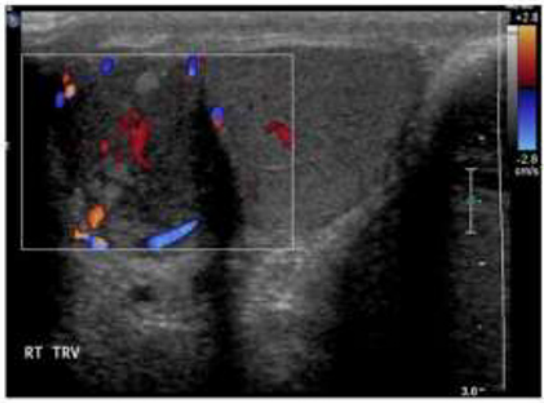

Right scrotal transverse ultrasound image demonstrates an extra-testicular intra-scrotal heterogeneously hypoechoic vascular lesion. The testicle was normal. Excisional biopsy showed granulomatous inflammation and granulomatous vasculitis

13-year-old male with right knee swelling and pain- patient is known to present with PAPA syndrome

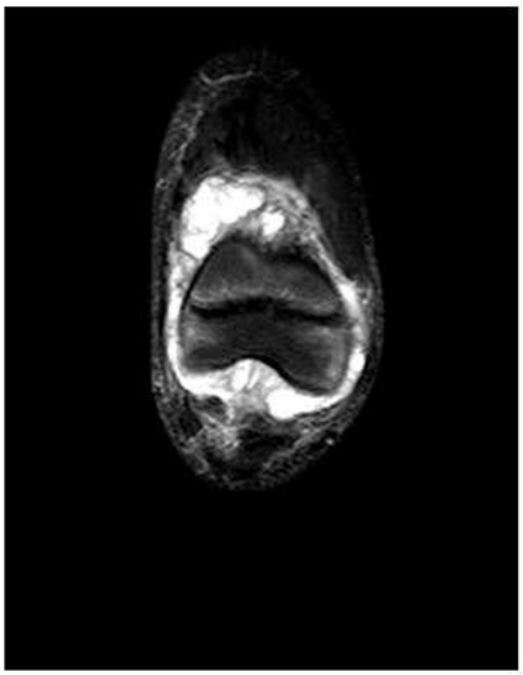

Coronal STIR through the anterior aspect of the right knee demonstrates moderate knee effusion with synovial thickening. Note the surrounding soft tissue edema.

8-week-old baby girl presents with abdominal distension and fever. Radiographs demonstrated markedly dilated bowel loops. To look for stenosis/ stricture

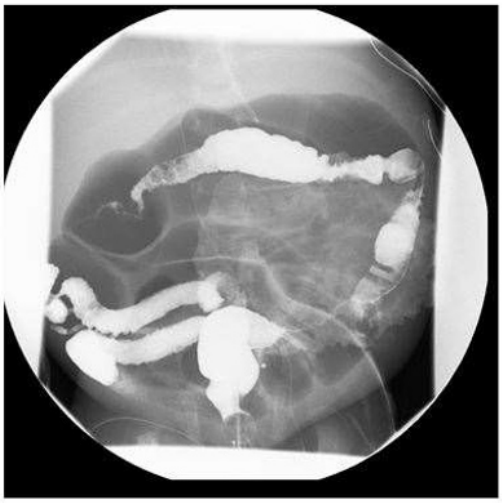

Frontal fluoroscopic view of lower GI contrast study with filling of the colon and terminal ileum. The image demonstrates mildly reduced caliber of the colon with multiple areas of wall irregularities. Terminal ileum demonstrates wall irregularity as well. Decompensating ileostomy was performed and intra-operative biopsies of the terminal ileum and colon showed acute on top of chronic inflammation with crypts remnants and apoptotic ileitis. Multiple endoscopic biopsies from the duodenum and stomach showed acute on top of inflammation. Note the massively dilated small bowels at the center of the abdomen.
DX: Early onset IBD- ulcerative colitis

Poster #: EDU-070 - *Withdrawn*

Poster #: EDU-071

Cerebral Blood Perfusion Reserve Assessment in Pediatric Sickle Cell Disease using ASL MRI and Acetazolamide Challenge

Cory Pfeifer, MD[1], *cpfeifer2018@gmail.com*; Jeffrey Miller[2]; [1]Diagnostic Radiology, University of Texas Southwestern Medical Center, Dallas, TX, [2]Phoenix Children's Hospital, Phoenix, AZ

Disclosures: All authors have disclosed no financial interests, arrangements or affiliations in the context of this activity.

Purpose or Case Report: Chronic cerebrovascular disease is common in pediatric sickle cell patients, and these children often require serial imaging to assess cerebral blood flow perfusion. ASL MRI has been shown to be an effective technique to assess cerebral blood flow, but the evaluation of perfusion reserve is also of value to ordering clinicians. This educational exhibit describes the use of the vasodilator acetazolamide to gauge potential changes in perfusion as determined by ASL MRI. The biochemical basis for cerebrovascular autoregulation and mechanism of acetazolamide are discussed.
Methods & Materials: Conventional MRI and Time-Of-Flight MRA is performed, and baseline cerebral blood flow perfusion is evaluated using dynamic pseudo-continuous Arterial Spin Labeling (pCASL). Acetazolamide (15 mg/kg) is given intravenously over a 3-5 minute period, and additional pCASL images are acquired 10-15 minutes after injection. Intravenous contrast is not given. Perfusion maps are calculated and compared. Cerebrovascular reserve is defined as the change in perfusion divided by the baseline perfusion.

Results: Perfusion changes in response to acetazolamide occur in three patterns. In the first, there is normal blood flow at baseline with acetazolamide-induced increased perfusion. Patients with the second pattern have a decreased baseline perfusion, but the vasodilator improves flow. In the third pattern, there is also a decreased baseline perfusion, but acetazolamide exacerbates the relative regional blood flow deficit. In the third pattern, the chronically ischemic territory is felt to be perfused by vessels that are already maximally dilated, and the apparent paradoxical response to the vasodilator is due to a steel phenomenon.
Conclusions: Acetazolamide challenge is a useful technique in the diagnostic evaluation of pediatric sickle cell patients with chronic cerebrovascular disease. Arterial-spin labeling obviates the need for intravenous contrast which is an important factor in the sickle cell population due to the inherent renal vulnerability of these patients.

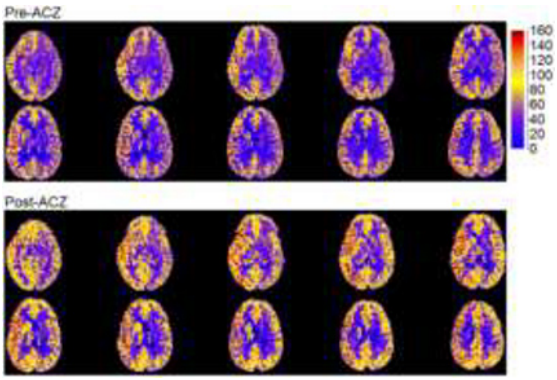

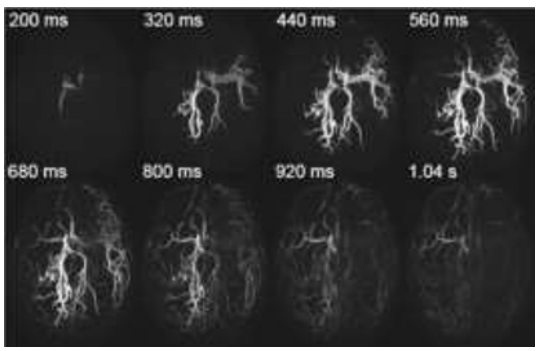

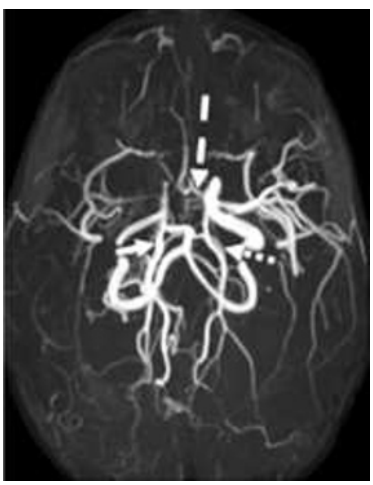

Poster #: EDU-072

Optimizing pediatric leptomeningeal metastasis detection: technical considerations

Julie Harreld, MD[1], *julie.harreld@stjude.org*; Muhammad Ayaz, PhD[1], Claudia Hillenbrand[1], Ralf Loeffler[1], Zoltan Patay, MD, PhD[1]; [1]Diagnostic Imaging, St. Jude Children's Research Hospital, Memphis, TN

Disclosures: All authors have disclosed no financial interests, arrangements or affiliations in the context of this activity.

Purpose or Case Report: Detection of leptomeningeal metastasis (LM) is critical to staging and prognosis of childhood CNS cancers like medulloblastoma and ependymoma. [1] Though CSF examination is the historical gold standard for diagnosis, technological advances have earned MRI a central role in metastasis detection; recent work finds MRI more predictive of survival than CSF analysis. [2-4] However, not all sequences are created equal for detection of tumor in the CSF, and pediatric MR imaging presents additional unique challenges such as patient motion, acoustic noise and scan time reduction. In this exhibit, we discuss the strengths and weakness of common sequences for LM detection; technical alternatives for reduction of motion, acoustic noise and scan time; and present a suggested targeted imaging protocol based on current best imaging practice.
With visual examples, we will discuss:
1. Signal characteristics of LM and role of complementary sequences for detection
2. Optimizing scan planes and slice thickness for tumor/metastasis location and patient size
3. Strengths and weaknesses of T1 FLAIR, SE, FSE/TSE, gradient echo and ultrafast spoiled gradient echo (VIBE/FAME/LAVA/THRIVE) sequences in terms of time, resolution, SNR and CSF artifact
4. Utility and optimization of post-contrast FLAIR, DWI, TrueFISP/bSSFP, and subtraction images for metastasis detection
5. Reducing imaging time: targeted sequences, k-space undersampling (HASTE, partial Fourier imaging), parallel imaging
6. Reducing acoustic noise: lowering bandwidth, longer echo spacing, modified gradient wave forms, alternate encoding (PETRA, SWIFT, zero-TE)
7. Reducing motion artifact: 2D vs. 3D, non-Cartesian acquisition schemes, motion correction
References:
1. Engelhard HH, Corsten LA. *Cancer Treat Res* 2005;125:71-85
2. Maroldi R, Ambrosi C, Farina D. *Eur Radiol* 2005;15:617-626
3. Pang J, Banerjee A, Tihan T. *Journal of neuro-oncology* 2008;87:97-102
4. Terterov S, Krieger MD, Bowen I, et al. *J Neurosurg Pediatr* 2010;6:131-136
Figure: Spine imaging at 3 Tesla. (a) Axial post-contrast T1-weighted VIBE images reconstructed at 3mm/0 gap show leptomeningeal metastasis to excellent advantage, without CSF pulsation artifact which obscures the same metastasis on axial (b) T1 TSE (3mm/0.3mm gap) with contrast. Metastasis was confirmed by CSF analysis.

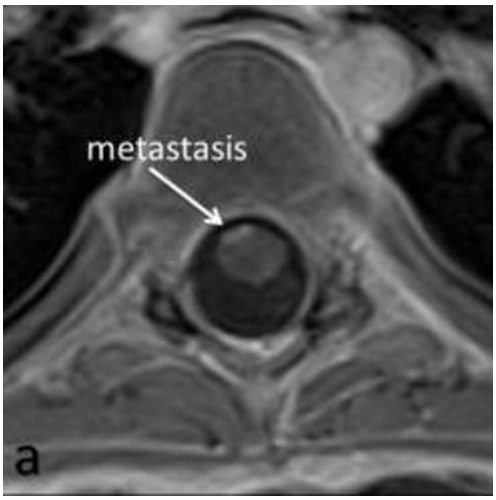

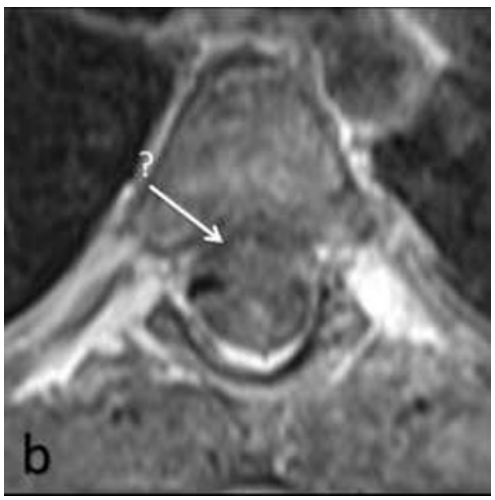

Poster #: EDU-073

Narrowing the differential diagnosis in pediatric patients with basal ganglia calcification based on associated musculoskeletal imaging findings

Lauren Averill, MD[1], *laverill@nemours.org*; Achala Donuru, MD[2], Vinay Kandula[1]; [1]Nemours Children's Health System, Wilmington, DE, [2]Thomas Jefferson University Hospital, Philadelphia, PA

Disclosures: All authors have disclosed no financial interests, arrangements or affiliations in the context of this activity.

Purpose or Case Report: The purpose of educational exhibit is to summarize the radiological appearances of various conditions causing basal ganglia (BG) calcification in children. The pathogenesis for symmetric BG calcification is diverse and ranges from benign physiological calcifications to a variety of pathological disorders including metabolic, infectious and genetic diseases. We present a practical approach to further narrow the differential diagnosis based on associated musculoskeletal imaging findings in patients with BG calcification.
Parathyroid disorders are the most common causes of pathological BG calcification. In hyperparathyroidism, distinctive subperiosteal bone resorption can be seen in phalanges on hand radiographs. Tapering of the clavicles, brown tumors and salt-and-pepper appearance of the skull are also classic radiographic features. In the Albright hereditary osteodystrophy phenotype of pseudohypoparathyroidism, shortening of the fourth and fifth metacarpals as well as advanced bone age can aid in diagnosis. Tumoral calcinosis is another radiographically distinct disease that can cause BG calcification, characterized in the extremities by periarticular calcific deposits. Cockayne syndrome is a rare autosomal recessive (AR) disorder with 4 overlapping subtypes, all with BG calcification as well as diffuse skeletal abnormalities that become apparent in the toddler years. Carbonic anhydrase deficiency type 2 is another rare AR disorder with intracranial calcification including the BG, as well as osteopetrosis and pathologic fractures. Coat's plus syndrome has characteristic rock-like intracranial calcifications paired with leukodystrophy and brain cysts. It manifests skeletally with osteopenia, delayed fracture healing, bowing of long bones, scoliosis, midface hypoplasia and femoral head avascular necrosis. Other common conditions such a Down syndrome and HIV, and rare disorders such Fahr's disease, malignant phenylketonuria, and Aicardi-Goutieres syndrome are in the differential diagnosis of BG calcifications.

Poster #: EDU-074

Sinonasal Tumors and Tumor-mimics in Children

Anjeza Chukus[1], *anjac18@gmail.com*; Arastoo Vossough, PhD, MD[2], Hisham Dahmoush, MD[1]; [1]Stanford University, Redwood City, CA, [2]Children's Hospital of Philadelphia, Philadelphia, PA

Disclosures: All authors have disclosed no financial interests, arrangements or affiliations in the context of this activity.

Purpose or Case Report: Sinonasal tumors in the pediatric population are uncommon. Tumors affecting the nasal cavity and paranasal sinuses in children can arise from either soft tissue or bony structures and differ substantially from adult sinonasal masses. The aim of our exhibit is to review imaging features of a myriad of sinonasal neoplasms and tumor-like masses unique to the pediatric population ranging from the more well-known rhabdomyosarcoma and Ewing's sarcoma to rarer lesions such as desmoplastic fibroma, nasal chondromesenchymal hamartoma, and melanotic neuroectodermal tumor of infancy.
Methods & Materials: A multimodality diagnostic imaging approach to sinonasal masses utilizing high-quality representative images with emphasis on CT and MRI will be highlighted. Histopathologically-proven cases from two large teaching children's hospitals will be presented encompassing an array of imaging modalities.
Results: 1. Highlight imaging features of tumors in the nasal cavity and paranasal sinuses that present in children either from soft tissue or bony origins. Lesions include but will not be limited to: melanotic neuroectodermal tumor, rhabdomyosarcoma, leukemia, lymphoma, pPNET/Ewing's sarcoma, nasal glioma, giant cell granuloma, nasal chondromesenchymal hamartoma, and lobular capillary hemangioma.
2. Distinguish benign and malignant sinonasal lesions in children and demonstrate cases where imaging features may overlap.
3. Review relevant anatomic landmarks and complications of sinonasal tumors such as invasion of adjacent critical structures and neurovascular involvement.
Conclusions: Sinonasal tumors are uncommon in children. They often present with nonspecific symptoms of nasal obstruction, pain, nasal secretions, or epistaxis. Imaging plays a crucial role in narrowing down the differential diagnosis when a child presents with clinical signs and symptoms referable to the sinonasal region. This review aims at familiarizing radiologists with the diagnostic possibilities in the pediatric population and raises awareness of the salient radiologic features.

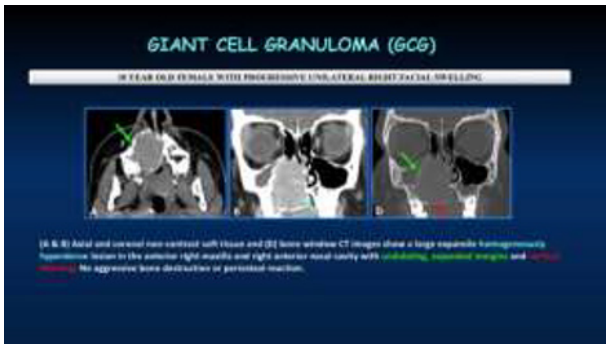

Poster #: EDU-075

Genetic Perforin Defect and Immunopathology: CNS Involvement and Imaging Manifestations

Alec Hedlund[2], *alec.hedlund@gmail.com*; Sara Stern, MD[3], John Bohnsack, MD[3], Gary Hedlund, DO[1]; [1]Primary Children's Hospital, Salt Lake, UT, [2]Boise State University, Boise, ID, [3]University of Utah, Salt Lake City, UT

Disclosures: All authors have disclosed no financial interests, arrangements or affiliations in the context of this activity.

Purpose or Case Report: To familiarize the pediatric radiologist with the important role that the perforin gene plays in lymphocyte cytotoxicity, to discuss the diversity in clinical presentation, and review the scope of neuroimaging abnormalities that may arise in the setting of a missense perforin genetic defect. The brain MRI findings and relevant clinical information of two remotely related children with the same novel missense mutation in the perforin gene represent the basis of this educational poster.

Perforin is a glycoprotein (encoded by the PRF-1 gene) involved in several human cellular functions, including, immune response and stored mainly in CD8-positive T-cells as well as natural killer (NK) cells. Normally, T-cells and NK cells are responsible for attacking dead cells. In the clinical setting of perforin deficiency, T-cells and NK cells attack the healthy immune system. This arises from a missense mutation of the PRF-1 gene. Links between perforin deficiency and the autoimmune clinical syndrome of hemophagocytic lymphohistiocytosis (HLH), have been reported.

MR imaging abnormalities in patients with perforin gene mutations, are diverse and complex as the defect may occur in the setting of familial hemophagocytic lymphohistiocytosis, primary necrotizing lymphocytic CNS vasculitis or associated with CNS infections such as the Epstein Barr virus.

To date, MRI abnormalities that have been reported include mimics of septic cerebral emboli, confluent white matter abnormalities involving the cerebral hemispheres and cerebellum invoking the consideration of diffuse demyelinating disease, and multifocal infratentorial and supratentorial intraaxial lesions with "necrotic-like" character and marginal enhancement. Multifocal sites of perivascular space pathological enhancement has also been reported. Common to many of these reports is cerebellar involvement.

The imaging differential diagnosis includes atypical infection, histocytic disorders of the CNS, lymphomatous granulomatosis, neurosarcoidosis, and primary CNS lymphoma.

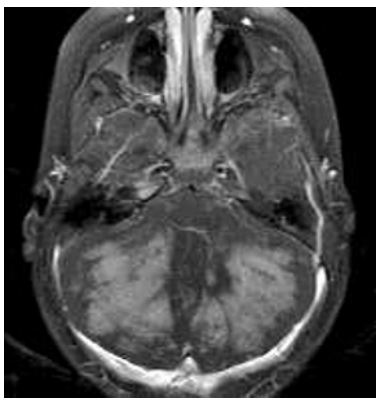

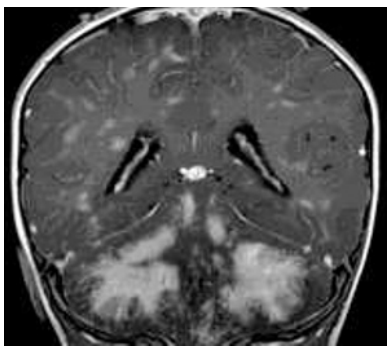

Poster #: EDU-076

Developmental abnormalities of the cerebral cortex: Simplifying a complex group of pathologies

Joshua Finkle, MD[1], *Joshua.Finkle@uchospitals.edu*; Thomas Tullius[1], Ariyan Javadi[1], Carina Yang, MD[1]; [1]Radiology, University of Chicago, Chicago, IL

Disclosures: All authors have disclosed no financial interests, arrangements or affiliations in the context of this activity.

Purpose or Case Report: Abnormalities of cortical development include a complex and often bewildering variety of pathologies. With substantial overlap in both imaging appearance and terminology, many radiology trainees and other

healthcare providers find these entities can be difficult to learn and efficiently retain. We aim to present a clear and streamlined approach to organizing these disorders within a differential. In the process we use high resolution imaging and original artwork to provide:
- A basic overview of the major steps of cortical development.
- A simplified classification of developmental abnormalities based on the affected stage of development.
- An overview of the underlying pathology, imaging appearance, and clinical relevance of each entity discussed.
- Tips for distinguishing malformations with similar imaging appearances and for understanding the nomenclature used in describing the abnormalities.
- Discussion of new and future imaging techniques for evaluating these lesions, including 3T and 3D DIR techniques.

OUTLINE:
- Cortical development: A basic overview
- Disorders of cell proliferation
— Microcephaly and cortical-related findings
— Hemimegalencephaly
— Focal non-neoplastic processes
— — Focal cortical dysplasia
— — Cortical hamartomas
— Cortical neoplasms
— — Ganglioglioma and gangliocytoma
— — DNET
- Disorders of neuronal migration
— The lissencephalies
— Gray matter heterotopia
- Disorders of cortical organization
— Polymicrogyria
— Schizencephaly

Poster #: EDU-077

Neurocristopathies: An embryological link between seemingly unrelated conditions throughout the body

Atsuhiko Handa[1], *atsuhiko-handa@uiowa.edu*; Sarv Priya, MD[1], T. Shawn Sato[1], Yutaka Sato, MD[1]; [1]Department of Radiology, University of Iowa Hospitals and Clinics, Iowa City, IA

Disclosures: All authors have disclosed no financial interests, arrangements or affiliations in the context of this activity.

Purpose or Case Report: Neurocristopathies are a group of disorders characterized by a common origin in aberrant neural crest development. These include common pediatric disorders such as Hirschsprung's disease, Treacher Collins syndrome, Di George syndrome, MEN type 2A/2B as well as common pediatric tumors such as neuroblastoma, pheochromocytoma, Ewing's sarcoma, neurofibromatosis, medullary carcinoma of the thyroid and melanoma.
Neural crest cells are derived from discrete cell masses that arise at the junction between the neural and epidermal ectoderm in neurula-stage vertebrate embryos. Neural crest cells migrate extensively in an organized manner and spread widely throughout the body. Derivatives of neural crest cells include Schwann cells in the leptomeninges, nerve root ganglia in the central nervous system, thyroid C cells, bone formation in the mandible and skull base, dermis of the head and neck, myenteric nerve plexuses of the intestines, pigment cells of the skin, paravertebral sympathetic ganglia, and adrenal medulla cells. Developmental disturbances of the neural crest cells give rise to a variety of disorders as listed above and have collectively been termed neurocristopathies by Bolande in 1974. Patients with one neurocristopahty have an increased risk of having other neurocristopathies. Familial inheritance has also been shown. There is a variability in the combinations of lesions found in the same patient or family.Recent advances in genetics and developmental biology have provided deeper insights into these collection of conditions. New technologies in biology including iPS cell technology are expected to further advance our understanding of neurocristopathies.
Methods & Materials: 1. Review normal neural crest development and embryological basis of neurocristopathies
2. Demonstrate various manifestations of neurocristopathies by providing example cases
Results: Review of the embryological origin of neurocristopathies, and how these developmental abnormalies can lead to various manifestations by providing example cases.
Conclusions: Neurocristopathies are common among pediatric populations. However, the concept of neurocristopathies is not well known among pediatric radiologists. These diverse set of disorders seem unrelated; however, they share common developmental origin and certain imaging features. Understanding the embryological origins of these spectrums of conditions as well as their imaging appearance enables deeper understanding of these common pediatric disorders and associated conditions.

Poster #: EDU-078

Baby Got Back: Review of Neonatal Spine with MRI Correlation

Jeffrey Poot, DO[1], *pootjd2@upmc.edu*; Subramanian Subramanian, MD[1], Serter Gumus, MD[1], Judy Squires, MD[1]; [1]Children's Hospital of Pittsburgh of UPMC, Pittsburgh, PA

Disclosures: All authors have disclosed no financial interests, arrangements or affiliations in the context of this activity.

Purpose or Case Report: Ultrasound is a common screening examination performed in infants prior to closure of osseous posterior elements. Although radiologists with pediatric neuroradiology subspecialty training may be very familiar with many abnormalities encountered sonographically, pediatric radiologists without pediatric neuroradiology subspecialty training are often less familiar. Further, the ultrasound appearance of abnormalities of infant spine may be less well known than appearance on MRI. The purpose of this educational review is to demonstrate normal appearance of infant spine and illustrate abnormalities that are frequently and infrequently encountered during screening ultrasound evaluation, with MRI for comparison.
Methods & Materials: An institutional review was conducted to identify neonatal patients with abnormal spine ultrasounds and subsequent MRI examinations. Imaging findings were correlated with clinical signs and symptoms, as well as treatment when available.
Results: A spectrum of congenital and acquired cases are presented including simple tethered cord, closed spinal dysraphism (dorsal dermal sinus, lipomyelomeningocele, diastematomyelia), open spinal dysraphism (meningocele, myelomeningocele), dermoid cyst, spinal lipoma, infantile hemangioma, sacrococcygeal teratoma, caudal regression syndrome, and hematoma. Cutaneous stigmata of spinal dysraphism are reviewed as well.
Conclusions: It is important to recognize sonographic appearance of normal and abnormal neonatal spine to appropriately diagnose and/or properly route to MRI for further evaluation.

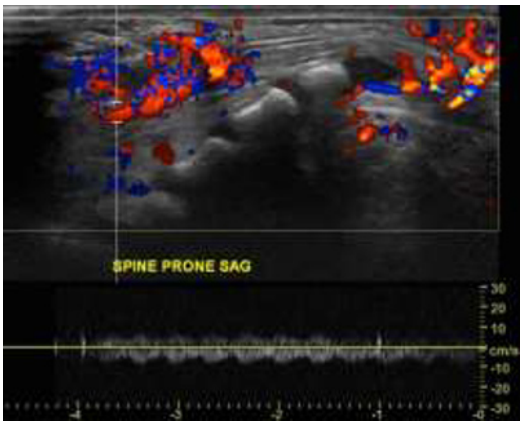

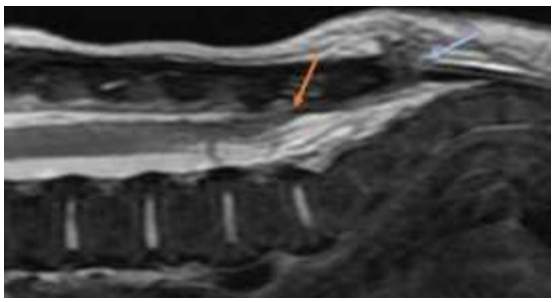

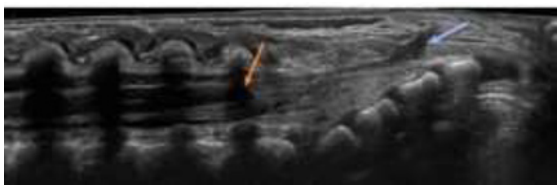

Poster #: EDU-079

Spectral Multi-energy Computed Tomography; Preliminary Experience in Pediatric Neuroradiology

Dianna Bardo, MD[1], *dbardo@phoenixchildrens.com*; Richard Southard, MD[1], Carla Williams, RT[1], Robyn Augustyn, BSRT RT(R)(CT)[1], Marrit Thorkelson[1], John Curran, MD[1], Jeffrey Miller[1], Lingyun Chen, PhD[1]; [1]3D Innovation Lab, Phoenix Children's Hospital, Phoenix, AZ

Disclosures: Robyn Augustyn has indicated a relationship with Koninklijke Philips, NV as a consultant and a speaker. Richard Southard has indicated a relationship with Philips Healthcare for consultant/ honoraria, speaking and receiving a research grant. All other authors have disclosed no financial interests, arrangements or affiliations in the context of this activity.

Purpose or Case Report: Spectral or multi-energy CT (MECT), obtains raw data at more than one energy spectra which allows the decomposition of materials into their constituent elements. As opposed to conventional CT which yields data based on linear attenuation, MECT yields both structural and material-specific information. Only limited experience and literature are available regarding use and applications of MECT in the pediatric patient population. Our institution has recently installed a spectral MECT scanner which uses a single x-ray source modified multilayered detector CT, in our emergency department (ED). It is currently the only such scanner used for routine clinical pediatric imaging in the US, and 4th such unit in a children's hospital in the world. In this educational exhibit we will review the basic physics of MECT, the benefits and limitations of the single-source multi-layered detector geometry, and clinical applications of MECT and our experience to date in the pediatric population.

Methods & Materials: An IQon Spectral MECT (Philips Healthcare, Cleveland, OH) was installed in our facility in October, 2017. Though positioned in the ED, routine inpatients and outpatients are also examined.

Results: We present brain, spine, facial trauma, and neck cases in which MECT aided in diagnosis through use of spectral data and propose areas of further clinical diagnoses and research. Clinical cases thus far examined include children suffering acute trauma, headache, and tumor.

Features of MECT advantageous to pediatric patients include reconstruction of virtual non-contrast images, perfusion imaging, mitigation of beam-hardening artifact with high mono-energetic imaging, the use of low mono-energetic imaging to boost iodine density to improve angiographic images which may be limited by contrast or bolus timing, and urinary stone analysis and renal mass characterization.

Conclusions: The use of Spectral MECT at our institution has provided a significant advance in our ability to confidently diagnose various disease processes. As we gain more experience in the use of MECT in the pediatric population, we will be able to better define its role and uncover further areas of research.

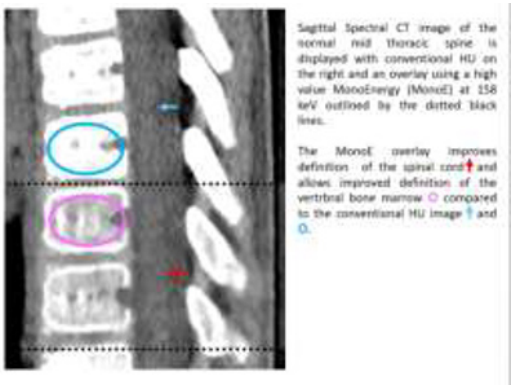

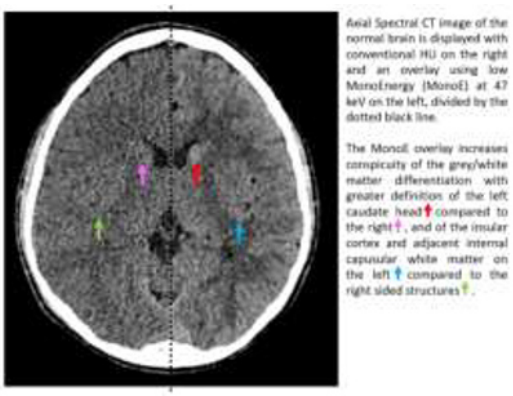

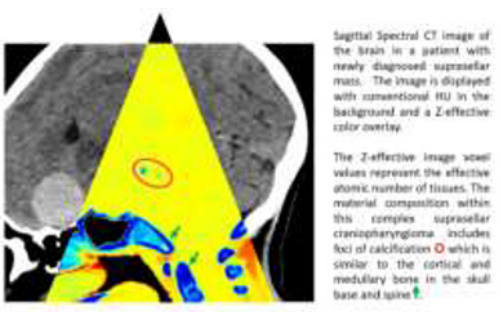

Poster #: EDU-080

Pediatric neurosurgical shunts: a primer for the radiologist and radiology resident

Gregory Vorona, MD[2], *gregory.vorona@vcuhealth.org*; Shareh Hallaji[1], John Collins[2], Ann Ritter[2], Gary Tye[2]; [1]Radiology, Virginia Commonwealth University, Richmond, VA, [2]The Children's Hospital of Richmond at Virginia Commonwealth University, Richmond, VA

Disclosures: All authors have disclosed no financial interests, arrangements or affiliations in the context of this activity.

Purpose or Case Report: Shunts are near-ubiquitous in the world of pediatric neuroimaging, and it is incumbent on radiologists who interpret pediatric neuroimaging to have a basic understanding of the different shunt types and components. In this educational poster we will review the appearance of a shunt with its three parts. We will correlate this to the imaging appearance of different shunt valves (programmable and non-programmable), and appropriate proximal and distal catheter positioning. We will describe the more common complications (i.e. shunt failure, subdural collections, slit ventriclular syndrome, etc.) associated with shunts in pediatric patients. The poster will also briefly highlight some of the relative advantages and disadvantages of computed tomography (CT) and magnetic resonance (MR) imaging in the assessment of hydrocephalus.

Poster #: EDU-081

Quiz Yourself! Imaging Features of Phakomatoses

Amy Farkas, MD[1], *afarkas@umc.edu*; Jeffrey Hooker, MD[1], David Joyner[1]; [1]Department of Radiology, University of Mississippi Medical Center, Jackson, MS

Disclosures: All authors have disclosed no financial interests, arrangements or affiliations in the context of this activity.

Purpose or Case Report: The phakomatoses, or neurocutaneous syndromes, are the classically described congenital disorders with involvement of structures derived from the ectoderm. While the cutaneous manifestations of these conditions often establish their diagnosis, imaging characteristics can indicate the extent of disease and signify prognosis and potential complications related to the disorders. This educational poster reviews key multimodality imaging features and examples of infrequently encountered phakomatoses, including Sturge-Weber, von-Hippel Lindau disease, hereditary hemorrhagic telangiectasia, neurocutaneous melanosis, PHACES syndrome, basal cell nevus, and Parry-Romberg in pediatric patients. This case-based review of these syndromes will focus on relevant imaging findings with self-testing. After this electronic exhibit, residents will be able to describe the common imaging features of the less common phakomatoses.

Poster #: EDU-082

Mimics of hypoxic ischemic encephalopathy: Infectious, metabolic, congenital, Oh My!

Anne Misiura, MD[1], Jaqueline Urbine[1], Mea Mallon[1], Archana Malik[1], Faaiza Kazmi[1], Erica Poletto, MD[1]; [1]Radiology, St. Christopher's Hospital for Children, Philadelphia, PA

Disclosures: All authors have disclosed no financial interests, arrangements or affiliations in the context of this activity.

Purpose or Case Report: Hypoxic-ischemic encephalopathy is a potentially devastating neurological diagnosis for which prompt recognition is crucial for patient management. The appearance of HIE on imaging depends on the duration and severity of the hypoperfusion injury, which can range from global to subtle. As such, the differential diagnosis is wide, including infectious, metabolic, and congenital dysmyelination causes. It is also critical for the pediatric radiologist to be aware of possible confounding cases when presented with imaging features seen in HIE which would significantly change management.
Methods & Materials: A retrospective analysis of multimodality imaging in neonatal patients demonstrating imaging features similar to that of HIE with alternative diagnoses, who presented to an urban children's hospital since 2005 is performed. Imaging and clinical history are correlated with laboratory findings where applicable. A variety of HIE mimics are selected for imaging review.
Results: Review of mimics of HIE is provided with imaging examples. Examples include infectious, metabolic, and other disorders, including, but not limited to herpes infection, parechovirus infection, non-ketotic hyperglycemia, neonatal hypoglycemia, and disorders of myelination.
Conclusions: While HIE in itself is a crucial diagnosis to make, it is important for the pediatric radiologist to be familiar with the differential diagnoses that can mimic the findings of HIE, many of which require prompt recognition to improve patient outcomes.

Poster #: EDU-083

Intrathecal Baclofen Pump Therapy: Complication Presentations and Imaging

Huy Pham[2], *huy.p.pham@gmail.com*; Jeffrey Gardner[1], Zachary Stewart[2], Allison Thompson, MD[2]; [1]Mercer University of Medicine, Savannah, GA, [2]Memorial Health University Medical Center, Savannah, GA

Disclosures: All authors have disclosed no financial interests, arrangements or affiliations in the context of this activity.

Purpose or Case Report: Our educational poster will evaluate and present the complications of the Medtronic Intrathecal Baclofen Pump as seen by our institution. Intrathecal Baclofen pumps are indicated as the treatment for intractable spasticity secondary to cerebral palsy and spinal cord injuries. However, it is not without complications and thus, reserved only for those refractory to other medical interventions. After reviewing radiographs available at our institution, we seek to discuss the complications of baclofen pumps using a multi-case illustration. We present some interesting radiographs of complications seen during infusion pump aspiration studies. These complications include the inability to aspirate CSF, catheter disconnection, catheter fracture, and malposition of catheter tip. Other complications of baclofen pumps include CSF leakage, infections, and even death. It is important to understand these complications because rapid intervention decreases morbidity and mortality rates.

Poster #: EDU-084

A New World Order: A Pediatric Radiologist's guide to the 2016 Updates to the World Health Organization Brain Tumor Classification System

T. Shawn Sato, MD[1], *shawn-sato@uiowa.edu*; Yutaka Sato, MD[1]; [1]Diagnostic Radiology, University of Iowa, Iowa City, IA

Disclosures: All authors have disclosed no financial interests, arrangements or affiliations in the context of this activity.

Purpose or Case Report: The 2016 World Health Organization Classification of Tumors of the Central Nervous System has now incorporated molecular and genetic parameters in addition to histology to define many tumor entities. Significant restructuring has occurred for pediatric CNS tumors. For example, medulloblastomas are classified into four genetic subtypes. Other embryonal tumors such as embryonal tumor with multilayered rosettes (ETMR) and atypical teratoid/rhabdoid tumor (ATRT) are further defined by their molecular features. Also new entities have been added defined by both histology and molecular signatures including H3 K27M-mutant diffuse midline glioma, *RELA* fusion-positive ependymoma and diffuse leptomeningeal glioneuronal tumor (DLGNT).
These more homogeneous and narrowly defined entities are expected to facilitate better classification, prognostication and patient stratification for precision therapy. This also improves the design of clinical trials and experimental models.
In this presentation, we will review the new WHO classification scheme and review the imaging and as well as molecular/genetic features of pediatric CNS tumors.
Radiologists must keep up to date with updates to the WHO classification scheme to be able to better communicate with clinicians ensure optimal patient care and relevant research collaboration.

Poster #: EDU-085

Retroclival Hematoma: Significance of the space behind the slope.

Atsuhiko Handa[1], *atsuhiko-handa@uiowa.edu*; Robert Becker[1], Yutaka Sato, MD[1], T. Shawn Sato[1]; [1]Department of Radiology, University of Iowa Hospitals and Clinics, Iowa City, IA

Disclosures: All authors have disclosed no financial interests, arrangements or affiliations in the context of this activity.
Purpose or Case Report: Retroclival hematomas most often occur in pediatric patients following high speed motor vehicle accidents. Hematomas may involve the epidural, subdural, or subarachnoid spaces. Of these hematoma patterns, retroclival epidural hematomas are often associated with ligamentous injury to the tectorial membrane, transverse ligament, or alar ligament resulting in instability. Children's relatively large head size in proportion to their bodies, less muscular support and more superior fulcrum point of cranial vertebrae (C2-C3 in young children) relative to adults predispose pediatric patients to ligamentous injury. Retroclival subdural hematomas are the most often to be associated with non-accidental brain injuries. Therefore, when young non-ambulatory children present without significant trauma, it is not only imperative to recognize the radiographic findings of retroclival subdural hematomas, but to be cognizant of its association with child abuse.
Radiological evaluation should include reconstructed sagittal CT images in soft tissue window as well as bone window. Special attention should be paid to the soft tissue window since hematomas often show low or intermediate attenuation on CT and can be easily missed on bone window. If only CT of the head is performed, extension to the craniocervical junction should be included. MRI, especially T2 weighted thin cut images are best suited for evaluation of ligamentous injury. STIR sequence can also provide ligamentous details as well as bone marrow edema.
Methods & Materials: 1. Review craniovertebral junction anatomy as it pertains to retroclival hematomas.
2. Illustrate the retroclival hematoma injury patterns including epidural, subdural and subarachnoid bleeds.
3. Demonstrate the CT and MRI findings of retroclival hematoma and the significance of scrutiny of the soft tissue windows of the craniovertebral junction.
Results: Demonstration of multiple cases involving retroclival hematomas with review of pertinent anatomical landmarks to help establish the diagnosis.
Conclusions: It is important for pediatric radiologists to be familiar with this disease entity as findings can be subtle and therefore easily overlooked. Each of the hematoma patterns described is associated with certain traumatic injury to the spine or brain that requires different management. Retroclival hematomas among non-ambulatory children without significant trauma history should be considered as abusive injury until proven otherwise.

Poster #: EDU-086

Imaging of Central Precocious Puberty: Why, When and How.

Mohamad Gharavi, MD[1], *seyed.gharavi@gmail.com*; Jessica Record, MD[1], Lorenna Vidal, MD[1], Prashant Raghavan, MBBS[1], Robert Morales, MD[1]; [1]University of Maryland Medical Center, Baltimore, MD

Disclosures: All authors have disclosed no financial interests, arrangements or affiliations in the context of this activity.

Purpose or Case Report: Precocious puberty is defined as development of secondary sex characteristics before the age of 8 years in girls and 9 years in boys. Two types of precocious puberty have been recognized: central (CPP) and peripheral (PPP). The central precocious puberty is further divided into idiopathic or organic types. CNS imaging is indicated if CPP is diagnosed in boys at any age or in girls younger than 6 years. Different structural abnormalities are associated with CPP such as Hypothalamic hamartoma, Hypothalamic astrocytoma, germ cell tumors or suprasellar arachnoid cysts.
The goals and objectives of the current presentation are as follow:
1- To briefly review the pathophysiology, clinical presentation and different types of CPP
2- To review the indications for CNS imaging work-up in children with CPP and to discuss the appropriate imaging modality and imaging protocol
3- To review different brain pathologies that are associated with CPP followed by discussion of main imaging characteristics through an interactive case series
Methods & Materials: Review of the current literature and retrospectively research in our PACS database for patients scanned with clinical concern for central precocious puberty. Illustrative cases will be chosen and anonymized.
Results: The exhibit will provide a brief review of the causes of central precocious puberty. Then, suggestions for dedicated imaging protocols will be provided, followed by an interactive series of illustrative cases of CPP. Finally, a summary will be available for the viewer in quiz format.

Conclusions: This exhibit will allow the viewer to review the causes of CPP, understand why and when to scan those patients as well how to best use their imaging resources. After reviewing the interactive case series, the viewer will learn the imaging characteristics of the most common CPP pathologies and will be better equipped to identify these lesions in their work routine.

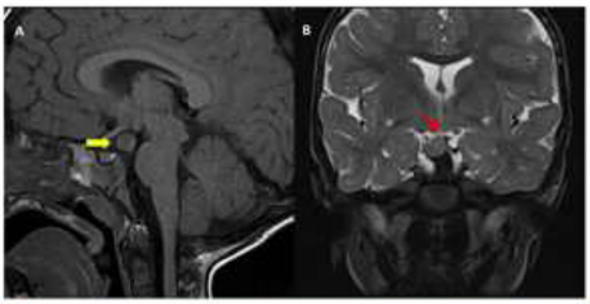

Fig A: Sagittal T1 weighted image shows a lesion arising from the region of the tuber cinereum (yellow arrow) demonstrating similar signal intensity to the cortex
Fig B: Coronal T2 weighted image show this lesion to be pedunculated (red arrow) slightly asymmetric to the right.

Pathology	Pathophysiology	MR characteristics
Hypothalamic Hamartoma	Most commonly associated with CPP Sessile and Pedunculated	Expand or arise from the floor of hypothalamus; T1 and T2 isointense with no enhancement
Hypothalamic-chiasmatic Astrocytoma	Occurs in 15%-20% of NF-1 Usually pilocytic or fibrillary	T1 iso/hypo and T2/FLAIR hyper intense; thickening and enhancement of the involved optic nerve or chiasm
Germ Cell Tumor	Can be pineal or Suprasellar or both; 70% germinoma and 30% non-germinoma	T1 and T2 signal heterogeneity; cystic and solid components; variable degree of contrast material enhancement of its solid elements; can spread through CSF
Arachnoid cyst	Can be congenital or acquired	Cystic lesions that follow CSF signal without enhancement and with mass effect on the adjacent calvarium
Traumatic brain injury		Diffuse micro-hemorrhages on susceptibility weighted images
Central midline abnormalities e.g. septo-optic dysplasia		Absent septum pellucidum; hypoplastic optic nerves

Poster #: EDU-087

Extra! Extra!! Read All About Extra-axial CNS Lesions!!!

Mary Mallon, MD[1], *mgm95@drexel.edu*; Bernard Goldwasser, MD[1], Archana Malik[1], Erica Poletto, MD[1], Jacqueline Urbine, MD[1], Faaiza Kazmi[1]; [1]St. Christopher's Hospital for Children, Philadelphia, PA

Disclosures: All authors have disclosed no financial interests, arrangements or affiliations in the context of this activity.

Purpose or Case Report: When evaluating the pediatric neuroaxis, it is important to include the extra-axial spaces in the radiologists' search pattern. The purpose of the presentation is to show a multimodality pictorial review of characteristic findings of extra-axial CNS lesions detected on CT and MRI.
Methods & Materials: A search for extra-axial CNS lesions was performed by reviewing studies stored on the picture archiving and communication system of an urban children's hospital between 2006 and 2017. A variety of cases were identified in the head and spine. A literature search on current information related to the diagnoses was performed. The presented cases include: lipoma, epidermoid, ruptured dermoid, transitional meningioma with brain invasion, inflammatory pseudotumor, lymphoma, atypical teratoid rhabdoid tumor, craniopharyngioma, arachnoid cyst, epidural abscess, neurofibroma and ganglioneuroblastoma metastases.
Results: A broad range of pathologies can occur in the extra-axial spaces, including benign and malignant lesions. By observing characteristics as described in the pictorial review, an appropriate differential diagnosis may be made enabling appropriate and efficient clinical management.
Conclusions: Many extra-axial CNS lesions demonstrate characteristic features that may help narrow the differential diagnosis affecting clinical decision making. This presentation will help the radiologist recognize these characteristic features. At times, a definitive diagnosis cannot be given and tissue sampling is required to make this determination.

Poster #: EDU-088

Pearls and Pitfalls of Craniosynostoses

Amy Farkas, MD[1], *afarkas@umc.edu*; Jeffrey Hooker, MD[1], David Joyner[1]; [1]Department of Radiology, University of Mississippi Medical Center, Jackson, MS

Disclosures: All authors have disclosed no financial interests, arrangements or affiliations in the context of this activity.

Purpose or Case Report: The clinical implications of craniosynostoses reach far beyond their striking cosmetic deformities. If untreated, craniosynostoses can lead to increased intracranial pressure, restriction of brain growth, and developmental delay, making the recognition of the findings and appropriate diagnosis critical. This electronic poster will provide an overview of various craniosynostoses including trigonocephaly, scaphocephaly, plagiocephaly, brachycephaly, and the various combinations of abnormally fused sutures, with an emphasis on 3D reconstruction imaging. In addition, the expected timing of the fusion of sutures will be described, as well as potential pitfalls in the interpretation of craniosynostosis, including metopic ridge. A brief review of Crouzon, Pfeiffer, and Apert syndromes, those syndromes most commonly associated with craniosynostosis, will be provided.

Poster #: EDU-089

Pediatric Epileptogenic Tumors

Amy Farkas, MD[1], *afarkas@umc.edu*; Jeffrey Hooker, MD[1], David Joyner[1]; [1]Department of Radiology, University of Mississippi Medical Center, Jackson, MS

Disclosures: All authors have disclosed no financial interests, arrangements or affiliations in the context of this activity.

Purpose or Case Report: Epilepsy can be a progressive, debilitating illness, particularly in the pediatric population. More than half of brain tumors are associated with epilepsy, and 30% of these tumors will not respond to pharmacologic therapy. Recognizing lesions that cause seizures is imperative, as providing an accurate diagnosis can identify patients with surgically treatable disease. In the appropriate patient population, epilepsy surgery can be an effective management option that prevents significant morbidity and mortality from epilepsy and dramatically improves quality of life.
This electronic poster will provide an overview of pediatric epileptogenic tumors including gangliogliomas, dysembryoplastic neuroepithelial tumors, pleomorphic xanthoastrocytoma, papillary glioneuronal tumor, pilocytic astrocytoma, and oligodendroglioma. Cases featuring these tumors and their distinguishing characteristics will be reviewed, as both tumor subtype and location contribute to the epileptogenicity of pediatric brain tumors.
The goal of this poster is to provide a framework for the evaluation of pediatric epileptogenic tumors to establish a

focused differential diagnosis when these lesions are identified. This is particularly important for trainees and well as those who do not commonly encounter epileptogenic tumors in their practice.

Poster #: EDU-090

Pediatric cervical spine trauma revisited.

Yasmin Akbari, MD[1], *akbariys@upmc.edu*; Subramanian Subramanian, MD[1], Andre Furtado[1], Ashok Panigrahy[1], Giulio Zuccoli[1]; [1]Diagnostic Radiology, UPMC, Pittsburgh, PA

Disclosures: All authors have disclosed no financial interests, arrangements or affiliations in the context of this activity.

Purpose or Case Report: Pediatric cervical spine trauma, although rare with an incidence of only 1-2%, can have very high morbidity and mortality. The leading causes are motor vehicle collision, sports related injury and child abuse in infants. The incidence of upper cervical spine injury is more common in children than adults due to differences in biomechanics, with the pediatric head size being proportionally larger when compared to adults. Although conventional radiographs remain the standard initial imaging evaluation, CT has become an important modality to detect bony injury and subtle signs of underlying ligamentous injury and hemorrhage (although consideration must be made for the increased radiation exposure). The presence of ligamentous injury, dens synchondrosis fracture, spinal cord evaluation, and spinal cord injury without radiographic abnormality (SCIWORA), meanwhile, are better evaluated with MRI. We will review the normal appearance of the pediatric cervical spine including normal measurements on radiographs and CT, including the importance of the basion-dens interval, powers ratio, and atlanto-occipital distance with illustrations. The normal development of the cervical spine as well as CT and MRI anatomy of cervical spine ligaments will be reviewed with illustrations. Imaging findings of atlanto-occipital and atlanto-axial distraction and pediatric cervical spine fractures including clay shoveler's fracture and dens synchondrosis fractures will be illustrated with CT and MRI. Finally, a review of clinical decision criteria for pediatric cervical spine trauma and imaging approach will be presented. The importance of obtaining MRI in children under 5 years and appropriate use of imaging will also be discussed.

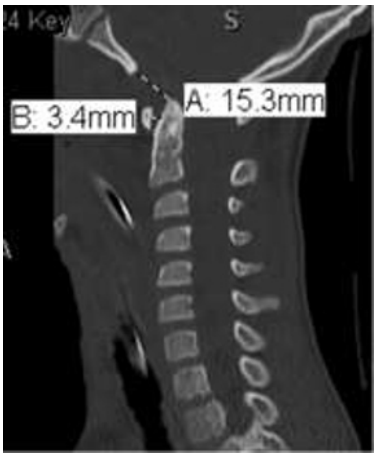

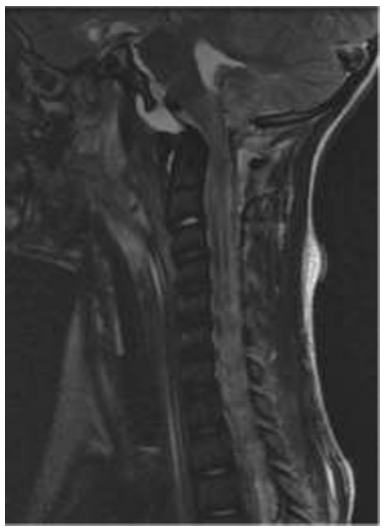

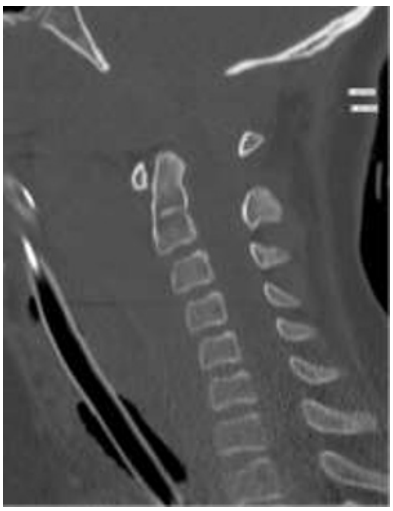

Image 1: Sagittal CT image demonstrates increased basion to dens distance and normal atlanto-dental interval, consistent with atlanto-occipital dissociation.
Image 2: T2-weighted sagittal MR image demonstrates injuries to the tectorial and posterior atlanto-occipital membranes with atlanto-occipital dissociation. There is associated epidural hemorrhage.
Image 3: Sagittal CT reconstruction demonstrates a powers ratio greater than 1, raising suspicion for anterior atlanto-occipital dissociation.

Poster #: EDU-091

Epidural Hematoma Revisited

Aparna Joshi, MD[1], *ajoshi@dmc.org*; Sheena Saleem, DNB, MBBS[1]; [1]Pediatric Imaging, Children's Hospital of Michigan, Detroit, MI

Disclosures: All authors have disclosed no financial interests, arrangements or affiliations in the context of this activity.

Purpose or Case Report: Epidural hematomas are typically seen after accidental head trauma in children, though they can also be seen in abusive head trauma. Most often they are arterial but venous hematomas can occur in posterior fossa and vertex locations.
This educational exhibit will review the pathophysiology and common imaging features on CT and MR of intracranial and intraspinal epidural hematomas. Illustrative examples of unusual types of epidural hematomas such as retroclival epidural hematoma and epidural hematoma crossing calvarial sutures will be included.

Poster #: EDU-092

MRI in the pediatric patient with a cochlear implant

Karuna Shekdar, MD[1], *shekdar@email.chop.edu*; Erin Simon Schwartz, MD, FACR[1]; [1]Radiology, Children's Hospital of Philadelphia, Philadelphia, PA

Disclosures: All authors have disclosed no financial interests, arrangements or affiliations in the context of this activity.

Purpose or Case Report:
To review magnetic resonance imaging (MRI) safety considerations in pediatric patients with cochlear implants (CIs) and to demonstrate feasibility of safely performing MRI of the brain in pediatric patients with CIs that have been deemed MRI conditional by the manufacturer.
Conclusions: MRI scanners use powerful magnets to create high resolution images. MRI safety is always paramount, and patients with implanted devices that are deemed MRI conditional, such as particular types of CIs, may be safely scanned with MRI only under very specific conditions, which will be reviewed in detail. Artifacts created by the implants can be extensive and we will also review artifact-reduction strategies. It must be emphasized that scanning patients with CIs without strictly adhering to the stipulated manufacturer's guidelines may result in severe patient injury and/or device malfunction.

Poster #: EDU-093

Pediatric vascular tumors: the innocent and the sinister. An educational poster reviewing vascular tumors according to the ISSVA classification.

Andrew Harrison, DO[1], *andrew.harrison@childrenscolorado.org*; Lorna Browne[1]; [1]Diagnostic Radiology, Children's Hospital Colorado, Aurora, CO

Disclosures: All authors have disclosed no financial interests, arrangements or affiliations in the context of this activity.

Purpose or Case Report: Vascular tumors are commonly encountered in infants and children, the vast majority being infantile hemangiomas with less frequent congenital hemangiomas. Less commonly encountered vascular tumors are challenging due to their rarity. However, these often have distinguishing clinical, imaging, and histologic features which enable diagnosis and dictate management.
The objective of this electronic exhibit is to present the clinical and imaging findings of vascular tumors encountered in a large children's hospital over a 10-year period. These will be grouped according to the ISSVA benign, locally-aggressive, and malignant classification of vascular tumors.
We will include unusual presentations of infantile and congenital hemangiomas, as well as the clinical features and imaging appearances of the less commonly encountered vascular tumors (tufted angioma, spindle cell hemangioma, pyogenic granuloma, epithelioid hemangioma, kaposiform hemangioendothelioma, and angiosarcoma). Treatment options and prognosis will also be discussed.

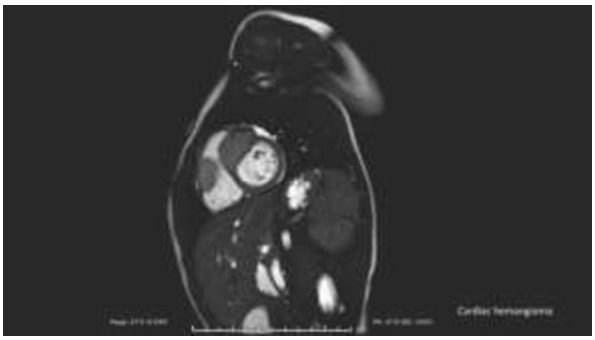

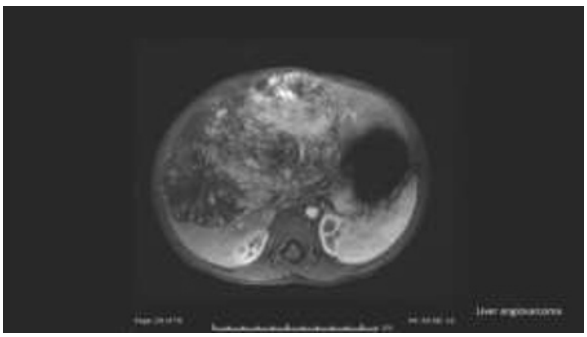

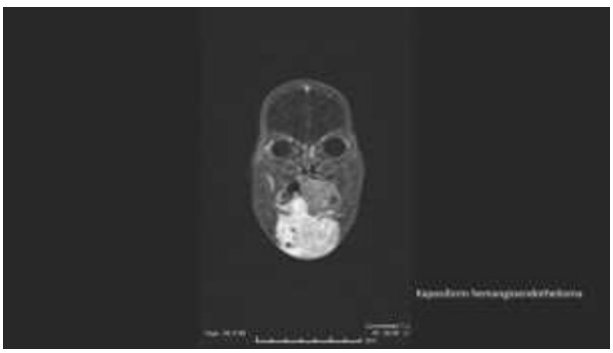

Poster #: EDU-094

Pearls and Pitfalls in FDG PET Brain Imaging in Pediatric Epilepsy

Daniel Nahl[1], *dannynahl@gmail.com*; Marvin Nelson[1], Rachel Berkovich[1], Fariba Goodarzian, MD[1], Lillian Lai, MD[1]; [1]Children's Hospital Los Angeles and Keck School of Medicine University of Southern California, Los Angeles, CA

Disclosures: All authors have disclosed no financial interests, arrangements or affiliations in the context of this activity.

Purpose or Case Report: The goal of this educational exhibit is to explore the utility of interictal FDG PET brain imaging in the evaluation of intractable, drug-resistant cases of pediatric epilepsy and to clarify its role in pre-surgical seizure focus localization. We will also explore the salient pearls and pitfalls of FDG PET brain imaging.

Methods & Materials: Retrospective review of key cases of interictal FDG PET brain imaging in pediatric epilepsy:

Normal brain FDG PET uptake in children:

- Normal distribution at different ages
- Normal variance in temporal lobes

Indications for FDG PET in epilepsy:

-When initial MRI is negative, interictal FDG PET can spotlight an area of concern and second-look MRI may uncover an inconspicuous seizure focus. (***Figure 1.*** Initial MRI was negative except for hippocampal inversion. Hypometabolic activity was seen on FDG PET throughout the left temporal lobe, and on second look MRI, corresponding FLAIR abnormality was seen in the temporal lobe.

-Evaluation of post-operative areas difficult to assess with EEG (***Figure 2.*** Hypometabolic activity was seen in the occipital lobe, which extended beyond the resection cavity and corresponded to areas of abnormal EEG activity).

-Isolating a target lesion when there is more than one area of abnormality (i.e. focal nodular heterotopia or tuberous sclerosis)

-Differentiate inflammation/limbic encephalitis from other seizure etiologies (i.e. focal cortical dysplasia or low grade glioma)

Utility of fusion techniques, comparison with ictal SPECT, and other hybrid imaging:

-Fusing PET with MRI enhances detection of subtle structural abnormalities

-Comparison of sensitivity with ictal SPECT

-Other hybrid imaging such as fusion with EEG or stereo grids can help localize seizure focus

Major artifacts and pitfalls in interpretation:

-metallic and motion artifact

-areas of ictal activity

-calculated attenuation difference due to skull thickness

-hyperglycemia

-drug related hypo- or hypermetabolism

The future:

-New tracers

-Utility of quantitative evaluation to confirm areas of hypometabolism

Results: This exhibit will review indications for interictal FDG-PET brain imaging and its utility in the multimodal work-up of pediatric epilepsy. Pearls and pitfalls in imaging will be discussed, including review of the normal distribution of FDG PET and major artifacts.

Conclusions: Recognizing the utility of FDG PET of the brain, as well as its shortcomings and potential pitfalls, will help radiologists and clinicians better utilize this modality in the evaluation of pediatric epilepsy.

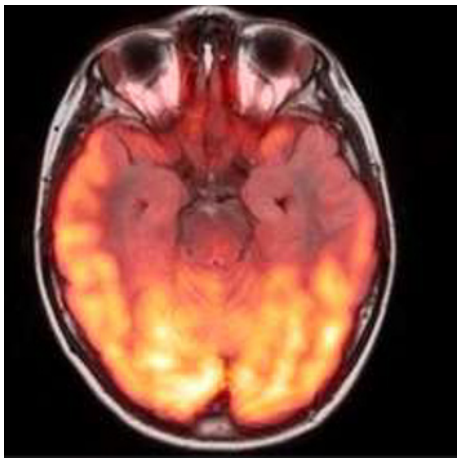

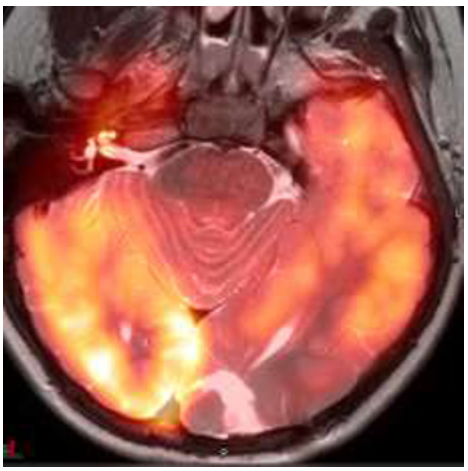

Poster #: EDU-095 - *Withdrawn*

Poster #: EDU-096

Image Defined Risk Factors in Neuroblastoma: An Overview of the Terminology with Key Imaging Features.

Alex Lionberg, MD[1], *alionbe@gmail.com*; Seng Ong, MD[1]; [1]University of Chicago, Chicago, IL

Disclosures: All authors have disclosed no financial interests, arrangements or affiliations in the context of this activity.

Purpose or Case Report: Neuroblastoma is recognized as having a broad spectrum of clinical behavior in children diagnosed with the disease. Some tumors exhibit aggressive characteristics and portend a poor prognosis, while others that appear aggressive spontaneously regress. Accurately identifying high risk neuroblastoma is important in determining which patients will benefit most from intense chemotherapy, which unfortunately carries a risk of significant adverse effects later in life. Historically this has been difficult, as the classification schemes vary in different parts of the world, limiting the ability to pool data and improve prognostication. In recent years, efforts among experts around the globe have led to a consensus on the most evidenced based approach to staging. The aim of this educational exhibit is to describe the new standardized language for radiology reports, which will contribute to accurate staging and improve treatment for patients with neuroblastoma. Additionally, key imaging features highlighting image defined risk factors will be presented.

Methods & Materials: The International Neuroblastoma Risk Group Task Force is a group of leading pediatric oncologists, radiologists, researchers and statisticians from around the world. In 2009, the group published a new classification system based on data collected from a large cohort of patients, representing a consensus among global experts in the field.
Results: The INRG Staging System (INRGSS) was introduced to replace the now decades-old International Neuroblastoma Staging System. The new system shifts away from surgicopathologic classification to describe tumors according to radiologic findings. In addition to differentiating local from metastatic disease, the new system further delineates local disease based on the presence or absence of "image defined risk factors" (IDRF). With this, there is a recommendation for specific terminology to be used in order to accurately characterize an IDRF. These include the words: separation, contact, encasement, compression, infiltration, and invasion.
Conclusions: As the care for Neuroblastoma patients evolves, radiologists must continue to provide value in the multidisciplinary efforts to advance the most up to date approach to staging of the disease. Now more than ever, the use of accurate and uniform language in reports will have a significant impact on the treatment of these patients.

Poster #: EDU-097

Not Your Typical Nashville Blues: An Education Review of Small Round Blue Cell Tumors."

Susan Yoon, DO[1], Stacy White, MD[1], Erica Poletto, MD[2], Jaqueline Urbine[2], Archana Malik[2], Mea Mallon[2], Faaiza Kazmi[2]; [1]Albert Einstein Medical Center, Philadelphia, PA, [2]St. Christopher's Hospital for Children, Philadelphia, PA

Disclosures: All authors have disclosed no financial interests, arrangements or affiliations in the context of this activity.

Purpose or Case Report: Small round blue cell tumors (SRBCT) are a category of malignant tumors that share the characteristic histologic feature of small round undifferentiated cells. These tumors predominantly affect the pediatric population. While SRBCT are similar at the cellular level, their location, imaging characteristics, clinical manifestations, and outcomes are widely variable. The purpose of this educational exhibit is to provide a pictorial review of small round cell blue tumors and to highlight key imaging findings that will aid the radiologist when faced with such tumors.
Methods & Materials: A retrospective review of SRBCT was performed at St. Christopher's Hospital for Children. A series of cases with pathologically confirmed SRBCT were collected for review and presentation.
Results: A multimodality approach including radiographs, CT, MRI, and nuclear scintigraphy is used to illustrate key imaging features of the various SRBCT. Cases to be presented include: medulloblastoma, primitive neuroectodermal tumor, atypical teratoid rhabdoid tumor, non-Hodgkin lymphoma, pineoblastoma, retinoblastoma, neuroblastoma, Wilm's tumor, hepatoblastoma, Ewing's sarcoma, rhabdomyosarcoma, synovial sarcoma, and desmoplastic small round blue cell tumor. Clinical manifestations, distinguishing imaging characterstics, metastatic patterns, prognosis, and treatment will be discussed for each tumor.
Conclusions: Small round blue cell tumors encompass a wide variety of malignant tumors that have a similar histologic appearance. It is critical for the radiologist to be able to identify the imaging features of these tumors to aid in prompt diagnosis and proper treatment.

Poster #: EDU-098

Imaging defined risk factors in neuroblastoma: A pictorial review based on MR imaging

Alan Chen[1], *amchen2107@gmail.com*; Andrew Trout[1], Alexander Towbin, MD[1]; [1]Cincinnati Children's Hospital Medical Center, Cincinnati, OH

Disclosures: All authors have disclosed no financial interests, arrangements or affiliations in the context of this activity.

Purpose or Case Report: Neuroblastoma is the most common extracranial solid malignancy in children. It can have a variety of clinical outcomes, ranging from spontaneous resolution without therapy to fatal outcomes resistant to maximal therapy. Historically, neuroblastoma has been staged using the International Neuroblastoma Staging System (INSS). While this staging system has been used in clinical trials since its introduction in 1989, its reliance on surgical staging is problematic. Surgical resection can vary between surgeons and between tumors and occurs at an interval from diagnosis. This method complicates the process of standardizing therapy. Additionally, some patients have a disease that spontaneously regresses and does not require surgical management and thus cannot be staged.
To combat these problems, the International Neuroblastoma Risk Group (INRG) created a new staging system for use in clinical trials in 2009. This staging system relies on preoperative imaging for up-front staging. This helps standardize neuroblastoma staging and helps to guide a more standard approach to management. The INRG staging system is comprised of twenty image-defined risk factors (IDRF), across multiple organ systems, which help predict surgical outcomes and can be combined with clinical data to provide up-front risk stratification.
Even though the INRG staging system has been in use since 2009, many pediatric radiologists remain unfamiliar with its definitions and application. Additionally, MR has now become an essential imaging tool for diagnosis, staging, and follow-up of patients with neuroblastoma. The purpose of this poster is to compare the INSS and INRG staging system, describe the limitations of each system, and illustrate the definitions and IDRFs that comprise the INRG staging system.

Poster #: EDU-099

Dual-Energy CT–Based Perfusion Imaging of the Lungs in Children: Acquisition Technique, Post-processing, and Interpretation

Jordan Rapp, MD[1], *jrapp24@gmail.com*; David Saul, MD[1], Summer Kaplan, MD MS[1], Christian Barrera[1], Hansel Otero, MD[1]; [1]Children's Hospital of Philadelphia, Philadelphia, PA

Disclosures: All authors have disclosed no financial interests, arrangements or affiliations in the context of this activity.

Purpose or Case Report: Background: Dual source dual-energy CT scanners (DECT) has allowed for the collection of two data sets with a single scan, opening the potential for functional data acquisition. The technique combines two energy beams at distinct voltages applied concurrently during a single scanning phase. The source data can be combined to generate a single mixed composite image, or iodine can be subtracted to create a contrast map or a virtual non-contrast image. The result is functional information in the setting of decreased radiation dose when replacing a biphasic scan, or dose neutral when compared to conventional single source CT. Post processing lung perfusion software allows for imaging display (qualification) and

quantification of iodinated contrast volumes in the lungs, a surrogate for lung perfusion.
Purpose:
This educational exhibit will demonstrate: 1. How to perform DECT in children, 2. How to use postprocessing software, and 3. How to interpret lung perfusion results through clinical examples of current pediatric clinical indications including pulmonary embolism, lung hypoplasia, pulmonary AV malformation, and pulmonary hypertension.
Conclusion:
Through this exhibit, readers will gain familiarity with technical aspects of DECT of the lungs in children, understand the basics of post processing and recognize focal or regional perfusion defects, segmented perfusion analysis, and focal lesion perfusion characteristics as well as identify future applications.

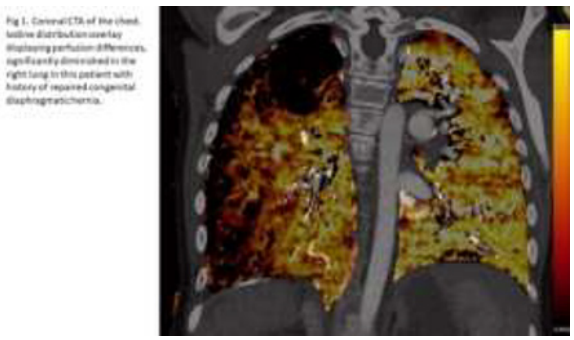

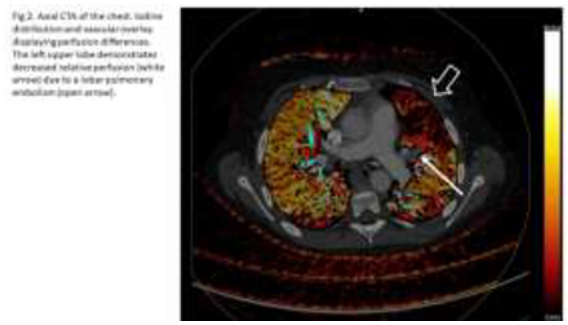

Poster #: EDU-100

Back to the Future: Perfluorochemical Liquid Ventilation and its Imaging Appearances

Andrew Degnan, MD, MPhil[1], *degnan.andrew@gmail.com*; David Biko, MD[1], Ammie White[1], Sabah Servaes[1], Hansel Otero, MD[1], William Fox[1], Thomas Shaffer, PhD[2], Huayan Zhang, MD[1], David Saul, MD[1]; [1]Children's Hospital of Philadelphia, Philadelphia, PA, [2]Nemours Research Lung Center, Wilmington, DE

Disclosures: All authors have disclosed no financial interests, arrangements or affiliations in the context of this activity.

Purpose or Case Report: With advances in intensive care, increasing numbers of premature neonates with severe respiratory distress have led to major challenges related to prolonged mechanical ventilation and chronic bronchopulmonary dysplasia. Acute lung injury and acute respiratory distress syndrome in children still confer significant morbidity and mortality despite advances in ventilation and resuscitative therapies.
Much of the damage attributed to mechanical ventilation in critically ill infants and children is due to surface tension and ventilation of atelectatic lung. First reported clinically in neonates in 1989, partial liquid ventilation involves the endotracheal administration of an inert volatile perfluorochemical liquid. These perfluorocarbons aid in gas exchange due to their large oxygen and carbon dioxide carrying capacity. In addition, these chemicals possess low surface tension that allows for greater alveolar recruitment and improved lung compliance through clearance of debris and secretions. Early trials in preterm neonates and neonates with congenital diaphragmatic hernia suggested a role for liquid ventilation as salvage therapy for patients not responding to conventional mechanical ventilation and extracorporeal membrane oxygenation. Currently, efforts are underway to reassess its clinical utility in bronchopulmonary dysplasia. With this renewed clinical interest, it is important for pediatric radiologists at institutions utilizing these perfluorocarbons to be familiar with the clinical use and radiographic appearance of liquid ventilation.
Conclusions: This presentation summarizes the imaging evaluation of liquid ventilation including information on the qualitative assessment of ventilation status and clinical relevance of particular imaging findings. Due to the presence of bromine, these perfluorocarbons demonstrate a strikingly radiopaque appearance on chest radiographs and computed tomography that can be confusing to radiologists unfamiliar with liquid ventilation. Understanding the radiographic distribution and clearance of perfluorocarbons from the lungs can be important in assessing the effectiveness of this experimental therapy. In addition, radiologists should be aware of the occasional retention of perfluorocarbons in extra-pulmonary tissues following discontinuation of liquid ventilation.

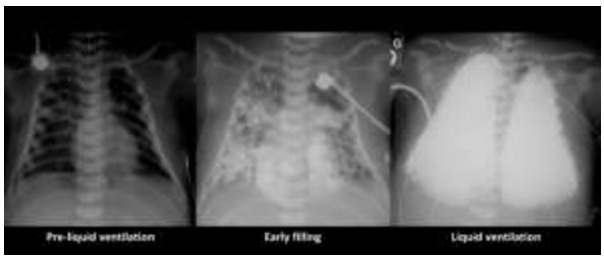

Poster #: EDU-101

Pediatric CXR - The forgotten art.

Renato Ferreira da Silva, MD[1], *renato-silva@uiowa.edu*; Prashant Nagpal, MBBS[1], Sarv Priya, MD[1], T. Shawn Sato[1], Yutaka Sato, MD[1]; [1]Department of Radiology, University of Iowa, Iowa City, IA

Disclosures: All authors have disclosed no financial interests, arrangements or affiliations in the context of this activity.

Purpose or Case Report: Interpretation of chest radiographs requires a good understanding of anatomy, the physiology of the lungs and cardiovascular system as well as good pattern recognition. Additionally, it requires a systematic approach to

search for pathologies and pertinent clinical details for interpretation. With frequent use of CT / MRI, the residents (and even practicing radiologists) have become less skilled in the interpretation of chest x-rays, making one of the most commonly ordered exams the most challenging.
With challenges of decreasing radiation exposure (especially in pediatric population), it is important that the relatively lost skill set of chest radiographs interpretation be revisited, for trainees (radiology and non-radiology services) and the practitioners.
OUTLINE
● Historical perspective.
● Overall approach towards a chest x-ray and importance of clinical details.
● PA/AP and lateral radiograph anatomy and radiographic lines and stripes.
● Fleischer society standard terminology for radiographs.
● Radiographic appearance of abnormalities and pearls for differentiation. The abnormalities to be categorized as:
○ Pneumonia
○ Effusion
○ Atelectasis
○ Big heart
○ Pulmonary vascularity (plethora and oligemia)
○ Lucencies (Pneumo: thorax, mediastinum and cardia)
○ Masses

Poster #: EDU-102 - *Withdrawn*

Poster #: EDU-103

Role of Sonography in a Proposed Imaging and Management Algorithm for Pediatric Patients with Suspected Post-traumatic Intercostal Lung Herniation

Denise Castro[1], *denisecastro22@gmail.com*; Mila Kolar[2], Don Soboleski, MD[2]; [1]The Hospital for Sick Children, University of Toronto, Kingston, ON, Canada, [2]Kingston General Hospital, Queen's University, Kingston, ON, Canada

Disclosures: All authors have disclosed no financial interests, arrangements or affiliations in the context of this activity.

Purpose or Case Report: Post-traumatic intercostal lung herniation (ICLH) is defined as a protrusion of lung tissue through a defect in the intercostal space musculature and is a rare result of chest trauma. Due to its rarity, the management and imaging work up has been based on the adult experience, with Computed Tomography (CT) the most common diagnostic tool and surgery the primary management approach.
The purpose of this study is to describe the sonographic appearance and technique utilized in diagnosis of post-traumatic ICLH and to support their inclusion in a proposed imaging algorithm to aid in management in the pediatric population.
Methods & Materials: We present a recent case of post-traumatic ICLH with follow-up and systematic review of all 15 cases in the literature found through a Pubmed, Embase, Ovid, Scopus and Cochrane search. Extracted data includes mechanism of trauma, clinical presentation, imaging performed, treatment and outcomes. Data was compared with the adult population.
Results: On Sonography, ICLH typically appears as loss of fascial plane delineation involving the external, internal and innermost intercostal muscles. The degree of disruption of this latticework of structures and the resulting loss of structural support determines the severity of the lung herniation, which is best depicted on real time assessment with utilization of maneuvers to increase intrathoracic pressures. ICLH usually presents as a soft non-tender mass exaggerated by coughing and/or straining and may present long after the initial injury. ICLH was located in the anterior chest wall in 81% of pediatric patients. The most common mechanism of trauma was blunt handlebar injury. Chest radiograph was used to diagnosis in 88% and CT scanning in 44% of patients. Sonography was utilized in 19% of cases. Management was surgical in 63% of patients, with thoracotomy with primary closure the preferred treatment. The remainder of the patients received non-surgical management with chest strapping, with resolution in 2-6 weeks.
Conclusions: Given the rarity of ICLH in pediatric patients and the lack of diagnostic and management guidelines, pediatric surgeons have mostly relied on published reports in the adult literature to guide work-up and management. The recent literature supports the feasibility of non-surgical management and the proposed imaging guidelines (Fig. 1) expanding the use of Sonography are meant to aid in the determination of surgical vs conservative treatment.

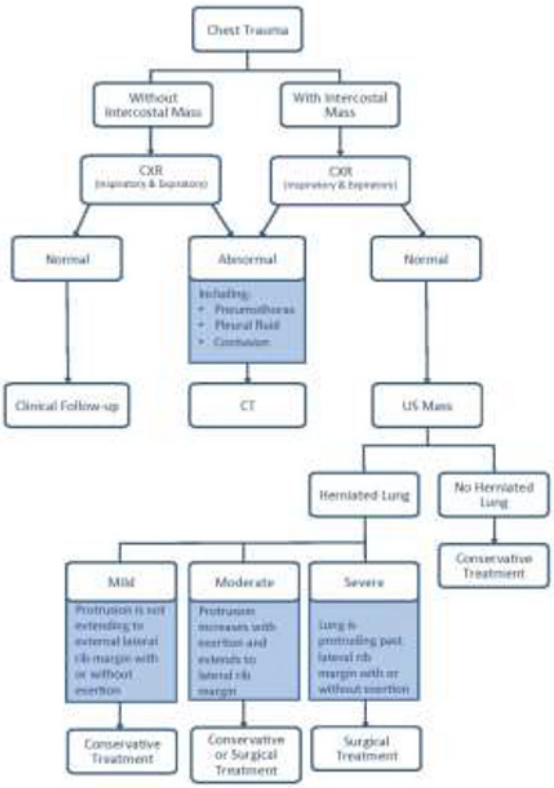

Poster #: EDU-104

Early Implementation of a Postmortem MRI Program: The Beaumont Experience

James Davis[1] *james.davis@beaumont.org*; ; [1]Diagnostic Radiology, Beaumont Health, Beverly Hills, MI

Disclosures: All authors have disclosed no financial interests, arrangements or affiliations in the context of this activity.

Purpose or Case Report: Stillbirth is a sad complication of pregnancy. Establishing the cause of death in intrauterine fetal demise (IUFD) is important to bring psychological closure to the family and crucial for reproductive counseling. The gold standard to establish the cause of IUFD is perinatal autopsy. However, perinatal autopsy rates are falling worldwide, largely attributed to patients and physicians discomfort with death and discussion of postmortem examinations as well as social and religious reasons. There is a lack of experience with minimally invasive perinatal autopsy in the United States and even more limited publications in the subject. Our main goal was to

investigate the added value of postmortem MRI to conventional autopsy in the clinical setting. Our program has had successes and failures, of which learning opportunities exist for other institutions that desire to implement similar programs. This paper will discuss the timeline of our progress and share examples of potential roadblocks and keys to success in implementing such a program.
Methods & Materials: In 2013, our research team at Beaumont Health realized that we have the capability to implement a postmortem MRI program here in the United States, similar to those already underway in the United Kingdom. We sought out a partnership with the anatomic pathology department to brainstorm how we could work together to contribute to the growing body of research in the postmortem diagnostic branch of medicine. We received IRB approval in 2014 and started meeting with the bereavement specialists and maternal fetal medicine physicians to identify prospective subjects.
Results: Since then, we have continued to adjust our protocol and inclusion criteria to optimize our number of subjects. This paper will discuss the hurdles that we have overcome and detail ways we have optimized this project in hopes of smoothing the transition period for institutions that aspire to contribute to this growing field of research.
Conclusions: Through our experiences with implementation of a post mortem MRI program at Beaumont Health, we have found early successes and failures. We have worked closely with the multidisciplinary team involved to overcome the early roadblocks that we had faced and continue to fine-tune our program in order to further the knowledge in this growing field. We hope that our experiences will be enlightening to other institutions that wish to join us in this venture.

Poster #: SCI-001

Comprehensive Analysis of Pediatric Scanning Parameters from Adult-Focused Practices: Are Settings Adjusted and Appropriate for Pediatric Patients?

Ashishkumar Parikh, MD[2], *ashishckt@gmail.com*; Sumit Pruthi, MBBS[1], Marta Hernanz-Schulman, MD[1]; [1]Radiology, Vanderbilt Children's Hospital, Nashville, TN, [2]Nemours Children's Health System, Jacksonville, FL

Disclosures: All authors have disclosed no financial interests, arrangements or affiliations in the context of this activity.

Purpose or Case Report: Recently JACHO proposed to address double scanning in pediatric chest CT, yet there are no data to determine whether this takes place; similarly, there is discussion regarding validity of sending pediatric patients to adult-focused practices for routine imaging by third party payors. Our purpose is to review the technical factors that impact upon radiation dose and image quality in CT scans of children referred from adult-focused practices to a children's hospital, referenced to pre-Image Gently values. To our knowledge this is the first such review that includes body and neuro scans and extensive technique and exposure data
Methods & Materials: This IRB-approved study assessed 100 randomly selected external CT scans. The study CDs were uploaded into Sante DICOM software for viewing and analysis. Study type, indication, gender, age, use of oral or IV contrast, number of phases, reformats, slice thickness (ST) DLP, CTDIvol, kV, mA, mAs, phantom size, iterative reconstruction (IR) vs filtered back projection (FBP)
Results: Of the 100 scans, 56% were body; 44% were neuro. Mean patient age was 9.4 years [0-24]. 38/51 (75%) A/P scans were done for pain, and of these 6 (16%) were done without IV contrast. Head CT was done for trauma in 15 (48%) and for seizure, H/A, N/V in 15 (48%). Of 51 A/P studies, 10 (20%) were multiphase, 3 were triple phase; of the 44 neuro studies, 3 (7%) were multiphase. Biplane reformats were available in less than half (43%) of body scans. The mean DLP for body scans was 496mGy*cm [32-2583], and for neuro 662 [102-2355]. Phantom size was available in 47/56 body scans, and a 16 inch phantom was used in only 1; phantom size was available in 39/44 neuro studies, and the 32 inch phantom was used in 6. Mean mA, mAs, kV, ST and DLP for neuro and body scans in 3 age groups: 0-6; 7-10 and >10 years are outlined in Table
Conclusions: Since 2001 (Paterson AJR 2001;176:297) our data indicate that adjustment for size is not universally applied in scan settings, or choice of ST; phantom size used in estimation of DLP is chosen more based on the body part scanned than on the patient size; the variation in dose is extremely high, with DLP's in the greater than 2000 range in some children; despite the multiphase examinations, triplane reformats are not universally provided.

Pediatric CT Parameters from Adult Focused Practices

		Tube Current (mA)		Exposure (mAs)		Kilovolt (kV)		Slice Thickness (ST) (mm)		DLP (mGy*cm)	
Age (years)	Neuro or Body	Mean	Range	Mean	Range	Mean	Range	Mean	Range	Mean	Range
0-6	Neuro	234	100-400	146	40-215	116	100-120	4.7	2.0-5.0	459	153-1308
7-10	Neuro	214	105-300	217	90-403	122	100-140	3.9	1.0-5.0	630	125-2356
> 10	Neuro	231	86-400	200	86-356	119	100-140	4.7	1.25-5.0	739	103-1862
0-6	Body	155	35-307	102	42-258	150	80-140	3.8	2.0-5.0	265	32-1405
7-10	Body	152	50-372	90	38-298	120	100-140	3.8	3.0-5.0	317	74-906
> 10	Body	224	55-451	155	28-418	116	100-135	4.4	2.0-5.0	674	52-1554

Poster #: SCI-002

Utility of Chest CT in Evaluation of Spontaneous Pneumomediastinum in Pediatric Patients

Brittany Albers, MD[1] *brittany.albers@gmail.com*; [1]Pediatric Radiology, Mallinckrodt Institute of Radiology, St. Louis, MO

Disclosures: All authors have disclosed no financial interests, arrangements or affiliations in the context of this activity.

Purpose or Case Report: Pneumomediastinum is a relatively common cause of hospitalization in the pediatric population. In this study, we evaluate the effect of chest CT on the management of spontaneous pneumomediastinum in the pediatric age group. If chest CT can be shown to have no significant effect on management, then radiation dose to the patient can be decreased.
Methods & Materials: We searched the hospital radiology database (RIS) for the word "pneumomediastinum" between September 2005 to March 2016. Medical record and imaging was reviewed. Patients with pneumothorax in addition to pneumomediastinum were not included.
Results: We found 14 pediatric patients with spontaneous, or non-traumatic, pneumomediastinum during this time period. Underlying causes included respiratory illness, asthma, drug overdose, extreme breath-holding and some truly idiopathic cases. All patients had at least one chest radiograph. 6 patients had chest CT in addition to a radiograph. Chest CT demonstrated pneumomediastinum in all patients but did not provide any additional information relative to the radiograph or clinical exam. The results of the chest CT therefore did not change management
Conclusions: Many pediatric patients with spontaneous pneumomediastinum are evaluated with chest CT. In our series, CT did not change patient management or outcome. In keeping with the surgical literature, we recommend against the routine use of CT to evaluate patients with spontaneous pneumomediastinum.

Poster #: SCI-003

Enabling Free-Breathing Real-Time Cine in Pediatric Patients with Compressed Sensing

Ramkumar Krishnamurthy, PhD[1], *ramkumar.krishnamurthy@nationwidechildrens.org*; Yingmin Liu, PhD[2], Houchun Hu, PhD[1], Rajesh Krishnamurthy[1], Kan Hor, MD[1], Rizwan Ahmad, PhD[2]; [1]Radiology, Nationwide Children's Hospital, Columbus, OH, [2]Ohio State University, Columbus, OH

Disclosures: Kan Hor has indicated a relationship with Medtronics and Capricor as a consultant/honoraria. All other authors have disclosed no financial interests, arrangements or affiliations in the context of this activity.

Purpose or Case Report: Conventional cardiac MRI (CMR) acquisitions in children are limited by long acquisition time, need for sedation, and an inefficient workflow. A conventional cine SSFP short-axis stack typically takes 5-7 minutes to complete and is ineffective for subjects with arrhythmias. Available alternatives like free-breathing, real-time cine (RT-cine) SSFP have suboptimal temporal and spatial resolution. Recent advances in compressed sensing (CS) MRI techniques may overcome this limitation. We hypothesize that a CS-based approach will allow the scan time for a short axis RT-cine stack to be shortened to less than a minute without compromising spatial or temporal resolution.
Methods & Materials: Five patients (Age: 14-44 years; 4 males) underwent CMR study with both conventional breath-held cine SSFP (BH-cine) as well as CS-based free-breathing, cardiac-triggered RT-cine acquisitions (Ahmad and Schniter, DOI: 10.1109/TCI.2015.2485078). The short-axis of the ventricles was covered with 14 slices in each patient. The spatial resolution for both acquisitions was 1.8x1.8x8 mm^3; temporal resolution was 32 ms (BH-cine) and 32 ms (RT-cine) per cardiac phase. End-diastolic volume (EDV), end-systolic volume (ESV), ejection fraction (EF), and scan duration were computed using established methods, and compared between BH-cine and RT-cine acquisitions using paired Student's t-test.
Results: Both BH-cine and RT-cine images were deemed of diagnostic quality by two expert readers. The EDV, ESV and EF showed good agreement (Mean EDV (BH-cine first): 144 ± 27 vs 137 ± 27 ml, p = 0.03; mean ESV: 58.8 ± 10.4 ml vs. 54.9 ± 6.4, p = 0.29; and mean EF = 58.8 ± 5% vs 54.9 ± 6.4 % ;p = 0.03); see figure 1. The scan times were significantly shorter for RT-cine (2 heart beats/slice; ~45 seconds for entire 14 slice acquisition) compared with BH-cine acquisition (6-8 beats/slice; ~5:38 minutes for 14-slice acquisition, p< 0.01). Figure 2 shows representative images acquired.
Conclusions: CS-based free-breathing RT-cine technique is feasible and provides images of comparable quality and diagnostic value when compared to conventional BH-cine SSFP, while significantly reducing scan time. It offers a potential solution to avoid the need for sedation for functional evaluation, improve diagnostic utility of MRI in arrhythmia, and improve CMR efficiency and workflow. Future reduction in reconstruction times, is needed prior to implementation of CS-based RT techniques into clinical practice.

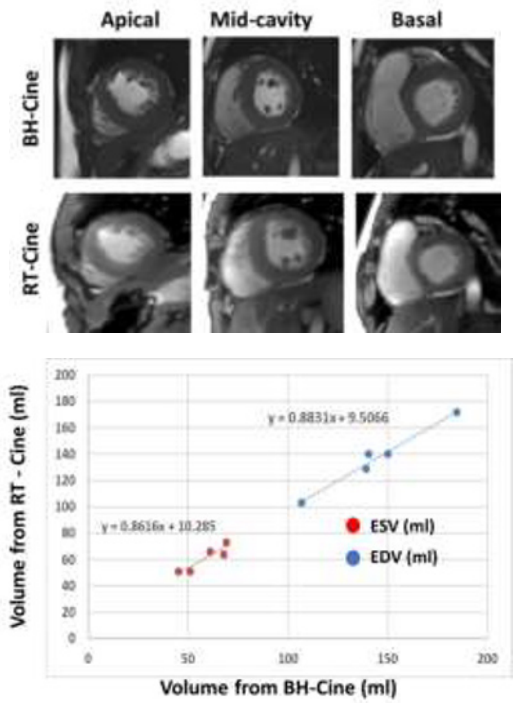

Poster #: SCI-004

Diagnostic accuracy of MSCT in Children with Abernethy Malformation

Chen Guo[1], *guochen0028@163.com*; Qian Wang[1], Li-Wei Hu[1], Yu-Min Zhong[1]; [1]Radiology, Shanghai Children's Medical Center affiliated with Shanghai Jiao Tong University Medical School, Shanghai, China

Disclosures: All authors have disclosed no financial interests, arrangements or affiliations in the context of this activity.

Purpose or Case Report: The purpose of this study was to demonstrate manifestations of MSCT in Abernethy malformation and its diagnostic value.
Methods & Materials: Twelve pediatric cases of Abernethy malformation were admitted to the center between July 2011 and September 2016. All the 12 patients (seven males and five females) performed MSCT and DSA. The patient ages ranged from 3 and 14 years old (median age 9 years old). The clinical records of the patients were thoroughly analyzed. MSCT angiography was performed on a 16-row CT scanner (Lightspeed 16, General Electric Medical Systems) or 64-row CT scanner (GE Discovery CT 750 HD, Waukesha, WI). CT raw data were transferred to an Advantage Windows 4.2 or 4.6 workstation (General Electric Medical Systems, Waukesha, WI). Maximum intensity projection (MIP) and multiplanar reformation (MPR) were the primary methods of visualization for evaluation. DSA was performed with a digital subtraction angiography machine (LC-LP biplane machine, General Electric Medical Systems) in all patients.
Results: Three cases were type Ib Abernethy malformation and nine cases were type II Abernethy malformation. Two cases of type II Abernethy malformation were misdiagnosed to type Ib Abernethy malformation in MSCT. Among the twelve patients, nine presented with single vessel shunt between portal vein and IVC, one with shunt between portal vein and left renal vein, one with shunt between splenic vein and right iliac vein, one with shunt between splenic vein and left iliac vein. Other clinical information of these patients includes congenital heart disease, pulmonary hypertension, diffuse pulmonary arteriovenous

fistula, abnormal liver function, hepatic nodules, elevated blood ammonia, hepatic encephalopathy.
Conclusions: MSCT can exactly diagnose type II Abernethy malformation and show the exact location of the portacaval shunt. Sometimes it is hard to make the certain diagnosis between Abernethy type Ib and II in MSCT, then DSA will help while necessary.

Table 1. Summary of findings in patients with Abernethy Malformation

Case No.	Age(y)/Sex	Presenting symptoms	Fistula classification and anatomy	Main clinical manifestations
1	11 years/Female	Physical examination	Type Ib(PV-IVC)	CHD, Hyperammonemia, Abnormal liver function
2	6 years/Female	Physical examination	Type Ib(PV-IVC)	CHD, Nodular liver lesions
3	12 years/Male	Hematochezia	Type Ib(SV-duc vein-IVC)	PH, Hyperammonemia
4	11 years/Female	Cyanosis	Type II(PV-IVC)	Pulmonary arteriovenous fistula, Hyperammonemia
5	9 years/Male	Fatigue	Type II(PV-IVC)	CHD
6	4 years/Male	Pulmonary hypertension	Type II(PV-IVC)	Hyperammonemia
7	9 years/Male	Fatigue	Type II(PV-IVC)	PH, Hepatic encephalopathy, Heart insufficiency, Hyperammonemia
8	14 years/Male	Fatigue	Type II(PV-IVC)	CHD, Hyperammonemia, Nodular liver lesions
9	5 years/Male	Cyanosis	Type II(PV-IVC)	Pulmonary arteriovenous fistula, Hyperammonemia
10	10 years/Female	Hematuria	Type II(SV-duc vein-IVC)	Renal vascular malformation, Hyperammonemia
11	1 years/Female	Pulmonary hypertension	Type II(PV-IVC)	CHD,PH, Abnormal liver function
12	1 years/Male	Cyanosis	Type II(PV-LKV-IVC)	CHD, Pulmonary arteriovenous fistula, Hyperammonemia

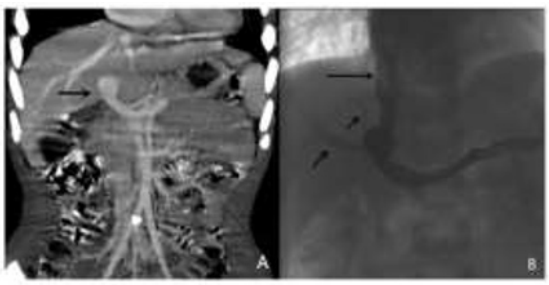

Fig. 1. Male, 3 years old, Abernethy II. A : Abdominal CT angiography maximum intensity projection (MIP) image (portal phase) shows the presence of extrahepatic portosystemic shunt (arrow) with absence of intrahepatic portal veins and diagnoses Abernethy Ib ; B : DSA image shows the shunt (long arrow) and the tiny intrahepatic portal veins (short arrow) and confirms Abernethy II.

Accuracy of Classification of Abernethy malformation in MSCT Compared with DSA

DSA	MSCT			Accuracy (%)
	Ia	Ib	II	
Ia(n=0)	0	0	0	/
Ib(n=3)	0	3	0	100
II(n=9)	0	2	7	77.8

Poster #: SCI-005

Comparison of Fetal Radiation Dose Estimation Methods

Ivey Royall, MD[1], *Ivey.Royall.MD@flhosp.org*; Vincent Grekoski[2], Matthew Hough, MS[1], William Sensakovic, PhD[1]; [1]Florida Hospital, Orlando, FL, [2]University of Central Florida, Orlando, FL

Disclosures: All authors have disclosed no financial interests, arrangements or affiliations in the context of this activity.

Purpose or Case Report: To compare methods of estimating the fetal radiation dose delivered during computed tomography (CT) scanning. Further, to assess sources of variability in estimation methods.
Methods & Materials: A database of 40 CT scans of pregnant patients was collected. Mean gestational age was 159±63 days (7 first, 19 second, and 14 third trimester). Mean maternal weight was 78±18kg. All patients underwent abdomen (n=10) or abdomen/pelvis (n=30) scanning.
Four estimation methods were investigated: 1) Classic calculation (Felmlee, et al. AJR 154:1990), 2) updated calculation (Angel, et al. Radiology 249(1): 2008), 3) iPad app (Sahbaee, et al. Medical Physics 41: 2014), and 4) dose tracking software (Radimetrics, Bayer).
Two observers made measurements necessary for dose calculation. These included fetal depth, maternal circumference, and maternal diameter.
Agreement among methods was assessed using regression and Bland-Altman analysis. Causes of disagreement between methods and variability within methods was also investigated.
Results: Fetal dose ranged from <1mGy to 32mGy. Differences between methods were significant ($p<0.05$), but generally small (<10mGy). Bias between methods was <5mGy and 95% Confidence Intervals (CI) were less than ±15mGy for pairwise method comparison. Regression between methods demonstrated typical slopes between 0.8 and 1.2 and R2 values between 0.3 and 0.8. When datasets were limited to avoid violating method assumptions both bias and 95%CI were cut by 50% or more. Complete patient circumference was not visible in the CT field of view for 30 of 40 patients (75%). This likely causes overestimation of fetal dose due to underestimation of the maternal size. Differences in measurement between the observers generally resulted in fetal dose estimate changes of <10mGy, though several outliers demonstrated larger changes.
Conclusions: Fetal dose estimation methods demonstrated good agreement; however, variability and outliers exist. A qualified medical physicist should review dose estimates to ensure proper calculation. Differences between methods could become important if combined with other dose data in a dose index tracking system as it could elevate estimated dose above threshold considered acceptable for fetal scanning.

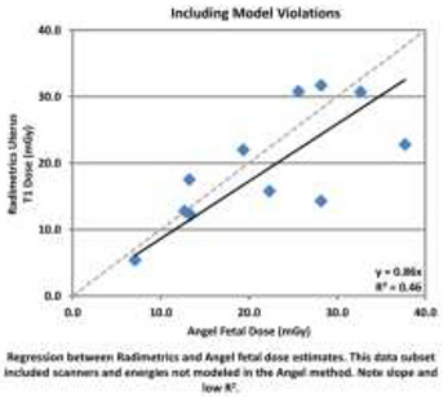

Regression between Radimetrics and Angel fetal dose estimates. This data subset included scanners and energies not modeled in the Angel method. Note slope and low R².

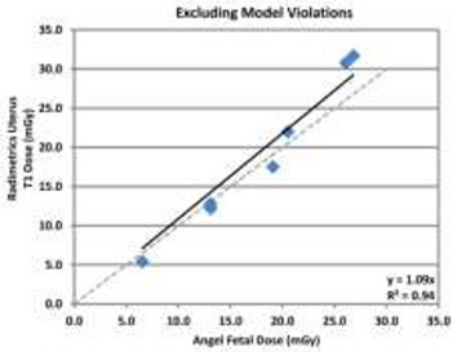

Regression between Radiometrics and Angel fetal dose estimates with incorrect data removed. Note improved slope and R^2.

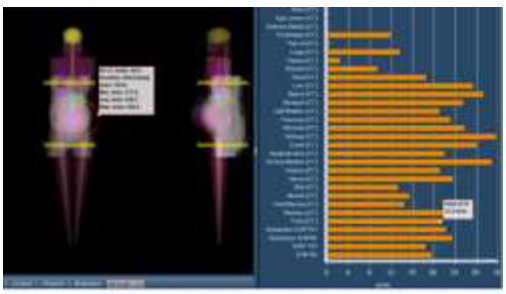

Radiometrics output demonstrating model with localizer overlay and organ/fetal dose estimates. Note the slight misregistration between computational model and localizer in both the lateral and anteroposterior directions. Currently there is no method to manually correct the registration.

Poster #: SCI-006

Measurement of Prenatal MRI Lung Volumes as a Prognostic Tool for Patients with Prenatally Diagnosed Giant Omphalocele

Alexis Maddocks, MD[1], *Alexis.Rothenberg@gmail.com*; Rama Ayyala, MD[1], Jesus Jimenez[1], Russell Miller[1], Vincent Duron, MD[1]; [1]Radiology, Columbia University Medical Center, West Nyack, NY

Disclosures: All authors have disclosed no financial interests, arrangements or affiliations in the context of this activity.

Purpose or Case Report: Giant omphaloceles are large in size and contain a significant portion of liver. Giant omphaloceles are often associated with other co-morbidities, such as pulmonary hypoplasia, which can lead to respiratory insufficiency, prolonged intensive care support, assisted ventilation, and death. The purpose of this study is to develop a prognostic model for prediction of post-natal outcomes in patients with giant omphaloceles using fetal MRI calculated observed to expected total lung volumes (O/E TLV).
Methods & Materials: After IRB approval, a retrospective search was performed to identify patients with giant omphalocele who underwent fetal MRI and received pre- and post-natal care at our institution from 2007 to 2017. Patients with other anterior abdominal wall defects, including OEIS complex, were excluded. After review of the fetal MR images, 3D lung volumes and O/E TLV were calculated. Statistical analysis was performed using Chi-square and Student's t-test.
Results: 14 patients met our inclusion criteria. Two of these patients died shortly after birth and two died in utero (one due to termination of pregnancy). 4 were female and 9 were male (1 was non-identified). Mean gestational age at fetal MRI was 26.5 ± 5.49 weeks with a mean O/E TLV of 0.56 ± 0.37. Mean gestational age at birth was 37.2 ± 1.89 weeks. O/E TLV did not significantly correlate with sex (p=0.53), pulmonary hypertension (p=0.69), need for tracheostomy (p=0.92), need for supplemental oxygen at discharge (p=0.16), or incidence of chronic lung disease (p=0.13). O/E TLV approached significance with regard to fetal distress at birth (p=0.06) and number of days intubated (p=0.057). O/E TLV did significantly correlate with the incidence of hypoxia at birth (p=0.005) and in-utero or neonatal death (p=0.004). Infants with hypoxia at birth had a mean O/E TLV of 0.53 ± 0.25. All infants with O/E TLV of less than 0.23 died in utero or around time of birth.
Conclusions: Fetal MRI calculated O/E TLV ratio may be helpful in predicting respiratory prognosis and survival in patients with giant omphalocele.

Poster #: SCI-008

Malrotation of the Bowel-Is Prenatal MRI Diagnosis Possible?

Kimberly Fagen, MD[1], *kimbopootsie@gmail.com*; Anna Blask, MD[2], Eva Rubio, MD[2], Judyta Loomis, MD[2], Dorothy Bulas, MD[2]; [1]Walter Reed National Military Medical Center, Bethesda, MD, [2]Children's National Medical Center, DC

Disclosures: All authors have disclosed no financial interests, arrangements or affiliations in the context of this activity.

Purpose or Case Report: To assess if malrotation of the bowel can be detected on prenatal MRI.
Methods & Materials: Nine cases of malrotation diagnosed postnatally by UGI in 8 cases and autopsy in 1 case had prenatal MRI imaging. Postnatal imaging (including SBFT/ KUB) was utilized to determine the position of small bowel and colon and to determine if obstruction was present. Prenatal MRIs were retrospectively reviewed to determine if bowel position matched the postnatal position. Prenatal factors documented: Gestational age, reason for MRI, AFI, small bowel and colon position, and bowel dilatation. Postnatal factors recorded include: reason for the UGI, bowel orientation and obstruction, and surgical findings. A control group of 98 prenatal MRIs was prospectively evaluated to determine if normal bowel orientation could be visualized.
Results: Prenatal MRI was performed for heterotaxy 5/9, congenital heart disease 3/9, and skeletal dysplasia 1/9. Indications for postnatal UGI included emesis 3/9, peritonitis 1/9, distended abdomen 1/9, and asymptomatic heterotaxy 4/9. Gestational age at MRI ranged from 23-37 weeks. AFI's were normal and no cases had dilated bowel. Prospectively, malrotation was suspected in 5 cases. Retrospectively on MRI, small bowel position was best assessed on T2 coronal images; colon T1 coronal images. Small bowel was nonrotated in 9/9 cases with small bowel positioned contralateral to stomach situs. Colon was nonrotated in 7/9 cases, contralateral to the small bowel in 6/7 and on the same side as the small bowel in 1/7. Colon position was indeterminate in 1/9; not seen 1/9. Prenatal small bowel position corresponded to the UGI/SBFT or autopsy in all cases with nonrotation in 8/9; partial rotation of the duodenum in 1/9. Colon prenatal position corresponded to the SBFT/KUB or autopsy with nonrotation in 7/7 cases. Of the 2/9 with indeterminate prenatal colon position, postnatal colon was nonrotated. No postnatal cases were obstructed. Surgery confirmed diagnosis in 4/9; autopsy 1/9 cases. The prenatal MRI control group had GA ranging from 21 to 38 weeks and normal bowel rotation seen in all cases.
Conclusions: Detection of bowel malrotation on prenatal MRI is possible with careful analysis of the small bowel and colon position. In a fetus with heterotaxy, prenatal analysis of the position of the bowel is useful secondary to the increased incidence of malrotation. If malrotation is suspected prenatally, postnatal evaluation prior to onset of symptoms may minimize potential for subsequent complication.

Poster #: SCI-009

Free-Breathing Motion Insensitive 3D T1-Weighted Post-Contrast Spine and Abdominal MRI Using a Golden Angle Radial Acquisition

Houchun Hu, PhD[1], *houchun.hu@nationwidechildrens.org*; Thomas Benkert, PhD[2], Ramkumar Krishnamurthy, PhD[1], Mark Smith, MS[1], Jerome Rusin[1], Cody Young, DO[1], Brent H. Adler, MD[1], Kathryn Milks, MD[1], Rajesh Krishnamurthy[1], Kai Tobias Block, PhD[3]; [1]Radiology, Nationwide Children's Hospital, Columbus, OH, [2]Siemens Healthineers, Enlargen, Germany, [3]New York University Medical Center, New York, NY

Disclosures: Thomas Benkert has indicated a relationship with Siemens Healthineers for receiving a salary. All other authors have disclosed no financial interests, arrangements or affiliations in the context of this activity.

Purpose or Case Report: Free-breathing MRI scans are attractive in pediatric imaging as they reduce the need for sedation and breath-holds. In this work, we evaluate a 3D T1w radial "stack of stars" gradient echo (GRE) acquisition (RAVE-RAdial Volumetric Encoding) in post-contrast abdomen and spine protocols and compare results with conventional Cartesian MRI of similar spatial resolution and volume coverage.
Methods & Materials: Studies were performed on a 3T Siemens Prisma. With radial MRI, data are acquired along k-space spokes during repetitions of the sequence. Consecutive spokes are rotated in-plane by the golden-angle (111.25 deg) to maximize k-space coverage. The center of k-space is oversampled and this feature affords RAVE's robustness to motion. When coupled with compressed sensing and parallel imaging, the radial data further yields dynamic images, (i.e., during contrast passage). We have evaluated free-breathing RAVE in 20 patients referred for non-sedated abdominal and spine MRI exams with contrast. In the abdomen, we have acquired RAVE in both axial and coronal orientations (i.e., liver, enterography). In the spine, we have acquired RAVE in the axial plane. Three radiologists compared RAVE to conventional breath-hold GRE in abdomen scans and free-breathing fast-spin-echo (FSE) images in the spine. A 3-point scale was used to evaluate diagnostic image quality: -1=RAVE is superior, 0=equivalent, +1=RAVE is inferior.
Results: In all cases, RAVE images were considered robust to respiratory, cardiac, and gastrointestinal motion, and no artifacts that impacted diagnostic image quality were noted. In the spine, RAVE was consistently superior to FSE ($p<0.01$) in delineating nerve tracts and roots against CSF. In the abdomen, RAVE was comparable to breath-hold GRE scans. Fig 1 shows a series of cervical, thoracic, and lumbar spine comparisons between FSE and RAVE in a 14y patient. Note the lack of motion-related artifacts in RAVE, without the use saturation bands. Fig 2 shows coronal RAVE dynamic frames ~15s apart, highlighting contrast uptake, in a 10y patient. A breath-hold post-contrast GRE image is shown for comparison. Figure 3 shows pre- and post-contrast axial RAVE images in a 14y patient.
Conclusions: Our data demonstrates the potential utility of a free-breathing accelerated 3D T1w RAVE sequence in unsedated pediatric imaging. The technique is particularly useful in patients who are unable to follow breath-hold instructions and suspend respiration, and it is 30-50% faster in scan time than conventional methods.

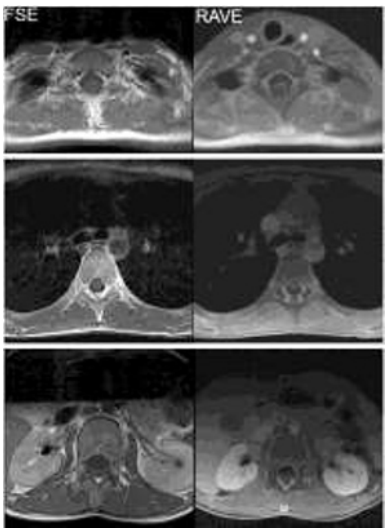

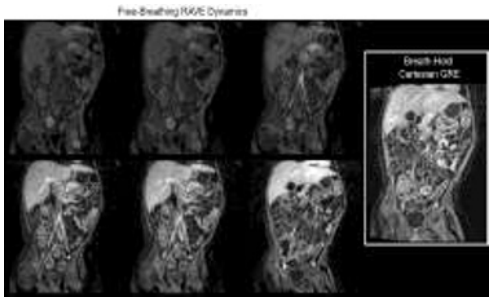

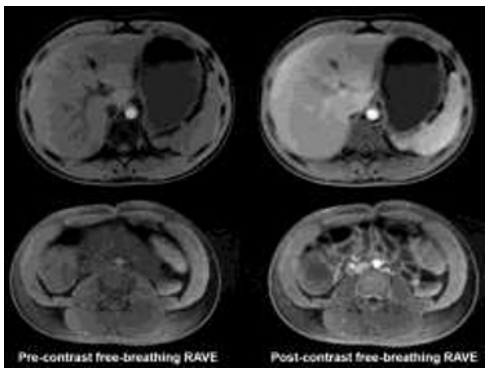

Poster #: SCI-010

The Utilization and Efficacy of a Staged US/CT Algorithm in Suspected Appendicitis in Pediatric Patients

Caroline Hubbard, BS[1], *hubbarca@musc.edu*; Jeanne Hill, MD[1], William Russell, MD[1], Robert Cina, MD[1]; [1]Radiology and Radiological Science, Medical University of South Carolina, Charleston, SC

Disclosures: Caroline Hubbard has indicated a relationship the NIH National Institute of Diabetes and Digestive and Kidney Disease for receiving a research grant. All authors have disclosed no financial interests, arrangements or affiliations in the context of this activity.

Purpose or Case Report: A multi-disciplinary team of physicians developed a clinical practice guideline (CPG) in June 2010 to standardize the diagnosis and management of suspected appendicitis in pediatric patients (< 18 years) who presented to a single institution's emergency room. This study evaluated the utilization and efficacy of the CPG,

comprised of Pediatric Appendicitis Score (PAS) and staged ultrasound (US) and computed tomography (CT) imaging, from 1/1/13-12/31/16. Using baseline data from the first year after implementation, we hypothesized that increased US and PAS utilization would result in improved US performance and a concomitant decrease in CT utilization without loss of diagnostic accuracy.
Methods & Materials: With IRB approval, a retrospective review of patients who had US for appendicitis was performed using Epic and AGFA Impax 6.6.1.3525. Analysis of the utilization and efficacy of US, CT, and the staged US/CT approach was conducted by determining the sensitivity, specificity, and positive and negative predictive values.
Results: 1,466 patient encounters, representing 1,390 different patients, met inclusion criteria. 1,466 US and 261 CT scans were performed; 6 CTs with indications for other acute abdomen etiologies were excluded. 219 US were interpreted as positive, 1,085 as negative, and 162 as equivocal for appendicitis (Table 1). Abdominal US had a sensitivity, specificity, positive predictive value, and negative predictive value of 80.9%, 98.5%, 92.7%, and 95.5% respectively. Abdominal CT had a sensitivity, specificity, positive predictive value, and negative predictive value of 98.4%, 98.9%, 96.9%, and 99.4% respectively. The staged US/CT algorithm had a sensitivity of 97.9%, specificity of 97.7%, positive predictive value of 91.3%, and negative predictive value of 99.5% (Table 2).
Conclusions: Experience and refinement of the appendicitis CPG led to improved US performance as sensitivity increased from 63.9% to 80.9% and specificity from 92.6% to 98.5%. CT utilization decreased overall, with CT use in only 17.4% of patient encounters; however, there was a trend of increasing CT use over time. Of the 316 with an appendectomy, 24.1% had CT (previously 45.5%). An algorithm strength was continuous patient reevaluation by clinicians. Thus, 60.5% of equivocal scans did not have CT, avoiding 98 CT scans. However, despite a negative US, 174 patients (16%) had a CT, only 32 of which proved to have appendicitis. 17 CTs were performed after a positive US, 15 of which characterized suspected ruptured appendicitis.

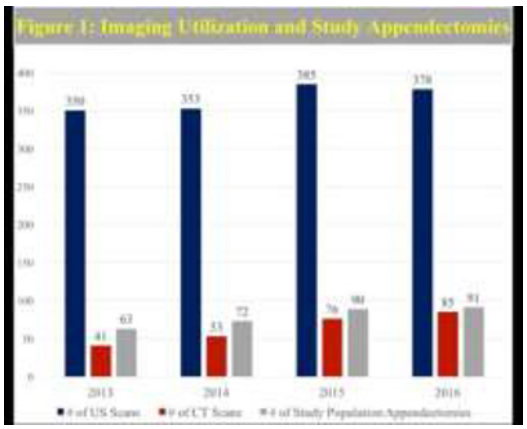

Table 1: Imaging Results

Modality	Negative	Positive	Equivocal
US	1085 (74.0%)	219 (14.9%)	162 (11.1%)
CT	65 (25.5%)	178 (69.8%)	12 (4.7%)

Table 2: US, CT, and Algorithm Performance

Modality	Sensitivity	Specificity	Positive Predictive Value	Negative Predictive Value
Abdominal US	80.9%	98.5%	92.7%	95.5%
Abdominal CT	98.4%	98.9%	96.9%	99.4%
Staged US/CT	97.9%	97.7%	91.3%	99.5%

Poster #: SCI-011

Evaluation of non-contrast MR enterography for pediatric inflammatory bowel disease assessment

Michael Lanier, MD[1], *mlanier@wustl.edu*; Anup Shetty[1], Amber Salter[1], Geetika Khanna[1]; [1]Washington University, St. Louis, MO

Disclosures: All authors have disclosed no financial interests, arrangements or affiliations in the context of this activity.

Purpose or Case Report: Gadolinium deposition in normal tissues is an increasingly recognized consequence of intravenous gadolinium contrast agents. Children with inflammatory bowel disease (IBD) undergo frequent surveillance imaging with contrast enhanced MR enterography (MRE).
Purpose: To determine the benefit (if any) of IV contrast in evaluation of IBD by MRE.
Methods & Materials: This was a retrospective, IRB approved study. The radiology information system was searched to identify all children who had undergone MRE and endoscopy within 6 weeks of each other in 2016. Imaging studies were interpreted by 2 radiologists, blinded to all clinical information, in 2 sessions 6 weeks apart (session 1 pre-contrast MRE; session 2 pre/post contrast MRE). The pre- and pre/post contrast assessment of bowel inflammation was assessed with respect to endoscopy.
A logistic regression model was evaluated using receiver operating characteristics curves and expressed by c-statistics. The concordance of each assessment with endoscopy was compared by the c-statistics using the DeLong method. Agreement between the raters was evaluated using a Cohen's or the weighted kappa statistics, as appropriate, and 95% confidence interval. A two-sided P-value < 0.05 was considered statistically significant. Descriptive statistics were used for assessment of IBD complications, with pre/post MRE as the reference standard.
Results: 52 children (46% female), mean age 13.2 (SD 3.42) years formed the study cohort. 77% (40/52) had evidence of inflammation on endoscopic biopsy. Pre/post contrast MRE showed no significant increase in the c-statistics compared to pre contrast MRE (Table 1). Intravenous contrast showed no significant change in interobserver agreement for assessment of inflammation in either the small (kappa 0.92 pre MRE, 0.88 pre/post MRE) or large bowel (kappa 0.83 pre MRE, 0.73 pre/post MRE). IV contrast had no significant impact on interobserver agreement for length of small bowel inflamed (kappa 0.90 pre MRE, 0.95 pre/post MRE). Assessment of IBD complications was improved with IV contrast, with 3/5 cases with perianal penetrating disease not recognised on pre MRE.
Conclusions: Routine administration of IV gadolinium has no impact on assessment of small or large bowel inflammation. However, there is potential for missing perianal penetrating disease using a non contrast protocol.

	Rater 1	Rater 2
Small Bowel		
c-statistic pre contrast MRE	0.62 (CI 0.48,0.75)	0.64 (CI 0.51, 0.78)
c-statistic pre/post contrast MRE	0.65 (CI 0.52, 0.79)	0.64 (CI 0.51, 0.78)
p-value	0.56	1.0
Large Bowel		
c-statistic pre contrast MRE	0.73 (CI 0.65, 0.80)	0.70 (CI 0.62, 0.78)
c-statistic pre/post contrast MRE	0.70 (CI 0.62, 0.78)	0.70 (CI 0.62, 0.78)
p-value	0.42	1.0

Table 1 C-statistics for pre contrast MRE, pre/post contrast MRE for both readers in assessment of bowel inflammation.

Poster #: SCI-012

Intestinal Stricture Formation Following Medically Treated Necrotizing Enterocolitis: A 10-year Experience at a Tertiary Care Children's Hospital

Erica Poletto, MD[1], *eweinberg2@hotmail.com*; Matthew Richards, MD[2], Bernard Goldwasser, MD[1], Teerin Meckmongkol, MD[1], Sean Ciullo, MD[1], Rajeev Prasad, MD[1]; [1]St. Christopher's Hospital for Children, Philadelphia, PA, [2]Hahnemann University Hospital, Philadelphia, PA

Disclosures: All authors have disclosed no financial interests, arrangements or affiliations in the context of this activity.

Purpose or Case Report: The formation of one or more intestinal strictures is a known complication of necrotizing enterocolitis (NEC). Multiple prior investigations have found that the occurrence of colonic strictures is higher than small intestinal strictures, at an approximate ratio of 2-3:1. We hypothesized that small intestinal strictures may be more prevalent than colonic strictures at our urban, academic, tertiary care children's hospital.
Our first aim was to determine the incidence of small intestinal and colonic strictures in patients with prior medically treated NEC who had not undergone previous surgical intervention. Second, we attempted to evaluate for differences in demographics and other clinical variables between the group of patients with small intestinal strictures versus the group with colonic strictures.
Methods & Materials: Infants who had undergone fluoroscopic imaging studies for the evaluation of intestinal strictures following medically treated NEC were included in the study. Of the 49 patients identified, 15 patients were confirmed to have had stricture formation during subsequent surgical exploration. For each subject the following demographic and clinical data were collected: gender, birth weight, gestational age at birth, age at first diagnosis of NEC, number of episodes of medical NEC, and age at surgery for evaluation of stricture.
Results: 5/15 (33%) subjects had strictures limited to the colon, 8/15 (53%) subjects had strictures limited to the small intestine, and 2/15 (13%) subjects had both small intestinal and colonic strictures. Therefore, the overall incidence of colonic stricture was 7/15 (46.7%; confidence interval: 25-70%) and the overall incidence of small intestinal stricture was 10/15 (66.7%; confidence interval: 42-85%). There was no statistically significant difference in gender, birth weight, gestational age at birth, age at first diagnosis of NEC, number of episodes of medical NEC, or age at surgery between the group of patients with small intestinal strictures versus the group with colonic strictures (p-values range from 0.13 to 0.77).
Conclusions: Small intestinal strictures are more common than colon strictures in our population of patients with medically treated NEC. This is contrary to the findings of most prior investigations that found colonic strictures to be most common. There was no statistically significant difference in patient demographics between the groups, limiting our ability to predict what type of stricture a patient might develop.

Poster #: SCI-013

Incidence and importance of portal venous gas in patients with hypertrophic pyloric stenosis

Sarah Milla, MD[1], *sarahsarvismilla@gmail.com*; Cera Cantu[1], Edward Richer, MD[1], Kiery Braithwaite, MD[1], Leann Linam[1], Erica Riedesel, MD[1], Jonathan Loewen, MD[1], Stephen Simoneaux[1]; [1]Radiology, Emory, Atlanta, GA

Disclosures: All authors have disclosed no financial interests, arrangements or affiliations in the context of this activity.

Purpose or Case Report: Idiopathic thickening of the pyloric muscle can occur in young infants, causing projectile vomiting, electrolyte abnormalities, and necessity for surgical intervention to relieve the gastric outlet obstruction. Case reports have been published describing infants with HPS who also have portal venous gas (PVG) visualized within the liver. The presence of PVG in other clinical scenarios often indicates a severe and potentially life threatening bowel condition. The purpose of this study was to determine the incidence of infants with hypertrophic pyloric stenosis (HPS) and concurrent portal venous gas (PVG), as well as whether there are unique clinical features or different outcomes in the HPS patients with PVG versus without PVG.
Methods & Materials: IRB approval with waiver of consent was granted for this retrospective study. Institutional report search was performed for infant ultrasound reports containing the words "pyloric stenosis", excluding a negative descriptor. Attending pediatric radiologists reviewed sonographic reports and images to confirm positive diagnosis of HPS and collect imaging data. Imaging data recorded included: length of pylorus, thickness of pylorus, sonographic evaluation of liver, presence of portal venous gas, and whether any additional imaging was performed. Clinical data included demographic information, days of symptomatology, presence of electrolyte abnormality, and length of hospital stay.
Results: Between 11/2010-9/2017, 559 ultrasounds were found to be positive for pyloric stenosis at our institution. 343 studies were deemed to have sufficient hepatic imaging to evaluate for portal venous gas. 6 out of the 343 HPS cases demonstrated PVG (1.8%). Pyloric thickness and length measured 4.4 mm and 18.9 mm respectively in HPS patients without PVG, versus 4.2 mm and 19.9 mm with PVG. Male gender predominance was seen in both groups. Average length of stay for both groups was approximately 2 days, with average length of symptoms and electrolyte abnormalities slightly decreased for the 6 patients with PVG than the group without PVG.
Conclusions: Our retrospective study showed an incidence of PVG in approximately 1.8% of our patient population with HPS. Imaging and clinical characteristics were similar between the HPS patients without and with PVG, suggesting that the presence of portal venous gas does not portend overall worse clinical condition or outcome in HPS patients.

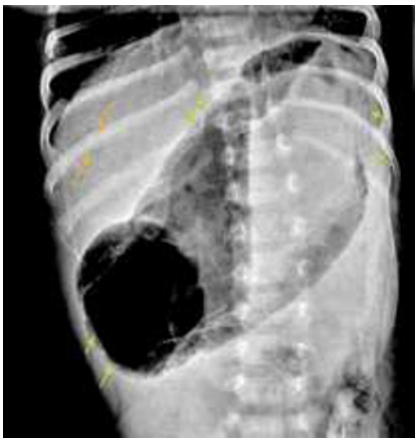

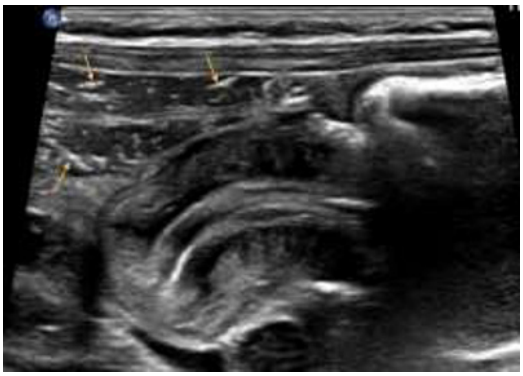

Poster #: SCI-014

Can ultrasound differentiate between right diaphragmatic hernia and eventration?

Andrew Schold, Medical student[2], *ashold@iu.edu*; Megan Marine, MD[1], Brandon Brown, MD, MA[1], Brian Gray, MD[1], Boaz Karmazyn, MD[1]; [1]Radiology, Riley Hospital for Children, Indianapolis, IN, [2]Indiana University School of Medicine, Indianapolis, IN

Disclosures: All authors have disclosed no financial interests, arrangements or affiliations in the context of this activity.

Purpose or Case Report: Radiographic findings of right diaphragmatic eventration may overlap with true hernia if only liver herniates without bowel. We thus wanted to know the accuracy of ultrasonography (US) in the diagnosis of right diaphragmatic hernia.

Methods & Materials: We identified all patients (2007-2016) who had US of the right diaphragm, and surgery for eventration or hernia. The medical record was reviewed for clinical presentation and surgical or pathologic diagnosis. US studies were reviewed for any diaphragm abnormalities. Surgical or pathology diagnosis was considered the gold standard.

Results: 16 children (8 females, age range birth-16 months, mean 5.2 months) had US as well as surgery for eventration (n=7) or hernia (n=9; 6 Bochdalek and 3 Morgagni). The most common presentation was respiratory distress (12/16, 75%). US correctly diagnosed all 9 patients with hernia and misdiagnosed 3 patients with eventration, yielding 100% sensitivity for hernia, 57% specificity, and 81% accuracy. Presence of at least one of the following US findings increased the specificity to 86% with 100% sensitivity, and 94% accuracy: folding of the free diaphragmatic edge (n=8) or liver seen cranial to the diaphragm muscle (n=7).

Conclusions: US imaging can be useful in the diagnosis of diaphragmatic hernia, although it is important to recognize presence of folding of free diaphragmatic edge and liver above the diaphragm muscle to improve specificity and overall accuracy.

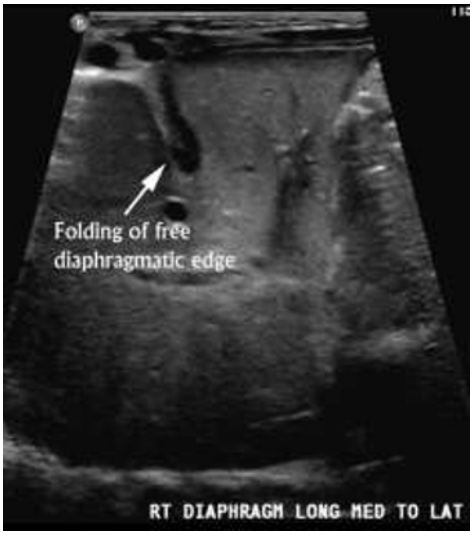

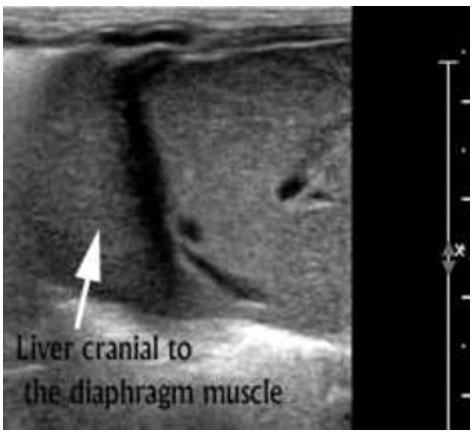

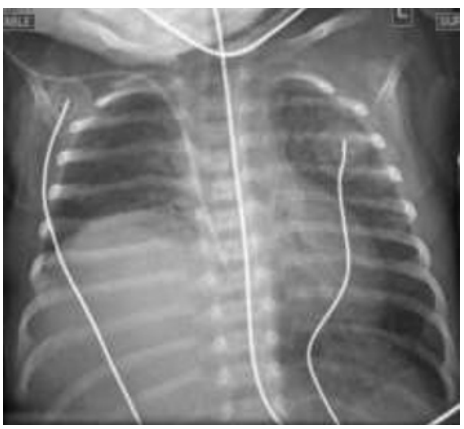

Poster #: SCI-015

Should non pediatric radiologists use ultrasound as the primary study for evaluation of hypertrophic pyloric stenosis?

Daniel Sassoon, PhD[1], *dsassoon@iupui.edu*; Matthew Wanner[1], Megan Marine, MD[1], Boaz Karmazyn, MD[1]; [1]Radiology, Indiana University, Indianapolis, IN

Disclosures: All authors have disclosed no financial interests, arrangements or affiliations in the context of this activity.

Purpose or Case Report: To evaluate false positive rate of community hospital ultrasound (US) diagnosis of hypertrophic pyloric stenosis (HPS)
Methods & Materials: Our institutional review board approved this HIPAA-compliant study; informed consent was waived. We identified all patients (1/2015-12/2016) who performed US for newly diagnosed HPS at an outside hospital (OSH), referred to our children's hospital. Only positive studies were included. Confidence of OSH diagnosis was grouped based on key words as follows: high confidence (compatible, positive, diagnostic of, consistent with, meet criteria for, highly suspicious), low (favor, concern, suspicious, suggesting, may represent), or equivocal (equivocal, non-diagnostic, borderline). OSH imaging and reports for discrepant cases were reviewed by a pediatric radiologist to determine reasons for false diagnosis.
Surgical results were used as the gold standard for positive HPS, while the gold standard for negative HPS utilized was successful non operative management with no readmission for surgery on follow-up chart review.
Results: 65 cases were referred from OSHs to our children's hospital. 6/65 (9.2%) were equivocal for HPS and 59 (90.8) positively identified HPS. Of the 59 cases that identified HPS, 30 (50.8%) did so with high confidence and 29 (49.2%) with low. 11/59 (18.6%) of cases diagnosed with HPS at OSH were not found to be HPS on further evaluation at our institution. Of discrepant cases 2/11 (18.2%) were diagnosed with high confidence by OSH and 9/11 (81.8%) low confidence. The most common 7/11 (%) reason for false positive results was misinterpretation of pylorospasm as HPS.
In 13/59 (22.0%) the US were repeated in our children's hospital as the OSH study was considered technically limited.
Conclusions: US for evaluation of HPS performed by non-pediatric radiologist is a limited study. About half of the positive studies were read with low confidence and 18% of the studies were false positives.

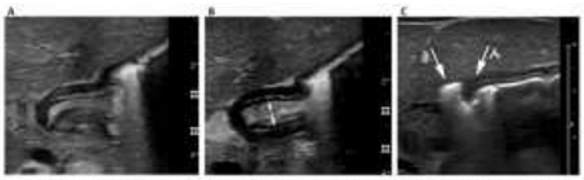

5 weeks old boy with vomiting suspected in a community hospital ultrasound of hypertrophic pyloric stenosis. Outside ultrasound shows elongated antropyloric canal (15 mm) with thickened (2.5 mm) muscle (a) and intermittent opening of the antropyloric lumen (b, double head arrow). A repeated US in our children hospital (b) confirmed pylorospasm demonstrating normal passage of gas from the antrum (A) to the duodenal bulb (B) with no elongation or thickening of the pylorus.

Poster #: SCI-016

Pediatric Transabdominal Ultrasound and Magnetic Resonance Cholangiopancreatography: Inpatient Imaging and Clinical Management

Daniel Nahl[1], *dannynahl@gmail.com*; Justin Glavis-Bloom[1], Amit Sura, MD, MBA[1]; [1]Radiology, Children's Hospital Los Angeles, Santa Monica, CA

Disclosures: All authors have disclosed no financial interests, arrangements or affiliations in the context of this activity.

Purpose or Case Report: Transabdominal ultrasound (TUS) is a fast, safe, and well-established screening modality for identifying pancreas, liver, and biliary tract pathology in the pediatric population. A subset of patients with findings that are incompletely characterized by ultrasound or who have no sonographic evidence of disease but persistent clinical suspicion may receive magnetic resonance cholangiopancreatography (MRCP). Pediatric inpatients who obtain an MRCP often experience longer inpatient stays, higher costs and delays in management. Relying on the sonographic findings or pursuing more advanced imaging as an outpatient may be a better option. To our knowledge, there have been no studies that have assessed whether inpatient MRCP performed following TUS in pediatric patients resulted in significant changes to additional inpatient treatment rendered. Our group ultimately looks to develop interdepartmental guidelines on when pursuit of an inpatient MRCP after TUS is indicated.
Methods & Materials: Our hospital is a pediatric, tertiary referral, level I trauma center with multiple transplantation services and approximately 80,000 emergency department visits each year. We sought to evaluate imaging data and clinical records for all patients at our hospital who received TUS followed by inpatient MRCP evaluation in 2016. This allowed us to investigate if MRCP studies performed after transabdominal ultrasound changed inpatient clinical management in pediatric patients with suspected pancreatohepatobiliary disease. The change was assessed by either an additional inpatient procedure or new treatment administered based on MRCP findings.
Results: There were a total of 101 inpatient MRCPs performed in 2016, of which 84 had a preceding abdominal ultrasound performed. Of these 84 MRCPs, 28 (33.3%) resulted in additional diagnostic information not seen on the ultrasound. Of these 28 studies, there were only eight cases in which the additional information obtained from the MRCP lead to an additional inpatient procedure or new treatment during the course of the patients hospital stay (Figure 1 and Table 1).
Conclusions: Transabdominal ultrasound is the primary screening modality for pediatric pancreatohepatobiliary disease. For some patients, obtaining ultrasound alone, serial ultrasound evaluations, or outpatient MRCP may be sufficient for evaluation. Inpatient MRCP may be over utilized, as only 8 out of 101 (7.9%) of MRCPs performed lead to a significant change in inpatient clinical management.

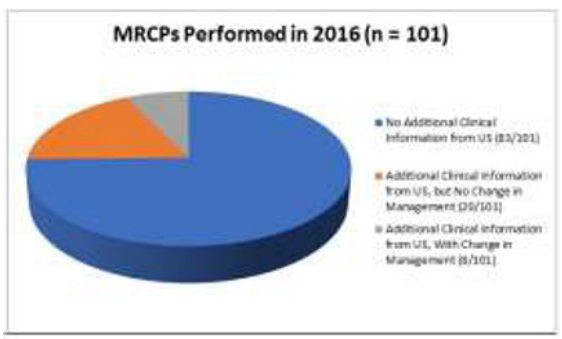

Indication	Abdominal US Findings	Additional Findings on MRCP	Change in Management
16-year-old female, history of biliary atresia and Kasai presenting with jaundice elevated LFTs and GGT in the setting of decompensated chronic liver disease.	Coarse hepatic echotexture.	Periportal edema and mildly dilated, diffusely irregular/beaded intrahepatic biliary ducts.	Yes: Liver biopsy
11-month-old male status post liver transplant, suspected cholangitis.	Normal appearing transplant liver.	Mild intra and extrahepatic biliary dilatation and mild periportal edema.	No
14-year-old male with jaundice, elevated LFTs, suspected Wilson's disease or hepatitis.	Hepatosplenomegaly, gallbladder wall thickening.	Soft tissue thickening at the porta hepatis, extending into the liver along the periportal regions.	Yes: Liver biopsy
19-year-old male with recurrent pancreatitis.	Periportal edema, heterogeneous hepatic parenchyma, gallbladder polyp.	Peripancreatic edema, intra and extrahepatic biliary ductal dilatation, and pericholecystic fluid.	No
16-year-old female with cholecholithiasis.	Cholelithiasis. Enlarged common bile duct with no obstructing gallstone visualized.	Choledocholithiasis and extrahepatic/central intrahepatic biliary ductal dilatation.	Yes: ERCP
12-year-old male with history of Gardner's syndrome, chronic colitis, and liver lesions presenting with abdominal swelling.	Hepatosplenomegaly. Focal lesions within the right hepatic lobe.	Further evaluation of liver lesions suggest hepatic adenomas.	No
8-year-old female status post liver transplant with elevated liver enzymes.	New intrahepatic biliary ductal dilatation within transplanted liver.	Moderate intrahepatic biliary ductal dilatation with the point of narrowing at the hepaticojejunostomy.	No
6-month-old female with choledocholithiasis status post cyst excision, cholecystectomy and choledochoduodenostomy.	Status post resection of choledochal cyst with stable mild intrahepatic biliary ductal dilatation.	Mild intrahepatic ductal dilatation most significant at the porta hepatis and likely at the site of anastomosis.	No
20-year-old male with chromosome deletion and recent abdominal pain.	Limited exam due to body habitus. The gallbladder was not visualized.	Gallbladder visualized and filled with sludge.	No
14-year-old male with hereditary spherocytosis, increased jaundice and conjugated bilirubin.	Hepatosplenomegaly. Echogenic liver. Mild intra and extrahepatic biliary ductal dilatation.	Cholelithiasis and choledocholithiasis.	Yes: ERCP
16-year-old female with ALL, status post bone marrow transplant, elevated lipase.	Mild hepatosplenomegaly. Mild dilatation of the common bile duct.	Cholelithiasis. Linear area of decreased signal in the common bile duct: artifact versus sludge.	No
13-year-old male with pancreatitis and suspected cholelithiasis.	Enlarged, edematous pancreas. Gallbladder wall thickening. Moderate ascites.	Acute pancreatitis with pseudocyst.	No
18-year-old female with ovarian cancer status post bilateral oophorectomies and recent peritonitis. Suspected cholangitis.	Limited visualization of known hepatic tumors secondary to body habitus. No ductal dilatation seen.	Mild intrahepatic biliary ductal dilatation. Nonvisualization of the common bile duct with significant adenopathy at the porta hepatis.	No
10-year-old male with history of hereditary pancreatitis presenting with acute pancreatitis.	Heterogeneous hepatic echogenicity with echogenic portal triads.	MRI findings of acute pancreatitis with mild dilatation of the pancreatic duct.	No
6-year-old female with pancreatitis.	Heterogeneous hepatic parenchyma.	Hepatosplenomegaly with iron deposition.	Yes: treatment for iron overload.
11-year-old male with recurrent acute pancreatitis.	Echogenic pancreatic head.	Normal appearance of the pancreas. Mild intrahepatic biliary ductal dilatation.	No
13-year-old female with Trisomy 21, recurrent pancreatitis.	Mildly dilated common bile duct and pancreatic duct.	Two separate ducts in the pancreatic head which could reflect pancreas divisum or represent interstitial changes from chronic pancreatitis.	No
14-year-old female with acute pancreatitis.	Prominent pancreatic duct with otherwise unremarkable appearing pancreas.	MRI findings of acute pancreatitis with mild dilatation of the pancreatic duct.	No
7-month-old male with recent liver transplant for biliary atresia.	Receiving hematoma lateral to transplant liver.	Mild intrahepatic biliary dilatation in the left lobe of the transplant liver.	No
4-year-old male with vomiting and elevated liver enzymes.	Increased parenchymal echogenicity of the pancreas. Coarse hepatic echotexture.	No MRI evidence of pancreatitis. Mild intrahepatic biliary ductal dilatation.	No
15-Year-old female status post cholecystectomy now with pancreatitis.	Dilated common bile duct and pancreatic duct. Mild hepatosplenomegaly.	Choledocholithiasis with two obstructing stones in the distal common bile duct.	Yes: ERCP
18-year-old female with right upper quadrant pain.	Cholelithiasis and mild pericholecystic fluid.	Mild dilatation of the common bile duct.	No
5-year-old boy with worsening coagulopathy and hyperbilirubinemia. History of cryptosporidia.	Punctate echogenic focus in gallbladder that may relate to small adherent stone versus polyp.	Choledocholithiasis and moderate dilatation of the common bile duct.	Yes: ERCP
10-month-old female with biliary atresia status post liver transplantation.	Heterogeneous hepatic echotexture with minimal intrahepatic ductal dilatation.	Moderate dilatation of intrahepatic bile ducts. Periportal edema and enhancement suggesting cholangitis.	Yes: ERCP
17-year-old female with history of recurrent pancreatitis, concern for pancreatic cyst.	Echogenic pancreas. No organized fluid collection.	Variant pancreas anatomy with identification of an accessory pancreatic lobe. Acute pancreatitis.	Yes: Endoscopic ultrasound.
11-year-old female with pancreatitis.	Mild hepatomegaly. Mild ascites.	Pancreatitis with pseudocyst.	No
7-year-old male with pancreatic contusion and elevated lipase. History of liver transplant.	Echogenic pancreas with adjacent fluid collection.	Focal disruption of the pancreatic duct near the head-neck junction.	No
13-year-old female with right upper quadrant pain, history of recurrent pancreatitis.	New complex fluid collection adjacent to the pancreas.	Dilated pancreatic duct and mild dilatation of the common bile duct.	No

Poster #: SCI-017

Optimizing Magnetic Resonance Enterography for Inflammatory Bowel Disease Based on Incidence of Unsuspected Perirectal Disease

Amie Robinson, BSRT(R)(MR)[1], *alrobinson@cmh.edu*; Nidhi Reddy, BA[2], Sherwin Chan, MD, PhD[1], Neil Mardis, DO[1], Amy Dahl, MD[1], Kristin Fickenscher, MD[1]; [1]Radiology, The Children's Mercy Hospital, Kansas City, MO, [2]University of Missouri - Kansas City, Kansas City, MO

Disclosures: All authors have disclosed no financial interests, arrangements or affiliations in the context of this activity.

Purpose or Case Report: Inflammatory bowel disease (IBD), including Crohn disease, is a cause of significant morbidity in the pediatric population. Perirectal disease is a Crohn related complication affecting as many as 62% of children. Magnetic resonance enterography (MRE) is being increasingly utilized in characterizing the extent of IBD. Dedicated perirectal disease imaging, such as a T2 SPACE, requires an additional 10-15 minutes of imaging time on an already time constrained modality. The goal of our study was to determine the best imaging protocol for patients without clinically suspicious perirectal disease based on the incidence in this population.
Methods & Materials: A retrospective chart review on patients up to 22 years of age who underwent an MRE examination between 1/2015 and 9/2017 for IBD were included in our study. A single reviewer evaluated all included patients' electronic medical records looking for documented clinical suspicion or colonoscopy/pathology findings of perirectal disease prior to MRE. Patients with prior history of perirectal disease or who had clinically suspected perirectal disease by the treating gastrointestinal physician were excluded. All patients in our study population received dedicated perirectal sequences in addition to the conventional MRE sequences. The study population was evaluated for presence of perirectal disease on MRE. Local institutional review board was approved for this study.
Results: A total of 301 patients had MRE for IBD during our two year time frame. Forty-two patients were excluded due to prior clinical suspicion of perirectal disease, yielding 267 patients in our total population. Fourteen patients (5%) had MRE findings of perirectal disease, five (35%) were found to have perirectal abscess and seven (50%) had a perirectal fistula or fistulous tract.
Conclusions: Our study found a 5% incidence rate of perirectal disease in IBD patients without clinical suspicion of perirectal disease. Thus, radiologists need to be aware of this population to add on perirectal sequences where needed to conventional MRE examinations. However, it is an inefficient use of resources to routinely perform perirectal sequences on this group of patients.

Poster #: SCI-018

Use of MRI in risk stratification, diagnosis, and monitoring of Pediatric Non-alcoholic Fatty Liver Disease

Zachary Swenson[1], *zjs4ge@virginia.edu*; Lydia Kuo-Bonde, MD, PhD[1]; [1]Radiology, University of Virginia, Charlottesville, VA

Disclosures: All authors have disclosed no financial interests, arrangements or affiliations in the context of this activity.

Purpose or Case Report: Non-alcoholic fatty liver disease (NAFLD) is now the most common form of pediatric chronic liver disease. This disease can have profound effects on overall health and is associated with diabetes, heart disease, and an

increased risk of hepatocellular carcinoma. The exact pathogenesis of NAFLD remains poorly understood, though it is known to progress to various chronic liver diseases, the most prevalent being hepatic fibrosis. The current gold standard for quantifying fat in the liver is via a core biopsy, which is expensive and carries an inherent risk of morbidity and mortality which makes it unsuitable for screening and monitoring purposes. We propose that MRI can be an effective, fast, and non-invasive method of screening and monitoring pediatric NAFLD. This would allow for earlier diagnosis and monitoring of pediatric NAFLD which would aid in treatment and management of this disease.
Methods & Materials: Children between the ages of 7 and 17 years old with a BMI > 85th percentile were recruited and consented for a fast MRI. Each of these patients underwent a limited MRI of the abdomen which included a Multi-echo 2-point Dixon imaging protocol covering the liver using a 3T Skyra MR-scanner (Siemens, Germany). The liver proton density fat fraction (PDFF) is calculated based upon the multi-echo method estimation where the fat fraction is based upon multiple pairs of opposed phase and in-phase echoes.
Results: Preliminary data in 10 patients shows that in a high risk pediatric population (BMI > 85th percentile) signs of NAFLD are present. The fat fraction in these patients ranged from 6.2% to 33.7% with an average of 18.8%. A fat fraction of > 5% is generally considered to be pathologic with higher numbers indicating more severe disease.
Conclusions: In a high risk pediatric population (BMI > 85th percentile), MRI can be used as a fast and non-invasive way of screening for pediatric NAFLD. This can be used to provide earlier diagnosis and monitoring of pediatric NAFLD helping to treat and manage this disease.

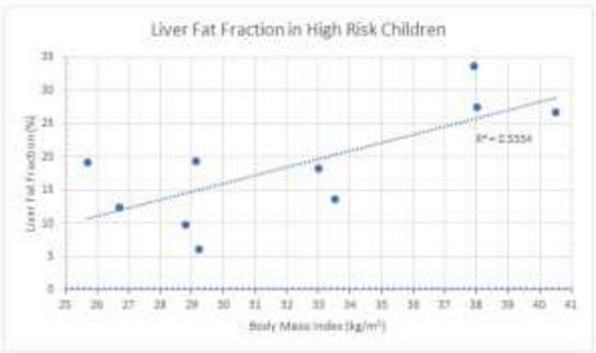

Poster #: SCI-019

Bowel Patterns on the Abdominal Radiograph Complicated by the Simple Sump

Rachelle Durand, DO[1], *durandr@email.chop.edu*; Michael Francavilla, MD[1], Christopher Edgar[1], Carolina Maya, MD[1], Summer Kaplan, MD, MS[1]; [1]Radiology, Children's Hospital of Philadelphia, Philadelphia, PA

Disclosures: All authors have disclosed no financial interests, arrangements or affiliations in the context of this activity.

Purpose or Case Report: Although ultrasound has advantages for bowel assessment in infants, the majority of bowel evaluation still takes place by radiograph. Although radiographic signs of advanced necrotizing enterocolitis (NEC) have been well documented, there is poor understanding of gas patterns in less severe NEC or other causes of feeding intolerance. Progressively abnormal appearance of gas patterns in NEC has been described, but it is unclear what role a gastric sump plays. Because a sump decompresses bowel and changes the gas pattern, its role in the progression of abnormal bowel gas patterns warrants attention.
Methods & Materials: We retrospectively reviewed bowel gas patterns in babies < 1 year old in the neonatal intensive care unit (NICU) over a one-year period. We selected infants whose abdomen or chest/abdomen radiographs were performed for reasons including: NEC, necrotizing, enterocolitis, pneumatosis, distension, or perforation. To assess how the sump affected progression of bowel gas pattern, we randomly selected 11 infants with 5 - 20 radiographs for the above indications performed < 24 hours from each prior. We evaluated supine radiographs using the Duke Abdominal Assessment Score (DAAS) and noted sump presence in the images. Chi-square tests assessed differences in proportions of infants with presence/absence of sump having positive/negative DAAS score.
Results: Our review included 107 exams on 11 patients. DAAS score 4 (Separation or focal thickening of bowel loops) was associated with presence of a sump in 88% of exams ($p = 0.01$). DAAS scores 0 (Normal gas pattern) and 2 (Moderate distention) were associated with absence of a sump in 62% of exams ($p < 0.01$) and 78% of exams ($p < 0.05$), respectively. DAAS score 3 (Focal moderate distention of bowel loops) had a trending significance with a sump present in 77% of exams ($p = 0.07$). Remainder of the DAAS scores ≤ 7 had no association with sump. No DAAS scores > 7 were recorded in our study.
Conclusions: Presence of a sump was associated with the appearance of separation or focal thickening of bowel loops and may correlate with focal moderate distention in a larger sample. It is therefore worth considering whether these gas patterns truly represent progression of disease or simply bowel decompression with a sump. In such cases, ultrasound may help differentiate fluid-filled bowel from partially decompressed bowel. A better understanding of the pathophysiology underlying these gas patterns may help guide management before the advanced stage of NEC.

Poster #: SCI-020

Intussusceptions along Gastrojejunostomy tubes: Known complication or new issue?

Kelly Dietz, MD[2], *diet0148@umn.edu*; Elissa Downs, MD[1], Alan Baldridge, MD[1]; [1]University of Minnesota Masonic Children's Hospital, Department of Gastroenterology, Minneapolis, MN, [2]University of Minnesota Masonic Children's Hospital, Department of Radiology, Minneapolis, MN

Disclosures: All authors have disclosed no financial interests, arrangements or affiliations in the context of this activity.

Purpose or Case Report: Gastrojejunostomy (GJ) tubes are a convenient way to provide nutrition to children with complex medical issues. A known complication is development of a small bowel intussusception. We perceived an increase in GJ tube intussusceptions (GJIs) at our quaternary care hospital. The purpose of our study was to identify cases of GJI, risk factors for development, and determine if there was a safety device issue.
Methods & Materials: After Institutional Review Board approval, cases of GJI were identified over a 24 month period (2014-2016). Patient records were reviewed for pertinent clinical information and information related to the GJ-tube including type of tube, presenting symptoms of GJI, and management of the GJI.
Results: During the study period, a total of 123 patients had at least one GJ-tube tube placed or replaced. Of those patients, 17 developed a GJI. The median patient age was 3.3 years (range 0.4-15.1 years). All patients had complex medical histories (Table 1). The last tube manipulation prior to intussusception occurred a median of 38 days prior to GJI, with 8 occurring <30 days after manipulation, and 5 occurring between 30-60 days

after manipulation. Imaging was obtained after suspicious signs and symptoms (Table 2). Abdominal ultrasound was ordered and diagnosed 10 cases (56%), CT 6 cases, and MRI 2 cases. There was a wide variety of tubes seen in patients with GJI (Table 3). The initial management plan included GJ-tube removal in 11 patients, removal and replacement of a different tube in 3 patients, and monitoring in 4 patients, 2 of which were asymptomatic. A total of 9 patients either kept or required their GJ-tube be replaced, with replacement an average of 10.8 days after GJI. In 50% of patients, gastrostomy tube feeds were tolerated and replacement of the GJ-tube was not required.
Conclusions: Given intussusceptions were observed across various GJ tubes, a specific device safety issue was not identified. We found a 14% rate of intussusception in our complex patient population, which is similar to previously published GJI rates. An unexpected finding was that 50% of patients went on to tolerate gastrostomy tube feeds, not requiring replacement of their GJ tube. A positive outcome of our research project has been an increased awareness of this complication throughout the hospital, and after education an increased utilization of abdominal ultrasound in patients with GJ-tubes and any suspicious symptoms.

Table 1

Presenting symptom	Number of patients
Agitation/pain	11 (65%)
Vomiting or bilious g-tube output	6 (35%)
Bloody stool	3 (18%)
Diarrhea	3 (18%)
Desaturations	3 (18%)
Asymptomatic	2 (12%)
Lethargy	1 (6%)

Table 2

Size of tube (french)	Length of tube (cm)	Number of patients
14	22 30	4 2
16	22 30 45 unknown	1 4 4 1
18	45 unknown	1 1

Table 3

Medical History	Number of patients
Cardiac issue	8 (35%)
Chronic or acute pancreatitis	6 (35%)
Prematurity	6 (35%)
Status Post Transplant Bone Marrow Transplant TPIAT Liver Heart	9 total (53%) 2 5 1 1
Other procedures	3 (18%)

Poster #: SCI-021 - *Withdrawn*

Poster #: SCI-022

The Correlation between Serial Ultrasound and Diuretic Renography in Children with Unilateral High-Grade Hydronephrosis

Carl Flink, MD[1], *flinkcc@uc.edu*; Deborah Jacobson[2], Earl Cheng, MD[2], Emilie Johnson, MD, MPH[2], Elizabeth Yerkes, MD[2], Max Maizels[2], Bruce Lindgren[2], Dennis Liu[2], Ilina Rosoklija, MPH[2], Edward Gong[2]; [1]University of Cincinnati, Cincinnati, OH, [2]Lurie Children's Hospital/Northwestern University, Chicago, IL

Disclosures: All authors have disclosed no financial interests, arrangements or affiliations in the context of this activity.

Purpose or Case Report: Serial renal ultrasound (RUS) is often used as a surrogate for functional renal imaging among patients followed for hydronephrosis. However, it is unclear whether a lack of progression on serial RUS safeguards against loss of renal function. This study was performed to better characterize the association between findings on serial RUS and diuretic renography (DR) among children with unilateral high-grade hydronephrosis.
Methods & Materials: We retrospectively reviewed imaging among children <18 years with a history of unilateral Society of Fetal Urology (SFU) 3-4/Urinary Tract Dilation (UTD) P2-3 hydronephrosis. All patients underwent 2 RUS and 2 DR. Patients were excluded for comorbidities associated with bladder-level dysfunction, uninterpretable DR, or diuretic usage during only one RUS. Each RUS was paired with a contemporaneous DR and compared with a subsequent study pair. All studies were reviewed by an independent, blinded diagnostic radiologist. Change in hydronephrosis was determined by either (1) change in SFU/UTD grade or (2) any change noted by the radiologist. This was compared with change in DR, with a ≥5% change considered significant. Chi-squared and Spearman's correlation analyses were performed.
Results: 85 patients aged 0-14 years (mean 12 months) were included in the final analysis. Patients were predominantly male (73%) with SFU 3/UTD P2 hydronephrosis (85%). Time between DR ranged from 1-112 months (mean 20). Worsening hydronephrosis was noted in 10/85 patients (12%) by SFU/UTD grade and in 28/85 patients (33%) by radiologist interpretation. Differential renal function decreased by ≥5% in 15/85 patients (18%). Changes in DR were significantly associated with changes in SFU/UTD grade on RUS among all patients (p=0.004, Table 1) and among patients with SFU 3/UTD P2 hydronephrosis (p=0.005, Table 2). Less substantial changes were not associated with DR findings (p=0.2). 10/70 (13%) patients with stable or improved SFU/UTD grade developed worsening renal function during the study period. When RUS and DR were directly compared, the Spearman's correlation was poor (r=0.2, CI [0.03-0.4]).
Conclusions: While substantial changes in RUS findings were associated with corollary changes on DR, the overall correlation between imaging modalities was poor. 13% of children with SFU 3-4/UTD P2-3 hydronephrosis experienced a loss of renal function despite stable longitudinal RUS imaging. These findings are important to consider when counseling conservatively managed patients followed without DR.

Anatomic Imaging: Renal Ultrasound	Functional Imaging: Diuretic Renogram: No Change in Split Differential Function		≥5% Change in Split Differential Function		Totals	p-value
SFU/UTD Grade Change						
Stable/Improved	65	(86.7%)	10	(13.3%)	75	0.004
Worsened	5	(50.0%)	5	(50.0%)	10	
Radiologist Interpretation						
Stable/Improved	49	(86.0%)	8	(14.0%)	57	0.21
Worsened	21	(75.0%)	7	(25.0%)	28	

Anatomic Imaging: Renal Ultrasound	Functional Imaging: Diuretic Renogram: No Change in Split Differential Function		≥5% Change in Split Differential Function		Totals	p-value
SFU/UTD Grade Change						
Stable/Improved	54	(87.1%)	8	(12.9%)	62	0.005
Worsened	5	(50.0%)	5	(50.0%)	10	
Radiologist Interpretation						
Stable/Improved	40	(85.1%)	7	(14.9%)	47	0.34
Worsened	19	(76.0%)	6	(24.0%)	25	

Poster #: SCI-023

Detection of ovarian torsion on pelvic ultrasound using multiple features including ovary medialization

Jeffrey Otjen, MD[1], *Jeffrey.otjen@seattlechildrens.org*; A. Luana Stanescu, MD[1], David Ansdell[2], Adam Alessio[1], Marguerite Parisi, MD, MS[1]; [1]Radiology, Seattle Children's Hospital, Seattle, WA, [2]Kapiolani Medical Center, Honolulu, HI

Disclosures: Adam Alessio has indicated a relationship with GE Healthcare and Philips Healthcare for receiving research grants. All other authors have disclosed no financial interests, arrangements or affiliations in the context of this activity.

Purpose or Case Report: Pelvic ultrasound is commonly used to detect ovarian torsion, but the diagnosis remains challenging as there is no single pathognomonic feature. This retrospective case-controlled study aims to identify an algorithm to detect torsion based on common ultrasound imaging features.
Methods & Materials: In this IRB approved retrospective study, patients who underwent pelvic ultrasound because of abdominal or pelvic pain between 2005 and 2015 were identified and classified as either torsion-absent or torsion-confirmed, based on final radiologic and surgical evidence. Of patients with torsion, patients less than 1 year of age were excluded as infants with torsion have different presentation and imaging features than older patients. In total, 99 torsion-confirmed and 331 sequential torsion-absent cases from 2015 were included. Radiologic features extracted from the ultrasound images included binary variables of presence of Doppler flow, free fluid, peripheral follicles, as well as ovary medialization and the continuous variables of right and left ovarian size. These features were fed into supervised learning systems to find viable decision algorithms. Data was divided into 60% training and 40% validation data sets and performance was assessed using sub-sets of the validation set.
Results: All variables had statistically significant differences between the torsion-confirmed and torsion-absent groups with p-values < 0.005 (Table 1). Using single variables to identify torsion provided only modest detection performance with areas under the curve (AUC) for medialization, peripheral follicles, and absence of flow of 0.76+/-.16, 0.66+/-0.14, and 0.82 +/-.14 respectively. The best decision tree (Fig. 1) using a combination of variables yielded an AUC of 0.96 +/- 0.07 and required knowledge of the presence of flow, peripheral follicles, the volume of both ovaries, and presence of cysts.
Conclusions: An algorithm combining multiple ultrasound imaging features associated with ovarian torsion performs better than simple approaches relying on singular features. While complex combinations using multiple interaction models provide slightly better performance, a clinically pragmatic decision tree can be employed to detect torsion and provide sensitivity levels of 95+/-14% with a specificity of 92 +/-2%.

Table 1. Summary statistics of measurement variables for all patients greater than 1 year old. p-values calculated using fisher exact test for binary variables (Medialized, Flow, Cyst, Free Fluid, Right Dominant, Follicles) and one sided t-test with unequal variance for continuous variables.

	Torsion	Normal	p-value	# Missing Torsed	# Missing Normal
Number	99	331			
Age (yrs)	11.8 +/- 4.1	14.2 +/- 3.6	<0.001	0	0
Right Dominant	56.60%	55.60%	0.91	0	0
Medialized	59.60%	1.20%	<0.001	0	0
Flow	30.20%	99.40%	<0.001	13	0
Cyst	68.70%	7.30%	<0.001	0	0
Free Fluid	58.20%	67.60%	0.09	1	1
Periph Follicles Present	41.20%	0.60%	<0.001	2	0
Volume Current Ovary (cc)	185.8 +/- 286.6	7.6 +/- 11.0	<0.001	0	0
Ratio Current to Contralateral Ovary Volume	30.7 +/- 41.2	1.4 +/- 2.1	<0.001	9	0
Ratio Volume Current Ovary to Age (cc/yrs)	15.9 +/- 22.3	0.5 +/- 0.7	<0.001	0	0

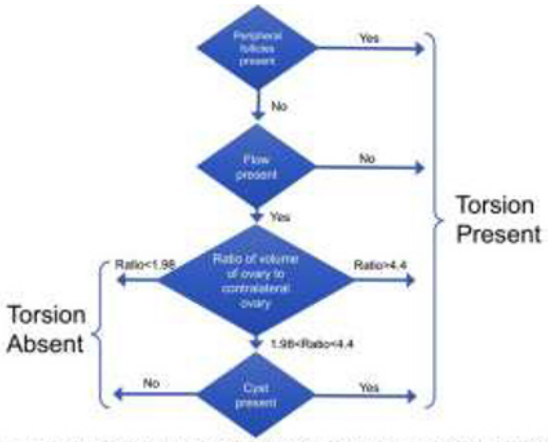

Figure 1. Optimal decision tree to identify torsion based on multiple features from pelvic ultrasound. Tree was learned from a training set of 258 exams. The decision process starts at the top and leads to a high sensitivity decision algorithm with a sensitivity of 95%+/-14% with the validation data set of 172 exams.

Poster #: SCI-024

Normal ovarian size on gray-scale ultrasound in the pediatric population: an update.

Jeffrey Otjen, MD[1], *Jeffrey.otjen@seattlechildrens.org*; David Ansdell[2], A. Luana Stanescu, MD[1], Adam Alessio[1], Marguerite Parisi, MD, MS[1]; [1]Radiology, Seattle Children's Hospital, Seattle, WA, [2]Kapiolani Medical Center for Women and Children, Honolulu, HI

Disclosures: Adam Alessio has indicated a relationship with GE Healthcare and Philips Healthcare for receiving research grants. All other authors have disclosed no financial interests, arrangements or affiliations in the context of this activity.

Purpose or Case Report: Ultrasound has long been a readily available, noninvasive, and accurate means of evaluating the female pelvis and is widely used in the emergency setting for girls with abdominal and pelvic pain. One key element in evaluating for pathology is to measure ovarian size and compare left and right ovaries. Normative volume data stratified by age are available; however, these studies suffer from lack of numbers, and frequently older equipment. Technological advances in ultrasonic hardware and software have increased the resolution of both gray-scale and Doppler imaging. Increases in

spatial resolution allow for better identification and measurement of ovaries and precise measurements and depictions of anatomic details. The purpose of this study was to re-evaluate normal pediatric ovarian volumes in relation to patient age with a larger dataset and newer technology.
Methods & Materials: After IRB approval at a freestanding children's hospital, a database of radiology examinations was queried to pull sequential pelvic ultrasounds for girls that presented to the emergency room with abdominal or pelvic pain from April 2015 to May 2016. Due to limited numbers of younger patients, the database was re-queried for girls from 2006-2017, ages 6 years old or less. Cases with identified ovarian or pelvic pathology including torsion, masses, cysts, and also those with appendicitis were excluded, as were patients with prior oophorectomy. In total, 420 cases were evaluated.
Results: In this cohort the average patient age was 12.2±5.1 years old. A slight majority of the patients had larger right ovaries (53.3%) with on average the dominant ovary being 2.1±3.1 times larger than the contralateral side. Ovarian size was found to increase with age with a linear fit to the data revealing an approximate 0.7 cc increase in volume per year of age (figure 1). For increasing age categories of 0-3, 4-6, 7-10, 11-15, >16 years old, the average ovarian volume was 1.1±1.4, 1.2±1.2, 1.3±0.9, 8.1±8.9 and 9.3±8.4 cc respectively.
Conclusions: An updated case series for normal ovarian sizes is presented. This is useful, particularly in the setting of emergency evaluation for torsion and other pelvic pathology, and can reasonably be extrapolated to the outpatient setting.

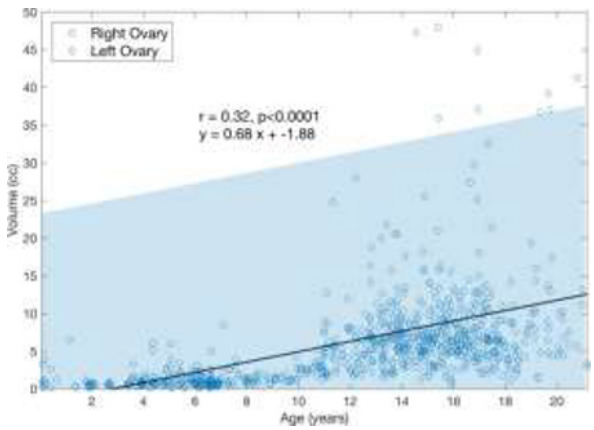

Poster #: SCI-025- *Withdrawn*

Poster #: SCI-026

Comparison of Ultrasound versus Computed Tomography for the Detection of Kidney Stones in the Pediatric Population: a Clinical Effectiveness Study

Nathaniel Roberson[1], *robersnp@mail.uc.edu*; Jonathan Dillman, MD, MSc[2], Sara O'Hara, MD[2], William DeFoor[3], Pramod Reddy[3], Richard Giordano[2], Andrew Trout[2]; [1]University of Cincinnati College of Medicine, Cincinnati, OH, [2]Cincinnati Children's Hospital Medical Center: Department of Radiology, Cincinnati, OH, [3]Cincinnati Children's Hospital Medical Center: Division of Pediatric Urology, Cincinnati, OH

Disclosures: William DeFoor has indicated a relationship with United Medical Systems for receiving stock options. All other authors have disclosed no financial interests, arrangements or affiliations in the context of this activity.
Purpose or Case Report: To determine the diagnostic performance of renal ultrasound for diagnosing nephrolithiasis in children using a clinical effectiveness approach.
Methods & Materials: Institutional review board approval with a waiver of informed consent was obtained for this retrospective, HIPAA-complaint investigation. Billing records and imaging reports were used to identify children (≤18 years-old) evaluated for nephrolithiasis by both ultrasound and unenhanced CT within 24 hours between March 2012 and March 2017. Imaging reports were reviewed for presence, number, size, and location of kidney stones. Diagnostic performance of ultrasound (reference standard = CT) was calculated per renal unit (left/right kidney) and per renal sector (four sectors per kidney). For sector analysis, ultrasound was considered truly positive if a stone was identified at CT in the same or an adjacent sector.
Results: There were 68 renal stones by CT in 30/69 patients (43%). Mean patient age was 14.7±3.6 years, and 35 were boys. For detecting nephrolithiasis in any kidney, ultrasound was 66.7% (48.8-80.8%) sensitive and 97.4% (86.8-99.9%) specific (positive predictive value [PPV]=95.2% [77.3-99.8%], negative predictive value [NPV]=79.2% [65.7-88.3%], and positive likelihood ratio [PLR]=26.0). Per renal sector, ultrasound was 59.7% (46.7-71.4%) sensitive and 97.4% (95.5-98.5%) specific (PPV=72.3% [58.2-83.1%], NPV=95.4% [93.2-96.9%], PLR=22.5). Of the 30 stones not detected by ultrasound, only three were >3 mm at CT.
Conclusions: In clinical practice, ultrasound has high specificity for detecting nephrolithiasis in children but only moderate sensitivity and false negatives are common.

Poster #: SCI-027

Fluoroscopic practice patterns during pregnancy in Pediatric Radiologists

Jane Kim, MD[1], *janekim80@gmail.com*; Jennifer Son, MD[1], Erica Poletto, MD[2], Andrew Phelps, MD[4], Terry Levin, MD[3]; [1]University of Maryland Medical Center, Baltimore, MD, [2]St. Christopher's Hospital for Children, Philadelphia, PA, [3]Montefiore Medical Center, Bronx, NY, [4]UCSF Benioff Children's Hospital, San Francisco, CA

Disclosures: All authors have disclosed no financial interests, arrangements or affiliations in the context of this activity.

Purpose or Case Report: To describe the fluoroscopic practice patterns during pregnancy in pediatric radiologists and potential impact on professional relationships and career.
Methods & Materials: An anonymous online survey was sent to SPR members via email.
Results: Of 398 responses (65% female, 35% male), most females (78%) reported being pregnant while practicing radiology. The majority (72%) announced their pregnancy during the first trimester. Factors affecting the timing and decision to announce pregnancy included fear of miscarriage (43%), impact of co-workers having to perform extra work during maternity leave (42%), impact of co-workers having to perform extra fluoroscopy during pregnancy (32%), negative reaction from co-workers (22%), and fear of negative impact on career (21%).
The majority (85%) performed fluoroscopy during pregnancy. Forty percent felt they had a choice whether to perform fluoroscopy; 28% said it depended on the pregnancy; and 32% felt they had no choice. Most performed fluoroscopy during all 3 trimesters (1st 78%, 2nd 90%, 3rd 87%). The majority (81%) double leaded; 45% asked a coworker to cover fluoroscopy; 38% observed trainees performing fluoroscopy; 37% used a lead shield. Forty-six percent felt their fluoroscopic responsibilities during pregnancy were stressful. Physical demands included lead aprons being too heavy (42%) or not fitting (29%), and back pain (38%), and 26% described no extra physical demands.
Of all male and female survey respondents, 56% have had to cover fluoroscopy for a pregnant co-worker; a majority (76%) did not consider this burdensome. Twenty percent of women

who opted to perform less fluoroscopy felt it negatively impacted their professional relationships and/or career. After witnessing a pregnant co-worker perform less fluoroscopy,16% of female and 0.04% of male respondents observed a subsequent negative impact on her professional relationships and/or career.
Conclusions: The majority of responding SPR female members have performed fluoroscopy during pregnancy. Of the respondents who performed less fluoroscopy during pregnancy, twenty percent reported a negative impact on their professional relationships and/or career. Interestingly, even fewer respondents reported witnessing a negative impact on a co-worker with significant differences in male and female responses. The negative impact of avoiding fluoroscopy during pregnancy is either under-discussed or over-estimated by pregnant radiologists.

Poster #: SCI-028

Imaging properties of Additive Manufactured (3D Printed) Materials for potential use for Phantom Models

Elizabeth Silvestro, MSE[1], *silvestre1@email.chop.edu*; Raymond Sze[1]; [1]Radiology- CHAMP Lab, Children's Hospital of Philadelphia, Philadelphia, PA

Disclosures: All authors have disclosed no financial interests, arrangements or affiliations in the context of this activity.

Purpose or Case Report: Additive manufacturing (also called 3D printing and rapid prototyping) in medical research and clinical applications is expanding. This study aims to quantify the imaging characteristics (Ultrasound, Magnetic Resonance Imaging, and Computed Tomography scan) of available materials on a common additive manufacturing technology and discuss potential opportunities to fabricate imaging phantoms, which can be utilized in:
-Training residents and technologists on the equipment and techniques
-Practice for unique case studies and interventions
-Planning procedures for complex surgical and interventional cases
-Quality assurance of equipment for safety
These would be high accuracy and cost-effective models, providing significant savings for purchased phantoms, which can cost over $3k. Moreover, printed phantoms allow custom phantoms for specific applications or anatomy unique to specific patient beyond pre-fabricated options.
Methods & Materials: A material sample phantom was fabricated by embedding printed materials and blends into silicon. Technologists scanned the material phantom using 3 scanning modalities (Ultrasound, Magnetic Resonance Imaging, and Computed Tomography). The images were then evaluated for echogenicity, relaxation, and radiodensity, respectively. Dimensional accuracy of the printed phantoms was also evaluated.
Results: Ultrasound phantom scanning produced clearly defined edges of the material but did not provide a range of different echogenicities. MRI scanning showed distinct signal intensity between model (14.7 grayscale value) and printer support (789.33 grayscale value), but no distinguishing signal between different print materials. CT scans showed variation in plastic and rubber materials between 93 to 160 Hounsfield units. Dimensional measurements confirmed the accuracy of printed phantoms to the original design.
Conclusions: The imaging properties of additive manufacturing offer an opportunity to create simple phantoms applicable. These materials cannot currently be extended to complex multi-material application as realistic as the imaging properties of human tissue. However, in this developing field, we anticipate new density varied materials that will better approximate the imaging characteristics of the anatomy. Particularly promising are the ongoing studies into composites and fiber laced materials. This report supports the potential of additive manufacturing to create simple, accurate, and cost-effective imaging phantoms, which could expand with further material research.

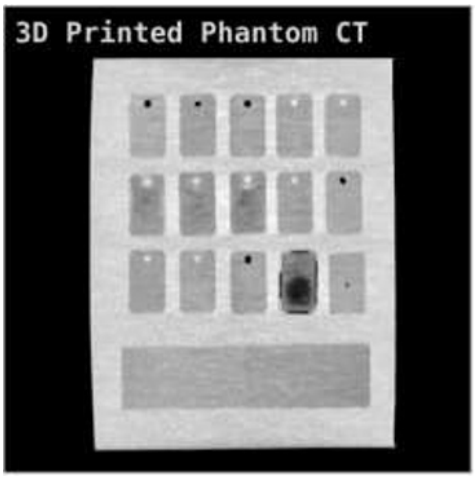

Poster #: SCI-029

Second Opinion Interpretation of Outside Imaging by Radiology Residents and Pediatric Radiologists at a Tertiary Children's Hospital

Justin Glavis-Bloom[1], *justingb@gmail.com*; Daniel Nahl[1], Amit Sura, MD, MBA[1]; [1]Children's Hospital Los Angeles, Los Angeles, CA

Disclosures: All authors have disclosed no financial interests, arrangements or affiliations in the context of this activity.

Purpose or Case Report: To study the frequency of discrepancies between interpretations of radiologists at outside referring hospitals, overnight residents preliminarily interpreting imaging, and pediatric fellowship trained attending radiologists at a tertiary children's hospital.
Methods & Materials: We retrospectively reviewed all requests for second opinion interpretations of plain film and computed tomography (CT) imaging at our institution in 2016 that occurred between the hours of 4:30pm to 6:00am, when on-call radiology residents provide preliminary interpretation. Our hospital is a pediatric, tertiary referral, level I trauma center with multiple transplantation services and approximately 80,000 emergency department visits each year. Patients are frequently

transferred to our emergency department and inpatient services from a large catchment area extending to Northern California, Nevada, and Arizona, and often arrive with outside hospital diagnostic imaging and radiologist interpretations. Using the RADPEER Scoring System (Table 1), we compared the interpretations of the outside hospital radiologist, overnight radiology resident, and attending pediatric radiologist.
Results: There were 158 requests for second opinion interpretations, of which 149 were CT scans and 9 were plain films. The overnight radiology resident and attending pediatric radiologist concurred in their interpretations (RADPEER score 1) in 145 studies (92%), had discrepancies that were not ordinarily expected to be made (RADPEER 2) in 12 studies (8%), and had a discrepancy that should have been made and was likely clinically significant (RADPEER 3b) in 1 study. Of the 12 RADPEER 2 studies, 9 were likely clinically significant (2b). The radiologist at the outside referring hospital and attending pediatric radiologist concurred in their interpretations (RADPEER score 1) in 146 studies (92%), had discrepancies that were not ordinarily expected to be made and were likely clinically significant (RADPEER 2b) in 11 studies (7%), and had a discrepancy that should have been made but was likely not clinically significant (RADPEER 3a) in 1 study.
Conclusions: There was a high degree of concordance between interpretations provided by outside hospitals, overnight radiology residents, and attending pediatric radiologists at our institution.

Table 1: RADPEER Scoring System (May 2016)

Score	Meaning	Optional
1	Concur with interpretation	
2	Discrepancy in interpretation/not ordinarily expected to be made (understandable miss)	a. Unlikely to be clinically significant b. Likely to be clinically significant
3	Discrepancy in interpretation/should be made most of the time	a. Unlikely to be clinically significant b. Likely to be clinically significant

Poster #: SCI-030

IR service impact in developing a clinical pathway for parapneumonic effusion.

Nancy Ghaleb[1], *NAGHALEB@uams.edu*; Shobit Sharma[1], Charles James, MD[1], Malik Dawoud[1], Paul Lewis[1], Mary Moore[1], Jim Parks[2], Emily White[2], Paula Roberson[3], Amir Pezeshkmehr[1]; [1]Pediatric Radiology, Arkansas Children's Hospital; University of Arkansas for Medical Sciences, Little Rock, AR, [2]Arkansas Children's Hospital, Little Rock, AR, [3]University of Arkansas for Medical Sciences, Little Rock, AR

Disclosures: Charles James has indicated a relationship with Acetaminophen Toxicity Diagnostics for receiving a research grant, Acetaminophen Toxicity Diagnostics and Bioventures for partner's ownership and partner's research grant. All other wuthors have disclosed no financial intersts, arrangements or affiliations in the context of this activity.

Purpose or Case Report: Evaluate IR service performance and patient outcomes following implementation of a clinical pathway for parapneumonic effusion.
Methods & Materials: *Background:* Upon completing a 2.5 year IRB approved observational study (control, Group A), the IR team developed the following dosing protocol for pleural tPA based on chest ultrasound findings: Grade 1, <50% pleural echogenicity, 1 mg BID; Grade 2, > 50% pleural echogenicity, 2 mg BID. *Study period:* IRB modification was obtained to review subsequent retrospective data and prospective data of patient characteristics and treatment responses during two discrete time periods: Group B - during pathway development: (July 2015-April 2017); and Group C - following pathway implementation: (May 2017-October 2017). Data elements of the review included diagnostic ultrasound, IR procedure note and daily IR rounding notes for chest tubes inserted exclusively for pneumonia. The following patient information was captured: age, gender, weight, tPA dose (1mg, 2mg), dose frequency, duration of tPA therapy, positive culture/PCR, subsequent IR procedure, need for surgery and hospital stay. Findings of the retrospective data review (Table 1) were leveraged to develop a hospital-wide clinical pathway for parapneumonic effusion. Statistical analysis included comparison of ultrasound grade and outcomes of the two discrete times periods listed above. In calculating hospital stay, subjects with co-morbid conditions that may have prolonged the hospital stay were excluded from the analysis.
Results: In Group B, duration of tPA therapy for Grade 1 (2.1 days) was lower than that of Grade 2 (3.8 days, p=0.03); positive cultures/PCR were more common in Grade 2 patients (p=0.03). In Group B, patients received the correct tPA protocol dose based on ultrasound grade (Grade 1 p<0.0001, Grade 2, p<0.0001). In the study period, days of BID dosing (84.6%) was greater compared to the control period (24.2%, p<0.0001) and more patients were Grade 2 (74.4%) compared to the control period (30.3%, p=0.0003). Duration of tPA therapy for Grade 1 (1.95 days) was lower than that of Grade 2 (3.64 days, p=0.004). Median hospital stay (8 days) did not differ compared to the control period (p=0.18).
Conclusions: An IR team standardized hospital-wide BID pleural tPA dosing by developing a clinical pathway. Despite treating more complex Grade 2 patients, hospital stay remained unchanged.

ANALYSES OF STUDY DATA VERSUS CONTROL				
	Group A+B+C (n=72)	Group A (n=33)	Group B+C (n=39)	p-value comparing Group A vs Group B+C
BID days (#; %)	41 (56.9%)	8 (24.2%)	33 (84.6%)	<0.0001
Patients skipping dose at least 1 day (#; %)	12 (16.7%)	8 (24.2%)	4 (10.3%)	0.12
Patients who are Grade 2 (#; %)	39 (54.2%)	10 (30.3%)	29 (74.4%)	0.0003
ANALYSES OF STUDY DATA BY GRADE				
	Group B+C (n=39)	Grade 1 Ultrasound (n=10)	Grade 2 Ultrasound (n=29)	p-value comparing Grade 1 vs Grade 2
Duration of tPA therapy (days) (mean; std dev)	3.21 2.04	1.95 1.19	3.64 2.11	0.004
ANALYSES OF STUDY DATA VERSUS CONTROL (LESS CO-MORBIDITIES)				
	Group A+B+C (n=54)	Group A (n=29)	Group B+C (n=25)	p-value comparing Group A vs Group B+C
Length of hospital stay (days) (median; (min, max))	8 (4,23)	8 (4,23)	8 (4,17)	0.18
ANALYSES OF STUDY DATA BY GROUP (LESS CO-MORBIDITIES)				
	Group B+C (n=25)	Group B (n=19)	Group C (n=6)	p-value comparing Group B vs Group C
Length of hospital stay (days) (median; (min, max))	8 (4,17)	8 (4,17)	6.5 (4,11)	0.31

p-value for mean duration of tPA is from t-test using the Satterthwaite correction; for median duration of tPA and length of stay is from Wilcoxon rank sum test. Those for categorical/count data are from Fisher's Exact test.

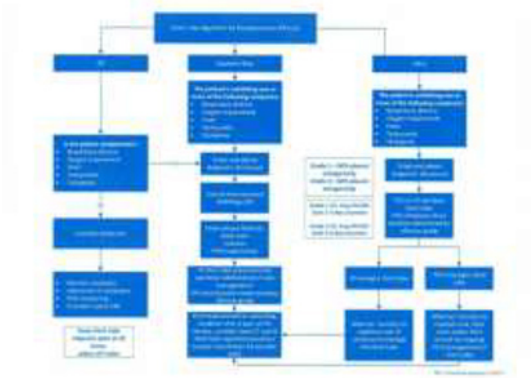

ANALYSES OF GROUP B BY ULTRASOUND GRADE

	Entire Group (n=31)	Grade 1 Ultrasound (n=7)	Grade 2 Ultrasound (n=24)	p-value comparing Grade 1 vs Grade 2
Patients needing 2nd procedure (#; %)	6 (19%)	1 (14%)	5 (21%)	1.0
Patients requiring surgical Drainage (#; %)	0 (0%)	0 (0%)	0 (0%)	1.0
Age (months) (mean/ std dev)	113.5 103.4	133.0 86.2	107.9 108.8	0.54
Weight (kg) (mean/ std dev)	37.8 31.6	53.3 42.6	33.3 27.1	0.28
Patients skipping dose at least 1 day (#; %)	4 (13%)	2 (29%)	2 (8%)	0.21
Duration of tPA therapy (days) (mean; std dev)	3.4 2.2	2.1 1.4	3.8 2.2	0.03
Patients culture or PCR positive (#; %)	17 (55%)	1 (14%)	16 (67%)	0.03
Patients receiving 1mg tPA (#; %)	7 (23%)	7 (100%)	0 (0%)	<0.0001
Patients receiving 2mg tPA (#; %)	25 (81%)	1 (14%)	24 (100%)	<0.0001

p-values for continuous variables are from t-tests using the Satterthwaite correction. Those for categorical/count data are from Fisher's Exact test.

Poster #: SCI-031

Retrospective Study of Hematologic Complications in Patients with Localized Intravascular Coagulopathy Undergoing Sclerotherapy

Manish Patel, DO[1], *manish.patel@cchmc.org*; Kiersten Ricci, MD[1], Paula Mobberley-Schuman, MS[1], Adrienne Hammill, MD[1], Roshni DasGupta[1]; [1]Radiology, Cincinnati Children's Hospital Medical Center, Cincinnati, OH

Disclosures: All authors have disclosed no financial interests, arrangements or affiliations in the context of this activity.

Purpose or Case Report: Slow-flow vascular malformations, most commonly multifocal or diffuse venous (VM), venous-lymphatic (VLM) and capillary-lymphatic-venous malformations (CLVM), are associated with coagulation abnormalities affecting hemostasis and thrombosis and increase risk of hematological complications with procedural interventions. Although not completely understood, pathogenesis of this coagulopathy, termed localized intravascular coagulopathy (LIC), is presumed secondary to stagnant blood in abnormal vessels and consumption of coagulation factors. LIC is characterized by elevated D-dimer, low fibrinogen, and/or mild thrombocytopenia and may progress to disseminated intravascular coagulopathy following surgical procedures. In patients with high-risk malformations, hematologic complications of sclerotherapy and use of low molecular weight heparin (LMWH) as a preventative measure have not been well studied.
Methods & Materials: This study reviewed medical records of patients with slow-flow vascular malformations who underwent sclerotherapy at our institution from July 2008 to December 2016 with LIC as defined by high D-dimer (5 times upper limit of normal), fibrinogen <150mg/dL and/or platelet count <150K/mcL. Hematologic complications included any clinically relevant bleeding or clotting abnormality that occurred 2 weeks post-sclerotherapy and/or while on LMWH prophylaxis, up to 2 weeks, prior to sclerotherapy. Relevant hematuria included gross and large microscopic hematuria. Use of LMWH including dose, frequency and course length was evaluated.
Results: Forty of 300 patients had slow-flow vascular malformations with associated LIC and underwent a total of 241 sclerotherapy procedures. In 87% of cases, LMWH was administered at 0.5mg/kg/dose once daily for 2 weeks before and after sclerotherapy. One patient on LMWH developed pulmonary emboli, presumably from deep vein thrombosis of the treated extremity. Two patients developed transient, asymptomatic hematuria. In 5 patients fibrinogen levels dropped below 100 mg/dL post-sclerotherapy for which cryoprecipitate was administered. No intra-op bleeding or thrombotic events occurred.
Conclusions: Prophylactic LMWH use was common in this patient population and did not appear to increase the risk of significant bleeding before, during or after sclerotherapy. In children receiving LMWH, thrombotic complications after sclerotherapy appear rare but may still occur.

Poster #: SCI-032

The Necessity of Routine Tract Embolization Following Ultrasound-Guided Percutaneous Liver Biopsy

Amie Robinson, BSRT(R)(MR)[1], *alrobinson@cmh.edu*; Keerthi Gondi[2], Brent Cully, MD[1], Brenton Reading, MD[1], Stephanie Theut[1], Richard Hendrickson, MD[1], Kimberly Reid, MS[1], Douglas Rivard, DO[1]; [1]Radiology, The Children's Mercy Hospital, Kansas City, MO, [2]University of Missouri - Kansas City, Kansas City, MO

Disclosures: All authors have disclosed no financial interests, arrangements or affiliations in the context of this activity.

Purpose or Case Report: Ultrasound guided percutaneous liver biopsy is frequently performed in pediatric patients. Published post-biopsy complication rates range between 0.3 - 3.3% according to Society of Interventional Radiology Standards of Practice. Post-biopsy tract embolization has been prophylactically used to theoretically decrease the bleeding risk, but is not the current standard of care at our institution. The goal of this study is to determine if there is a need for prophylactic biopsy tract-embolization after ultrasound guided liver biopsy in the pediatric population.
Methods & Materials: Retrospective chart review on patient's ages 0-18 years, who received an ultrasound guided percutaneous liver biopsy for routine standard of care between January 2008 and August 2016 at dedicated academic pediatric institution. Clinical, radiographic, procedural and pathology data were collected on each subject meeting inclusion criteria. Subjects with a focal liver mass were excluded. Local institutional review board approval was obtained for this study.
Results: A total of 512 liver biopsy procedures on 209 subjects were evaluated for post-procedural complications. The average age was 8.3 (SD ± 6.1) years and a little over half of the patients were male (n=119, 56.5%). Majority of patients had a liver biopsy for increased liver enzymes (n=115, 55.8%) and 74 (5.4%) for prior liver transplant. Pre- and post-biopsy hemoglobin (Hgb) values were evaluated and one (0.2%) subject experienced a Hgb drop of >2.0 g/dL, twenty (3.6%) subjects experienced a Hgb drop of >1.0 g/dL and six (7.23%) subjects did not have a change in Hgb pre- and post-biopsy. We examined the average platelet count and INR for biopsies resulting in a drop of >1.0 g/dL. No statistically significant difference was observed between the pre- and post-procedure

coagulation labs between patients with and without an Hgb drop of >1.0 g/dL. Average platelet count drop was 230 mL for those with >1.0 g/dL drop in Hgb and 226.5 mL for those without a change in Hgb (p=0.918). INR (normal <1.10) was 1.05 for those with >1.0 g/dL drop in Hgb and 1.03 for those without >1.0 g/dL drop (p=0.459).
Conclusions: Ultrasound guided liver biopsies are safe and routinely performed by pediatric interventional radiology practices. Our results indicate that prophylactic track-embolization in pediatric liver biopsy patients is not necessary in patients with normal coagulation parameters.

Poster #: SCI-033

Single-center longitudinal experience with percutaneous management of biliary stenosis complicating pediatric liver transplantation.

Cecil Qiu[2], *cecil.qiu@northwestern.edu*; James Donaldson, MD[1], Shankar Rajeswaran[1], Stanley Kim[3], Riccardo Superina[1], Saeed Mohammad[1], Bridget Whitehead[1], Jared Green, MD[1]; [1]Medical Imaging, Ann & Robert H. Lurie Children's Hospital of Chicago, Chicago, IL, [2]Feinberg School of Medicine - Northwestern University, Chicago, IL, [3]Valley Children's Hospital, Fresno, CA

Disclosures: All authors have disclosed no financial interests, arrangements or affiliations in the context of this activity.

Purpose or Case Report: Biliary stenosis continues to be an important source of morbidity in pediatric liver transplantation. Percutaneous transhepatic cholangiography (PTC) with cholangioplasty and placement of an internal/external biliary drainage catheter has been the standard of care for biliary stenosis at our institution for over twenty years. The purpose of this article is to present the largest and most comprehensive pediatric series to date detailing the percutaneous management of liver transplants complicated by biliary stenosis.
Methods & Materials: We retrospectively reviewed a consecutive series of 74 patients with liver transplant complicated by biliary stenosis who underwent PTC with cholangioplasty and internal/external biliary drain placement between 1997 and 2013. Each biliary drain was evaluated for possible removal after a standard three-month dwell time. Absence of a symptomatic biliary stricture for at least two years post biliary drain removal was considered a treatment success. Management of recurrent biliary stenosis, percutaneous or surgical, was tracked. Variables of interest included transplant graft type, location of biliary stricture, time to drainage catheter removal, and number of recurrences.
Results: Subjects included 32 males and 41 females with a mean age at transplant of 3.4 years and median follow-up of 5.7 years. The most common etiology of liver failure leading to liver transplant was biliary atresia (n=37). 64% of patients (n=47) were successfully managed percutaneously, including 43% (n=32) successfully managed via a single trial. Success rate did not significantly decrease with subsequent trials of percutaneous treatment. Success rate of PTC was higher in anastomotic strictures than in non-anastomotic strictures (71% vs. 31% success rate, p<0.01).
Conclusions: Percutaneous management of biliary strictures complicating pediatric liver transplantation allows for successful treatment of most patients, precluding the need for surgical revision. An optimal treatment protocol remains unknown, but we have shown that a minimal dwell time of 3 months is sufficient.

Poster #: SCI-034

Intrathecal Access in Spinal Muscular Atrophy Patients with Scoliosis and Complex Spinal Hardware Including the Trans-Forminal Approach

Manish Patel, DO[1], *manish.patel@cchmc.org*; Judith Weiss, RN[1], Ali Kandil, DO[1], Neil Johnson, MBBS[1]; [1]Radiology, Cincinnati Children's Hospital Medical Center, Cincinnati, OH

Disclosures: All authors have disclosed no financial interests, arrangements or affiliations in the context of this activity.

Purpose or Case Report: Patients with Spinal Muscular Atrophy (SMA) may have scoliosis requiring spinal hardware for spinal fixation. The scoliosis in addition to the spinal hardware makes intrathecal access difficult with conventional approaches. With recent FDA approval of nusinersen (SpinrazaÒ) for SMA, intrathecal access is required for administration of this meditation. We describe our experience in these patients using a variety of lumbar puncture approaches (intra-spinous process, trans-pedicle, and trans-foraminal) utilizing conventional fluoroscopy, cone-beam CT (CBCT) with fluoroscopy overlay and/or conventional CT with CT fluoroscopy. Approach to the type of access and image guidance is based on the presence of spinal hardware and degree of scoliosis and spinal fusion.
Methods & Materials: An IRB approved retrospective review was performed of our data base of SMA patients having such injection. The technique, technical success and complications were reviewed.
Results: To date, there have been 25 patients receiving 73 procedures. 15 of the 25 patients had spinal hardware (10 patients with conventional rods; 5 with expandable rods). 15 procedures (6 patients) all with conventional spinal rods and some degree of spinal fusion required either CT or CBCT. The remainder of the procedures were performed with conventional fluoroscopy. 14 procedures (5 patients with conventional spinal rods), required trans-foraminal approach. After initial procedures were performed with CBCT or CT guidance, several patients had subsequent procedure performed with conventional fluoroscopy utilizing a trans-foraminal approach.
71 of the 73 procedures (97%) were technically successful with intrathecal injection. The two non-successful procedures were initially performed with conventional fluoroscopy and subsequently performed with technical success using CT (one with trans-foraminal approach). One complication of a CSF leak and one complication of persistent back pain 5 days post procedure were identified. Both complications were self-limited and resolved.
Conclusions: In SMA patients with complex scoliosis or extensive spinal hardware with fusion, successful intrathecal can be achieved utilizing a trans-formainal or trans-pedicle approach. Some patients may require CBCT with fluoroscopy overlay or conventional CT with CT fluoroscopy and laser guide.

Poster #: SCI-035

Differentiating stable buckle fractures from unstable distal radius fractures: The 1cm Rule

Benjamin Iles, DO[1], *bwdiles@gmail.com*; Julie Samora, MD, PhD, MPH[2], Satbir Singh, BS[2], Lynne Ruess, MD[1]; [1]Radiology, Nationwide Children's Hospital, Columbus, OH, [2]Orthopaedic Surgery, Nationwide Children's Hospital, Columbus, OH

Disclosures: All authors have disclosed no financial interests, arrangements or affiliations in the context of this activity.

Purpose or Case Report: Treatment pathways for isolated distal radius fractures in children are evolving and becoming more tailored to specific fracture types, including different management plans for stable buckle fractures (BFs) versus unstable distal radius fractures (DRFs). We propose a measurement rule to aid differentiation of stable BFs from unstable DRFs in children.
Methods & Materials: IRB approval was waived for this retrospective QI project. Medical record search identified children with closed radius fractures during a 14month period. Demographic and other study data were collected and recorded using REDCap. Original radiology reports were compared to consensus diagnosis of two senior readers, which was used as the reference standard. Agreement was calculated using Cohen's Kappa statistic. Fracture to distal radial physis distance was measured in mm on PA and Lateral (LAT) views. Diagnostic accuracy using fracture distance as a predictor for buckle fractures was analyzed on both views. An ROC curve was used to determine the cutoff values tested.
Results: There were 148 BFs (73%), 55 isolated DRFs (27%). Agreement between the original report and final diagnosis was 'slight' (κ=0.120, SE=0.058, n=203). The BF to physis distance was < 1cm in only 1 of 106 (0.9%) children 7-16y on PA view. No older children had a BF to physis distance <1 cm on LAT view and the sensitivity, specificity and accuracy for BF diagnosis were all above 82% using a cut off of 14mm (PA) and 13 mm (LAT). The BF to physis distance was < 1cm in 1 (2.4%) of 42 children 3-6y on PA view and another 1(2.4%) on LAT view. Diagnostic accuracy was low for children <7 years old for all tested distances. The areas under the ROC curve increased after excluding patients <7y: 0.822 to 0.867 (PA) and 0.819 to 0.874 (LAT). Diagnostic odds ratios also increased when excluding patients < 7y: from 11.375 to 24.612 (>14mm PA) and from 10.095 to 22.815 (>13mm LAT).
Conclusions: An isolated distal radius fracture in a child is not likely to be a BF if the fracture to physis distance is < 1 cm. We propose measurement cut offs to increase diagnostic accuracy in children ≥ 7y. Using measurements to differentiate stable BFs and unstable DRFs is less reliable in younger children.

Poster #: SCI-036

Consensus-driven development of a standardized WB-MRI scoring system for assessment of disease activity in JIA: Special Interest Group from the MRI in JIA in OMERACT

Jyoti Panwar, MD, FRCR[1], *drjyoticmch@gmail.com*; Mirkamal Tolend[1], Jonathan Akikusa, MBBS[2], Nele Herregods, MD, PhD[5], Kerri Highmore, MD[3], Emilio Inarejos Clemente, MD[4], Lennart Jans, MD, PhD[5], Jacob Lester Jaremko, MD, PhD[6], Thekla von Kalle, MD[7], Eva Kirkhus, MD, PhD[8], Arthur Meyers, MD[9], Hiten Patel, MBChB[11], Marion van Rossum, MD, PhD[10], Jennifer Stimec, MD[12], Shirley Tse, MD[12], Marinka Twilt, MD, MSCE, PhD[13], Nikolay Tzaribachev, MD[14], Andrea Doria, MD, PhD, MSc[12]; [1]University of Toronto, Toronto, ON, Canada, [2]Royal Children's Hospital Melbourne, Melbourne, VIC, Australia, [3]Children's Hospital of Eastern Ontario, Ottawa, ON, Canada, [4]Hospital Sant Joan de Deu, Barcelona, Spain, [5]Ghent University, Ghent, Belgium, [6]University of Alberta, Edmonton, AB, Canada, [7]Radiologisches Institut, Olgahospital Klinikum, Stuttgart, Germany, [8]Oslo University Hospital, Oslo, Norway, [9]Nemours Children's Hospital, Orlando, FL, [10]Academic Medical Center, Amsterdam Rheumatology and Immunology Center, Amsterdam, Netherlands, [11]Birmingham Children's Hospital, Birmingham, United Kingdom, [12]The Hospital for Sick Children, Toronto, ON, Canada, [13]Alberta Children's Hospital, Calgary, AB, Canada, [14]Pediatric Rheumatology Research Institute, Bad Bramstedt, Germany

Disclosures: All authors have disclosed no financial interests, arrangements or affiliations in the context of this activity.

Purpose or Case Report: Whole body (WB) MRI is a valuable method for surveying the overall burden of systemic diseases such as juvenile idiopathic arthritis (JIA), directing further diagnostic and treatment approaches. Consensus-driven development and validation of a standardized WB-MRI scoring system for JIA has important clinical utility in timely detection and monitoring of disease activity, and serves as an outcome measure in research. We describe our experience utilizing a formal consensus approach amongst imaging and/or clinical JIA experts towards developing a novel WB MRI scoring system to assess disease activity in JIA.
Methods & Materials: Three rounds of anonymous, iterative Delphi surveys were used to determine the relevant anatomic joints for assessment, diagnostic item selection, definition and grading, and selection of appropriate imaging planes and sequences. These surveys were completed independently by an international expert group consisting of pediatric musculoskeletal radiologists and rheumatologists. The rates of agreement for potential choices, and additional suggestions were discussed amongst the group after each survey, ultimately yielding to a structured WB-MRI scoring system for JIA.
Results: Eighteen to 22 experts participated in three rounds of Delphi surveys and a concluding consensus meeting. A first iteration scoring system was developed that ultimately included assessment of 40 joints, representation of both axial and peripheral joints, 2-5 diagnostic items graded in each, and inclusion of levels from binary (presence/absence) to 4-level ordinal scoring. Recommendations specific to the imaging of each joint, consisting of anatomical planes and MRI sequences were constructed as a preliminary, minimally necessary imaging protocol to supplement the scoring system.
Conclusions: A novel WB-MRI scoring system for JIA was developed by consensus. Further iterative refinements, feasibility, reliability and responsiveness testing are warranted in upcoming studies.

Poster #: SCI-037

SPICA MRI predictors for epiphyseal osteonecrosis after closed reduction treatment of DDH

J. Kan, MD[1], Lee Haruno, BS[1], Michael Rivlin, MD[1], Scott Rosenfeld[1], Vinitha Shenava[1], Huirong Zhu[1], Erica Schallert, MD[1]; [1]Radiology, Texas Children's Hospital, Houston, TX

Disclosures: All authors have disclosed no financial interests, arrangements or affiliations in the context of this activity.

Purpose or Case Report: SPICA MRI with gadolinium contrast administration is routinely performed after closed reduction for the treatment of developmental dysplasia of the hip (DDH). Quantifying the degree of femoral head enhancement and abduction angles are routinely performed to identify and stratify those patients who may be at risk for epiphyseal osteonecrosis. The purpose of our study is to evaluate predictors for epiphyseal osteonecrosis based on percentage enhancement and abduction angles evaluated based on SPICA MRI.
Methods & Materials: Retrospective descriptive study for all patients identified through text word query through our electronic medical record who underwent closed hip reduction for the treatment of DDH followed by gadolinium enhanced MRI between 7/11 and 11/14. Patient demographics were recorded and follow-up data inclusive of development of epiphyseal osteonecrosis and need for re-intervention after the initial reduction. MRI data recorded included hip abduction angles after the initial closed reduction and percentage of femoral head enhancement.

Results: 25 hips in 21 patients (16 female, 5 males, mean age 0.99 years, range 0.4-3.1 years) were included in our study. The mean follow-up period was 2.7 years (range 0.7-5.1 years). 8 of 25 hips (32%) went on to develop osteonecrosis. The development of epiphyseal osteonecrosis was more likely with <80% enhancement (sensitivity 87.5%, specificity 88.25%, positive predictive value 78%, negative predictive value 94%). The mean contrast enhancement for patients developing osteonecrosis compared to those who did not was 37.5% and 86.5% respectively; p=0.001. The development of epiphyseal osteonecrosis trended, but was not statistically significant when the abduction angle was greater than 55 degrees (P=0.1). The odds of osteonecrosis is 9% lower with every 1% increase of perfusion. There were 3 hips (12%) that underwent re-intervention based on the immediate post-reduction SPICA MRI results. For this subset, one (33%) went on to develop epiphyseal osteonecrosis.
Conclusions: Immediate post-SPICA MRI with gadolinium is a useful prognostic tool for determining future risk for epiphyseal osteonecrosis in children treated for DDH. Our data complements existing literature, and suggests that even in cases where there may be partial epiphyseal enhancement, epiphyseal osteonecrosis may still develop which has not been well explored in the literature. When epiphyseal enhancement is less than 80%, it is recommended that SPICA cast revision be considered.

Poster #: SCI-038

The influence of age on pediatric fracture healing: a radiographic approach

Diana Messer, MS[1], *dianamesser@gmail.com*; Brent H. Adler, MD[2], Farah Brink, MD[2], Henry Xiang, PhD, MPH, MD[2], Amanda Agnew, PhD[1]; [1]Division of Anatomy, The Ohio State University, Erie, PA, [2]Nationwide Children's Hospital, Columbus, OH

Disclosures: All authors have disclosed no financial interests, arrangements or affiliations in the context of this activity.

Purpose or Case Report: Skeletal fractures may go undetected and untreated in physically abused children for significant periods of time. When discovered later through radiographic survey, the time since injury (TSI) may be important for the medical diagnosis of physical abuse and have implications for child protection. Prior research suggests that clinical and biological variables, such as fracture location and age, may influence pediatric fracture healing. However, radiographic determination of TSI has been poorly studied until recently. It has been commonly understood that in general younger patients heal faster and lower extremity fractures heal slower than upper extremity fractures. However, the influence of patient age and fracture location on fracture healing has only been explored on a limited scale and not between pediatric age groups. This study examines the effect of age on specific features of pediatric fracture healing through radiographic analysis.
Methods & Materials: Four hundred ninety-eight upper and lower limb skeletal fractures (>1355 radiographs) of children ages 0 to 5.99 years old were evaluated for features of fracture healing at a large tertiary care center. Abuse-related fractures and individuals with co-morbidities or disorders affecting bone were excluded. Subperiosteal new bone formation (SPNBF) and callus were evaluated along with the time to complete healing. The presence, thickness, matrix, and character were recorded based on modified parameters set by Walters et al. (2014).
Results: Independence and goodness of fit frequency tests revealed correlations between age and the thickness and character of SPNBF as well as callus matrix and fracture margin definition, in addition to within bone location and bone type and rate of healing. Mean comparisons reveal significant differences in callus matrix thickness between younger and older age groups ($p < 0.001$). Statistical tests reveal no significant differences between sex and other variables of fracture healing.
Conclusions: These results may provide an improved method of determining the age of fractures and TSI. Future research may provide better guidelines for radiographic characterization of fracture healing, and improved confidence in the estimation of TSI.

Poster #: SCI-039

Evaluation of MRI Sequences for Detection of Intraarticular Damage of the Hip

Michael Fadell, MD[1], *michael.fadell@childrenscolorado.org*; Jonathan Flug, MD[2], Tatum McArthur, MD[2], Anne Skelton, BS[1], Patrick Carry, BS[1], Stephanie Mayer, MD[1]; [1]Radiology, Children's Hospital Colorado, Aurora, CO, [2]University of Colorado, Aurora, CO

Disclosures: All authors have disclosed no financial interests, arrangements or affiliations in the context of this activity.
Purpose or Case Report: This study compares the accuracy of three MRI acquisitions commonly used to assess intra articular pathology in identifying labral, transition zone, and articular cartilage injuries.
Methods & Materials: Two musculoskeletal radiologists evaluated high resolution (HR), 3-dimensional with multiplanar reconstruction (MPR), and radially reformatted (RR) magnetic resonance images (MRI) of 33 patients who later underwent surgical treatment for FAI. Raters reviewed each MRI sequence for the presence of labral tear or injury to the transition zone or true acetabular cartilage as well as the size of the injury. An orthopedic surgeon reviewed intra operative images to assess for intra articular injury. Bland-Altman methods were used to estimate agreement between the percentage of hips affected by injury as measured by MRI relative to direct visualization. Bias or mean difference between MRI and arthroscopic visualization as well as the limit of agreement was also calculated for each of the three formats in assessing size of injury. The 12 o'clock to 2 o'clock positions within the acetabulum were used for comparison, the most common locations for intra-articular pathology in femoroacetabular impingement (FAI).
Results: MPR was most accurate at identifying labral injuries (accuracy: 88%, sensitivity: 92%, specificity: 25%) compared to HR (accuracy: 82%, sensitivity: 87%, specificity: 0%) and RR (accuracy: 83%, sensitivity: 89%, specificity: 0%). MPR (accuracy: 38%, sensitivity: 38%, specificity: 50%) and RR formats (accuracy: 38%, sensitivity: 38%, specificity: 50%) were also more accurate at identifying transition zone injuries compared to HR images (accuracy: 29%, sensitivity: 27%, specificity: 100%). HR was more accurate at identifying articular cartilage injuries (accuracy: 65%, sensitivity: 40%, specificity: 76%) compared to MPR (accuracy: 56%, sensitivity: 30%, specificity: 67%) and RR (accuracy: 61%, sensitivity: 40%, specificity: 70%) formats. MPR had performed best in determining the size of labral injury (bias -0.10), while MPR and RR performed best in identifying transition zone (bias -0.06) and acetabular cartilage (bias -0.31) injuries.
Conclusions: Labral injuries were best identified with the MPR format while transition zone cartilage injuries were best identified with MPR and RR formats, and the HR format was best to identify true articular cartilage pathology. 3D with MPR and RR are a less commonly utilized though beneficial approach in the evaluation of the labrum and transition zone injuries.

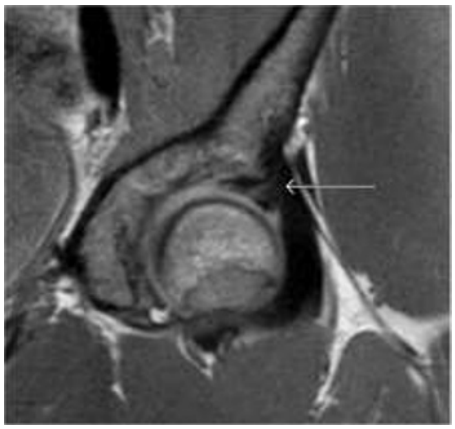

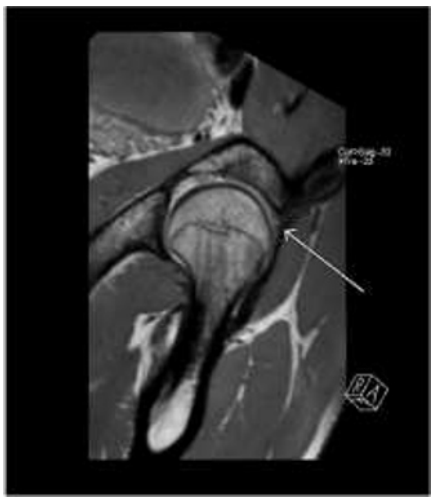

Poster #: SCI-040

"The Seven Day Rule": MRI for detection of bone marrow edema in acute hematogenous osteomyelitis of the pelvis in children

Osamu Miyazaki, MD[1], *miyazaki-o@ncchd.go.jp*; Hidekazu Aoki, MD[1], Mikiko Miyasaka, MD[1], Reiko Okamoto, MD[1], Yoshiyuki Tsutsumi, MD[1], Shunsuke Nosaka, MD[1]; [1]Radiology, National Center for Child Health and Development, Setagaya-ku, Japan

Disclosures: All authors have disclosed no financial interests, arrangements or affiliations in the context of this activity.

Purpose or Case Report: MRI is the gold standard for the diagnosis of acute septic sacroiliitis. However, appropriate timing of the procedure has not been addressed in the literature. MRI is highly sensitive for detecting long tubular bone osteomyelitis as early as 24-48 hours of symptom onset. The hypothesis of this study is that the onset of bone marrow edema of acute hematogenous osteomyelitis (AHO) of pelvis might be delayed as compared with long bone. The purpose of this study is to evaluate the optimum timing of MRI examination from the onset of disease.

Methods & Materials: Nine patients (8 - 16 years, median 14 years, four male and five female) with AHO of pelvis were selected from our radiology database between 2004 and 2016. We compared signal intensity of sacral/iliac bone marrow (BM) and gluteal muscle (M) (BM/M ratio) on the fat suppressed T2Weighted image (T2WI) and T1weighted image (T1WI) respectively. We also calculated the days elapsed from onset to MRI examination. Regression methods were used to evaluate the relationship between BM/M ratio and days elapsed. We also evaluated other five findings (subperiosteal infiltration, muscle infiltration, laba cleft phenomenon, erosive destruction, joint space enhance).

Results: BM/M ratio and elapsed days in patients with AHO of pelvis showed a statistically correlation (R^2= 0.57). In five cases where MRI was performed twice, the BM/M ratio increased without exception. This tendency seemed to be more prominent in those who underwent initial MRI before day 7. The average BM/M ratio within the first 7 days was 3.6 ± 0.7 (mean ± SD), but increased markedly in those who underwent MRI more than one week after onset (6.5 ± 0.7 [mean ± SD]). There was a statistically significant difference in the BM/M ratio before and after day 7 ($p \leq 0.001$). The BM/M ratio on the T1WI showed an inverse relationship to that on the T2WI with a statistically correlation (R^2= 0.59) on the T2WI as well. All nine cases showed bone marrow edema, otherwise, un-even incidence of other five findings were identified.

Conclusions: The present research suggests that until day 7 there might be false negative or subtle finding of bone marrow edema in AHO. A follow-up MRI should be performed after seven days where the diagnosis is still in doubt.

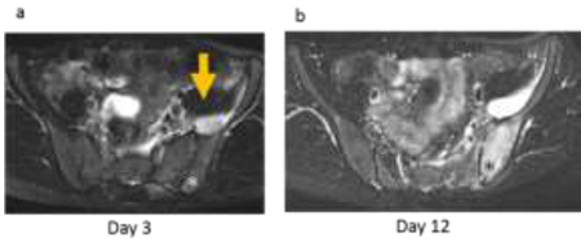

The initial fat suppressed T2WI (a) showed focal fluid collection between iliac muscle and iliac bone as abscess (→), although the bone marrow signal was normal (*). Follow-up MRI depicts increased signal in iliac bone marrow (b*)

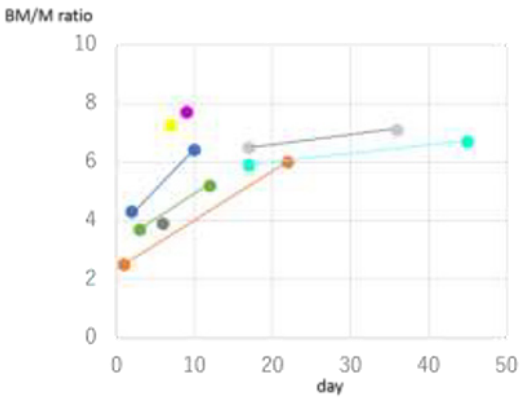

Fig. 2. Relationship between BM/M ratio and days elapsed for patients; five colored lines depict the interval change in those who underwent two examinations

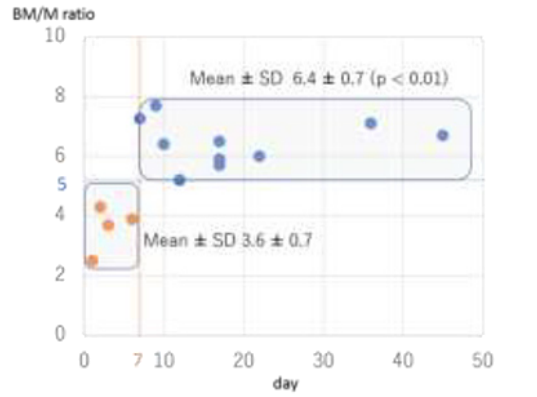

Fig. 3. Proposed "7 day rule" and statistical evaluation of two groups (before and after day 7)

Poster #: SCI-041

Evaluation of Bone Mineralization of Lumbar Vertebrae by QCT in Children Less Than 6 Years

Liliane Gibbs, MD[1], Joyce Keyak, PhD[1]; [1]University of California Irvine, Anaheim, CA

Disclosures: All authors have disclosed no financial interests, arrangements or affiliations in the context of this activity.

Purpose or Case Report: Determining the underlying etiology of bone fracture in children is an essential part of patient care. Very young patients who may be victims of child abuse, but who may not be able to express themselves, must be distinguished from those who have low bone mineralization due to disease. Quantitative computed tomography (QCT) has been used to evaluate volumetric bone mineral density (BMD) in children, but there is little information on BMD in very young subjects.[1,2] The goal of this study was to demonstrate the feasibility of using QCT to evaluate BMD and volume (Vol) of lumbar vertebral bodies in children and to establish the need for a separate comparative database to evaluate these parameters in subjects less than 6 years.

Methods & Materials: We obtained anonymized QCT scans (80-120kVp, 9.6-580.8mAs, 0.416-0.977mm pixel size, 2-4mm slice thickness) of lumbar vertebrae of 24 male subjects, 15 less than 6 years old (<6yo) and 9 between 13 and17 years old (13-17 yo), who were imaged for unrelated medical reasons in the ER of our institution (Image Analysis INTable phantom; Philips BrillianceTM iCT 3.2, 256 slice scanner). IRB approval to study anonymous data is not required. BMD and Vol of the vertebral body were evaluated on one image in a region of interest (ROI) through the mid-vertebral body (Figure 1). Volume was computed using an assumed 3-mm slice thickness. Student's t-tests were performed to determine if BMD and Vol at each level differed between subjects of different groups. Linear regression analysis of the two groups separately was used to determine if BMD and Vol at each level were associated with age. A significance level of $p<0.05$ was used.

Results: BMD was virtually independent of age in the younger group but increased with age at multiple levels in the older group (Tables 1-2, Figure 2). In contrast, Vol in 13-17yo was more than twice that in <6yo at all levels ($p<0.002$). Volume increased 0.09 to 0.29 cm^3/yr in subjects <6yo ($0.33 \le R^2 \le 0.61$, $p \le 0.04$), but was not associated with age in 13-17yo ($p>0.7$).

Conclusions: This study demonstrated a QCT method for evaluating bone mineralization in very young subjects and showed that a separate normative database is needed for subjects less than 6 years. With future work, this method may be helpful for distinguishing very young patients who may be victims of child abuse from those with low bone mineralization due to disease or a metabolic process.

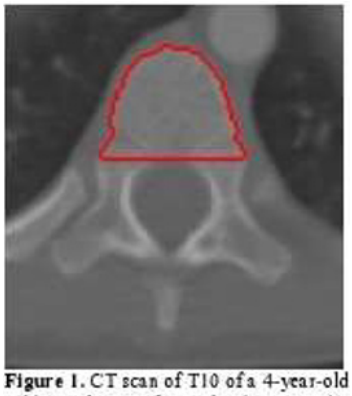

Figure 1. CT scan of T10 of a 4-year-old subject. The ROI for evaluating BMD is shown in red.

Table 1. BMD regression results, <6yo. NS=not significant

Level	Slope (mg/cm³/yr)	R^2	p
L1 – L3	–	0.002 – 0.03	0.58 – 0.87
L4	5.66 (NS)	0.28	0.053
L5	**7.32**	**0.50**	**0.005**

Table 2. BMD-age regression results, 13-17yo.

Level	Slope (mg/cm³/yr)	R^2	p
L1 – L3	10.5 – 13.9 (NS)	0.35 – 0.40	0.067 – 0.095
L4	**15.3**	**0.54**	**0.024**
L5	**24.1**	**0.72**	**0.004**

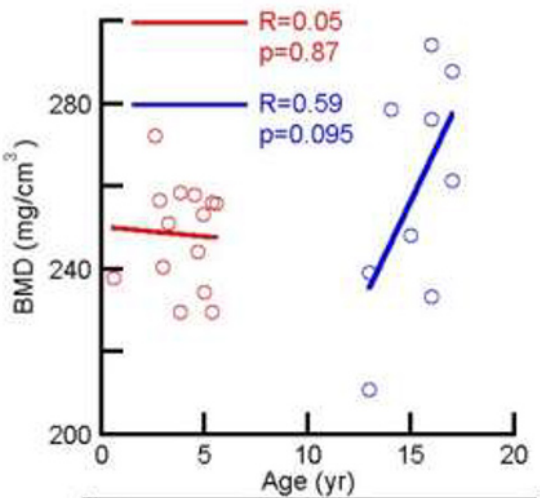

Figure 2. Linear regression results for L1

Poster #: SCI-042

Pediatric Hip Labrum with MRA and Arthroscopic Correlation.

Tracey Mehlman, MD[1], *gloxinia09@hotmail.com*; Pat Riley, Jr., MD[1], Allison Person, MD[1]; [1]Radiology, Akron Children's Hospital, Copley, OH

Disclosures: All authors have disclosed no financial interests, arrangements or affiliations in the context of this activity.

Purpose or Case Report: Hip pain in the active adolescent can be a diagnostic challenge. Labral tears are a common cause of pain, but on average, a lag time of greater than 2 years exists before a diagnosis is achieved. Leading etiologies of labral pathology include: trauma, femoroacetabular impingement, and dysplasia. A better understanding of hip pathology, in this age group and the development of less-invasive hip arthroscopy and surgical repair, has led to an increased number of pediatric MR hip arthrograms (MRA) being performed.
The purpose of this investigation was to evaluate the accuracy of our MRA reports with arthroscopic findings and create a pictorial radiologic-arthroscopic correlation. This study will assist both radiologists whom may be formally trained in pediatric radiology but have variable experience and/or training in musculoskeletal radiology, as well as our clinical colleagues to better understand the diagnostic utility of MRA.
Methods & Materials: A retrospective review of the MRA reports was performed at our institution between January 1, 2015 and October 1, 2017. The EMR was utilized to ascertain clinical management. The diagnostic efficacy of the MRA radiology reports is determined based on the arthroscopic report findings; the absence or presence of labral pathology is identified. A third category separating labral pathology into either definite labral tear verses labral fraying/irregularity is also evaluated. The appearance of the adolescent acetabular labrum is demonstrated in a pictorial review including MRA and arthroscopic images.
Results: 99 MRA exams were performed during the study time frame. Most common indication for the MRA was hip pain and/or signs of impingement. 78% of the patients who obtained an MRA were female. The average age at the time of imaging was 16 years (from 12 to 22 years). More than 50% of the patients had labral pathology on MRA, and at least 29 underwent arthroscopic repair at our institution. The overall agreement was 79% between MRA and arthroscopic findings, with three false negatives and three false positives. Free marginal Kappa coefficient was 0.59.
Conclusions: A labral tear is a not infrequent cause of hip pain in the adolescent, and an increasing number of MRA exams are routinely being performed. MRA can accurately diagnose the presence of labral pathology and is a useful tool prior to arthroscopy. The pediatric radiologist plays a key role in the diagnosis of labral pathology.

Poster #: SCI-043

Normative, Age-matched FDG PET Brain Analysis to Identify Epileptic Foci in Children

Sandra Poliachik, PhD[1],
sandra.poliachik@seattlechildrens.org; Adam Alessio, PhD[1], Seth Friedman, PhD[1], Jason Wright, MD[1]; [1]Radiology, Seattle Children's Hospital, Seattle, WA

Disclosures: Adam Alessio has indicated a relationship with GE Healthcare and Philips Healthcare for receiving research grants. All other authors have disclosed no financial interests, arrangements or affiliations in the context of this activity.

Purpose or Case Report: Purpose: The evaluation of epileptic foci with FDG PET can be challenging, particularly when epileptic foci are subtle. We sought to determine if an age-matched database of normative cerebral FDG PET uptake can be used to automatically identify epileptic foci.
Methods & Materials: Materials and Methods: Through an IRB-approved study, we constructed an in-house normative database for FDG cerebral uptake using the brain portion of total Body PET scans (n=84) performed for oncology assessment with no known neurologic pathology. We separated the data into age bins (0-2, 3-5, 6-8, 9-11, 12-14, 15-17 years), and nonlinearly co-registered the studies to an age-matched MRI atlas by age (18 mo, 4 yr, 7 yr, 10 yr, 13 yr, 16 yr) using BioImage Suite. Within each age bin, each registered brain image was normalized such that the mean of the PET voxels within the MRI mask was the same across patients. The mean and standard deviation for each age bin formed the normative atlas. This atlas was applied to PET brain studies performed for epilepsy assessment (n=10). Assessment of the epilepsy studies followed the same processing as entries for the atlas (registration, normalization within each age bin), and were then compared to the normative atlas in terms of ratio from mean and number of standard deviations from mean (z-scoring). The detection performance was evaluating by comparing the automatically identified epileptic zones to the original radiologist report.
Results: Results: The FDG PET atlas was generated with 84 normal studies and tested with 10 abnormal epilepsy exams (age 2-16 yrs). The radiologist reports identified 15 epileptic foci in the abnormal studies. Using regions exceeding 4 standard deviations as a threshold for epileptic foci, the automatic identification with the normative atlas identified 14 of these sites (93% Sensitivity) and also identified 7 additional false positive sites.
Conclusions: Conclusions: An age-matched normative FDG PET Brain database can provide a highly sensitive tool to help identify FDG PET abnormalities in epilepsy exams. Additional refinements are needed to improve the specificity of this approach.

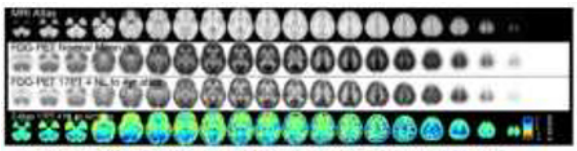

Figure 1: FDG PET data for a 4 year-old epilepsy patient in 4 year atlas space. Compared to mean normalized FDG PET data, z-scores indicate hypometabolism in the right temporal and left frontal regions. The radiologist's report noted hypometabolism in the right lateral temporal lobe and left frontal cortex.

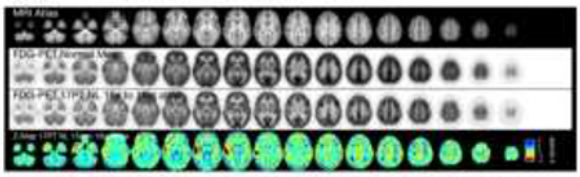

Figure 2: FDG PET data for a 15 year-old epilepsy patient in 16 year atlas space. Patient FDG PET data is hypometabolic in the region of the right temporal lobe compared to the normative atlas. The radiologist's report notes hypometabolism in the right anterolateral temporal lobe and right perisylvian region.

Poster #: SCI-044

Improved Pediatric fMRI Success Rates in Clinical Epilepsy Patients Using Intensive Patient Preparation Methods

Alexander Long, Bachelors[1],
Alexander.long@nationwidechildrens.org; Tricia Buskirk, Master of Science in Child and Family Studies[1], Mark Smith, MS[1], Ramkumar Krishnamurthy, PhD[1], Houchun Hu, PhD[1], Mark Halverson, MD[1]; [1]Radiology, Nationwide Children's Hospital, Columbus, OH

Disclosures: All authors have disclosed no financial interests, arrangements or affiliations in the context of this activity.

Purpose or Case Report: Functional MRI (fMRI) for preoperative language mapping of Wernicke's and Broca's areas in clinical pediatric epilepsy presents various challenges resulting in poor patient compliance. We hypothesized that higher fMRI success rates can be achieved using intensive patient preparation in a fMRI practice session using a mock MRI scanner.

Methods & Materials: We performed a retrospective IRB approved review of epilepsy patients that received preoperative language fMRI between 2010 and 2017. We recorded age, FSIQ scores, scan information and the radiologist's reports. We defined success of the fMRI by the radiologist's ability to locate Broca's and Wernicke's areas in their report.
Under the old protocol, patient preparation consisted of a 10-minute verbal explanation before the MRI consisting of 2 language tasks. Under the new protocol, the practice session lasted 60 minutes using a mock MRI scanner. Tasks were first practiced seated and then supine in the mock scanner. Coaching with real-time feedback was given during the practice and exam. Information from practice was used to select and modify tasks according to patient's ability. We increased the number of language tasks, and an additional specialist was responsible for task practice and coaching during the exam. On average 6 language tasks were administered during the MRI, increasing total length over the old protocol.
Results: We identified 33 preoperative language-mapping fMRI scans of children with epilepsy. 13 of 33 were done under the old protocol with a mean age of 16 (range 12 - 19 years). FSIQ scores were available for 10 of the 14 patients with a mean score of 84 (range 62 - 108). 19 of 33 scans were done after institution of an new protocol with mean age of 14 (range 8 - 19 years). FSIQ scores were available for 14 of the 19 patients with a mean score of 75 (range 49 - 111).
The radiologist could identify Broca's area in 9 of 14 scans (64%) under the old protocol, and 18/19 (95%) with the new protocols. The radiologist could identify Wernicke's area in 9 of 14 scans (64%) under the old protocol, and 19/19 (100%) of scans with the new protocol. Using the z-statistic for two group proportions, the success rate between new and old protocols were significantly different ($p<0.05$), with $p=0.035$ for Broca's and $p=0.005$ for Wernicke's.
Conclusions: Higher pediatric fMRI success rates can be achieved with intensive patient preparation in an fMRI practice session using a mock scanner.

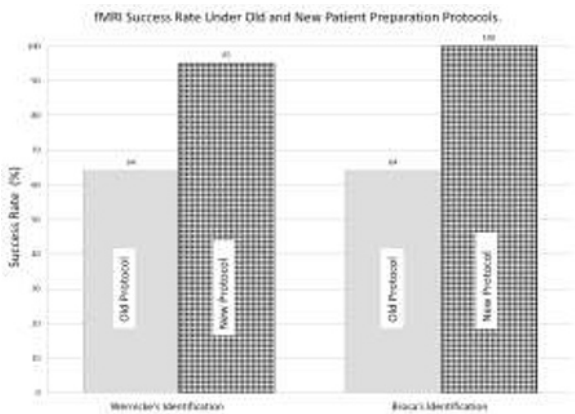

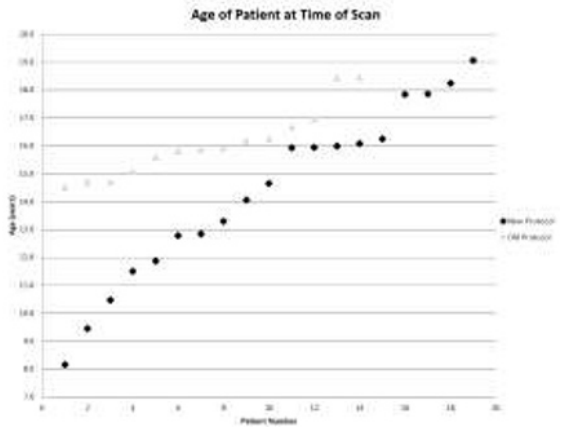

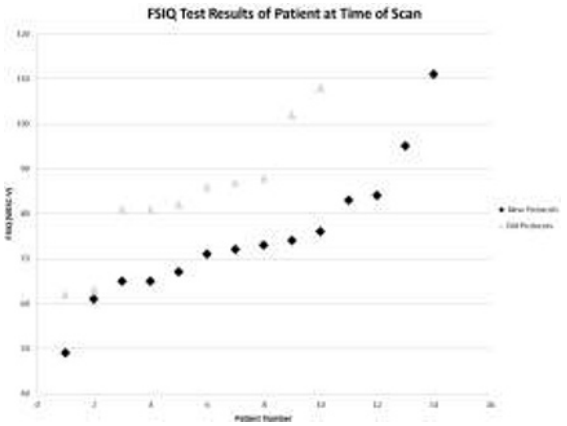

Poster #: SCI-045

The Pediatric Upper Airway: Thoroughfares and Road blocks

Mark Whitehead, PA[2], *markallenwhitehead@gmail.com*; Matthew Whitehead, MD[1]; [1]Neuroradiology, Children's National Medical Center, Washington, DC, [2]Just 4 Kids Pediatrics, Hohenwald, TN

Disclosures: All authors have disclosed no financial interests, arrangements or affiliations in the context of this activity.

Purpose or Case Report: The human airway is fundamental to respiratory gas transmission and oxygen exchange. The pediatric upper airway is subject to a number of specific age and location related disease processes that can cause alarming morbidity and could be deadly by impairing normal air movement. In this exhibit, we guide the learner on a fantastic journey thorough the pediatric upper airway from nose to cords illustrated thorough neuroimages. Congenital and acquired anatomic and pathologic barriers to airflow will be reviewed.
Methods & Materials: CT, MRI, ultrasound and radiographic images with didactic value will be procured from the teaching file of a pediatric medical center in order to demonstrate anatomy and pathology of the pediatric upper airway.
Results: Specific entities illustrated and discussed as follows:
1. Sinuses
a. Congenital:
-variants
b. *Acquired:*
-Sinusitis and its complications
-Cystic fibrosis
-Polyposis
-Allergic fungal sinusitis

-Trauma/hemorrhage/fracture
-Pott's puffy tumor
-Granulomatosis with polyangitis
-Lymphoma
2. Nose and Nasopharynx
a. Congenital:
-Choanal atresia
-Piriform aperture stenosis
-Tumor (dermoid, nasopharyngeal angiofibroma, rhabdomyosarcoma)
-Encephalocele
b. Acquired:
-Penetrating trauma: palate
-Infection: adenoiditis
-Foreign bodies
3. Oral Cavity and Oropharynx:
a. Congenital:
-Congenital deformities: Pierre Robin sequence
-Ranula
-Teratoma
-Lymphangioma
-Thyroglossal duct cyst (TGDC)/lingual thyroid
b. Acquired:
-Trauma
-Tonsillitis/abscess/pharyngitis
-Epiglottitis
4. Hypopharynx/larynx:
a. Congenital:
-Hemangioma
-TGDC
-Dermoid
-Laryngomalacia
-Vocal cord paralysis
b. Acquired
-Retropharyngeal abscess
-Trauma with air leak
-Pertussis, Croup

Conclusions: A variety of diseases may affect the pediatric upper airway. Location and imaging characteristics are primary determinants of the differential diagnosis.

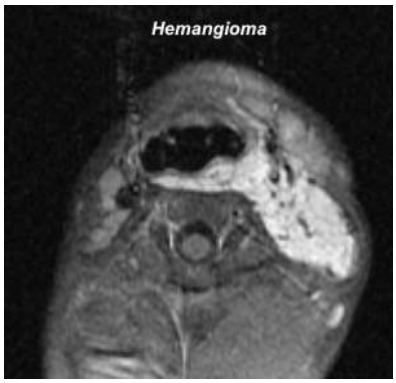

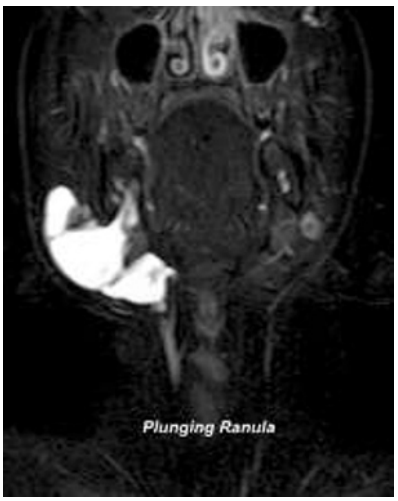

Poster #: SCI-046

Clival Malformations in CHARGE syndrome

Eman Mahdi, M.D[1], *emahdi@childrensnational.org*; Matthew Whitehead, MD[1]; [1]Radiology, Children National Health System, Arlington, VA

Disclosures: All authors have disclosed no financial interests, arrangements or affiliations in the context of this activity.

Purpose or Case Report: CHARGE syndrome is a genetic disorder with multisystemic congenital anomalies, most commonly including coloboma, heart malformations, choanal atresia, developmental delay, and genital and ear anomalies. The diagnostic criteria for CHARGE syndrome has been refined over the years. However, there are limited reports describing skullbase and craniocervical junction abnormalities. Recently, a coronal clival cleft has been identified in association with CHARGE syndrome. The aim of our study is to assess the prevalence of coronal clival clefts in patients with CHARGE syndrome.
Methods & Materials: In this retrospective study, the CT/MRI database at a single academic children's hospital was queried for the phrase "CHARGE syndrome" over a 17-year period (2001-2017). Electronic medical records were reviewed to confirm the diagnosis. Images were assessed for skull base anomalies, specifically clival hypoplasia and dysplasia.
Results: The search yielded 42 exams (21 CTs and 21 MRIs) from 15 distinct patients (mean ages 4.1 ± 5.6 years; range 2 days to 19 years). Diagnosis of CHARGE syndrome was confirmed either by clinical and genetic testing (n=6) or by clinical diagnosis only (n=9). A coronal clival cleft was identified in 87% of patients (n=13; 37 exams), either partial

(53%) or complete (33%). Clival hypoplasia without clefting was present in all 5 exams from the remaining 2 patients.
Conclusions: Clival pathology is universal in CHARGE syndrome. Coronal clival clefts are extremely common, representing a useful diagnostic feature. Detection of a clival cleft should alert the radiologist to examine the ears, eyes, palate, choana, and olfactory centers for other signs of CHARGE syndrome.

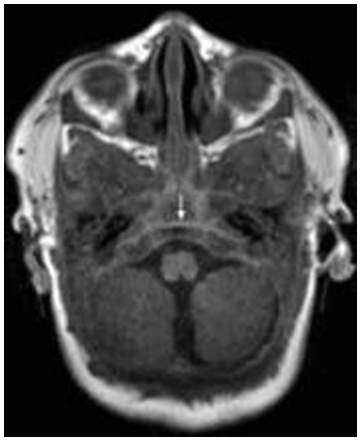

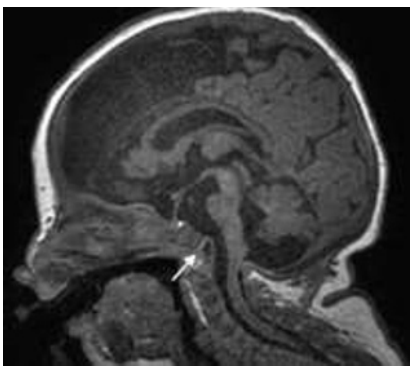

Poster #: SCI-047

Chronic Subdural Hemorrhage: What We Have Learned

Jeffrey Tutman, MD[2], *jeffreytutman@gmail.com*; Gary Hedlund, DO[1]; [1]Medical Imaging, Primary Children's Hospital, Salt Lake, UT, [2]University of Utah, Salt Lake City, UT

Disclosures: All authors have disclosed no financial interests, arrangements or affiliations in the context of this activity.

Purpose or Case Report: Accurate imaging characterization of chronic subdural hemorrhage (cSDH) has clinical and forensic implications, and continues to challenge the radiologist. The MRI characteristics of surgically proven cSDH were retrospectively reviewed in the context of known pathomorphology of the aging SDH.
Methods & Materials: A search of the pediatric neurosurgical database at a large children's hospital was performed with the terms "chronic subdural hemorrhage" and "subdural drainage". Data was available from 2010-2017. Chart review was performed. Operative findings, pertinent demographic and clinical information was recorded. Preoperative MR imaging of 14 patients with surgically confirmed cSDH was retrospectively reviewed. NECT was reviewed if available. Imaging was surveyed by a senior pediatric neuroradiologist and a senior radiology resident. This retrospective study is pending approval by the Institutional Review Board.

Results: 14 patients with 19 drained subdural compartments were identified. The majority of MR imaging was performed within 3 days antecedent to drainage (84%). Most cases were determined to be sequelae of non-accidental trauma (74%). Using gray matter as an internal control, the fluid signal characteristics were recorded (table 1). All cases showed internal membranes (figure 1). The majority of the membranes demonstrated post contrast enhancement and a minority of cases showed enhancement of the meningeal dura (table 2). A subjective determination was made as to which axial sequence showed the membranes most conspicuously. Membranes were determined to be most conspicuous on SWI (61%) or T2 (39%) in all cases. All sequences and planes were then evaluated to determine which best demonstrated membranes. Coronal T2 (31%), axial T2 (31%), and axial SWI (37%) were nearly equal.
Conclusions: Our data of the signal characteristics of cSDH shares some similarities with current literature. We chronicle the paradoxical signal features of T2* and SWI as well as the confounding variability of T1, T2, and FLAIR imaging. However, analysis of fluid characteristics alone provides an incomplete evaluation of cSDH. Importantly, in our cohort, all patients demonstrated internal membranes within the cSDH and assessment of these structures is critical. Our results showed the most useful sequences for detection of membranes to be T2 and SWI, particularly when obtained in orthogonal planes. The administration of intravenous contrast was of limited utility in the evaluation of cSDH.

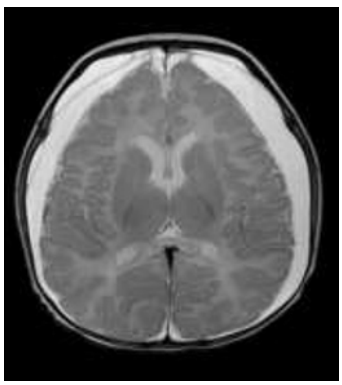

Chronic Subdural Hemorrhage MRI Signal Characteristics

	T1	T2	FLAIR	SWI	GRE	DWI	PD
Hypointense	16/19	0/19	13/19	6/15	0/4	19/19	2/4
Isointense	2/19	1/19	2/19	0/15	1/4	0/19	0/4
Hyperintense	1/19	18/19	4/19	9/15	3/4	0/19	2/4

Chronic Subdural Hemorrhage Enhancement and Architecture

	Endosteal Dura	Meningeal Dura	Internal Membranes
Enhancement	12/13	4/13	11/13
No Enhancement	1/13	9/13	2/13

Poster #: SCI-048

Performance of whole-body MRI in evaluation of pediatric oncology patients: a single center experience.

Perry Hampilos[1], *perry_hampilos@hms.harvard.edu*; Alison Friedmann, MD[2], Michael Gee, MD, PhD[2]; [1]Harvard Medical School, Boston, MA, [2]Massachusetts General Hospital, Boston, MA

Disclosures: All authors have disclosed no financial interests, arrangements or affiliations in the context of this activity.

Purpose or Case Report: Whole-body magnetic resonance imaging (WB-MRI) is an increasingly important tool in pediatric oncology. Optimized WB-MRI protocols allow for abbreviated imaging of young patients with excellent tissue contrast/resolution and without ionizing radiation exposure. Recent data suggest a role for WB-MRI in pediatric cancer staging, cancer predisposition syndrome (CPS) surveillance and evaluation for chemotherapy-related osteonecrosis. The purpose of this study is to evaluate the performance of WB-MRI in these populations.

Methods & Materials: A single institution IRB-approved retrospective review of radiology reports identified pediatric patients who underwent WB-MRI in the years 2002-2016. Electronic records were queried to identify patients undergoing WB-MRI for cancer staging, CPS surveillance or evaluation for osteonecrosis. A single pediatric radiologist reviewed all studies to confirm findings in the report. Electronic medical records of imaging and notes within one year of WB-MRI were reviewed to assess impact on clinical management.

Results: A total of 24 patients were included: 12 undergoing cancer staging (5 neuroblastoma, 2 Ewing sarcoma, 5 lymphoma), 5 undergoing CPS surveillance (4 hereditary paraganglioma-pheochromocytoma syndrome (HPPS), 1 Li-Fraumeni syndrome) and 7 undergoing evaluation for osteonecrosis. In the staging group, WB-MRI demonstrated known disease in 12 of 12 (100%) patients when compared to concurrent scintigraphy, PET, SPECT or CT/MR imaging (fig 1). In the CPS group, no new lesions were seen on follow-up imaging in 5 of 5 patients (fig 2). WB-MRI identified known lesions in 1 of 2 (50%) HPPS patients, failing to detect a vertebral lesion seen on PET imaging. In the osteonecrosis group, WB-MRI confirmed osteonecrosis in 6 of 7 patients (86%) and ruled it out in 1 of 7 (14%). Imaging affected the decision to continue, hold or restart steroids in all 6 patients with steroid-based treatment plans (fig 3). In one patient, WB-MRI identified an area of sub-clinical osteonecrosis in the femoral head.

Conclusions: This preliminary single-institution study demonstrates the value of WB-MRI in pediatric cancer staging, surveillance and chemotherapy-related osteonecrosis. Study limitations included population size and retrospective nature of the analysis. We note that WB-MRI was used as an adjunct to other imaging modalities in our population, and further studies will be needed to assess WB-MRI performance in the pediatric oncology population as the sole surveillance imaging modality.

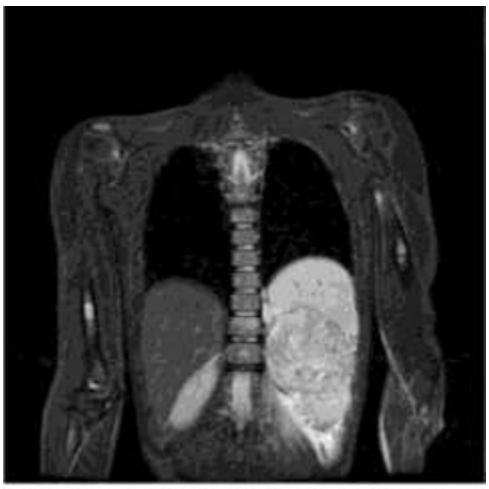

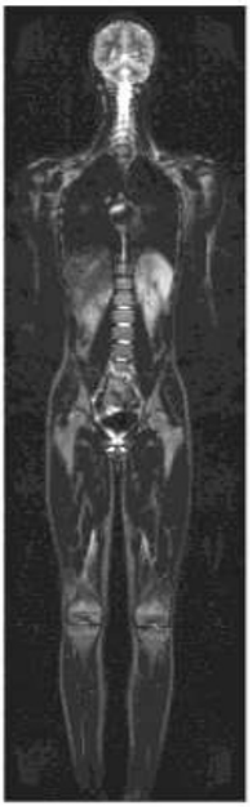

Figure 2: WB-MRI coronal STIR image of a 16 year-old male with hereditary paraganglioma-pheochromocytoma syndrome and known right cervical paraganglioma, demonstrating no new paragangliomas.

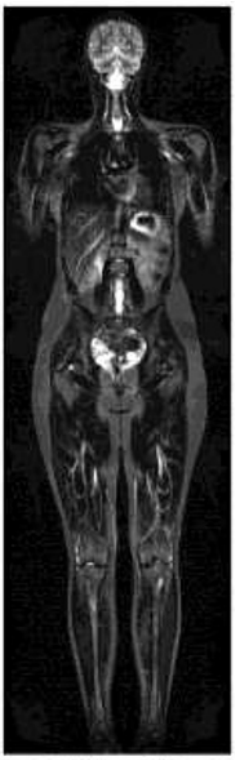

Figure 3: WB-MRI coronal STIR image of a 17 year-old female undergoing chemotherapy for Hodgkin lymphoma, demonstrating steroid related multifocal osteonecrosis.

Poster #: SCI-049

The Landscape of Pediatric Breast Imaging

Bonmyong Lee, MD[2], *blee111@jhmi.edu*; Matthew Whitehead, MD[1]; [1]Neuroradiology, Children's National Medical Center, Washington, DC, [2]Johns Hopkins Medical Institute, Baltimore, MD

Disclosures: All authors have disclosed no financial interests, arrangements or affiliations in the context of this activity.

Purpose or Case Report: Imaging evaluation of the pediatric breast is often necessary to evaluate suspected disease in immature and developing mammary tissue. The initial assessment of these patients commonly occurs at a children's hospital. In this retrospective study, we aim to demonstrate the landscape of pediatric breast imaging by providing the prevalence of various breast-related imaging techniques, diagnoses, and demographics encountered at an academic children's hospital over a 10 year period.
Methods & Materials: The imaging database at a single academic children's hospital was queried for all reports containing "breast" over 10 consecutive years (11/1/06-11/1/16). Each imaging report and electronic medical records were reviewed for demographics, clinical data, imaging findings, follow-up information, and histopathology when available.
Results: 1348 reports (595 inpatient, 124 ER, and 92 outpatient; 1129 ultrasound, 129 CT, and 90 MRI) from 1175 patients (1140 female, 208 male; mean 12 +/-6 years) were identified. The most common diagnoses were infection (abscess, cellulitis, mastitis) (n=244 patients), fibroadenoma (n=231 patients), gynecomastia (n=80 patients), breast buds (n=51 patients), ductal ectasia (n=30 patients), and hematoma (n=27 patients). Neoplastic disease was questioned in 16 patients; histopathology revealed 5 fibroadenomas, 1 hyperplastic lymph node, and 1 lipoma. The remaining 9 patients were either lost to follow-up (n=6) or considered to have benign disease after breast surgery consultation (n=3). There were no proven cases of breast carcinoma, sarcoma, or lymphoma.
Conclusions: Pediatric breast imaging encompasses an array of typically benign etiologies.
Breast disease in the pediatric population is generally benign; we found no proven cases of neoplastic breast disease in an academic children's hospital setting over 10 consecutive years.

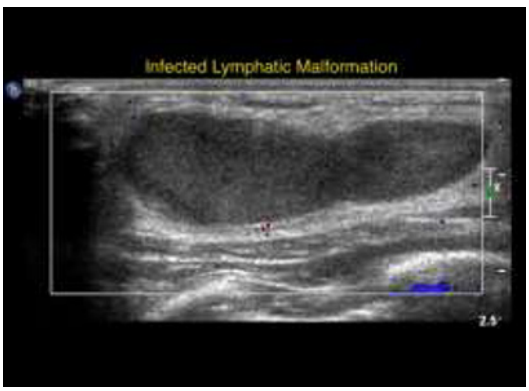

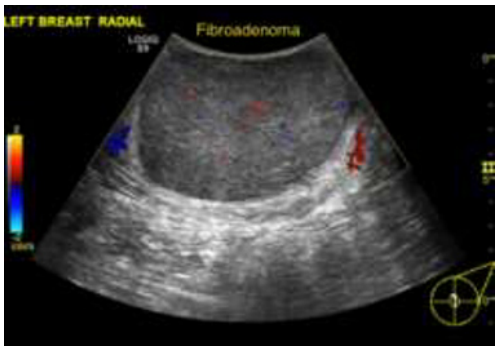

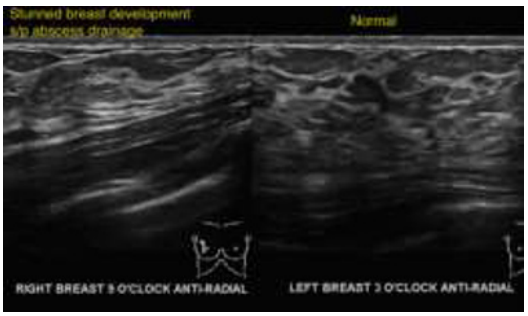

Poster #: SCI-050

Dynamic Ultrasound in Pediatric Patients with Suspected Slipping Rib Syndrome

Dane Van Tassel, MD[1], *vantasse@gmail.com*; Monique Riemann, RDMS RVT[1], Lisa McMahon, MD[1], Craig Barnes[1], Kevin Wong, DO[1]; [1]Radiology, Phoenix Children's Hospital, Chandler, AZ

Disclosures: All authors have disclosed no financial interests, arrangements or affiliations in the context of this activity.

Purpose or Case Report: Slipping Rib Syndrome (SRS) is a condition that affects adolescents and young adults. Dynamic Ultrasound imaging has a potential and likely significant role; however, limited data exists describing the protocol and techniques available for evaluating SRS. It is the intent of this study to describe the development of an effective and reproducible protocol for dynamic imaging in patients with SRS.
Methods & Materials: Retrospective review was performed of suspected SRS patients that presented either to the Radiology or Surgery department from March through October of 2017. 22 patients were evaluated utilizing a high frequency 12-5 linear transducer. Focused history was taken and imaging was performed at the site of pain. Images of the bilateral 7th-11th ribs were obtained in the parasagittal plane at rest and with dynamic maneuvers. Dynamic maneuvers included Valsalva, crunch, focal rib push/compression, and any other provocative movement that elicited pain per the patient. Imaging results were correlated with medical and surgical records generated by the pediatric surgeon specializing in treatment of slipping ribs.
Results: 86% (18/21) of patients had a clinical diagnosis of SRS with an average age of 17.4 years. 16 patients were female, while 6 were male. 73% (16/22) of patients were athletes, with average BMI 22.3. Dynamic ultrasound correctly detected the presence of SRS in 84% (16/19) of patients and correctly detected the absence of SRS in 100% of patients (3/3). Two of the three examinations which did not detect SRS did not utilize dynamic crunch or push maneuvers. In the last patient, crunch was performed, but push maneuver was not. All but one exam utilizing the crunch and push maneuver correctly detected SRS.
Conclusions: Dynamic Ultrasound imaging of the ribs,

particularly with utilization of crunch and push maneuvers, is an effective and reproducible tool for the diagnosis of SRS.

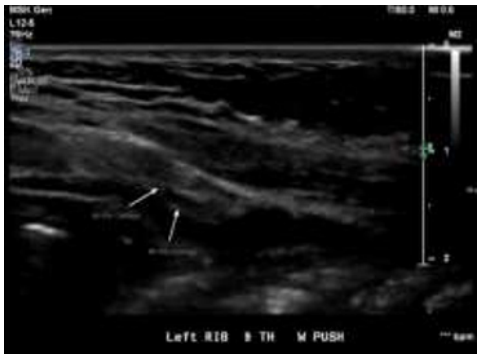

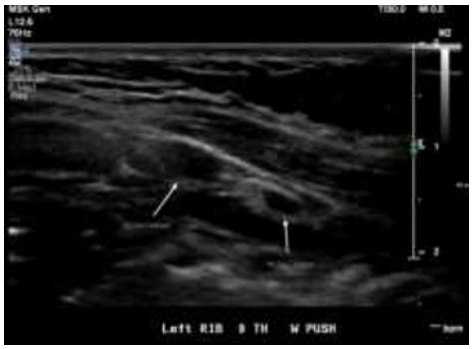

CASE REPORT, EDUCATIONAL AND SCIENTIFIC POSTERS - TECHNOLOGISTS

(T) indicates an Imaging Technologist Program Submission

Poster #: CR-001 (T)

MRI fetal exams for sacrococcygeal teratomas

Silvia Acevedo, Bachelor of Science[1], *sacevedo@luriechildrens.org*; Kimberly Ritze[1]; [1]Medical Imaging, Ann & Robert H. Lurie Children's Hospital of Chicago, Chicago, IL

Disclosures: All authors have disclosed no financial interests, arrangements or affiliations in the context of this activity.

Purpose or Case Report: To provide MRI staff education on MRI fetal exams for sacrococcygeal teratomas. Sacrococcygeal teratoma (SCT) is a congenital germ cell tumor located at the base of the tailbone in newborns. This birth defect is generally not malignant. A SCT is most often diagnosed prenatally using routine obstetric ultrasonography, and further anatomical evaluation may require MRI. A SCT can grow during pregnancy and develop large blood vessels requiring more work for the fetal heart. SCT are more common in females than in males and occur in about 1 in 35,000 live births.
Methods & Materials: Ann & Robert H. Lurie Children's Hospital of Chicago scanned approximately 100 fetal MRI exams in fiscal year 2016. Lurie Children's new Chicago Institute of Fetal Health program has increased the volume of fetal cases being performed in our MR department. Now with more cases being scanned we are seeing more rare pathology and diagnosis than prior. One of the recent cases was diagnosed as a fetal sacrococcygeal teratoma. Evaluation of this case has led to a modification of our fetal scanning protocol to accommodate previously identified SCT.
Results: MR staff will need to identify and properly scan sacrococcygeal teratomas that may be indicated amongst our fetal cases. Sacrococcygeal teratoma requires the technologist to identify the pathology and extend the scan field of view to include the extent of the tumor. Patient position may need to be modified to optimize the image quality. Radiologist surveillance at the scanner may assist in ensuring images are of sufficient diagnostic quality.
Conclusions: Fetal sacrococcygeal teratomas are rare but the imaging performed in MRI may yield helpful results to prepare for the next steps if the MRI protocol is adjusted appropriately.

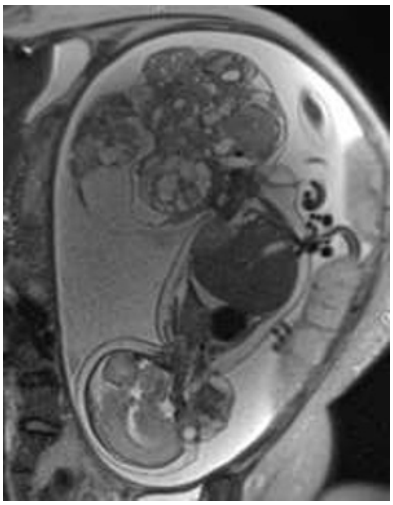

Poster #: CR-002 (T)

Title: Role of Ultrasound in Diagnosis Pediatric Acute Appendicitis with a secondary sign of an early perforation

Falguni Patel, Associates[1] *fpatel0807@yahoo.com*; ; [1]Medical Imaging (Ultrasound), Lurie Children's Hospital of Chicago, Chicago, IL

Disclosures: All authors have disclosed no financial interests, arrangements or affiliations in the context of this activity.

Purpose or Case Report: To demonstrate Pediatric Acute Appendicitis with a secondary sign of an early perforation based on ultrasound findings.
Methods & Materials: 11 years old patient presented to our Emergency department with severe abdominal pain for past two days, constipation for four days, inability to tolerate food intake and non-bloody emesis. STAT portable abdomen ultrasound was ordered on this patient to rule out Acute Appendicitis by the Emergency department.
Results: Ultrasound findings demonstrated markedly dilated appendix with the AP diameter of 2.5cm in right lower quadrant with a large shadowing Appendicolith near the tip of the appendix. It also demonstrated a small echogenic focus near the wall of the appendix which could represent an early perforation. After ultrasound findings, patient was rushed to the Operating room without further imaging and post-operative diagnosis demonstrated perforated appendix with fecalith and extensive pus in the intraperitoneal cavity.
Conclusions: Ultrasound should be an initial imaging study of choice for pediatric appendicitis. With the presence of secondary signs such as appendicolith, periappendiceal fat, free fluid and extra luminal air along the margin of the appendicular wall. Ultrasound plays an important role in diagnosis acute appendicitis in pediatric patients.

Poster #: CR-003 (T)

Do you know how to do MR Lymphangiography?

Stacy Kikke[1], *skikke@luriechildrens.org*; Kimberly Ritze[1]; [1]Medical Imaging, Ann and Robert H. Lurie Children's Hospital of Chicago, Chicago, IL

Disclosures: All authors have disclosed no financial interests, arrangements or affiliations in the context of this activity.

Purpose or Case Report: The purpose of this submission is to educate technologists in performing magnetic resonance (MR) lymphangiography in conjunction with intranodal gadolium contrast injection in the pediatric patient. MR lymphangiography is a new procedure in the pediatric population. The lymphatic system plays the important role of transporting fluid from tissue back into the venous system via lymphovenous connections. Despite this key role, there has been a poor understanding of lymphatic flow physiology. The recent development of dynamic contrast intranodal MR lymphangiography, which provides quick and reliable access to the central lymphatic system, has provided insight into understanding the pathophysiology of several lymphatic flow disorders and provides guidance for interventional procedures. It also makes it possible to see central lymphatic anatomy with high spatial and temporal resolution. This allows clinicians to map the anatomy of the lymphatic system to determine the location of lymphatic leaks. MR lymphangiography may reduce the need for conventional IR lymphangiogram and spare patient's radiation exposure.
Methods & Materials: Multiplanar multisequence MR is performed with and without the administration of intranodal gadolinium. Precontrast sequences include coronal T2 "Sampling Perfection with Application Optimized Contrasts using Different Flip Angle Evolution" (SPACE), axial coronal and sagittal with "True Fast Imaging with Steady State Free Precession" (TRUFI) and precontrast coronal T1 "Volumetric Interpolated Breathhold Examination" (VIBE). Subsequently, under ultrasound guidance, 22-gauge spinal needles are inserted into bilateral inguinal lymph nodes and gadolinium followed by saline is injected into the lymph nodes timed over a duration of 15 minutes. TWIST sequences are acquired as well as delayed postcontrast sequences.
Results: MR lymphangiography was performed in several patients who received conventional IR lymphangiogram contemporaneously. Qualitative evaluation of these cases indicates that MR lymphangiography may be diagnostically adequate for evaluation of lymphatic disorders.
Conclusions: MR lymphangiography requires complex coordination between anesthesia, interventional radiology (IR) and the MR divisions. Despite these challenges, our recently developed MR lymphangiography protocol has been successfully performed in several patients and early validation looks promising.

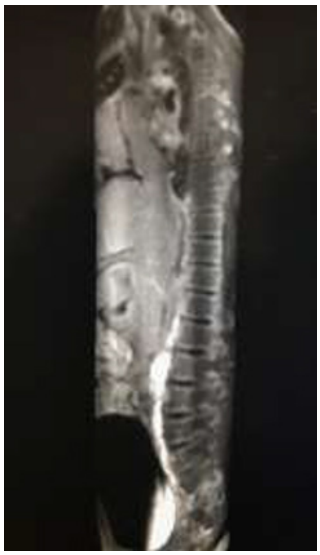

Poster #: CR-004 (T)

Extra-osseous uptake of Tc^{99m}-HDP on bone scintigraphy in a paediatric patient with hepatoblastoma

Laura Mannix[1] *lauramannix15@gmail.com* ; [1]Nuclear Medicine, Our Lady's Children's Hospital Crumlin, Dublin, Ireland

Disclosures: All authors have disclosed no financial interests, arrangements or affiliations in the context of this activity.

Purpose or Case Report: A three year old child was referred to the Nuclear Medicine Department for bone scintigraphy for staging. This patient was diagnosed with hepatoblastoma. Imaging findings showed no bony disease, however, radiotracer uptake was demonstrated throughout the liver.
Methods & Materials: A whole body bone scene was performed, Supplemental Data File 1, followed by SPECT of the abdomen with low dose co-registering CT through the liver, to further assess a lesion seen on planar imaging.
Results: No evidence of local bony disease or distant metastasis. Multiple small focal accumulations of Tc-99 HDP radiotracer are demonstrated throughout the liver with some CT abnormalities, Supplemental Data File 2. This is related to calcifications within the hepatoblastoma.
Conclusions: Demonstration of calcified lesions within the liver of a paediatric patient with hepatoblastoma.

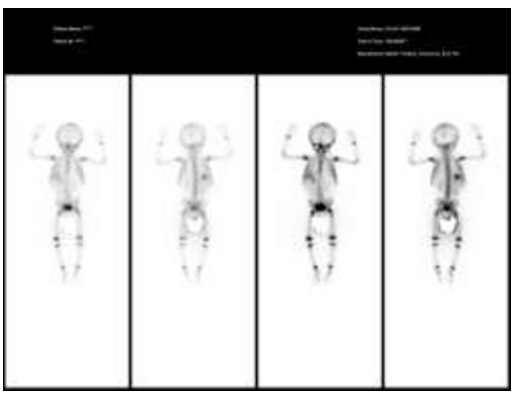

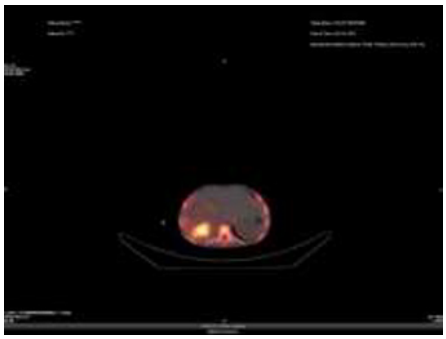

Poster #: EDU-001 (T) - *Withdrawn*

Poster #: EDU-002 (T)

Transcranial Doppler of the Neonatal and Infant Brain: How, When, and Why

Tara Cielma[1], *tcielma@cnmc.org*; Anjum Bandarkar[2], Lesley Demshur[1], Dorothy Bulas, MD[1]; [1]Children's National Health System, Manassas, VA, [2]Mid-Atlantic Permanente Medical Group, Reston, VA

Disclosures: All authors have disclosed no financial interests, arrangements or affiliations in the context of this activity.

Purpose or Case Report: Background: Duplex sonography is a critical portion of intracranial hemodynamics evaluation. Serial Doppler examination allows real-time assessment of disease progression or improvement.
The goals of this exhibit are:
1. Describe the technical approach of performing neonatal/infant transcranial Doppler ultrasound.
2. Review tips, and up to date technology that assist in optimizing studies.
3. Discuss changes in flow patterns with various pathologies, providing examples of clinical indications.
4. Review future potential techniques and applications.
Methods & Materials: Neonatal/infant cranial ultrasounds performed with Doppler at our institute were reviewed retrospectively with selected representative cases chosen to illustrate technical aspects and clinical indications for this procedure. Correlation was made with follow up radiology studies, clinical and/or surgical outcomes.
Major intracranial cerebral arterial (PSV/RI/PI) values with hypoxic ischemic encephalopathy, hydrocephalus, vascular malformations and brain death; terminal vein flow; dural venous sinus flow, and compression of the fontanelle for intracranial pressure assessment will be described.
Results: Typical findings in normal and abnormal infant transcranial Doppler exams will be illustrated. Emphasis on appropriate technique and methodology for serial examinations is described. Tips including utilization of a high frequency linear transducer, choosing optimal window of insonation will be discussed.
Conclusions: Through this exhibit, participants will learn to utilize cranial Doppler as an effective adjuvant tool when performing infant neurosonography.

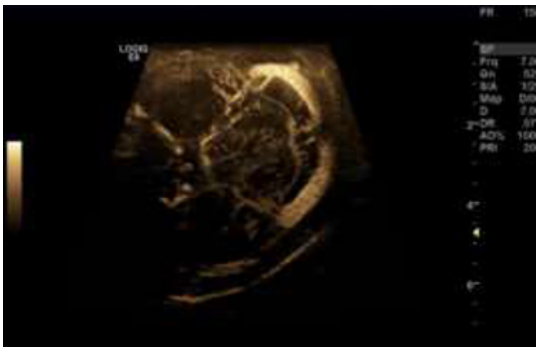

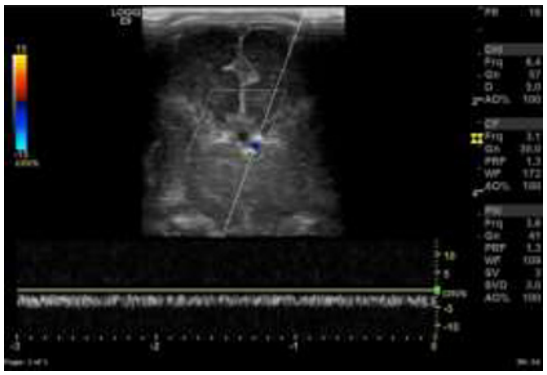

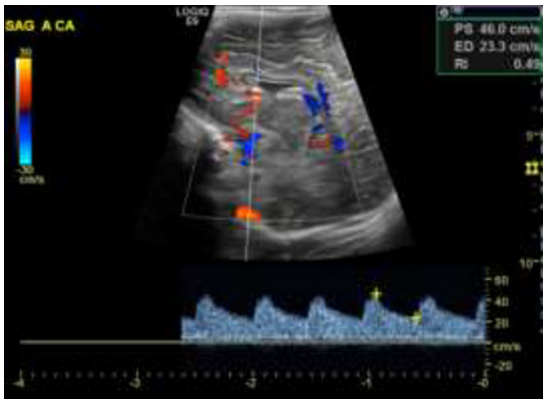

Poster #: EDU-003 (T)

The Impact of One Volume Acquisition

Tara Cielma[1], *tcielma@cnmc.org*; Kadine Linden[1]; [1]Children's National Health System, DC

Disclosures: All authors have disclosed no financial interests, arrangements or affiliations in the context of this activity.

Purpose or Case Report: Background: Volume acquisition in ultrasound is recognized as a helpful tool in prenatal sonography, but notorious for having a steep learning curve. At times, utilizing this technology may be the *only* way to visualize anatomy due to factors such as maternal body habitus or fetal position. Our goal is provide the audience with the information and techniques required to take a volume sweep acquisition and obtain numerous rendering modes to evaluate the fetal craniofacial area.
Aims:
1. To describe utility and benefit of acquiring volume ultrasound in detection of craniofacial anomalies in prenatal patients.
2. To describe tips, tricks, and current technology to optimize imaging and assist in minimizing equivocal exams.

3. Provide examples of soft tissue lesions, hydrocephalus, craniosynostosis, micrognathia and midline cleft cases.
4. To look into future technology and potential applications.
Methods & Materials: Second and third trimester prenatal ultrasound exams were performed on patients referred for suspected abnormalities. Volume sweeps were acquired on each patient and representative cases chosen to illustrate technical aspects and clinical indications for this procedure were selected. Post-acquisition rendering was performed to illustrate modes to analyze the skeletal system, fluid filled structures, soft tissue, and internal structure contours. Correlation was made with follow up radiology studies, clinical and/or surgical outcomes.
Results: Thorough evaluation and timely diagnosis is essential for optimal management and site of delivery.
Common sites for multiplanar imaging include the bony face and soft tissue anatomy. Demonstration of the methods will be explored and the impact of their clinical application discussed.
Conclusions: Through this exhibit, participants will gain familiarity with the use of multiplanar and spatial volume imaging, and utilize volume imaging as an effective adjuvant tool to routine 2D cross-sectional imaging.

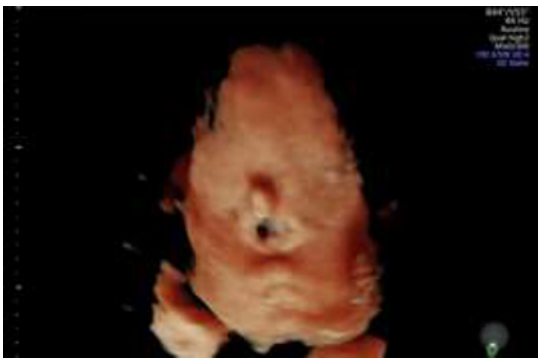

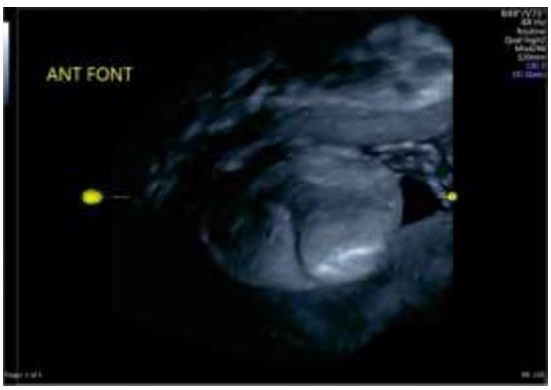

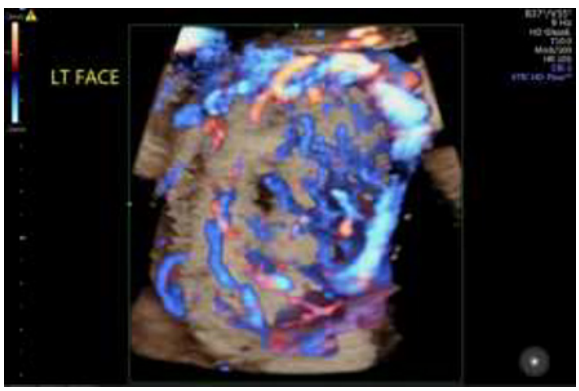

Poster #: EDU-004 (T) - *Withdrawn*

Poster #: EDU-005 (T)

Radiographic features of Necrotizing Enterocolitis (NEC), one of the most common gastrointestinal diseases in premature neonates.

Ewelina Ulikowska, RT (R) [1] *eulikowska@luriechildrens.org*; [1]Medical Imaging, Ann & Robert Lurie Children's Hospital, Des Plaines, IL

Disclosures: All authors have disclosed no financial interests, arrangements or affiliations in the context of this activity.

Purpose or Case Report: Necrotizing enterocolitis (NEC) is one of the most leading causes of morbidity and mortality in premature infants. It usually develops within the first days following birth. NEC is a gastrointestinal disease, that can affect any part of the large or small bowel but most commonly affects the terminal ileum and colon. It causes inflammation and tissue death of the affected area and can lead to bowel perforations and a need for surgical resections. In severe cases, bacteria and waste products can pass through the perforated intestine and enter the baby's bloodstream or abdominal cavity which can cause a life threatening infection and shock. In a pediatric hospital, that treats premature infants, signs and symptoms of necrotizing enterocolitis are very important to diagnose quickly. Most common symptoms include poor feeds, bloating or swelling in the abdomen, bloody stools and diarrhea. In order to manage the disease medically and surgically, prompt diagnostic tests such as ultrasounds and xrays need to be performed. Abdominal X-rays are the gold standard of diagnosis and treatment planning. Therefore it is crucial, to recognize the radiographic signs of NEC. The purpose of this abstract is to describe radiographic appearances associated with NEC, which include: dilated bowel loops, thickened bowel walls with edema, pneumatosis intestinalis, abdominal free air, portal venous gas, absence of bowel gas. I will present confirmed cases that show radiographic signs of NEC.

Poster #: EDU-006 (T)

Optimal techniques in fluoroscopy when determining intestinal malrotation versus normal intestinal variants.

Lynn Gazzi, associates[1] *gazzi@sbcglobal.net* ; [1]Lurie Children's Hospital, Chicago, IL

Disclosures: All authors have disclosed no financial interests, arrangements or affiliations in the context of this activity.

Purpose or Case Report: Intestinal malrotation is a defect that occurs in the 10th week of gestation. During this stage the intestines normally migrate back into the abdominal wall following a brief period where they are temporarily located in the base of the umbilical cord. As the intestines returns to the abdomen it makes two rotations and becomes fixed into its normal position. The small bowel is located in the center of the abdomen and the large intestine drapes around the top and sides of the small intestine. When rotation is incomplete and intestinal fixation does not occur, this creates a defect known as malrotation. Malrotation occurs in one of every 500 births in the United States. Up to 40 percent of patients with this show signs of the disease within the first week of life. By one month of age 50-60 percent are diagnosed. 75 to 90 percent are diagnosed by age 1. The remaining cases are diagnosed into adulthood. Some symptoms of malrotation include vomiting and bilious emesis, fussiness, crying in pain, a swollen abdomen that's tender to the touch, fever, diarrhea and bloody stool or none at all. If malrotation is not treated, it can lead or turn into a midgut

vovulus. This is when the gut twists counterclockwise around the superior mesenteric artery and vein causing a narrowing. This may cause abdominal distention and pain or acute bowel necrosis. It can also be life threatening or lead to a lifelong dependence on total parenteral nutrition, so surgical correction is the dependent treatment. When medical history and physical examination indicate a suspicion of malrotation and vovulus, patients must undergo blood tests and diagnostic imaging studies to evaluate the position of the intestine to determine if there is blockage or twisting. The imaging modality of choice remains the upper GI study. This is a fluoroscopic study using barium contrast to look at the upper and middle sections of the gastrointestinal tract. A radiologist's knowledge of normal anatomy is important in performing and interpreting the upper GI series. From a technical standpoint common pitfalls during this test that can lead to a misdiagnosis would be imaging quality. Improper patient positioning, nonsufficient images taken and the wrong amount of contrast administered during the most crucial part of the study can lead to false findings. The purpose of this abstract is to present case studies and imaging which mimic intestinal rotation but are a normal variant vs. actual cases of malrotation.

Poster #: EDU-007 (T) – *Withdrawn*

Poster #: EDU-008 (T)

Recognizing and Reducing Imaging Artifacts in Pediatric Digital Radiography

Patty Myefski, RTR, RDMS[1], *pmyefski@luriechildrens.org*; Christina Sammet, PhD, DABR[1]; [1]Medical Imaging, Lurie Children's, Chicago, IL

Disclosures: All authors have disclosed no financial interests, arrangements or affiliations in the context of this activity.

Purpose or Case Report: To recognize imaging artifacts that are unique to digital radiography (DR) and to learn techniques to reduce the most common image quality issues. DR systems in medical imaging have transformed planar xray, one of the oldest imaging modalities. Computed radiography (CR) and DR share some of the same image quality challenges including poor positioning, inappropriate techniques, and motion. There are image quality issues unique to DR that may be unfamiliar to new operators. Although, artifacts have been a part of imaging since the use of film-screen xray, with DR, the technologists have to be aware of new artifacts related to digital acquisition and processing. At times, pediatric DR imaging can present even bigger challenges. Technologists must learn methods to avoid DR imaging artifacts, and how to identify them before sending the image to the Picture Archiving and Communication System (PACS). This exhibit will review how to identify common DR imaging artifacts, explain the reason they occur, and suggest methods to reduce their interference with image quality.
Methods & Materials: Common DR artifacts were identified by review of recent literature and a retrospective review of images acquired at our institution. A physicist was consulted regarding the source of these DR image quality issues. A radiologist was consulted to assess how much these artifacts interfere with clinical interpretation. Image quality issues were evaluated for their appearance on both image viewing station and the radiologist viewing station in order to assess differences in conspicuity and appearance. Example cases were identified where DR artifacts are significantly more prominent on high resolution PACS monitors than they appear at the technologists work station. A case-based technologist staff education was developed.
Results: A case-based educational module was developed that reviews common artifacts in DR, the physical principles behind these artifacts, and their effect on diagnostic quality. Methods to reduce or eliminate these artifacts were reviewed and summarized. A protocol to communicate with Radiologists regarding digital artifacts was developed including best practices for determining when repeat imaging is required.
Conclusions: Technologists familiar with CR may face challenges when learning DR because image artifacts are different. Case based education on artifacts unique to digital imaging may reduce image quality issues and the need for repeat imaging leading to reduced radiation exposure in children.

Poster #: EDU-009 (T)

Reduction in Sedation of Patients Five Years and Younger Receiving CT Imaging of Thorax and/or Abdomen/Pelvis on a Siemens SOMATOM Force

Crystal Blake, AAS, RT(R)(CT)[1], *crystal.blake@choa.org*; Laura Chastain, RN, BS, BSN[1]; [1]Radiology, Children's Healthcare of Atlanta, Buford, GA

Disclosures: All authors have disclosed no financial interests, arrangements or affiliations in the context of this activity.

Purpose or Case Report: Pediatric patients five years and younger often require sedation to successfully complete CT imaging of the thorax and/or abdomen/pelvis. Sedation of pediatric patients poses certain risks and should be avoided when possible. In August of 2017, Children's Healthcare of Atlanta installed a new CT scanner - a Siemens SOMATOM Force. The SOMATOM Force posesses a Turbo Flash mode which results in sub second scan times for CT imaging of the thorax and/or abdomen/pelvis.
Methods & Materials: Historically, patients that are five years and younger are often sedated for CT exams of the thorax and/or abdomen/pelvis. In August, 2017, Children's Healthcare of Atlanta installed a Siemens SOMATOM Force CT scanner, capable of imaging the thorax and/or abdomen/pelvis with scan times averaging 0.56 seconds. To identify a decrease in sedations after the installation of the SOMATOM Force, we analyzed sedation percentages before the installation to the sedation percentages after installation. A report was created within our EMR system to identify patients five years and younger that received CT imaging of the thorax and/or abdomen/pelvis. An additional report was generated by the sedation physicians' data regarding the number of sedations for the same time reference. These reports were analyzed and compared to generate the overall percentage of sedations.
Results: Four months of data prior to the installation of the Siemens SOMATOM Force revealed sedation percentages on an average of 34.5% of patients aged five years and younger. The first full month after installation of the Siemens SOMATOM Force revealed a decrease in sedations to 15% of patients aged five years and younger.
Conclusions: Installation of the Siemens SOMATOM Force at Children's Healthcare of Atlanta at Scottish Rite has resulted in a decrease in the sedation of patients five years and younger receiving CT imaging of the thorax and/or abdomen/pelvis.

Poster #: EDU-010 (T)

Mobile CT Utilization during CT Renovation at a Children's Hospital: Patient Safety Consideration

Angie Wright[1], *angie.wright@choa.org*; Stephen Simoneaux[1]; [1]Radiology, Children's Healthcare of Atlanta, Atlanta, GA

Disclosures: All authors have disclosed no financial interests, arrangements or affiliations in the context of this activity.

Purpose or Case Report: During a recent CT renovation, a mobile CT scanner had to be used at a major urban children's hospital which also is a Level 1 trauma center. Performing exams while maintaining patient safety and providing quality diagnostic imaging involved the collaborative efforts of the radiology team, the project manager, the construction team, and the hospital service line leaders. The purpose of this exhibit is highlight the anticipated and unanticipated considerations which had to be addressed prior to the use of the mobile CT scanner. Knowing how these environmental and patient safety issues were identified and addressed may be a help with future radiology equipment replacement projects.
Methods & Materials: Environmental concerns: As the unit was outside, the construction team had to design and build an adequate overhead awning to protect patients from inclement weather. An approaching hurricane meant the area had to be reassessed for its ability to be used during violent weather.
Inpatient imaging: Patient simulations were performed to determine which pieces of medical equipment could fit onto the mobile CT lift when transporting the patient from ground level into the scanner. Earlier communication to pertinent hospital personnel, notably Emergency Department and ICU staff, would have allowed for more education in preparation for transporting patients to the mobile CT. Issues around severe trauma and unstable ICU patients would have been addressed with more time for preparation. With more notice and simulations, staff in these critical areas would have been more prepared for the utilization of the mobile CT scanner.
Emergency and Sedation Preparation: Anesthesiology and Sedation Services were involved in the process. Ultimately, Anesthesia decided that patients could not be safely performed at the mobile location, and these patients were performed on a PET/CT scanner. The sedation team was able to provide its services off-site, but again, simulations and early involvement were key. Security and the Code Team were also engaged to ensure that responses to codes were prompt and the site well-known.
Conclusions: The use of the mobile CT scanner during the removal and installation of a new CT scanner was an educational experience to those involved. This radiology project may have gone more smoothly if many of these concerns were addressed prior to the start of the project. The information contained in this presentation will help other sites who have to use a mobile CT unit for scanning.

Poster #: EDU-011 (T)

The Stop Sign Method: An Alternative Radiographic Position for the True Lateral Elbow Projection.

Allister Ramrattan, RT, BSN, RN, BSN[1]
allister.mark.r@gmail.com; [1]Radiology, Children's National Medical Center, Gaithersburg, MD

Disclosures: All authors have disclosed no financial interests, arrangements or affiliations in the context of this activity.

Purpose or Case Report: The purpose of this retrospective observational study is to provide an alternative if not optimal lateral elbow projection method to be considered for use in traumatic injuries with suspected distal humeral fractures and/or observable deformity at the distal humerus.
The true lateral radiograph of the distal humerus commonly contributes to the decision of Gartland classification of supracondylar fractures and other distal humerus fractures. This is important when deciding which elbow fractures require invasive surgery and anesthesia as opposed to a reduction with conscious sedation. While the Elbow Lateral Projection (Lateromedial) in current practice typically results in a perfect lateral radiograph for adult patients, this method does not result in a true lateral of the distal humerus in pediatric patients. The condyles are rarely superimposed and the signature "hour glass" sign is imperfect. The Stop Sign Method is a medial to lateral projection that routinely results in a true lateral of diagnostic quality and meeting textbook qualification. Not only is positioning in the Stop Sign method more comfortable for trauma clients, it produces a more consistent radiograph when utilized on follow-up orthopaedic visits and enables clinicians to better track reduction retention and healing.
Methods & Materials: Review of past radiographs of distal humeral fractures performed by a team of blind, radiologic technologists imaging pediatric clients in a busy Emergency Department setting, utilizing current procedures and a specific protocol of radiographic positioning. Use of a mediolateral projection was used in patients that were unable to comply with the lateromedial projection due to immobility attributable to injury or other underlying condition.
Results: Noted success in achieving a true lateral elbow radiograph by utilizing the stop sign method instead of the conventional methods as outlined in the current radiologic technologist's curriculum.
Conclusions: Utilization of the Stop Sign method for imaging of pediatric patients results in a true lateral as evidenced by fewer films needed to achieve a true lateral of the distal humerus both post trauma and on serial visits and cast changes.

Poster #: EDU-012 (T)

Shared Governance - The Radiology technologist's journey to Implementation

Chris Harris, RT (R) (MR)[1] *Harrisc@email.chop.edu*; [1]Children's Hospital of Philadelphia, Philadelphia, PA

Disclosures: All authors have disclosed no financial interests, arrangements or affiliations in the context of this activity.

Purpose or Case Report: Introduction:
Shared governance is a specific leadership style which incorporates commitment to the value of shared decision-making among key stakeholders around issues that affect the work environment. It also provides a dynamic staff-leader partnership that promotes collaboration, shared decision making and accountability for improving quality of care, safety and enhancing work life
Methods & Materials: Around 2009, CHOP's Radiology Department attempted to implement the nursing professional practice model with a core group of technologist's, but failed after only one year of implementation. Failure was attributed to the following: Model driven by upper management vs staff driven; Model was presented without collaboration; and No interest from staff
To better understand what engaged our staff, we conducted an employee satisfaction survey. After conclusion of the survey, staff presented concerns to leadership within Radiology as well as to the VP of the hospital. These concerns were then categorized into themes:

Recognition/retention, education opportunities for staff, staff support to our patients, having input into decisions and communication within the department.
Results: With this knowledge at hand, we relooked at our past shared governance model and design a program by which these themes could be addressed, while improving patient care and the work environment. We set up eight committees which balanced staff and the following leadership concerns:
Recognition and retention, Patient centered care, Policy and procedures, Ancillary partnerships, Education, Quality improvement, Research/Equipment and Imaging protocols. Each group provided a mission, developed by them. Meetings and, topics are managed by staff. . Committees are supported by Team Leaders in the form of coverage to attend meetings, time to work on projects, dollars for projects, and ensuring that solutions meet hospital standards and policies. Leadership views this as a great opportunity to vet complaints and process and work issues to these groups to look for solutions.
Conclusions: Challenges associated with the introduction of a nurse driven professional practice model into a technologist practice model suggests that greater attention to implementation may be required much more than a top down approach. Understanding what drives your staff, collaboration on these ideals and supporting this practice model makes for a successful program.

Poster #: EDU-013 (T)

Driving the path to easing anxiety for pediatric Radiology patients

Dana Brinson, BHA, RT(R)(ARRT)[1], *Dana.brinson@choa.org*; Nikki Butler, BMSc, RT(R)(QM)[1]; [1]Radiology, Children's Healthcare of Atlanta, Atlanta, GA

Disclosures: All authors have disclosed no financial interests, arrangements or affiliations in the context of this activity.

Purpose or Case Report: For pediatric patients, the hallway leading to a radiology imaging room may be just as anxiety-inducing as the exam itself. In an effort to counteract a child's anxiety, rideable remote control cars were purchased to begin the distraction process at the child's first step towards the Radiology Department.
Methods & Materials: Through charitable donations, two cars were purchased for $400 each to be used in a trial for patient transport throughout Radiology. Six staff members, across different shifts, were identified as Super Users and trained based on the Operation Manual provided by the manufacturer. Competency was deemed through staff demonstration of operating the remote control cars safely and practicing all safety measures associated with patient riders. The riders must wear the safety belt, keep all body parts inside the vehicle, be age three years or older and weigh under 60 pounds. There is a switch to deactivate the foot pedals; however there is not a mechanism to deactivate the steering wheel. Therefore, patients are asked to place their hands by their sides. Another consideration was storage of the cars, as multiple cars require a significant amount of space for parking and electrical outlet needs for recharging the batteries. Storing the cars in a publicly accessible location was not ideal for safety concerns. Ultimately, an alcove by a set of elevators was selected for easy access by staff during the day and the MRI Mock Scanner Room was utilized for recharging at night.
Results: The success of the rideable remote control car program was evident through positive feedback received on customer service surveys. A video posting on Facebook resulted in a local news story highlighting the cars and the fun experience for one patient, thus providing marketing exposure affirmative of the care being provided. The project returned favorable results, prompting the facility to add the rideable cars to a wish list that is shared with charitable donors. A total of 20 cars are now available for use throughout Radiology and other departments across the system.
Conclusions: While the project initially centered on the reduction of patient anxiety, additional benefits identified were stress alleviation for the parents and entertainment for patient's siblings. The ride from the Radiology Waiting Room to the exam room also allowed the technologists to develop a rapport with the patient that allowed for more cooperation during the imaging study.

Poster #: EDU-014 (T)

Low Dose Imaging for Feeding Tube Confirmation

Colleen Flowers, Associates Degree[1], *flowers@email.chop.edu*; Summer Kaplan, MD, MS[1], Xiaowei Zhu[1]; [1]Radiology, Children's Hospital of Philadelphia, Philadelphia, PA

Disclosures: All authors have disclosed no financial interests, arrangements or affiliations in the context of this activity.

Purpose or Case Report: The objective for a low dose imaging protocol was to eliminate patient risks and to reduce radiation doses. Tube placements are confirmed via imaging thereby avoiding utilization of malpositioned tubes. Reduced technical parameters lessen the absorbed skin dose. A limited field of view which includes distal espohagus and airway allows accurate assessment of feeding tube position. The new region of interest eliminates unnecessary exposure to hypersensitive organs including, thyroid and reproductive structures. This coned down view requires a lower image quality thereby allowing a lower dose approach.
Methods & Materials: A multidisciplinary team discussed current workflows, process improvements. and anticipated obstacles. Workflows were mapped out for all patient visit types, providers and services. Exam codes were developed with associated CPT charges. Order panels for providers were updated. Macro templates for the Radiologist were developed and loaded at workstations.
Lucite block and phantom testing were conducted using equivalent sized infant, toddler and adolescent phantoms on dedicated and portable units. Testing concentrated on portable units but table bucky techniques were also established. A 40" source to image distance (SID) was used for table (grid) testing and a 36" SID for portable/tabletop. A 6fr feeding tube was used to simulate placement. Established abdomen techniques were selected for corresponding phantom. The KVP factors were unchanged and mAS settings were decreased to lowest outputs by the units. The lowest mAs 1.25 mAs (table grid) was 0.32 for portable (non-grid). The field of view was mid-chest to iliac crest with proper collimation. Radiologist reviewed images and approved for trial. Exams performed using the new protocol. Image quality remained comparable to phantom testing with same technical factors.
Results: The ongoing trial of portable images reflects optimal for tube confirmation using the lowest mAs setting on unit (0.32 mAs). The abdominal KVP settings remained constant for adequate penetration.
Conclusions: The new protocol has a huge benefit to patients. The objective for chest and abdomen imaging is impressively different than a tube check therefore less dose can be utilized. Full dose images are essential for accurate clinical correlations. Mid chest to crest region reduces potential risk of malpositioned tubes as well as significantly reduces unnecessary dose to hypersensitive organs. This is vital when multiple images are required to confirm tube placements.

Poster #: EDU-015 (T)

Pediatric Shielding Education for Imaging Staff

Barbara Karl[1], *bkarl@luriechildrens.org*; Christina Sammet, PhD, DABR[1], Caitlin Maher[1]; [1]Medical Imaging, Ann & Robert H. Lurie Children's of Chicago, IL

Disclosures: All authors have disclosed no financial interests, arrangements or affiliations in the context of this activity.

Purpose or Case Report: The goal of this study was to develop and share a consistent policy and procedure for the appropriate use of patient shielding in the pediatric environment. Education was developed to increase the level of awareness and skill sets to properly shield, or not shield, pediatric patients. The education was distributed to adult affiliated hospitals and within our institution to ensure consistency of care and safety measures.
Methods & Materials: A comprehensive patient shielding policy was developed by a team of technologists, medical physicists, and managers within our institution. An educational presentation was created to standardize acceptable shielding practices for CT, fluoroscopy and diagnostic radiology. The education was based on a retrospective review of cases from our radiation dose monitoring system and PACS, as well as literature searches for best practices in patient shielding. We provided examples of proper and improper shielding on diagnostic images and demonstrate the impact of shielding on both image quality and radiation dose. A competency quiz was developed to capture understanding of the material.
Results: ● Staff were educated on how to accurately shield patients for diagnostic imaging.
● Staff have a document on proper patient shielding to reference when needed.
● Staff were better prepared to address shielding concerns with parents and patients.
● Staff have more consistent shielding practices across the enterprise.
Conclusions: The Pediatric Shielding Education improved consistency of shielding practices at our institution.
● Staff are now competent on what constitutes appropriate shielding in diagnostic imaging, CT and fluoroscopy.
● Staff demonstrated an improved understanding of our shielding practices post education.
● Staff feel more empowered to discuss shielding practices with parents and are aware of their resources for more complex questions.
● Image quality and safety has improved in our pediatric patient population.

Poster #: EDU-016 (T) - *Withdrawn*

Poster #: EDU-017 (T) – *Withdrawn*

Poster #: EDU-018 (T)

Intussusception: How to Reduce the Problem

Dawn Whitson[1] *dwhitson@luriechildrens.org*; [1]Medical Imaging - X-ray, Ann & Robert H. Lurie Children's Hospital of Chicago, Chicago, IL

Disclosures: All authors have disclosed no financial interests, arrangements or affiliations in the context of this activity.

Purpose or Case Report: The purpose of this education is to describe Therapeutic Enema reduction of Intussusception using Hydrostatic and Pneumatic methods. The benefits of Delayed Repeated Enema (DRE) instead of immediate surgical intervention after a failed reduction will be reviewed.

2018 AUTHOR INDEX BY ABSTRACT

I

J

2018 KEYWORD INDEX BY ABSTRACT

D

T

U